Functional and Structural Characterization of the RNase II-family of enzymes

Rute Gonçalves Matos

Dissertation presented to obtain the Ph.D degree in Biology

Instituto de Tecnologia Química e Biológica | Universidade Nova de Lisboa

Oeiras,
September, 2011

INSTITUTO
DE TECNOLOGIA
QUÍMICA E BIOLÓGICA
/UNL

Knowledge Creation

Functional and Structural Characterization of the RNase II-family of enzymes

Rute Gonçalves Matos

Dissertation presented to obtain a Doctoral Degree in Biology by Instituto de Tecnologia Química e Biológica, Universidade Nova de Lisboa

Oeiras, September 2011

Financial Support from **Fundação para a Ciência e Tecnologia (FCT)**.
Doctoral Grant - SFRH/BD/36024/2007

Cover image
By Doutor Nuno Micaêlo,
Molecular Modelling and Simulation Lab, University of Minho

Adapted from the cover of Journal of Biological Chemistry
Volume 284 Issue 31, July 31, 2009

Work performed at:
Control of Gene Expression Laboratory
Instituto de Tecnologia Química e Biológica
Av^{a} da República
2781-901 Oeiras - Portugal
Tel: +351 21 446 95 62
Fax: +351 21 446 95 49
http://www.itqb.unl.pt/Research/Biology/Control_of_Gene_Expression/

Supervisor:

Professora Doutora Cecília Maria Pais de Faria de Andrade Arraiano: Investigadora Coordenadora, Instituto de Tecnologia Química e Biológica, Universidade Nova de Lisboa.
(Head of the Control of Gene Expression Laboratory, where the work of this Dissertation was performed)

Co-Supervisor:

Doutora Ana Lúcia Freitas de Mesquita Barbas Sant'Ana de Miranda: Investigadora do Instituto de Biologia Experimental e Tecnológica.

President of the Jury

Professora Doutora Maria Helena Dias dos Santos: Professora Catedrática do Instituto de Tecnologia Química e Biológica da Universidade Nova de Lisboa.

Examiners

Professor Doutor Kenneth John McDowall: Investigador, Astbury Centre for Structure Molecular Biology, Faculty of Biological Sciences, University of Leeds, United Kingdom.

Professora Doutora Isabel Maria de Sá Correia Leite de Almeida: Professora Catedrática do Instituto Superior Técnico da Universidade Técnica de Lisboa.

Professora Doutora Claudina Amélia Marques Rodrigues-Pousada: Professora Catedrática Convidada do Instituto de Tecnologia Química e Biológica da Universidade Nova de Lisboa.

"O mundo está nas mãos daqueles que têm a coragem de sonhar e correr o risco de viver seus sonhos"

"A cada momento de nossa existência temos que escolher entre um caminho e o outro. Uma simples decisão pode afectar uma pessoa para o resto da vida."

Paulo Coelho

Group photo with the members of the jury: Professora Doutora Isabel Sá-Correia, Professor Doutor Kenneth McDowall, Professora Doutora Cecília Arraiano, Rute Matos, Professora Claudina Rodrigues-Pousada, Doutora Ana Barbas, Professora Doutora Helena Santos.

To my family, Mom, Dad and Sónia, for your love and support. Especially to Miguel, for your unconditional love and patience, for being always there for me.

Acknowledgments

I would like to thank to all the people that contributed and supported my work during the past four years. I also would like to thank for all the conditions given to me, which helped me to perform a better work.

Fist of all, I would like to thank **Instituto de Tecnologia Química e Biológica (ITQB)** from **Universidade Nova de Lisboa** for making possible to perform such a good work. Especially, I would like to thank all the ITQB directors, namely **Professor Doutor Miguel Teixeira** for accepting me at this institute to develop my research, **Professor Doutor José Artur Martinho Simões** for all his effort to improve the excellence of this Institute, our work conditions and for care about the students. Finally, to **Professor Doutor Luís Paulo Rebelo**, the present Director, for continuing the good work started by the previous directors. I also want to thank all the people that work at ITQB which, with their continuous work, provided us a better place to work, namely the Economato guys, **Carlos**, **Bruno**, **Ricardo** and **João**, for all their patience with our orders, for taking good care of our packages and for all the laughter and joy downstairs. To the Lab Manager, for taking care of all the ITQB equipments and for being efficient in the resolution of any problem regarding them. To the account department, the security guards, the Academic Office, namely to **Ana Maria Portocarrero**, the Maintenance, the responsible for our mail and archive, the staff from the Computer System Support Office, the washing room ladies and their responsible, and to all that continue to keep ITQB working every day.

A vital contribute to this work was the financial support given by **Fundação para a Ciência e a Tecnologia (FCT)** to whom I express my sincerely acknowledge.

A special thank to **Professor Cecília Arraiano**, for accepting me in her lab to do my Master and my Ph.D., for believing in me and in my work, for trusting in my capabilities to develop the work by myself when Ana left; for all the opportunities to attend several important meetings and to present my work there; for all the scientific discussions and for the opportunity to collaborate with other scientists abroad. More particularly, thank you for

being a friend, for worrying and for all the rides back home (when home was in Lisbon).

To **Ana Barbas**, a deeply and truly thank you: for choosing me as your lab partner, and for open a little space for me in your life as a friend. Thank you for all the support during my Master and also in the beginning of my Ph.D. Thank you for sharing all your knowledge and expertise with me, and, more importantly, for letting me "fly" in science and letting me know that you were always there for me. The scientist that I am today, I owe it also to you.

I would also like to thank **Mónica Amblar**, **Eduardo Lopéz-Viñas** and **Professor Paulino Gomez-Puertas** for all their help in the discussion of our biochemical data, for the modelling experiments and for accepting our strangest requests. It was a pleasure to be a co-author with all of you.

A special acknowledgment to **Prof. Arsénio Fialho** and **Nuno Bernardes**, **Prof. Isabel Sá Correia**, **Nuno Mira** and **Sílvia Henriques** from Instituto Superior Técnico, and **Prof. Kenny McDowall** from University of Leeds for the opportunity to collaborate with you, for all the scientific discussions, and also for your interest in my work.

To my colleagues in the lab, the former and the present ones, which supported and helped me during these last years, thanks for your help when I started in the lab, for all you patience with me, for all your enthusiasm, joy and friendship. Thank you for sharing all my joys and successes but also the less good moments. I am sure that your presence in my life contributed to the person and scientist that I am today.

Specially, I would like to thank **Inês BG**. We met while we were at the University and our paths crossed once again during our Ph.D. It was a pleasure to be part of your life again, to see you growing as a person and, especially as a scientist, fighting against million obstacles to obtain some results. I think that your presence in this lab was important to everyone and taught us a lot. Thank you for being my friend and for supporting me

during the period that we had together; for all the good moments, all the tears and laughters, for all the outflows, for your shoulder when I needed it, for sharing a paper with me and for all the rides to the train station. You will be forever in my heart. I wish you all the best for your future at LNIV.

Andreia, thank you for all your joy and happiness that cheers our side of the lab. Thank you for reminding me how good is to be young. Thank you for all your help as a lab technician but also as friend, for all the good moments that we had and for all the laughter. I cannot imagine how it would be to work in the lab without your presence here. I wish you all the best for you future and I hope to stay a little bit longer to see you succeed.

Cátia, although your presence in the lab is very recent, sooner we became friends. It is really a pleasure to share the lab and also my life with you. Thank you for all your joy and happiness, for being a special friend, for taking care of my look, and for giving me support in one of the most important periods of my life.

Sandra, thank you very much for your support, for all the rides back home and from home when there was a strike. For being my roommate and pin ball mate at FASEB, where we shared good and unforgettable moments. Thanks for your shoulder when I needed it. Thank you for your patience with me (and with my temper) when I came to the lab, for insisting on being my friend and for sharing all my joys in the lab.

To **Inês Silva**, **Margarida** and **Susana**, thanks for your good mood, all the jokes and laughter and crazy conversations. Thanks for all the good moments that we had and for your support in the hardest ones. For believe in me and in my work and for sharing these last years of my life with me.

To all my colleagues at ITQB, namely the ones that did the Ph.D. classes with me, thank you for all your help when I needed and for sharing ideas and your expertise with me. For all the dinners and lunches that we had, full of joy and happiness, for all the conversations and for hearing and sharing funny stories.

To all my friends apart from science, **Vera**, **Cristina**, **Irmã Natália**, **Irmã Conceição**, **Paulina**, **Sofia**, **Sarita** and many others, a huge thank you for caring about my work, even though most of the time you were not able to understand what I was doing. Thank you for reminding me which are the most important things in life, for being there when I needed, for sharing my achievements and for letting me be part of your lives. A special thank to my dance friends, specially to my partner **Paulo**, and to all the dance teachers (**Rui**, **Paulo**, **Alberto**, **Telma**, **Catarina**, **Sofia** and **Gonçalo**) for all the good moments lived during our dance classes, all joy, jokes and friendship that were crucial for the hardest moments in my life and that helped me to forget the world and just enjoy the magic of the dance.

I want to leave a special acknowledgment to all my family, **Matos** and **Gonçalves**, for their eternal love and support.

To my **Mum**, thank you for all your patience with me, for preparing me my lunch everyday, and for being always there. I' am sorry for the less good moments, but they were also necessary for us to grow as a family.
To my **Dad**, for showing me that we need to work really hard to get what we want and make our dreams come true, for your example of life, for being proud of me and of my achievements.
To my sister **Sónia**, thank you for your help during the crises. For trying to show me the right way, even though mine was not the same as yours…

My final but not less important thank you goes to **Miguel**: for your unconditional love, support and patience; for all the times that I could not be with you due to work or a meeting outside Lisbon. For all the cartoons that you prepared for my papers and presentations, for pushing me to be a better scientist, for all your good advice. Thank you for being my best friend and for sharing these last years with me. Love you.

Table of Contents

List of Publications

Scientific articles in international peer reviewed journals in September 2011:

Barbas, A. *****, **Matos, R.G.***, Amblar, M.,Lopez-Viñas, E., Gomez-Puertas, P., and Arraiano, C.M. 2009. Determination of Key Residues for Catalysis and RNA-Cleavage Specificity: One Mutation Turns RNase II into a "Super-Enzyme". ***J. Biol. Chem.*** 284(31):20486-20498. *****authors contributed equally. This article was the cover of this JBC issue.

Matos, R.G., Barbas, A., and Arraiano, C.M. 2009. RNase R mutants elucidate the catalysis of structured RNA: RNA-binding Domains select the RNAs targeted for degradation**.** ***Biochemical Journal.*** 423 (2): 291-301.

Matos, R.G., Barbas, A. and Arraiano, C.M. 2010. Comparison of EMSA and SPR for the characterization of RNA-RNase II complexes. ***The Protein Journal***. 29(6): 394-397.

Matos, R.G., Barbas, A. and Arraiano, C.M. 2011. Swapping the domains of exoribonucleases RNase II and RNase R: conferring upon RNase II the ability to degrade dsRNA. ***Proteins***. 79: 1853-1867.

Barbas, A., **Matos, R.G.**, Amblar, M., Lopez-Viñas, E., Gomez-Puertas, P., and Arraiano, C.M. 2008. New insights into the mechanism of RNA degradation by ribonuclease II: identification of the residue responsible for setting the RNase II end-product. ***J. Biol. Chem.*** 283:13070-13076.

Domingues, S., **Matos, R.G.**, Reis, F.P., Fialho, A.M., Barbas, A. and Arraiano, C.M. 2009. Biochemical characterization of the hydrolytic exoribonucleases from the human pathogens *Salmonella typhimurium* and *Streptococcus pneumoniae*. ***Biochemistry.*** 48(50): 11848-11857.

Arraiano, C.M., **Matos, R.G**. and Barbas, A. 2010. RNase II: The finer details of the *Modus operandi* of a molecular killer. ***RNA Biology***. 7(3): 276-281.

Arraiano C.M., Andrade J.M., Domingues, S., Freire, P., Guinote, I., **Matos, R.G.**, Moreira, R.N., Pobre, V., Reis, A.F., Silva, I.J., and Viegas, S.C. 2010. The Critical Role of RNA Processing and Degradation in the Control of Gene Expression. ***FEMS Microbiology Reviews***. 34(5): 883-923.

Guinote, I.B., **Matos, R.G.**, Freire, P., and Arraiano, C.M. 2011. BolA affects growth and binds to the promoters of Penicillin-Binding Proteins 5 and 6 regulating their expression. ***Journal of Microbiology and Biotechnology***. 21(3): 243-251.

Mira, N., Henriques, S., Keller, G., Teixeira, M., **Matos, R.G.**, Arraiano, C.M., Winge, D. and Sá-Correia, I. 2011. Identification of a DNA binding site for the transcription factor Haa1p, required for *Saccharomyces cerevisiae* response to acetic acid stress. ***Nucleic Acid Research***. 39(16):6896-6907.

Book chapters

Matos, R.G., Pobre, V., Reis, F.P., Malecki, M., Andrade, J.M., and Arraiano, C.M. 2011. Structure and degradation mechanisms of 3' to 5' exoribonucleases. **Ribonucleases, Nucleic Acids and Molecular Biology** (Springer). 26: 193-222. Edited by Professor Allen Nicholson.

Dissertation Outline

The author of this dissertation, Rute G. Matos, has worked on 13 manuscripts that were submitted during her Doctoral work and she has others in preparation. She is the first author in seven of these manuscripts, and second author in 4 of them. In this dissertation, she has decided to focus on four manuscripts in which she was the first author (Chapters 1 to 4). Then, she discusses work and purposes future perspectives (Chapter 5). In the last chapter, she annexes all the manuscripts published, in press or submitted. Accordingly, this dissertation is divided into six chapters:

The first chapter is composed of a brief introduction about exoribonucleases and their importance in RNA metabolism. A particular emphasis is given to RNase II and RNase R, the two members of the RNB family which were the main focus of this dissertation. Most of this section will be published in a chapter called "Structure and degradation mechanisms of 3' to 5' exoribonucleases" within the book "Ribonucleases" from Springer. Rute G. Matos is the first author of this book chapter.

In chapter two we discuss the role of several highly conserved residues in RNA degradation mechanism by *E. coli* RNase II. This paper was published in *Journal of Biological Chemistry* and the author of this dissertation had a major contribution in this manuscript and was considered first author. It describes a mutational analysis where several amino acids were changed in order to determine their role in catalysis. The most prominent finding was the discovery of an enzyme that was more than 100 times more active when compared to the wild-type enzyme and which was named "super-enzyme". This work was very important to improve the RNA degradation model previous proposed.

Chapter three describes a work published on *Biochemical Journal* in which the author of this dissertation is the first author. It was determined the functional role of each protein domain of RNase R regarding its catalytic activity and ability to bind to RNA. It was also performed a mutational analysis to confirm the role of two highly conserved residues. The findings

presented were important to decipher the mechanism of double-stranded RNA degradation by RNase R.

Chapter four focuses in the catalytic differences observed between RNase II and RNase R deciphering which domains could be responsible for those differences. To understand why these proteins behave so differently regarding the degradation of double-stranded substrates and the product released, we constructed a set of hybrid proteins by swapping domains between RNase II and RNase R. With this work we were able to discover which RNase R domains were contributing for the degradation of double-stranded RNA and further understand the mechanism of action of this protein. This work was published in *Proteins*, with Rute G. Matos as first author.

Chapter five comprises a final discussion where the major discoveries performed during this dissertation are brought together. Considering the results obtained, new experiments are also proposed.

Chapter six is an appendix with the printed version of the papers published, in press or submitted during this doctoral work.

Abbreviations

3D three dimensional
Å angstrom
Ala alanine
Amp ampicilin
Arg arginine
Asn asparagine
Asp aspartate
ATP adenosine triphosphate
bp base pair
BSA bovin serum albumine
ºC degree Celsius
Ca calcium
Co Cobalt
cpm counts per minute
CR3 three cysteine-rich domain
CSD cold shock domain
Cu copper
Δ deletion
Da dalton
DTT dithiothreitol
DNA deoxyribonucleic acid
DNase deoxyribonuclease
dsRNA double-stranded RNA
E. coli Escherichia coli
EDTA ethylenediaminetetraacetic acid
EMSA electrophoretic mobility shift assay
fmol femtomoles
g relative centrifugal force
Glu glutamate
h hour
His histidine
HPLC High-performance liquid chromatography
HRDC helicase and RNaseD C-terminal
HTH Helix-turn-Helix
IPTG IsoPropyl-β-D-thiogalactopyranoside
K Kelvin
kb kilobase
k_a association rate constant
k_{cat} first-order rate constant
k_d dissociation rate constant
K_D dissociation constant
kDa kilodalton
K_m michaelis constant
l liter
LB luria-bertani broth
Lys lysine
M molar/molarity (mol/L)
mg milligram
µg microgram
µl microliter
µM micromolar
MD molecular Dynamics
mer oligomer
Mg magnesium
min minute
mJ milijoule
ml mililiter
mM miliMolar
Mn manganese
Mol mole
mRNA messenger RNA
Na sodium
NBS nucleic acid binding sequence
Ni nickel
nm nanometer
nM nanomolar
nmol nanonole
ns nanosecond
nt nucleotide
OD optical density
Oligo oligonucleotide
o.n. over nigth
^{32}P phosphorus 32 radioactive
PAA polyacrylamide
PAP I poly(A) polymerase I
PCR polymerase chain reaction

PDB protein data bank
Phe phenylalanine
PIN pilT N-terminal
pM picomolar
pmol picomol
PMSF phenylmethylsulfonyl fluoride
PNPase polynucleotide phosphorylase
Poly(A) polyadenylate
ppGpp Guanosine 3' diphosphate 5'diphosphate
Ps picosecond
psi pressure units
REP repetitive extragenic palindromic
RNA ribonucleic acid
RNase ribonucleases
rpm rotations per minute
rRNA ribosomal RNA
s second
SA streptavidine
SD standard deviation
SDS sodium dodecyl sulphate
SOV suppressor of varicose
SPR surface plasmon resonance
sRNA small RNA
ssRNA single-stranded RNA
Tris tris(hydroxymethyl)aminomethane
tRNA transfer RNA
Tyr tyrosine
UV ultraviolet radiation
V volt
V_{max} maximum velocity
vol volume
wt wild type
Zn zinc

Abstract

Ribonucleases (RNases) are ubiquitous and have a central role in the control of gene expression. They are involved in the maturation of functional RNAs as well as their degradation. RNases are also involved in quality control mechanisms and are crucial to the recycling of ribonucleotides, key cellular metabolites. Ribonucleases can be broadly classified as endoribonucleases, which cleave at sites internal to the RNA, or exoribonucleases, which remove nucleotides from either the 5' end or 3' end of the RNA molecule. Enzymes from the RNase II-family of exoribonucleases are present in all domains of life, and processively degrade RNA in the 3' to 5' direction with a hydrolytic activity that releases 5'-nucleotide monophosphates. They play a crucial role in RNA metabolism and have been shown to be required for normal growth and viability, virulence, mitotic control and chloroplast biogenesis.

E. coli RNase II is the prototype of this family of enzymes, which also comprises *E. coli* RNase R. All members of the RNase II family share a similar domain organization.

The broad objective of this Doctoral work was to investigate the relationship between the structures of these enzymes and their functions. This was approached by comparing the effects on introducing mutations into *E. coli* RNase II and its paralogue RNase R, which by contrast is relatively insensitive to secondary structures that are significant barriers to the processivity of RNase II. Highly conserved residues within the active site of RNase II were mutated, and the effects on RNA binding and degradation were assayed. It was found that residue Asp209 is critical for catalytic activity, Tyr253 controls the size of the final end-product, and a Glu542Ala substitution increase the activity greater than 100 fold. The latter may have a great biotechnology potential. These and other results allowed refinement of the model previously proposed for the RNA degradation by RNase II. Equivalent residues within RNase R were also mutated. As found for Asp209 in RNase II, Asp280 in RNase R is crucial for the activity of the protein without changing its binding ability. Similarly, Tyr324 sets the size of the end product in RNase R.

RNase R is composed of two CSDs at the N-terminal region, which are preceded by an HTH motif, a central RNB domain, and a C-terminal S1 domain, which is followed by a lysine-rich tail. The HTH motif and Lysine-rich tail are both absent in RNase II. To analyze the contribution of functional domains from RNase R to the degradation of RNA, truncated proteins were constructed. The CSDs and S1 were found to be important for RNA binding. The CSDs are possibly involved in the initial recruitment of RNA substrates, while the S1 domain could stabilise the binding of RNA following the initial interaction with the CSDs. Interestingly, and unexpectedly, the RNB domain from RNase R was found to be sufficient to degrade double-stranded substrates including those without a 3' single-stranded overhang. Thus, it appears that the RNA-binding domains are specificity determinants, i.e. direct RNase R to particular substrates.

To decipher which domains are responsible for the biochemical differences between RNase II and RNase R, six chimeric proteins were constructed and assayed using both single- and double-stranded substrates. The results confirmed that RNB domain from RNase R conveys the ability to degrade double-stranded substrates. Evidence was also obtained that the RNB domain is assisted in dsRNA degradation by the Lys-rich tail, and that the requirement for a 3' overhang is imparted by the S1 domain. Despite the lack of a 3D structure for RNase R, the biochemical studies described here along with homology modelling have revealed for the first time structural differences between RNase R and RNase II that explain their different substrate requirements, as well as revealing further insight into the molecular recognition events that control catalysis.

This work provides a platform for investigating the functions of the many other RNase II-family members, which are found in all divisions of life.

Resumo

As Ribonucleases (RNases) são ubíquas e têm um papel central no controlo do metabolismo do RNA. Elas processam e degradam moléculas de RNA e são o principal factor responsável pela determinação dos níveis de mRNA funcional na célula. As RNases podem também estar envolvidas em mecanismos de controlo de qualidade e desempenham um papel importante na reciclagem de ribonucleótidos na célula. As enzimas podem ser classificadas em endoribonucleases (clivam a molécula de RNA internamente) ou exoribonucleases (removem os nucleótidos a partir das extremidades 5' ou 3' da molécula de RNA).

As enzimas da família da RNase II encontram-se presentes em todos os domínios da vida. As enzimas desta família degradam o RNA da extremidade 3' para a 5' de uma forma hidrolítica e processiva, libertando 5'-monofosfatos. Estas desempenham uma função crucial no metabolismo do RNA e já se mostrou que estão envolvidas em vários processos, tais como virulência, crescimento e viabilidade, controlo mitótico e biogénese de cloroplastos.

A RNase II de *E. coli* é o protótipo desta família de enzimas, à qual também pertence a RNase R. Todos os membros desta família apresentam uma organização de domínios semelhante e o seu mecanismo de acção poderá ser também similar.

O primeiro objectivo deste trabalho Doutoral foi a análise do papel de alguns resíduos altamente conservados na degradação do RNA pela RNase II. Para tal, inseriram-se várias mutações pontuais nesta enzima e analisou-se o seu efeito na actividade da enzima e também na sua capacidade de ligação ao RNA. Os resultados mostram que os resíduos que formam o centro activo da RNase II desempenham diferentes funções durante a catálise, e que o aspartato na posição 209 é o único aminoácido essencial para a actividade da proteína. Descobrimos também que a tirosina na posição 253 é o aminoácido responsável pela formação do produto final da reacção. Explicámos também porque é que a RNase II é capaz de se ligar a moléculas de DNA sem as degradar. Um dos resultados obtidos mais interessantes foi a construção de uma proteína com 110 vezes

mais actividade quando comparada com a proteína selvagem. Esta proteína foi obtida quando se alterou o glutamato na posição 542 por uma alanina e poderá ter um grande impacto biotecnológico. Com este estudo, foi possível melhorar o modelo previamente proposto da degradação do RNA pela RNase II.

Na segunda parte deste trabalho, tivemos como objectivo o estudo da outra proteína da família da RNase II em *E. coli*: a RNase R. Começámos por mutar os resíduos equivalentes aos que se mostraram cruciais para a actividade da RNase II. À semelhança do que aconteceu com o Asp209 da RNase II, também na RNase R o resíduo equivalente (Asp280) mostrou ser essencial para a actividade da enzima sem alterar a sua capacidade para se ligar ao RNA. Verificámos ainda que a Tyr324 também é responsável pela determinação do produto final da reacção na RNase R. Como membro da família da RNase II, a RNase R é composta por dois CSD na região N-terminal, os quais são precedidos por um motivo HTH (que não existe na RNase II), um domínio RNB central e um domínio S1 na região C-terminal (ao qual se segue uma cauda rica em lisinas, também ausente na RNase II). Fomos então de seguida analisar a importância destes domínios para a degradação do RNA na RNase R. Para tal, construímos proteínas truncadas o que nos permitiu observar que, de facto, os domínios CSD e S1 são importantes para a ligação ao RNA mas desempenham funções diferentes: os domínios CSD parecem ser mais importantes para o recrutamento das moléculas de RNA enquanto que o domínio S1 poderá desempenhar um papel na estabilização da molécula de RNA. No entanto, a descoberta mais importante foi a de que o domínio catalítico da RNase R, por si só, é capaz de degradar substratos em cadeia dupla. Mais ainda, na ausência dos domínios de ligação ao RNA, a proteína truncada é capaz de degradar substratos estruturados mesmo na ausência de uma cauda em cadeia simples na extremidade 3', o que não se observa para a proteína selvagem. Esta descoberta levou-nos a concluir que os domínios de ligação ao RNA são muito importantes para escolher as moléculas de RNA que estão marcadas com uma cauda para serem degradadas.

Finalmente, o último objectivo desta dissertação foi perceber quais os domínios responsáveis pelas diferenças catalíticas que se observam entre a RNase II e a RNase R. Para tal, trocámos os domínios entre estas duas proteínas e construímos seis proteínas quiméricas. De seguida, fomos analisar a actividade destas proteínas usando diferentes substratos de RNA, tanto em cadeia simples como em cadeia dupla. Os resultados obtidos confirmam que, de facto, o domínio responsável pela degradação de RNA em cadeia dupla é o RNB da RNase R. No entanto e para nossa surpresa, verificámos que o domínio S1 da RNase R, mais precisamente a cauda rica em lisinas, também está envolvida neste processo. Mais ainda, a degradação dos substratos em cadeia dupla é efectuada de uma forma diferente de acordo com o domínio que está envolvido nessa degradação: enquanto a degradação efectuada pelo domínio RNB é independente da existência de uma cauda de RNA em cadeia simples na extremidade 3', para o domínio S1 poder efectuar essa degradação necessita da presença dessa cauda de forma a conseguir "desenrolar" o substrato. Na ausência da estrutura da RNase R, apenas através de estudos bioquímicos e de modelação poderemos ter uma ideia do mecanismo de acção desta proteína e só assim tentar revelar as diferenças existentes entre a RNase II e a RNase R. Com este trabalho foi-nos possível ir mais longe na explicação do mecanismo de acção da RNase R e aumentar o conhecimento que temos acerca desta ribonuclease.

Com esta dissertação obtivemos resultados muito importantes que nos permitiram aprofundar o conhecimento sobre o mecanismo de reacção dos dois membros da família da RNase II que existem em *E. coli*. Estes resultados podem ser depois extrapolados para melhor compreender o modo de acção de outras proteínas da mesma família noutros organismos.

Chapter 1

Introduction

This chapter was based on the manuscripts below:

Matos, R.G., Pobre, V., Reis, F.P., Malecki, M., Andrade, J.M., and Arraiano, C.M. 2011. Structure and degradation mechanisms of 3' to 5' exoribonucleases. **Ribonucleases, Nuclei Acids and Molecular Biology** (Springer). 26: 193-222 Edited by Professor Allen Nicholson.

Arraiano, C.M., **Matos, R.G**. and Barbas, A. 2010. RNase II: The finer details of the *Modus operandi* of a molecular killer. RNA Biology. **7(3)**: 276-281.

Arraiano, C.M., Andrade, J.M., Domingues, S., Guinote, I., Malecki, M., **Matos, R.G.**, Moreira, R.N., Pobre, V., Reis, A.F., Saramago, M., Silva, I.J. and Viegas, S.C.. 2010. The Critical Role of RNA Processing and Degradation in the Control of Gene Expression. FEMS Microbiology Reviews. **34(5)**: 883-923.

INTRODUCTION

The RNA levels in the cell depend on the efficiency of the transcription, and the rate of degradation. Although transcription is important to determine RNA steady state levels, the processing and degradation of RNA are also key factors in the regulation of gene expression.

Ribonucleases (RNases) are the enzymes that are able to process and degrade RNA. Moreover, they have a critical role in the maturation of ribosomal and transfer RNA (Arraiano *et al.*, 2010a; Régnier and Arraiano, 2000). They are also involved in the quality control of all types of RNA, allowing the recycling of the ribonucleotides in the cell (Arraiano *et al.*, 2010a; Li *et al.*, 2002). RNases are present in all domains of life, and play a central role in the control of gene expression by determining the levels of functional RNA in the cell (Arraiano and Maquat, 2003; Parker and Song, 2004; Régnier and Arraiano, 2000). Many of the RNases in the cell are essential and others have overlapping functions (Régnier and Arraiano, 2000). RNases can act alone or they can be part of RNA degradation complexes, namely the degradosome and the exosome.

Ribonucleases can be divided into endoribonucleases (which cleave the RNA molecules internally) and exoribonucleases (which degrade the RNA by removing terminal nucleotides from the 3' end or the 5' end of the RNA molecules). In this chapter, we will focus on exoribonucleases, namely those which degrade the RNA from the 3' to the 5' end.

Exoribonucleases can act hydrolytically releasing nucleoside monophosphates, or phosphorolytically if they use inorganic phosphate to cleave the molecules releasing nucleoside diphosphates (Zuo and Deutscher, 2001). The nucleotides released after the action of exoribonucleases are very important for turnover since they can be reutilized for the synthesis of new RNA molecules.

Exoribonucleases are involved in many RNA metabolic events, namely in RNA maturation and degradation (Andrade *et al.*, 2009b). According to their sequence and structural characteristics, exoribonucleases can be

divided into four families: RNB, PDX, DEDD, and 5PX (the last family does not have any representatives in bacteria) (Table 1). In this chapter we will summarize the available information about all families of exoribonucleases that degrade RNA from the 3' to the 5' end, and discuss the latest findings and their relevance in RNA metabolism.

PDX-FAMILY

The PDX-family of 3'-5' exoribonucleases includes PNPase, RNase PH from bacteria, and the core of the exosome in archaea and eukaryotes (Pruijn, 2005) (Figure 1). These enzymes, contrary to the other exoribonucleases, are phosphate dependent enzymes, and release a dinucleotide as an end-product of degradation. Beside their role as exoribonucleases the enzymes from this family can also catalyze other reactions like the addition of heteropolymeric tails to RNA substrates (Slomovic *et al.*, 2008). In fact, the polymerization activity of PNPase was essential for the deciphering of the genetic code and this discovery led to the award of a Nobel Prize to Severo Ochoa in 1959 (Grunberg-Manago *et al.*, 1955).

PNPase

PNPase is a multifunctional protein. Its activity is stalled by the presence of double-stranded structures and a minimal 3' overhang of 7-10 unpaired ribonucleotides is required to PNP to bind to the RNA molecule (Spickler and Mackie, 2000). However, under conditions of low inorganic phosphate concentration, PNPase catalyzes the inverse reaction, i.e. polymerization of single-stranded RNA from nucleoside diphosphates (Littauer and Soreq, 1982). Contrary to the homopolymeric poly(A) tails added by PAP I (Poly(A) Polymerase I), the tails synthesized by PNPase are heteropolymeric, containing all four nucleotides (Littauer and Soreq, 1982). In spinach chloroplasts, cyanobacteria and Gram-positive bacteria, PNPase is suggested to be the main polyadenylating enzyme (Campos-Guillén *et al.*, 2005; Rott *et al.*, 2003; Sohlberg *et al.*, 2003; Yehudai-Resheff *et al.*, 2001).

TABLE 1. Family of 3' to 5' Exoribonucleases

Family	*E. coli* members	Eukaryotic members	Catalytic mechanism	Comments
RNB	RNase II RNase R	Rrp44 (Dis3) Tazman	Hydrolytic	These enzymes are processive in the 3' to 5' direction; distributed in all domains of life
DEDD	RNase D	Rrp6	Hydrolytic	Proteins from this family are distributive or processive in the 3' to 5' direction; some have DNase activity
	RNase T	-		
	Oligoribonuclease	Ynt20 (Rex2)		
	-	Pan2, ERI-1 Rex1, 3, 4		
PDX	PNPase	-	Phosphorolytic	The activity is processive in the 3' to 5' direction and phosphate dependent
	RNase PH	Rrp41-43, 45, 46 Mtr3		The activity is distributive in the 3' to 5' direction and phosphate dependent
		Csl4		

Adapted from (Matos *et al.*, 2011b)

The archaeal exosome, which is very similar to PNPase (see below), has also been demonstrated to be responsible for the addition of heteropolymeric tails in *Sulfolobus* (Portnoy et al., 2005). More recently it was described that human PNPase also regulates RNA translocation into mitochondria (Wang *et al.*, 2010).

PNPase can form complexes with other enzymes to easily degrade RNA. The main complex in which PNPase is involved is the degradosome. The degradosome is a large, multiprotein complex involved in RNA degradation. In *E. coli*, this multiprotein complex is composed of the endoribonuclease RNase E, the 3'-5' exoribonuclease PNPase, the DEAD-box RNA helicase B (RhlB) and the glycolytic enzyme enolase (Carpousis *et al.*, 1994; Miczak *et al.*, 1996; Py *et al.*, 1996; Vanzo *et al.*, 1998). RNase E provides the scaffold for the degradosome. Recent findings showed that *E. coli* PNPase and RNase E are present in the degradosome in an equimolar ratio (Nurmohamed *et al.*, 2009). However, PNPase content can change in response to phosphosugar stress, temperature

shock and growth stage (Beran and Simons, 2001). In other organisms, the degradosome content might be different. In *Pseudomonas syringiae* PNPase is substituted by RNase R, and the DEAD-box helicase present in the degradosome is RhlE (Purusharth *et al.*, 2005).

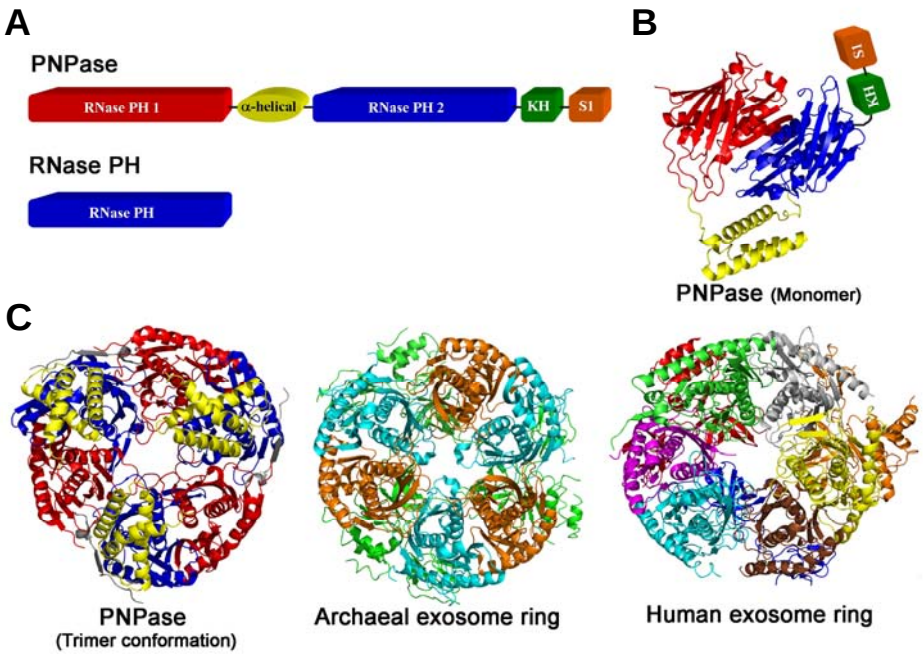

FIGURE 1. The PDX-family of enzymes. A. Linear representation of *E. coli* PNPase and RNase PH domains (note that the figures are not in scale). **B.** View of PNPase crystal structure in the monomer organization (PDB ID 3CDI - this PDB does not include the KH and S1 domains) (Shi *et al.*, 2008). **C.** Comparison of PNPase trimer structure (PDB ID 3GCM - this PDB does not include the KH and S1 domains) (Nurmohamed *et al.*, 2009) with the archaeal exosome ring from *Sulfolobus solfataricus* (Rrp41 is represented in light blue, Rrp42 in orange and Rrp4 in green; PDB ID 3L7Z) (Lu *et al.*, 2010) and with the human exosome ring (Rrp4 is represented in orange, Rrp40 in red, Rrp41 in grey, Rrp42 in yellow, Rrp43 in light blue, Rrp45 in green, Rrp46 in magenta, Mtr3 in brown, and Csl4 in blue; PDB ID 2NN6) (Liu *et al.*, 2006). Adapted from Matos *et al.*, 2011b.

X-ray crystal structures of *E. coli* and *Streptomyces antibioticus* PNPase reveal a homotrimeric subunit organization with a ring-like architecture (Figure 1) (Nurmohamed *et al.*, 2009; Shi *et al.*, 2008; Symmons *et al.*, 2000). Each monomer exhibits a five-domain arrangement: at the N-terminus two RNase PH domains (PH1 and PH2) are linked by a α-helical domain, and at the C-terminal end there are two RNA-binding domains (KH and S1) (Figure 1A and B). The three monomers associate via trimerization interfaces of the core domains, forming a central channel, where catalysis occurs (Figure 1C). The catalytic site of PNPase is composed of structural elements of the first and second core domains (PH1 and PH2) (Briani *et al.*, 2007; Nurmohamed *et al.*, 2009; Shi *et al.*, 2008; Symmons *et al.*, 2000).

PNPase lacking either the S1 or KH domains retained phosphorolytic activity and still has some RNA-binding capacity, but the truncated enzymes are much less active. Although PNPase lacking the S1 domain, KH domain, or both domains could still be assembled in the degradosome and their presence in the degradosome is vital at low temperature, the domains were shown to be essential to support growth in the cold. Nevertheless, the presence of both KH and S1 domains is required for proper RNA binding (Briani *et al.*, 2007; García-Mena *et al.*, 1999; Goverde *et al.*, 1998; Matus-Ortega *et al.*, 2007; Shi *et al.*, 2008; Zangrossi *et al.*, 2000). Shi and co-authors demonstrated that these RNA-binding domains also have a major role in the formation of a more stable trimeric structure, and are essential for the constriction of the central channel (Shi *et al.*, 2008). This is in agreement with a previous study where PNPase S1 domain was able to induce trimerization of an RNase II-PNPase chimeric protein (Amblar *et al.*, 2007).

PNPase is encoded by the *pnp* gene that is located downstream of the *rps*O gene (encoding ribosomal protein S15), and is transcribed from two promoters (one upstream of the *rps*O gene and another upstream of *pnp* gene. *pnp* expression is negatively autoregulated at the post-transcriptional level. This autoregulation only occurs after an initial

cleavage by RNase III at the 5' end of the *pnp* message (Carzaniga *et al.*, 2009; Jarrige *et al.*, 2001; Portier *et al.*, 1987; Robert-Le Meur and Portier, 1992). PNPase levels are also affected by polyadenylation but not by PAP I itself (Jarrige *et al.*, 2001). PNPase and RNase II are inter-regulated. In the absence of RNase II, PNPase levels are increased and PNPase overexpression leads to a decrease in RNase II activity (Zilhão *et al.*, 1996a; Zilhão *et al.*, 1996b). More recently it was shown that guanosine 5' diphosphate 3' diphosphate (ppGpp) inhibits *Nonomuraea sp.* and *Streptomyces* PNPase phosphorolytic and polymerization activities (Gatewood and Jones, 2010; Siculella *et al.*, 2010). In conclusion, PNPase has a complex regulation and its expression is finely controlled both at transcriptional and post-transcriptional levels (Andrade *et al.*, 2009b).

PNPase does not seem to be indispensable to *E. coli* at optimal temperature, unless either RNase II or RNase R are also missing (Cheng *et al.*, 1998; Donovan and Kushner, 1986). However, PNPase is essential for *E. coli* growth at low temperatures (Luttinger *et al.*, 1996; Piazza *et al.*, 1996; Zangrossi *et al.*, 2000).

PNPase has been implicated in the establishment of virulence in several pathogens, namely in *Salmonella*, *Dichelobacter nodosus*, *Dickeya dadantii*, *Yersinia*, *Campylobacter jejuni* and *Streptococcus pyogenes*. However, PNPase role in virulence can be contradictory, while in some pathogens PNPase seems to act as a virulence repressor, in others PNPase is important for the establishment of virulence (Arraiano *et al.*, 2010a).

RNase PH

RNase PH is encoded by the *rph* gene and is co-transcribed with pyrE, a gene necessary for pyrimidine synthesis which is located upstream of *rph* (Ost and Deutscher, 1991). RNase PH is not essential for cell growth, unless RNase T or PNPase are also missing. In fact, the *rph* mutation only results in inviability in a strain already lacking RNases I, II, D, BN and T (Kelly *et al.*, 1992). Contrary to PNPase, which is mainly involved in RNA degradation, RNase PH is involved in tRNA metabolism, namely in the processing of tRNA precursors (Deutscher *et al.*, 1988; Kelly and

Deutscher, 1992b), and in ribosome metabolism (Redko and Condon, 2010; Zhou and Deutscher, 1997).

RNase PH can act as a phosphorolytic ribonuclease (removing nucleotides following the CCA terminus of tRNA) or as a nucleotidyltransferase (adding nucleotides to the ends of RNA molecules) (Bralley *et al.*, 2006; Kelly and Deutscher, 1992b; Wen *et al.*, 2005). RNase PH can also modify the 3' end of other small RNA, including M1, 6 S, and 4.5 S RNA (Li *et al.*, 1998).

The crystal structures of RNase PH from *Aquifex aeolicus*, *B. subtilis* and *Pseudomonas aeruginosa* were determined. All the three proteins crystallized as a hexamer arranged as a trimer of dimers (Choi *et al.*, 2004; Harlow *et al.*, 2004; Ishii *et al.*, 2003). The formation of the RNase PH hexameric ring is essential for the binding of precursor tRNA and also for the exoribonucleolytic activity (Choi *et al.*, 2004).

The Exosome and the PDX-family

The exosome is a multiprotein complex with a 3'-5' RNase activity that is involved in RNA degradation and processing (van Hoof and Parker, 1999). In Archaea, the exosome consists of two RNase PH subunits (Rrp41 and Rrp42) and two RNA-binding subunits (Rrp4 and Csl4) (Buttner *et al.*, 2005; Evguenieva-Hackenberg *et al.*, 2003). The crystal structure of the archaeal exosomes from the *Sulfolobus solfataricus*, *Archaeoglobus fulgidus* and *Pyrococcus abyssi* were solved. These structures revealed a hexameric ring-like assembly formed by three Rrp41 and Rrp42 subunits. This hexameric ring is "capped" by a trimer of the RNA-binding proteins Rrp4 and/or Csl4 (Figure 1C) (Buttner *et al.*, 2005; Lorentzen and Conti, 2005). Both Rrp41 and Rrp42 are involved in substrate binding, however only the Rrp41 has catalytic activity (Lorentzen and Conti, 2005). A model for the RNA processing by the archaeal exosome as been proposed, which is very similar to the one proposed for RNase II (Frazão *et al.*, 2006).

The eukaryotic core exosome is also formed by a six subunit PH domains ring, Rrp41, Rrp45, Rrp46, Rrp42, Rrp43, and Mtr3. However, and contrary to what happens in archaeal organisms, these proteins appear to

lack catalytic activity. In fact, both yeast and human exosome cores do not present any catalytic activity (Dziembowski *et al.*, 2007; Liu *et al.*, 2006). In this case, the RNase PH homologues in eukaryotes may have a role in substrate binding and recruitment.

THE RNase II/RNB-FAMILY

The RNB-family of enzymes is present in all domains of life and exhibits the same modular organization (Figure 2). These enzymes processively degrade RNA in the 3' to the 5' direction. They have a hydrolytic activity, releasing 5' nucleoside monophosphates. *E. coli* RNase II is the prototype of this family of enzymes, which also comprises RNase R and the eukaryotic Rrp44/Dis3 (Table 1) (Mian, 1997; Zuo and Deutscher, 2001). Members of this family play very important functions in the cell: they are essential for growth (Mitchell *et al.*, 1997), they can be developmentally regulated (Cairrão *et al.*, 2005), and mutations in its gene have been linked with abnormal chloroplast biogenesis (Bollenbach *et al.*, 2005), mitotic control and cancer (Figure 3) (Lim *et al.*, 1997).

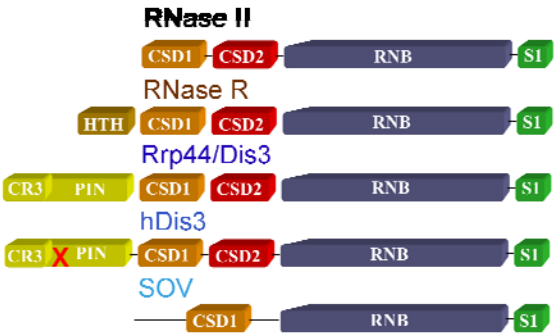

FIGURE 2. Schematic representation of RNB-family members (note that the figures are not in scale). RNase II and RNase R from *E. coli* are both represented. As eukaryotic example, we have Rrp44 from yeast. We also represented the human homologue hDis3L, which does not have endoribonucleolytic activity in its PIN domain. SOV proteins from *Arabidopsis* doesn't have PIN domain and lack one CSD. Adapted from Matos *et al.*, 2011b.

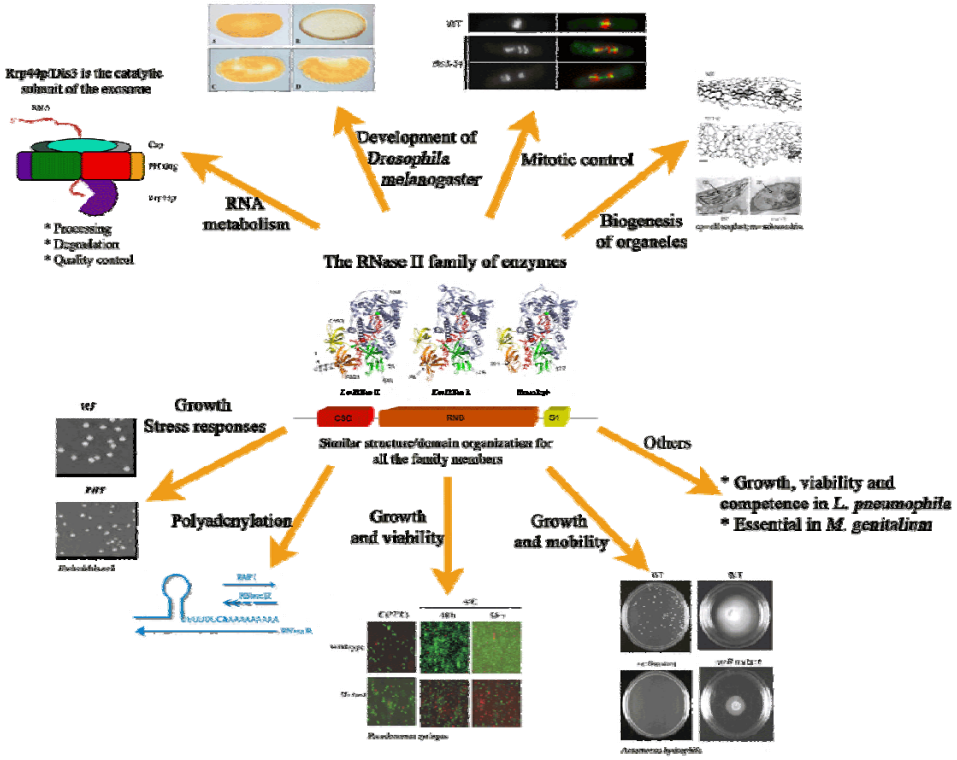

FIGURE 3. The multiple roles of RNase II-family of enzymes. RNase II-family of enzymes is ubiquitous, share the same modular organization and many of its members are crucial in RNA metabolism. In eucaryotes, RNase II-like enzymes (Rrp44/Dis3) are the only catalytic subunit of the exosome, a crucial protein complex involved in processing, degradation and quality control; Tazman is the RNase II *Drosophila melanogaster* homologue that is differentially expressed during development; RNase II-like enzymes can also be involved in mitotic control and in the biogenesis of chloroplasts. In prokaryotes, RNase II and RNase R have been shown to be involved in poly(A)-mediated RNA degradation mechanisms; in *E. coli* RNase R is involved in growth and stress responses, in growth and viability in *P. syringae*, in growth and motility of *A. hydrophila*, and in growth and competence of *L. pneumophila*. Adapted from Arraiano *et al.*, 2010b.

They were also shown to be important for stress responses, RNA and protein quality control, and required for virulence in several organisms (Figure 3) (Andrade *et al.*, 2006; Cairrão *et al.*, 2003; Cairrão and Arraiano, 2006; Charpentier *et al.*, 2008; Cheng *et al.*, 1998; Cheng and Deutscher, 2003, 2005; Erova *et al.*, 2008; Purusharth *et al.*, 2007).

In eukaryotes, RNase II homologues can act independently or can be associated in multiprotein complexes, like the exosome, a complex of exoribonucleases crucial for the maintenance of the correct levels of RNA in the cell (Figure 3) (van Hoof and Parker, 1999).

RNase II

E. coli RNase II is the prototype of this family of enzymes. This 72 kDa protein encoded by gene *rnb* is the major hydrolytic enzyme, responsible for 90% of the exoribonucleolytic activity in crude extracts (Deutscher and Reuven, 1991). RNase II is expressed from two different promoters, P1 and P2, which implies a differential regulation of the *rnb* gene at the level of transcription (Zilhão *et al.*, 1996b). This protein is also regulated at post-transcriptional levels (Cairrão *et al.*, 2001). Other ribonucleases, such as RNase III, RNase E and PNPase, are involved in the modulation of RNase II levels (Zilhão *et al.*, 1995; Zilhão *et al.*, 1996a). It was also shown that there is a post-translational regulation of RNase II levels by the *gmr* gene (Gene Modulating RNase II), located downstream of the *rnb* gene (Cairrão *et al.*, 2001). Gmr seems to control RNase II at the level of protein stability. In the absence of Gmr, RNase II is more stable. Furthermore, RNase II levels change accordingly to different growth conditions and in the *gmr* mutant these changes are abolished (Cairrão *et al.*, 2001).

RNase II is a hydrolytic enzyme which processively degrades RNA in the 3' to 5' direction releasing 5' nucleoside monophosphates, and the final product released is a 4 nt fragment. The activity of this protein is sequence independent but sensitive to secondary structures (Figure 4) (RNase II stalls around seven nucleotides before it reaches the double-stranded region) (Spickler and Mackie, 2000). Ten nucleotides is the minimum of length of the RNA molecule needed for the processivity of the

enzyme. For fragments less than 10 nt, the activity of RNase II becomes distributive (Cannistraro and Kennell, 1994). Although being specific for RNA, RNase II is able to bind to DNA molecules without being able to cleave them (Barbas *et al.*, 2009; Cannistraro and Kennell, 1994). It seems that the DNA oligonucleotides can act as inhibitors of RNase II action since they bind its specific binding site (Cannistraro and Kennell, 1994).

RNase II activity does not depend on the RNA sequence, however, it has a marked preference for poly(A) substrates. Polyadenylation is responsible for the control of mRNA stability in several organisms. The poly(A) tails are synthesized by PAP I to target RNA to be degraded by exoribonucleases. Since RNase II has preference for poly(A) substrates, it will rapidly degrade these tails. The degradation process proceeds until a secondary structure, such as a Rho independent terminator, is found. By rapidly degrading these poly(A) tails, RNase II can impede the binding of other exoribonucleases to the RNA molecule, since no overhang is left to allow the binding of other ribonucleases, thus preventing the RNA degradation. With this behaviour, RNase II is acting paradoxically by protecting some messages (Andrade *et al.*, 2009b; Marujo *et al.*, 2000).

By sequence analysis, it was proposed that RNase II has a modular organization, with three conserved domains: a CSD at the N-terminal region, a central catalytic RNB domain, and a C-terminal S1 domain (Figure 2) (Andrade *et al.*, 2009b; Arraiano *et al.*, 2010a; Arraiano *et al.*, 2010b). The RNB domain is well conserved and it is exclusive to RNase II-like proteins. It contains four highly conserved motifs (I to VI) with several invariant amino acids (Mian, 1997). The function of each domain was determined and it was shown that the RNB domain is responsible for the catalytic activity, whereas CSD and S1 domains are responsible for the binding to RNA (Amblar *et al.*, 2006). The resolution of the crystal structure of RNase II (the first of an RNB-family member) revealed the existence of four domains instead of the three previously proposed: two N-terminal CSD, the central RNB domain and the S1 domain at the C-

terminal region (Frazão *et al.*, 2006). Moreover, it was possible to see that the RNB domain presents an unprecedented fold which is characteristic of this family. The RNA-binding domains (CSD1, CSD2 and S1) are grouped together on one side of the structure, while the active site is on the other side of the molecule (Figure 5A) (Frazão *et al.*, 2006).

An RNase II mutant found in nature (D209N) was previously described and it was showed to encode an inactive protein still able to bind to RNA (Amblar and Arraiano, 2005). The structure of this mutant was also solved, and the crystallization proceeded with a RNA molecule that was inside. This allowed the co-crystalization of the RNA molecule inside the protein, which was very important since enabled the visualization of RNA-protein contacts, and gave the explanation of its mode of action (Frazão *et al.*, 2006).

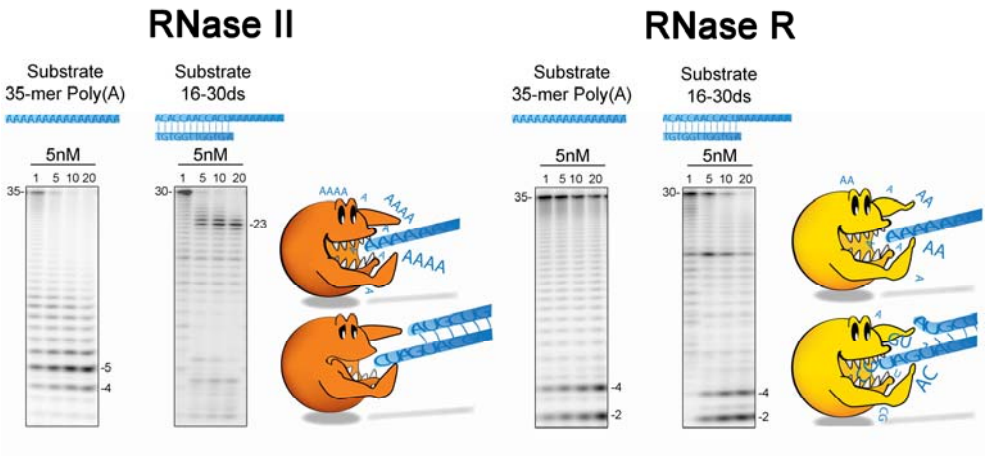

FIGURE 4. Comparing the catalysis of *E. coli* RNase II and RNase R with different substrates. RNase II releases a 4 nt fragment as end-product when degrading single-stranded substrates. For structured substrates, the product released by RNase II has an overhang of 4-7 nt before the duplex. RNase R is able to degrade both single- and double-stranded substrates releasing a 2 nt fragment as end-product. Adapted from Matos *et al.*, 2011b.

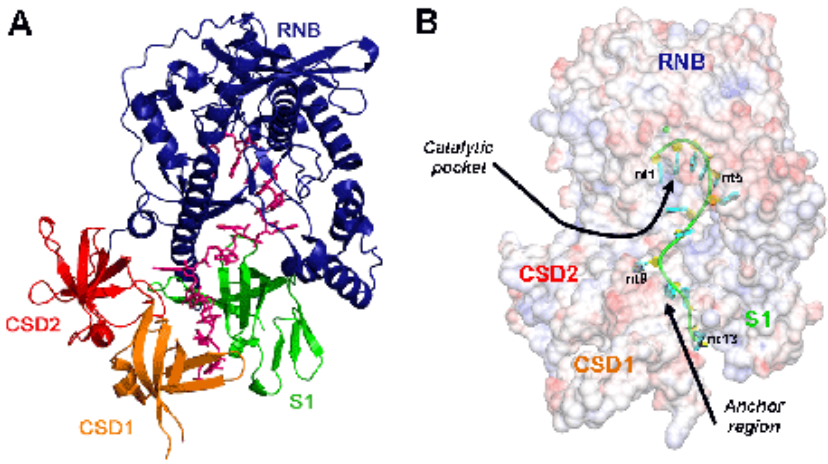

FIGURE 5. RNase II 3D structure. A. RNase II crystal structure shows that it is comprised of two N-terminal Cold Shock Domains (CSD1 in orange and CSD 2 in red), a central RNB domain (in blue) and a C-terminal S1 domain (in green); the RNA molecule is also represented (in pink) (PDB ID 2IX0 and 2IX1). **B.** The RNA molecule contacts with the protein at two different regions: the anchoring region (which contacts with nucleotides 9 to 13 of the RNA molecule) and the catalytic region (which contacts with the first five nucleotides counting from the 3' end. Adapted from Frazão *et al.*, 2006.

The RNA contacts RNase II at two different and non-contiguous regions (Figure 5B), which act synergistically to provide a processive degradation: the anchoring region, constituted by the three RNA-binding domains (CSD1, CSD2 and S1), and the catalytic region, which is buried inside the catalytic RNB domain (Figure 5B) (Frazão *et al.*, 2006). The shortest RNA substrate that is able to contact both anchor and catalytic regions is a 10 nt fragment. In fact, this is the minimum size necessary for the enzyme to

be processive. For shorter RNA fragments, fewer contacts with the protein are established and the enzyme becomes distributive (Frazão *et al.*, 2006). The access to the catalytic pocket is restricted to ssRNA due to the steric hindrance at its entrance and explains why RNase II is not able to cleave double-stranded substrates (Frazão *et al.*, 2006; Spickler and Mackie, 2000). The first five nucleotides counting from the 3' end are stacked between the two aromatic residues Tyr253 and Phe358 (Figure 6): when the RNA molecule is shorter than five nucleotides, the stacking no longer occurs, and the 4 nucleotide end-product is released (Frazão *et al.*, 2006). A mutational analysis identified residue Tyr253 as responsible for setting the final end-product in RNase II. The substitution of this residue by an alanine changed the RNase II product from 4 to 10 nt and it was also shown to be crucial for the RNA binding at the 3' end (Arraiano *et al.*, 2010b; Barbas *et al.*, 2008; Matos *et al.*, 2010). The active site of RNase II has four highly conserved aspartic acids in positions 201, 207, 209, and 210 and an arginine in position 500 (Figure 6), which were postulated to assist in catalysis, namely by fixing the RNA molecule correctly. The Arg500 was also proved to have a crucial role in RNA degradation (Arraiano *et al.*, 2010b; Barbas *et al.*, 2009). It was shown that the four aspartates are not equivalent in their function, with Asp209 being the only one essential for catalysis (Arraiano *et al.*, 2010b; Barbas *et al.*, 2008). The same result was obtained with other members of this family (Dziembowski *et al.*, 2007; Matos *et al.*, 2009). The residue Glu542 is in close proximity with the leaving nucleotide (Figure 6), and it was proposed that, after cleavage, it helped to release the last nucleotide. However, its substitution in *E. coli* RNase II by an alanine led to a mutant which is 110 fold more active and with a 20 fold higher RNA affinity when compared to the wild-type protein (Arraiano *et al.*, 2010b; Barbas *et al.*, 2009; Matos *et al.*, 2010). This mutant protein constructed was described as an RNase II "Super-Enzyme" (Figure 7). This result showed that, in fact, Glu542 slows down the activity of the protein (Arraiano *et al.*, 2010b; Barbas *et al.*, 2009). As mentioned previously, RNase II is able to bind to DNA but it

cannot cleave it. The resolution of RNase II structure allowed to see the interaction between Tyr313 and Asp201 and the O2' ribose oxygen of the second ribose and Glu390 with the O2' ribose oxygen of the fourth ribose (Frazão *et al.*, 2006) (Figure 6). It was also demonstrated that RNase II has a strict requirement for a ribose at the second and/or the fourth nucleotide from the 3' end of the molecule (Arraiano *et al.*, 2010b; Barbas *et al.*, 2009). These contacts are responsible for the RNA specificity (Barbas *et al.*, 2009).

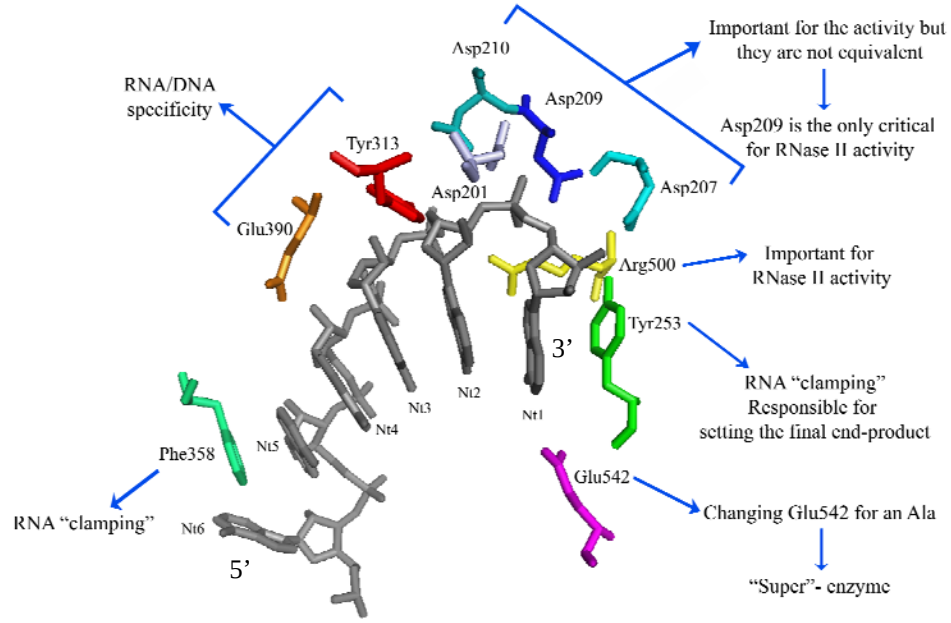

FIGURE 6. Zooming into the catalytic cavity of RNase II: critical residues in the mechanism of RNA degradation. The last 5 nucleotides of the 3' end of the RNA molecule are stacked between the aromatic residues Tyr253 and Phe358. The conserved aspartates 201, 207, 209 and 210 and arginine 500 are located in the active site of RNase II. The last nucleotide establishes contacts with Glu542, while Tyr313 and Glu390 contact with nucleotides 2 and 4 being the amino acids responsible for the RNA/DNA specificity. Adapted from Arraiano *et al.*, 2010b.

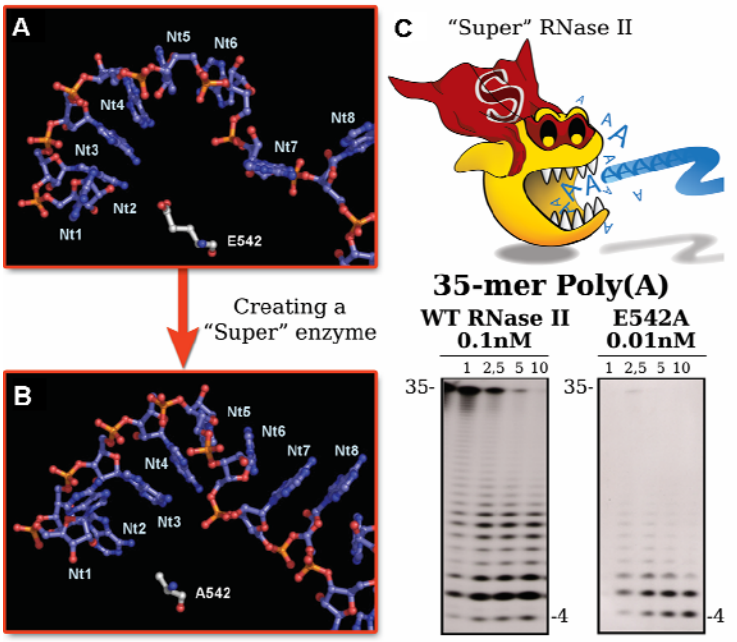

FIGURE 7. The making of a 'super-enzyme'. A. Zooming the catalytic cavity of RNase II. **B.** Modelling the E542A mutant with the poly(A) RNA strand in the RNB domain. Substitution in position 542 of the negatively charged glutamic side-chain for the smaller neutral methyl group of alanine could reduce significantly both electrostatic and steric surfaces in the RNA-binding interface. **C.** Exoribonuclease activity with the poly(A) substrate: comparison of wild-type and E542A proteins. It is possible to see that we need to use higher concentrations of RNase II when compared with the E542A mutant, which is 110 fold more active when compared with the wild-type. Adapted from Arraiano *et al.*, 2010a.

RNase R

RNase R-like enzymes have a wide impact in RNA metabolism in many different organisms. RNase II stalls when reaching near a duplex, and PNPase needs association with a helicase to overcome such structures. However, RNase R has the remarkable feature of degrading double-stranded RNA (Figure 4). The substrate list for RNase R includes defective

tRNA (Li *et al.*, 2002) or rRNA (Cheng and Deutscher, 2003) as well as mRNA with REP-containing sequences (Cheng and Deutscher, 2005) or small RNA like the stable SsrA/tmRNA (Cairrão *et al.*, 2003). Degradation of a RNA duplex occurs provided there is a single-stranded 3' overhang of at least 7 nt (Figure 8) (Vincent and Deutscher, 2006) and RNase R was shown to be a key enzyme involved in the degradation of polyadenylated RNA (Andrade *et al.*, 2009a).

The activity of RNase R is modulated according to environmental stimuli and its protein levels are up regulated under several stresses, namely stationary phase of growth and in cold shock (Andrade *et al.*, 2006; Cairrão and Arraiano, 2006). RNase R was shown to be involved in the degradation of the *omp*A transcript specifically in the stationary phase of growth, while no effect is detected in exponentially growing cells (Andrade *et al.*, 2006). *E. coli* RNase R deficient colonies are smaller especially in the cold (Cairrão *et al.*, 2003) and this enzyme is even essential for survival at low temperatures in pathogenic strains like *P. syringae* (Purusharth et al., 2005) or *A. hydrophila* (Figure 3) (Erova *et al.*, 2008). In addition to its role in stress response, RNase R has also been implicated in virulence mechanisms (Figure 3) (Erova *et al.*, 2008; Lalonde *et al.*, 2007; Tobe *et al.*, 1992; Tsao *et al.*, 2009). The stress-induction of RNase R levels can in fact be highly advantageous, enabling pathogens to adapt to environmental challenges imposed prior and during the infection process. Accordingly, most RNase R deficient bacteria have been shown to be less virulent than the wild-type strains. How this is achieved is still unclear but it has been suggested that RNase R may control the export of proteins involved in virulence mechanisms (Tobe *et al.*, 1992). A common trait of pathogenic RNase R mutants seems to be impaired motility (Erova *et al.*, 2008; Tsao *et al.*, 2009). RNase R also affects other cellular processes, like the development of competence in *L. pneumophila* (Charpentier et al., 2008) or the expression of apoptosis genes in *Helicobacter pylori* (Tsao et al., 2009). This is probably related to critical RNA degradation pathways mediated by RNase R.

Currently, the structure of RNase R remains unknown, which represents a major drawback in understanding RNase R mechanism of action. Most of the knowledge on RNase R structure is inferred from the available structures of its close counterparts, RNase II and Rrp44. RNase R follows the typical modular organization found on RNase II-family members: a RNB catalytic domain flanked by RNA-binding domains (CSD1 and CSD2 located at the N-terminus and a C-terminal S1 domain) (Figure 2). Furthermore, additional features are exclusively found in the RNase R sequence, namely a predicted nucleic acid binding motif (Helix-turn-Helix) at the N-terminal and a highly basic extended region after the S1 domain (Figure 2). All these regions must combine in a way that makes RNase R unique amongst exoribonucleases.

The majority of the residues interacting with the 3' end of the RNA are conserved throughout the RNase II-family of exoribonucleases, suggesting a similar mechanism for hydrolysis (Barbas *et al.*, 2008; Bonneau *et al.*, 2009). Structural differences might help explaining the divergence in substrate recognition between the members of RNase II-family. Despite the biochemical similarities many uncertainties remain concerning the pathway followed to effect the degradation of structured substrates.

A three-dimensional model of RNase R has been proposed based on the structure of its paralogue RNase II (Barbas *et al.*, 2008). Mutational analysis identified the highly conserved acid residues located in the active center responsible for catalysis: D272, D278 and D280 (Awano *et al.*, 2010; Matos *et al.*, 2009). As in the other members of the RNase II-family, these highly conserved aspartates are involved in coordination of divalent metal ions (preferably Mg^{2+}) essential to catalysis. In particular, the RNase R D280N mutant showed no exonucleolytic activity although RNA binding was not affected, analogous to what was reported with the D209N mutant in RNase II (Amblar and Arraiano, 2005; Awano *et al.*, 2010; Matos *et al.*, 2009). The highly conserved tyrosine 324 was found to be responsible for setting the final end-product of RNase R. Mutation Y342A altered the final end-product from 2 to 5 nucleotides, probably due to

loose packing of the 3' terminal nucleotides in the catalytic cavity (Matos *et al.*, 2009). Overall, the structural model of RNase R when compared to RNase II and Rrp44 structures identified the critical residues located in similar catalytic environments (Barbas *et al.*, 2008). However, mutagenic studies revealed that despite all similarities, the catalytic channel is not alike between these enzymes. RNase R was shown to bind RNA more tightly within its catalytic channel than does RNase II. The amino acid residue Arg572 located in the nuclease domain channel strongly affects RNase R catalytic properties. Mutation to a lysine (the equivalent residue found in RNase II) greatly impaired RNase R activity on structured RNA (Vincent and Deutscher, 2009a). Surprisingly, just the nuclease domain of RNase R (but not the one from RNase II) without accessory domains is able to degrade a double-stranded RNA (Matos *et al.*, 2009; Vincent and Deutscher, 2009b). A truncated form of RNase R expressing only the RNB domain degrades a blunt dsRNA (Figure 8) although with a low level of activity when compared to wild-type protein. However, the presence of the auxiliary domains for substrate binding completely inhibits this activity, probably by "blocking" the entrance of dsRNA into the catalytic channel (Figure 8). In the presence of CSD1, CSD2 and S1 domains, a short 3' unpaired overhang is required to allow the degradation of dsRNA (Figure 8). Available data indicates that RNA-binding domains actually discriminate the substrates that can be targeted by RNase R, favouring the selection of RNA molecules tagged with a 3' linear tail (Matos *et al.*, 2009).

Remarkably, RNA-binding domains may have an intrinsic ability to help to unwind the double-stranded RNA molecules. As an additional probe of the resourceful enzyme that RNase R is, it has been suggested that it can function both as an exoribonuclease as well as an RNA "helicase" (Awano *et al.*, 2010). RNase R intrinsic "helicase" unwinding activity is dependent on RNA-binding regions (namely on CDS2). *In vitro* studies showed that exonuclease and "helicase" activities are distinct and independent being located in separate domains. Like CsdA and other DEAD-box RNA

helicases, RNase R was shown to be more active at unwinding short (10-bp) rather than longer RNA duplexes. Not surprisingly, only a double stranded RNA with a 3' linear overhang was shown to be a suitable substrate for RNase R "helicase" action. Moreover, the additional motifs exclusively found in RNase R may expand the known functions of the anchor domains (Andrade *et al.*, 2009b; Zuo *et al.*, 2006). The helix-turn-helix predicted in the N-terminus is a potential nucleic acid binding motif although there is no experimental evidence of this role yet. The extended region found in the C-terminal end contains a positively charged surface patch formed by basic arginine and lysine residues. This suggests a possible role in nucleic acid binding through electrostatic interactions. These potential extra protein:RNA interactions might contribute to "melting" of secondary RNA structures, and help to explain the impressive RNase R mode of action. However, this is quite speculative at the moment. In fact it was proven that these "extra" domains in RNase R are not there merely for cosmetic purposes; the basic region in the C-terminal region was found to control the stability of RNase R through interactions with components of the *trans*-translation machinery. RNase R is an unstable protein but is highly stabilized if SmpB and/or tmRNA are prevented from interacting with the C-terminal region of RNase R (Liang and Deutscher, 2010). It is still not clear how binding of SmpB and tmRNA to RNase R leads to its destabilization. Possible structural changes of the complex might help explaining these observations. More recently, it was also shown that the C-terminal lysine-rich region is necessary for the recruitment of RNase R to stalled ribosomes and to the selective decay of defective transcripts (Ge *et al.*, 2010). It was also shown that chimeric proteins with the catalytic region from RNase II and the S1 domain from RNase R were able to degrade structured substrates. This result indicates that the C-terminal region of RNase R is involved in the degradation of structured substrates, probably by helping to unwind the substrate (Matos *et al.*, 2011a).

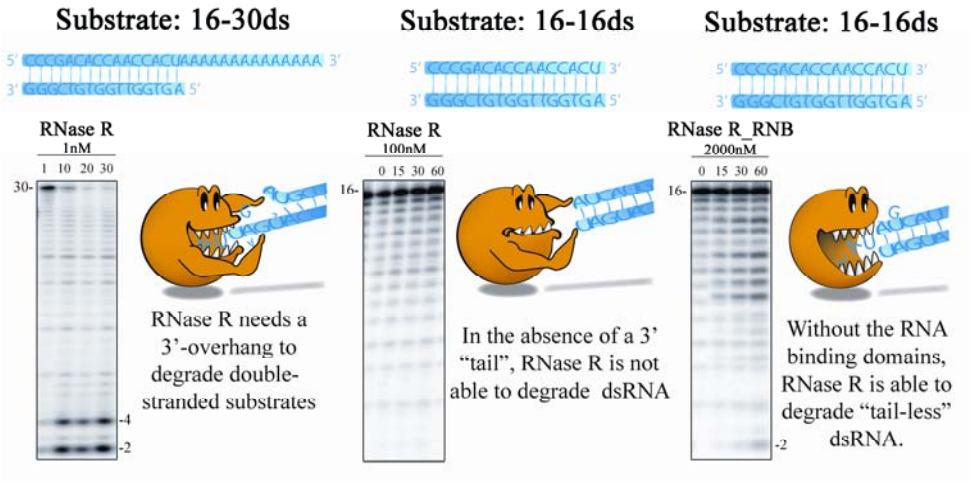

FIGURE 8. Degradation of double-stranded substrates by *E. coli* RNase R. RNase R needs a 3' single-stranded overhang to degrade double-stranded substrates. In the absence of the RNA-binding domains, the protein can degrade "tail-less" RNA. Adapted from Matos *et al.*, 2011b.

A definitive model for RNA degradation by RNase R is still open, and it seems clear that only the resolution of RNase R structure will answer the many questions about its remarkable mode of action.

Rrp44 (Dis3)

Rrp44, also a member of the RNB-family of enzymes, degrades RNA hydrolytically from 3' to 5' in a processive manner to a final product of 3 to 5 nucleotides. In addition to single-stranded RNA, Rrp44 is able to degrade secondary structures provided that it has a 3' end overhang with at least 4 nucleotides (Bonneau *et al.*, 2009; Dziembowski *et al.*, 2007).

In addition to the domains described for RNase II and RNase R, Rrp44 contains in the N-terminus a region with three conserved cysteines (CR3 region) and a highly conserved pilT N-terminal (PIN) domain (Figure 2) with endonucleolytic activity (Cairrão *et al.*, 2005; Lebreton *et al.*, 2008;

Schaeffer *et al.*, 2009; Schneider *et al.*, 2009). The two active sites responsible for both exo and endonucleolytic activity coordinate to degrade and process exosome substrates.

In *Saccharomyces cerevisiae*, the crystallographic structure of a single aminoacid mutant (D551N) of Rrp44ΔPIN in complex with RNA was determined (Bonneau *et al.*, 2009). It showed that there is a structural conservation in all domains when compared to RNase II. However, there is a difference concerning the relative orientation of the binding domains, with implications on the route of RNA access to the catalytic site. In Rrp44, the RNA is threaded to the catalytic site by binding the CSD1 and the RNB domains, while in RNase II the RNA is threaded by binding S1 and CSD2 domains. It was suggested that these different routes are responsible for the difference in RNA unwinding properties and activity on structured RNA substrates between RNase II and Rrp44 enzymes (Bonneau *et al.*, 2009).

Rrp44 is the only active component of the yeast cytoplasmic exosome (Dziembowski *et al.*, 2007; Liu *et al.*, 2006; Schneider *et al.*, 2007). Electron microscopic analysis of the *S. cerevisiae* exosome showed that Rrp44 binds to the bottom of the exosome PH ring through the interaction of the PIN domain and Rrp41, and the RNase II-like region contacts with Rrp41, Rrp43 and Rrp45 (Figure 9) (Wang *et al.*, 2007). Biochemical results showed that the interaction between the PIN domain and Rrp41 is the strongest between Rrp44 and the exosome. These interactions seem to be conserved in other species.

Usually cells present a single Rrp44 ortholog, however there are cases where two or more orthologues of Rrp44 exist. In *S. cerevisiae* the unique Rrp44 is present in the nucleus and the cytoplasm (Houseley *et al.*, 2006). In humans, there are two Rrp44 homologues, hDIS3 and hDIS3L, which interact with the exosome and display processive exonuclease activity (Staals *et al.*, 2010; Tomecki *et al.*, 2010). hDIS3 mainly localizes in the nucleoplasm, has endonucleolytic activity, and complements lower levels of yeast Rrp44, while hDIS3L is strictly cytoplasmic and has no

endonucleolytic activity, probably due to several mutations in the PINc domain (Figure 2) (Tomecki *et al.*, 2010). Recently, a protein that contains the RNase II-like region, without one or more of the CSD domains, but lacks the PIN domain was identified in *Arabidopsis thaliana* (Figure 2) (Zhang *et al.*, 2010). This protein, named suppressor of varicose (SOV), is a major cytoplasmic protein with mRNA decay activity *in vivo*. Like RNase II-like proteins, it was proposed to have 3' to 5' exoribonuclease activity, but the absence of the PIN domain suggests that it is not one of the components of the exosome. SOV-like proteins have been conserved in distant lineages, namely in *Mus musculus*, *Drosophila melanogaster*, *Oryza sativa*, *Selaginella moellendorffii* and *Caenorhabditis elegans*.

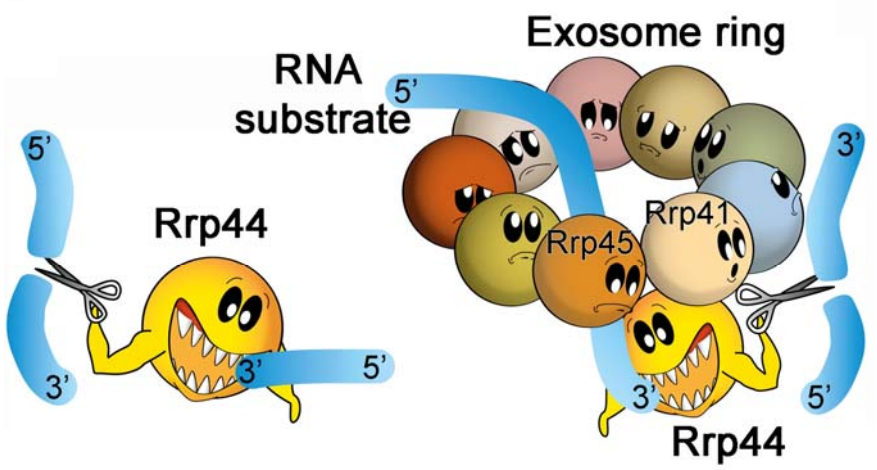

FIGURE 9. Schematic representation of the exosome ring. The Rrp44 protein is the only active subunit in the yeast exosome and has both exo and endonucleolytic activity. This protein can act as a member of the exosome and it is also possible that it may act alone. Adapted from Matos *et al.*, 2011b.

In *Drosophila*, the Rrp44/Dis3 homologue was characterized and named Tazman. It was shown to be more similar to RNase R and Rrp44 than to RNase II, and, similarly to Rrp44, it has an N-terminal PINc domain and a CR3 region (Cairrão *et al.*, 2005). This N-terminal region is sufficient for the endoribonucleolytic activity and also contributes to the interaction with the exosome and with protein localization (Mamolen *et al.*, 2010). This protein was also shown to be differentially expressed during the *Drosophila* life cycle, suggesting that it may play an important role in the modulation of RNA levels important for development (Cairrão *et al.*, 2005).

DEDD-FAMILY

This family of enzymes includes both RNA and DNA exonucleases. These proteins have a characteristic core with four invariant acidic amino acids (which are responsible for the designation of this family) and other conserved residues which are distributed in three distinct sequence motifs. In motif III, the presence of a tyrosine or histidine led to the division of this family into two subgroups, DEDDy and DEDDh, respectively. All proteins of this family share a common mechanism of action which involves two metal ions (Zuo and Deutscher, 2001).

Oligoribonuclease

Pioneering work identified Oligoribonuclease as the "finishing enzyme" in RNA metabolism. The degradative activity of other exoribonucleases result in final RNA fragments ranging from 2-5 nt whose accumulation could be deleterious to the cell. Oligoribonuclease acts at the final steps of RNA degradation, converting the small oligoribonucleotides to mononucleotides (Ghosh and Deutscher, 1999).

Oligoribonuclease (OligoRNase/Orn) is a 3'-5' RNase member of the DnaQlike/DEDD exonuclease superfamily. The DnaQ-like exonuclease domain contains three well conserved ExoI, ExoII and ExoIII sequence motifs clustered around the active site. Like all members of this family, Orn contains four highly conserved acidic residues (DEDD) in the active

center. These amino acids are proposed to be essential for binding divalent metal ions and thus for catalytic activity (Steitz and Steitz, 1993). Only a preliminary X-ray crystal study of *E. coli* Oligoribonuclease was published (PDB 1YTA) (Fiedler *et al.*, 2004), although a more refined structure is available in the PDB database (PDB 2IGI). A more detailed structural work concerning Orn was done with the plant pathogen *Xanthomonas campestris*, which oligoribonuclease XC847 shares a 52.6% identity with *E. coli* Orn (Chin *et al.*, 2006).

Oligoribonuclease functions as a homodimeric enzyme (Zhang *et al.*, 1998). The dimeric architecture of Oligoribonuclease is very similar to the arrangement seen in RNase T (Figure 10). The two DEDD domains appear to complement each other with one monomer providing the substrate binding surface leading into the catalytic center of the other monomer (Zuo *et al.*, 2005). Destabilization of the dimer conformation can alter protein activity and possibly cause its inactivation.

Oligoribonuclease is a processive enzyme and its nuclease activity is inversely proportional to the length of the single-stranded substrate with a 5-mer oligoribonucleotide being a preferable substrate. Orn is insensitive to 5' RNA phosphorylation state but the molecule must have a free 3' OH end (Datta and Niyogi, 1975).

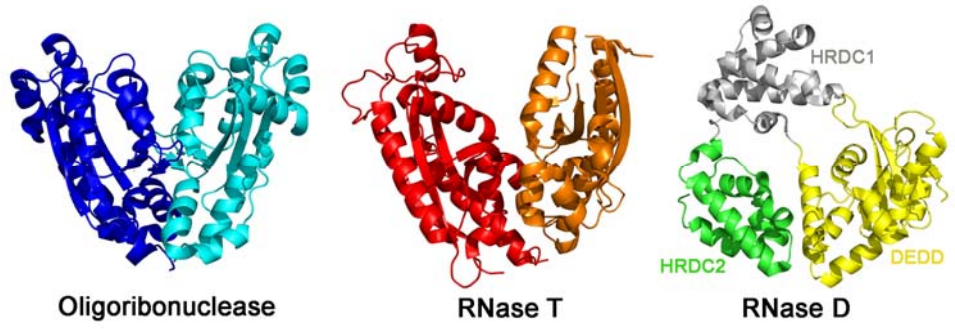

FIGURE 10. Comparison of the structures of the three members of the DEDD-family from *E. coli*: oligoribonuclease (PDB ID 2IGI), RNase T (PDB ID 2IS3) and RNase D (PDB ID 1YT3). Adapted from Matos *et al.*, 2011b.

Oligoribonucleases are found in the Proteobacteria (β and γ divisions) and have not been detected in archaea, although are present in all eukaryotes (Zuo and Deutscher, 2001). *E. coli* Oligoribonuclease is encoded by the *orn* gene and is the only essential exoribonuclease required for cell viability in this organism (Ghosh and Deutscher, 1999). *Bacillus subtilis* lacks an Orn homologue (Mechold *et al.*, 2006). However, *B. subtilis* has at least two functional analogues of Orn, termed nanoRNases NrnA and NrnB that can complement *in vivo* a defective *E. coli orn* mutant.

Yeast homologue Ynt20/Rex2 is localized in mitochondria whereas its function there remains unclear (Hanekamp and Thorsness, 1999). It was also reported to function in the nucleus, namely in the processing of some stable and small RNA (van Hoof *et al.*, 2000). The human homologue was proposed to exist in two isoforms that arise from alternatively spliced transcripts, one of them, Sfnα, contains mitochondrial targeting sequences, while the other protein, referred as Sfn, was shown to be oligoribonuclease *in vitro* and, in contrast to the bacterial enzyme, is able to digest both DNA and RNA substrates (Nguyen *et al.*, 2000).

RNase D

RNase D is a 40 kDa protein encoded by the *rnd* gene. As a member of DEDD-family of enzymes, it requires divalent metal ions for its activity and has a high degree of substrate specificity (Cudny *et al.*, 1981). This enzyme was initially discovered through its action on "denatured" and damaged tRNA but it also acts on tRNA precursors with extra 30 residues following the CCA sequence, 5S rRNA and other small-structured RNA but not ssRNA (Cudny and Deutscher, 1980; Zhang and Deutscher, 1988a). RNase D is not an essential protein for the cell however, is crucial for viability when RNase II, BN, T, and PH are absent, which may indicate that is a backup enzyme when the principal ribonucleases are missing (Kelly and Deutscher, 1992a). RNase D overexpression seems to be deleterious for the cell (Zhang and Deutscher, 1988b). In the cell, the *rnd* expression may be limited because: the chromosomal gene uses UUG as

the initiation codon; it has an abnormally high level of rare codons; its expression is negatively regulated at the translational level by the initiation codon (Zhang and Deutscher, 1989).

The resolution of the RNase D crystal structure showed that this protein has one C-terminal DEDD catalytic domain and two HRDC domains at the N-terminal region. The interactions between HRDC2 and DEDD are responsible for bringing the three domains into a funnel-shaped ring structure, which is very flexible, and suggests a processive activity (Figure 10). RNase D is not able to degrade short oligonucleotides, possibly due to their weak binding at the active center (Zuo *et al.*, 2005).

RNase D homologues have been found in many bacterial organisms, while in archeal genomes it was not possible to find any RNase D homologue. In eukaryotes there is, at least, one RNase D homologue, named Rrp6, which is one of the exosome ring proteins (Zuo and Deutscher, 2001).

Rrp6 structure of the yeast enzyme was solved and shows similarity with the nuclease domain of RNase D with the presence of one HRDC domain (Midtgaard *et al.*, 2006). Rrp6 is a distributive single-strand specific RNA nuclease. In yeast, it plays a role in nuclear mRNA surveillance and in the degradation of rRNA maturation by-products or intergenic transcripts (Houseley *et al.*, 2006). It is also involved in the final step in processing several non-coding RNA (Allmang *et al.*, 1999).

In plants, it was shown that there are three different Rrp6-like proteins, which are localized in nucleus, nucleolus and cytoplasm, respectively. Each of them seems to serve some specific and unique function (Lange *et al.*, 2008).

RNase T

RNase T, also a member of the DEDD superfamily of RNases, is a single-strand specific exoribonuclease which also has DNA exonuclease activity (Viswanathan *et al.*, 1998). It has a distributive activity, which depends on the presence of divalent metal ions, such as Mg^{2+} or Mn^{2+}, and has an unusual base specificity, discriminating against pyrimidines and, particularly, C residues. This sequence specificity is determined by the

last four nucleotides at the 3' end (Deutscher and Marlor, 1985; Zuo and Deutscher, 2002a, b). When compared to other ribonucleases, RNase T is the only enzyme capable of removing nucleotides near the duplex structure without unwinding the substrate, generating blunt-ended RNA. RNase T is involved in the final step of maturation of many stable RNA (Li and Deutscher, 1995, 1996; Li *et al.*, 1998): it is essential for the maturation of the 3' ends of 5S and 23S rRNA genes (Li and Deutscher, 1995; Li *et al.*, 1999), and it is also involved in the end turnover of tRNA (Deutscher and Marlor, 1985).

In order to be functional, RNase T needs to form a dimer, both *in vivo* and *in vitro* (Li et al., 1996). Mutational analysis identified three NBS (nucleic acid binding sequences) segments important for substrate binding (Zuo and Deutscher, 2002a). The resolution of crystal structure of RNase T from both *E. coli* and *Pseudomonas aeruginosa* show that the protein has an oligoribonuclease-like homodimer architecture (Figure 10) (Zuo *et al.*, 2007). The two monomers face in opposite directions, i. e., the NBS segment from one monomer is located in the vicinity of the DEDD active center pocket of the other monomer. This arrangement allows the binding of the RNA molecule from one monomer to be close to the active site of the other, and also helps us to explain why the enzyme requires the formation of the homodimer in order to be active (Zuo *et al.*, 2007). Despite its critical role in RNA metabolism, RNase T orthologues are only found in the γ division of Proteobacteria (Zuo and Deutscher, 2001).

CONCLUDING REMARKS

To maintain the correct RNA levels in the cell, RNA metabolism must be tightly controlled. One of the factors involved are ribonucleases, which will determine the degradation pathway for each RNA molecule. Exoribonucleases play an important role in the mechanism of RNA degradation, and they behave differently regarding RNA recognition and degradation. While some RNases are important for RNA degradation,

others are specialized in the processing and maturation of some types of RNA. The determination of crystal structures of these enzymes has allowed investigators to better understand their mechanism of action and further our knowledge of RNA metabolism. The similarities between prokaryotes and eukaryotes were shown to be much higher than initially expected.

AIM OF THIS DISSERTATION STUDY

This dissertation is mainly focused on the two members of RNase II-family that exist in *E. coli*, RNase II and RNase R, since their study was the main objective proposed for this Doctoral work.

After the resolution of the crystal structure of RNase II and its RNA-bound complex, it was possible to verify which residues were in close contact with the RNA molecule (Frazão *et al.*, 2006). In a preliminary work, the role of some highly conserved residues was elucidated. In the catalytic cavity, the last 5 nucleotides from the 3´ end of the RNA molecule is stacked between the two aromatic residues Tyr253 and Phe358. Also, the active site of the protein is constituted by four aspartate residues that could play an important role in catalysis (Frazão *et al.*, 2006). By mutational analysis, it was shown that tyrosine in position 253 is very important for the activity of the protein and is responsible for setting the final end-product of RNase II. Moreover, the four highly conserved aspartates located in the active site are not equivalent in their function and only the one is position 209 was crucial for the activity of the protein (Barbas *et al.*, 2008).

Although the role of these residues was already determined, other important amino acids were still having an unknown function. As such, the first phase of the work was to determine the role of the remaining highly conserved residues (Y313, E390, R500 and E542) which are located in the catalytic cavity. For this purpose, we mutated those amino acids and constructed several single, double and triple mutants. Then,

the resultant proteins were tested regarding their ability to degrade single- and double-stranded molecules. Their affinity for RNA and DNA was also analysed using different substrates. We were also interested in understanding why RNase II binds to DNA but is not able to cleave these molecules. This led us to analyse some mutants using chimeric substrates, where some bases were DNA and others RNA.

In the second phase of the work, we focused on RNase R protein. Little was known regarding the mechanism of action of this protein. Similarly to what was performed with RNase II (Amblar *et al.*, 2006), we wanted to confirm the specific role of each domain from RNase R in RNA degradation mechanism. Moreover, considering that RNase R is able to cleave double-stranded substrates and RNase II is sensitive to these substrates, we were also interested to know which domain(s) is(are) responsible for the degradation of structured substrates. In order to address this question, we constructed a set of truncated proteins and analyzed them regarding their ability to degrade single and double-stranded substrates. We also characterized their ability to bind to RNA molecules. Considering the results obtained with RNase II regarding the role of some highly conserved residues, we also performed a mutational analysis. However, for this purpose, we chose just the residues that were shown to be important for the mechanism of action of RNase II (Asp209 and Tyr253) and we mutated the corresponding amino acids in RNase R (Asp280 and Tyr324).

Although belonging to the same family of enzymes, RNase II and RNase R present some differences regarding the RNA degradation mechanism, namely in the end-product released and their ability to degrade double-stranded molecules (Arraiano *et al.*, 2010a). In the final step of this work, we wanted to unravel where the differences between RNase II and RNase R (namely regarding the final product release and the ability do degrade structured substrates) were localized. With this purpose, we constructed a set of chimeric proteins where we swapped domains between RNase II and RNase R. This allowed us to determine which are the domains

responsible for setting the final end-product in both enzymes and also to understand why RNase R is able to degrade double-stranded substrates.
In summary, the worked developed in this dissertation aimed to deeply understand the mechanism of action of proteins from the RNase II-family of enzymes. For that purpose, we mainly focused on RNase II and RNase R proteins from *E. coli*, since they where shown to be good models that may help us to understand the mode of action of these proteins in other organisms, including in eukaryotes.

ACKNOWLEDGMENTS

We thank Miguel Luís for graphical assistance in Figures 4, 7, 8 and 9.

REFERENCES

Allmang, C., Kufel, J., Chanfreau, G., Mitchell, P., Petfalski, E., and Tollervey, D. (1999) Functions of the exosome in rRNA, snoRNA and snRNA synthesis. *EMBO J* **18**: 5399-5410.

Amblar, M., and Arraiano, C.M. (2005) A single mutation in *Escherichia coli* ribonuclease II inactivates the enzyme without affecting RNA binding. *FEBS J* **272**: 363-374.

Amblar, M., Barbas, A., Fialho, A.M., and Arraiano, C.M. (2006) Characterization of the functional domains of *Escherichia coli* RNase II. *J Mol Biol* **360**: 921-933.

Amblar, M., Barbas, A., Goméz-Puertas, P., and Arraiano, C.M. (2007) The role of the S1 domain in exoribonucleolytic activity: substrate specificity and multimerization. *RNA* **13**: 317-327.

Andrade, J.M., Cairrão, F., and Arraiano, C.M. (2006) RNase R affects gene expression in stationary phase: regulation of ompA. *Mol Microbiol* **60**: 219-228.

Andrade, J.M., Hajnsdorf, E., Régnier, P., and Arraiano, C.M. (2009a) The poly(A)-dependent degradation pathway of rpsO mRNA is primarily mediated by RNase R. *RNA* **15**: 316-326.

Andrade, J.M., Pobre, V., Silva, I.J., Domingues, S., and Arraiano, C.M. (2009b) The role of 3'-5' exoribonucleases in RNA degradation. *Prog Mol Biol Transl Sci* **85**: 187-229.

Arraiano, C.M., and Maquat, L.E. (2003) Post-transcriptional control of gene expression: effectors of mRNA decay. *Mol Microbiol* **49**: 267-276.

Arraiano, C.M., Andrade, J.M., Domingues, S., Guinote, I.B., Malecki, M., Matos, R.G., Moreira, R.N., Pobre, V., Reis, F.P., Saramago, M., Silva, I.J., and Viegas, S.C. (2010a) The critical role of RNA processing and degradation in the control of gene expression. *FEMS Microbiol Rev*.

Arraiano, C.M., Matos, R.G., and Barbas, A. (2010b) RNase II: The finer details of the Modus operandi of a molecular killer. *RNA Biol* **7**: 276-278.

Awano, N., Rajagopal, V., Arbing, M., Patel, S., Hunt, J., Inouye, M., and Phadtare, S. (2010) *Escherichia coli* RNase R has dual activities, helicase and RNase. *J Bacteriol* **192**: 1344-1352.

Barbas, A., Matos, R.G., Amblar, M., Lopez-Viñas, E., Goméz-Puertas, P., and Arraiano, C.M. (2008) New insights into the mechanism of RNA degradation by ribonuclease II: identification of the residue responsible for setting the RNase II end product. *J Biol Chem* **283**: 13070-13076.

Barbas, A., Matos, R.G., Amblar, M., Lopez-Vinas, E., Gomez-Puertas, P., and Arraiano, C.M. (2009) Determination of key residues for catalysis and RNA cleavage specificity: one mutation turns RNase II into a "SUPER-ENZYME". *J Biol Chem* **284**: 20486-20498.

Beran, R.K., and Simons, R.W. (2001) Cold-temperature induction of *Escherichia coli* polynucleotide phosphorylase occurs by reversal of its autoregulation. *Mol. Microbiol.* **39**: 112-125.

Bollenbach, T.J., Lange, H., Gutierrez, R., Erhardt, M., Stern, D.B., and Gagliardi, D. (2005) RNR1, a 3'-5' exoribonuclease belonging to the RNR superfamily, catalyzes 3' maturation of chloroplast ribosomal RNAs in *Arabidopsis thaliana*. *Nucleic Acids Res* **33**: 2751-2763.

Bonneau, F., Basquin, J., Ebert, J., Lorentzen, E., and Conti, E. (2009) The yeast exosome functions as a macromolecular cage to channel RNA substrates for degradation. *Cell* **139**: 547-559.

Bralley, P., Gust, B., Chang, S., Chater, K.F., and Jones, G.H. (2006) RNA 3'-tail synthesis in Streptomyces: in vitro and in vivo activities of RNase PH, the SCO3896 gene product and polynucleotide phosphorylase. *Microbiology* **152**: 627-636.

Briani, F., Del Favero, M., Capizzuto, R., Consonni, C., Zangrossi, S., Greco, C., De Gioia, L., Tortora, P., and Dehò, G. (2007) Genetic analysis of polynucleotide phosphorylase structure and functions. *Biochimie* **89**: 145-157.

Buttner, K., Wenig, K., and Hopfner, K.P. (2005) Structural framework for the mechanism of archaeal exosomes in RNA processing. *Mol. Cell* **20**: 461-471.

Cairrão, F., Chora, A., Zilhão, R., Carpousis, A.J., and Arraiano, C.M. (2001) RNase II levels change according to the growth conditions: characterization of *gmr*, a new *Escherichia coli* gene involved in the modulation of RNase II. *Mol Microbiol* **39**: 1550-1561.

Cairrão, F., Cruz, A., Mori, H., and Arraiano, C.M. (2003) Cold shock induction of RNase R and its role in the maturation of the quality control mediator SsrA/tmRNA. *Mol Microbiol* **50**: 1349-1360.

Cairrão, F., Arraiano, C., and Newbury, S. (2005) *Drosophila* gene tazman, an orthologue of the yeast exosome component Rrp44p/Dis3, is differentially expressed during development. *Dev Dyn* **232**: 733-737.

Cairrão, F., and Arraiano, C.M. (2006) The role of endoribonucleases in the regulation of RNase R. *Biochem Biophys Res Commun* **343**: 731-737.

Campos-Guillén, J., Bralley, P., Jones, G.H., Bechhofer, D.H., and Olmedo-Alvarez, G. (2005) Addition of poly(A) and heteropolymeric 3' ends in *Bacillus subtilis* wild-type and polynucleotide phosphorylase-deficient strains. *J. Bacteriol.* **187**: 4698-4706.

Cannistraro, V.J., and Kennell, D. (1994) The processive reaction mechanism of ribonuclease II. *J Mol Biol* **243**: 930-943.

Carpousis, A.J., Van Houwe, G., Ehretsmann, C., and Krisch, H.M. (1994) Copurification of *E. coli* RNAase E and PNPase: evidence for a specific association between two enzymes important in RNA processing and degradation. *Cell* **76**: 889-900.

Carzaniga, T., Briani, F., Zangrossi, S., Merlino, G., Marchi, P., and Dehò, G. (2009) Autogenous regulation of *Escherichia coli* polynucleotide phosphorylase expression revisited. *J Bacteriol* **191**: 1738-1748.

Charpentier, X., Faucher, S.P., Kalachikov, S., and Shuman, H.A. (2008) Loss of RNase R induces competence development in *Legionella pneumophila*. *J Bacteriol* **190**: 8126-8136.

Cheng, Z.F., Zuo, Y., Li, Z., Rudd, K.E., and Deutscher, M.P. (1998) The *vacB* gene required for virulence in *Shigella flexneri* and *Escherichia coli* encodes the exoribonuclease RNase R. *J Biol Chem* **273**: 14077-14080.

Cheng, Z.F., and Deutscher, M.P. (2003) Quality control of ribosomal RNA mediated by polynucleotide phosphorylase and RNase R. *Proc Natl Acad Sci U S A* **100**: 6388-6393.

Cheng, Z.F., and Deutscher, M.P. (2005) An important role for RNase R in mRNA decay. *Mol Cell* **17**: 313-318.

Chin, K.H., Yang, C.Y., Chou, C.C., Wang, A.H., and Chou, S.H. (2006) The crystal structure of XC847 from *Xanthomonas campestris*: a 3'-5' oligoribonuclease of DnaQ fold family with a novel opposingly shifted helix. *Proteins* **65**: 1036-1040.

Choi, J.M., Park, E.Y., Kim, J.H., Chang, S.K., and Cho, Y. (2004) Probing the functional importance of the hexameric ring structure of RNase PH. *J Biol Chem* **279**: 755-764.

Cudny, H., and Deutscher, M.P. (1980) Apparent involvement of ribonuclease D in the 3' processing of tRNA precursors. *Proc Natl Acad Sci U S A* **77**: 837-841.

Cudny, H., Zaniewski, R., and Deutscher, M.P. (1981) *Escherichia coli* RNase D. Catalytic properties and substrate specificity. *J Biol Chem* **256**: 5633-5637.

Datta, A.K., and Niyogi, K. (1975) A novel oligoribonuclease of *Escherichia coli*. II. Mechanism of action. *J. Biol. Chem.* **250**: 7313-7319.

Deutscher, M.P., and Marlor, C.W. (1985) Purification and characterization of *Escherichia coli* RNase T. *J Biol Chem* **260**: 7067-7071.

Deutscher, M.P., Marshall, G.T., and Cudny, H. (1988) RNase PH: an *Escherichia coli* phosphate-dependent nuclease distinct from polynucleotide phosphorylase. *Proc Natl Acad Sci U S A* **85**: 4710-4714.

Deutscher, M.P., and Reuven, N.B. (1991) Enzymatic basis for hydrolytic versus phosphorolytic mRNA degradation in *Escherichia coli* and *Bacillus subtilis*. *Proc Natl Acad Sci U S A* **88**: 3277-3280.

Donovan, W.P., and Kushner, S.R. (1986) Polynucleotide phosphorylase and ribonuclease II are required for cell viability and mRNA turnover in *Escherichia coli* K-12. *Proc Natl Acad Sci U S A* **83**: 120-124.

Dziembowski, A., Lorentzen, E., Conti, E., and Seraphin, B. (2007) A single subunit, Dis3, is essentially responsible for yeast exosome core activity. *Nat Struct Mol Biol* **14**: 15-22.

Erova, T.E., Kosykh, V.G., Fadl, A.A., Sha, J., Horneman, A.J., and Chopra, A.K. (2008) Cold shock exoribonuclease R (VacB) is involved in *Aeromonas hydrophila* pathogenesis. *J Bacteriol* **190**: 3467-3474.

Evguenieva-Hackenberg, E., Walter, P., Hochleitner, E., Lottspeich, F., and Klug, G. (2003) An exosome-like complex in *Sulfolobus solfataricus*. *EMBO Rep* **4**: 889-893.

Fiedler, T.J., Vincent, H.A., Zuo, Y., Gavrialov, O., and Malhotra, A. (2004) Purification and crystallization of *Escherichia coli* oligoribonuclease. *Acta Crystallogr. D. Biol. Crystallogr.* **60**: 736-739.

Frazão, C., McVey, C.E., Amblar, M., Barbas, A., Vonrhein, C., Arraiano, C.M., and Carrondo, M.A. (2006) Unravelling the dynamics of RNA degradation by ribonuclease II and its RNA-bound complex. *Nature* **443**: 110-114.

García-Mena, J., Das, A., Sánchez-Trujillo, A., Portier, C., and Montañez, C. (1999) A novel mutation in the KH domain of polynucleotide phosphorylase affects autoregulation and mRNA decay in *Escherichia coli*. *Mol. Microbiol.* **33**: 235-248.

Gatewood, M.L., and Jones, G.H. (2010) (p)ppGpp inhibits polynucleotide phosphorylase from streptomyces but not from *Escherichia coli* and increases the stability of bulk mRNA in *Streptomyces coelicolor*. *J Bacteriol* **192**: 4275-4280.

Ge, Z., Mehta, P., Richards, J., and Karzai, A.W. (2010) Non-stop mRNA decay initiates at the ribosome. *Mol Microbiol* **78**: 1159-1170.

Ghosh, S., and Deutscher, M.P. (1999) Oligoribonuclease is an essential component of the mRNA decay pathway. *Proc Natl Acad Sci U S A* **96**: 4372-4377.

Goverde, R.L., Huis in't Veld, J.H., Kusters, J.G., and Mooi, F.R. (1998) The psychrotrophic bacterium *Yersinia enterocolitica* requires expression of *pnp*, the gene for polynucleotide phosphorylase, for growth at low temperature (5 degrees C). *Mol. Microbiol.* **28**: 555-569.

Grunberg-Manago, M., Oritz, P.J., and Ochoa, S. (1955) Enzymatic synthesis of nucleic acidlike polynucleotides. *Science* **122**: 907-910.

Hanekamp, T., and Thorsness, P.E. (1999) YNT20, a bypass suppressor of yme1 yme2, encodes a putative 3'-5' exonuclease localized in mitochondria of *Saccharomyces cerevisiae*. *Curr Genet* **34**: 438-448.

Harlow, L.S., Kadziola, A., Jensen, K.F., and Larsen, S. (2004) Crystal structure of the phosphorolytic exoribonuclease RNase PH from *Bacillus subtilis* and implications for its quaternary structure and tRNA binding. *Protein Sci* **13**: 668-677.

Houseley, J., LaCava, J., and Tollervey, D. (2006) RNA-quality control by the exosome. *Nat Rev Mol Cell Biol* **7**: 529-539.

Ishii, R., Nureki, O., and Yokoyama, S. (2003) Crystal structure of the tRNA processing enzyme RNase PH from *Aquifex aeolicus*. *J Biol Chem* **278**: 32397-32404.

Jarrige, A.C., Mathy, N., and Portier, C. (2001) PNPase autocontrols its expression by degrading a double-stranded structure in the *pnp* mRNA leader. *EMBO J.* **20**: 6845-6855.

Kelly, K.O., and Deutscher, M.P. (1992a) The presence of only one of five exoribonucleases is sufficient to support the growth of *Escherichia coli*. *J Bacteriol* **174**: 6682-6684.

Kelly, K.O., and Deutscher, M.P. (1992b) Characterization of Escherichia coli RNase PH. *J Biol Chem* **267**: 17153-17158.

Kelly, K.O., Reuven, N.B., Li, Z., and Deutscher, M.P. (1992) RNase PH is essential for tRNA processing and viability in RNase-deficient *Escherichia coli* cells. *J Biol Chem* **267**: 16015-16018.

Lalonde, M.S., Zuo, Y., Zhang, J., Gong, X., Wu, S., Malhotra, A., and Li, Z. (2007) Exoribonuclease R in *Mycoplasma genitalium* can carry out both RNA

processing and degradative functions and is sensitive to RNA ribose methylation. *RNA* **13**: 1957-1968.

Lange, H., Holec, S., Cognat, V., Pieuchot, L., Le Ret, M., Canaday, J., and Gagliardi, D. (2008) Degradation of a polyadenylated rRNA maturation by-product involves one of the three RRP6-like proteins in *Arabidopsis thaliana*. *Mol Cell Biol* **28**: 3038-3044.

Lebreton, A., Tomecki, R., Dziembowski, A., and Seraphin, B. (2008) Endonucleolytic RNA cleavage by a eukaryotic exosome. *Nature* **456**: 993-996.

Li, Z., and Deutscher, M.P. (1995) The tRNA processing enzyme RNase T is essential for maturation of 5S RNA. *Proc Natl Acad Sci U S A* **92**: 6883-6886.

Li, Z., and Deutscher, M.P. (1996) Maturation pathways for *E. coli* tRNA precursors: a random multienzyme process in vivo. *Cell* **86**: 503-512.

Li, Z., Zhan, L., and Deutscher, M.P. (1996) *Escherichia coli* RNase T functions in vivo as a dimer dependent on cysteine 168. *J Biol Chem* **271**: 1133-1137.

Li, Z., Pandit, S., and Deutscher, M.P. (1998) 3' exoribonucleolytic trimming is a common feature of the maturation of small, stable RNAs in *Escherichia coli*. *Proc Natl Acad Sci U S A* **95**: 2856-2861.

Li, Z., Pandit, S., and Deutscher, M.P. (1999) Maturation of 23S ribosomal RNA requires the exoribonuclease RNase T. *RNA* **5**: 139-146.

Li, Z., Reimers, S., Pandit, S., and Deutscher, M.P. (2002) RNA quality control: degradation of defective transfer RNA. *EMBO J.* **21**: 1132-1138.

Liang, W., and Deutscher, M.P. (2010) A novel mechanism for ribonuclease regulation: transfer-messenger RNA (tmRNA) and its associated protein SmpB regulate the stability of RNase R. *J Biol Chem* **285**: 29054-29058.

Lim, J., Kuroki, T., Ozaki, K., Kohsaki, H., Yamori, T., Tsuruo, T., Nakamori, S., Imaoka, S., Endo, M., and Nakamura, Y. (1997) Isolation of murine and human homologues of the fission-yeast dis3+ gene encoding a mitotic-control protein and its overexpression in cancer cells with progressive phenotype. *Cancer Res* **57**: 921-925.

Littauer, Y.Z., and Soreq, H. (1982) *Polynucleotide Phosphorylase.* New York: Academic Press.

Liu, Q., Greimann, J.C., and Lima, C.D. (2006) Reconstitution, activities, and structure of the eukaryotic RNA exosome. *Cell* **127**: 1223-1237.

Lorentzen, E., and Conti, E. (2005) Structural basis of 3' end RNA recognition and exoribonucleolytic cleavage by an exosome RNase PH core. *Mol Cell* **20**: 473-481.

Lu, C., Ding, F., and Ke, A. (2010) Crystal structure of the *S. solfataricus* archaeal exosome reveals conformational flexibility in the RNA-binding ring. *PLoS One* **5**: e8739.

Luttinger, A., Hahn, J., and Dubnau, D. (1996) Polynucleotide phosphorylase is necessary for competence development in *Bacillus subtilis*. *Mol Microbiol* **19**: 343-356.

Mamolen, M., Smith, A., and Andrulis, E.D. (2010) *Drosophila melanogaster* Dis3 N-terminal domains are required for ribonuclease activities, nuclear localization and exosome interactions. *Nucleic Acids Res* **38**: 5507-5517.

Marujo, P.E., Hajnsdorf, E., Le Derout, J., Andrade, R., Arraiano, C.M., and Régnier, P. (2000) RNase II removes the oligo(A) tails that destabilize the rpsO mRNA of *Escherichia coli*. *RNA* **6**: 1185-1193.

Matos, R.G., Barbas, A., and Arraiano, C.M. (2009) RNase R mutants elucidate the catalysis of structured RNA: RNA-binding domains select the RNAs targeted for degradation. *Biochem J* **423**: 291-301.

Matos, R.G., Barbas, A., and Arraiano, C.M. (2010) Comparison of EMSA and SPR for the characterization of RNA-RNase II complexes. *Protein J* **29**: 394-397.

Matos, R.G., Barbas, A., Goméz-Puertas, P., and Arraiano, C.M. (2011a) Swapping the domains of exoribonucleases RNase II and RNase R: conferring upon RNase II the ability to degrade ds RNA. *Proteins* **79**: 1853-1867.

Matos, R.G., Pobre, V., Reis, F.P., Malecki, M., Andrade, J.M., and Arraiano, C.M. (2011b) Structure and degradation mechanisms of 3′ to 5′ exoribonucleases. *Ribonucleases (Springer)* ***In press***.

Matus-Ortega, M.E., Regonesi, M.E., Pina-Escobedo, A., Tortora, P., Dehò, G., and García-Mena, J. (2007) The KH and S1 domains of *Escherichia coli* polynucleotide phosphorylase are necessary for autoregulation and growth at low temperature. *Biochim. Biophys. Acta* **1769**: 194-203.

Mechold, U., Ogryzko, V., Ngo, S., and Danchin, A. (2006) Oligoribonuclease is a common downstream target of lithium-induced pAp accumulation in *Escherichia coli* and human cells. *Nucleic Acids Res.* **34**: 2364-2373.

Mian, I.S. (1997) Comparative sequence analysis of ribonucleases HII, III, II PH and D. *Nucleic Acids Res* **25**: 3187-3195.

Miczak, A., Kaberdin, V.R., Wei, C.L., and Lin-Chao, S. (1996) Proteins associated with RNase E in a multicomponent ribonucleolytic complex. *Proc Natl Acad Sci U S A* **93**: 3865-3869.

Midtgaard, S.F., Assenholt, J., Jonstrup, A.T., Van, L.B., Jensen, T.H., and Brodersen, D.E. (2006) Structure of the nuclear exosome component Rrp6p reveals an interplay between the active site and the HRDC domain. *Proc Natl Acad Sci U S A* **103**: 11898-11903.

Mitchell, P., Petfalski, E., Shevchenko, A., Mann, M., and Tollervey, D. (1997) The exosome: a conserved eukaryotic RNA processing complex containing multiple 3'-->5' exoribonucleases. *Cell* **91**: 457-466.

Nguyen, L.H., Erzberger, J.P., Root, J., and Wilson, D.M., 3rd (2000) The human homolog of *Escherichia coli* Orn degrades small single-stranded RNA and DNA oligomers. *J Biol Chem* **275**: 25900-25906.

Nurmohamed, S., Vaidialingam, B., Callaghan, A.J., and Luisi, B.F. (2009) Crystal structure of *Escherichia coli* polynucleotide phosphorylase core bound to RNase E, RNA and manganese: implications for catalytic mechanism and RNA degradosome assembly. *J Mol Biol* **389**: 17-33.

Ost, K.A., and Deutscher, M.P. (1991) *Escherichia coli orf*E (upstream of *pyr*E) encodes RNase PH. *J Bacteriol* **173**: 5589-5591.

Parker, R., and Song, H. (2004) The enzymes and control of eukaryotic mRNA turnover. *Nat Struct Mol Biol* **11**: 121-127.

Piazza, F., Zappone, M., Sana, M., Briani, F., and Dehò, G. (1996) Polynucleotide phosphorylase of *Escherichia coli* is required for the establishment of bacteriophage P4 immunity. *J Bacteriol* **178**: 5513-5521.

Portier, C., Dondon, L., Grunberg-Manago, M., and Régnier, P. (1987) The first step in the functional inactivation of the *Escherichia coli* polynucleotide phosphorylase messenger is a ribonuclease III processing at the 5' end. *EMBO J.* **6**: 2165-2170.

Portnoy, V., Evguenieva-Hackenberg, E., Klein, F., Walter, P., Lorentzen, E., Klug, G., and Schuster, G. (2005) RNA polyadenylation in Archaea: not observed in *Haloferax* while the exosome polynucleotidylates RNA in *Sulfolobus*. *EMBO Rep* **6**: 1188-1193.

Pruijn, G.J. (2005) Doughnuts dealing with RNA. *Nat. Struct. Mol. Biol.* **12**: 562-564.

Purusharth, R.I., Klein, F., Sulthana, S., Jager, S., Jagannadham, M.V., Evguenieva-Hackenberg, E., Ray, M.K., and Klug, G. (2005) Exoribonuclease R interacts with endoribonuclease E and an RNA helicase in the psychrotrophic bacterium *Pseudomonas syringae Lz4W*. *J. Biol. Chem.* **280**: 14572-14578.

Purusharth, R.I., Madhuri, B., and Ray, M.K. (2007) Exoribonuclease R in *Pseudomonas syringae* is essential for growth at low temperature and plays a novel role in the 3' end processing of 16 and 5 S ribosomal RNA. *J Biol Chem* **282**: 16267-16277.

Py, B., Higgins, C.F., Krisch, H.M., and Carpousis, A.J. (1996) A DEAD-box RNA helicase in the *Escherichia coli* RNA degradosome. *Nature* **381**: 169-172.

Redko, Y., and Condon, C. (2010) Maturation of 23S rRNA in *Bacillus subtilis* in the absence of Mini-III. *J Bacteriol* **192**: 356-359.

Régnier, P., and Arraiano, C.M. (2000) Degradation of mRNA in bacteria: emergence of ubiquitous features. *Bioessays* **22**: 235-244.

Robert-Le Meur, M., and Portier, C. (1992) *E.coli* polynucleotide phosphorylase expression is autoregulated through an RNase III-dependent mechanism. *EMBO J.* **11**: 2633-2641.

Rott, R., Zipor, G., Portnoy, V., Liveanu, V., and Schuster, G. (2003) RNA polyadenylation and degradation in cyanobacteria are similar to the chloroplast but different from *Escherichia coli*. *J. Biol. Chem.* **278**: 15771-15777.

Schaeffer, D., Tsanova, B., Barbas, A., Reis, F.P., Dastidar, E.G., Sanchez-Rotunno, M., Arraiano, C.M., and van Hoof, A. (2009) The exosome contains domains with specific endoribonuclease, exoribonuclease and cytoplasmic mRNA decay activities. *Nat Struct Mol Biol* **16**: 56-62.

Schneider, C., Anderson, J.T., and Tollervey, D. (2007) The exosome subunit Rrp44 plays a direct role in RNA substrate recognition. *Mol Cell* **27**: 324-331.

Schneider, C., Leung, E., Brown, J., and Tollervey, D. (2009) The N-terminal PIN domain of the exosome subunit Rrp44 harbors endonuclease activity and tethers Rrp44 to the yeast core exosome. *Nucleic Acids Res* **37**: 1127-1140.

Shi, Z., Yang, W.Z., Lin-Chao, S., Chak, K.F., and Yuan, H.S. (2008) Crystal structure of *Escherichia coli* PNPase: central channel residues are involved in processive RNA degradation. *RNA* **14**: 2361-2371.

Siculella, L., Damiano, F., di Summa, R., Tredici, S.M., Alduina, R., Gnoni, G.V., and Alifano, P. (2010) Guanosine 5'-diphosphate 3'-diphosphate (ppGpp) as a negative modulator of polynucleotide phosphorylase activity in a 'rare' actinomycete. *Mol Microbiol* **77**: 716-729.

Slomovic, S., Portnoy, V., Yehudai-Resheff, S., Bronshtein, E., and Schuster, G. (2008) Polynucleotide phosphorylase and the archaeal exosome as poly(A)-polymerases. *Biochim. Biophys. Acta* **1779**: 247-255.

Sohlberg, B., Huang, J., and Cohen, S.N. (2003) The *Streptomyces coelicolor* polynucleotide phosphorylase homologue, and not the putative poly(A) polymerase, can polyadenylate RNA. *J. Bacteriol.* **185**: 7273-7278.

Spickler, C., and Mackie, G.A. (2000) Action of RNase II and polynucleotide phosphorylase against RNAs containing stem-loops of defined structure. *J Bacteriol* **182**: 2422-2427.

Staals, R.H., Bronkhorst, A.W., Schilders, G., Slomovic, S., Schuster, G., Heck, A.J., Raijmakers, R., and Pruijn, G.J. (2010) Dis3-like 1: a novel exoribonuclease associated with the human exosome. *EMBO J* **29**: 2358-2367.

Steitz, T.A., and Steitz, J.A. (1993) A general two-metal-ion mechanism for catalytic RNA. *Proc. Natl. Acad. Sci.* **90**: 6498-6502.

Symmons, M.F., Jones, G.H., and Luisi, B.F. (2000) A duplicated fold is the structural basis for polynucleotide phosphorylase catalytic activity, processivity, and regulation. *Structure* **8**: 1215-1226.

Tobe, T., Sasakawa, C., Okada, N., Honma, Y., and Yoshikawa, M. (1992) vacB, a novel chromosomal gene required for expression of virulence genes on the large plasmid of *Shigella flexneri*. *J Bacteriol* **174**: 6359-6367.

Tomecki, R., Kristiansen, M.S., Lykke-Andersen, S., Chlebowski, A., Larsen, K.M., Szczesny, R.J., Drazkowska, K., Pastula, A., Andersen, J.S., Stepien, P.P., Dziembowski, A., and Jensen, T.H. (2010) The human core exosome interacts with differentially localized processive RNases: hDIS3 and hDIS3L. *Embo J* **29**: 2342-2357.

Tsao, M.Y., Lin, T.L., Hsieh, P.F., and Wang, J.T. (2009) The 3'-to-5' exoribonuclease (encoded by HP1248) of *Helicobacter pylori* regulates motility and apoptosis-inducing genes. *J Bacteriol* **191**: 2691-2702.

van Hoof, A., and Parker, R. (1999) The exosome: a proteasome for RNA? *Cell* **99**: 347-350.

van Hoof, A., Lennertz, P., and Parker, R. (2000) Three conserved members of the RNase D family have unique and overlapping functions in the processing of 5S, 5.8S, U4, U5, RNase MRP and RNase P RNAs in yeast. *Embo J* **19**: 1357-1365.

Vanzo, N.F., Li, Y.S., Py, B., Blum, E., Higgins, C.F., Raynal, L.C., Krisch, H.M., and Carpousis, A.J. (1998) Ribonuclease E organizes the protein interactions in the *Escherichia coli* RNA degradosome. *Genes Dev* **12**: 2770-2781.

Vincent, H.A., and Deutscher, M.P. (2006) Substrate recognition and catalysis by the exoribonuclease RNase R. *J Biol Chem* **281**: 29769-29775.

Vincent, H.A., and Deutscher, M.P. (2009a) Insights into how RNase R degrades structured RNA: analysis of the nuclease domain. *J Mol Biol* **387**: 570-583.

Vincent, H.A., and Deutscher, M.P. (2009b) The roles of individual domains of RNase R in substrate binding and exoribonuclease activity. The nuclease domain is sufficient for digestion of structured RNA. *J Biol Chem* **284**: 486-494.

Viswanathan, M., Dower, K.W., and Lovett, S.T. (1998) Identification of a potent DNase activity associated with RNase T of *Escherichia coli*. *J Biol Chem* **273**: 35126-35131.

Wang, G., Chen, H.W., Oktay, Y., Zhang, J., Allen, E.L., Smith, G.M., Fan, K.C., Hong, J.S., French, S.W., McCaffery, J.M., Lightowlers, R.N., Morse, H.C., 3rd, Koehler, C.M., and Teitell, M.A. (2010) PNPase regulates RNA import into mitochondria. *Cell* **142**: 456-467.

Wang, H.W., Wang, J., Ding, F., Callahan, K., Bratkowski, M.A., Butler, J.S., Nogales, E., and Ke, A. (2007) Architecture of the yeast Rrp44 exosome complex suggests routes of RNA recruitment for 3' end processing. *Proc Natl Acad Sci U S A* **104**: 16844-16849.

Wen, T., Oussenko, I.A., Pellegrini, O., Bechhofer, D.H., and Condon, C. (2005) Ribonuclease PH plays a major role in the exonucleolytic maturation of CCA-containing tRNA precursors in *Bacillus subtilis*. *Nucleic Acids Res* **33**: 3636-3643.

Yehudai-Resheff, S., Hirsh, M., and Schuster, G. (2001) Polynucleotide phosphorylase functions as both an exonuclease and a poly(A) polymerase in spinach chloroplasts. *Mol Cell Biol* **21**: 5408-5416.

Zangrossi, S., Briani, F., Ghisotti, D., Regonesi, M.E., Tortora, P., and Dehò, G. (2000) Transcriptional and post-transcriptional control of polynucleotide phosphorylase during cold acclimation in *Escherichia coli*. *Mol Microbiol* **36**: 1470-1480.

Zhang, J.R., and Deutscher, M.P. (1988a) Transfer RNA is a substrate for RNase D in vivo. *J Biol Chem* **263**: 17909-17912.

Zhang, J.R., and Deutscher, M.P. (1988b) Cloning, characterization, and effects of overexpression of the *Escherichia coli rnd* gene encoding RNase D. *J Bacteriol* **170**: 522-527.

Zhang, J.R., and Deutscher, M.P. (1989) Analysis of the upstream region of the *Escherichia coli rnd* gene encoding RNase D. Evidence for translational regulation of a putative tRNA processing enzyme. *J Biol Chem* **264**: 18228-18233.

Zhang, W., Murphy, C., and Sieburth, L.E. (2010) Conserved RNase II domain protein functions in cytoplasmic mRNA decay and suppresses *Arabidopsis* decapping mutant phenotypes. *Proc Natl Acad Sci U S A* **107**: 15981-15985.

Zhang, X., Zhu, L., and Deutscher, M.P. (1998) Oligoribonuclease is encoded by a highly conserved gene in the 3'-5' exonuclease superfamily. *J Bacteriol* **180**: 2779-2781.

Zhou, Z., and Deutscher, M.P. (1997) An essential function for the phosphate-dependent exoribonucleases RNase PH and polynucleotide phosphorylase. *J Bacteriol* **179**: 4391-4395.

Zilhão, R., Caillet, J., Régnier, P., and Arraiano, C.M. (1995) Precise physical mapping of the *Escherichia coli* rnb gene, encoding ribonuclease II. *Mol Gen Genet* **248**: 242-246.

Zilhão, R., Cairrão, F., Régnier, P., and Arraiano, C.M. (1996a) PNPase modulates RNase II expression in *Escherichia coli*: implications for mRNA decay and cell metabolism. *Mol Microbiol* **20**: 1033-1042.

Zilhão, R., Plumbridge, J., Hajnsdorf, E., Régnier, P., and Arraiano, C.M. (1996b) *Escherichia coli* RNase II: characterization of the promoters involved in the transcription of *rnb*. *Microbiology* **142 (Pt 2)**: 367-375.

Zuo, Y., and Deutscher, M.P. (2001) Exoribonuclease superfamilies: structural analysis and phylogenetic distribution. *Nucleic Acids Res* **29**: 1017-1026.

Zuo, Y., and Deutscher, M.P. (2002a) Mechanism of action of RNase T. I. Identification of residues required for catalysis, substrate binding, and dimerization. *J Biol Chem* **277**: 50155-50159.

Zuo, Y., and Deutscher, M.P. (2002b) Mechanism of action of RNase T. II. A structural and functional model of the enzyme. *J Biol Chem* **277**: 50160-50164.

Zuo, Y., Wang, Y., and Malhotra, A. (2005) Crystal structure of *Escherichia coli* RNase D, an exoribonuclease involved in structured RNA processing. *Structure* **13**: 973-984.

Zuo, Y., Vincent, H.A., Zhang, J., Wang, Y., Deutscher, M.P., and Malhotra, A. (2006) Structural basis for processivity and single-strand specificity of RNase II. *Mol Cell* **24**: 149-156.

Zuo, Y., Zheng, H., Wang, Y., Chruszcz, M., Cymborowski, M., Skarina, T., Savchenko, A., Malhotra, A., and Minor, W. (2007) Crystal structure of RNase T, an exoribonuclease involved in tRNA maturation and end turnover. *Structure* **15**: 417-428.

Chapter 2

Determination of Key Residues for Catalysis and RNA Cleavage Specificity: *One mutation turns RNase II into a "super-enzyme"*

This chapter contains data published in:
Barbas, A.*, **Matos, R. G.***, Amblar, M., López-Viñas, E., Gómez-Puertas, P., and Arraiano, C.M. 2009. Determination of Key Residues for Catalysis and RNA Cleavage Specificity: One mutation turns RNase II into a "super-enzyme" Journal of Biological Chemistry **284**: 20486-20498.
***** Authors contributed equally
This Article was the cover of this JBC issue

The author had a major contribution in this manuscript, namely in the planning of the experimental work and in the performance of the experiments.

The modeling experiments and the Molecular Dynamics simulations were performed by Professor Paulino Gómez-Puertas and Dr. Eduardo Lopéz-Viñas from Centro de Biologia Molecular “Severo Ochoa”, Madrid, Spain. Mónica Amblar from Centro Nacional de Microbiología - Instituto de Salud Carlos III, Madrid, Spain helped in the discussion of the results obtained.

Abstract

RNase II is the prototype of a ubiquitous family of enzymes that are crucial for RNA metabolism. In *Escherichia coli* this protein is a single-stranded-specific 3' exoribonuclease with a modular organization of four functional domains. In eukaryotes, the RNase II homologue Rrp44 (also known as Dis3) is the catalytic subunit of the exosome, an exoribonuclease complex essential for RNA processing and decay. In this work we have performed a functional characterization of several highly conserved residues located in the RNase II catalytic domain to address their precise role in the RNase II activity. We have constructed a number of RNase II mutants and compared their activity and RNA binding to the wild-type using different single- or double-stranded substrates. The results presented in this study substantially improve the RNase II model for RNA degradation. We have identified the residues that are responsible for the discrimination of cleavage of RNA versus DNA. We also show that the Arg500 residue present in the RNase II active site is crucial for activity but not for RNA binding. The most prominent finding presented is the extraordinary catalysis observed in the E542A mutant that turns RNase II into a "super-enzyme."

Introduction

Exoribonuclease II (RNase II) is one of the major exoribonucleases involved in the degradation of RNA (Andrade *et al.*, 2009). This protein degrades RNA hydrolytically in the 3' to 5' direction, releasing 5' nucleoside monophosphates in a processive manner. Its activity is sequence independent but sensitive to secondary structures, and poly(A) is the preferential substrate for this enzyme (Amblar and Arraiano, 2005; Coburn and Mackie, 1996; Gupta *et al.*, 1977; Marujo *et al.*, 2000; McLaren *et al.*, 1991). In *Escherichia coli* RNase II is responsible for 90% of the hydrolytic activity in crude extracts (Deutscher and Reuven, 1991). Moreover, its expression is differentially regulated at the transcriptional and post-transcriptional levels (Cairrão *et al.*, 2001; Zilhão *et al.*, 1993; Zilhão *et al.*, 1996), and the protein can be regulated by environmental conditions (Cairrão *et al.*, 2001). The *E. coli* enzyme is the prototype of a widespread family of exoribonucleases, and RNase II homologues can be found in prokaryotes and eukaryotes (Mian, 1997). In the nucleus and in the cytoplasm of eukaryotic cells, RNase II homologues (Rrp44/Dis3) are part of the exosome, an essential multiprotein complex of exoribonucleases involved in processing, turnover, and quality control of different types of RNA (Mitchell *et al.*, 1997). Rrp44 is the only catalytically active nuclease in the human and yeast core exosome (Dziembowski *et al.*, 2007; Liu *et al.*, 2006). Moreover, it was recently demonstrated that apart from the RNB catalytic domain, Rrp44 has a second nuclease domain, the PINc domain that confers endonucleolytic activity to the protein (Lebreton *et al.*, 2008; Schaeffer *et al.*, 2009). In prokaryotic cells, apart from RNase II, there is an additional RNase II-like enzyme, RNase R that is involved in RNA degradation and RNA and protein quality control (Andrade *et al.*, 2006; Cairrão *et al.*, 2003; Cairrão and Arraiano, 2006; Cheng and Deutscher, 2005). RNase R has also been shown to be required for virulence (Cheng *et al.*, 1998).

The determination of *E. coli* RNase II structure (Frazão *et al.*, 2006; McVey *et al.*, 2006; Zuo *et al.*, 2006) showed that, contrary to the sequence predictions, RNase II consisted of four domains; they are two N-terminal cold shock domains (CSD1 and CSD2) involved in RNA binding, one central RNB catalytic domain, and a third RNA-binding domain at the C-terminus, the S1 domain (Figure 1A). Inside RNase II the RNA contacts the enzyme at two different and non-contiguous regions, the anchoring region (formed by the three RNA-binding domains) and the catalytic region (buried inside the catalytic domain) (Cannistraro and Kennell, 1994; Frazão *et al.*, 2006). The shortest RNA molecule able to retain contacts with these two regions simultaneously is a 10 nucleotide fragment, and this is also the minimum length necessary to maintain the processivity of the enzyme (Barbas *et al.*, 2008; Cannistraro and Kennell, 1994; Frazão *et al.*, 2006). Therefore, simultaneous binding of substrate to both sites is necessary for a processive degradation. Moreover, the structure of the RNA-bound complex revealed a tight packing of the five 3' terminal nucleotides in the catalytic cavity, mediated by the conserved aromatic residues Tyr253 and Phe358 (Frazão *et al.*, 2006). When the RNA substrate is shorter than 5 nucleotides the required packing of the bases can no longer occur, impeding the translocation of the RNA and generating the typical 4 nt fragment as the end-product for RNase II. A mutational analysis of *E. coli* RNase II has been reported (Barbas *et al.*, 2008), confirming the crucial role of Tyr253 in setting the end-product of RNase II degradation. In addition, this analysis showed that conserved acidic residues in the active site can have a different role during the degradation mechanism (Barbas *et al.*, 2008).

RNase II is specific for RNA. However, although it does not degrade DNA, it is still able to bind it. DNA oligonucleotides have been shown to act as reaction inhibitors of the *E. coli* RNase II, suggesting that both DNA and RNA compete for the same binding sites of the enzyme (Cannistraro and Kennell, 1994). Previous reports have demonstrated that the ribose specificity of RNase II is not for the scissile bond but for the nearby

nucleotides (Cannistraro and Kennell, 1994; Frazão *et al.*, 2006). The presence of a ribose between positions 2 through 5 from the 3' end of the RNA substrate is required for cleavage to occur (Cannistraro and Kennell, 1994). The crystal structure of the RNase II-RNA-bound complex (Frazão *et al.*, 2006) revealed direct contacts between the residues Asp201, Tyr313, and Glu390 and the O2' ribose oxygens of nucleotides in positions 2, 4, and 6 (Figure 1B). Such interactions seem to be responsible for the proper orientation of the RNA at the catalytic cavity and may account for the specificity of RNA *versus* DNA in RNase II.

Structural data also revealed that there are two other conserved residues at the active site that seem to be crucial for RNase II activity, Arg500 and Glu542 (Frazão *et al.*, 2006). In the RNA-complexed structure, the Arg500 is positioned between the two nucleotides at the 3' end interacting with their phosphate backbones (Figure 1B). It was postulated that Arg500 could assist in catalysis by fixing the phosphodiester bond at the cleavage position and enhancing the susceptibility of the leaving phosphorous atom to a nucleophilic attack (Frazão *et al.*, 2006). Glu542 is in close proximity to the nitrogen atoms of the leaving nucleotide (Figure 1B) and was suggested to facilitate the elimination of this nucleotide upon phosphor-ester cleavage by pulling it out of the base-stacked position (Frazão *et al.*, 2006).

In this report we analyze the role of some of these highly conserved amino acids in RNase II activity. We studied the function of Asp201, Tyr313, and Glu390 in the cleavage discrimination of RNA *versus* DNA. Our results showed that only Tyr313 and Glu390 are crucial for RNA specificity of RNase II. We also demonstrate that Arg500 is essential for RNase II activity, but it is not involved in RNA binding. Moreover, the most prominent findings presented are the extraordinary catalysis and binding abilities observed in the E542A mutant that turns RNase II into a "super-enzyme".

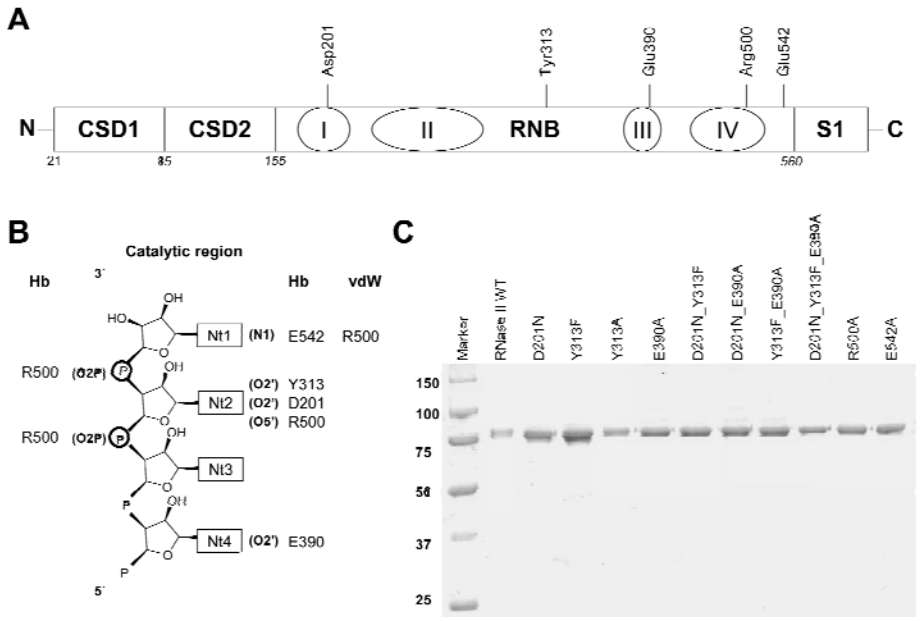

FIGURE 1. RNase II and mutant proteins. ***A.*** Linear representation of RNase II domains with the specification of the position of the conserved residues within RNB domain. ***B.*** Atomic interactions scheme between RNA and protein residues. *Hb* indicates hydrogen bonds up to 3.2 Å, and *vdW* indicates van der Waals interactions up to 3.6 Å. The labeling of the nucleotides starts from the 3' end of the RNA, inversely to previous reports where the nucleotides at the 3' end was labeled as nt 13 (Frazão *et al.*, 2006). ***C.*** Purity of the enzymes. 0.5μg of purified His6-RNase II, His6-D201N, His6-Y313F, His6-Y313A, His6-E390A, His6-D201N/Y313F, His6-D201N/E390A, His6-Y313F/E390A, His6-D201N/Y313F/ E390A, His6-R500A, and His6-E542A were applied and visualized by Coomassie Blue staining. Molecular weights of standard proteins are indicated on the left.

Experimental Procedures

Materials

Restriction enzymes, T4 DNA ligase, *Pfu* DNA polymerase, and T4 polynucleotide kinase were purchased from Fermentas. Unlabeled oligonucleotide primers were synthesized by STAB Vida, Portugal.

Strains

The *E. coli* strains used were DH5α (F' *fhuA2*Δ(*argF-lacZ)U169 phoA glnV44* Φ*80* Δ(*lacZ)M15 gyrA96 recA1 relA1 endA1 thi-1 hsdR17*a) (Taylor *et al.*, 1993) for cloning experiments and BL21(DE3) (F$^-$ *rB*$^-$ *mB*$^-$ *gal ompT* (*int*::*PlacUV5 T7 gen1 imm21 nin5*) (Studier and Moffatt, 1986) for expression and purification of enzymes.

Construction of RNase II Mutants by Overlapping PCR

The point mutations Y313F, Y313A, E390A, R500K, R500A, and E542A, the double mutations D201N/Y313F, D201N/E390A, and Y313F/E390A, and the triple mutation D201N/Y313F/E390A were introduced into pFCT6.9 (Cairrão *et al.*, 2001) or in the pFCT6.9/D201N (Barbas *et al.*, 2008) by overlapping PCR (Higuchi, 1990).

The primers used in this study were the following (base changes are indicated in small letters): forward primer Y313Fa, 5'-GCAAAGCTtGTGTtT GACCAGGTTTCTGAC-3', and reverse primer Y313Fb; 5'-GTCAGAAACCT GGTCAaACACaAGCTTTGC-3'; forward primer, Y313Aa, 5'-GCAAAGCTtGT GgcTGACCAGGTTTCTGAC-3', and reverse primer, Y313Ab; 5'-GTCAGAAA CCTGGTCAgcCACaAGCTTTGC-3', forward primer, E390Aa, 5'-CCAACCG TATCGTCGctGAAGCGATGATTGCC-3', and reverse primer, E390Ab, 5'-G GCAATCATCGCTTCagCGACGATACGGTTGG-3'; forward primer, R500Ka, 5'-CCACCTGGACgTCGCCGATCaagAAATATG-3', and reverse primer, R500Kb, 5'-CATATTTcttGATCGGCGAcGTCCAGGTGG-3'; forward primer, R500Aa, 5'-CGCCACCTGGACTTCGCCGATCgcTAAATA-3', and reverse primer, R500Ab, 5'-CCATATTTAgcGATCGGCGAAGTCCAGGTG-3'; forward primer, E542Aa, 5'-CGCCGgCTCAACCGGATGGCAGcACGTGATGTT-3', and reverse primer, E542Ab, 5'-AACATCACGTgCTGCCATCCGGTTGAGcC GGCG-3'. All mutant constructs were confirmed by DNA sequencing at STAB Vida, Portugal.

Overexpression and Purification of Wild-Type RNase II and Mutants

The plasmid used for expression of wild-type *E. coli* histidine-tagged RNase II protein was pFCT6.9 plasmid (Cairrão *et al.*, 2001). This plasmid contains the *rnb* gene cloned into pET-15b vector (Novagen) under the control of φ10 promoter, allowing the expression of the His6-tagged RNase II fusion protein. All other plasmids bearing mutations were transformed into BL21(DE3) *E. coli* strain (Novagen) to allow the expression of the recombinant proteins. Cells were grown at 37 °C in 100 ml of LB medium supplemented with 150 μg/ml ampicillin to an *A*600 of 0.45 and then induced for 2 h by addition of 1 mM isopropyl 1-thio-β-D-galactopyranoside. Cell cultures were pelleted by centrifugation and stored at -80 °C. Purification of all proteins was performed by histidine affinity chromatography using HiTrap Chelating HP columns (GE Healthcare) and the AKTA fast protein liquid chromatography system (GE Healthcare) following the protocol previously described. Briefly, cell suspensions were lysed using a French press at 9000 p.s.i. in the presence of 0.1 mM phenylmethylsulfonyl fluoride. The crude extracts were treated with 150 units of Benzonase (Sigma) during 30 min to degrade the nucleic acids and clarified by a 30 min centrifugation at 10,000 *g*. The clarified extracts were then added to a HiTrap chelating-Sepharose 1 ml column equilibrated in buffer A (20 mM Tris-HCl, 0.5 M NaCl, pH 8, 20 mM imidazole and 2 mM β-mercaptoethanol). Protein elution was achieved by a continuous imidazole gradient (from 20–500 mM) in buffer A. The fractions containing the purified protein were pooled together, and buffer was exchanged to buffer B (20 mM Tris-HCl, pH 8, 100 mM KCl, and 2 mM β-mercaptoethanol) using a desalting 5 ml column (GE Healthcare). Eluted proteins were concentrated by centrifugation at 15 °C with Amicon Ultra Centrifugal Filter Devices of 30,000 molecular weight cut off (Millipore). Protein concentration was determined by spectrophotometry, and glycerol was added to the final

fractions before storage at -20 °C to a final concentration of 50 %. 0.5 μg of each purified protein was applied in a SDS-PAGE gel with 8 % of polyacrylamide 37:5:1 and visualized by Coomassie Blue staining (Figure 1C).

Activity Assays

Exoribonucleolytic activity was assayed using different RNA oligoribonucleotides as substrates (Amblar *et al.*, 2006): a poly(A) chain of 35 nt as a single-stranded substrate, a 30-mer oligoribonucleotide (5'-CC CGACACCAACCACUAAAAAAAAAAAAAA-3') annealed to the complementary 16-mer oligodeoxyribonucleotide (5'-AGTGGTTGGTGTCG GG-3') as a double-stranded substrate with a 3' single-stranded extension, and the DNA-RNA chimeric substrates Chi1 (5'-dTdTdTdTdTdT dTdTdTdTdTrCrCdTdT-3') and Chi2 (5'-dTdTdTdTdTdTdTdTdTdTdTrCdT rCdT-3'). All the oligoribonucleotides were labeled at the 5' end with [γ-^{32}ATP] and T4 polynucleotide kinase and further purified with Microcon YM-3 Centrifugal Filter Devices (Millipore) to remove the unincorporated nucleotides. The hybridization between 30-mer and 16-mer oligomers was performed in a 1:1 (mol:mol) ratio by 5 min of incubation at 68 °C followed by 45 min as room temperature. The exoribonucleolytic reactions were carried out in a final volume of 10 μl containing 30 nM concentrations of substrate, 20 mM Tris-HCl, pH 8, 100 mM KCl, 1 mM $MgCl_2$, and 1 mM dithiothreitol. The amount of each enzyme added to the reaction was adjusted to obtain linear conditions and is indicated in the respective figures (Figures 2 to 4). Reactions were started by the addition of the enzyme and incubated at 37 °C. Samples were withdrawn at the time points indicated in the figures (Figures 2 to 4), and the reaction was stopped by adding formamide-containing dye supplemented with 10 mM EDTA. Reaction products were resolved in a 20 % polyacrylamide 19:1, 7 M urea and analyzed by autoradiography. Autoradiograms were scanned, and the densities of the bands were quantified using ImageQuant 5.0 software. The exoribonucleolytic activity of the enzymes was determined

by measuring and quantifying the disappearance of the substrate from gels in several distinct experiments, and each value obtained represents the mean of at least three independent assays. The specific activity of each enzyme is given as the nmol of substrate consumed/min/nmol of protein at 37 °C. Results obtained are shown in Table 1.

Formal Kinetic Analysis

To determine the 3'-5' exoribonuclease rates of the WT and the E542A mutant, the reactions were carried out in 20 mM Tris-HCl, pH 8, 100 mM KCl, 1 mM $MgCl_2$, and 1 mM dithiothreitol using the 35 nt poly(A) RNA oligonucleotide as a substrate. Preliminary assays (not shown) showed that product formation proceeded linearly at the protein concentrations and for the incubation times used in the experiments reported here. As such, the protein activities were measured at the following substrate concentrations: 10, 25, 50, 100, 150, 200, 250 and 300 nM. The protein concentrations used were 5 pM and 0.1 fM for the WT and the E542A mutant, respectively. The reactions were carried out at 37 °C for 2 min with these protein concentrations as under these conditions less than 20 % of substrate was degraded. Reactions were stopped by adding formamide-containing dye supplemented with 10 mM EDTA. Reaction products were resolved in a 20 % polyacrylamide 19:1, 7 M urea and analyzed by autoradiography. Autoradiograms were scanned, and the densities of the bands were quantified using ImageQuant 5.0 software. The amount of product was calculated by using the original substrate concentration and the final ratio of remaining substrate and product formed. Lineweaver-Burk plots (Lineweaver and Burk, 1934) were used to estimate kinetic parameters: K_m, V_{max}, and k_{cat}. Each value obtained represents the mean of at least three independent assays, and the S.D. was calculated from these data sets.

Surface Plasmon Resonance Analysis-BIACORE

Biacore SA chips were obtained from Biacore Inc. (GE Healthcare). The flow cells of the SA streptavidin sensor chip were coated with a low concentration of the following substrates. On flow cell 1 no substrate was

added so this cell could be used as the control blank cell. On flow cell 2 a 5' biotinylated 25 nucleotide RNA oligomer (5'-CCCGACACCAACCACUAA AAAAAAA-3') was added to allow the study of the protein interaction with a single-stranded RNA molecule. On flow cell 3 a 5' biotinylated 16-nucleotide DNA oligomer (5'-AGTGGTTGGTGTCGGG-3') was added to allow the study of the protein interaction with a single-stranded DNA molecule. On flow cell 4 a 5' biotinylated 35 nucleotide poly(A) oligomer was added to allow the study of the protein interaction with a single-stranded RNA molecule composed only of adenosines. The target RNA and DNA substrates were immobilized on flow cells 2 and 3 by injecting 20 μl of a 500 nM solution of the target RNA or DNA in 1 M NaCl at a 10 μl/min flow rate as described in previous reports (Arraiano *et al.*, 2008; Park *et al.*, 2000). We obtained a response of ~400RU for the RNA substrates and 270 RU for the DNA substrate. The biosensor assay was run at 4 °C in 20 mM Tris-HCl, pH 8, 100 mM KCl, 1 mM DTT, and 25 mM EDTA. The proteins were injected over the flow cells for 2 min at concentrations of 10, 20, 30, 40, and 50 nM using a flow rate of 20 μl/min. All experiments included triple injections of each protein concentration to determine the reproducibility of the signal and control injections to assess the stability of the RNA or DNA surface during the experiment. Bound protein was removed with a 60 s wash with 2 M NaCl, which did not damage the substrate surface. Data from flow cell 1 were used to correct for refractive index changes and nonspecific binding. Rate constants and equilibrium constants were calculated using the BIA EVALUATION 3.0 software package according to the fitting model 1:1 Languimir binding.

Modeling of Wild-type RNase II and E542A Mutant

Using standard comparative modeling methods and the software DeepView (Guex and Peitsch, 1997), three-dimensional models of wild-type *E. coli* RNase II (RNB/ECOLI) and E542A mutant proteins were built up from the x-ray structure (PDB code 2IX1 (Frazão *et al.*, 2006)) of RNase II D209N mutant complexed with a 13 nt poly(A) RNA.

Molecular Dynamics (MD) Simulation of the E542A Mutant and RNase II Models Based on the 2ix1 Structure

To obtain a fine-grained theoretical model of wild-type RNase II and E542A mutant enzymes bound to a 13 nt poly(A) RNA, a 4 ns MD simulation was performed. To readjust side chains and domain conformations, the recreation was calculated using the PMEMD module of the AMBER9 package (Case *et al.*, 2004; Case *et al.*, 2005) and the *parm99* parameter set from this distribution. Dynamically stabilized 2IX1 crystal structure model of RNase II in complex with RNA described elsewhere (Barbas *et al.*, 2008) was taken into consideration for subsequent molecular dynamics trajectory analyses. The details on MD methodology applied to the models were described (Barbas *et al.*, 2008).

MD Models of the Wild-Type RNase II and E542A Mutant Proteins Bound to RNA

Theoretical models of RNase II wild-type and E542A mutant enzymes bound to a 13 nt poly(A)RNA were, respectively, built up from an energy-minimized average structure of the stabilized molecular dynamics simulation of the x-ray structure of RNase II D209N mutant complexed with a 13 nt poly(A) RNA (PDB code 2IX1 (Frazão *et al.*, 2006)), previously published (Barbas *et al.*, 2008). To obtain biophysically consistent models, 4 ns MD simulations were performed with each model. Calculations were done by using the PMEMD module and the *parm99* parameter set in the AMBER9 package (Case *et al.*, 2005; Case *et al.*, 2006; Pearlman *et al.*, 1995). MD simulations of both RNase II systems included the four RNase II domains (CSD1, CSD2, RNB, and S1), the RNA molecule, and the magnesium atom of the active center reported in the real structure of D209N mutant. To neutralize the electrostatic charge of the system, Na^+ counterions were placed in a shell around the system using a grid of coulombic potentials. Electrostatically neutralized complexes where then embedded in a truncated octahedron solvation

box, keeping a distance of 12 Å between the limits of the box and the closest atom of the solute. Both counterions and solvent were added using the LEAP module in AMBER9. Initial relaxation of each complex was completed by performing 10,000 steps of energy minimization with a cut off of 10.0 Å. Initial heating and equilibration were performed simultaneously by raising the temperature in two stages; a first one from 0 to 5 K to induce a slow adaptation of the system to the force field represented in parm99 and a second up to 298 K in 200 ps continuous heating phases. During this procedure stage velocities were reassigned at each new temperature according to the Maxwell-Boltzmann distribution, and positions of the Cα and P atoms of the solute were constrained with a force constant of 20 Kcal.mol^{-1} to impede spurious disorganizations of protein and RNA backbone structures. During the last 100 ps of the equilibration phase of the MD, the force constant was reduced stepwise down to 0 for all constrained atoms to progressively allow the stabilization of the system. Consecutively, a MD simulation of 4 ns over the complete systems was completed.

RESULTS

Comparing the Exoribonucleolytic Activity of the Different Mutant Proteins

E. coli RNase II is the prototype of the RNase II superfamily of exoribonucleases, and this protein has shown to be a good study model for all family members, as they share a similar mode of action (Barbas *et al.*, 2008; Lorentzen *et al.*, 2008; Schaeffer *et al.*, 2009; Schneider *et al.*, 2007; Wang *et al.*, 2007). To better understand the reaction mechanism of *E. coli* RNase II and the processes underlying the specificity of RNA cleavage, we constructed a set of single-, double-, and triple-mutants of RNase II and studied their effect in RNA binding and in catalytic activity. We introduced the following point mutations in RNase II: Y313F, Y313A, E390A, R500A, R500K, and E542A, the double mutations D201N/Y313F,

D201N/E390A, and Y313F/E390A, and the triple mutation D201N/Y313F/E390A. All these mutant proteins were introduced in *E. coli* BL21(DE3) and were overproduced by IPTG induction. The optimal induction conditions were standardized for each mutant by analysis of protein production and solubility at different times of IPTG treatment. All the mutants were shown to be more than 80% soluble after induction, except for R500K, which was mainly in the insoluble fraction (data not shown). All mutant proteins, with the exception of R500K were, purified (Figure 1C) as described under "Experimental Procedures." The exoribonucleolytic activity of the purified mutant proteins was analyzed and compared with the wild-type by performing activity assays using two different types of RNA substrates as described under "Experimental Procedures."

As previously demonstrated, the wild-type enzyme was able to degrade the single-stranded RNA substrate, and the end-product was a 4 nt fragment (Amblar *et al.*, 2007; Barbas *et al.*, 2008) (Figure 2). With the R500A mutant the shortest product observed was a 11 nt, even with 1000 nM of protein concentration after a 30 min reaction. The double-mutant D201N/Y313F was only able to degrade a few nucleotides in the conditions tested (1000 nM concentration of protein in a 30 min reaction). Previous reports had shown that D201N mutant accumulated a 10 –11 nt fragment as a major degradation product, although longer reaction times resulted in the usual 4 nt fragment as a secondary product (Barbas *et al.*, 2008). This is probably because of a higher dissociation rate of RNA fragments shorter than 11 nt. A similar behaviour was also observed for the double D201N/E390A and triple D201N/Y313F/E390A mutants, which confirm the important role played by Asp201 in the RNase II activity. Y313F, Y313A, Y313F/E390A, and E542A generated a 4 nt fragment like wild-type RNase II (Figure 2). In the conditions tested (1 nM concentrations of protein in a 10 min reaction), the E390A mutant was able to degrade the substrate until it reached a 6 nt fragment (Figure 2). However, in more extreme conditions (*i.e.* longer reaction times and/or

higher enzyme concentrations) the mutant was also able to reach the typical final end-product of 4 nt (data no shown).

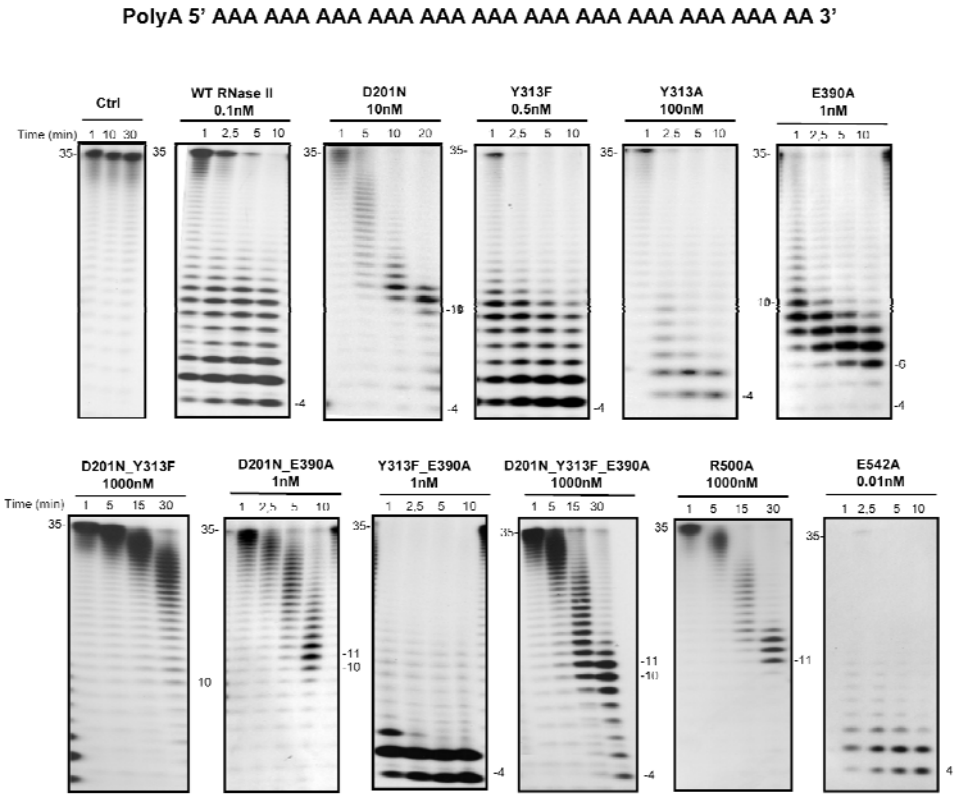

FIGURE 2. Exoribonuclease activity with single-stranded RNA substrate; comparison of wild-type and mutant proteins. Activity assays were performed as described under "Experimental Procedures" using a poly(A) chain of 35 nt as substrate. The mutants used and their respective protein concentrations are shown. The wild-type enzyme was used as control. Samples were taken during the reaction at the time points indicated, and reaction products were analyzed in a 20 % polyacrylamide 19:1, 7 M urea gel. Control reactions with no enzyme added (*Ctrl*) were incubated at the maximum reaction time for each protein. Length of substrates and degradation products are indicated in the figure.

When the substrate tested was a double-stranded molecule with a 3' single-stranded extension (16–30ds), the wild-type enzyme degraded the single-stranded portion, generating 23–25-nt oligomers (Amblar *et al.*, 2006). This shows that the enzyme stalls 7–9 nt before reaching the double-stranded region (Amblar *et al.*, 2006; Amblar *et al.*, 2007) (Figure 3). Similarly, most of the mutant enzymes rendered products ranging between 21 and 25 nt in length behaving like the wild-type does against secondary structures. The D201N, D201N/E390A, and R500A mutants, however, generated longer products than the wild-type, with 26–27 nt in length. The E542A mutant was able to go closer to the double-stranded portion of the RNA, rendering a 19 nt product. The exoribonucleolytic activity of wild-type and mutant enzymes was determined by measuring the substrate disappearance from the activity gels (Table 1). The results obtained suggested that although fully conserved in all domains of life, Glu390 is not essential for RNase II catalysis because the activity of E390A was very similar to that of the wild-type enzyme (0.30 and 0.36 $nmol.min^{-1}.nmol^{-1}$ for the wild-type and E390A mutant, respectively) (Table 1). In the case of Tyr313, its substitution by Phe did not alter the enzymatic activity, whereas its replacement by an Ala resulted in a 100 fold reduction (Table 1). These observations imply that the aromatic moiety of Tyr313, but not the hydroxyl group, is important for the maintenance of the enzymatic activity. Accordingly, the exoribonucleolytic activity of the double-mutant Y313F/E390A was not affected by the presence of the two mutations simultaneously (Table 1). As previously reported, the activity of D201N was highly impaired (only 0.2 % of the activity of wild-type enzyme), confirming the importance of this residue in RNase II activity (Barbas *et al.*, 2008). This effect was also reflected in the D201N/Y313F and the D201N/Y313F/E390A mutants, which showed less than 0.1 % of the activity present in the wild-type (Table 1). However, the D201N mutation did not have such a pronounced effect on the activity of the double-mutant D201N/E390A, which had a very similar specific activity to the wild-type (0.30 and 0.31 $nmol.min^{-1}.nmol^{-1}$ for the

wild-type and D201N/E390A double-mutant, respectively) (Table 1). This mutant was able to degrade the poly(A) substrate in a very processive manner until generating the 10 nt oligomer, as does the wild-type enzyme. However, further degradation of this 10 nt oligomer into shorter products seemed to occur with much more difficulty, and higher concentrations of enzyme were required to generate the typical 4 nt product. One explanation for the results obtained is the possible reconstitution of the catalytic site around the Mg^{2+} atom and the D201N, induced by the E390A mutation. The electrostatic environment in the catalytic center and in the cleft has to be preserved for the enzyme to continue to function; as such, an uncertain number of casual rearrangements might have taken place.

TABLE 1. Specific exoribonucleolytic activity of wild-type and mutant enzymes Exoribonucleolytic activity was assayed using a 35 nt poly(A) chain as substrate. Activity assays were performed in triplicate as described under "Experimental Procedures." Each value represents nmol of substrate oligoribonucleotide consumed per min and per nmol of protein, and the exoribonucleolytic activity of the wild-type enzyme was taken as 100 %.

Protein	Protein Activity *nmol min^{-1} $nmol^{-1}$*	Relative Activity *%*
wt RNase II	0.30 ± 0.04	100
Y313F	0.35 ± 0.04	117
Y313A	<0.01	1
E390A	0.36 ± 0.03	120
D201N	<0.01	0.2
D201N/Y313F	<0.01	<0.1
D201N/E390A	0.31 ± 0.06	103
Y313F/E390A	0.33 ± 0.01	110
D210N/Y313F/E390A	<<0.01	<<0.1
E542A	33.75 ± 3.90	11,250
R500A	<<0.01	<<0.1

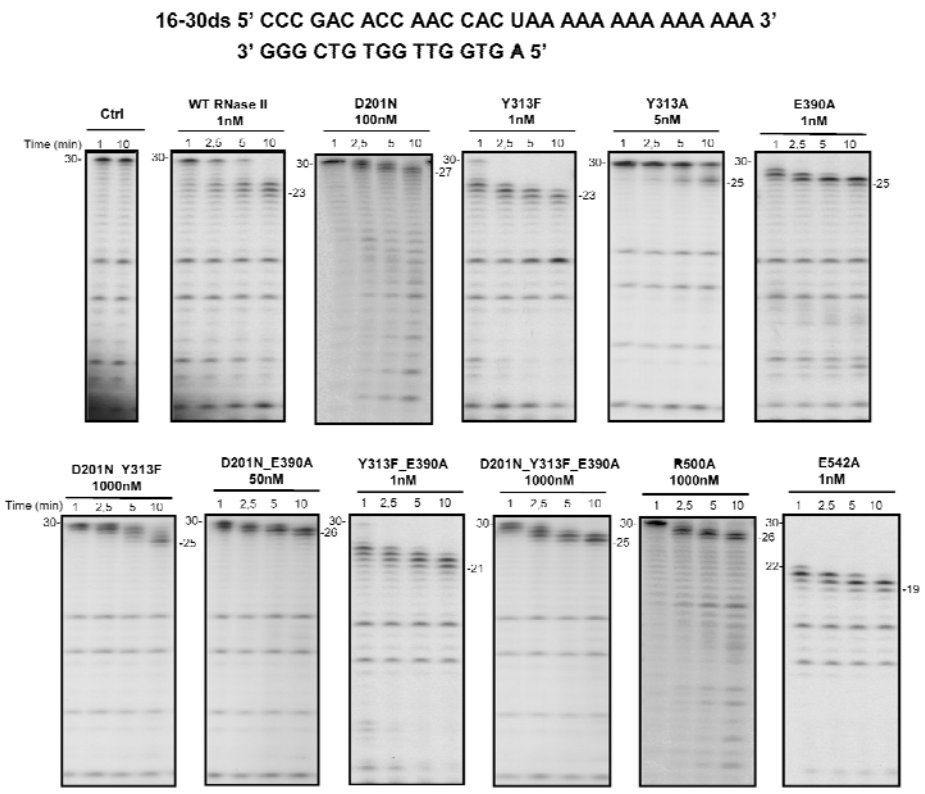

FIGURE 3. Exoribonuclease activity with ds16–30 substrate; comparison of wild-type and mutant proteins. Activity assays were performed as described under "Experimental Procedures" using a 30-mer oligoribonucleotide hybridized to the complementary 16-mer oligodeoxyribonucleotide, thus obtaining the corresponding double-stranded substrate 16–30ds. The mutants used and their respective protein concentrations are shown. The wild-type enzyme was used as control. Samples were taken during the reaction at the time points indicated, and reaction products were analyzed in a 20 % polyacrylamide 19:1, 7 M urea gel. Control reactions with no enzyme added (*Ctrl*) were incubated at the maximum reaction time for each protein. Length of substrates and degradation products are indicated in the figure.

The Arg500 residue seems to be very important for the RNase II activity, as the R500A mutant showed more than a 40,000 fold reduction in activity when compared with the wild-type ($7.0x10^{-6}$ *versus* 0.30 $nmol.min^{-1}.nmol^{-1}$) (Table 1). In fact, the side chain of this residue interacts with the phosphate backbone of the two nucleotides at the 3' end of the RNA molecule, and it was postulated to assist in catalysis by fixing the phosphodiester bond at the cleavage position and enhancing the susceptibility of the leaving phosphorous atom to a nucleophilic attack (Frazão *et al.*, 2006). Its substitution by Ala would, therefore, prevent such an interaction, resulting in the inactivation of the enzyme.

Finally, the substitution of the Glu542 by Ala rendered a mutant version of the RNase II that was much more active than the wild-type enzyme, with more than a 100 fold increase in the exoribonucleolytic activity. This residue is in close proximity to the leaving nucleotide and was suggested to facilitate the elimination of this nucleotide upon phosphor-ester cleavage by pulling it out of the base-stacked position (Frazão *et al.*, 2006). The elimination of the cleaved nucleotide from the catalytic cavity is essential for the enzymatic process to continue, and an alanine residue in this position seems to facilitate this process even more.

Determination of RNA Dissociation Constants (K_D) by Surface Plasmon Resonance Analysis

To determine the contribution of each residue in RNA binding, we calculated the dissociation constants (K_D) of the wild-type and the mutant proteins by surface plasmon resonance analysis with Biacore 2000 using two different single-stranded RNA substrates as described under "Experimental Procedures." The results obtained are presented in Table 2. The dissociation constants for the 25-mer single-stranded RNA substrate of the wild-type RNase II and D201N enzymes were previously determined (6.5 ± 0.4 and 11.4 ± 0.7 nM, respectively) (Barbas *et al.*, 2008). When assaying the 25-mer single-stranded RNA substrate, almost all the mutant proteins tested in this work showed K_D values similar to that of the wild-type enzyme, except for the E542A mutant. This mutant enzyme

presented a significant increase in RNA binding affinity with a much lower K_D value when compared with the wild-type (0.5 ± 0.08 *versus* 6.5 ± 0.4 nM) (Table 2). When a poly(A) substrate was used almost all enzymes showed a moderate reduction on K_D values, indicating a higher affinity for this substrate. When compared with the wild-type, most of the mutant enzymes showed no significant differences in K_D values except for the triple mutant, which showed a 9 fold reduction in poly(A) binding affinity. Once more, the E542A mutant presented a significant increase in RNA affinity for poly(A), with a ~20 fold higher K_D value when compared with that of the wild-type (Table 2). The same result was obtained by electrophoretic mobility shift assay, with this mutant showing RNA-protein complex formation at much lower protein concentration than wild-type enzyme (Supplementary Figure S1). This means that the high level of activity of this mutant is, at least in part, because of a higher RNA binding affinity than the wild-type.

TABLE 2. RNA binding affinity of wild-type and mutant enzymes The dissociation constants (K_D) were determined by SPR using the 25 nt RNA oligomer (5' Biotin-CCCGACACCAACCACUAAAAAAAAA-3') and 35 nt poly(A) RNA oligomer.

Proteins	25mer ssRNA		Poly(A) ssRNA	
	K_D *nM*	Relative K_D	K_D *nM*	Relative K_D
RNase II WT	6.5 ± 0.4	1.0	1.3 ± 0.4	1.0
D201N	11.4 ± 0.7	1.8	1.1 ± 0.1	0.8
Y313F	12.9 ± 2.4	2.0	4.4 ± 0.1	3.4
Y313A	17.1 ± 0.8	2.6	4.2 ± 0.7	3.2
E390A	8.7 ± 1.4	1.3	2.3 ± 0.4	1.8
D201N/Y313F	3.4 ± 0.3	0.5	4.4 ± 0.6	3.4
D201N/E390A	17.8 ± 1.7	2.7	1.6 ± 0.1	1.2
Y313F/E390A	7.3 ± 0.3	1,1	6.0 ± 0.7	4.6
D201N/Y313F/E390A	22.1 ± 7.2	3.4	12.0 ± 2.9	9.2
R500A	10.9 ± 1.2	1.7	3.3 ± 0.6	2.5
E542A	0.5 ± 0.08	0.1	0.06 ± 0.005	0.05

Kinetic Analyses of Wild-Type and E542A Mutant

Given the extraordinary properties of the E542A mutant, we wanted to better characterize its catalytic properties. With this aim, we performed a kinetic analysis of this E542A mutant and the wild-type enzyme and determined their kinetic parameters. The experiments were carried out using the poly(A) RNA substrate as described under "Experimental Procedures." The results obtained were plotted, and the reaction proceeded according to a Michaelis-Menten equation, as indicated by linearity in the Lineweaver-Burk plots (Lineweaver and Burk, 1934) (data not shown). From this plot we determined the kinetic parameters, V_{max}, K_m, and k_{cat} for the wild-type and the E542A mutant, which are presented in Table 3. The K_m values obtained were 1.25 ± 0.17 μM for the wild-type and 0.30 ± 0.05 μM for E542A (Table 3), suggesting that the E542A mutation significantly increased the affinity of RNase II enzyme for the poly(A) substrate and confirming the data obtained from the K_D values. In addition, the k_{cat} value of the E542A mutant was also much higher than that of the wild-type (~200,000 fold), thus giving a final k_{cat}/K_m ratio of ~1,000,000 fold higher in the E542A mutant than in the wild-type (Table 3). All these data explain why the E542A mutant is much more efficient in catalysis than the wild-type enzyme, confirming that, in fact, substitution of Glu542 by Ala resulted in a "super-enzyme".

TABLE 3. 3'-5'-Exoribonuclease kinetic constants of wild-type and E542A mutant enzymes The exoribonuclease rates were measured at different substrate concentrations using a 35 nt poly(A) chain as substrate, as indicated under "Experimental Procedures."

Proteins	V_{max} $\mu M.s^{-1}$	K_m μM	k_{cat} s^{-1}	k_{cat}/K_m $\mu M^{-1}s^{-1}$
RNase II WT	0.25 ± 0.02	1.25 ± 0.17	0.41 ± 0.01	0.23 ± 0.06
E542A	(1.14 ± 0.48) x 10^4	0.30 ± 0.05	(8.08 ± 0.84) x 10^4	(2.36 ± 0.38) x 10^5

Can the Discrimination of RNA Versus DNA by RNase II Be Dictated by Three Conserved Residues?

It was previously described that residues Asp201, Tyr313, and Glu390 are involved in ribose binding (Frazão *et al.*, 2006); therefore, they are probably important for the specificity of RNA cleavage. Particularly and starting from the 3' end of the RNA molecule, Tyr313 and Asp201 interact with the O2' ribose oxygen of the second nucleotide, and Glu390 interacts with the O2' ribose oxygen of the fourth nucleotide (Figure 1B). To determine the role of these residues in the discrimination of RNA *versus* DNA, the activity of these mutants was assayed using two different 15 nt chimeric DNA-RNA oligomers. In the first chimeric substrate (Chi1), the 3rd and 4th positions from the 3' end are occupied by ribonucleotides (rC) and the other 13 are deoxyribonucleotides (dT) (5'-dTdTdTdTdTdTdTdTdTdTrCrCdTdT-3'), whereas in the second substrate (Chi2) the ribonucleotides are located in the 2nd and 4th positions from the 3' end (5'-dTdTdTdTdTdTdTdTdTdTrCdTrCdT-3'). Our data showed that RNase II is only able to cleave DNA bases when having a ribose in the 2nd or the 4th positions. The results demonstrate that, with the Chi1 substrate, wild-type RNase II was only able to cleave three nucleotides, rendering a final degradation product of 12 nt (Figure 4A). After the first cleavage event the RNA translocates, and the riboses now occupy the 2nd and 3rd positions. Because one of the riboses is still in the 2nd position, cleavage can pursue. The riboses then move to positions 1 and 2, and cleavage is still allowed. Finally, once there is only one ribose present, in the 1st position, cleavage halts. This explains why after three cleavage events the 12 nt fragment is released. With the Chi2 substrate only one cleavage event occurred with wild-type RNase II, converting the 15-mer into a 14-mer oligonucleotide (Figure 4B and Supplementary Figure S2). After this first and unique cleavage event, the RNA translocates, the two riboses then occupy the 1st and the 3rd positions, and the enzyme is not able to continue degradation. Therefore, RNase II has a strict requirement for a

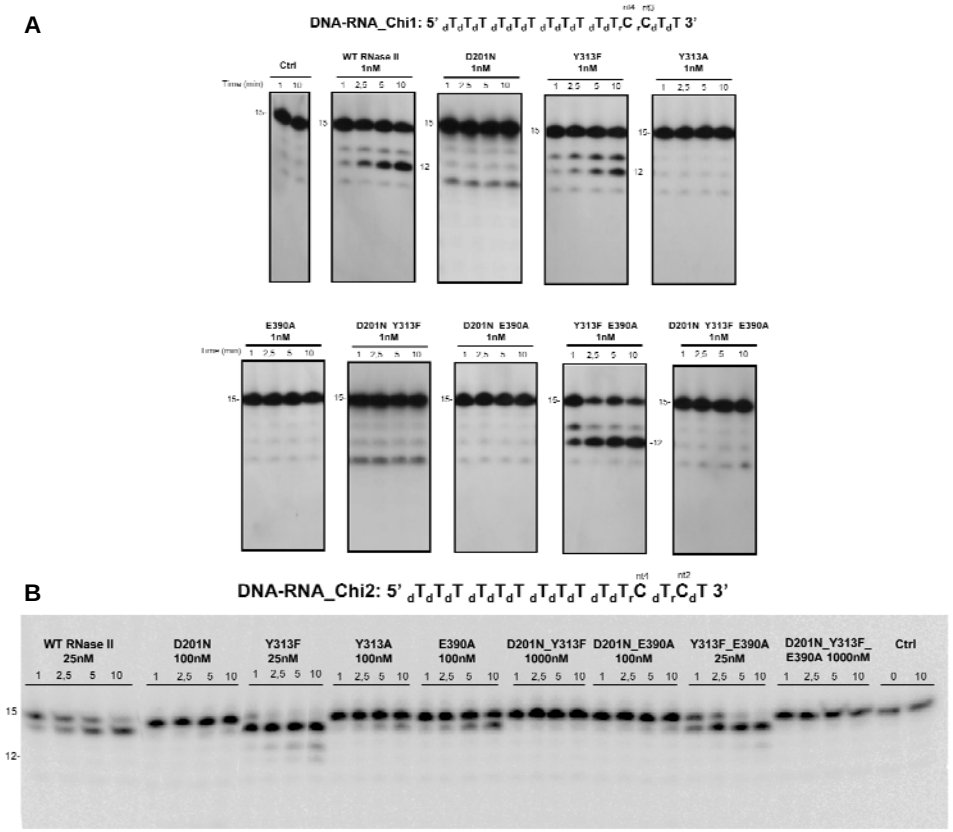

FIGURE 4. Exoribonuclease activity with DNA-RNA chimeric substrates; comparison of wild-type and mutant proteins. Activity assays were performed using two 15-mer chimeric substrates as described under "Experimental Procedures." ***A.*** activity assays with Chi 1 were the 3rd and 4th positions from the 3' end are occupied by ribonucleotides (rC), and the other 13 are deoxyribonucleotides (dT). ***B.*** activity assays with Chi2 were the 2nd and 4th positions from the 3' end are occupied by ribonucleotides, and the other 13 are deoxyribonucleotides. The mutants used and their respective protein concentrations are shown. The wild-type enzyme was used as control. Samples were taken during the reaction at the time points indicated, and reaction products were analyzed in a 20 % polyacrylamide 19:1, 7 M urea gel. Control reactions with no enzyme added (*Ctrl*) were incubated at the maximum reaction time for each protein. Length of substrates and degradation products are indicated in the figure.

ribose in the second and/or the fourth nucleotides from the 3' end of the molecule and not in other positions, as previously described (Cannistraro and Kennell, 2001). This fact confirms that the specific contacts observed in the RNase II structure with the O2' oxygen at these positions are essential for RNase II activity.

The substitution of the Asp201 by Asn inhibited the degradation activity with both DNA-RNA substrates used (Figure 4). However, this mutant has also been shown to be highly inactive in degradation of a poly(A) RNA substrate (with 0.2 % of the wild-type activity) because of the role of Asp201 in Mg^{2+} coordination (Barbas *et al.*, 2008; Frazão *et al.*, 2006) (Figure 2 and Table 1). Its role as an Mg^{2+} ligand at the active site of RNase II is so critical for the activity of the enzyme that we are unable to see the actual contribution of this residue in the interaction with the second ribose. The E390A mutant presented similar degradation efficiency over an RNA substrate, like that of the wild-type. However, this mutant was not able to degrade the Chi1 DNA-RNA substrate (Figure 4A). The substitution of Glu390 by Ala, which probably prevents the interaction with the 4th ribose, abolished the activity, confirming that the presence of a ribonucleotide in the 3rd position cannot support activity. With the Chi2 substrate, the E390A behaved like the wild-type, although with less efficiency (Figure 4B). Therefore, it seems that the single establishment of contacts with the ribose of 2nd nucleotide is enough to support catalysis to a certain extent. The importance of contacts between protein residues and the ribose of the 2nd nucleotide of the substrate for RNA recognition and cleavage was confirmed by mutations introduced in Tyr313. Based on the crystal structure, the side chain of this residue is hydrogen-bonded to the O2' oxygen of ribose of the 2nd nucleotide. Its substitution by Ala prevented the degradation of the Chi1 substrate, and the ability of the enzyme to degrade the Chi2 substrate was highly reduced, even at high protein concentrations (Figure 4). This reduction seems to be similar to that observed with the poly(A) RNA substrate (Table 1). However, Y313F was shown to be highly active in degradation of both

chimeric substrates (Figure 4), even more active than the wild-type over the Chi2. Furthermore, with this second substrate, Y313F was able to perform more than one cleavage event, behaviour that was also observed in the Y313F/E390A double mutant (Figure 4B and Supplementary Figure S2). Therefore, it seems that the absence of the side-chain hydroxyl group in Phe313 could favour the degradation of certain substrates. The presence of a Phe instead of a Tyr may induce a local rearrangement of the nucleotides and/or the protein residues at the catalytic cavity, thus allowing the establishment of new contacts with a ribose in the 3rd or the 1st positions of the substrate. Such contacts, which are not present in the wild-type, allow the enzyme to proceed in degradation of the Chi2 substrate even in the absence of the canonical interactions with the 2nd or the 4th riboses.

Determination of DNA Dissociation Constants (K_D) by Surface Plasmon Resonance Analysis

We wanted to explore the effect of these residues, Asp201, Tyr313, and Glu390, in general DNA binding affinity. For this purpose we determined the K_D values by surface plasmon resonance using a DNA substrate. The results obtained (Table 4) showed that all mutants tested have a similar DNA affinity as the wild-type, with the exceptions of E390A and Y313A derivatives, which showed a ~9 fold and a 100 fold reduction, respectively (Table 4). These results confirm that the contacts of Tyr313 and Glu390 with the 2nd and 4th riboses are important not only for catalysis but also for a proper substrate binding at the catalytic cavity in the absence of the canonical interactions. Our data indicate that inside the cavity the unique specific contacts for ribose established by RNase II are those with the 2nd and 4th nucleotides from the 3' end of the RNA molecule. Moreover, these contacts are necessary and sufficient for cleavage to occur, and therefore, they seem to be responsible for the RNA specificity *versus* DNA in RNase II.

TABLE 4. DNA binding affinity of wild-type and mutant enzymes The dissociation constants (K_D) were determined by SPR using 16 nt DNA oligomer (5' Biotin-AGTGGTTGGTGTCGGG-3').

Proteins	16mer ssDNA	
	K_D *nM*	Relative K_D
RNase II WT	8.7 ± 0.7	1.0
D201N	15.9 ± 2.4	1.8
Y313F	6.9 ± 0.3	0.8
Y313A	>>100	>>100
E390A	75.7 ± 8.8	8.7
D201N/Y313F	6.4 ± 0.5	0.7
D201N/E390A	12.8 ± 2	1.5
Y313F/E390A	12.0 ± 0.4	1.4
D201N/Y313F/E390A	10.7 ± 0.3	1.2
R500A	14.2 ± 0.2	1.6
E542A	6.1 ± 0.3	0.7

DISCUSSION

E. coli RNase II is the model of the RNase II-family of enzymes, whose homologues are present in all three domains of life (Andrade *et al.*, 2009; Grossman and van Hoof, 2006; Mian, 1997; Mitchell *et al.*, 1997; Zuo and Deutscher, 2001). The resolution of the structure of *E. coli* RNase II in the RNA-free and bound complex constituted a significant breakthrough (Frazão *et al.*, 2006; Zuo *et al.*, 2006). The structural study together with biochemical analysis helped to explain certain aspects of the enzyme activity and led to the proposal of a model for RNA degradation by RNase II that can be extrapolated to other family members (Barbas *et al.*, 2008; Dziembowski *et al.*, 2007; Frazão *et al.*, 2006; Schaeffer *et al.*, 2009; Schneider *et al.*, 2007). However, some essential features remain unknown.

The structure of the D209N mutant complexed with a 13 nt poly(A) oligomer revealed specific contacts of several residues at the active site with the RNA oligomer, with most of these residues being highly

conserved in RNase II-like enzymes of all domains of life (Barbas *et al.*, 2008; Frazão *et al.*, 2006). To identify the specific role of these amino acids and verify their precise function in RNase II activity, we introduced several single, double, and triple mutations in residues Asp201, Tyr313, Glu390, Arg500, and Glu542 and studied the exoribonucleolytic activity and substrate binding ability of the corresponding mutant proteins.

The results obtained in this report revealed that, except for the Glu542, none of the residues analyzed is crucial for RNA binding, as only slight differences in RNA binding affinity (K_D values) were observed upon mutation (Table 2). However, the Glu542 residue is very important in the prevention of the binding to the substrate, as its substitution by an Ala causes the protein to bind RNA more tightly than the wild-type enzyme. Moreover, our data demonstrate that, among the residues mutated in this study, Arg500 plays a central role in catalysis. The R500A mutation practically inactivated the enzyme, although the protein was still able to bind RNA efficiently. A similar result had previously been obtained when mutating the conserved Asp209 into an Asn (Amblar and Arraiano, 2005; Barbas *et al.*, 2008). Comparable results were obtained with the double-mutant D201N/Y313F and the triple-mutant D201N/Y313F/E390A, which also have their activities highly impaired.

The results obtained with R500A support the essential role of this residue in assisting catalysis (Frazão *et al.*, 2006). Arg500 has been described as interacting with the phosphate backbone of the two nucleotides at the 3' end of the substrate (Figure 1B). It was suggested that the role of Arg500 could be to fix the phosphodiester bond at the cleavage position, enhancing the susceptibility of the phosphorous atom of the leaving nucleotide to a nucleophilic attack. To confirm our experimental results, we performed a computational model of the putative binding mode of a 13 nt poly(A) RNA fragment to RNase II wild-type enzyme based on the x-ray structure of RNase II D209N-RNA-bound complex (Frazão *et al.*, 2006). The model obtained gave us precious information about the interactions established between the RNA substrate and protein residues and helped

to clarify certain aspects (Figure 5A). For instance, the computational model predicts that in the wild-type enzyme, the guanidinium group in the Arg500 residue would contact directly with the phosphate of nt 2 from the 3' end, stabilizing its position. This conformation keeps the enzyme catalytically competent and allows the outgoing nucleotide to remain coordinated with the magnesium atom and the rest of the active center elements. Thus, the model shows that changes in this position could induce an extensive reorganization of the region that would turn the enzyme catalytically incompetent, which correlates with the experimental results obtained for mutant R500A and confirms the hypothesis previously postulated (Frazão *et al.*, 2006).

The RNase II structure showed that Tyr313, Asp201, and Glu390 hydrogen-bonded with the O2' ribose oxygen of two nucleotides in the RNA molecule (Figure 1B). Because this oxygen is absent in a deoxyribose, the three residues were postulated to be involved in RNA discrimination *versus* DNA.

Previous studies showed that Asp201 residue was very important for RNase II activity but not for substrate binding (Barbas *et al.*, 2008). In this report we performed new experiments with the previously constructed D201N mutant, and we demonstrated that this mutant enzyme was unable to degrade DNA-RNA chimeras. The computational model performed in this report helped to explain all experimental data obtained with the D201N mutant, showing that different groups of the aspartate participate in different contacts. The carboxylic of its side chain coordinates the Mg^{2+} ion that is essential for catalysis, and therefore, its substitution by asparagine led to the loss of activity. However, interaction with the O2' ribose is mediated by polar contacts with the carbonyl oxygen in the backbone trace, indicating that any other residue could account for such interaction as long as the substrate and protein residue conformation is conserved. Therefore, although the actual contribution of Asp201 to the RNA cleavage specificity cannot be deciphered with the D201N mutant because of its inactivation, computational model confirms

the postulated contact between this residue and the 2nd ribose of the RNA molecule. According to our results Tyr313 and Glu390 seemed to be two essential contacts that RNase II establishes with the ribose of the substrate, demonstrating that these residues are responsible for the RNA cleavage specificity.

Substitution of Glu390 by Ala caused a significant loss of activity over the chimeric substrates but did not affect degradation of a RNA molecule. The model predicts polar contacts between the ribose 2' OH and the carbonyl oxygens of the glutamic acid. This means that its replacement by Ala should not destabilize the interaction. However, Glu390 is also involved in polar contacts with neighbouring arginine residues through its side chain. Therefore, E390A mutation will probably induce local conformational changes that may prevent the hydrogen bond formation between Ala (smaller residue than Glu) and the second ribose oxygen. The loss of this interaction would have a drastic effect in degradation of the chimeric substrate, where other canonical interactions may not be occurring. In the case of Tyr313, our experimental results suggested that its aromatic moiety but not its hydroxyl group is crucial for activity and for RNA specificity of RNase II, as the Y313A but not Y313F mutation produced a drastic reduction of RNA and DNA-RNA substrate degradation efficiency. In fact, the computational modelling predicts contacts between the Tyr313 aromatic ring and the OH of the ribose, but the hydroxyl group of the Tyr313 does not participate in such interactions, confirming this hypothesis. In addition, our results demonstrate that the contact with Tyr313 (or Phe) is critical for the degradation of DNA-RNA chimeric substrate and that this single contact is able to support catalysis of DNA bases. Therefore, the presence of a ribose in positions 2 or 4 from the 3' end of the nucleic acid is the unique requirement for RNase II to perform degradation. RNA specificity shown by this ribonuclease resides in these two positions and interaction with Tyr313 and Glu390.

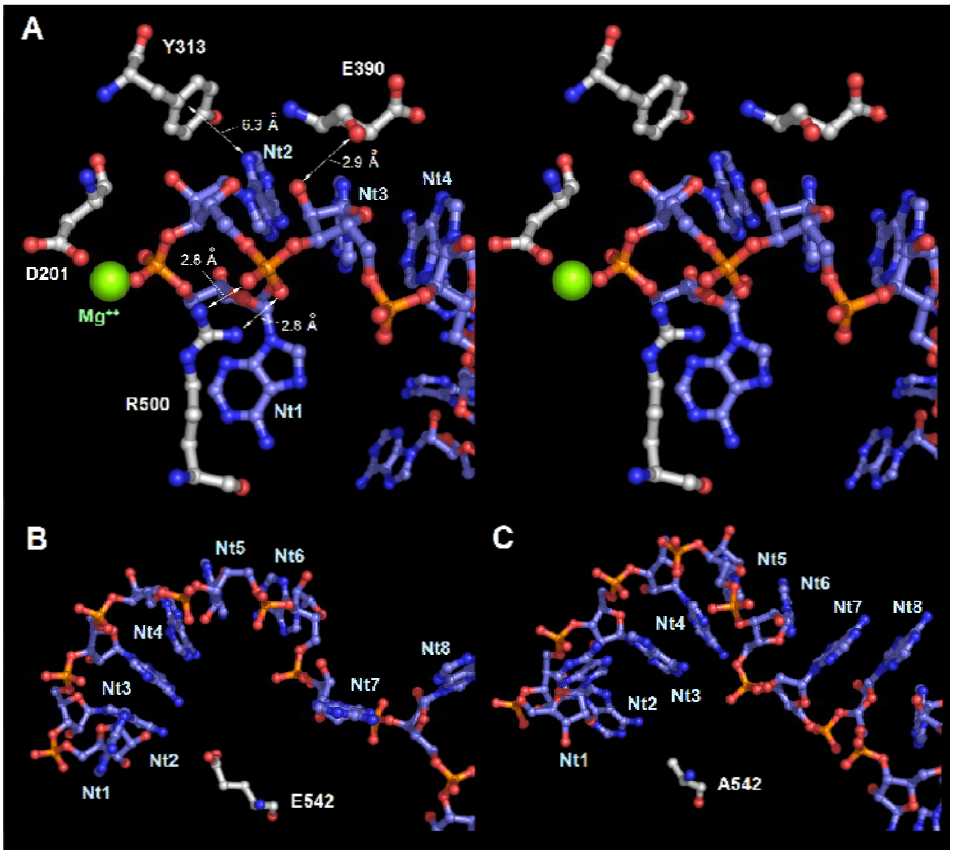

FIGURE 5. Modelling of RNase II and E542A mutant proteins in RNA-bound conformations. To obtain biophysically consistent models, minimal energy average structures of both models were obtained from stabilized trajectories of 4 ns molecular dynamics. Figures in sticks were depicted with Pymol© (DeLano Scientific LLC, San Carlos, CA). ***A.*** stereo diagram of wild-type protein active center showing Glu390, Tyr313, Arg500, and Asp201 residues from the RNB domain. Significant polar contacts distances and relative positions of Mg^{2+} atom and outgoing RNA nucleotides (nt 1) are also represented. Hydrogen bonding between the Glu390 backbone trace carbonyl oxygen and nt 3 ribose 2' OH group could be responsible for RNA *versus* DNA recognition. Mutation to alanine would have introduced soft changes in local RNB conformation that could affect RNA discrimination in chimeric substrates. The guanidinium phosphate-hydrogen-bonding network between Arg500 and nt 2 would essentially result in stabilizing the catalytic complex while keeping the outgoing nucleotide conformation correct.

Catalytic competence of mutant R500A would result in being completely abolished. Long range hydrogen-π facial interactions between nucleotide nt 12 and Tyr313 or Phe313 mutant aromatic side chains could contribute to avoiding harmful interactions in the active center during procession and/or catalysis. ***B*** and ***C.*** Modeled conformations of the poly(A) RNA strand in the RNB domain procession cleft in the wild-type and Ala542 mutant RNase II proteins, respectively. As depicted in *B*, after 4 ns of MD simulation, the RNB domain of RNase II Ala542 mutant could be able to deploy 6 stacked nucleotides (from nt 8 to 2) in progression, ready for cleavage. As shown in *C*, the same region in the wild-type model could only allocate 4 nucleotides (from nt 5 to 2) simultaneously in the cleft during a catalytic event. Substitution in position 542 of the negatively charged glutamic side chain for the smaller neutral methyl group of alanine could significantly reduce both electrostatic and steric surfaces in the RNA-binding interface.

Finally, Glu542 was shown to play a very important function in RNase II. The carboxylic group of this glutamate is in close proximity to the nitrogen atoms of the leaving nucleotide, and the establishment of one or more hydrogen-bonds between them could facilitate the elimination of this nucleotide after cleavage, thus allowing the degradation process to continue. Thus, Glu542 seemed to be very important for the degradation to occur. Our experimental results demonstrate that its substitution by Ala resulted in a 110 fold increase in RNA degradation efficiency compared to the wild-type enzyme (Table 1) and a 10–20 fold increase in RNA affinity (Table 2). Moreover, the kinetic data suggest that this mutant not only has a much higher affinity for the poly(A) RNA substrate but also presents a much higher catalytic rate, confirming its role in the catalytic event. Such intriguing results led us to perform computational modelling with the E542A mutant enzyme with the RNA bound and compared it with the model of the wild-type. The model predicts that substitution of the negatively charged glutamic acid side chain for a short quasi-apolar alanine residue seems to induce a subtle conformational change in the

Cα backbone of the RNB domain itself that leads to a reorganization of its RNA binding interface (Figure 5B). Comparing the E542A mutant and wild-type models in this region (Figure 5B), the RNA bound to E542A mutant shows that nucleotides in positions ranging from 2 to 8 are set out in a stable stacked conformation. In comparison, the wild-type model presents only nucleotides 2–6 in a similar conformation. The efficiency of E542A mutant to deploy 50% more residues within the catalytic domain in the model could determine an increased capability of binding the RNA substrate by the RNB domain during catalysis than the RNase II wild-type. In addition, the higher degree of organization and density of packing of the nucleotide chain in the E542A mutant could favour the RNA translocation upon cleavage, leading to higher degradation efficiency. These two aspects together may, therefore, be responsible for the high enzymatic activity experimentally determined of this mutant.

The results we present in this study substantially improve the RNase II model for RNA degradation. We have identified the residues that are responsible for the discrimination of cleavage of RNA *versus* DNA, which are fully conserved in all domains of life. We also show that the Arg500 residue, present in RNase II active site, is crucial for activity but not for RNA binding. Finally, we report a very interesting mutant that acts as a "super-enzyme", in which the substitution of Glu542 by Ala leads to an outstanding catalytic efficiency, because of the high increase of both the exoribonucleolytic activity and substrate binding.

Because Rrp44/Dis3 protein (an RNase II homologue) is the only catalytically active nuclease in the exosome, the understanding of the degradation mechanism will have a large impact in future studies of the exosome. Moreover, the recent determination of the structure of yeast Rrp44 showed that *E. coli* RNase II is a good study model (Lorentzen *et al.*, 2008; Wang *et al.*, 2007). Also, yeast Rrp44/Dis3 has a similar linear arrangement of domains in the sequence when compared with *E. coli* RNase II. Both proteins share a high degree of identity as their conservation is the highest at the active site. This suggests that these two

exoribonucleases share a similar hydrolytic mechanism (Lorentzen *et al.*, 2008). As such, the results from this report on RNase II mutants can be extrapolated for the comprehension of the mode of action of other members of the RNase II-family.

ACKNOWLEDGMENTS

We thank Ambro Van-Hoof for critical reading. We also thank to Biomol-Informatics SL for bioinformatics consulting. Ana Barbas is a recipient of a post-doctoral fellowship from the Fundação para a Ciência e Tecnologia, Portugal, and Rute G. Matos is a recipient of a Ph.D. fellowship from the Fundação para a Ciência e Tecnologia, Portugal. The work was supported by Ministerio de Educación y Ciencia, Spain, Grant SAF2007-61926, an institutional grant from the "Fundación Ramón Arecesm," and by Fundação para a Ciência e Tecnologia, Portugal.

SUPPLEMENTARY INFORMATION

Supplementary methods

Electrophoretic Mobility Shift Assay (EMSA)

EMSA were performed with a poly(A) chain of 35 nt RNA oligomer as described previously (Amblar *et al.*, 2006; Arraiano *et al.*, 2008). Briefly, after substrate labelling described at Experimental Procedures, binding reactions were performed in 10 µl of volume containing 20 mM Tris-HCl pH8, 100 mM KCl, 1 mM DTT, 0.5 µg/µl BSA and 10 mM EDTA, 1 fmol of substrate and increasing concentration of enzyme. Mixtures containing increasing concentration of each enzyme were incubated for 10 min at 37 ºC and then subjected to UV crosslinking (600 mJ, 10 min, 254 nm) at 4 ºC. The samples were analyzed in a 10 % nondenaturing polyacrylamide 19:1 gel, and the RNA-protein complexes were detected by using the phosphorImager system from Molecular Dynamics

Supplementary figures

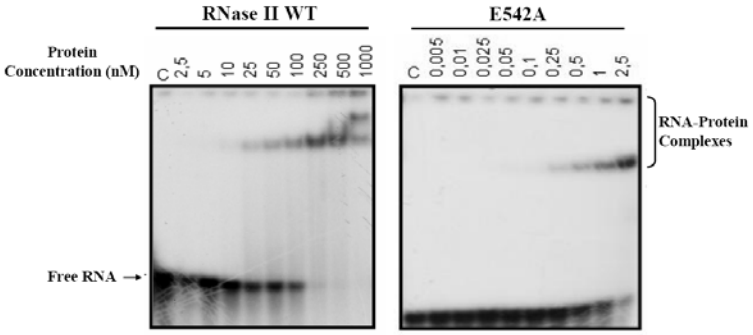

SUPPLEMENTARY FIGURE S1. Comparison of RNA binding ability of RNase II wt and E542A mutant. 10,000 cpms of polyA 35 nt were incubated under the conditions described above. The enzyme concentrations used are indicated in the Figure. A control reaction without enzyme added was performed (C).

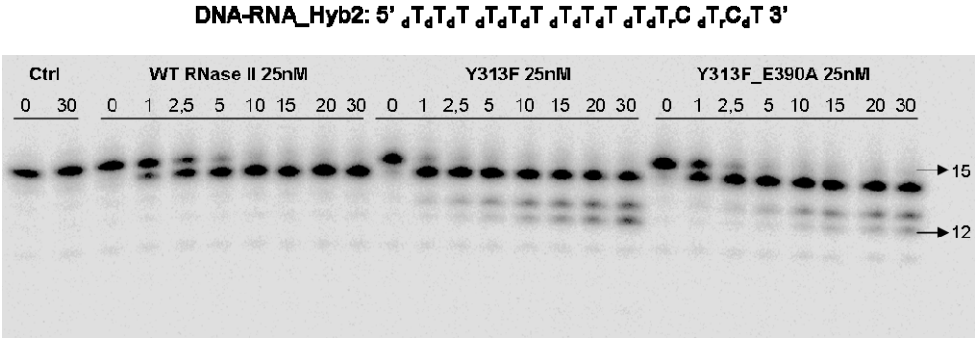

SUPPLEMENTARY FIGURE S2. Exoribonuclease activity with DNA-RNA Chimera2 substrate: comparison of wild-type and mutants. Activity assays were performed as described under "Experimental Procedures" using a 15-mer chimeric substrate Chi2 were the 2nd and 4th positions from the 3' end are occupied by ribonucleotides, and the other 13 are deoxiribonucleotides. The mutants used and their respective protein concentrations are shown. The wild-type enzyme was used as control. Samples were taken during the reaction at the time points indicated, and reaction products were analyzed in a 20 % polyacrylamide19:1/7 M urea gel. Control reactions with no enzyme added (*Ctrl*) were incubated at the maximum reaction time for each protein. Length of substrates and degradation products are indicated in the figure.

REFERENCES

Amblar, M., and Arraiano, C.M. (2005) A single mutation in *Escherichia coli* ribonuclease II inactivates the enzyme without affecting RNA binding. *FEBS J* **272**: 363-374.

Amblar, M., Barbas, A., Fialho, A.M., and Arraiano, C.M. (2006) Characterization of the functional domains of *Escherichia coli* RNase II. *J Mol Biol* **360**: 921-933.

Amblar, M., Barbas, A., Goméz-Puertas, P., and Arraiano, C.M. (2007) The role of the S1 domain in exoribonucleolytic activity: substrate specificity and multimerization. *RNA* **13**: 317-327.

Andrade, J.M., Cairrão, F., and Arraiano, C.M. (2006) RNase R affects gene expression in stationary phase: regulation of ompA. *Mol Microbiol* **60**: 219-228.

Andrade, J.M., Pobre, V., Silva, I.J., Domingues, S., and Arraiano, C.M. (2009) The role of 3'-5' exoribonucleases in RNA degradation. *Prog Mol Biol Transl Sci* **85**: 187-229.

Arraiano, C.M., Barbas, A., and Amblar, M. (2008) Characterizing ribonucleases in vitro examples of synergies between biochemical and structural analysis. *Methods Enzymol* **447**: 131-160.

Barbas, A., Matos, R.G., Amblar, M., Lopez-Viñas, E., Goméz-Puertas, P., and Arraiano, C.M. (2008) New insights into the mechanism of RNA degradation by ribonuclease II: identification of the residue responsible for setting the RNase II end product. *J Biol Chem* **283**: 13070-13076.

Cairrão, F., Chora, A., Zilhão, R., Carpousis, A.J., and Arraiano, C.M. (2001) RNase II levels change according to the growth conditions: characterization of *gmr*, a new *Escherichia coli* gene involved in the modulation of RNase II. *Mol Microbiol* **39**: 1550-1561.

Cairrão, F., Cruz, A., Mori, H., and Arraiano, C.M. (2003) Cold shock induction of RNase R and its role in the maturation of the quality control mediator SsrA/tmRNA. *Mol Microbiol* **50**: 1349-1360.

Cairrão, F., and Arraiano, C.M. (2006) The role of endoribonucleases in the regulation of RNase R. *Biochem Biophys Res Commun* **343**: 731-737.

Cannistraro, V.J., and Kennell, D. (1994) The processive reaction mechanism of ribonuclease II. *J Mol Biol* **243**: 930-943.

Cannistraro, V.J., and Kennell, D. (2001) *Escherichia coli* ribonuclease II. *Methods Enzymol* **342**: 309-330.

Case, D.A., T.A. Darden, T.E. Cheatham, r., C.L. Simmerling, J. Wang, R.E. Duke, R. Luo, K.M. Merz, D.A. Pearlman, M. Crowley, R.C. Walker, W. Zhang, B. Wang, S. Hayik, A. Roitberg, G. Seabra, K.F. Wong, F. Paesani, X. Wu, S. Brozell, V. Tsui, H. Gohlke, L. Yang, C. Tan, J. Mongan, V. Hornak, G.

Cui, P. Beroza, D.H. Mathews, C. Schafmeister, W.S. Ross, and Kollman, P.A. (2004) AMBER 8. *University of California, San Francisco.* .

Case, D.A., Cheatham, T.E., 3rd, Darden, T., Gohlke, H., Luo, R., Merz, K.M., Jr., Onufriev, A., Simmerling, C., Wang, B., and Woods, R.J. (2005) The Amber biomolecular simulation programs. *J Comput Chem* **26**: 1668-1688.

Case, D.A., T.A. Darden, T.E. Cheatham, r., C.L. Simmerling, J. Wang, R.E. Duke, R. Luo, K.M. Merz, D.A. Pearlman, M. Crowley, R.C. Walker, W. Zhang, B. Wang, S. Hayik, A. Roitberg, G. Seabra, K.F. Wong, F. Paesani, X. Wu, S. Brozell, V. Tsui, H. Gohlke, L. Yang, C. Tan, J. Mongan, V. Hornak, G. Cui, P. Beroza, D.H. Mathews, C. Schafmeister, W.S. Ross, and Kollman, P.A. (2006) AMBER 9. *University of California, San Francisco.* .

Cheng, Z.F., Zuo, Y., Li, Z., Rudd, K.E., and Deutscher, M.P. (1998) The *vacB* gene required for virulence in *Shigella flexneri* and *Escherichia coli* encodes the exoribonuclease RNase R. *J Biol Chem* **273**: 14077-14080.

Cheng, Z.F., and Deutscher, M.P. (2005) An important role for RNase R in mRNA decay. *Mol Cell* **17**: 313-318.

Coburn, G.A., and Mackie, G.A. (1996) Overexpression, purification, and properties of *Escherichia coli* ribonuclease II. *J Biol Chem* **271**: 1048-1053.

Deutscher, M.P., and Reuven, N.B. (1991) Enzymatic basis for hydrolytic versus phosphorolytic mRNA degradation in *Escherichia coli* and *Bacillus subtilis*. *Proc Natl Acad Sci U S A* **88**: 3277-3280.

Dziembowski, A., Lorentzen, E., Conti, E., and Seraphin, B. (2007) A single subunit, Dis3, is essentially responsible for yeast exosome core activity. *Nat Struct Mol Biol* **14**: 15-22.

Frazão, C., McVey, C.E., Amblar, M., Barbas, A., Vonrhein, C., Arraiano, C.M., and Carrondo, M.A. (2006) Unravelling the dynamics of RNA degradation by ribonuclease II and its RNA-bound complex. *Nature* **443**: 110-114.

Grossman, D., and van Hoof, A. (2006) RNase II structure completes group portrait of 3' exoribonucleases. *Nat Struct Mol Biol* **13**: 760-761.

Guex, N., and Peitsch, M.C. (1997) SWISS-MODEL and the Swiss-PdbViewer: an environment for comparative protein modeling. *Electrophoresis* **18**: 2714-2723.

Gupta, R.S., Kasai, T., and Schlessinger, D. (1977) Purification and some novel properties of *Escherichia coli* RNase II. *J Biol Chem* **252**: 8945-8949.

Higuchi, R. (1990) Recombinant PCR. *In PCR Protocols. A Guide to Methods and Applications (Innis, M. A., Gelfand, D. H., Sninsky, J. J. & White, T. J., eds.), pp. 177-183. Academic Press, Inc. Harcourt Brace Jovanovich, Publishers, San Diego.*

Lebreton, A., Tomecki, R., Dziembowski, A., and Seraphin, B. (2008) Endonucleolytic RNA cleavage by a eukaryotic exosome. *Nature* **456**: 993-996.

Lineweaver, H., and Burk, D. (1934) The Determination of Enzyme Dissociation Constants. *Journal of the American Chemical Society* **56**: 658–666.

Liu, Q., Greimann, J.C., and Lima, C.D. (2006) Reconstitution, activities, and structure of the eukaryotic RNA exosome. *Cell* **127**: 1223-1237.

Lorentzen, E., Basquin, J., Tomecki, R., Dziembowski, A., and Conti, E. (2008) Structure of the active subunit of the yeast exosome core, Rrp44: diverse modes of substrate recruitment in the RNase II nuclease family. *Mol Cell* **29**: 717-728.

Marujo, P.E., Hajnsdorf, E., Le Derout, J., Andrade, R., Arraiano, C.M., and Régnier, P. (2000) RNase II removes the oligo(A) tails that destabilize the rpsO mRNA of *Escherichia coli*. *RNA* **6**: 1185-1193.

McLaren, R.S., Newbury, S.F., Dance, G.S., Causton, H.C., and Higgins, C.F. (1991) mRNA degradation by processive 3'-5' exoribonucleases *in vitro* and the implications for prokaryotic mRNA decay in vivo. *J Mol Biol* **221**: 81-95.

McVey, C.E., Amblar, M., Barbas, A., Cairrão, F., Coelho, R., Romão, C., Arraiano, C.M., Carrondo, M.A., and Frazão, C. (2006) Expression, purification, crystallization and preliminary diffraction data characterization of *Escherichia coli* ribonuclease II (RNase II). *Acta Crystallogr Sect F Struct Biol Cryst Commun* **62**: 684-687.

Mian, I.S. (1997) Comparative sequence analysis of ribonucleases HII, III, II PH and D. *Nucleic Acids Res* **25**: 3187-3195.

Mitchell, P., Petfalski, E., Shevchenko, A., Mann, M., and Tollervey, D. (1997) The exosome: a conserved eukaryotic RNA processing complex containing multiple 3'-->5' exoribonucleases. *Cell* **91**: 457-466.

Park, S., Myszka, D.G., Yu, M., Littler, S.J., and Laird-Offringa, I.A. (2000) HuD RNA recognition motifs play distinct roles in the formation of a stable complex with AU-rich RNA. *Mol Cell Biol* **20**: 4765-4772.

Pearlman, D.A., Case, D.A., Caldwell, J.W., Ross, W.S., Cheatham, T.E., DeBolt, S., Ferguson, D., Seibel, G., and Kollman, P. (1995) AMBER, a package of computer programs for applying molecular mechanics, normal mode analysis, molecular dynamics and free energy calculations to simulate the structural and energetic properties of molecules. *Computer Physics Communications* **91**: 1-41.

Schaeffer, D., Tsanova, B., Barbas, A., Reis, F.P., Dastidar, E.G., Sanchez-Rotunno, M., Arraiano, C.M., and van Hoof, A. (2009) The exosome contains domains with specific endoribonuclease, exoribonuclease and cytoplasmic mRNA decay activities. *Nat Struct Mol Biol* **16**: 56-62.

Schneider, C., Anderson, J.T., and Tollervey, D. (2007) The exosome subunit Rrp44 plays a direct role in RNA substrate recognition. *Mol Cell* **27**: 324-331.

Studier, F.W., and Moffatt, B.A. (1986) Use of bacteriophage T7 RNA polymerase to direct selective high-level expression of cloned genes. *J Mol Biol* **189**: 113-130.

Taylor, R.G., Walker, D.C., and McInnes, R.R. (1993) *E. coli* host strains significantly affect the quality of small scale plasmid DNA preparations used for sequencing. *Nucleic Acids Res* **21**: 1677-1678.

Wang, H.W., Wang, J., Ding, F., Callahan, K., Bratkowski, M.A., Butler, J.S., Nogales, E., and Ke, A. (2007) Architecture of the yeast Rrp44 exosome complex suggests routes of RNA recruitment for 3' end processing. *Proc Natl Acad Sci U S A* **104**: 16844-16849.

Zilhão, R., Camelo, L., and Arraiano, C.M. (1993) DNA sequencing and expression of the gene rnb encoding *Escherichia coli* ribonuclease II. *Mol Microbiol* **8**: 43-51.

Zilhão, R., Cairrão, F., Régnier, P., and Arraiano, C.M. (1996) PNPase modulates RNase II expression in *Escherichia coli*: implications for mRNA decay and cell metabolism. *Mol Microbiol* **20**: 1033-1042.

Zuo, Y., and Deutscher, M.P. (2001) Exoribonuclease superfamilies: structural analysis and phylogenetic distribution. *Nucleic Acids Res* **29**: 1017-1026.

Zuo, Y., Vincent, H.A., Zhang, J., Wang, Y., Deutscher, M.P., and Malhotra, A. (2006) Structural basis for processivity and single-strand specificity of RNase II. *Mol Cell* **24**: 149-156.

Chapter 3

RNase R Mutants Elucidate the Catalysis of Structured RNA: *RNA-Binding Domains Select the RNA Targeted for Degradation*

This chapter contains data published in:

Matos, R. G., Barbas, A. and Arraiano, C.M. 2009. RNase R Mutants Elucidate the Catalysis of Structured RNA: RNA-Binding Domains Select the RNA Targeted for Degradation. Biochemical Journal **423**: 291-301.

The author of this dissertation is the first author of the published manuscript.

Abstract

The RNase II superfamily is a ubiquitous family of exoribonucleases that are essential for RNA metabolism. RNase II and RNase R degrade RNA in the 3' to 5' direction in a processive and sequence-independent manner. However, although RNase R is capable of degrading highly structured RNA, the RNase II activity is impaired by the presence of secondary structures. RNase II and RNase R share structural properties and have a similar modular domain organization. The eukaryotic RNase II homologue, Rrp44/Dis3, is the catalytic subunit of the exosome, one of the most important protein complexes involved in the maintenance of the correct levels of cellular RNA. In the present study, we constructed truncated RNase II and RNase R proteins and point mutants and characterized them regarding their exoribonucleolytic activity and RNA binding ability. We report that Asp280 is crucial for RNase R activity without affecting RNA binding. When Tyr324 was changed to alanine, the final product changed from 2 to 5 nt in length, showing that this residue is responsible for setting the end-product. We have shown that the RNB domain of RNase II has catalytic activity. The most striking result is that the RNase R RNB domain itself degrades double-stranded substrates even in the absence of a 3' overhang. Moreover, we have demonstrated for the first time that the substrate recognition of RNase R depends on the RNA-binding domains that target the degradation of RNA that are 'tagged' by a 3' tail. These results can have important implications for the study of poly(A)-dependent RNA degradation mechanisms.

Introduction

Escherichia coli RNase II is the prototype of the RNase II superfamily of exoribonucleases. Homologues of RNase II/R are present in all domains of life (Grossman and van Hoof, 2006; Mian, 1997; Mitchell *et al.*, 1997; Zuo and Deutscher, 2001). RNase R is a member of this family that is involved in mRNA degradation, in RNA and protein quality control and has been shown to be required for virulence (Andrade *et al.*, 2006; Cairrão *et al.*, 2003; Cairrão and Arraiano, 2006; Cheng *et al.*, 1998; Cheng and Deutscher, 2005). In the nucleus and cytoplasm of eukaryotic cells, the RNase II homologue Rrp44/Dis3 is a subunit of the exosome, an essential multiprotein complex involved in the processing, turnover and quality control of different types of RNA (Mitchell *et al.*, 1997). Rrp44/Dis3 is the only catalytically active nuclease in the yeast core exosome (Dziembowski *et al.*, 2007), and it was shown recently that it has both exo- and endoribonuclease activities (Lebreton *et al.*, 2008; Schaeffer *et al.*, 2009).

RNase II and RNase R share catalytic properties: they both degrade RNA processively, in the 3' to 5' direction releasing 5' nucleoside monophosphates. These enzymes also share structural properties, including 60 % sequence similarity (Cheng and Deutscher, 2002). Their activity is sequence-independent, but whereas RNase II is sensitive to secondary structures, RNase R is capable of degrading highly structured RNA (Amblar *et al.*, 2006; Andrade *et al.*, 2006; Cheng and Deutscher, 2002, 2005). Another difference is that the final degradation product of RNase II is a 4 nt fragment, whereas the end-product of RNase R is a 2 nt fragment (Amblar *et al.*, 2006; Amblar *et al.*, 2007; Cannistraro and Kennell, 1994).

RNase R is a 92 kDa protein encoded by the *rnr* gene. It is involved in the degradation of different types of RNA, such as rRNA, sRNA (small non-coding RNA) and mRNA. It was shown that RNase R has *in vivo* affinity for polyadenylated RNA and that it can be a key enzyme involved in poly(A) metabolism (Andrade and Arraiano, 2008). RNase R is the only known 3'

to 5' exoribonuclease able to degrade double-stranded RNA without the aid of helicase activity (Andrade *et al.*, 2009). It is a cold-shock protein that is regulated transcriptionally and post-transcriptionally (Cairrão *et al.*, 2003; Cairrão and Arraiano, 2006). The activity of RNase R is modulated according to the growth conditions of the cell (Cairrão *et al.*, 2001), and its levels increase in stationary phase and under stress conditions (Andrade *et al.*, 2006; Cairrão *et al.*, 2003; Cheng and Deutscher, 2005). It has been shown that this protein is also involved in pathogenesis in different micro-organisms (Cheng *et al.*, 1998; Erova *et al.*, 2008; Tobe *et al.*, 1992; Tsao *et al.*, 2009).

RNase II is a 72 kDa protein encoded by the *rnb* gene. In *E. coli*, this protein is the major hydrolytic enzyme that is responsible for 90 % of the exoribonucleolytic activity in crude extracts (Deutscher and Reuven, 1991). RNase II expression is differentially regulated at the transcriptional and post-transcriptional levels, and the protein can be regulated by the environmental conditions (Cairrão *et al.*, 2001; Zilhão *et al.*, 1993; Zilhão *et al.*, 1996). The determination of the three-dimensional structure of *E. coli* RNase II showed that RNase II consists of four domains: two N-terminal CSD (cold-shock domains) (CSD1 and CSD2), one central RNB catalytic domain, and one C-terminal S1 domain (Frazão *et al.*, 2006; Zuo *et al.*, 2006) (Figure 1). Structural and biochemical analysis helped to explain the activity of the enzyme and led to the proposal of a model for RNA degradation by RNase II. RNA contacts RNase II in two different and non-contiguous regions: the anchoring (formed by the RNA-binding domains) and the catalytic (buried inside the RNB domain) regions (Cannistraro and Kennell, 1994; Frazão *et al.*, 2006). The shortest RNA substrate able to retain contacts with these two regions is a 10 nt fragment, and it was known that this was the minimum size necessary to maintain the processivity of the enzyme (Barbas *et al.*, 2008; Cannistraro and Kennell, 1994; Frazão *et al.*, 2006). It was demonstrated that Tyr313 and Glu390 are important to the discrimination of cleavage of RNA compared with DNA (Barbas *et al.*, 2009). During the determination of

key residues for catalysis, we have recently discovered that the substitution of alanine for Glu542 leads to a 100 fold increase in the exoribonucleolytic activity, turning RNase II into a "super-enzyme" (Barbas *et al.*, 2009).

The structure of the RNA-bound complex led to the explanation of why a 4 nt fragment is the final degradation product for RNase II (Frazão *et al.*, 2006). This is a result of the tight packing of the five 3' terminal nucleotides in the catalytic cavity, mediated by the aromatic residues Tyr253 and Phe358 (Frazão *et al.*, 2006). It was reported that the highly conserved Tyr253 is the residue responsible for setting the end-product of RNase II and it is extremely important for the maintenance of the RNA "clamping" in the catalytic site of RNase II (Barbas *et al.*, 2008).

The structural model of *E. coli* RNaseR protein was constructed on the basis of the RNase II structure; the two enzymes share a common three-dimensional arrangement, with all the critical residues for exoribonucleolytic activity being located in equivalent spatial positions (Barbas *et al.*, 2008). By comparing the protein models, it was noteworthy that these two proteins have a common arrangement of the "clamping" tyrosine residue, but, in contrast, the presence of Phe358 is exclusive to RNase II. RNase R protein presents a phenylalanine residue in the immediate downstream position (Phe429), perhaps with a similar functionality in fixing the RNA. The differences in the equivalent Phe358 in RNase II and RNase R could explain their differences in regard to RNA degradation (Barbas *et al.*, 2008).

It was also shown that the conserved Asp209 is directly involved in RNA cleavage by RNase II. This is the only critical aspartate residue for RNase II activity (Amblar and Arraiano, 2005; Barbas *et al.*, 2008) and its replacement by asparagine was responsible for the total loss of protein activity without affecting its RNA binding ability (Amblar and Arraiano, 2005). Moreover, a similar mutation in the yeast RNase II homologue Rrp44/Dis3 (D551N) totally abolished activity without reducing substrate binding. This mutation was also responsible for a very strong growth

defect, suggesting that the phenotype of this mutant is very important for yeast physiology (Dziembowski *et al.*, 2007; Schneider *et al.*, 2007).

In the present study, we constructed and analysed the equivalent mutants to Y253A and D209N of *E. coli* RNase II in RNase R, Y324A and D280N respectively. Our aim was to confirm their importance in the activity of the enzymes of the RNase II-family. We observed that the D280N mutant has no activity, but is still able to bind RNA efficiently, which confirms the importance of this aspartate residue in catalysis. When Tyr324 was changed into an alanine, we verified that the final product of RNase R changed from 2 to 5 nt, confirming the importance of this residue in setting the end-product in this family of enzymes.

Furthermore, we constructed a set of truncated proteins of RNase R lacking CSD and/or S1 domains in order to understand the contribution of each domain (Figure 1). We analysed the activity and the binding ability of the truncated proteins using different substrates and observed that the RNB domain of RNase R alone is capable of degrading RNA molecules. In addition, we show that this domain is sufficient for the degradation of structured substrates, and that is also able to bind to RNA, although with less efficiency when compared with the wild-type protein. We also observed that the CSD and S1 domains are responsible for the binding of the proteins to the substrate and that they are crucial for the recognition of which substrates are targeted to be degraded. In the absence of both of these domains, the protein is capable of degrading perfect double-stranded RNA that lack the 3' end overhang. To date, it had always been reported that the existence of a 3' end overhang of at least 5 nt in length for RNase R was essential for catalysis to occur; in the present study, we have unravelled why.

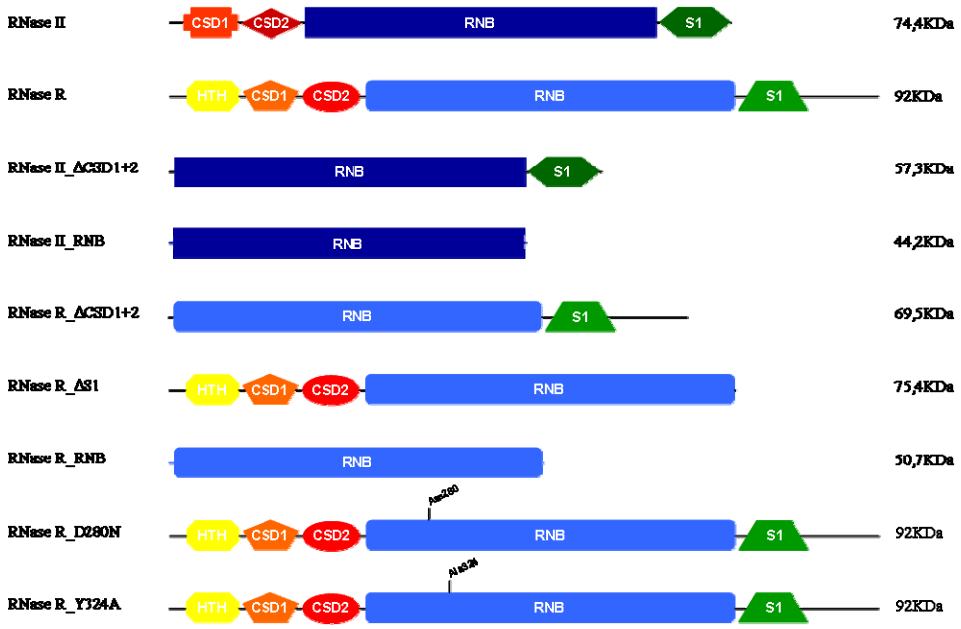

FIGURE 1. Linear representation of the domains of wild-type RNase II, RNase R and its derivative proteins

Experimental Procedures

Materials

Restriction enzymes, T4 DNA ligase, Pfu DNA polymerase and T4 polynucleotide kinase were purchased from Fermentas. Unlabelled oligonucleotide primers were synthesized by STAB VIDA.

Strains

The *E. coli* strains used were DH5α (F' *fhuA2*Δ(*argF-lacZ)U169 phoA glnV44* Φ*80* Δ(*lacZ)M15 gyrA96 recA1 relA1 endA1 thi-1 hsdR17*a) (Taylor *et al.*, 1993) for cloning experiments and BL21(DE3) (F^- rB^- mB^- *gal ompT* (*int*::*PlacUV5 T7 gen1 imm21 nin5*) (Studier and Moffatt, 1986) for expression and purification of enzymes.

TABLE 1. Plasmids used in the present study

Plasmid	Relevant characteristic	Reference
pFCT6.1	gene *rnb* cloned into pET15b, Amp^R	Cairrão *et al.*, 2001
pABA-RNR	gene *rnr* cloned into pET15b, Amp^R	Amblar *et al.*, 2007
pABA-RNR_D280N	Expresses RNase R where the Asp280 was changed by an Asn	The present study
pABA-RNR_Y324A	Expresses RNase R where the Tyr324 was changed by an Ala	The present study
pFCT_XhoI521	pFCT6.1 with a *Xho*I restriction site in position 521 of *rnb* gene	The present study
pABA-RNR_NdeI549	pABA-RNR with a *Nde*I restriction site in position 549 of *rnr* gene	The present study
pFCT_ΔCSD	Expresses RNase II lacking CSD1 and CSD2 domains	The present study
pFCT_RNB	Expresses RNase II lacking CSD1, CSD2 and S1 domains	The present study
pABA-RNR_ΔCSD	Expresses RNase R lacking HTH, CSD1 and CSD2 domains	The present study
pABA-RNR_ΔS1	Expresses RNase R lacking S1 domain	The present study
pABA-RNR_RNB	Expresses RNase R lacking HTH, CSD1, CSD2 and S1 domains	The present study

Construction of RNase R Mutants by Overlapping PCR

The point mutations D280N and Y324A were introduced into pABA-RNR (Table 1) by overlapping PCR. The primers used in the construction of RNase R mutants were Asp280Asn_Fw, Asp280Asn_Rev, Tyr324Ala_Fw and Tyr324Ala_Rev (Table 2). All mutant constructs were confirmed by DNA sequencing at STAB VIDA.

Construction of Truncated Proteins

The truncated proteins were constructed by removing different regions of *rnb* and *rnr* genes in pFCT6.1 and pABA-RNR plasmids (Table 1). An XhoI restriction site was introduced into pFCT6.1 in the position 512 by overlapping PCR using the primers pFCT_XhoI512_Fw and pFCT_XhoI521_Rev (Table 2) originating the pFCT_XhoI521 plasmid. The natural occurrence of an XhoI recognition site at position 69 allowed us to construct pFCT_ΔCSD by digesting the plasmid pFCT_XhoI521 with

XhoI (producing cleavage products of 6955 and 456 bp, with the latter corresponding to CSD1 and CSD2 of RNase II) and circularizing the fragment of 6955 bp. The protein RNase II_RNB was constructed by introduction of a stop codon (TAA) at position 1735 in the plasmid pFCT_ΔCSD using the primers RNB_Stop1735_Fw and RNB_Stop1735_Rev (Table 2).

In the pABA-RNR plasmid (Table 1) an NdeI restriction site was introduced at position 549 by overlapping PCR using the primers RNR_NdeI549_Fw and RNR_NdeI549_Rev (Table 2) creating the pABA-RNR_NdeI549 plasmid. The natural occurrence of an NdeI recognition site at position 60 allowed us to construct pABA-RNR_ΔCSD by digesting the plasmid pABA-RNR_NdeI549 with NdeI [producing cleavage products of 7624 and 651 bp, with the latter corresponding to HTH (helix–turn–helix), CSD1 and CSD2 of RNase R] and circularizing the fragment of 7624 bp. The proteins RNR_ΔS1 and pABA-RNR_RNB were constructed by introduction of a stop codon (TAA) at position 1927 in the plasmids pABA-RNR and pABA-RNR_ΔCSD respectively, using the primers RNR_Stop1927_Fw and RNR_Stop1927_Rev (Table 2).

Overexpression and Purification of Wild-type RNase II, RNase R and RNase II and RNase R Mutants

The plasmid used for expression of wild-type *E. coli* His6-tagged RNase II protein was pFCT6.1 plasmid (Cairrão *et al.*, 2001) (Table 1). This plasmid contains the *rnb* gene cloned into pET-15b vector (Novagen) under the control of φ10 promoter, allowing the expression of the His6-tagged RNase II fusion protein. The plasmid used for expression of wild-type *E. coli* His6-tagged RNase R protein was pABA-RNR plasmid (Amblar *et al.*, 2007) (Table 1) that contains the *rnr* gene cloned into pET15b vector (Novagen) under the control of φ10 promoter, allowing the expression of the His6-tagged RNase R fusion protein.

All plasmids were transformed into BL21(DE3) *E. coli* strain (Novagen) to allow the expression of the recombinant proteins. Cells were grown at 30

TABLE 2. Primers used in the present study Bases underlined indicate restriction endonuclease sites. Bases in bold indicate amino acid changes

Primer	Sequence (5' → 3')[ab]	Purpose
Asp280Asn_Fw	5'-CGCCCGGGACTTT **A**ACGATGC-3'	Introduces D280N mutation into pABA-RNR
Asp280Asn_Rev	5'-GCATCGT**T**AAAGTC CCGGGCG-3'	Introduces D280N mutation into pABA-RNR
Tyr324Ala_Fw	5'-CCGTGGGACGTCGGTG**GC** CTTCCCTTCGC-3'	Introduces Y324A mutation into pABA-RNR
Tyr324Ala_Rev	5'-GCGAAGGGAAG**GC**CACC GACGTCCCACGG-3'	Introduces Y324A mutation into pABA-RNR
pFCT_XhoI512_Fw	5'-CATCACTTTTGGT**CT**CGA**G** CACTTTGTACCGT-3'	Introduces XhoI restriction site into pFCT6.1 at the position 512
pFCT_XhoI521_Rev	5'-ACGGTACAAAGTG**C**TCG **AG**ACCAAAAGTGATG-3'	Introduces XhoI restriction site into pFCT6.1 at the position 512
RNB_Stop1735_Fw	5'-GCCGGG**TAA**GACA CGCGTTTCGC-3'	Introduces stop codon into pFCT6.1 at the position 1735
RNB_Stop1735_Rev	5'-GCGAAACGCGT GTC**TTA**CCCGGC-3'	Introduces stop codon into pFCT6.1 at the position 1735
RNR_NdeI549_Fw	5'-GTCGAAGTGCTGGGC GAC**C**ATATGGGCACC-3'	Introduces NdeI restriction site into pABA-RNR at the position 549
RNR_NdeI549_Rev	5'-GGTGCC**C**ATAT**G**GTCG CCCAGCACTTCGAC-3'	Introduces NdeI restriction site into pABA-RNR at the position 549
RNR_Stop1927_Fw	5'-GTGTGACTTCATGCT CGACCAG**TA**AGG-3'	Introduces stop codon into pABA-RNR at the position 1927
RNR_Stop1927_Rev	5'-CCT**TA**CTGGTCGAG CATGAAGTCACAC-3'	Introduces stop codon into pABA-RNR at the position 1927

°C in 100 ml of LB (Luria–Bertani) medium supplemented with 150 μg/ml ampicillin to an OD_{600} of 1.5. Then, they were transferred to 18 °C for 30 min and then induced by addition of 0.5 mM IPTG (isopropyl β-D-thiogalactoside); induction proceeded for 20 h at 18°C. Cell cultures were pelleted by centrifugation at 8500 *g* for 15 min and stored at −80◦C.

Purification of all proteins was performed by histidine affinity chromatography using HiTrap Chelating HP columns (GE Healthcare) and ÄKTA HPLC system (GE Healthcare) following the protocol described previously (Amblar *et al.*, 2006; Arraiano *et al.*, 2008). Briefly, cell suspensions were lysed using a French press at 9000 psi (1 psi = 6.9 kPa)

in the presence of 0.1 mM PMSF. The crude extracts were treated with 150 units of Benzonase (Sigma) during 30 min to degrade the nucleic acids and clarified by a 30 min of centrifugation at 10000 g. The clarified extracts were then added to a 1 ml HiTrap Chelating Sepharose column equilibrated in buffer A (20 mM Tris/HCl and 0.5 M NaCl, pH 8) plus 20 mM imidazole and 2 mM 2-β-mercaptoethanol. Protein elution was achieved by a continuous imidazole gradient (from 20 to 500 mM) in buffer A. The fractions containing the purified protein were pooled together and buffer-exchanged to buffer B (20 mM Tris/HCl, pH 8, 100 mM KCl and 2 mM 2-β-mercaptoethanol) using a 5 ml desalting column (GE Healthcare). Eluted proteins were concentrated by centrifugation at 7000 g for 15 min at 15ºC with Amicon Ultra Centrifugal Filter Devices of 30000 Da molecular mass cut off (Millipore). Protein concentration was determined by spectrophotometry and glycerol was added to the final fractions before storage at −20 °C to a final concentration of 50 %. A 0.5 μg sample of each purified protein was separated by SDS/PAGE gel with 8 % of polyacrylamide 37:5:1 and visualized by Coomassie Blue staining.

Activity Assays

Exoribonucleolytic activity was assayed using three different RNA oligoribonucleotides as substrates (Amblar *et al.*, 2006; Arraiano *et al.*, 2008). The 30-mer oligoribonucleotide (5'-CCCGACACCAACCACUAAAAAA AAAAAAAA-3'), the 16-mer oligoribonucleotide (5'-CCCGACACCAACCACU -3') and the poly(A) chain of 35 nt were labelled at its 5' end with [γ ^{32}P]ATP and T4 polynucleotide kinase. The RNA oligomers were then purified using Microcon YM-3 Centrifugal Filter Devices (Millipore) to remove the unincorporated nucleotides. The labelled 30-mer and 16-mer oligoribonucleotides were hybridized to the complementary 16-mer oligodeoxiribonucleotide (5'-AGTGGTTGGTGTCGGG-3'), thus obtaining the corresponding double-stranded substrate, 16–30ds and 16–16ds respectively. The hybridization between 30-mer and 16-mer oligomers was performed in a 1:1 (mol:mol) ratio by 5 min of incubation at 68 °C

followed by 45 min as room temperature. The exoribonucleolytic reactions were carried out in a final volume of 10 μl containing 30 nM substrate, 20 mM Tris/HCl (pH 8), 100 mM KCl, 1 mM $MgCl_2$ and 1 mM DTT. The amount of each enzyme added to the reaction is indicated in the respective Figures. Reactions were started by the addition of the enzyme and the mixtures incubated at 37 ºC. Samples were withdrawn at the time points indicated in the Figures, and the reaction was stopped by adding formamide-containing dye supplemented with 10 mM EDTA. Reaction products were resolved in a 20 % polyacrylamide 19:1/7 M urea gel and analysed by autoradiography. The exoribonucleolytic activity of the enzymes was determined by measuring and quantifying the disappearance of the substrate in several distinct experiments in which the protein concentration was adjusted in order that, under those conditions, less than 25 % of substrate was degraded. Each value obtained represents the mean for these independent assays. The exoribonucleolytic activity of the wild-type enzymes was taken as 100 %.

SPR (Surface Plasmon Resonance) Analysis

Biacore SA chips were obtained from Biacore (GE Healthcare). The flow cells of the SA (streptavidin) sensorchip were coated with a low concentration of the following substrates. On flow cell 1, no substrate was added so this cell could be used as the control blank cell. On flow cell 2, a 5' biotinylated 25-mer RNA oligomer (5'-CCCGACACCAACCACUAAAAAAA AA-3') was added, and on flow cell 3, we added a 5' biotinylated 30-mer poly(A) oligomer to allow the study of the protein interaction with different single-stranded RNA substrates. The target substrates were captured on flow cells 2 and 3 by manually injecting 20 μl of a 500 nM solution of the substrates in 1 M NaCl at a 10 μl/min flow rate, as described previously (Arraiano *et al.*, 2008; Barbas *et al.*, 2008; Barbas *et al.*, 2009; Park *et al.*, 2000), and we obtained a response of ~400RU. The biosensor assay was run at 4 ºC in the buffer with 20 mM Tris/HCl (pH 8), 100 mM KCl, 1 mM DTT and 25 mM EDTA. The proteins were injected over flow cells 1, 2 and 3 for 2 min at concentrations of 10, 20, 30, 40 and 50 nM using a flow

rate of 20 μl/min. All experiments included triple injections of each protein concentration to determine the reproducibility of the signal and control injections to assess the stability of the RNA surface during the experiment. Bound protein was removed with a 60 s wash with 2 M NaCl. Data from flow cell 1 were used to correct for refractive index changes and non-specific binding. Rate constants and equilibrium constants were calculated using the BIA EVALUATION 3.0 software package, according to the 1:1 Langmuir binding fitting model.

Multiple Sequence Alignment

Homologous sequences belonging to the RNase II-family of proteins in protein databases were obtained using BLAST (Altschul *et al.*, 1997) and they were aligned using ClustalW (Thompson *et al.*, 1994) and T-Coffee (Notredame *et al.*, 2000) algorithms.

RESULTS AND DISCUSSION

Asp280 is Crucial for RNase R Activity Without Affecting RNA Binding Ability

The active site of RNase II has four conserved aspartate residues that are the responsible for positioning the RNA substrate correctly in order to promote the nucleophilic attack of the phosphodiester bond (Frazão *et al.*, 2006). Previous studies have shown that, in this protein, Asp209 is a crucial residue for the catalytic activity without affecting RNA binding (Amblar and Arraiano, 2005) and that this aspartate residue is the only one that is essential for the activity of RNase II (Barbas *et al.*, 2008). Since this is a highly conserved residue in this family of enzymes (Supplementary Figure S1), we also mutated the correspondent amino acid in RNase R, Asp280, to better understand the reaction mechanism of this exoribonuclease. For that, we introduced the point mutation D280N into the pABA-RNR (Amblar *et al.*, 2007), and overexpressed and purified the respective protein. The exoribonucleolytic activity of this mutant

protein was analysed and compared with the wild-type enzyme by performing activity assays using different types of RNA substrates.

Wild-type RNase R is able to degrade single- and double-stranded RNA substrates releasing a 2 nt fragment as the shortest end-product in both cases (Figure 2). In fact, the final product is a mixture of a 2 and 4 nt fragments (Figure 2). The structure of RNase II showed that, in the catalytic pocket, 5 nt of RNA were "clamped" between the aromatic residues Tyr253 and Phe358 (Frazão *et al.*, 2006). Tyr253 is highly conserved and equivalent residues are present in all RNase II-family members (Supplementary Figure S1). However, in RNase R, the equivalent residue to Phe358 does not exist and that could be a possible explanation for the differences regarding the end-product (Barbas *et al.*, 2008). In RNase R, there is a phenylalanine residue (Phe429) in the position immediately downstream of the equivalent residue (Phe358) in RNase II (Supplementary Figure S1). It is possible that some RNA fragments are still partially "clamped" and therefore they are released when they reach 4 nt. Others bind the catalytic cavity more efficiently and are able to be degraded up to a 2 nt fragment. This issue will be clarified when the RNase R crystal structure is solved. When the D280N mutant of RNase R was tested with both single- and double-stranded substrates, no activity was found (Figure 2), similarly to what happened with RNase II_D209N mutant (Amblar and Arraiano, 2005; Barbas *et al.*, 2008). Furthermore, we determined the exoribonucleolytic activity of wild-type RNase R and D280N mutant enzymes. Our results are consistent and confirm those obtained with the activity assays, i.e. the activity of D280N mutant is highly diminished when compared with the wild-type enzyme (Table 3). To determine the involvement of this residue in RNA binding, we calculated the dissociation constants of the wild-type and mutant proteins by SPR using two different RNA substrates, a 25-mer and a poly(A) oligomer. We observed that the binding ability of the protein is not affected by the presence of this mutation, since the D280N mutant presented a K_D value very similar to that of the wild-type RNase R protein

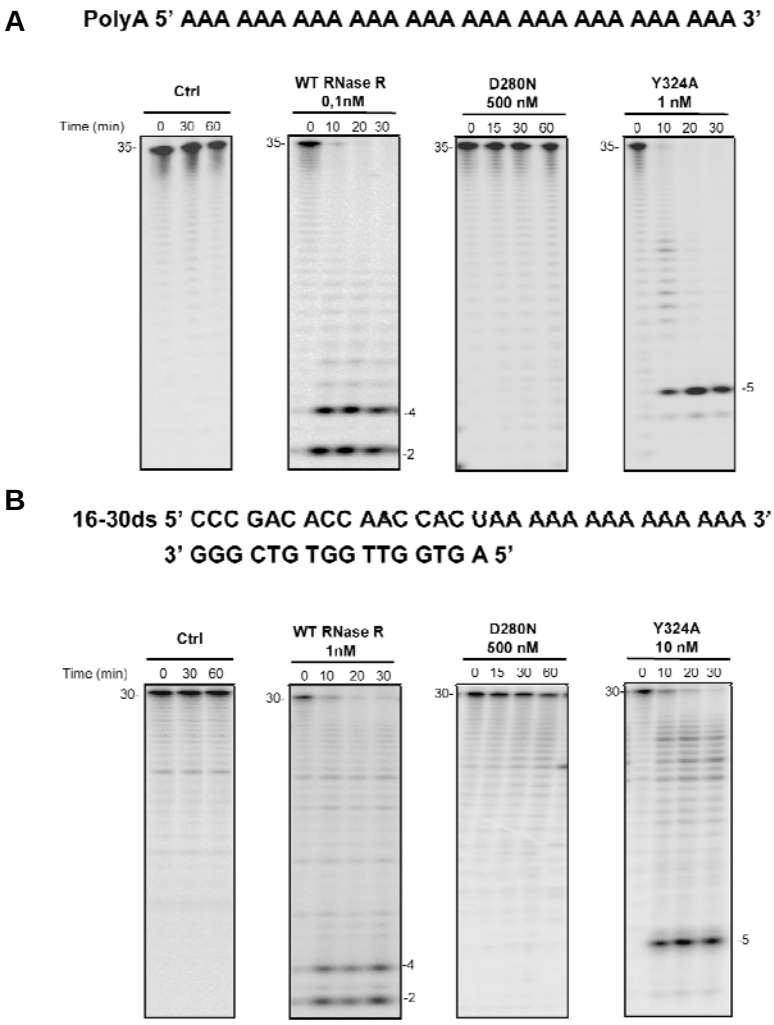

FIGURE 2. Exoribonuclease activity of RNase R wild-type and point mutant enzymes Activity assays were performed as described in the Experimental section using a poly(A) chain of 35 nt (**A**) or a 30-mer oligoribonucleotide hybridized to the complementary 16-mer oligodeoxyribonucleotide, thus obtaining the corresponding double-stranded substrate 16–30ds (**B**). The wild-type enzyme (WT RNase R) was used for comparison. Samples were taken during the reaction at the time points indicated and reaction products were analysed in a 20 % polyacrylamide 19:1/7 M urea gel. Control reactions with no enzyme added (*Ctrl*) were incubated at the maximum reaction time for each protein. Lengths of substrates and degradation products are indicated (in nt).

with both substrates tested: 2.2 ± 0.3 nM with 25-mer and 1.3 ± 0.2 nM with poly(A) for D280N compared with 3.2 ± 0.4 nM with 25-mer and 1.2 ± 0.1 nM with poly(A) for RNase R (Table 4). These results confirm that, similarly to what happens with RNase II, this aspartate residue is indeed essential for the activity of RNase R without affecting RNA binding.

In RNase R, the four aspartate residues in the active centre are located at positions 272, 278, 280 and 281, and, like Asp209 in RNase II, the equivalent Asp280 in RNase R may well be the only critical aspartate in this protein. Recent studies have shown that a mutation in Asp278 impairs RNase R activity, but the D278N mutant still retains 4 % of

TABLE 3. Exoribonucleolytic activity of wild-type RNase R and point mutant Enzymes Exoribonucleolytic activity was assayed using a 35 nt poly(A) chain as substrate. Activity assays were performed in triplicate as described in the Experimental Procedures section

Protein	Protein Activity *pmol.min^{-1}.nmol^{-1}*	Relative Activity %
wt RNase R	130.8 ± 6.3	100
D280N	<<0.01	<<0.01
Y324A	3.3 ± 0.2	2.5

TABLE 4. RNA-binding affinity of wild-type RNase R and point mutant enzymes The dissociation constants (K_D) were determined by SPR using Biacore 2000 with a 25 nt RNA oligomer (5' biotin-CCCGACAC CAACCACUAAAAAAAAA-3') and 30 nt poly(A) as substrates as described in the Experimental Procedures section.

Protein	K_D *nM* 25-mer	Relative K_D 25-mer	K_D *nM* poly(A)	Relative K_D poly(A)
wt RNase R	3.2 ± 0.4	1.0	1.2 ± 0.1	1.0
D280N	2.2 ± 0.3	0.7	1.3 ± 0.2	1.1
Y324A	20.4 ± 1.4	6.4	6.7 ± 0.3	5.6

activity (Vincent and Deutscher, 2009). Moreover, we can say that this residue plays a crucial role in the activity of all the proteins of this family, since a mutation in the equivalent residue in RNase R of *Legionella pneumophila*, Asp283, also led to the loss the exoribonucleolytic activity of the enzyme (Charpentier *et al.*, 2008).

Tyr324 is Responsible for Setting the Final End-Product in RNase R

In RNase II, the RNA molecule is stacked and "clamped" between two aromatic residues, Tyr253 and Phe358 (Frazão *et al.*, 2006), and it was shown previously that Tyr253 is important for setting the end-product of 4 nt. In the Y253A mutant, the final product released was a 10 nt fragment, which is the minimum length necessary for the RNA molecules to establish contacts between the catalytic and the anchoring regions simultaneously (Barbas *et al.*, 2008). In RNase R, the equivalent tyrosine is at position 324 (Supplementary Figure S1), and, in the present study, we wanted to see whether this residue also played such an important role in the mechanism of RNA degradation. For that purpose, we introduced the point mutation Y324A into the pABA-RNR plasmid (Amblar *et al.*, 2007) and purified the respective protein. The exoribonucleolytic activity was analysed with different RNA substrates and compared with the wild-type. As shown in Figure 2A, the mutant Y324A is capable of degrading the poly(A) substrate, rendering a final product of 5 nt instead of the usual 2 nt observed for the wild-type. The same behaviour is observed when we used the double-stranded 16–30ds substrate (Figure 2B). After this last cleavage event, the resultant 5 nt fragment is no longer capable of establishing the necessary contacts with the protein in order achieve the cleavage of the substrate and is released. As such, and similarly to what was shown with Tyr253 in RNase II, the Y324A mutant (Barbas *et al.*, 2008), the corresponding residue in RNase R, Tyr324, is also responsible for the establishment of the end-product of this protein. When we measured the activity of Y324A, we observed that it retains only 2.5 % of activity when compared with the wild-type (3.3 ± 0.2 and 130.8 ±

6.3 pmol.min^{-1}.nmol^{-1} respectively) (Table 3), whereas, in RNase II, the equivalent mutation retained approximately 25 % of activity (Barbas *et al.*, 2008). However, when we compared the dissociation constants (K_D values) obtained by SPR, the mutant presented a ~6 fold reduction for both substrates tested (Table 4), a similar result to the one obtained for the Y253A mutant in RNase II (Barbas *et al.*, 2008). These results suggest that the tyrosine residue in RNase R is also important for the binding of the RNA molecule at the 3' end, but has a much more important function in the activity of the enzyme than in RNase II. This could be due to the fact that the second residue involved in the RNA "clamping" in RNase II, Phe358, has no equivalent in RNase R, which can confer on Tyr324 a more important function in RNA "clamping".

The RNB Domain of RNase II has Catalytic Activity and is Able to Bind to RNA

When the *E. coli* RNase II structure was solved, it was possible to see that it is composed of four domains instead of the three initially proposed. This protein is formed by two CSD at the N-terminal region, a central catalytic RNB domain and a S1 domain at the C-terminal region (Frazão *et al.*, 2006). Before the RNase II structure was known, previous studies were performed with truncated RNase II proteins, where the ΔCSD and RNB mutants included the regions that corresponded to the CSD2 (Amblar *et al.*, 2006). In the present study, we constructed the genuine ΔCSD1+2 and RNB mutants lacking both CSD1/CSD2 and CSD1/CSD2/S1 domains respectively (Figure 1). We then induced and purified the truncated RNase II proteins and performed activity assays using different substrates.

When we analysed the two truncated RNase II proteins regarding their ability to degrade the single-stranded poly(A) substrate, we observed that, like wild-type RNase II, both RNase II_ΔCSD1+2 and RNase II_RNB were able to degrade the substrate until it reaches 4 nt as a final product (Figure 3A). However, the activity of these truncated RNase II proteins is

Table 5 Exoribonucleolytic activity of wild-type and truncated RNase II
Exoribonucleolytic activity was assayed using a 35 nt poly(A) chain as substrate. Activity assays were performed in triplicate as described in the Experimental Procedures section

Protein	Protein Activity *pmol.min^{-1}.nmol^{-1}*	Relative Activity %
wt RNase II	299.4 ± 36.0	100
RNase II_ΔCSD	0.1 ± 0.01	0.03
RNase II_RNB	<<0.01	<<0.01

very diminished when compared with the wild-type enzyme, with RNase II_ΔCSD1+2 retaining only 0.03 % of the enzyme's activity and RNase II_RNB less than 0.01 % (Table 5). Taking into account that the two CSD and S1 are the domains responsible for the RNA binding (Amblar *et al.*, 2006; Frazão *et al.*, 2006), we can clearly say that the loss of activity observed in these mutants is caused by the decrease in their ability to bind to the RNA molecule. The determination of the K_D values showed that these mutants are able to bind to RNA molecules less efficiently than the wild-type enzyme for both substrates tested. While RNase II presents a K_D value of 6.5 ± 0.4 and 1.3 ± 0.4 nM for the 25-mer and poly(A) substrate respectively (Barbas *et al.*, 2009), the absence of both CSD causes a 4 fold increase in the K_D value, with RNase II_ΔCSD1+2 presenting K_D values of 24.1 ± 2.9 and 5.2 ± 0.6 nM for the 25-mer and poly(A) substrates respectively (Table 6). The absence of all of the RNA-binding domains of the protein is responsible for a more pronounced reduction in RNA affinity, with the RNase II_RNB protein presenting almost a 10 fold increase in the K_D values when compared with the wild-type enzyme (Table 6).

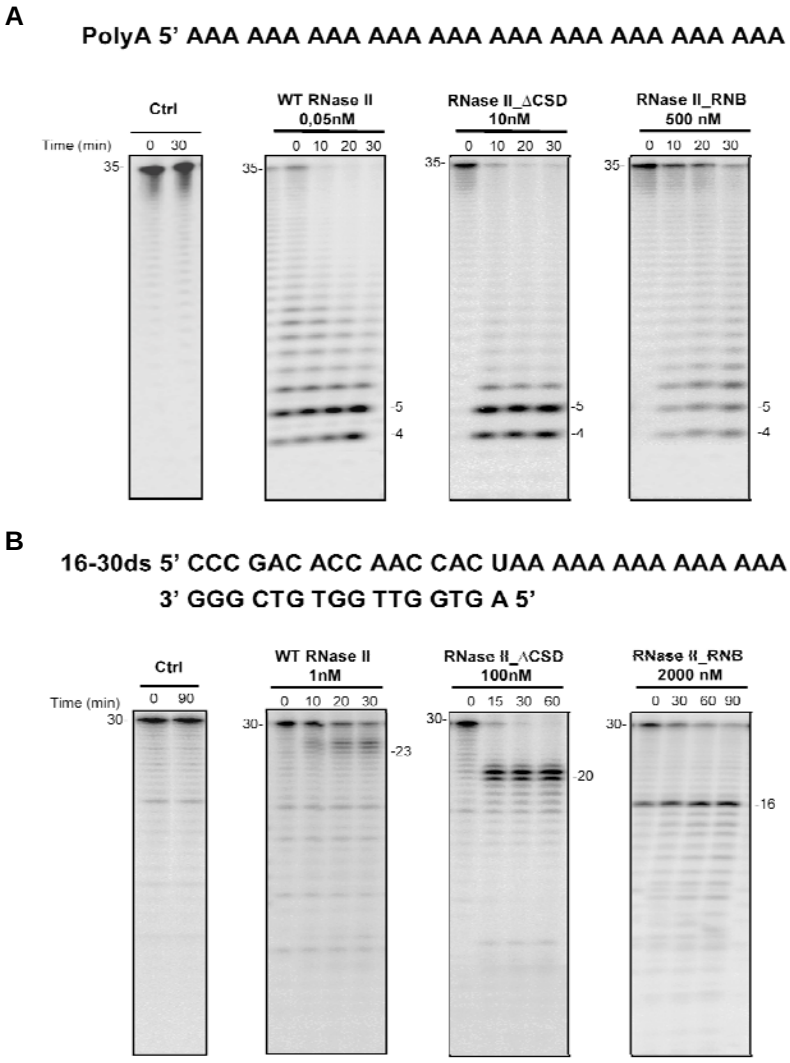

FIGURE 3. Exoribonuclease activity of wild-type and truncated RNase II enzymes Activity assays were performed as described in the Experimental section using a poly(A) chain of 35 nt (**A**) or a 30-mer oligoribonucleotide hybridized to the complementary 16-mer oligodeoxyribonucleotide, thus obtaining the corresponding double-stranded substrate 16–30ds (**B**). The wild-type enzyme (WT RNase II) was used for comparison. Other details were as in Figure 2.

TABLE 6. RNA-binding affinity of wild-type and truncated RNase II The dissociation constants (K_D) were determined by SPR using Biacore 2000 with a 25 nt RNA oligomer (5' biotin-CCCGACACCAACCACUAAAAAAAAA-3') and 30 nt poly(A) as substrates as described in the Experimental Procedures section

Protein	K_D *nM* 25-mer	Relative K_D 25-mer	K_D *nM* poly(A)	Relative K_D poly(A)
wt RNase II	6.5 ± 0.4	1.0	1.3 ± 0.4	1.0
RNase II_ΔCSD	24.1 ± 2.9	3.7	5.2 ± 0.6	4.0
RNase II_RNB	59.9 ± 6.0	9.2	11.7 ± 2.1	9.0

When we analysed the activity using a double-stranded substrate, 16–30ds, we verified that RNase II_ΔCSD1+2 is able to degrade a few more nucleotides than the wild-type enzyme, releasing fragments of 20–22 nt compared with the 23–25 nt released by RNase II (Figure 3B). This suggests that this mutant can get closer to the double-stranded region, maybe because the absence of both domains results in less steric hindrance, and allows the better entrance of double-stranded molecules into the catalytic cavity. A similar result was obtained with the mutant lacking only the CSD1 (Amblar *et al.*, 2006). However, when we tested the same substrate with the RNase II_RNB mutant, we observed that it was capable of degrading the entire single-stranded 3' overhang of the substrate. The reaction stopped when RNase II_RNB mutant reached the single-strand/double-strand junction and released a 16 nt blunt ended fragment (Figure 3B). It is possible to see that the band that corresponds to the 16 nt fragment is to a small extent present in all reactions, even in the control. However, since the intensity of the bands is clearly more pronounced in the RNase II_RNB mutant, and no other products are observed, this indicates that the substrate is being degraded. As such, we can say that the 16 nt product is the final one that is being released by the mutant. Previous studies have shown that wild-type RNase II has more difficulty in degrading the nucleotides adjacent to the double-

stranded region (Vincent and Deutscher, 2009). Our results confirm that the RNA binding channel formed by the CSD and S1 domains in RNase II could be the initial barrier for the degradation of double-stranded substrates (Amblar *et al.*, 2006). In fact, removal of the RNA-binding domains does allow RNase II to proceed further and the RNase II_RNB mutant protein is able to degrade all the way up to the double-stranded region.

The Cleavage of Double-Stranded RNA is a Property of the RNB Domain of RNase R

The structural model of *E. coli* RNase R indicates that this protein shares a common three-dimensional arrangement with *E. coli* RNase II and both enzymes have the same domain organization (Barbas *et al.*, 2008). However, RNase R has an additional HTH domain at the N-terminal region and a basic region after the S1 domain (Figure 1). It is already known that the CSD and S1 domains of RNase II are involved in RNA binding and that RNB domain is responsible for the catalytic activity of the enzyme (Amblar *et al.*, 2006). This modular domain organization has also been postulated for RNase R and the domains predicted to have the same function (Barbas *et al.*, 2008). In order to confirm this hypothesis, we constructed truncated RNase R proteins which lack both CSD and HTH and/or S1 domains as described in Figure 1.

In order to see the contribution of each domain to the activity and binding of the enzyme, we performed activity assays with a 35-mer poly(A) substrate, calculated the exoribonucleolytic activity and determined the K_D values.

RNase R is able to degrade single-stranded substrates, releasing a 2 nt fragment as the final product of the reaction (Amblar *et al.*, 2007) (Figure 4A). The same behaviour is observed for all the truncated proteins, RNase R_ΔCSD1+2, RNase R_ΔS1 and RNase R_RNB (Figure 4A). However, when we compared the activity of the different enzymes with the wild-type, it was possible to verify that all the truncated proteins analysed presented a

significant decrease in their activity (Table 7). The absence of both CSD in RNase R_ΔCSD1+2 protein causes a decrease of the activity of the enzyme more than 1000 fold, from 130.8 ± 6.3 to 0.2 ± 0.04 pmol.min^{-1}.nmol^{-1}. This reduction is more pronounced when the S1 domain is absent, with RNase R_ΔS1 presenting an activity of 0.02 ± 0.002 pmol.min^{-1}.nmol^{-1}. When only the RNB domain is present, the activity of the enzyme decreases more than 10000 fold, to values lower than 0.01 pmol.min^{-1}.nmol^{-1}. These results show that both the CSD and the S1 domains are important for the activity of the enzyme, with the S1 domain having a more important role.

Since it is postulated that CSD and the S1 domain are involved in RNA binding, the decrease in the activity observed in the truncated proteins can be due to a decrease in RNA binding ability. To confirm this hypothesis, we determined the K_D values of each protein by SPR using two different substrates. In fact, all of the truncated proteins showed a decrease in their K_D values when compared with the wild-type enzyme for both substrates tested (Table 8). By analysing the K_D values obtained for the truncated proteins, it is possible to see that the CSD are more important for the RNA binding when compared with the S1 domain.

TABLE 7. Exoribonucleolytic activity of wild-type and truncated RNase R
Exoribonucleolytic activity was assayed using a 35 nt poly(A) chain as substrate. Activity assays were performed in triplicate as described in the Experimental Procedures section.

Protein	**Protein Activity** ***pmol.min^{-1}.nmol^{-1}***	**Relative Activity** ***%***
wt RNase R	130.8 ± 6.3	100
RNase R_ΔCSD	0.2 ± 0.04	0.1
RNase R_ΔS1	0.02 ± 0.002	0.02
RNase R_RNB	<<0.01	<<0.01

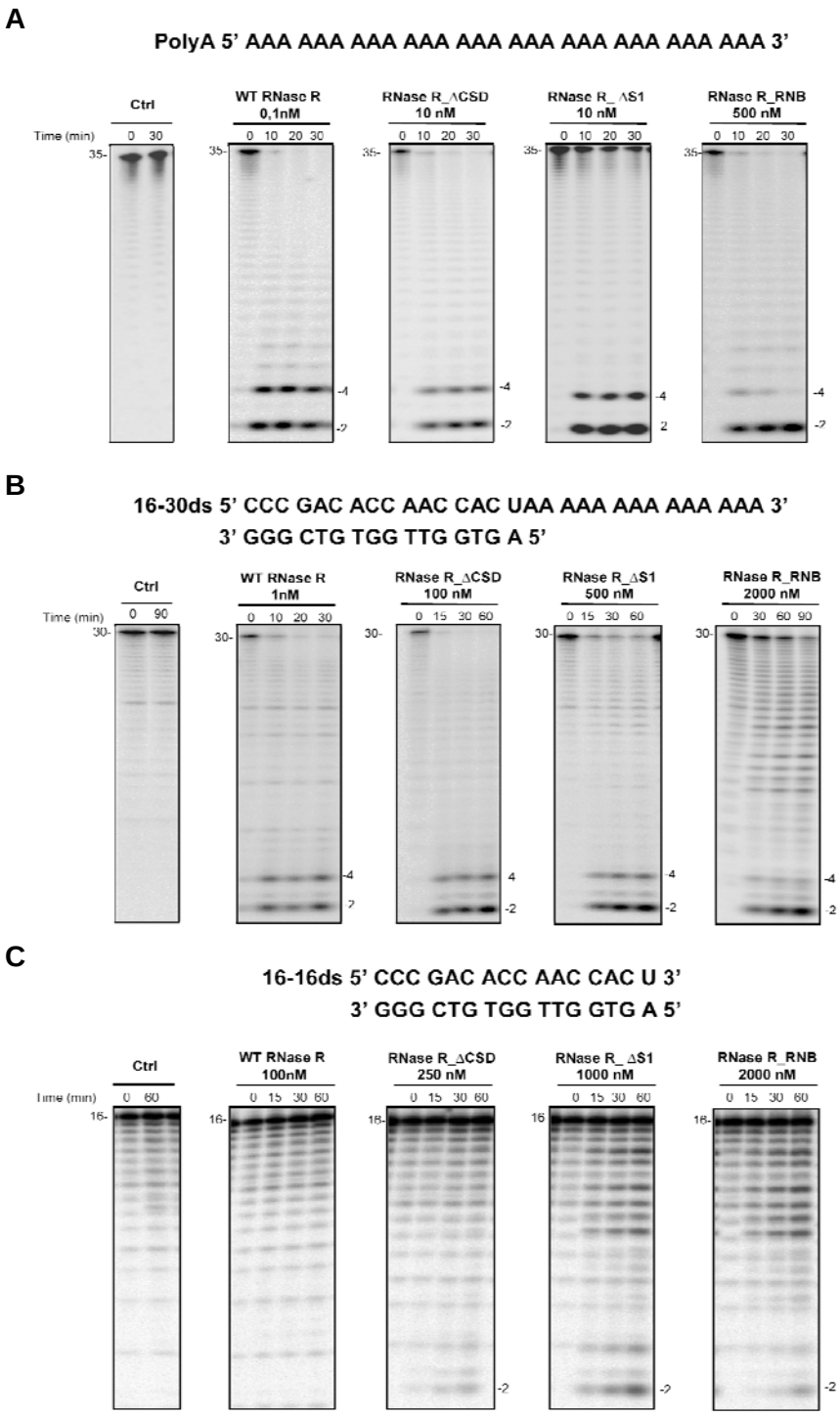
A
PolyA 5' AAA AAA AAA AAA AAA AAA AAA AAA AAA AAA 3'
Ctrl
WT RNase R 0,1nM
RNase R_ΔCSD 10 nM
RNase R_ ΔS1 10 nM
RNase R_RNB 500 nM
Time (min)
0 30
0 10 20 30
35-
-4
-7
B
16-30ds 5' CCC GAC ACC AAC CAC UAA AAA AAA AAA AAA 3'
3' GGG CTG TGG TTG GTG A 5'
Ctrl
WT RNase R 1nM
RNase R_ΔCSD 100 nM
RNase R_ΔS1 500 nM
RNase R_RNB 2000 nM
Time (min)
0 90
0 10 20 30
0 15 30 60
0 30 60 90
30-
-4
-2
C
16-16ds 5' CCC GAC ACC AAC CAC U 3'
3' GGG CTG TGG TTG GTG A 5'
Ctrl
WT RNase R 100nM
RNase R_ΔCSD 250 nM
RNase R_ ΔS1 1000 nM
RNase R_RNB 2000 nM
Time (min)
0 60
0 15 30 60
16-
-2

FIGURE 4. Exoribonuclease activity of wild-type and truncated RNase R enzymes Activity assays were performed as described in the Experimental section using a poly(A) chain of 35 nt (**A**), a 30-mer oligoribonucleotide hybridized to the complementary 16-mer oligodeoxyribonucleotide, thus obtaining the corresponding double-stranded substrate 16–30ds (**B**) or a 16-mer oligoribonucleotide hybridized to the complementary 16-mer oligodeoxyribonucleotide, thus obtaining the corresponding double-stranded substrate 16–16ds (**C**). The wild-type enzyme (WT RNase R) was used as control. Other details were as in Figure 2.

This is illustrated by the fact that the RNase R_ΔCSD1+2 protein presented a 3 fold reduction in its binding ability, whereas the absence of S1 domain was responsible for only a 2 fold reduction (Table 8). When the three domains are absent, the reduction in the ability to bind RNA molecules is much more significant, with RNase R_RNB protein presenting a K_D value of 20.7 ± 2.8 nM for the 25-mer substrate and 7.4 ± 0.4 nM for the poly(A) substrate, values that are approximately 6 fold higher than those described for RNase R (Table 8). In RNase R_ΔS1 protein, the reduction in the activity is more pronounced than that verified for the RNase R_ΔCSD1+2 (Table 7), whereas the dissociation constants obtained for both substrates tested are just 2 fold higher for this protein when compared with wild-type compared with 3 fold higher for the RNase R_ΔCSD1+2 protein. This result led us to conclude that the CSD and the S1 domains have different roles in RNA binding. The CSD must be more important for the recruitment of the substrate, whereas the S1 domain might help in the orientation and stabilization of the substrate in the catalytic cavity. It is interesting that the RNB domain is able to bind to RNA, although with a 6 fold decrease when compared with the wild-type. This also helps to explain the residual activity found in the RNase R_RNB protein.

TABLE 8. RNA-binding affinity of wild-type and truncated RNase R The dissociation constants (K_D) were determined by SPR using Biacore 2000 with a 25 nt RNA oligomer (5' biotin-CCCGACACCAACCACUAAAAAAAAA-3') and 30 nt poly(A) as substrates as described in the Experimental Procedures section

Protein	K_D *nM* 25-mer	Relative K_D 25-mer	K_D *nM* poly(A)	Relative K_D poly(A)
wt RNase R	3.2 ± 0.4	1.0	1.2 ± 0.1	1.0
RNase R_ΔCSD	9.6 ± 1.4	3.0	3.1 ± 0.1	2.6
RNase R_ΔS1	5.4 ± 0.3	1.7	2.1 ± 0.2	1.8
RNase R_RNB	20.7 ± 2.8	6.5	7.4 ± 0.4	6.2

As referred above, RNase R is able to degrade the double-stranded substrate 16–30ds, releasing a final product of 2 nt (Figure 4B) (Amblar *et al.*, 2007). When the truncated RNase R proteins were analysed with the same substrate, we verified that all of them were able to degrade it, releasing the characteristic 2 nt fragment (Figure 4B).

RNase R RNA-Binding Domains Discriminate Which RNA Molecules Will be Targeted for Degradation

It has been suggested that RNase R needs a single-stranded 3' overhang at least 5 nt in length in order to degrade structured RNA molecules (Vincent and Deutscher, 2006). Then, cleavage occurs at the single-stranded 3' overhang and proceeds processively in the 5' direction, degrading the secondary structure (Vincent and Deutscher, 2006; Worrall and Luisi, 2007). To verify which domains are responsible for the 3' overhang requirement in RNase R, we performed activity assays with the truncated RNase R proteins using a 16–16ds substrate (which lacks a 3' overhang). As expected, wild-type RNase R is not able to degrade the blunt-ended substrate that was tested (Figure 4C). Previous reports have also shown that the enzyme is not capable of degrading other blunt ended substrates, even using more extreme reaction conditions (i.e. higher concentrations of enzyme and longer incubation periods) (Vincent and

Deutscher, 2006). Surprisingly, the absence of CSD and/or the S1 domain resulted in the ability to degrade the 16–16ds substrate as shown in Figure 4C. These results show that the binding domains (CSD1, CSD2 and S1) are blocking the entrance of the double-stranded substrates into the catalytic channel. In their absence, the substrate is free to enter into the catalytic cavity and cleavage can occur.

Together, these results show that the RNB domain of RNase R is sufficient for the activity of the enzyme. This domain is also capable of binding to RNA substrates, although with less efficiency, and this explains its decreased activity. The decrease in RNA affinity upon deletion of either the CSD or the S1 domain confirms that these regions indeed function as RNA-binding domains. They are also responsible for the selective degradation of double-stranded substrates that contain a single-stranded 3' overhang of five or more nucleotides. In fact, in both prokaryotes and eukaryotes, the RNA targeted for degradation usually contain a short poly(A) tail (Houseley *et al.*, 2006). In the case of RNase R, the presence of the binding domains is important for the degradation of only structured RNA molecules that have an overhang of at least 5 nt in length. This suggests that this protein is capable of degrading RNA molecules only when they are targeted to that purpose. As such, the discrimination of which molecules are targeted for decay is made by the CSD1, CSD2 and S1 domains.

In conclusion, the results of the present study provide an important breakthrough in the understanding of the RNase R mechanism of action. We have identified Tyr324 as being responsible for setting the final end-product as 5 nt, instead of the usual 2 nt observed for the wild-type RNase R. This residue is fully conserved in all domains of life and was proved to have the same function in RNase II. We have also shown that Asp280, present in the RNase R active site, is crucial for the activity of the enzyme, but not for RNA binding.

We have demonstrated that RNB domains of RNase II and RNase R are able to degrade RNA, even in the absence of the RNA-binding domains.

The most striking result is that, in contrast with the existing literature, the RNB domain of RNase R is sufficient for the degradation of double-stranded substrates even in the absence of a 3' overhang. The RNA-binding domains present in the wild-type RNase R prevent the degradation of blunt-double-stranded RNA molecules. The discrimination of which molecules will be susceptible to degradation by RNase R is made by CSD1, CSD2 and the S1 domains that target the degradation of RNA that are "tagged" by a 3' tail. These results can have important implications for the study of poly(A)-dependent degradation mechanisms.

ACKNOWLEDGMENTS

We thank Miguel Luís for helping with the images. Rute G. Matos was a recipient of a Ph.D. fellowship and Ana Barbas was a recipient of a post-doctoral fellowship, both of them funded by Fundação para a Ciência e Tecnologia, Portugal. This work was supported by Fundação para a Ciência e Tecnologia, Portugal.

SUPPLEMENTARY INFORMATION

Supplementary figures

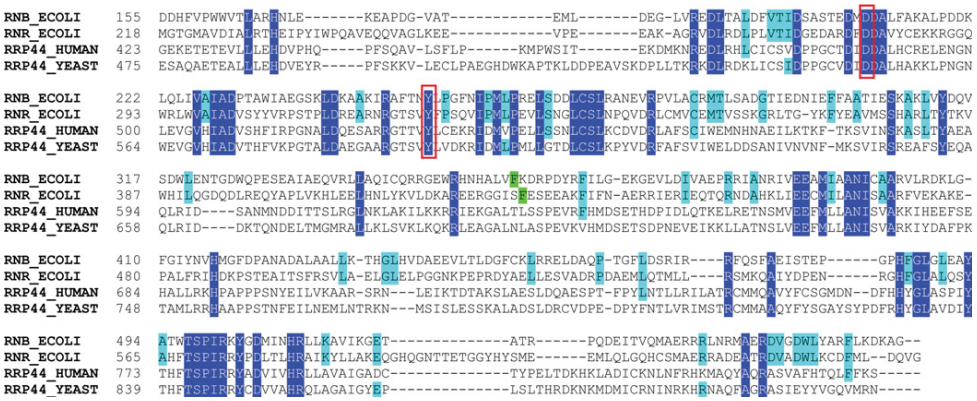

SUPPLEMENTARY FIGURE 1. Sequence alignment of RNB domains from RNase II, RNase R, human Rrp44 and yeast Rrp44 Residues highlighted in dark blue are fully conserved in all domains of life and residues highlighted in light blue are conserved in prokaryotes. The aspartate and tyrosine residues studied are boxed in red. Phe358 from RNase II and Phe429 from RNase R are highlighted in green.

REFERENCES

Altschul, S.F., Madden, T.L., Schaffer, A.A., Zhang, J., Zhang, Z., Miller, W., and Lipman, D.J. (1997) Gapped BLAST and PSI-BLAST: a new generation of protein database search programs. *Nucleic Acids Res* **25**: 3389-3402.

Amblar, M., and Arraiano, C.M. (2005) A single mutation in *Escherichia coli* ribonuclease II inactivates the enzyme without affecting RNA binding. *FEBS J* **272**: 363-374.

Amblar, M., Barbas, A., Fialho, A.M., and Arraiano, C.M. (2006) Characterization of the functional domains of *Escherichia coli* RNase II. *J Mol Biol* **360**: 921-933.

Amblar, M., Barbas, A., Goméz-Puertas, P., and Arraiano, C.M. (2007) The role of the S1 domain in exoribonucleolytic activity: substrate specificity and multimerization. *RNA* **13**: 317-327.

Andrade, J.M., Cairrão, F., and Arraiano, C.M. (2006) RNase R affects gene expression in stationary phase: regulation of ompA. *Mol Microbiol* **60**: 219-228.

Andrade, J.M., and Arraiano, C.M. (2008) PNPase is a key player in the regulation of small RNAs that control the expression of outer membrane proteins. *RNA* **14**: 543-551.

Andrade, J.M., Pobre, V., Silva, I.J., Domingues, S., and Arraiano, C.M. (2009) The role of 3'-5' exoribonucleases in RNA degradation. *Prog Mol Biol Transl Sci* **85**: 187-229.

Arraiano, C.M., Barbas, A., and Amblar, M. (2008) Characterizing ribonucleases in vitro examples of synergies between biochemical and structural analysis. *Methods Enzymol* **447**: 131-160.

Barbas, A., Matos, R.G., Amblar, M., Lopez-Viñas, E., Goméz-Puertas, P., and Arraiano, C.M. (2008) New insights into the mechanism of RNA degradation by ribonuclease II: identification of the residue responsible for setting the RNase II end product. *J Biol Chem* **283**: 13070-13076.

Barbas, A., Matos, R.G., Amblar, M., Lopez-Vinas, E., Gomez-Puertas, P., and Arraiano, C.M. (2009) Determination of key residues for catalysis and

RNA cleavage specificity: one mutation turns RNase II into a "SUPER-ENZYME". *J Biol Chem* **284**: 20486-20498.

Cairrão, F., Chora, A., Zilhão, R., Carpousis, A.J., and Arraiano, C.M. (2001) RNase II levels change according to the growth conditions: characterization of *gmr*, a new *Escherichia coli* gene involved in the modulation of RNase II. *Mol Microbiol* **39**: 1550-1561.

Cairrão, F., Cruz, A., Mori, H., and Arraiano, C.M. (2003) Cold shock induction of RNase R and its role in the maturation of the quality control mediator SsrA/tmRNA. *Mol Microbiol* **50**: 1349-1360.

Cairrão, F., and Arraiano, C.M. (2006) The role of endoribonucleases in the regulation of RNase R. *Biochem Biophys Res Commun* **343**: 731-737.

Cannistraro, V.J., and Kennell, D. (1994) The processive reaction mechanism of ribonuclease II. *J Mol Biol* **243**: 930-943.

Charpentier, X., Faucher, S.P., Kalachikov, S., and Shuman, H.A. (2008) Loss of RNase R induces competence development in *Legionella pneumophila*. *J Bacteriol* **190**: 8126-8136.

Cheng, Z.F., Zuo, Y., Li, Z., Rudd, K.E., and Deutscher, M.P. (1998) The *vacB* gene required for virulence in *Shigella flexneri* and *Escherichia coli* encodes the exoribonuclease RNase R. *J Biol Chem* **273**: 14077-14080.

Cheng, Z.F., and Deutscher, M.P. (2002) Purification and characterization of the *Escherichia coli* exoribonuclease RNase R: comparison with RNase II. *J Biol Chem* **277**: 21624-21629.

Cheng, Z.F., and Deutscher, M.P. (2005) An important role for RNase R in mRNA decay. *Mol Cell* **17**: 313-318.

Deutscher, M.P., and Reuven, N.B. (1991) Enzymatic basis for hydrolytic versus phosphorolytic mRNA degradation in *Escherichia coli* and *Bacillus subtilis*. *Proc Natl Acad Sci U S A* **88**: 3277-3280.

Dziembowski, A., Lorentzen, E., Conti, E., and Seraphin, B. (2007) A single subunit, Dis3, is essentially responsible for yeast exosome core activity. *Nat Struct Mol Biol* **14**: 15-22.

Erova, T.E., Kosykh, V.G., Fadl, A.A., Sha, J., Horneman, A.J., and Chopra, A.K. (2008) Cold shock exoribonuclease R (VacB) is involved in *Aeromonas hydrophila* pathogenesis. *J Bacteriol* **190**: 3467-3474.

Frazão, C., McVey, C.E., Amblar, M., Barbas, A., Vonrhein, C., Arraiano, C.M., and Carrondo, M.A. (2006) Unravelling the dynamics of RNA degradation by ribonuclease II and its RNA-bound complex. *Nature* **443**: 110-114.

Grossman, D., and van Hoof, A. (2006) RNase II structure completes group portrait of 3' exoribonucleases. *Nat Struct Mol Biol* **13**: 760-761.

Houseley, J., LaCava, J., and Tollervey, D. (2006) RNA-quality control by the exosome. *Nat Rev Mol Cell Biol* **7**: 529-539.

Lebreton, A., Tomecki, R., Dziembowski, A., and Seraphin, B. (2008) Endonucleolytic RNA cleavage by a eukaryotic exosome. *Nature* **456**: 993-996.

Mian, I.S. (1997) Comparative sequence analysis of ribonucleases HII, III, II PH and D. *Nucleic Acids Res* **25**: 3187-3195.

Mitchell, P., Petfalski, E., Shevchenko, A., Mann, M., and Tollervey, D. (1997) The exosome: a conserved eukaryotic RNA processing complex containing multiple 3'-->5' exoribonucleases. *Cell* **91**: 457-466.

Notredame, C., Higgins, D.G., and Heringa, J. (2000) T-Coffee: A novel method for fast and accurate multiple sequence alignment. *J Mol Biol* **302**: 205-217.

Park, S., Myszka, D.G., Yu, M., Littler, S.J., and Laird-Offringa, I.A. (2000) HuD RNA recognition motifs play distinct roles in the formation of a stable complex with AU-rich RNA. *Mol Cell Biol* **20**: 4765-4772.

Schaeffer, D., Tsanova, B., Barbas, A., Reis, F.P., Dastidar, E.G., Sanchez-Rotunno, M., Arraiano, C.M., and van Hoof, A. (2009) The exosome contains domains with specific endoribonuclease, exoribonuclease and cytoplasmic mRNA decay activities. *Nat Struct Mol Biol* **16**: 56-62.

Schneider, C., Anderson, J.T., and Tollervey, D. (2007) The exosome subunit Rrp44 plays a direct role in RNA substrate recognition. *Mol Cell* **27**: 324-331.

Studier, F.W., and Moffatt, B.A. (1986) Use of bacteriophage T7 RNA polymerase to direct selective high-level expression of cloned genes. *J Mol Biol* **189**: 113-130.

Taylor, R.G., Walker, D.C., and McInnes, R.R. (1993) *E. coli* host strains significantly affect the quality of small scale plasmid DNA preparations used for sequencing. *Nucleic Acids Res* **21**: 1677-1678.

Thompson, J.D., Higgins, D.G., and Gibson, T.J. (1994) CLUSTAL W: improving the sensitivity of progressive multiple sequence alignment through sequence weighting, position-specific gap penalties and weight matrix choice. *Nucleic Acids Res* **22**: 4673-4680.

Tobe, T., Sasakawa, C., Okada, N., Honma, Y., and Yoshikawa, M. (1992) vacB, a novel chromosomal gene required for expression of virulence genes on the large plasmid of *Shigella flexneri*. *J Bacteriol* **174**: 6359-6367.

Tsao, M.Y., Lin, T.L., Hsieh, P.F., and Wang, J.T. (2009) The 3'-to-5' exoribonuclease (encoded by HP1248) of *Helicobacter pylori* regulates motility and apoptosis-inducing genes. *J Bacteriol* **191**: 2691-2702.

Vincent, H.A., and Deutscher, M.P. (2006) Substrate recognition and catalysis by the exoribonuclease RNase R. *J Biol Chem* **281**: 29769-29775.

Vincent, H.A., and Deutscher, M.P. (2009) The roles of individual domains of RNase R in substrate binding and exoribonuclease activity. The nuclease

domain is sufficient for digestion of structured RNA. *J Biol Chem* **284**: 486-494.

Worrall, J.A., and Luisi, B.F. (2007) Information available at cut rates: structure and mechanism of ribonucleases. *Curr Opin Struct Biol* **17**: 128-137.

Zilhão, R., Camelo, L., and Arraiano, C.M. (1993) DNA sequencing and expression of the gene rnb encoding *Escherichia coli* ribonuclease II. *Mol Microbiol* **8**: 43-51.

Zilhão, R., Cairrão, F., Régnier, P., and Arraiano, C.M. (1996) PNPase modulates RNase II expression in *Escherichia coli*: implications for mRNA decay and cell metabolism. *Mol Microbiol* **20**: 1033-1042.

Zuo, Y., and Deutscher, M.P. (2001) Exoribonuclease superfamilies: structural analysis and phylogenetic distribution. *Nucleic Acids Res* **29**: 1017-1026.

Zuo, Y., Vincent, H.A., Zhang, J., Wang, Y., Deutscher, M.P., and Malhotra, A. (2006) Structural basis for processivity and single-strand specificity of RNase II. *Mol Cell* **24**: 149-156.

Chapter 4

Swapping the domains of exoribonucleases RNase II and RNase R: *Conferring upon RNase II the ability to degrade dsRNA*

This chapter contains data published in:

Matos, R. G., Barbas, A., Gómez-Puertas, P. and Arraiano, C.M. 2011. Swapping the domains of exoribonucleases RNase II and RNase R: Conferring upon RNase II the ability to degrade dsRNA. Proteins **79**: 1853-1867.

The author of this dissertation is the first author of the manuscript published.

The protein modelling and multiple sequence alignment were performed by Professor Paulino Gómez-Puertas from Centro de Biologia Molecular “Severo Ochoa”, Madrid, Spain.

Abstract

RNase II and RNase R are the two *E. coli* exoribonucleases that belong to the RNase II superfamily of enzymes. They degrade RNA hydrolytically in the 3' to 5' direction in a processive and sequence independent manner. However, while RNase R is capable of degrading structured RNA, the RNase II activity is impaired by dsRNA. The end-product of these two enzymes is also different, being 4 nt for RNase II and 2 nt for RNase R. RNase II and RNase R share structural properties, including 60 % of amino acid sequence similarity and have a similar modular domain organization: two N terminal cold shock domains (CSD1 and CSD2), one central RNB catalytic domain, and one C-terminal S1 domain. We have constructed hybrid proteins by swapping the domains between RNase II and RNase R to determine which are the responsible for the differences observed between RNase R and RNase II. The results obtained show that the S1 and RNB domains from RNase R in an RNase II context allow the degradation of double-stranded substrates and the appearance of the 2 nt long end-product. Moreover, the degradation of structured RNA becomes tail-independent when the RNB domain from RNase R is no longer associated with the RNA-binding domains (CSD and S1) of the genuine protein. Finally, we show that the RNase R C-terminal lysine-rich region is involved in the degradation of double-stranded substrates in an RNase II context, probably by unwinding the substrate before it enters into the catalytic cavity.

Introduction

RNase II and RNase R are the two *Escherichia coli* exoribonucleases that belong to the RNase II superfamily of enzymes. RNase II is the prototype of this family of exoribonucleases, and RNase II/R homologues are present in all domains of life (Arraiano *et al.*, 2010a; Grossman and van Hoof, 2006; Mian, 1997; Mitchell *et al.*, 1997; Zuo and Deutscher, 2001). The other member of the RNase II-family, RNase R, has been shown to be required for virulence and is involved in mRNA degradation, and RNA and protein quality control (Andrade *et al.*, 2006; Arraiano *et al.*, 2010a; Cairrão *et al.*, 2003; Cairrão and Arraiano, 2006; Cheng *et al.*, 1998; Cheng and Deutscher, 2005). In the nucleus and the cytoplasm of eukaryotic cells, the RNase II homologue Rrp44/Dis3 is part of the exosome, an essential multiprotein complex of exoribonucleases, involved in processing, turnover, and quality control of different types of RNA (Mitchell *et al.*, 1997). Most importantly, this enzyme was reported to be the only catalytically active nuclease in the yeast core exosome (Dziembowski *et al.*, 2007), and studies have shown that this protein has a dual function since it comprises both exo- and endoribonucleolytic activity (Arraiano *et al.*, 2010a; Lebreton *et al.*, 2008; Schaeffer *et al.*, 2009).

RNase II and RNase R share catalytic properties: they both processively degrade RNA hydrolytically in the 3' to 5' direction releasing 5' nucleosite monophosphates. Both enzymes share structural properties, including 60 % amino acid sequence similarity, and 29 % protein sequence identity (Cheng and Deutscher, 2002). Their activity is sequence independent but while RNase II is sensitive to secondary structures, RNase R is capable of degrading highly structured RNA (Amblar *et al.*, 2006; Andrade *et al.*, 2006; Cheng and Deutscher, 2002, 2005). In fact, recent studies have shown that the RNB domain of RNase R is the one responsible for the degradation of double-stranded substrates (Matos *et al.*, 2009; Vincent and Deutscher, 2009). It is known that RNase R needs a 3' single-

stranded overhang of at least five nucleotides in length to be able to attach to the substrate and proceed to the degradation of the structured RNA molecules (Vincent and Deutscher, 2006). However, it was recently shown that the CSD and S1 domains are those responsible for the selective degradation of double-stranded substrates that contain a 3' single-stranded overhang of five or more nucleotides (Matos *et al.*, 2009). Another difference between these two *E. coli* enzymes is that the final degradation product of RNase II is a 4 nucleotide fragment, whereas the end-product of RNase R is a 2 nucleotide fragment (Amblar *et al.*, 2006; Amblar *et al.*, 2007; Cannistraro and Kennell, 1994). The same differences have been observed in *Salmonella*, which also has both RNase II and RNase R-like proteins (Domingues *et al.*, 2009). In *Streptococcus pneumoniae*, only one member of this family of enzymes is present. Its characterization showed that it behaves like RNase R, since it is able to degrade double-stranded substrates releasing a 2 nt fragment as its end-product (Domingues *et al.*, 2009).

RNase II is a protein encoded by gene *rnb* with 72 kDa. In *E. coli*, this protein is the major hydrolytic enzyme that is responsible for 90 % of the exoribonucleolytic activity in crude extracts (Deutscher and Reuven, 1991). RNase II expression is differentially regulated at the transcriptional and post-transcriptional levels and the protein can be regulated by the environmental conditions (Arraiano *et al.*, 2010b; Cairrão *et al.*, 2001; Zilhão *et al.*, 1993; Zilhão *et al.*, 1996). The determination of the 3D structure of *E. coli* RNase II showed that RNase II consists of 4 domains: two N-terminal cold shock domains (CSD1 and CSD2), one central RNB catalytic domain, and one C-terminal S1 domain (Frazão *et al.*, 2006; Zuo *et al.*, 2006) (Figure 1). The final degradation product of RNase II is 4 nt. The structure of the RNA bound complex showed that there is a tight packing of the five 3' terminal nucleotides in the catalytic cavity, and the RNA "clamping" is mediated by the aromatic residues Tyr253 and Phe358 (Frazão *et al.*, 2006). Subsequently, it was demonstrated that Tyr253 is the residue responsible for setting the end-product of RNase II (Arraiano

et al., 2010b; Barbas *et al.*, 2008). It was also demonstrated that Tyr313 and Glu390 are important for the discrimination of cleavage of RNA versus DNA (Arraiano *et al.*, 2010b; Barbas *et al.*, 2009). During the determination of key residues for catalysis, we have recently discovered that the substitution of the Glu542 by alanine lead to a 110 fold increase in the exoribonucleolytic activity and 20 fold in RNA binding, turning RNase II into a "super-enzyme" (Arraiano *et al.*, 2010b; Barbas *et al.*, 2009; Matos *et al.*, 2010).

RNase R is a 92 kDa protein encoded by the *rnr* gene that is involved in the degradation of different types of RNA such as rRNA, small RNA and mRNA. It was shown that RNase R has *in vivo* affinity for polyadenylated RNA and can be a key enzyme involved in poly(A) metabolism (Andrade and Arraiano, 2008). It is a cold shock protein that is regulated at the transcriptional and post-transcriptional levels (Cairrão *et al.*, 2003; Cairrão and Arraiano, 2006). The activity of RNase R is modulated according the growth conditions of the cell (Cairrão *et al.*, 2001) and its levels increase in stationary phase and under other stress conditions (Andrade *et al.*, 2006; Cairrão *et al.*, 2003; Cheng and Deutscher, 2005). It has been shown that this protein is also involved in pathogenesis in different micro-organisms (Cheng *et al.*, 1998; Erova *et al.*, 2008; Tobe *et al.*, 1992; Tsao *et al.*, 2009). The structural model of *E. coli* RNase R protein has been constructed based on the RNase II structure. It clearly indicates that these enzymes share a common three-dimensional arrangement, with all the critical residues for exoribonucleolytic activity located in equivalent spatial positions (Barbas *et al.*, 2008). In fact, recent studies have shown that like in RNase II D209N mutant, Asp280 in RNase R is important for the activity of the enzyme but not for the RNA binding. Also it has been described that Tyr324 is also the conserved residue responsible for setting the final product in RNase R, comparable with what is observed with RNase II (Matos *et al.*, 2009).

The aim of this work was to determine if the catalytical differences observed between RNase II and RNase R could be assigned directly to one

of the domains. As such, we wanted to investigate which domain could be accounted for the setting of the different end-products (4 nt for RNase II and 2 nt for RNase R), and which domain could be responsible for the discrimination between single- and double-stranded RNA cleavage. For that, we constructed a set of six different hybrid proteins by swapping the cold shock domains, the catalytic domains, and the S1 domains between RNase II and RNase R (Figure 1). The results presented here show that in fact the RNB domain from RNase R is the one responsible for the degradation of double-stranded substrates. However and more interestingly, our data shows that the C-terminal region from RNase R has a very important role in the degradation of double-stranded substrates. We show that this domain might contribute to the unwinding of the secondary structures, and this can explain why RNase R is capable of degrading RNA structured substrates.

Experimental Procedures

Materials

Restriction enzymes, T4 DNA ligase, Pfu DNA polymerase and T4 Polynucleotide Kinase were purchased from Fermentas. Unlabeled oligonucleotide primers were synthesized by STAB Vida, Portugal.

Strains

The *E. coli* strains used were DH5α (F' *fhuA2*Δ(*argF-lacZ)U169 phoA glnV44* Φ*80* Δ(*lacZ)M15 gyrA96 recA1 relA1 endA1 thi-1 hsdR17*a) (Taylor *et al.*, 1993) for cloning experiments and BL21(DE3) (F^- rB^- mB^- *gal ompT* (*int*::*PlacUV5 T7 gen1 imm21 nin5*) (Studier and Moffatt, 1986) for expression and purification of enzymes.

Construction of Hybrid Proteins

The hybrid proteins were constructed by swapping the N-terminal region (corresponding to the cold shock domains), the catalytic domain RNB or the C-terminal region (S1 domain) between (His)6-RNase II and (His)6-RNase R, thus obtaining the following six proteins: RNase II_CSD_R,

RNase II_RNB_R, RNase II_S1_R, RNase R_CSD_II, RNase R_RNB_II, and RNase R_S1_II (Figure 1).

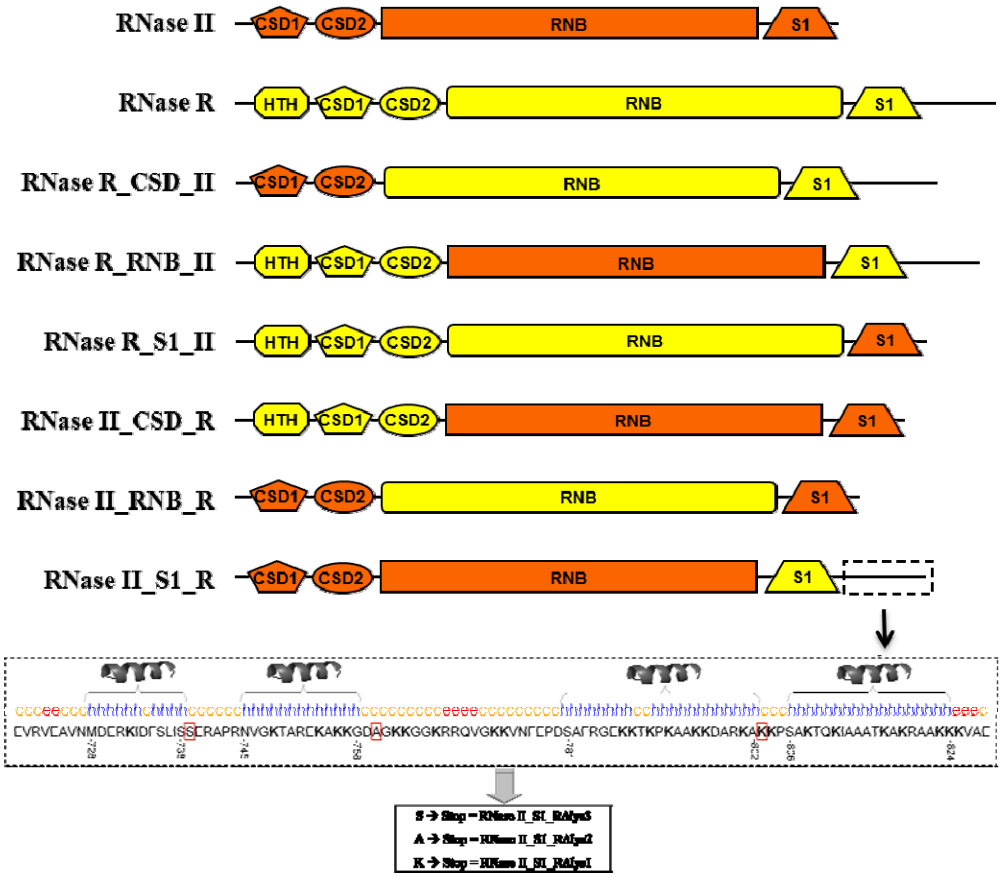

FIGURE 1. Linear representation of the domains of wild-type RNase II, RNase R and its derivatives proteins. The lysine-rich tail of the S1 domain from RNase R is highlighted, and the protein structure is represented. The aminoacids that were substituted by stop codons to construct the proteins RNase II_S1_RΔLys1, RNase II_S1_RΔLys2, and RNase II_S1_RΔLys3 are boxed. On the top of the protein structure is the secondary structure prediction using the GOR 4 method of NPS@ as described in Experimental Procedures. h stands for alpha helix, e stands for extended strand and c stands for random coil.

For this purpose, the *Spe*I and *Sma*I restriction sites were introduced into the pFCT6.1 plasmid (Table 1) at the 514 nt and 1729 nt positions respectively and in the pABA-RNR plasmid (Table 1) at the 547 nt and 1924 nt positions respectively by overlapping PCR. The mutagenic primers used were pFCT_SpeI514_Fw, pFCT_SpeI514_Rev, pFCT_SmaI1729_Fw, pFCT_SmaI1729_Rev, RNR_SpeI547_Fw, RNR_SpeI547_Rev, RNR_SmaI1924_Fw, and RNR_SmaI1924_Rev (Table 2). To construct the hybrid proteins RNase II_RNB_R and RNase R_RNB_II, the resulting plasmids pFCT_SpeI514_SmaI1729 and pABA-RNR_SpeI547_SmaI1924 (Table 2) were digested with *Spe*I and *Sma*I, obtaining cleavage products of 6195 bp and 1216 bp for pFCT_SpeI514_SmaI1729 and 7005 bp and 1270 bp for pABA-RNR_SpeI547_SmaI1924. The restriction fragment with 1216 bp resultant of the restriction of pFCT_SpeI514_SmaI1729 was ligated to the restriction fragment of 7005 bp resultant of the digestion of pABA-RNR_SpeI547_SmaI1924, originating the hybrid protein RNase R_RNB_II. The restriction fragment with 6195 bp resultant of the restriction of pFCT_SpeI514_SmaI1729 was ligated to the restriction fragment of 1270 bp resultant of the digestion of pABA-RNR_SpeI547_SmaI1924, originating the hybrid protein RNase II_RNB_R. To construct the hybrid proteins RNase II_CSD_R and RNase R_CSD_II, the plasmids with the insertion of *Spe*I restriction site only, pFCT_SpeI514 and pABA-RNR_SpeI547 (Table 1) were digested with *Spe*I and *Xba*I (the restriction enzyme *Xba*I cleaves the pET15b plasmid upstream the insertion of the *rnb* or *rnr* genes), obtaining cleavage products of 6860 bp and 551 bp for pFCT_SpeI514 and 7529 bp and 746 bp for pABA-RNR_SpeI547. The restriction fragment with 551 bp resultant of the restriction of pFCT_SpeI514 was ligated to the restriction fragment of 7529 bp resultant of the digestion of pABA-RNR_SpeI547, originating the hybrid protein RNase R_CSD_II. The restriction fragment with 6860 bp resultant of the restriction of pFCT_SpeI514 was ligated to the restriction fragment

of 746 bp resultant of the digestion of pABA-RNR_SpeI547, originating the hybrid protein RNase II_CSD_R.

TABLE 1. Plasmids used in this study

Plasmid	Relevant characteristic	Reference
pFCT6.1	gene *rnb* cloned into pET15b, Amp^R	Cairrão *et al.*, 2001
pABA-RNR	gene *rnr* cloned into pET15b, Amp^R	Amblar *et al.*, 2007
pFCT_SpeI514	pFCT6.1 with a SpeI restriction site in position 514 of *rnb* gene	This work
pFCT_SmaI1729	pFCT6.1 with a *Sma*I restriction site in position 1729 of *rnb* gene	This work
pFCT_SpeI514_SmaI1729	pFCT_SpeI514 with a *Sma*I restriction site in position 1729 of *rnb* gene	This work
pABA-RNR_SpeI547	pABA-RNR with a *Spe*I restriction site in position 547 of *rnr* gene	This work
pABA-RNR_SmaI1924	pABA-RNR with a SmaI restriction site in position 1924 of *rnr* gene	This work
pABA-RNR_ SpeI547_SmaI1924	pABA-RNR_SpeI547 with a *Sma*I restriction site in position 1924 of *rnr* gene	This work
pFCT_CSD_R	Expresses RNase II with HTH, CSD1 and CSD2 domains from RNase R	This work
pFCT_RNB_R	Expresses RNase II with RNB domain from RNase R	This work
pFCT_S1_R	Expresses RNase II with S1 domain from RNase R	This work
pABA-RNR_CSD_II	Expresses RNase R with CSD1 and CSD2 domains from RNase II	This work
pABA-RNR_RNB_II	Expresses RNase R with RNB domain from RNase II	This work
pABA-RNR_S1_II	Expresses RNase R with S1 domain from RNase II	This work
pFCT_S1_R_ΔLys1	Expresses RNase II with S1 domain from RNase R without the last 26 aa	This work
pFCT_S1_R_ΔLys2	Expresses RNase II with S1 domain from RNase R without the last 67 aa	This work
pFCT_S1_R_ΔLys3	Expresses RNase II with S1 domain from RNase R without the last 87 aa	This work

TABLE 2. Primers used in this study Bases underlined indicate restriction endonuclease sites. Bases in bold indicate amino acid changes

Primer	Sequence (5' → 3')[ab]	Purpose
pFCT_SpeI514_Fw	5'-CACAATACATCACT **AG**TGGTGACG-3'	Introduces SpeI restriction site into pFCT6.1 at the position 514
pFCT_SpeI514_Rev	5'-CGTCACCA**CT**AGT GATGTATTGTG-3'	Introduces SpeI restriction site into pFCT6.1 at the position 514
pFCT_SmaI1729_Fw	5'-CCTGAAAGACAAA**C**CC GGGACCGACACCCG-3'	Introduces SmaI restriction site into pFCT6.1 at the position 1729
pFCT_SmaI1729_Rev	5'-CGGGTGTCGGTCCCGG **G**TTTGTCTTTCAGG-3'	Introduces SmaI restriction site into pFCT6.1 at the position 1729
RNR_SpeI547_Fw	5'-GTCGAAGTGCTGGGC **ACTAG**TATGGGCACC-3'	Introduces SpeI restriction site into pABA-RNR at the position 547
RNR_SpeI547_Rev	5'-GGTGCCCATA**CTAGT** GCCCAGCACTTCGAC-3'	Introduces SpeI restriction site into pABA-RNR at the position 547
RNR_SmaI1924_Fw	5'-GTGTGACTTCATG C**C**CG**GG**CAGGTAGG-3'	Introduces SmaI restriction site into pABA-RNR at the position 1924
RNR_SmaI1924_Rev	5'-CCTACCTG**CC**CG**G**G CATGAAGTCACAC-3'	Introduces SmaI restriction site into pABA-RNR at the position 1924
Δlys1_Fw	5'-TTTAGCCTGATCTCC **TAA**GAACGCGCACCG-3'	Introduces stop codon into pFCT_S1_R at the position 2172
Δlys1_Rev	5'-CGGTGCGCGTTC**TTA** GGAGATCAGGCTAAA-3'	Introduces stop codon into pFCT_S1_R at the position 2172
Δlys2_Fw	5'-GAAAAAAGGCGAT**TA**A GGTAAAAAAGGCGG-3'	Introduces stop codon into pFCT_S1_R at the position 2049
Δlys2_Rev	5'-CCGCCTTTTTTACCT **TA**ATCGCCTTTTTTC-3'	Introduces stop codon into pFCT_S1_R at the position 2049
Δlys3_Fw	5'-GCGAGAAAAGCG**T** AAAAGCCATCGG-3'	Introduces stop codon into pFCT_S1_R at the position 1989
Δlys3_Rev	5'-CCGATGGCTTTT**A** CGCTTTTCTCGC-3'	Introduces stop codon into pFCT_S1_R at the position 1989

To construct the hybrid proteins RNase II_S1_R and RNase R_S1_II, the plasmids with the insertion of *Sma*I restriction site only, pFCT_SmaI1729 and pABA-RNR_SmaI1924 (Table 1) were digested with *Sma*I and *Hind*III (the restriction enzyme *Hind*III cleaves the pET15b plasmid downstream the insertion of the *rnb* or *rnr* genes), obtaining cleavage products of 7076 bp and 335 bp for pFCT_SmaI1729 and 7325 bp and 950 bp for pABA-RNR_SmaI1924. The restriction fragment with 335 bp resultant of the restriction of pFCT_SmaI1729 was ligated to the restriction fragment of

7325 bp resultant of the digestion of pABA-RNR_SmaI1924, originating the hybrid protein RNase R_S1_II. The restriction fragment with 7076 bp resultant of the restriction of pFCT_SmaI1729 was ligated to the restriction fragment of 950 bp resultant of the digestion of pABA-RNR_SmaI1924, originating the hybrid protein RNase II_S1_R. The Δlys mutations in the RNase II_S1_R_Δlys1, RNase II_S1_R_Δlys2, and RNase II_S1_R_Δlys3 proteins were introduced into the pFCT_S1_R (Table 1) by overlapping PCR. The primers used in the constructions were Δlys1_Fw, Δlys1_Rev, Δlys2_Fw, Δlys2_Rev, Δlys3_Fw, and Δlys3_Rev (Table 2).

Overexpression and Purification of Wild-type and Hybrid Proteins

The plasmid used for expression of wild-type *E. coli* histidine-tagged RNase II protein was pFCT6.1 plasmid (Table 1). The plasmid used for expression of wild-type *E. coli* histidine-tagged RNase R protein was pABA-RNR (Table 1).

All plasmids were transformed into BL21(DE3) *E. coli* strain (Novagen) to allow the expression of the recombinant proteins. Cells were grown at 30 ºC in 100 mL LB medium supplemented with 150 μg/mL ampicillin to an OD_{600} of 1.5. Then, they were transferred to 18ºC for 30 min and then induced by addition of 0.5 mM IPTG; induction proceeded for 20 h at 18 ºC. Cell cultures were pelleted by centrifugation at 6000 rpms for 15 min and stored at -80 ºC.

Purification of all proteins was performed by histidine affinity chromatography using HiTrap Chelating HP columns (GE Healthcare) and AKTA HPLC system (GE Healthcare) following the protocol previously described (Amblar *et al.*, 2006; Arraiano *et al.*, 2008). Protein concentration was determined by spectrophotometry using a Nanodrop device and measuring the OD at 280nm. Finally, glycerol was added to the final fractions prior storage at -20ºC to a final concentration of 50 %. 0.5 μg of each purified protein was applied in an SDS PAGE gel with 8 % of polyacrilamide 37:5:1 and visualized by Coomassie Blue staining.

Activity Assays

Exoribonucleolytic activity was assayed using three different RNA oligoribonucleotides as substrates (Amblar *et al.*, 2006; Arraiano *et al.*, 2008). The 30-mer oligoribonucleotide (5'-CCCGACACCAACCACUAAAAAA AAAAAAAA-3'), the 16-mer oligoribonucleotide (5'-CCCGACACCAACCAC U-3') and the poly(A) chain of 35 nt were labelled at its 5' end with [γ-^{32}ATP] and T4 polynucleotide kinase. The RNA oligomers were then purified using Microcon YM-3 Centrifugal Filter Devices (Millipore) to remove the unincorporated nucleotides. The labelled 30-mer and 16-mer oligoribonucleotides were hybridized to the complementary 16-mer oligodeoxyribonucleotide (5'-AGTGGTTGGTGTCGGG-3'), thus obtaining the corresponding double-stranded substrate 16–30ds and 16-16ds, respectively. The hybridization between 30-mer and 16-mer oligomers was performed in a 1:1 (mol:mol) ratio by 5 min of incubation at 68 °C followed by 45 min as room temperature. The exoribonucleolytic reactions were carried out in a final volume of 10 μl containing 30 nM of substrate, 20 mM Tris-HCl pH 8, 100 mM KCl, 1 mM $MgCl_2$, and 1 mM DTT. The amount of each enzyme added to the reaction was adjusted to obtain linear conditions and is indicated in the respective figures. Reactions were started by the addition of the enzyme and incubated at 37 ºC. Samples were withdrawn at the time points indicated in the figures, and the reaction was stopped by adding formamide-containing dye supplemented with 10 mM EDTA. Reaction products were resolved in a 20 % polyacrylamide 19:1/7 M urea and analyzed by autoradiography. The exoribonucleolytic activity of the enzymes was determined by measuring and quantifying the disappearance of the substrate in several distinct experiments in which the protein concentration was adjusted in order that, under those conditions, less than 25 % of substrate was degraded. Each value obtained represents the mean of these independent assays.

Surface Plasmon Resonance analysis - BIACORE

Surface plasmon resonance analysis was developed for the study of the interaction between RNases and RNA molecules as previously described (Arraiano *et al.*, 2008). Biacore SA chips were obtained from Biacore Inc. (GE Healthcare). The flow cells of the SA streptavidin sensor chip were coated with a low concentration of the following substrates. On flow cell 1, no substrate was added so this cell could be used as the control blank cell. On flow cell 2, a 5' biotinylated 25 nucleotide RNA oligomer (5'-CCCG ACACCAACCACUAAAAAAAAA-3') was added to allow the study of the protein interaction with a single-stranded RNA molecule. On flow cell 3, a 5' biotinylated 30-mer poly(A) substrate. The target substrates were captured on flow cells 2 and 3 by manually injecting 20 μl of a 500 nM solution of the substrates in 1 M NaCl at a 10 μl/min flow rate, as described in previous reports (Arraiano *et al.*, 2008; Arraiano *et al.*, 2010b; Park *et al.*, 2000), obtaining ~400 RU of response. The biosensor assay was run at 4 ºC in the buffer with 20 mM Tris-HCl pH8, 100 mM KCl, 1 mM DTT and 25 mM EDTA. The proteins were injected over flow cells 1, 2, and 3 for 2 min at concentrations of 10, 20, 30, 40, and 50 nM using a flow rate of 20 μl/min. All experiments included triple injections of each protein concentration to determine the reproducibility of the signal and control injections to assess the stability of the RNA surface during the experiment. Bound protein was removed with a 60 s wash with 2 M NaCl, which did not damage the substrate surface. Data from flow cell 1 were used to correct for refractive index changes and nonspecific binding. Rate constants and equilibrium constants were calculated using the BIA EVALUATION 3.0 software package, according to the fitting model 1:1 Languimir Binding.

Secondary Structure Prediction of the Lysine-Rich Tail of RNase R, Protein Modelling and Multiple Sequence Alignment

To predict the secondary structure of the lysine-rich tail of RNase R, we used the NPS@ server (Network Protein Sequence Analysis) (Combet *et al.*,

2000) with the GOR4 method (Garnier *et al.*, 1996) (http://npsa-pbil.ibcp.fr).

Structural model of the *E. coli* RNase R protein as well as RNase II_S1_R and RNase R_RNB_II constructions were performed by standard comparative modelling methods and the software DeepView (Guex and Peitsch, 1997), using the crystal structures of wild-type RNase II and the RNase II D209N mutant complexed with a 13 nucleotide poly(A) RNA as templates (PDB codes: 2IX1 and 2IX0 (Frazão *et al.*, 2006)). To optimize geometries, models were energy minimized using the GROMOS 43B1 force field implemented in DeepView (Guex and Peitsch, 1997), using 500 steps of steepest descent minimization followed by 500 steps of conjugate-gradient minimization. Sequence identity between RNase II and modelled RNase R was 26 %, with a Blast e-value of 3.3×10^{-43}. The quality of the model was checked using the analysis programs (Anolea, Gromos and Verify3D) provided by the SWISSMODEL server (http://swissmodel.expasy.org/) (Arnold *et al.*, 2006; Kiefer *et al.*, 2009; Schwede *et al.*, 2003). Structures were manipulated using the Swiss PDB viewer and were rendered using Pymol (DeLano, 2002).

Homologous sequences belonging to the RNase II-family of proteins in protein databases were obtained using Blast (Altschul *et al.*, 1997), and they were aligned using Clustal W (Thompson *et al.*, 1994) and T-COFFEE (Notredame *et al.*, 2000) algorithms.

RESULTS

Characterizing the Exoribonucleolytic Activity of the Hybrid Proteins Using a Poly(A) Substrate

RNase II and RNase R are members of the same family of exoribonucleases and therefore share catalytic and structural properties. However, they behave differently regarding the final product released: while RNase II releases a 4 nt fragment as its end-product, RNase R releases a mixture of 2 nt and 4 nt fragments, but 2 nt is the

predominant product (Figure 2, panels a and b) (Amblar *et al.*, 2006; Amblar *et al.*, 2007; Cannistraro and Kennell, 1994). The mechanism of RNase II has been elucidated and the size of the final product released depends on the aromatic residues Tyr253 and Phe358 that "clamp" the RNA (Barbas *et al.*, 2008; Frazão *et al.*, 2006). In RNase R, Phe429 is located in the position immediately downstream of the equivalent residue of Phe358 in RNase II (Barbas *et al.*, 2008). This residue may allow a partial "clamp" of the RNA and a 4 nt end-product is released. However, other oligoribonucleotides may still bind to the catalytic cavity and are able to be degraded up to the final 2 nt fragment (Matos *et al.*, 2009). Since these two enzymes also share a common 3D arrangement and have the same domain organization (Barbas *et al.*, 2008) we were interested in studying which domain(s) would be responsible for these differences. For this purpose, we exchanged the domains between RNase II and RNase R and constructed six hybrid proteins. In the designation chosen, the first word represents the protein that "received" the other domain as explained in Figure 1. The constructed proteins are: RNase II_CSD_R, which consists of RNase II with the two cold shock domains and the helix-turn-helix region from RNase R; RNase II_RNB_R, which consists of RNase II with the RNB domain of RNase R; RNase II_S1_R that is RNase II with the S1 and basic region from RNase R; RNase R_CSD_II, in which the CSDs from RNase II substitute those of RNase R; RNase R_RNB_II, which consists of RNase R with the RNB from RNase II; and finally, RNase R_S1_II, in which the S1 domain from RNase II substitutes the S1 domain from RNase R (Figure 1).

We started to analyze the protein activity by using a single-stranded poly(A) substrate. This substrate was chosen to determine the activity of the proteins, since it has been shown that RNase II-family members reflect a marked preference for poly(A) substrates (Barbas *et al.*, 2009; Matos *et al.*, 2009). To determine the activity of the hybrid proteins, we tested several different protein concentrations, and performed the calculations in triplicate using the values where less than 25 % of the

substrate was degraded. The results obtained are presented in Table 3 and the units of activity refer to the pmol of substrate which is degraded by 1 nM of protein in 1 min. When compared with their wild-type counterparts, we can see that the six engineered proteins have a reduced activity (Table 3). The decrease in the activity of the hybrid proteins ranges from 600 fold (RNase II_CSD_R protein) to 7000 fold (RNase II_S1_R protein). However, when compared with the inactive mutants RNase II D209N and RNase R D280N (Table 3), we can safely say that, although bearing a low activity, these proteins are still able to degrade RNA substrates. Since we are working with engineered proteins that do not exist in nature, we also need to consider the possibility that only a fraction of the hybrid proteins adopt a catalytically active conformation. In this case, the determination of the activity could be underestimated.

TABLE 3. Exoribonucleolytic Activity of Wild-type and Hybrid Proteins
Exoribonucleolytic activity was assayed using a 35 nt poly(A) chain as substrate. Activity assays were performed in triplicate.

Protein	Protein Activity *pmol subst.nmol prot^{-1}.min^{-1}*
wt RNase II	299,4 ± 36,0
RNase II_CSD_R	0,5 ± 0,05
RNase II_RNB_R	0,05 ± 0,002
RNase II_S1_R	0,04 ± 0,001
RNase II _S1_R_ΔLys1	0,01 ± 0,001
RNase II _S1_R_ΔLys2	0,01 ± 0,001
RNase II _S1_R_ΔLys3	0,01 ± 0,001
RNase II D209N	<0.0001
wt RNase R	130,8 ± 6,3
RNase R_CSD_II	0,04 ± 0,001
RNase R_RNB_II	0,02 ± 0,001
RNase R_S1_II	0,08 ± 0,002
RNase R D280N	<0.0001

Another objective of this work was to identify the end-product of each of these engineered proteins. To do so, we tested different conditions to ensure that all the enzymes had reached their end-product. As a consequence, we had to use higher protein concentrations for the hybrid proteins than those used for both RNase II and RNase R. Figures 2 to 5 show the representative assays from the several ones performed that we believe better illustrate the results obtained.

In RNase II_CSD_R, when we changed the CSD of RNase II by the ones from RNase R we observed that the protein behaved like RNase II (Figure 2, panel c). However, when we changed the RNB or S1 domains of RNase II by the equivalents of RNase R (as is the case in the RNase II_RNB_R and RNase II_S1_R proteins), we were able to see that the final product changed to 2 nt (Figure 2, panels d and e).

For RNase II_S1_R protein, it was possible to observe that the majority of the product released was a 4 nt fragment and only a small portion of substrate was able to be degraded until the 2 nt of length, contrary to what happened for RNase R (Figure 2, panel e). Thus, we can conclude that the S1 and RNB domains from RNase R are each sufficient to allow RNase II to behave like RNase R, and generate the 2 nt end-product.

When we changed the RNase R domains by the ones in RNase II (RNase R_CSD_II, RNase R_RNB_II and RNase R_S1_II proteins), we observed that the final product released was always a 2 nt (Figure 2, panels f to h). These results indicate that the RNB domain of RNase R is responsible for setting the final end-product. However, when the RNB domain of RNase II was inserted into RNase R (RNase R_RNB_II), the final product was not altered as expected, which suggested to us that the RNA-binding domains of RNase R are also involved, probably by inducing a different conformation of the protein.

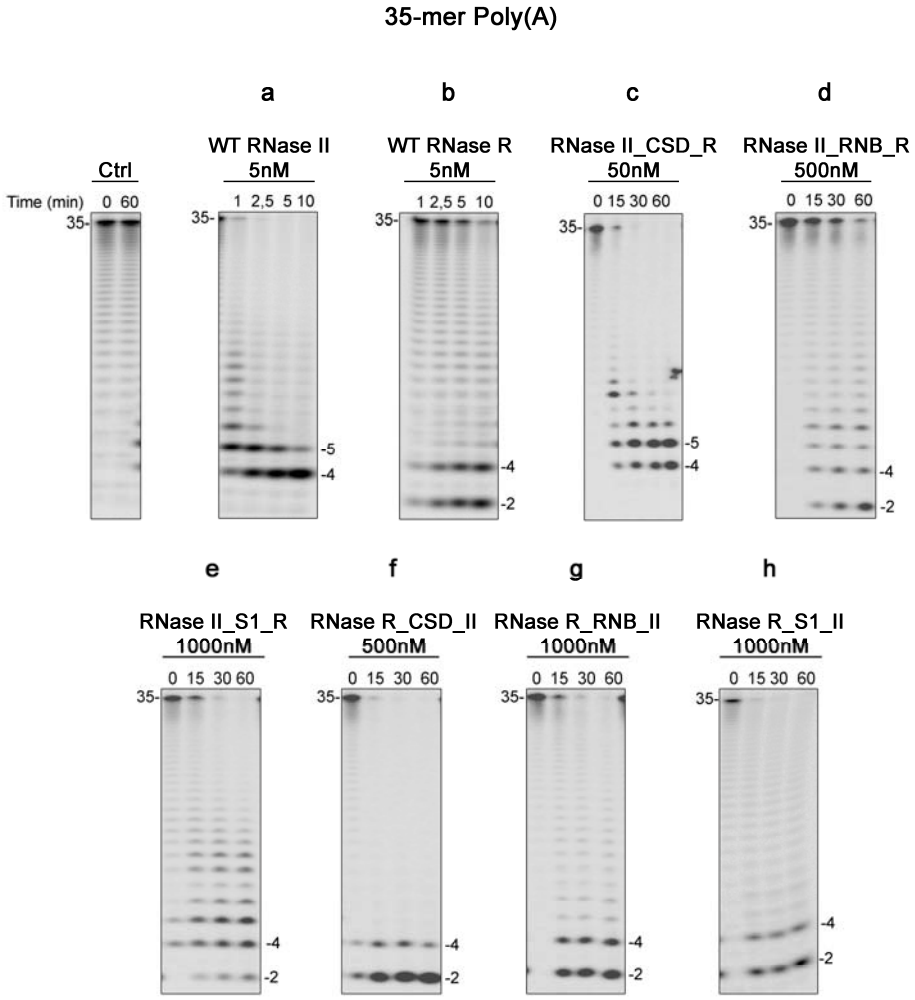

FIGURE 2. Exoribonuclease activity with a 35ss Poly(A) substrate: comparison of wild-type with hybrid enzymes. Activity assays were performed as described under Experimental Procedures using a poly(A) chain of 35 nt. The proteins used and their respective concentrations are shown. The wild-type enzymes were used as control. Samples were taken during the reaction at the time points indicated, and reaction products were analyzed in a 20 % polyacrylamide 19:1/7 M urea gel. Control reactions with no enzyme added (*Ctrl*) were incubated at the maximum reaction time for each protein. Length of substrates and degradation products are indicated in the figure.

The Hybrid Proteins Prefer Poly(A) Substrates

To see if the binding ability was affected in the hybrid proteins, we determined the dissociation constants by SPR using two different single-stranded substrates, a 25 nt RNA oligomer and a 30 nt poly(A) oligomer and compared them with the wild-type enzymes (Table 4). In all the cases, and for all the proteins, the affinity constants determined using the 30 nt poly(A) substrate were always lower when compared with those detected using the other ssRNA substrate. This was expected, and indicates that, like in the cases of wild-type RNase II and RNase R, the hybrid proteins constructed reflect their preference for poly(A) type substrates. However, in the case of RNase R_RNB_II and RNase II_S1_R that preference is not so marked (Table 4). The results obtained also showed that, for almost all proteins, the affinity is slightly reduced for both substrates when compared with the wild-type enzymes (Table 4). These differences are not significant however, they can help us explain the reduction in the activity of the hybrid proteins. However, the affinity of a protein is not always correlated with its activity. For example, the RNase II_D209N and RNase R_D280N mutants were inactive but the RNA affinity was not altered (Amblar and Arraiano, 2005; Barbas *et al.*, 2008; Matos *et al.*, 2009).

Degradation of Double-Stranded Substrates by Hybrid Proteins

To study which domains could be responsible for the differences regarding the ability to cleave double-stranded substrates, we tested the hybrid proteins against a 16–30ds substrate, that consists of a 30-mer ribonucleotide hybridized with a complementary 16-mer oligonucleotide, as described in Experimental Procedures. To detect the ribonucleolytic activity with this substrate, we tested several different concentrations of the various proteins to find the optimal conditions. In our assays, the hybrid proteins were active with double-stranded substrates when using as little as 10 nM of protein. However, in such conditions it was difficult to determine which was the real final product released and if, in fact, the protein was degrading the substrate. For this reason, in Figure 3 the protein concentrations used in the assays are extremely high.

Table 4. RNA Binding Affinity of the Hybrid Proteins. The dissociation constants (K_D) were determined by surface plasmon resonance using BIACORE 2000 with a 25 nt RNA oligomer (5' Biotin-CCCGACACCAACCACUAAAAAAAAA-3') and a 30 nt poly(A) RNA oligomer.

Protein	K_D *nM* 25-mer	K_D *nM* Poly(A)
wt RNase II	6.5 ± 0.4	1.3 ± 0.4
RNase II_CSD_R	16.0 ± 0.4	4.3 ± 0.3
RNase II_RNB_R	7.0 ± 0.9	2.0 ± 0.3
RNase II_S1_R	3.2 ± 0.5	1.3 ± 0.1
wt RNase R	3.2 ± 0.4	1.2 ± 0.1
RNase R_CSD_II	8.6 ± 0.7	5.1 ± 0.1
RNase R_RNB_II	5.4 ± 0.6	4.4 ± 0.1
RNase R_S1_II	10.1 ± 1.4	3.2 ± 0.2

The results showed that when RNase II has the N-terminal region of RNase R (RNase II_CSD_R) the hybrid protein behaved like RNase II since it was not able to degrade double-stranded substrates. However, the protein was capable to degrade a few more nucleotides than RNase II, releasing a 20 nt fragment instead of the usual 23 nt fragment (Figure 3, panels a to c). RNase II_RNB_R protein was able to cleave the 16–30ds substrate just like RNase R (Figure 3, panel d). It was previously described that RNase R needs a 3' single-stranded overhang of at least 7 nucleotides of length to attach to the substrate and proceed with the degradation (Vincent and Deutscher, 2006) and it is not able to cleave a substrate in the absence of a 3' end tail (Figure 4, panel a). However, the hybrid protein RNase II_RNB_R did not present this requirement since it was able to degrade double-stranded substrates in the absence of a 3' overhang (Figure 4, panel c). Even though only a small percentage of the 16–16ds substrate was degraded, this fact confirms that, as previously demonstrated (Matos *et al.*, 2009), the RNB domain from RNase R is the

one responsible for the degradation of double-stranded substrates. The substitution of only one RNase R binding domain (CSD or S1 domains) eliminates the requirement of a 3' single-stranded overhang for the degradation of dsRNA substrates. Surprisingly, the RNase II_S1_R protein was also able to cleave double-stranded substrates releasing a fragment with 2 nt of length (Figure 3, panel e). Nevertheless, for this protein the requirement for a 3' overhang was essential since it was not able to cleave the perfect double-stranded substrate (Figure 4, panel d). This suggests that the catalytic cavity of the protein is only accessible to single-stranded substrates, similarly to that which occurs with RNase II (Frazão *et al.*, 2006). This implies that the RNA is entering into the catalytic cavity in a single-stranded form, which means that the substrate is being unwound before its entry. Thus, the domain responsible for this action must be the S1 domain from RNase R. RNase R_CSD_II, RNase R_RNB_II and RNase R_S1_II proteins were able to cleave the double-stranded substrates similar to RNase R (Figure 3, panels f to h). When the RNB domain of RNase R was substituted by the one of RNase II (RNase R_RNB_II), the protein was still able to cleave the double-stranded substrate (Figure 3, panel g). In this case, the requirement for a 3' overhang was also verified, since the protein was not able to degrade the 16–16ds substrate (Figure 4, panel f). This suggests that the RNB domain from RNase R is not the only one responsible for the degradation of structured RNA.

In our work, we showed that the simple substitution of the RNB domain in RNase II for that of RNase R lead to the construction of a protein that was active against double-stranded substrates. The RNB domain does not seem to be acting alone in this process, because when switching the S1 domain from RNase II for the S1 domain from RNase R, the respective protein is also able to cleave double-stranded substrates (Figure 3). However, it seems that the RNB and S1 domains may act differently against structured RNA when they are in an RNase II context. While RNase R S1 domain requires a 3' single-stranded overhang to bind to the

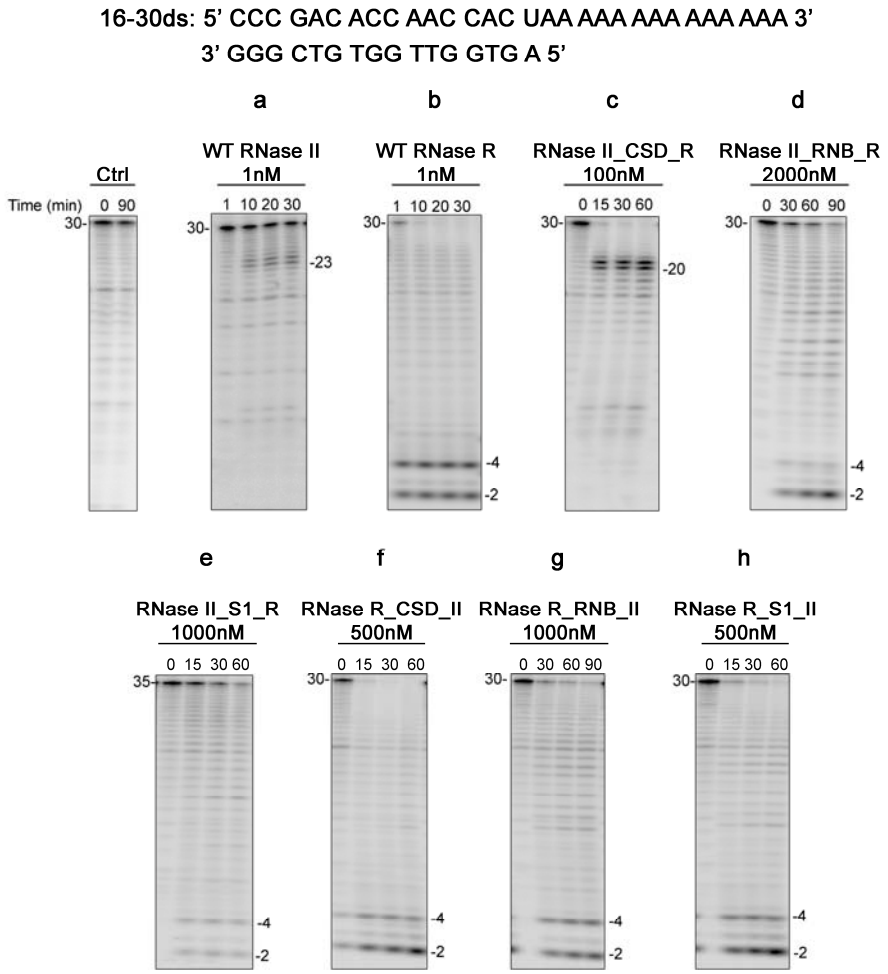

FIGURE 3. Exoribonuclease activity with 16–30ds substrate: comparison of wild-type with hybrid enzymes. Activity assays were performed as described under Experimental Procedures using a 30-mer oligoribonucleotide hybridized to the complementary 16-mer oligodeoxyribonucleotide, thus obtaining the corresponding double-stranded substrate 16–30ds. The proteins used and their respective concentrations are shown. The wild-type enzymes were used as control. Samples were taken during the reaction at the time points indicated, and reaction products were analyzed in a 20 % polyacrylamide 19:1/7 M urea gel. Control reactions with no enzyme added (*Ctrl*) were incubated at the maximum reaction time for each protein. Length of substrates and degradation products are indicated in the figure.

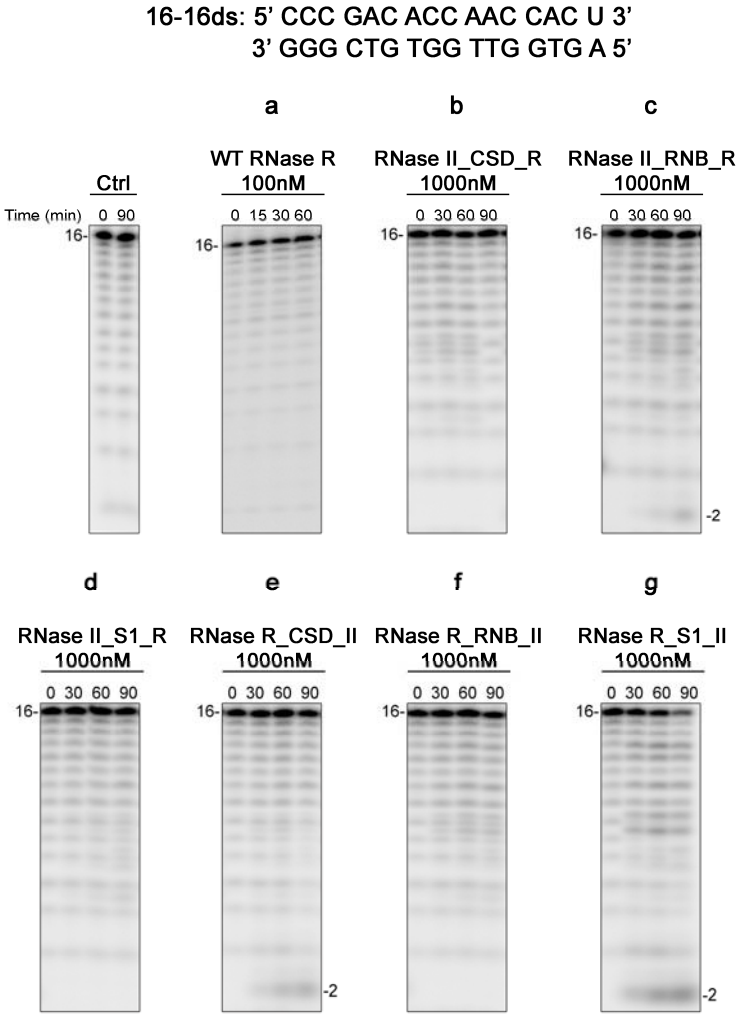

FIGURE 4. Exoribonuclease activity with 16–30ds substrate: comparison of wild-type with hybrid enzymes. Activity assays were performed as described under Experimental Procedures using a 16-mer oligoribonucleotide hybridized to the complementary 16-mer oligodeoxyribonucleotide, thus obtaining the corresponding double-stranded substrate 16–16ds. The proteins used and their respective concentrations are shown. The wild-type enzymes were used as control. Samples were taken during the reaction at the time points indicated, and reaction products were analyzed in a 20 % polyacrylamide 19:1/7 M urea gel. Control reactions with no enzyme added (*Ctrl*) were incubated at the maximum reaction time for each protein. Length of substrates and degradation products are indicated in the figure.

substrate and degrade it, the RNB domain from RNase R is able to bind and degrade structured RNA in the absence of a tail, as previously demonstrated (Matos *et al.*, 2009). The results obtained led us to further analyze the role of the C-terminal region of RNase R in the mechanism of degradation of double-stranded substrates.

Unravelling the Role of the Lysine-Rich Tail of RNase R

Since the S1 domain from RNase R is allowing the cleavage of double-stranded substrates, we wanted to discriminate which region could be conferring that property. By comparing the C-terminal region of both RNase II and RNase R proteins, it is possible to observe that, apart from the S1 domain, RNase R has an extra lysine-rich tail (Figure 1). To understand the role of this region in RNA degradation, we predicted its secondary structure in the Network Protein Sequence Analysis as described in Experimental Procedures. The results predicted showed that this region is formed by four alpha-helices: the first (from the C-terminal end) comprises the last 22 aa of the protein, the second is formed by the aa 781 to 802, the third comprises aa 745 to 758 and the fourth, which is smaller when compared with the others, is constituted by aa 728 to 738 (note that this numbering refers to RNase R and not to the hybrid protein, as indicated in the figure) (Figure 1). To investigate the contribution of the three major alpha-helices in the degradation of double-stranded substrates, we introduced three stop codons into the hybrid protein RNase II_S1_R as indicated in Figure 1, thus obtaining the three proteins, RNase II_S1_RΔlys1, RNase II_S1_RΔlys2 and RNase II_S1_RΔlys3, which lack one, two or three alpha-helices, respectively. The determination of the role of the C-terminal region of the S1 domain from RNase R in the degradation of double-stranded substrates was performed in an RNase II context, using the hybrid protein RNase II_S1_R. The mutations were introduced in this protein and not in RNase R wt because the RNB domain of RNase R by itself is able to degrade double-stranded substrates (Matos *et al.*, 2009) and this characteristic could bias the results

obtained. The proteins were then analyzed regarding their activity against single- and double-stranded substrates and RNA affinity.

We also determined the exoribonucleolytic activity of these three proteins, and we could observe that the activity is 4 fold reduced when we compare with RNase II_S1_R (Table 3). This indicates that the lysine-rich tail is also contributing for the activity of RNase II_S1_R protein. When the substrate used was the single-stranded one, the results obtained were similar to those obtained for the RNase II_S1_R hybrid protein, since all the three proteins tested released a 2 nt fragment as end-product (Figure 5A). When we tested the double-stranded substrate 16–30ds, we could observe some differences between these proteins. As already mentioned, the RNase II_S1_R is able to cleave double-stranded substrates. The same behaviour is observed when the first and second alpha helices are absent (in RNase II_S1_R_Δlys1 and RNase II_S1_R_Δlys2 proteins) (Figure 5B, panels b and c). However, when we removed all three helices, the protein RNase II_S1_R_Δlys3 was not able to degrade the substrate tested (Figure 5B, panel d). These results indicate that the lysine-rich region can be involved in the degradation of double-stranded substrates in RNase R. We also measured the RNA affinity of these proteins with the two different substrates tested previously and compared the data with the values obtained with the RNase II_S1_R protein (Table 5). For both substrates used it was possible to see that the K_D value rose slightly when the helices were removed. In the case of the 25ss substrate, the hybrid protein II_S1_R presented a K_D value that was equivalent to the one presented by RNase R, which was 3.2 nM for both proteins (Table 5). When the three helices were absent, the K_D value presented by the II_S1_R_Δlys3 protein became closer to the one presented by RNase II wt (6.9 ± 0.2 and 6.5 ± 0.4 nM, respectively). The results obtained indicate that the lysine rich tail from RNase R is also responsible for a higher affinity for some RNA substrates.

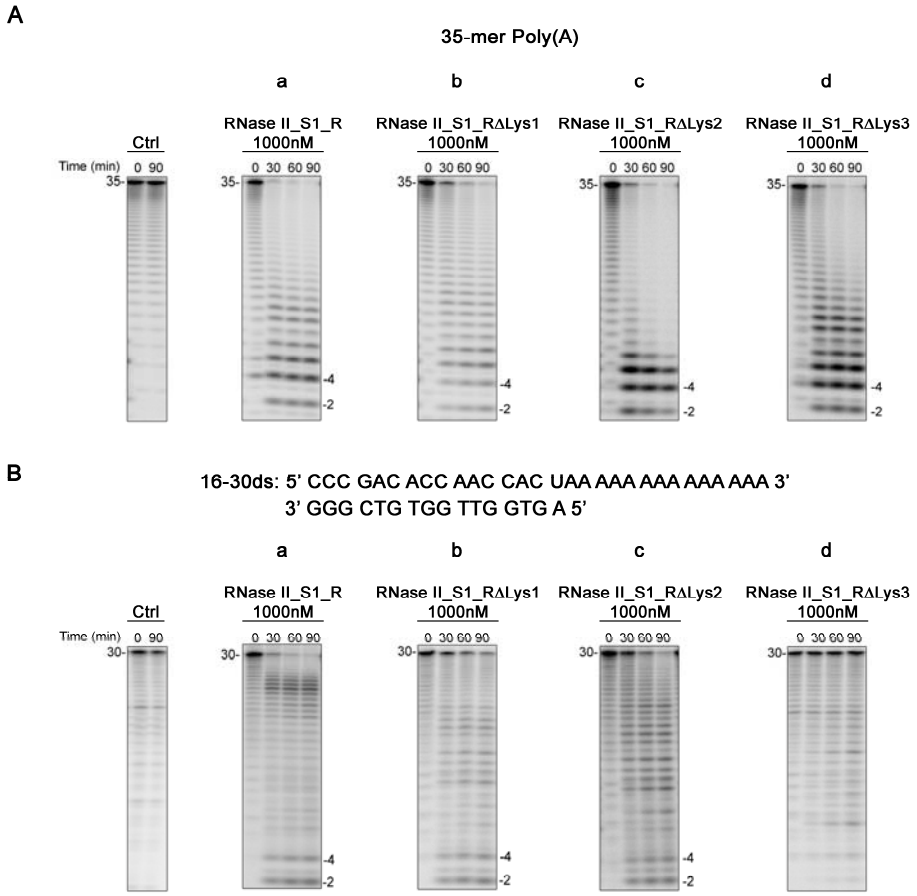

FIGURE 5. Exoribonuclease activity of RNase II_S1_R and ΔLys mutants. Activity assays were performed as described under Experimental Procedures using a poly(A) chain of 35 nt (A), and a 30-mer oligoribonucleotide hybridized to the complementary 16-mer oligodeoxyribonucleotide, thus obtaining the corresponding double stranded substrate 16–30ds (B). The proteins used and their respective concentrations are shown. The wild-type enzyme was used as control. Samples were taken during the reaction at the time points indicated, and reaction products were analyzed in a 20 % polyacrylamide 19:1/7 M urea gel. Control reactions with no enzyme added (*Ctrl*) were incubated at the maximum reaction time for each protein. Length of substrates and degradation products are indicated in the figure.

TABLE 5. RNA Binding Affinity of the Δlys Hybrid Proteins. The dissociation constants (K_D) were determined by surface plasmon resonance using BIACORE 2000 with a 25 nt RNA oligomer (5' Biotin-CCCGACACCAACCACUAAAAAAAAA-3') and a 30 nt poly(A) RNA oligomer.

Protein	K_D *nM* 25-mer	K_D *nM* Poly(A)
RNase II_S1_R	3.2 ± 0.5	1.3 ± 0.1
RNase II _S1_RΔLys1	4.2 ± 0.4	1.4 ± 0.3
RNase II _S1_RΔLys2	5.5 ± 0.9	1.4 ± 0.1
RNase II _S1_RΔLys3	6.9 ± 0.2	2.4 ± 0.3

DISCUSSION

To understand which domains are responsible for the differences observed between RNase II and RNase R regarding the RNA degradation, we switched domains between them and analyzed the activity of the six hybrid proteins against single- and double-stranded substrates.

When we used a single-stranded substrate, we observed that the presence of the RNB domain from RNase R in RNase II changed the final product from 4 to a mixture of 4 and 2 nt (Figure 2, panel d). This result clearly indicates that it is in the RNB domain of both proteins that resides the difference regarding the releasing of the final product after cleavage. However, when the RNB domain from RNase II was inserted into RNase R, the end-product was not altered to 4 nt as expected by the previous result (Figure 2, panel g). One possible explanation for this could be the fact that the differences in both RNB domains can not be related with the amino acid sequence but with the conformation that the protein acquires when it is folded. In the RNase R_RNB_II protein, the presence of the CSD and S1 domains of RNase R can lead to a subtle conformational rearrangement of the catalytic cavity in the RNB domains of RNase II. To elucidate this question, we modelled both proteins and compared them with RNase II structure (Frazão *et al.*, 2006) and RNase R model (Barbas

et al., 2008) (Figure 6A). In fact, by comparing the four models, it is possible to see that all proteins share an almost identical structure. If we analyze in more detail the catalytic cavity of all proteins, no dramatic changes are observed (data not shown). So, it appears that the differences observed in the activity of these enzymes are not due to changes in the overall protein structure. A suitable explanation could be the different nature of the residues located in S1 domain in close contact to RNA (Figure 6B to D, purple residues). In RNase II, the residues in S1 domain which are in close contact with the RNA molecule are Ser572, Gly574, Phe588, Pro590, Pro592, Phe593, Arg632, Thr635, and Ser637 as indicated in Figure 6B. In the protein RNase II_S1_R, the residues from the S1 domain from RNase R that contact the RNA molecule are different (Thr655, Phe657, Leu671, His673, Ser675, Ser676, Asn714, Glu717, Lys719), that implies differences in the properties of the relationship between RNA and S1 (Figure 6C). When compared with other proteins of the family, the nature of RNA-contacting residues is, as expected, more conserved among members of the same sub-family (RNase II sub-family versus RNase R sub-family) and, to some extent, different between these sub-families (Figure 6D). Moreover, when comparing the interactions between the RNB and the S1 domains of RNase II (Figure 6B) and the RNB of RNase II with the S1 from RNase R (Figure 6C), it is possible to observe differences regarding the residues involved in the contact of the S1 domain with the RNB. While in S1 domain from RNase II the residues in contact with the RNB domain are Arg577, Arg579, Asn583, Glu606, Lys619, Val620, and Thr621, in the RNase II_S1_R protein we can see that Phe660, Arg662, Leu666, Ile668, Gln689, Arg701, Leu702, and Gly703 are the ones involved in this interaction (Figure 6B to D). The residues responsible for the domain-domain interactions in the S1 domain are conserved between sub-families but not conserved in RNase II and RNase R (Figure 6D). The different nature of the residues in S1 domain that contact to the same residues in RNB domain (as this domain is conserved both in RNase II and RNase II_S1_R proteins) could be

responsible for changes in the relative position of S1 domain in the overall structure of the RNase II_S1_R protein (Figure 6C). It could not be discarded that the alterations in the interactions of the RNB and S1 domains in this hybrid protein may induce a subtle conformational change in some residues near the catalytic cavity. These modifications may result in a higher affinity for RNA in the catalytic cavity, and a fraction of the 4 nt fragments can still bind to the protein and be cleaved until they reach the 2 nt of length.

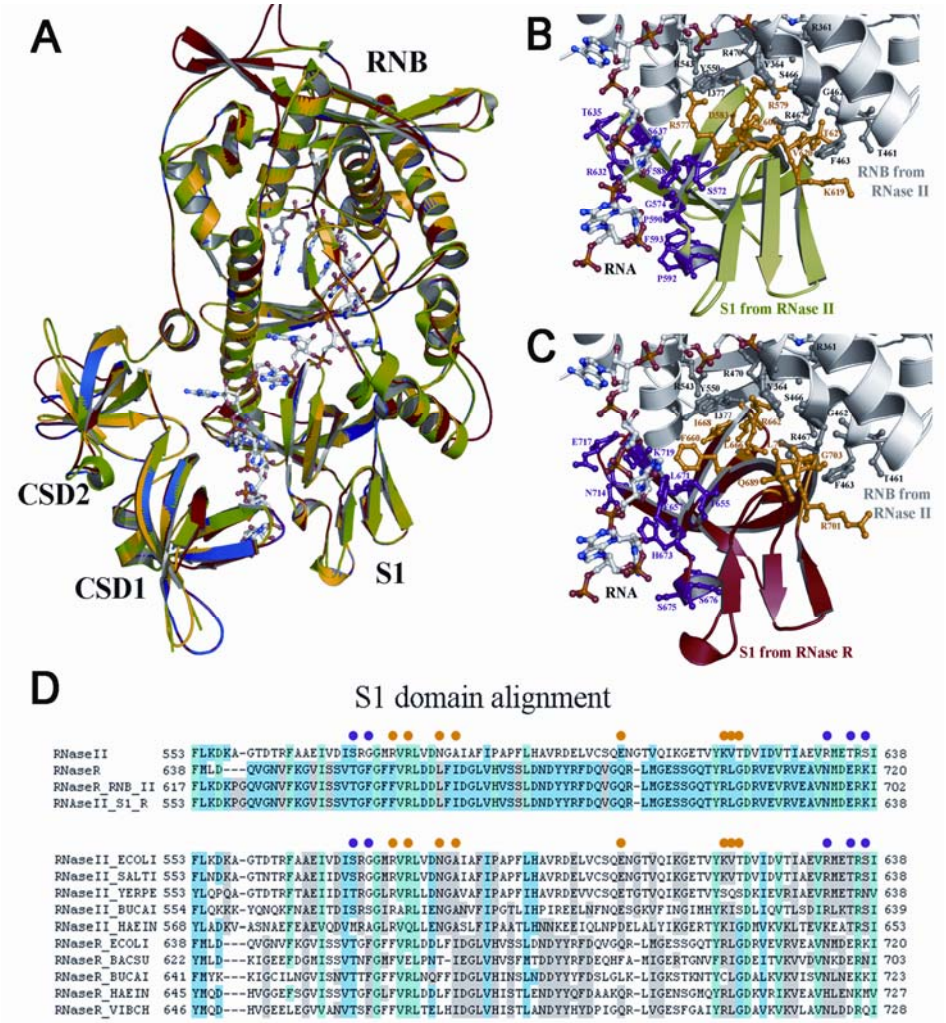

FIGURE 6. Modelling the hybrid proteins RNase II_S1_R and RNase R_RNB_II. A. Representation of RNase II structure (green) and the predictive 3D models of the *E. coli* RNase R (red), RNase II_S1_R (yellow) and RNase R_RNB_II (blue) proteins **B.** Residues of S1 domain from RNase II (green cartoon, residues in purple) in close contact to RNA: Ser572, Gly574, Phe588, Pro590, Pro592, Phe593, Arg632, Thr635 and Ser637; Residues of S1 domain from RNase II (residues in orange: Arg577, Arg579, Asn583, Glul606, Lys619, Val620 and Thr621) in close contact to RNB domain from RNase II (residues in dark grey: Arg361, Tyr364, Ile377, Thr461, Gly462, Phe463, Ser466, Arg467, Arg470, Arg543, and Tyr550). **C.** Residues of S1 domain from RNase R (red cartoon, residues in purple) in close contact to RNA: Thr655, Phe657, Leu671, His673, Ser675, Ser676, Asn714, Glu717 and Lys719); Residues of S1 domain from RNase R (residues in orange: Phe660, Arg662, Leu666, Ile668, Gln689, Arg701, Leu702 and Gly703) in close contact to RNB domain from RNase II (residues in dark grey: Arg361, Tyr364, Ile377, Thr461, Gly462, Phe463, Ser466, Arg467, Arg470, Arg543, and Tyr550). **D.** Top: structure alignment of the S1 domain of RNase II, RNase R and the constructed polypeptides RNase R_RNB_II and RNaseII_S1_R. Bottom: alignment of the S1 domain of RNase II and RNase R from different bacteria (*Escherichia coli* –ECOLI-, *Salmonella typhimurium* –SALTI-, *Yersinia pestis* –YERPE-, *Buchnera aphidicola* -BUCAI-, *Haemophilus influenzae* –HAEIN-, *Bacillus subtilis* –BACSU- and *Vibrio cholerae* –VIBCH-). Sequences from *E. coli* are included in both alignments for comparison purposes. Multiple alignments are coloured according to conservation. Position of some important residues is highlighted: purple dots: residues in S1 domain contacting RNA molecule; orange dots: residues in S1 domain contacting RNB domain.

When we determined the K_D values of the hybrid proteins we observed that with the poly(A) substrate the affinity was reduced when compared with the 25-mer. This indicates that, like for wild-type RNase II and RNase R, the hybrid proteins also reflect their marked preference for poly(A) type substrates.

Regarding the degradation of the double-stranded substrate, five of the six hybrid proteins tested were able to overcome the secondary structures

and degrade the substrates totally. It was previously described that the RNB domain from RNase R is able, by itself, to degrade double-stranded substrates (Matos *et al.*, 2009; Vincent and Deutscher, 2009). So, it was not a surprise to see that when we switched the RNB domain from RNase II for the one from RNase R, the resultant protein was able to cleave double-stranded substrates. The same was valid for the hybrid proteins where the RNB of RNase R is present (RNase R_CSD_II and RNase R_S1_II). We also observed that the requirement of a single-stranded 3' overhang to degrade dsRNA is a property resulting from the association of the RNB domain with the CSD and S1 RNA-binding domains of RNase R. The most intriguing result was obtained with the RNase II_S1_R and RNase R_RNB_II proteins. In both cases, the RNB from RNase R is not present and the proteins are still able to overcome secondary structures (Figure 3). The common element between these proteins is the S1 domain from RNase R, thus this domain has to be the one responsible for the behaviour observed for these proteins. Moreover, the degradation of structured RNA molecules by the S1 domain implies the existence of a 3' single-stranded overhang for cleavage to occur. In fact, in the C-terminal region of RNase R there is a lysine-rich region positioned after the S1 domain and this feature is absent in S1 from RNase II (Figure 1). Recently it was shown that the lysine-rich region of RNase R is important for recruitment of stalled ribosomes and for the selection of defective transcripts to be degraded (Ge *et al.*, 2010). If we analyze other proteins from the RNase II-family of enzymes, we can see that this lysine-rich tail is only present in RNase R-like proteins, which led us to hypothesize that it could be also involved in the degradation of structured RNA. The results obtained confirm that, in an RNase II context, the lysine-rich region is important for the degradation of double-stranded substrates. Our results are in agreement with recent findings that show that RNase R could have some "helicase" activity which is conferred by the binding domains (Awano *et al.*, 2010). Our experiments indicate that the "helicase" activity could be of the responsibility of the S1 domain of RNase

R, namely of the lysine-rich tail in the C-terminus of the protein, which can be responsible for the unwinding of the substrate. Moreover, we showed that this activity is intrinsic to RNase R, since this protein was able to degrade double-stranded substrates in the absence of ATP, in contrast to other helicases.

With this work we intended to unravel the different modes of action between the two major *E. coli* exoribonucleases, RNase II and RNase R, namely we aimed to explain their different behaviours. With the lack of the 3D structure of RNase R, only biochemical and modelling studies can help disclose the differences between these two homologue enzymes, belonging to the same RNase II family of proteins. In this report we show that both S1 and RNB domains from RNase R, in separate, allow the appearance of the characteristic 2 nt end-product and the degradation of double-stranded substrates. Finally, we demonstrated that the degradation of structured RNA is tail-independent when the catalytic domain from RNase R is no longer associated with the RNA-binding domains from RNase R. As such, the results obtained in this report can be extrapolated for the comprehension of the mode of action of other members of the RNase II family. Moreover, this work represents a major breakthrough in the distinction between these two so close but yet so different exoribonucleases.

ACKNOWLEDGMENTS

We thank Prof. Arsénio M. Fialho for the critical reading, and Miguel Luís for helping with the images. We also thank Biomol-Informatics SL <www.biomolinformatics.com> for bioinformatics advising. R. G. Matos was a recipient of a PhD fellowship and A. Barbas was a recipient of a Post Doctoral fellowship, both of them funded by FCT- Fundação para a Ciência e Tecnologia, Portugal.

REFERENCES

Altschul, S.F., Madden, T.L., Schaffer, A.A., Zhang, J., Zhang, Z., Miller, W., and Lipman, D.J. (1997) Gapped BLAST and PSI-BLAST: a new generation of protein database search programs. *Nucleic Acids Res* **25**: 3389-3402.

Amblar, M., and Arraiano, C.M. (2005) A single mutation in *Escherichia coli* ribonuclease II inactivates the enzyme without affecting RNA binding. *FEBS J* **272**: 363-374.

Amblar, M., Barbas, A., Fialho, A.M., and Arraiano, C.M. (2006) Characterization of the functional domains of *Escherichia coli* RNase II. *J Mol Biol* **360**: 921-933.

Amblar, M., Barbas, A., Goméz-Puertas, P., and Arraiano, C.M. (2007) The role of the S1 domain in exoribonucleolytic activity: substrate specificity and multimerization. *RNA* **13**: 317-327.

Andrade, J.M., Cairrão, F., and Arraiano, C.M. (2006) RNase R affects gene expression in stationary phase: regulation of ompA. *Mol Microbiol* **60**: 219-228.

Andrade, J.M., and Arraiano, C.M. (2008) PNPase is a key player in the regulation of small RNAs that control the expression of outer membrane proteins. *RNA* **14**: 543-551.

Arnold, K., Bordoli, L., Kopp, J., and Schwede, T. (2006) The SWISS-MODEL workspace: a web-based environment for protein structure homology modelling. *Bioinformatics* **22**: 195-201.

Arraiano, C.M., Barbas, A., and Amblar, M. (2008) Characterizing ribonucleases in vitro examples of synergies between biochemical and structural analysis. *Methods Enzymol* **447**: 131-160.

Arraiano, C.M., Andrade, J.M., Domingues, S., Guinote, I.B., Malecki, M., Matos, R.G., Moreira, R.N., Pobre, V., Reis, F.P., Saramago, M., Silva, I.J., and Viegas, S.C. (2010a) The critical role of RNA processing and degradation in the control of gene expression. *FEMS Microbiol Rev*.

Arraiano, C.M., Matos, R.G., and Barbas, A. (2010b) RNase II: The finer details of the Modus operandi of a molecular killer. *RNA Biol* **7**: 276-278.

Awano, N., Rajagopal, V., Arbing, M., Patel, S., Hunt, J., Inouye, M., and Phadtare, S. (2010) *Escherichia coli* RNase R has dual activities, helicase and RNase. *J Bacteriol* **192**: 1344-1352.

Barbas, A., Matos, R.G., Amblar, M., Lopez-Viñas, E., Goméz-Puertas, P., and Arraiano, C.M. (2008) New insights into the mechanism of RNA degradation by ribonuclease II: identification of the residue responsible for setting the RNase II end product. *J Biol Chem* **283**: 13070-13076.

Barbas, A., Matos, R.G., Amblar, M., Lopez-Vinas, E., Gomez-Puertas, P., and Arraiano, C.M. (2009) Determination of key residues for catalysis and

RNA cleavage specificity: one mutation turns RNase II into a "SUPER-ENZYME". *J Biol Chem* **284**: 20486-20498.

Cairrão, F., Chora, A., Zilhão, R., Carpousis, A.J., and Arraiano, C.M. (2001) RNase II levels change according to the growth conditions: characterization of *gmr*, a new *Escherichia coli* gene involved in the modulation of RNase II. *Mol Microbiol* **39**: 1550-1561.

Cairrão, F., Cruz, A., Mori, H., and Arraiano, C.M. (2003) Cold shock induction of RNase R and its role in the maturation of the quality control mediator SsrA/tmRNA. *Mol Microbiol* **50**: 1349-1360.

Cairrão, F., and Arraiano, C.M. (2006) The role of endoribonucleases in the regulation of RNase R. *Biochem Biophys Res Commun* **343**: 731-737.

Cannistraro, V.J., and Kennell, D. (1994) The processive reaction mechanism of ribonuclease II. *J Mol Biol* **243**: 930-943.

Cheng, Z.F., Zuo, Y., Li, Z., Rudd, K.E., and Deutscher, M.P. (1998) The *vacB* gene required for virulence in *Shigella flexneri* and *Escherichia coli* encodes the exoribonuclease RNase R. *J Biol Chem* **273**: 14077-14080.

Cheng, Z.F., and Deutscher, M.P. (2002) Purification and characterization of the *Escherichia coli* exoribonuclease RNase R: comparison with RNase II. *J Biol Chem* **277**: 21624-21629.

Cheng, Z.F., and Deutscher, M.P. (2005) An important role for RNase R in mRNA decay. *Mol Cell* **17**: 313-318.

Combet, C., Blanchet, C., Geourjon, C., and Deleage, G. (2000) NPS@: network protein sequence analysis. *Trends Biochem Sci* **25**: 147-150.

DeLano, W.L. (2002) The PyMOL Molecular Graphics System, 0.83 ed. *DeLano Scientific, San Carlos, CA.*

Deutscher, M.P., and Reuven, N.B. (1991) Enzymatic basis for hydrolytic versus phosphorolytic mRNA degradation in *Escherichia coli* and *Bacillus subtilis*. *Proc Natl Acad Sci U S A* **88**: 3277-3280.

Domingues, S., Matos, R.G., Reis, F.P., Fialho, A.M., Barbas, A., and Arraiano, C.M. (2009) Biochemical characterization of the RNase II family of exoribonucleases from the human pathogens *Salmonella typhimurium* and *Streptococcus pneumoniae*. *Biochemistry* **48**: 11848-11857.

Dziembowski, A., Lorentzen, E., Conti, E., and Seraphin, B. (2007) A single subunit, Dis3, is essentially responsible for yeast exosome core activity. *Nat Struct Mol Biol* **14**: 15-22.

Erova, T.E., Kosykh, V.G., Fadl, A.A., Sha, J., Horneman, A.J., and Chopra, A.K. (2008) Cold shock exoribonuclease R (VacB) is involved in *Aeromonas hydrophila* pathogenesis. *J Bacteriol* **190**: 3467-3474.

Frazão, C., McVey, C.E., Amblar, M., Barbas, A., Vonrhein, C., Arraiano, C.M., and Carrondo, M.A. (2006) Unravelling the dynamics of RNA

degradation by ribonuclease II and its RNA-bound complex. *Nature* **443**: 110-114.

Garnier, J., Gibrat, J.F., and Robson, B. (1996) GOR method for predicting protein secondary structure from amino acid sequence. *Methods Enzymol* **266**: 540-553.

Ge, Z., Mehta, P., Richards, J., and Karzai, A.W. (2010) Non-stop mRNA decay initiates at the ribosome. *Mol Microbiol* **78**: 1159-1170.

Grossman, D., and van Hoof, A. (2006) RNase II structure completes group portrait of 3' exoribonucleases. *Nat Struct Mol Biol* **13**: 760-761.

Guex, N., and Peitsch, M.C. (1997) SWISS-MODEL and the Swiss-PdbViewer: an environment for comparative protein modeling. *Electrophoresis* **18**: 2714-2723.

Kiefer, F., Arnold, K., Kunzli, M., Bordoli, L., and Schwede, T. (2009) The SWISS-MODEL Repository and associated resources. *Nucleic Acids Res* **37**: D387-392.

Lebreton, A., Tomecki, R., Dziembowski, A., and Seraphin, B. (2008) Endonucleolytic RNA cleavage by a eukaryotic exosome. *Nature* **456**: 993-996.

Matos, R.G., Barbas, A., and Arraiano, C.M. (2009) RNase R mutants elucidate the catalysis of structured RNA: RNA-binding domains select the RNAs targeted for degradation. *Biochem J* **423**: 291-301.

Matos, R.G., Barbas, A., and Arraiano, C.M. (2010) Comparison of EMSA and SPR for the characterization of RNA-RNase II complexes. *Protein J* **29**: 394-397.

Mian, I.S. (1997) Comparative sequence analysis of ribonucleases HII, III, II PH and D. *Nucleic Acids Res* **25**: 3187-3195.

Mitchell, P., Petfalski, E., Shevchenko, A., Mann, M., and Tollervey, D. (1997) The exosome: a conserved eukaryotic RNA processing complex containing multiple 3'-->5' exoribonucleases. *Cell* **91**: 457-466.

Notredame, C., Higgins, D.G., and Heringa, J. (2000) T-Coffee: A novel method for fast and accurate multiple sequence alignment. *J Mol Biol* **302**: 205-217.

Park, S., Myszka, D.G., Yu, M., Littler, S.J., and Laird-Offringa, I.A. (2000) HuD RNA recognition motifs play distinct roles in the formation of a stable complex with AU-rich RNA. *Mol Cell Biol* **20**: 4765-4772.

Schaeffer, D., Tsanova, B., Barbas, A., Reis, F.P., Dastidar, E.G., Sanchez-Rotunno, M., Arraiano, C.M., and van Hoof, A. (2009) The exosome contains domains with specific endoribonuclease, exoribonuclease and cytoplasmic mRNA decay activities. *Nat Struct Mol Biol* **16**: 56-62.

Schwede, T., Kopp, J., Guex, N., and Peitsch, M.C. (2003) SWISS-MODEL: An automated protein homology-modeling server. *Nucleic Acids Res* **31**: 3381-3385.

Studier, F.W., and Moffatt, B.A. (1986) Use of bacteriophage T7 RNA polymerase to direct selective high-level expression of cloned genes. *J Mol Biol* **189**: 113-130.

Taylor, R.G., Walker, D.C., and McInnes, R.R. (1993) *E. coli* host strains significantly affect the quality of small scale plasmid DNA preparations used for sequencing. *Nucleic Acids Res* **21**: 1677-1678.

Thompson, J.D., Higgins, D.G., and Gibson, T.J. (1994) CLUSTAL W: improving the sensitivity of progressive multiple sequence alignment through sequence weighting, position-specific gap penalties and weight matrix choice. *Nucleic Acids Res* **22**: 4673-4680.

Tobe, T., Sasakawa, C., Okada, N., Honma, Y., and Yoshikawa, M. (1992) vacB, a novel chromosomal gene required for expression of virulence genes on the large plasmid of *Shigella flexneri*. *J Bacteriol* **174**: 6359-6367.

Tsao, M.Y., Lin, T.L., Hsieh, P.F., and Wang, J.T. (2009) The 3'-to-5' exoribonuclease (encoded by HP1248) of *Helicobacter pylori* regulates motility and apoptosis-inducing genes. *J Bacteriol* **191**: 2691-2702.

Vincent, H.A., and Deutscher, M.P. (2006) Substrate recognition and catalysis by the exoribonuclease RNase R. *J Biol Chem* **281**: 29769-29775.

Vincent, H.A., and Deutscher, M.P. (2009) The roles of individual domains of RNase R in substrate binding and exoribonuclease activity. The nuclease domain is sufficient for digestion of structured RNA. *J Biol Chem* **284**: 486-494.

Zilhão, R., Camelo, L., and Arraiano, C.M. (1993) DNA sequencing and expression of the gene rnb encoding *Escherichia coli* ribonuclease II. *Mol Microbiol* **8**: 43-51.

Zilhão, R., Cairrão, F., Régnier, P., and Arraiano, C.M. (1996) PNPase modulates RNase II expression in *Escherichia coli*: implications for mRNA decay and cell metabolism. *Mol Microbiol* **20**: 1033-1042.

Zuo, Y., and Deutscher, M.P. (2001) Exoribonuclease superfamilies: structural analysis and phylogenetic distribution. *Nucleic Acids Res* **29**: 1017-1026.

Zuo, Y., Vincent, H.A., Zhang, J., Wang, Y., Deutscher, M.P., and Malhotra, A. (2006) Structural basis for processivity and single-strand specificity of RNase II. *Mol Cell* **24**: 149-156.

Chapter 5

Discussion and Future Perspectives

THE ROLE OF CONSERVED AMINO ACIDS IN THE MECHANISM OF DEGRADATION BY RNase II

Structural and functional studies have helped unravelling the mechanism of RNA degradation by RNase II. During catalysis there are some highly conserved residues which are in close contact with RNA molecule (Frazão *et al.*, 2006). It was already known that Asp209, located in the active site of the protein, was essential for the activity of the enzyme, since its substitution by an asparagine completely abolished the activity without affecting RNA binding (Amblar and Arraiano, 2005). The same results were also obtained with the eukaryotic homologue from yeast, the Rrp44/Dis3 protein (Dziembowski *et al.*, 2007). Other three aspartate residues can be found in the active center of RNase II, Asp201, Asp207 and Asp210. Together with Asp209, they were postulated to position the RNA molecule correctly and promote the nucleophilic attack of the phosphodiester bond (Frazão *et al.*, 2006). By mutational analysis, it was shown that the aspartates are important for the activity of RNase II. However, they are not equivalent in their function, with D209 being the only essential for the activity of the enzyme (Barbas *et al.*, 2008). Analysing the binding ability of the D201N, D207N and D210N mutant proteins, we were able to see that it was slightly reduced and the amino acid change led to the formation of unstable complexes. This indicated that, although not directly involved in RNA binding, Asp 201, 207 and 210 are contributing to the stabilization of the RNA-RNase II complexes (Barbas *et al.*, 2008; Matos *et al.*, 2010).

The last five nucleotides counting from the 3' end of the RNA molecules are stacked between the aromatic residues Tyr253 and Phe358 (Frazão *et al.*, 2006). The role of these residues was also previously determined. It was suggested that Phe358 may function as a "propeller" by helping to push the last nucleotide into the catalytic site. In the absence of this residue, the protein is ~2 fold more active than the wild-type and lead to an accumulation of a 5 nt fragment (Barbas *et al.*, 2008). The most

surprisingly result was obtained when we changed the Tyr253 into an alanine. In this case, we were expecting that the protein could not be active, since the "clamping" of the RNA molecule at the 3' end was not possible any more. However, the mutant protein still retained 25 % of the activity and the final product released changed from 4 to 10 nt (Barbas *et al.*, 2008). The 3D structure of RNase II showed that 10 nt is the minimum size necessary to the RNA molecule to be able to contact with both anchoring and catalytic regions. For fragments shorter than 10 nt, the RNA will only contact with the catalytic pocket, and RNase II becomes distributive (Cannistraro and Kennell, 1994; Frazão *et al.*, 2006). The absence of Tyr253 may cause the loosening of the substrate in the catalytic region, suggesting that the binding to the anchoring region is essential to maintain the RNA molecule attached to the protein. The determination of the dissociation constants for this mutant showed that this residue is, in fact, important for the RNA binding at the 3' position (Barbas *et al.*, 2008). Moreover, by EMSA it was possible to see that the protein-RNA complex is less stable for the Y253 mutant than for the wild-type (Matos *et al.*, 2010).

The role of these residues was determined before this Doctoral work had started. However, other important amino acids located in the catalytic activity had an unknown function in the mechanism of degradation by RNase II. In the first part of this Doctoral work the aim was to continue the characterization of the role of the highly conserved amino acids in the mechanism of action of RNase II, namely their importance in catalysis and in the RNA *versus* DNA discrimination.

Besides the aspartates located in the active site, we can also find an arginine in the position 500. This residue was postulated to assist in catalysis by fixing the phosphodiester bond at the cleavage position (Frazão *et al.*, 2006). We then changed it into an alanine and the enzyme practically became inactive. In order to detect some activity we need to use higher protein concentrations and increase the reaction time. Even in these conditions, the mutant protein was not able to completely degrade

the RNA substrates until the typical end-product of 4 nt of length (Barbas *et al.*, 2009). Similarly to what was reported for Asp209 (which is also crucial for the activity of the protein) (Amblar and Arraiano, 2005), in the R500A mutant, no changes in the binding ability of this mutant were observed. However, R500A complexes are less stable when compared to the ones from the wild-type and D209N proteins (Barbas *et al.*, 2009; Matos *et al.*, 2010). These results support the role of this residue in assisting catalysis, since it is a crucial residue for the activity of the protein.

Although RNase II is an enzyme specific for RNA, it is still able to bind to DNA without cleave it. Previous results have shown that, for cleavage to occur, the presence of a ribose between positions 2 to 5 from the 3' end is mandatory (Cannistraro and Kennell, 1994). The resolution of the crystal structure helped us to understand why. In fact, it is possible to see that the residues Asp201 and Tyr313 are interacting with the O2' ribose oxygen of the second ribose and Glu390 with the O2' ribose oxygen of the forth ribose (Frazão *et al.*, 2006). In order to understand the importance of these residues for the specificity of RNase II to degrade RNA, we used two chimeric substrates (with RNA and DNA bases) to test the activity of the protein. The results obtained showed that RNase II has a strict requirement for a ribose in the second and/or in the fourth nucleotides counting from the 3' end and not in other positions. These contacts are necessary and sufficient for cleavage to occur (Barbas *et al.*, 2009). Taking this into account, we can say that Asp201, Tyr313, and Glu390 residues seem to be the responsible for the RNA specificity in RNase II. Since that these residues are highly conserved in all proteins of the RNase II family of enzymes and due to the structural similarity observed, the same conclusions can be extrapolated for other members of this family.

In RNase II, Glu542 is in close proximity with the leaving nucleotide. It was thought that it may be involved in nucleotide elimination after cleavage, thus allowing degradation to proceed (Frazão *et al.*, 2006). To

confirm the role of this residue in the mechanism of degradation, we mutated it into an alanine. This single change in RNase II led to a protein that was more than 110 fold more active when compared to the wild-type protein (Barbas *et al.*, 2009). Moreover, besides a higher catalytic rate confirmed by a kinetic analysis, this mutant also presented a higher affinity for RNA molecules when compared to the wild-type (Barbas *et al.*, 2009; Matos *et al.*, 2010). In fact, it seems that this residue is not involved in nucleotide elimination, but is preventing RNA degradation by slowing down the activity of RNase II.

In summary, the results obtained by this mutational analysis substantially improved the mechanism of RNA degradation by RNase II. It has been verified that the proteins which belong to this family share a high degree of identity and the mechanism of action is also conserved. In collaboration with Professor Paulino Goméz-Puertas from Centro de Biología Molecular "Severo Ochoa", we have built the models of RNase R and human Rrp44 based on RNase II structure (Barbas *et al.*, 2008). These models show that the three enzymes share a common 3D arrangement, with all the critical residues for activity located in equivalent spatial positions. As such, our results are extremely relevant since they can be extrapolated for the understanding of the mode of action of the other members of the family.

CHARACTERIZING THE ROLE OF RNase R FUNCTIONAL DOMAINS

In the second part of the work we focused in the study of RNase R. Contrary to what happens with RNase II, little was know about the mechanism of action of this enzyme. Taking into consideration the results obtained with RNase II protein, we went to check the role of two conserved amino acids in the mechanism of action of RNase R. It was already known that the changing of Asp209 by an Asn in RNase II lead to the inactivation of the protein without affecting the RNA binding ability

(Amblar and Arraiano, 2005). The same result was also obtained in the yeast counterpart Rrp44/Dis3, where a similar mutation was also responsible for a strong growth defect, showing the importance of this protein in yeast metabolism (Amblar and Arraiano, 2005; Dziembowski *et al.*, 2007; Schneider *et al.*, 2007). To confirm the role of this residue in RNase R protein, we mutated the equivalent residue, Asp280, into an alanine and analyzed its activity and ability to bind to RNA. Similarly to what happens with RNase II, also in RNase R Asp280 is crucial for the activity of the protein, without affecting RNA binding (Matos *et al.*, 2009). Also in RNase R from *Legionella pneumophila* (Charpentier et al., 2008) this aspartate was the only residue essential for the activity of the enzyme.

In RNase II we showed that the Tyr253 is responsible for setting the final end product, and considering the structure of the protein, we could easily understand the releasing of a 10 nt fragment (Barbas *et al.*, 2008). We decided to perform the same mutation in the equivalent residue of RNase R protein. As expected, the final product released was also changed. Instead of the usual 2 nt fragment, the Y324A mutant releases a 5 nt fragment and this behaviour was observed with single- and double-stranded substrates. While in RNase II we could easily understand the release of a 10 nt fragment, in RNase R we can not explain why it releases a 5 nt fragment. We believe that the resolution of the crystal structure from RNase R will help us to elucidate this and other questions regarding its mechanism of action. The binding ability of this protein was also reduced when compared to wild-type protein, indicating that this residue is important for the binding of the RNA molecule at the 3' end (Matos *et al.*, 2009). However, in RNase R, the substitution of Tyr residue led to a reduction of 40 fold in the activity of the protein, while in RNase II the substitution of the equivalent residue still retained 25% of the activity. This may indicate that the Tyr residue has a much important function in RNase R than in RNase II (Matos *et al.*, 2009). This can be due to the fact that the second residue involved in the RNA "clamping", Phe358, has no

equivalent in RNase R (Barbas *et al.*, 2008), which can confer to Tyr324 a more important function in RNA mechanism of degradation.

In order to understand the role of each domain from RNase R in the degradation mechanism, we constructed truncated proteins lacking CSD and/or S1 domains and analysed their activity. The results obtained showed that the RNA domain from RNase R, by itself, is still able to bind to RNA and cleave it, although with less efficiency. The activity of the RNB domain is highly reduced in the absence of the RNA-binding domains, indicating that they play an important role in catalysis (with S1 domain being more critical when compared to CSD): CSD seem to be more important for the recruitment of the substrate, since in their absence the affinity of the protein for RNA diminished; the S1 domain might help in the orientation and stabilization of the RNA molecule in the catalytic cavity. Moreover, we showed that the cleavage of double-stranded substrates is a property of the RNB domain, since it is able to cleave this substrate in the absence of the RNA-binding domains (Matos *et al.*, 2009).

It was previously shown that RNase R in order to degrade structured RNA needs a single-stranded 3' overhang of at least 5 nucleotides (Vincent and Deutscher, 2006). We also verified which domains were responsible for such requirements by performing activity assays with a blunt-ended double-stranded substrate, as previously described (Amblar *et al.*, 2006). The results showed that, in the absence of the CSD and/or S1 domains, the truncated proteins were able to cleave RNA molecules without a tail. In fact, it seems that these domains are blocking the entrance of the double-stranded substrates into the catalytic cavity. In their absence, the substrate is free to enter and cleavage can occur. We can then conclude that the RNA-binding domains are responsible for the selection of which RNA should be degraded in the cell, picking just the ones that are tagged with a 3' tail (Matos *et al.*, 2009). In fact, both in eukaryotes and prokaryotes, the RNA are tagged for degradation with short poly(A) tails (Arraiano *et al.*, 2010a). This signal will allow RNase R to detect which RNAs are "tagged", attach to them and proceed with degradation. In the

absence of the RNA-binding domains, the protein would degrade all RNA indiscriminately, which would be deleterious for the cell.

In conclusion, the results presented provided an important breakthrough in the understanding of the mechanism of action of RNase R. Moreover, the discovery that RNA-binding domains help discriminating which molecules are degraded can have important implications for the study of poly(A)-dependent degradation mechanism, in prokaryotes and eukaryotes.

UNRAVELLING THE DIFFERENCES BETWEEN RNase II AND RNase R

As members of the RNase II-family of enzymes, both RNase II and RNase R share some catalytic properties. However, some differences can be observed between them: while the activity of RNase II is impaired by the presence of secondary structures, RNase R is able to degrade them. Another difference between these two proteins resides in the final product that is released, which is 4 nt for RNase II and 2 nt for RNase R. The aim of the third part of this Doctoral work was to determine if the differences observed in the catalysis between RNase II and RNase R could be assigned to one of the domains that constitute each protein. With that purpose, we swapped the domains of RNase II by the ones from RNase R and *vice versa* and obtained 6 hybrid proteins. The activity and binding ability of those proteins was tested against different substrates.

The results obtained showed that, when RNase II has the RNB or the S1 domain from RNase R, the respective hybrid proteins were able to degrade the poly(A) substrate until it reached the 2 nt of length, contrary to what happened with RNase II, which released a 4 nt fragment. When we changed the RNB domain from RNase R for the one from RNase II we were expecting to see a final product characteristic of RNase II, since that the RNB domain is the one responsible for the activity of the protein.

However, that was not the result obtained and the hybrid protein was also able to cleave the substrate until it reaches the 2 nt. Together, these findings led us to conclude that the RNB domain from RNase R is responsible for setting the end-product in RNase R, but the S1 domain is also involved. We wanted to understand why the presence of the S1 domain from RNase R is causing these changes in the hybrid proteins. Accordingly, we collaborated with Professor Paulino Goméz-Puertas in order to model them and compare the obtained models with RNase II structure (Frazão *et al.*, 2006) and RNase R model (Barbas *et al.*, 2008). The results obtained showed that the overall structure is similar in all proteins and no dramatic changes are observed in the catalytic cavity. So, it appears that the differences observed in the catalysis are not due to drastic changes in the catalytic cavity. These changes in the interactions verified between both domains could induce a subtle conformational change in some residues near the catalytic cavity. These modifications would result in a higher affinity for RNA fragments shorter than 4 nt, allowing the hybrid proteins to degrade them until the 2 nt (Matos *et al.*, 2011). However, only the resolution of RNase R structure will allow us to clarify this question.

As mentioned in the discussion of the second part of this Doctoral work, we showed that the RNB domain from RNase R is able, by itself, to degrade double-stranded substrates. When we inserted the RNB domain from RNase R in RNase II we observed that the hybrid protein was also able to degrade structured substrates. The most intriguing results were obtained when the S1 domain from RNase R was inserted in RNase II and when RNB domain from RNase II was inserted into RNase R. Both proteins are still able to cleave double-stranded substrates in the absence of the RNB domain from RNase R. The common element between these proteins is the S1 domain from RNase R, so, we concluded that this domain must be the responsible for the new activity observed in hybrid proteins. We then looked more carefully into the C-terminal region of RNase R and, immediately after the S1 domain there is a lysine-rich

region. This region is absent in RNase II-like proteins and it is only found in RNase R-like proteins. In eukaryotes, RNase II homologues also do not have this region at the C-terminal end. Considering these results, we postulated that the lysine-rich region could be involved in the degradation of structured substrates, probably by helping to unwind the substrate before it enters into the catalytic cavity. To confirm the role of this region, we predicted its secondary structure and we saw that it is formed by three major alpha helices. We then decided to construct truncated forms of the lysine-rich region in the protein that has CSD and RNB domains from RNase II and the S1 domain is from RNase R. We chose this protein due to the absence of an RNB domain from RNase R, which was shown to be responsible for the degradation of double-stranded substrates (Matos *et al.*, 2009). The results obtained showed that, by deleting the three major alpha helices that constitute the lysine-rich tail, the protein was no longer able to cleave double-stranded substrates. This data confirmed our hypothesis that the S1 domain from RNase R, together with RNB domain, is involved in the degradation of structured substrates (Matos *et al.*, 2011). Moreover, the mechanism of degradation by both domains seem to be different: while RNB domain from RNase R is able to degrade dsRNA in the absence of a 3' single stranded overhang, the degradation by the S1 domain has this strict requirement (Matos *et al.*, 2011).
In summary, the results obtained in this chapter are very important for the understanding of the mode of action of other members of the family, namely those who are able to degrade double-stranded substrates. Moreover, it is an important step in the comprehension of the mechanism of action of these two so close but yet so different exoribonucleases.

Members from RNase II-family of enzymes play a crucial role in RNA metabolism. They are widespread in nature and are involved in several processes: they can be essential for growth, and mutations in its genes have been related with abnormal chloroplast biogenesis, mitotic control and cancer. It was already shown that proteins from this family are

required for expression of virulence in several pathogens (Arraiano *et al.*, 2010b). In eukaryotic organisms, the proteins of this family are part of a complex responsible for the RNA maturation and turnover, the exosome (van Hoof and Parker, 1999).

Due to the importance that the members of this family have shown, the findings that were presented in this dissertation were very important to understand the mechanism of action of these proteins. Due to the similar mode of action, we believe that most of the results can be extrapolated to the other proteins of the family.

FUTURE PERSPECTIVES

The results obtained with this Doctoral work helped us to elucidate the mechanism of action of the two members of the RNase II-family of enzymes present in *E. coli*: RNase II and RNase R.

Since RNase II and RNase R are important enzymes in the cell for the processing and degradation of RNA, in collaboration with Prof. Kenny McDowall from the University of Leeds, we are testing some compounds to see if we are able to inhibit the activity of these proteins. These compounds were screened by vHTS (virtual High Throughput Screening) as the best possible binders considering the architecture of RNase II catalytic cavity. At the moment we are already testing the compounds with the highest score. The ones that will be able to inhibit the activity of the proteins will then be used to perform *in vivo* studies to check the efficiency of the inhibitor molecule. Since proteins of this family of enzymes are involved in virulence, mitotic control, chloroplast biogenesis, stress responses and quality control, this work will have a great impact for future studies in this area. Moreover, we will also perform the same analysis with PNPase, the major phosphorolytic ribonuclease present in the cell.

In eukaryotes, the RNase II homologue (Rrp44) is part of exosome and, besides the CSD, RNB and S1 domains it has an extra PINc domain and a

cystein-Rich region (CR3) at the N-terminal region. It was shown that this extra N-terminal region acts as endoribonuclease and is important for the interaction with the exosome (Schaeffer *et al.*, 2009). In order to see the effect in the cell due to the presence of those extra domains in RNase II or RNase R, we constructed hybrid proteins which correspond to RNase II with the PINc and CR3 domains from yeast and the other which is RNase R with PINc and CR3. In the first step of this work, we tested the activity of the hybrid proteins *in vitro* and we were able to see that the exoribonucleolytic activity was not altered and these proteins also acquired the endoribonucleolytic activity conferred by the PINc domain. The next step will be the complementation in strains deficient in endoribonucleases to see if this new endoribonucleolytic activity is able to substitute *in vivo* the endo activities observed in *E. coli*. We are also interested in testing the effect of the activity of these proteins in some known substrates for RNase II and RNase R, but also if the hybrid proteins are able to process specific substrates from RNase E and RNase III, the two major endoribonucleases in the cell. It is known that RNase II, although being a degrading enzyme, can protect some RNases from being degraded (Marujo *et al.*, 2000). By having both endo and exoribonucleolytic activities we are expecting that this protecting behaviour disappears.

The studies described in this Doctoral work were performed with RNase II-family members from Eubacteria. We will also want to characterize proteins from other organisms. In Archaea, little is know about RNA degradation mechanisms. In methanogenic archaea it is known that the RNA degradation is perfomed by the exosome (Evguenieva-Hackenberg *et al.*, 2003). However, in halophilic archaea no homologues of the exosome components were found. It is possible to find only an RNase R-like protein, which is the only protein responsible for the 3' to 5' degradation in these organisms (Portnoy and Schuster, 2006). *Haloferax volcanii* is a representative halophilic archaeon. It was shown that RNase R is an essential protein in this organism and, therefore, plays an important role

in the mechanism of RNA degradation. Due to the importance on this protein in *Haloferax*, it is crucial to understand its role in the mechanism of RNA degradation. For that purpose, we intend to characterize the protein activity (salt, pH and divalent ions preference) and the test how the protein behaves regarding the degradation of single- and double-stranded substrates. When aligned with other members of RNase II-family of enzymes, RNase R from *H. volcanii* is a shorter protein and misses a CSD at the N-terminal region. Since no structure is available for RNase R-like proteins, in collaboration with Prof. Arun Malhotra from the University of Miami, we will try to crystallize the protein. We also want to analyse other homologues of RNase II in other organisms, such as *Synechocystis*.

Altogether, the information that we will obtain with these experiments will allow us to understand the evolution of this family of enzymes and their mode of action in different organisms.

REFERENCES

Amblar, M., and Arraiano, C.M. (2005) A single mutation in *Escherichia coli* ribonuclease II inactivates the enzyme without affecting RNA binding. *FEBS J* **272**: 363-374.

Amblar, M., Barbas, A., Fialho, A.M., and Arraiano, C.M. (2006) Characterization of the functional domains of *Escherichia coli* RNase II. *J Mol Biol* **360**: 921-933.

Arraiano, C.M., Andrade, J.M., Domingues, S., Guinote, I.B., Malecki, M., Matos, R.G., Moreira, R.N., Pobre, V., Reis, F.P., Saramago, M., Silva, I.J., and Viegas, S.C. (2010a) The critical role of RNA processing and degradation in the control of gene expression. *FEMS Microbiol Rev*.

Arraiano, C.M., Matos, R.G., and Barbas, A. (2010b) RNase II: The finer details of the Modus operandi of a molecular killer. *RNA Biol* **7**: 276-278.

Barbas, A., Matos, R.G., Amblar, M., Lopez-Viñas, E., Goméz-Puertas, P., and Arraiano, C.M. (2008) New insights into the mechanism of RNA degradation by ribonuclease II: identification of the residue responsible for setting the RNase II end product. *J Biol Chem* **283**: 13070-13076.

Barbas, A., Matos, R.G., Amblar, M., Lopez-Vinas, E., Gomez-Puertas, P., and Arraiano, C.M. (2009) Determination of key residues for catalysis and

RNA cleavage specificity: one mutation turns RNase II into a "SUPER-ENZYME". *J Biol Chem* **284**: 20486-20498.

Cairrão, F., Chora, A., Zilhão, R., Carpousis, A.J., and Arraiano, C.M. (2001) RNase II levels change according to the growth conditions: characterization of *gmr*, a new *Escherichia coli* gene involved in the modulation of RNase II. *Mol Microbiol* **39**: 1550-1561.

Cannistraro, V.J., and Kennell, D. (1994) The processive reaction mechanism of ribonuclease II. *J Mol Biol* **243**: 930-943.

Charpentier, X., Faucher, S.P., Kalachikov, S., and Shuman, H.A. (2008) Loss of RNase R induces competence development in *Legionella pneumophila*. *J Bacteriol* **190**: 8126-8136.

Dziembowski, A., Lorentzen, E., Conti, E., and Seraphin, B. (2007) A single subunit, Dis3, is essentially responsible for yeast exosome core activity. *Nat Struct Mol Biol* **14**: 15-22.

Evguenieva-Hackenberg, E., Walter, P., Hochleitner, E., Lottspeich, F., and Klug, G. (2003) An exosome-like complex in *Sulfolobus solfataricus*. *EMBO Rep* **4**: 889-893.

Frazão, C., McVey, C.E., Amblar, M., Barbas, A., Vonrhein, C., Arraiano, C.M., and Carrondo, M.A. (2006) Unravelling the dynamics of RNA degradation by ribonuclease II and its RNA-bound complex. *Nature* **443**: 110-114.

Marujo, P.E., Hajnsdorf, E., Le Derout, J., Andrade, R., Arraiano, C.M., and Régnier, P. (2000) RNase II removes the oligo(A) tails that destabilize the rpsO mRNA of *Escherichia coli*. *RNA* **6**: 1185-1193.

Matos, R.G., Barbas, A., and Arraiano, C.M. (2009) RNase R mutants elucidate the catalysis of structured RNA: RNA-binding domains select the RNAs targeted for degradation. *Biochem J* **423**: 291-301.

Matos, R.G., Barbas, A., and Arraiano, C.M. (2010) Comparison of EMSA and SPR for the characterization of RNA-RNase II complexes. *Protein J* **29**: 394-397.

Matos, R.G., Barbas, A., Goméz-Puertas, P., and Arraiano, C.M. (2011) Swapping the domains of exoribonucleases RNase II and RNase R: conferring upon RNase II the ability to degrade ds RNA. *Proteins* ***Accepted***

Piedade, J., Zilhão, R., and Arraiano, C.M. (1995) Construction and characterization of an absolute deletion mutant of *Escherichia coli* ribonuclease II. *FEMS Microbiol Lett* **127**: 187-193.

Portnoy, V., and Schuster, G. (2006) RNA polyadenylation and degradation in different Archaea: roles of the exosome and RNase R. *Nucleic Acids Res* **34**: 5923-5931.

Schaeffer, D., Tsanova, B., Barbas, A., Reis, F.P., Dastidar, E.G., Sanchez-Rotunno, M., Arraiano, C.M., and van Hoof, A. (2009) The exosome contains

domains with specific endoribonuclease, exoribonuclease and cytoplasmic mRNA decay activities. *Nat Struct Mol Biol* **16**: 56-62.

Schneider, C., Anderson, J.T., and Tollervey, D. (2007) The exosome subunit Rrp44 plays a direct role in RNA substrate recognition. *Mol Cell* **27**: 324-331.

van Hoof, A., and Parker, R. (1999) The exosome: a proteasome for RNA? *Cell* **99**: 347-350.

Vincent, H.A., and Deutscher, M.P. (2006) Substrate recognition and catalysis by the exoribonuclease RNase R. *J Biol Chem* **281**: 29769-29775.

Chapter 6

Appendix

Appendix I

Published papers related with this dissertation

1 - New Insights into the Mechanism of RNA Degradation by Ribonuclease II: Identification of the Residue Responsible for Setting the RNase II End-Product [JBC 2008, 283(19): 13070-13076]

2 - Determination of Key Residues for Catalysis and RNA Cleavage Specificity: One Mutation Turns RNase II into a "Super-Enzyme" [JBC 2009, 284(31): 20486-20498]

3 - RNase R Mutants Elucidate the Catalysis of Structured RNA: RNA-Binding Domains Select the RNAs Targeted for Degradation [Biochemical Journal 2009, 423: 291-301]

4 - Biochemical characterization of the RNase II family of exoribonucleases from the human pathogens *Salmonella typhimurium* and *Streptococcus pneumoniae* [Biochemistry 2009, 48: 11848-11857]

5 - RNase II: the finer details of the *Modus operandi* of a molecular killer [RNA Biology 2010, 7(3): 276-281]

6 - Comparison of EMSA and SPR for the characterization of RNA-RNase II complexes [Protein Journal 2010, 29: 394-397]

7 - The critical role of RNA processing and degradation in the control of gene expression [FEMS Microbiology Reviews 2010, 34(5):883-923]

8 - Swapping the Domains of Exoribonucleases RNase II and RNase R: Conferring upon RNase II the ability to Degrade dsRNA [Proteins 2011, 79: 1853-1867]

The *H. volcanii* RNase R Protein has a Dual Activity According to Temperature

Rute G. Matos[1], Paulino Goméz-Puertas[2] and Cecília M. Arraiano[1]✉

1 Instituto de Tecnologia Química e Biológica/Universidade Nova de Lisboa, Apartado 127, 2781-901 Oeiras, Portugal
2 Centro de Biología Molecular "Severo Ochoa" (CSIC-UAM), Cantoblanco, 28049 Madrid, Spain

Archaea are microscopic, single-celled organisms. Regarding mRNA, they seem to be more similar to bacteria than to eukaryotes but little is known regarding mRNA degradation mechanisms. In some archaeal organisms it was demonstrated the existence of an archaeal exosome. Halophilic archaea do not have an exosome but instead an RNase R-like protein, which may be the only exoribonuclease in these organisms. In *H. volcanii*, the RNase R homologue is the only enzyme described with exoribonucleolytic activity, which indicates that it may play a crucial role in the mechanism of RNA degradation in this organism. In this work we characterized the mechanism of action by *H. volcanii* RNase R and its implications for the RNA degradation process. The results obtained showed that, although named RNase R, at 37ºC, this protein behaves like an RNase II protein. However, at 42ºC, the optimum temperature of growth, this protein is now able to overcome secondary structures, acting like RNase R. This discovery has a great impact for RNA degradation, since this is the first case reported where a single enzyme has two different exoribonucleolytic activities according to temperature.

Archaea are microscopic, single-celled organisms with no nucleus, no mitochondria and no chloroplasts. Regarding mRNA, they seem to be more similar to bacteria than to eukaryotes: they have a polycistronic mRNA with no introns, which is not modified and does not have long stabilizing poly(A) tails at the 3' end (1). However, little is known regarding RNA degradation in these organisms.

In some archaeal organisms, such as *Sulfolobus* and *Methanothermobacter*, it was demonstrated the existence of an archaeal exosome, which shares some characteristics with the eukaryotic exosome (2,3). In *S. solfataricus* it was shown that the exosome has a dual function: it can work as an RNA-tailing and RNA-degrading complex, since it has both phosphorolytic and polyadenylating activity (4). Halophilic and many methanogenic archaeal genomes lack the genes for the orthologues of exosomal subunits and also for a poly(A) polymerase homologue. However, an RNase R-like protein is found and it may be the only enzyme responsible the exoribonucleolytic activity in these organisms (5). This information indicates that it may exist different RNA degradation mechanisms in archaeal organisms: one in thermophiles performed by the archaeal exosome, which involves polyadenylation, and the other in halophiles performed by other ribonucleases in the cell, which is poly(A)-independent (6). RNA degradation in bacteria initiates with an endonucleolytic cleavage, followed by the cleavage of the resultant fragments by exoribonucleases, with or without a polyadenylation step (7). In Archaea it seems that the mechanism is very similar, although some have an exosome complex, which is similar to the eukaryotic system. Most of the archaeal organisms have genes related to RNase E and RNase J (8,9), which can be responsible for the initial endonucleolytic cleavage in RNA degradation process. Then, depending on the organisms, the resultant fragments are degraded in a Poly(A)-dependent manner by the archaeal exosome in thermophiles or, in the case of halophilic organisms, the degradation is performed by RNase R homologue in a Poly(A)-independent process (4).

Haloferax volcanii, a bacterium isolated from the Dead Sea, is the type strain from halophilic archaea. It requires a high concentration of sodium chloride to replicate (1.7 to 2.5M) and its optimum temperature for growth is 42ºC, and was the first organism described that is able to degrade RNA molecules in the absence of polyadenylation. As an halophilic organism, *H. volcanii* does not have a exosome complex, but an RNase R-like protein which is essential for viability and, in the absence of PNPase and exosome components, may play a crucial role in RNA degradation in the absence of polyadenlylation (4,10,11). RNase R belongs to the RNase II-family of proteins, which are present in all domains of life and play a crucial role in RNA metabolism (7). In Eukaryotes, the RNase II homologue is the only active sub-unit of the exosome. In prokaryotes, proteins of this family are important for growth and stress responses and may also be involved in virulence (12). RNase II, the prototype of RNase II-family of enzymes, is composed by two N-terminal CSD domains and a C-terminal S1 domain involved in RNA binding, and a central RNB domain responsible for the catalytic activity of the protein (13,14). As member of the RNase II-family of enzymes, RNase R shares the same domain organization with RNase II and also an overall structural rearrangement, with all the important residues for cleavage located in the same spatial position (15). In RNase II, Tyr253 was shown to be important for setting the final end-product of RNase II, and the same was observed with the equivalent Tyr in RNase R (15,16). In the active site, there are four highly conserved aspartates with different roles in RNA degradation mechanism. The most critical aspartate for the activity of the enzyme is the one located in position 209 in RNase II. Its substitution by an asparagine in RNase II, RNase R or Rrp44 (the yeast homologue) completely abolished the activity of the protein without changing its binding ability (15-17). These results indicate that the mechanism of RNA degradation may be conserved in all members of this family. However, while RNase II is sensitive to secondary structures, RNase R is able to completely degrade structured substrates (18). Although the crystal structure of RNase R is yet unknown, the mechanism of dsRNA degradation by RNase R has been deciphered by biochemical studies. It was shown that the RNB domain of RNase R, by itself, is responsible for the degradation of double-stranded substrates (16,19), and that the RNA-binding domains are important to discriminate the molecules to be degraded, choosing only the RNAs that are tagged to be degraded (16). More recently, it was shown that the S1 domain from RNase R, namely the lysine-rich region (which is absent in RNase II), is

also involved in the degradation of structured substrates, probably by helping to unwind it (20). This region was also proved to be involved in the recruitment of RNase R to stalled ribosomes and to the selective decay of defective transcripts (21).

In *H. volcanii*, the RNase R homologue is the only enzyme described with exoribonucleolytic activity, which indicates that it may play a crucial role in the mechanism of RNA degradation in this organism. The aim of this work was the characterization of the mechanism of action by RNase R from *H. volcanii* and their implications for the RNA degradation process. The results obtained showed that, although named RNase R, at 37ºC, this protein behaves like an RNase II protein: it released a 4 nt fragment as final end-product and is sensitive to secondary structures. However, at 42ºC, the optimum temperature of growth, this protein is now able to overcome secondary structures, acting like RNase R. This discovery has a great impact for RNA degradation, since this is the first case reported where a single enzyme has two different exoribonucleolytic activities according to temperature.

MATERIAL AND METHODS

Overexpression and purification of recombinant RNase R from H. volcanii. The plasmid used for expression of *H. volcanii* RNase R was previously described (10). The plasmid was transformed into M15 (REP4) strain to allow the expression of the recombinant protein. Cells were grown at 37ºC in 100 ml LB medium supplemented with 150 μg/ml ampicillin to an A_{600} of 0.5 and induced by addition of 0,5 mM IPTG during 2h. Cell culture was pelleted by centrifugation and stored at -80°C. RNase II and RNase R overexpression and purification were performed as described previously (22-24).

Purification was performed by histidine affinity chromatography using HiTrap Chelating HP columns (GE Healthcare) and AKTA HLPC system (GE Healthcare) following the protocol previously described (22,24). The fractions containing the purified *H. volcanii* RNase R protein were pooled together to perform an anion exchange by injecting the fractions in a monoQ column (GE Healthcare) equilibrated in buffer composed by 20mM Tris pH8, 60mM KCl, 2mM $MgCl_2$ and 0,2mM EDTA. Protein elution was achieved by a continuous KCl gradient (from 60mM to 1M) in buffer B. Protein concentration was determined by spectrophotometry and 50% (v/v) glycerol was added to the final fractions prior storage at -20 ºC. 0.5 μg of the purified protein was applied in a 8% SDS-PAGE and visualized by Coomassie blue staining (data not shown).

Exoribonucleolytic Activity Assays. The exoribonucleolytic activity was determined using different substrates: a Poly(A) oligomer of 30 nts, a 16mer oligoribonucleotide (5'-CCCGACACCAACCACU-3'), and a 30mer oligoribonucleotide (5'-CCCGACACCAACCACUAAAAAAAA AAAAAA-3') hybridized to the complementary non labelled 16mer oligodeoxiribonucleotide (5'-AGTGGTTGGTGTC GGG-3'), in order to obtain the double stranded substrate 16-30ds (the hybridization was performed in a 1:1 (mol:mol) ratio by 5 min of incubation at 100ºC followed by 45 min at 37ºC). All RNA molecules were labelled at its 5'-end with [γ-^{32}ATP] and T4 polynucleotide kinase. The RNA oligomers were then purified using Microcon YM-3 Centrifugal Filter Devices (Millipore) to remove the non-incorporated nucleotide. The exoribonucleolytic reactions were carried out in a final volume of 12.5 μl containing 5 nM of substrate, 20 mM Tris-HCl (pH tested from 6,5 to 9), KCl or NaCl (from 10 to 200mM), $MgCl_2$ (from 1 to 10 mM), and 1 mM DTT. The amount of each enzyme added to the reaction was adjusted to obtain linear conditions and is indicated in the figures and respective legends. Reactions were started by the addition of the enzyme and incubated at 37ºC or 42ºC. Samples were withdrawn at the time points indicated and the reaction was stopped by adding formamide-containing dye supplemented with 10 mM EDTA. Reaction products were resolved in a 20% polyacrylamide/7 M urea and detected by using the Fuji Fluorescent Analyzer TLA-5100 from GE Healthcare. The exoribonucleolytic activity of the enzyme was determined by measuring and quantifying the disappearance of the substrate in several distinct experiments in which the protein concentration was adjusted in order that, under those conditions, less than 25% of substrate was degraded. Each value obtained represents the mean for these independent assays.

RESULTS AND DISCUSSION

Salt and pH preference of H. volcanii RNase R. *H. volcanii* is an organism that lives in Dead Sea, which has a salt concentration extremely high. In order to see if RNase R protein from *H volcanii* had adapted to be active in high salt concentrations, a previous experiment was performed using different KCl concentrations. The results obtained showed that the protein was shown to be active with low salt concentrations and the activity was reduced when the concentrations increased (10). We also went to analyse the activity of the protein using different salt concentrations and using two different types of salts, KCl and NaCl, in five different concentrations, 50, 100 and 500mM and 1 and 2M. The results obtained for KCl are in agreement with the ones previously published, since our experiments also show that RNase R from *H. volcanii* prefers lower KCl concentrations (Figure 1A) (10). When the buffer contains NaCl, the activity of the protein was highly impaired (Figure 1A). In order to determine the optimal concentration of KCl for the activity of the protein, we quantified its specific activity using five different concentrations: 50, 100 and 500mM, 1 and 2M. For this determination, we started by adjusting the conditions of the reaction to guarantee that less than 25% of the substrate was being degraded. The activity of the protein was then measured by quantifying the disappearance of the substrate along the time, and the results are presented in Figure 1B. This determination confirmed that RNase R protein prefers lower salt concentrations, being more active in the presence of 50 and 100mM when compared to the higher concentrations tested (Figure 1B). The activity of the protein is very similar at 50 and 100mM of KCl but slightly higher in the presence of 100mM of this salt, which led us to use this concentration for the following assays. Although being an organism which lives in the Dead Sea (which has salt concentration nearing saturation), and also has a high internal potassium concentration (~4M), these results demonstrate that this protein did not adapt to have an optimal activity inside the cell. This led us to agree with what was previously proposed: the activity that the protein presents at high salt concentrations, although reduced when compared to the one obtained at lower salt concentrations, is enough for the RNA degradation activity required by *H. volcanii* (10).

This first experiment allowed us to determine the optimal salt concentration for *H. volcanii* RNase R activity, which was shown to be 100mM of KCl. This condition was used for the following experiments. The next step was to determine of the preferred pH for the activity of the protein. For that purpose, we tested the activity of the recombinant protein using buffers with different pH, ranging from 6.5 to 9. The results obtained in the activity gel showed that the protein is active in all pH used. However, it seemed to have a higher accumulation of degradation products when the pH of the activity buffer was 8 (Figure 2A). In order to confirm this result, we quantified the activity of the protein by measuring the disappearance of the

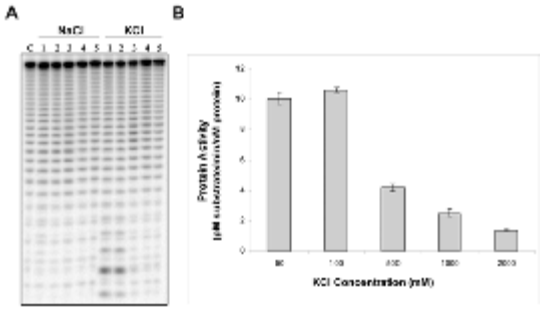

Figure 1. Salt dependence of RNase R homologue in *H. volcanii*. A. 100nM of recombinant protein were incubated with 10nM of Poly(A) at 37ºC for 5 minutes in a reaction buffer with different salt concentrations (lanes 1 =50mM, lanes 2 = 100mM, lanes 3 = 500mM, lanes 4 = 1M, and lanes 5 = 2M). **B.** Determination of the protein activity in the presence different KCl concentrations.

substrate. As explained above, the conditions used for this determination were different from the ones used to obtain figure 2A, since we needed to ensure that less than 25% of the substrate was being degraded. The results obtained through this measurement showed us that, in fact, the protein was more active at pH 8, although the activity at this condition was very similar to the one obtained at pH 8.5 and 9. For values lower than 8, the activity started to decrease until it reaches 30% of the optimal activity observed (Figure 2B).

These preliminary results allowed us to determine both salt and pH preference for RNase R from *H. volcanii*, which were shown to be 100mM of KCl and pH 8. These were the conditions used to perform the following experiments.

H. volcanii RNase R protein is active in the presence of a wide range of divalent ions. It was already demonstrated that exoribonucleases from the RNase II-family of enzymes need a divalent ion in order to proceed with catalysis. For *E. coli* RNase II and RNase R, the presence of Mg^{2+} was shown to be very important for the activity of the proteins (13). Other divalent ions can also contribute for the activity of these proteins, however, such experiments were not performed until now. Taking this into consideration, we performed activity assays with *E. coli* RNase II and RNase R in the presence of different divalent ions: Mg^{2+}, Mn^{2+}, Ca^{2+}, Zn^{2+}, Cu^{2+}, Co^{2+}, and Ni^{2+}.

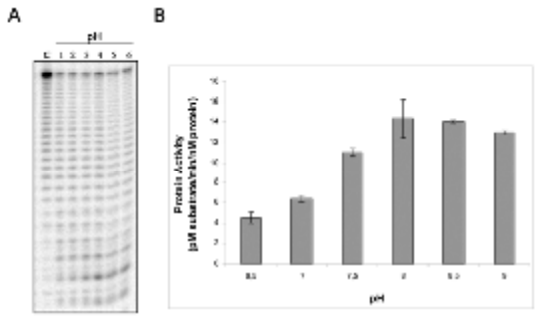

Figure 2. pH dependence of RNase R homologue in *H. volcanii*. A. 100nM of recombinant protein were incubated with 10nM of Poly(A) at 37ºC for 5 minutes in a reaction buffer with different pH, ranging from 6.5 to 9. **B.** Determination of the protein activity in the presence of different pH.

Surprisingly, both *E. coli* RNase II and RNase R showed activity in the presence of other divalent ions than Mg^{2+} (Figure S1). When *E. coli* RNase II was incubated with the substrate during 5 minutes in the presence of the different ions, we were able to see that is cleaves RNA when Mg^{2+} and Ca^{2+} are added to the reaction buffer. However, if we allow the reaction to occur during 60 minutes, we can see that RNase II is also able to degrade the Poly(A) substrate in the presence of Zn^{2+} and Ni^{2+} (Figure S1). On the other hand, the incubation of RNase R with the same ions tested during 5 minutes showed that this protein was only active in the presence of Mg^{2+}. Once again, if the reaction proceed during 60 minutes, we were able to see that the protein was also active in the presence of Ca^{2+}, Zn^{2+} and Ni^{2+} (Figure S1). We then performed the same experiment for RNase R from *H. volcanii* and the results obtained are presented in Figure 3A. Similarly to what was observed for both *E. coli* homologues, also RNase R from *H. volcanii* was shown to be active in the presence of other divalent ions than Mg^{2+} (Figure 3A), namely Ca^{2+}, Zn^{2+}, Cu^{2+} and Ni^{2+}. However, in this case, we did not need to increase the incubation period to observe the activity with the other ions, as it was the case of RNase II and RNase R from *E. coli*. This led us to determine the specific activity of the protein in these conditions (Figure 3A, right panel). The results obtained showed that the higher activity was obtained in the presence of Mg^{2+}. However, RNase R form *H. volcanii* showed a similar activity to the one obtained with Mg^{2+} also in a buffer with Ca^{2+}. Moreover, when the buffer had Ni^{2+} on its composition, RNase R protein retained 60% of its optimal activity, and about 30% in a buffer with Zn^{2+} or Cu^{2+} (Figure 3A, right panel). For the other two ions tested, Co^{2+} and Mn^{2+}, the activity detected was residual in the conditions tested (Figure 3A). We also tested the activity of the protein with these two

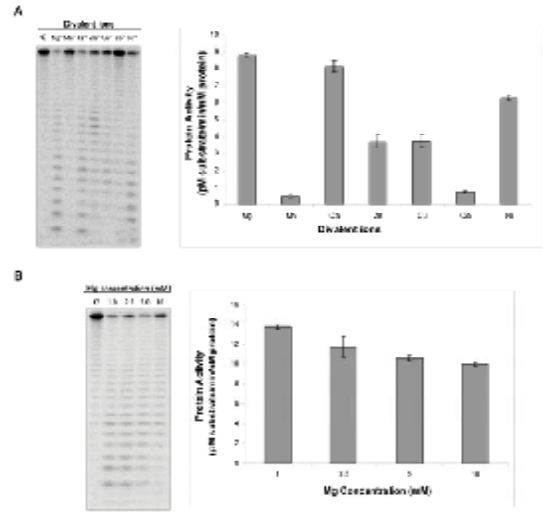

Figure 3. Divalent metal ion dependence of RNase R homologue in *H. volcanii*. A. Left panel: 100nM of recombinant protein were incubated with 10nM of Poly(A) at 37ºC for 5 minutes in a reaction buffer with different divalent metal ions. Right panel: Determination of the protein activity in the presence different divalent ions. **B.** Left panel: 100nM of recombinant protein were incubated with 10nM of Poly(A) at 37ºC for 5 minutes in a reaction buffer with different Mg^{2+}concentrations. Rigth panel: determination of the protein activity in the presence of different Mg^{2+} concentrations.

ions but increasing the reaction time and the protein concentration, and only residual activity was detected (data not shown). Considering all the results obtained, we can conclude that Mg^{2+} is the preferred ion for the activity of RNase II-family of enzymes. However, these proteins are still able to perform its function in the presence of other ions, such as Ca^{2+}, Ni^{2+} and Zn^{2+}. This ability can be very important, since it may allow the cell to regulate the activity of these ribonucleases when different divalent metals are available. This will also allow the cells to change their RNA metabolism in order to better adapt to new environmental conditions. Considering that the higher activity was obtained in a buffer with Mg^{2+}, we tested which could be the best Mg^{2+} concentration for the reaction to occur. For that purpose, we used four different buffers with concentrations ranging from 1 to 10mM of Mg^{2+}. As presented in figure 3B left panel, we were able to see that the protein decreased its activity when we increased the Mg^{2+} concentration. These results were confirmed when the activity of the protein was determined (Figure 3B, right panel). From the concentrations of Mg^{2+} tested, RNase R from *H. volcanii* showed to have preference for the lower one, which was 1mM.

Altogether, the results obtained allowed us to establish the optimal conditions for the activity of *H. volcanii* RNase R protein: 100mM of KCl, pH of 8 and 1mM of $MgCl_2$. We also showed that the protein was active in other conditions, namely in the presence of other divalent ions, but the activity was reduced when compared to the one obtained in these conditions. For the following experiments, we used the conditions described above.

RNase R from H. volcanii behaves like an RNase II-like protein. In the first part of these experiments, we wanted to determine the optimal conditions for the activity of RNase R from *H. volcanii*. This determination was important to further test the activity of the protein against different substrates. We used three substrates (two single-stranded and one double-stranded) to analyze the behaviour of RNase R from *H. volcanii*. Although RNase II and RNase R share some catalytic properties, they are different regarding the final-end product released and also in their ability to degrade structured molecules (7). RNase II degrades RNA molecules releasing a final end product with 4 nucleotides of length and stalls 5 to 7 nt before it reaches a double-stranded region. Contrary, RNase R is able to overcome secondary structures and degrades the RNA molecules releasing a final product of 2 nt (18,23).

When we tested the activity of RNase R protein from *H. volcanii* we were expecting that it would behave like RNase R, since it was previously described that, regarding the amino acid sequence, it is more similar to *E. coli* RNase R (34% of identity) than to RNase II (26% of identity) (10). However, these predictions were not verified when we analysed the RNA degradation bahaviour. As already mentioned, we tested the activity of RNase R protein from *H. volcanii* against two single-stranded substrates, the Poly(A) and the 16-mer. For both molecules, it is possible to verify that the protein behaves like RNase II regarding the end-product released (Figure 4). When the substrate used was the Poly(A), the enzyme accumulated an intermediary fragment of 5 nucleotides of length, which was then converted to the typical 4 nt fragment as the reaction proceeded (Figure 4). The same behaviour was already described for *E. coli* RNase II while *E. coli* RNase R is able to degrade a few more nucleotides releasing a 2 nt final product (Figure 4). If we increase the protein concentration or use longer incubation periods, we could observe that the intermediate fragment of 5 nt was completely converted into the 4 nt product (data not shown). For the 16-mer substrate, a similar result was obtained. However, the intermediate fragment observed had 6 nt of length and not the 5 nt fragment obtained in the degradation of the

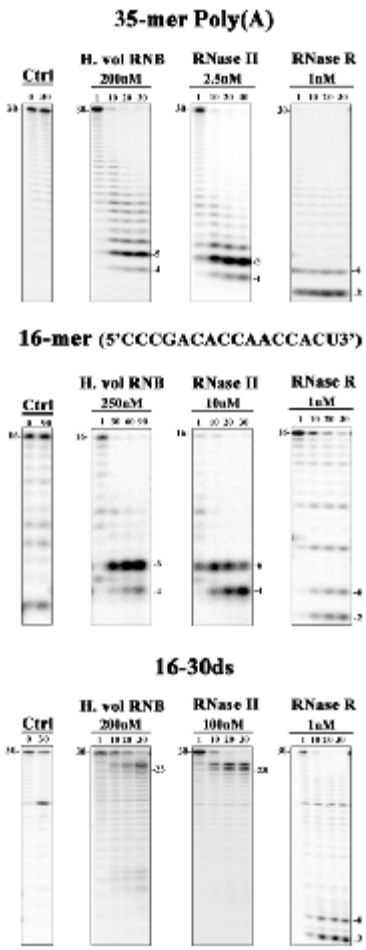

Figure 4. Exoribonucleolytic activity of RNase R from *H. volcanii*: comparison with *E. coli* RNase II and RNase R. Activity assays were performed at 37ºC as described in Materials and Methods using three different substrates: 30-mer poly(A), the 16-mer and the double-stranded substrate 16-30ds, as referred. The concentration of proteins used is indicated in the figure. Samples were taken during the reaction at the time points indicated and reaction products were analyzed in a 20% polyacrylamide/7M urea gel. Control reactions with no enzyme added (*Ctrl*) were incubated at the maximum reaction time for each protein. Length of substrates and degradation products are labelled.

Poly(A) substrate for both *E. coli* RNase II and *H. volcanii* RNase R (Figure 4). This may be related with substrate sequence, namely with the fact that the fifth nucleotide counting from the 5´ end is an adenine, which is the preferred substrates of these enzymes. For substrates smaller than 10 nucleotides of length, the activity of these proteins became distributive (13,25), which means that it degrades a nucleotide, releases the fragment and binds to other RNA molecule. In this case, when the sixth fragment is released (5'CCCGAC3') and the protein binds again to it and cleaves the C at the 3' end, then the nucleotide after is an adenosine. Since it was showed that proteins from the RNase II family have preference for Poly(A) substrates (15,26), the protein can have more affinity and bind more efficiently to the 5 nt fragment than to the 6 nt fragment, which would enable us to observe the 5 nt fragment as intermediate.

Considering the results obtained in the assays with the single-stranded substrates, we could observe that RNase R from *H. volcanii* behaves like an RNase II-like protein regarding the final product released and not an RNase R-like protein. We then went to test how this recombinant protein behaves regarding the degradation of double-stranded substrates. Once again, *H. volcanii* RNase R showed a behaviour similar to the one presented by *E. coli* RNase II protein, since it was not able to degrade structured molecules, stalling 7 nucleotides before it reached the double-stranded region (Figure 4). Considering that we are in the presence of an organism which lacks polyadelylation, we could expect that it would compensate the degrading activity on structured RNAs. However, this is not the case since that this protein is not able to degrade structured RNAs. The results obtained led us to conclude that, although the *H. volcanii* homologue presented a higher similarity to *E. coli* RNase R regarding its amino acid sequence (10), it behaves like an RNase II-like protein since it is not able to degrade double-stranded substrates and releases a fragment of 4 nt and end-product of the reaction.

RNase R from H. volcanii has a dual activity according to temperature. Although *H. volcanii* is able to grow at 37ºC, its optimal temperature of growth is around 42ºC (11). Since that the results described above were all performed at 37ºC, we also decided to test the activity of the protein in the same conditions and with the same substrates at 42ºC.

The results obtained with the single-stranded substrates were similar to the ones obtained at 37ºC. However, for the Poly(A) substrate we can see that the activity is reduced at 42ºC for the three proteins. For *H. volcanii* RNase R and *E. coli* RNase II, we were able to see that the proteins needed more time to completely degrade the RNA molecules until they reach the final product of 4 nt, which was not reached in the same conditions used at 37ºC (Figure 5) but only when higher incubation periods were used (data not shown). However, when we determined the activity of the protein at both temperatures, we could see that it was very similar for all the substrates tested (Figure 6). This determination was performed taking into account the amount of substrate degraded along time and not the formation of the 4 nt end-product. Probably, this was the reason why we did not detect any difference regarding the activity at both temperatures. For the 16-mer substrate, we did not detect any difference between the assays run at 37ºC and 42ºC (Figure 5).

Surprisingly, when we tested the activity of the RNase R form *H. volcanii* at 42ºC, the result was not similar to the one obtained at 37ºC. While at 37ºC the protein was not able to degrade double-stranded substrates, behaving like RNase II, at 42º the protein is now able to overcome secondary structures and degrade the 16-30ds substrate completely releasing a mixture of fragments with 4 and 6 nt of length. It is known that at high temperatures the RNA structures are less stable, which led us to ask if the result obtained could be due to a destabilization of the structure of the RNA molecule. In order to discard this hypothesis, we also tested RNase II as a negative control and RNase R as a positive control. At the same temperature we were able to see that RNase II was still not able to degrade the 16-30ds substrate, while RNase R, as expected, was able to overcome the secondary structure (Figure 5). This experiment allowed us to verify the integrity of our structured RNA at this temperature, since RNase II was not able to degrade it.

In *H. volcanii* there is no archaeal exosome and its genome lacks a number of proteins involved in RNA degradation, namely PNPase and PAP I. However, only one gene for a putative exoribonuclease is found and it was shown to have significant homology to RNase R. This protein is essential for

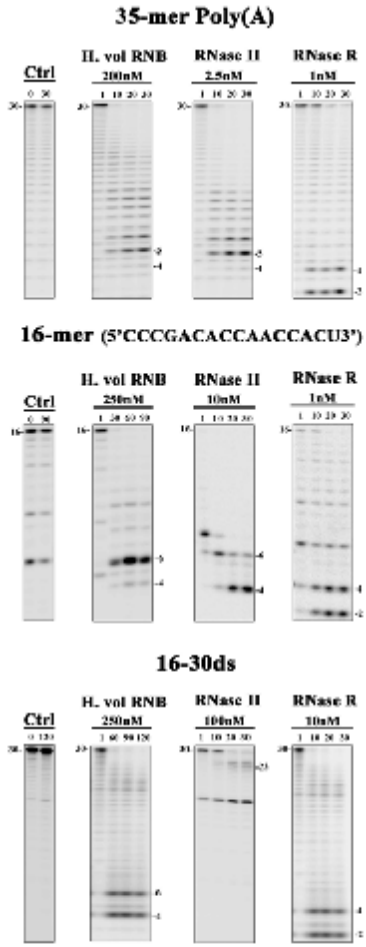

Figure 5. Exoribonucleolytic activity of RNase R from *H. volcanii*: comparison with *E. coli* RNase II and RNase R. Activity assays were performed at 42ºC as described in Materials and Methods using three different substrates: 30-mer poly(A), the 16-mer and the double-stranded substrate 16-30ds, as referred. The concentration of proteins used is indicated in the figure. Samples were taken during the reaction at the time points indicated and reaction products were analyzed in a 20% polyacrylamide/7M urea gel. Control reactions with no enzyme added (*Ctrl*) were incubated at the maximum reaction time for each protein. Length of substrates and degradation products are labelled.

cell survival, which indicates that plays a crucial role in RNA metabolism and it may be the only responsible for the exoribonucleolytic activity observed in *H. volcanii* (4,10). By analysing the activity of this protein, we could see that, although is more similar in its amino acid sequence to RNase R (10), at 37º C it behaves like RNase II and it not able to degrade structured RNAs. At high salt concentrations, RNA is encouraged to become more structured and we could wonder how *H. volcanii* is able to deal with RNA degradation in the absence of a protein able to overcome double-stranded substrates. One possible explanation could be that the RNA degradation could be maily performed by endoribonucleases which would cleave all double-stranded regions and leaving only singe-stranded substrates to be degraded by RNase R. However, in *H. volcanii* genome we can only find homologues from RNase Z and RNase H. RNase Z was already described as an

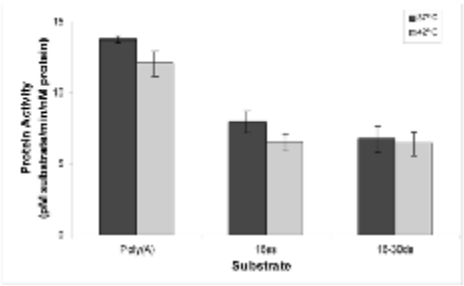

Figure 6. Determination of the activity of RNase R from *H. volcanii* at two different temperatures. The activity of the protein was determined at 37ºC and 42ºC using three different substrates: 30-mer poly(A), 16-mer and the double-stranded 16-30ds. All the activity assays were performed in triplicate.

endoribonuclease involved in tRNA processing and, more recently, in the maturation of 5S rRNA (27,28). RNase H from *H. volcanii* was not yet characterized but it is usually involved in the degradation of the RNA of RNA/DNA hybrids that are formed during replication and repair (7). This may implicate the existence of other ribonucleases in archaeal organisms which homology to the know ribonucleases was not detected or does not exist. However, at 42ºC, the optimal temperature of growth, we have a different scenario. At this temperature, we showed that RNase R from *H. volcanii* was able to degrade double-stranded molecules. We can then conclude that the role of RNase R is more important for RNA degradation at 42ºC, where is able to degrade a wide variety of molecules. In this case, we may have a conformational change of the RNA dependent of temperature, most likely thermal breathing of the duplex. This would allow the double-stranded structures to transiently open, which could facilitate the degradation of dsRNA at this temperature.

This work fully characterized RNase R protein form *H. volcanii*. Although is was predicted to be more similar to *E. coli* RNase R, the results presented here show that at 37ºC, it behaves like RNase II regarding the ability to degrade double stranded substrates and also in the final product released. Surprisingly, when we tested the activity of the protein at 42ºC, we could see that it was able to degrade dsRNAs. We are in the presence of a protein with dual activity, which can acts like RNase II or RNase R, according to the temperature. The results obtained are very important to help to decipher the RNA degradation mechanisms in *H. volcanii*, since RNase R seems to be the only enzyme involved in this process.

ACKNOWLEDGMENTS

We thank Andreia Aires for her technical support in the lab. Rute G. Matos was a recipient of a PhD fellowship funded by FCT- Fundação para a Ciência e a Tecnologia, Portugal. This work was supported by FCT-Fundação para a Ciência e a Tecnologia, Portugal.

REFERENCES

1.**Brown, J.W. and J.N. Reeve.** 1986. Polyadenylated RNA isolated from the archaebacterium Halobacterium halobium. Journal of bacteriology *166*:686-688.

2.**Evguenieva-Hackenberg, E., P. Walter, E. Hochleitner, F. Lottspeich, and G. Klug.** 2003. An exosome-like complex in *Sulfolobus solfataricus*. EMBO Reports *4*:889-893.

3.**Farhoud, M.H., H.J. Wessels, P.J. Steenbakkers, S. Mattijssen, R.A. Wevers, B.G. van Engelen, M.S. Jetten, J.A. Smeitink, et al.** 2005. Protein complexes in the archaeon *Methanothermobacter* thermautotrophicus analyzed by blue native/SDS-PAGE and mass spectrometry. Mol Cell Proteomics *4*:1653-1663.

4.**Portnoy, V., E. Evguenieva-Hackenberg, F. Klein, P. Walter, E. Lorentzen, G. Klug, and G. Schuster.** 2005. RNA polyadenylation in Archaea: not observed in *Haloferax* while the exosome polynucleotidylates RNA in *Sulfolobus*. EMBO Reports *6*:1188-1193.

5.**Zuo, Y. and M.P. Deutscher.** 2001. Exoribonuclease superfamilies: structural analysis and phylogenetic distribution. Nucleic acids research *29*:1017-1026.

6.**Koonin, E.V., Y.I. Wolf, and L. Aravind.** 2001. Prediction of the archaeal exosome and its connections with the proteasome and the translation and transcription machineries by a comparative-genomic approach. Genome research *11*:240-252.

7.**Arraiano, C.M., J.M. Andrade, S. Domingues, I.B. Guinote, M. Malecki, R.G. Matos, R.N. Moreira, V. Pobre, et al.** 2010. The critical role of RNA processing and degradation in the control of gene expression. FEMS Microbiology Reviews *34*:883-923.

8.**Anantharaman, V., E.V. Koonin, and L. Aravind.** 2002. Comparative genomics and evolution of proteins involved in RNA metabolism. Nucleic acids research *30*:1427-1464.

9.**Even, S., O. Pellegrini, L. Zig, V. Labas, J. Vinh, D. Brechemmier-Baey, and H. Putzer.** 2005. Ribonucleases J1 and J2: two novel endoribonucleases in *B.subtilis* with functional homology to *E.coli* RNase E. Nucleic acids research *33*:2141-2152.

10.**Portnoy, V. and G. Schuster.** 2006. RNA polyadenylation and degradation in different Archaea; roles of the exosome and RNase R. Nucleic acids research *34*:5923-5931.

11.**Mullakhanbhai, M.F. and H. Larsen.** 1975. *Halobacterium volcanii* spec. nov., a Dead Sea *Halobacterium* with a moderate salt requirement. Archives of microbiology *104*:207-214.

12.**Arraiano, C.M., R.G. Matos, and A. Barbas.** 2010. RNase II: The finer details of the *Modus operandi* of a molecular killer. RNA biology *7*.

13.**Frazão, C., C.E. McVey, M. Amblar, A. Barbas, C. Vonrhein, C.M. Arraiano, and M.A. Carrondo.** 2006. Unravelling the dynamics of RNA degradation by ribonuclease II and its RNA-bound complex. Nature *443*:110-114.

14.**Amblar, M., A. Barbas, A.M. Fialho, and C.M. Arraiano.** 2006. Characterization of the functional domains of Escherichia coli RNase II. Journal of molecular biology *360*:921-933.

15.**Barbas, A., R.G. Matos, M. Amblar, E. Lopez-Viñas, P. Gomez-Puertas, and C.M. Arraiano.** 2008. New insights into the mechanism of RNA degradation by ribonuclease II: identification of the residue responsible for setting the RNase II end product. The Journal of biological chemistry *283*:13070-13076.

16.**Matos, R.G., A. Barbas, and C.M. Arraiano.** 2009. RNase R mutants elucidate the catalysis of structured RNA: RNA-binding domains select the RNAs targeted for degradation. Biochem J *423*:291-301.

17.**Dziembowski, A., E. Lorentzen, E. Conti, and B. Seraphin.** 2007. A single subunit, Dis3, is essentially responsible for yeast exosome core activity. Nature structural & molecular biology *14*:15-22.

18.**Andrade, J.M., V. Pobre, I.J. Silva, S. Domingues, and C.M. Arraiano.** 2009. The role of 3'-5' exoribonucleases in RNA degradation. Prog Mol Biol Transl Sci *85*:187-229.

19.**Vincent, H.A. and M.P. Deutscher.** 2009. The Roles of Individual Domains of RNase R in Substrate Binding and Exoribonuclease Activity: THE NUCLEASE DOMAIN IS SUFFICIENT FOR DIGESTION OF STRUCTURED RNA. The Journal of biological chemistry *284*:486-494.

20.**Matos, R.G., A. Barbas, P. Goméz-Puertas, and C.M. Arraiano.** 2011. Swapping the domains of exoribonucleases RNase II and RNase R: conferring upon RNase II the ability to degrade dsRNA. Proteins.

21.**Ge, Z., P. Mehta, J. Richards, and A.W. Karzai.** 2010. Non-stop mRNA decay initiates at the ribosome. Molecular microbiology *78*:1159-1170.

22.**Amblar, M. and C.M. Arraiano.** 2005. A single mutation in Escherichia coli ribonuclease II inactivates the enzyme without affecting RNA binding. FEBS J *272*:363-374.

23.**Amblar, M., A. Barbas, P. Gomez-Puertas, and C.M. Arraiano.** 2007. The role of the S1 domain in exoribonucleolytic activity: substrate specificity and multimerization. RNA (New York, N.Y *13*:317-327.

24.**Arraiano, C.M., A. Barbas, and M. Amblar.** 2008. Characterizing ribonucleases *in vitro* examples of synergies between biochemical and structural analysis. Methods Enzymol *447*:131-160.
25.**Cannistraro, V.J. and D. Kennell.** 1994. The processive reaction mechanism of ribonuclease II. Journal of molecular biology *243*:930-943.
26.**Barbas, A., R.G. Matos, M. Amblar, E. Lopez-Vinas, P. Gomez-Puertas, and C.M. Arraiano.** 2009. Determination of Key Residues for Catalysis and RNA Cleavage Specificity: one mutation turns RNase II into a "super-enzyme". The Journal of biological chemistry *284*:20486-20498.
27.**Holzle, A., S. Fischer, R. Heyer, S. Schutz, M. Zacharias, P. Walther, T. Allers, and A. Marchfelder.** 2008. Maturation of the 5S rRNA 5' end is catalyzed in vitro by the endonuclease tRNase Z in the archaeon *H. volcanii*. RNA (New York, N.Y *14*:928-937.
28.**Schierling, K., S. Rosch, R. Rupprecht, S. Schiffer, and A. Marchfelder.** 2002. tRNA 3' end maturation in archaea has eukaryotic features: the RNase Z from *Haloferax volcanii*. Journal of molecular biology *316*:895-902.

SUPPLEMENTARY FIGURE

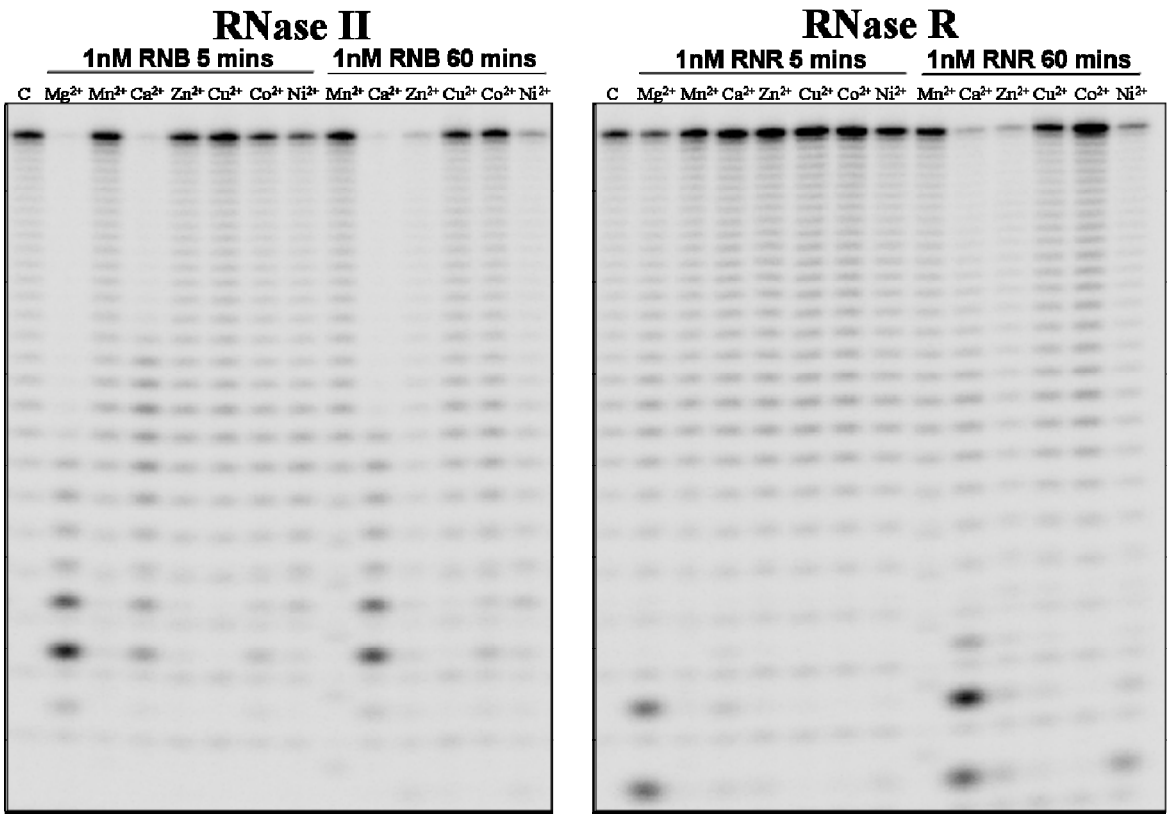

Figure S1: Activity of *E. coli* RNase II and RNase R in the presence of different divalent metal ions. 1nM of recombinant protein were incubated with 10nM of Poly(A) substrate at 37ºC for 5 and 60 minutes in a reaction buffer containing different divalent ions as indicated in figure. On the left we present the results obtained for *E. coli* RNase II and on the right the results obtained for *E. coli* RNase R.

The *rnb* Gene of *Synechocystis* PCC6803 Encodes an RNA Hydrolase Displaying RNase II and not RNase R Properties

Rute G. Matos[1], Arsénio M. Fialho[2], Gadi Schuster[3] and Cecília M. Arraiano[1]✉

1 Instituto de Tecnologia Química e Biológica/Universidade Nova de Lisboa, Apartado 127, 2781-901 Oeiras, Portugal
2 Institute for Biotechnology and Bioenineering Centre for Biological and Chemical Engineering/Instituto Superior Técnico, Lisboa, Portugal.
3 Faculty of Biology, Technion-Israel Institute of Technology, Haifa 32000, Israel

Cyanobacteria are photosynthetic prokaryotic organisms which share characteristics from bacteria and chloroplasts regarding mRNA degradation. *Synechocystis* PCC6803 is a model organism for cyanobacteria, and not much is known about the mechanism of RNA degradation in these organisms. In the genome of *Synechocystis sp*. it is possible to find only one member of the RNase II-family of proteins. This protein was shown to be essential for its viability, which indicates that may have a crucial role in *Synechocystis* metabolism. The aim of this work was to characterize the activity of RNase II/R homologue present in *Synechocystis* PCC6803. Although being the only member of this family present and contrary to what happens for other microorganisms where when only one member is found it behaves like RNase R, the results showed that this protein behaves like an RNase II-like protein. This is the first case reported where the only member of the RNase II family of enzymes present in an organism behaves like an RNase II and not like RNase R.

Cyanobacteria are photosynthetic prokaryotic organisms comprising the major biomass of living organisms in earth oceans, and believed to be related to the ancestor of chloroplasts. They share characteristics from bacteria and chloroplasts regarding mRNA degradation. *Synechocystis* PCC6803 is a model organism for cyanobacteria, and not much is known about the mechanism of RNA degradation in this class of organisms.

The *Synechocystis* genome contains genes that have a high homology to RNase E, PNPase, RNase II/R and PAP, the proteins involved in mRNA degradation and polyadenylation (1). The polyadenylation pathway was already studied and it was shown that the product of the putative PAP gene has nucleotidyltransferase and not polyadenylation activity. Instead, the reaction of polyadenylation in *Synechocystis* is performed by PNPase, which originates heterogenous poly(A)-rich tails (1). Previous results showing that in chloroplasts of higher plants there is no equivalent of *E. coli* PAP and the tails are also heterogeneous were subsequently corrected that there is a PAP in the chloroplast of higher plants and, together with PNPase, contributes to the polyadenylation activity (2,3). In *Synechocystis* the absence of PNPase is lethal for the cell (1). The same behaviour was observed by disrupting the genes for RNase II/R and RNase E (1). In *Synechocystis*, the RNase E homologue is more related with RNase G, and it is not associated in a multicomponent complex, such as the *E. coli* degradosome (1). However, *in vivo* assays showed that RNase E homologue from *Synechocystis* is able to complement the functions of both RNase E and RNase G in *E. coli*. Moreover, its endonucleolytic activity was confirmed *in vitro*, showing that cleavage is dependent on the primary target sequence and on the secondary structure of the mRNA to be degraded (4).

By analyzing *Synechocystis sp*. genome it is possible to see that there is only one member of the RNase II-family of proteins. Proteins from this family are present in all domains of life, are involved in several processes, and play a central role in the mechanism of gene expression (5). In Eukaryotes, RNase II homologues are part of a multiprotein complex, the exosome, where they are the catalytic subunit. Mutants in these homologues have shown defects in development, mitotic control and chloroplast biogenesis (6). In Prokaryotes, they are important for growth and stress responses and they are also involved in virulence (5,6). RNase II is the prototype of this family of enzymes, which also comprises RNase R in *E. coli*. They both act hydrolytically, degrading RNA molecules in the 3' to 5' direction, releasing 5'-nucleoside monophosphates (7). The resolution of RNase II crystal structure showed that it is composed of two N-terminal Cold Shock Domains (CSD) domains and a C-terminal S1 domain involved in RNA binding (8,9). The central RNB domain is the responsible for the catalytic activity of the protein (8-10). This domain organization is seen in all family members. In the RNase II catalytic cavity, the first five nucleotides of the RNA molecule counting from the 3' end RNA are stacked between two aromatic residues, Tyr253 and Phe358. After the last cleavage event, the 4 nt fragment is no longer able to be stacked between those residues, which explains why 4 nt is the final end-product released by RNase II (8). A mutational analysis showed that the Tyr253 is crucial for setting the final end product, not only in RNase II (11) but also in RNase R (10), indicating that its role may be conserved in all members of this family of enzymes. The active site is formed by four highly conserved aspartates (Asp201, Asp207, Asp209 and Asp210) and an arginine (Arg500), which were shown to be important for the activity of the protein and proper RNA binding/orientation (11-13). From these residues, Arg209 was the only one critical for the activity of RNase II, since its substitution for an asparagine totally abolished the activity without affecting RNA binding ability (12). The same results were obtained for other members of this family (10,14-16). However, the most intriguing finding which arise from this mutational study performed with RNase II was obtained when the Glu542, a residue postulated to be involved in nucleotide elimination, was changed into an alanine. This substitution resulted in a protein with an enhanced RNA affinity and >100 times more active when compared to the wild type, which was named as "super-enzyme" (13).

Although belonging to the same family and sharing structural and domain organization, *E. coli* RNase II and RNase R act differently on RNA substrates and have different specificities. RNase R was shown to have an intrinsic ability to unwind double-stranded RNAs (14,17), while RNase II is sensitive to these structures and stalls a few nucleotides before reaching the double-stranded region (5). RNase II is responsible

for 90% of the hydrolytic activity in *E. coli* (18), however, in stationary phase and stress conditions (like cold-shock induction), RNase R levels increase in the cell (19). This can be related to the crucial role that RNase R has in RNA quality control, namely in the degradation of defective tRNA and rRNA (20), and also in protein quality control (19). Contrary, RNase II is mainly involved in the terminal stages of mRNA degradation and its activity can be replaced by PNPase. It was also suggested that the main function of RNase II can be the protection of some mRNA transcripts by rapidly removing the poly(A) tail which is tagging them to be degraded (21).

In Cyanobacteria nothing is know about this family of enzymes, except that RNase II/R protein is essential for the viability of these organisms (1). This indicates that RNase II/R homologue may have a crucial role in *Synechocystis* metabolism. The aim of this work was to characterize the activity of RNase II/R homologue present in *Synechocystis* PCC 6803 as a first approach for the study of the role of this enzyme in RNA metabolism in cyanobacteria. Although being the only member of this family present and contrary to what happens for other microorganisms where when only one member is found it behaves like RNase R (e.g. *Mycoplasma genitallium* and *Streptococcus pneumoniae* (22,23)), the results showed that this protein behaves like an RNase II-like protein: the final product released is a 4 nt fragment and the protein is not able to degrade structured substrates. This is the first case reported where the only member of the RNase II family of enzymes present in an organism behaves like an RNase II and not like RNase R. However, while RNase II prefers Poly(A) substrates (11,13), RNase II from *Synechocystis* does not demonstrate such preference. This may happen because there is no PAP and the tails found are heterogeneous (1).

MATERIAL AND METHODS

Overexpression and purification of recombinant RNase II from Synechocystis sp. The plasmid used for expression of *Synechocystis sp.* histidine-tagged RNase II protein was pQE31synRNB. This plasmid contains the *rnb* gene of *Synechocystis sp.* cloned into pQE vector (Qiagen) that allows the expression of the $(His)_6$-tagged RNase II fusion protein.

The plasmid was transformed into M15 (REP4) strain to allow the expression of the recombinant protein. Cells were grown at 37ºC in 100 ml LB medium supplemented with 150 μg/ml ampicillin to an A_{600} of 0.5 and induced by addition of 0.5 mM IPTG for 2h. Cell culture was pelleted by centrifugation and stored at -80°C. *E. Coli* RNase II and RNase R overexpression were performed as described previously (12,24,25).

Purification was performed by histidine affinity chromatography using HiTrap Chelating HP columns (GE Healthcare) and AKTA HLPC system (GE Healthcare) following the protocol described previously (12,25). The fractions containing the purified *Synechocystis* protein were pooled and loaded to an anion exchange monoQ column (GE Healthcare) equilibrated in buffer composed by 20mM Tris pH 8, 60mM KCl, 2mM $MgCl_2$ and 0.2mM EDTA. Protein elution was achieved by a continuous KCl gradient (from 60mM to 1M) in buffer B. Protein concentration was determined by spectrophotometry by using the ND100 Spectrophotometer from Nanodrop and 50% (v/v) glycerol was added to the final fractions prior storage at -20 ºC. 0.5 μg of the purified protein was applied to 8% SDS-PAGE and visualized by Coomassie blue staining (data not shown).

Exoribonucleolytic Activity Assays. The exoribonucleolytic activity was determined using different substrates: a Poly(A) oligomer of 30 nts, a 16-mer oligoribonucleotide (5'-CCCGACACCAACCACU-3'), and a 30-mer oligoribonucleotide (5'-CCCGACACCAACCACUAAAAAAA AAAAAAA-3') hybridized to the complementary non labelled 16mer oligodeoxiribonucleotide (5'-dAGTGGTTGGTGTCGG G-3'), in order to obtain the double stranded substrate 16-30ds (the hybridization was performed in a 1:1 (mol:mol) ratio by 5 min incubation at 100ºC followed by 45 min at 37ºC). All RNA molecules were labelled at 5' end with [γ-^{32}ATP] and T4 polynucleotide kinase. The RNA oligomers were then purified using Microcon YM-3 Centrifugal Filter Devices (Millipore) to remove the non-incorporated nucleotide. The exoribonucleolytic reactions were carried out in a final volume of 12.5 μl containing 5 nM of substrate, 20 mM Tris-HCl (pH tested from 6.5 to 9), KCl or NaCl (from 10 to 200mM), $MgCl_2$ (from 1 to 10 mM), and 1 mM DTT. The amount of each enzyme added to the reaction was adjusted to obtain linear conditions and is indicated in the figures and respective legends. Reactions were started by the addition of the enzyme and incubated at 30ºC or 37ºC. Samples were withdrawn at the time points indicated and the reaction was stopped by adding formamide-containing dye supplemented with 10 mM EDTA. Reaction products were resolved in a 20% polyacrylamide/7 M urea and detected by using the Fuji Phosphorimager Analyzer TLA-5100 from GE Healthcare. The exoribonucleolytic activity of the enzyme was determined by measuring and quantifying the disappearance of the substrate in several distinct experiments in which the protein concentration was adjusted in order that, under those conditions, less than 25% of substrate was degraded. Each value obtained represents the mean for these independent assays.

Surface plasmon resonance analysis - BIACORE. Biacore SA chips were obtained from Biacore Inc. (GE Healthcare). The Flow cells of the SA streptavidin sensor chip were coated with a low concentration of the following substrates. On flow cell 1 no substrate was added so this cell could be used as the control blank cell. On flow cell 2 a 5' biotinylated 25-nucleotide RNA oligomer (5'-CCCGACACCAACCACUAAAAAAAA A-3') was added to allow the study of the protein interaction with a single-stranded RNA molecule. On flow cell 3 a 5' biotinylated 30-mer PolyA substrate. On flow cell 4 the biotinylated 25mer hybridized with the complementary 16mer oligodeoxiribonucleotide (5'-AGTGGTTGGTGTCGGG-3') was immobilized, originating the double-stranded substrate 16-25ds. The target substrates were captured on flow cells 2 to 4 by manually injecting 20 μl of a 500 nM solution of the substrates in the reaction buffer at a 20 μl/min flow rate. The biosensor assay was run at 4°C in the buffer with 20 mM Tris-HCl pH7,5, 50 mM KCl, 1 mM DTT and 25 mM EDTA. The proteins were injected over flow cells 1, 2, 3 and 4 for 2.5 min at concentrations of 10, 20, 30, 40 and 50 nM using a flow rate of 20μl/min. All experiments included triple injections of each protein concentration to determine the reproducibility of the signal and control injections to assess the stability of the RNA surface during the experiment. Bound protein was removed with a 30s wash with 2 M NaCl. Data from flow cell 1 were used to correct for refractive index changes and non-specific binding. Rate and equilibrium constants were calculated using the BIA EVALUATION 3.0 software package, according to the fitting model 1:1 Languimir Binding.

Protein Modelling. The model structures were built using the Swiss Model web server (http://swissmodel.expasy.org/ (26-28)). 3D models for the hybrid proteins were based on the crystal structures of wild-type RNase II and the RNase II D209N mutant complexed with a 13-nucleotide poly(A) RNA (Protein Data Bank entries 2IX1 and 2IX0(8)). Figures of the structure and models were generated with Pymol (29).

RESULTS AND DISCUSSION

Salt and pH preference of the RNase II-family protein in Synechocystis sp. In order to characterize the activity of the RNase II/R homologue from *Synechocystis* and determine the optimal conditions for the catalysis, we analysed the optimal concentrations for activity of the protein for NaCl and KCl. We also determined the pH preference of the protein by varying this parameter.

To assess the effect of salt type and concentration, we performed activity assays with 10, 50, 100, 150 and 200 mM of NaCl and KCl as described in materials and methods. The activity of the protein was measured by quantifying the disappearance of the substrate along the time. The conditions used for this and the following determinations were adjusted to guarantee that less than 25 % of the substrate was being degraded. The results obtained are presented in Figure 1. When the salt used was NaCl, the protein seemed inactive for all the concentrations tested, while in the presence of KCl we were able to detect activity with all the concentrations used, although the proteins preferred 50 mM KCl (Figure 1A). However, by quantifying the activity of the protein along time, we were able to see that, in fact, the protein was active in the presence of NaCl, but the cleavage efficiency was 10 times lower when compared to KCl (Figure 1B). We were also able to confirm that, in fact, the preferred KCl concentration was 50 mM. For higher salt concentrations, the activity of the protein starts to decrease (Figure 1B). Taking these results into consideration, we used an activity buffer with a salt concentration of 50 mM of KCl for the remaining experiments.

After establishing the optimal salt concentration for the activity of the protein, we analyzed the effect of pH in catalysis to determine which was the preferred for the activity. For that purpose, we tested the activity of the recombinant protein using different activity buffers with a pH ranging from 6.5 to 9 in the presence of 50 mM of KCl, as previously determined. The results obtained showed that at lower pH levels the activity of the protein was impaired, it raised and reached the maximum activity at 8 and then the activity started to decrease again (Figure 2). From these experiments we could conclude that the optimal activity from RNase II/R from *Synechocystis sp.* is achieved at a pH of 8, although the activity at 7.5 and 8.5 is not so different from pH=8 (Figure 2B).

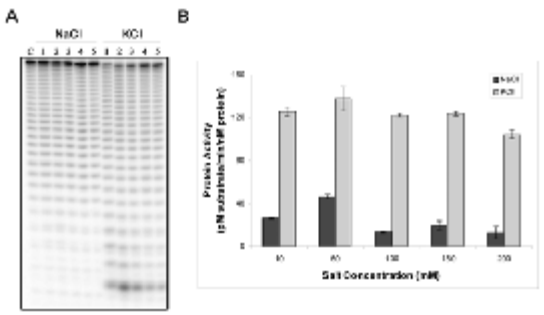

Figure 1. Salt dependence of *Synechocystis* RNase II/R homologue. A. 5nM of recombinant protein were incubated with 10nM of Poly(A) at 37ºC for 5 minutes in a reaction buffer with different salt concentrations (lanes 1 =10mM, lanes 2 = 50mM, lanes 3 = 100mM, lanes 4 = 150mM, and lanes 5 = 200mM). **B.** Determination of the protein activity in the presence of NaCl and KCl in different concentrations.

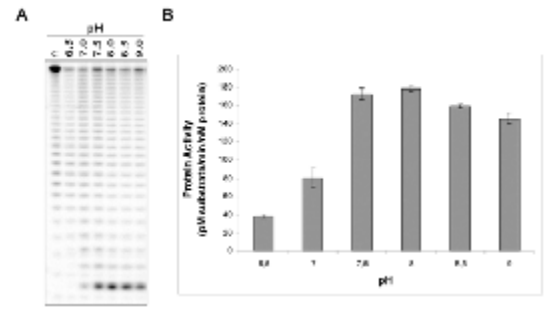

Figure 2. pH dependence of *Synechocystis* RNase II/R homologue. A. 5nM of recombinant protein were incubated with 10nM of Poly(A) at 37ºC for 5 minutes in a reaction buffer with different pH, ranging from 6.5 to 9. **B.** Determination of the protein activity in the presence of different pH.

This initial analysis allowed us to determine that the optimal salt and pH conditions for the activity of the RNase II/R homologue in *Synechocystis sp.* are 50 mM of KCl and pH=8.0, respectively. These conditions were the ones used for the following experiments.

RNase II/R protein from Synechocystis sp. prefers Mg^{2+} for its activity. Exoribonucleases from the RNase II-family of enzymes need a divalent ion in order to proceed with catalysis. For *E. coli* RNase II and RNase R, the presence of Mg^{2+} is crucial for the activity of the proteins (8), however, catalysis can also occur in the presence of other divalent ions (unpublished results). We then tested the activity of the *Synechocystis* homologue with different divalent metal ions: Mg^{2+}, Mn^{2+}, Ca^{2+}, Zn^{2+}, Cu^{2+}, Co^{2+}, and Ni^{2+}. As shown in figure 3A, incubating the RNA with 10nM of protein during 5 minutes we can only detect activity in the presence of Mg^{2+} (Figure 3A). In the presence of Ca^{2+}, it seems that the protein has some residual activity. To confirm this, we increased the time of the reaction, and saw that, after one hour of incubation in a buffer with Ca^{2+}, the protein is also able to cleave the substrate (Figure 3A). In the same conditions no activity can be detected for all the other divalent ions tested (Figure 3A).

These experiments allowed us to conclude that the RNase II/R homologue from *Synechocystis* needs an Mg^{2+} ion for the catalysis, but is also able to cleave RNA in the presence of Ca^{2+}, although with less efficiency. Taking these results into consideration, we then tested the activity of the protein using different Mg^{2+} concentrations (1, 2.5, 5 and 10mM). As shown in figure 3B and C, we were able to determine that the protein is more active in the presence of 1mM of Mg^{2+} and that for higher concentrations, the protein activity started to decrease (Figure 3B and C).

All these experiments allowed us to determine the optimal conditions for the activity of RNase II/R homologue from *Synechocystis sp*. The protein preferred KCl in a concentration of 50mM and was substantially less active with NaCl. It was shown to be more active in a pH of 8, although it showed a similar activity with pH 7.5 and 8.5. We also tested the activity of the protein with different cations and, from the ones tested, we saw that the protein presented higher activity in the presence of 1mM of Mg^{2+}, but it was also shown to be able to degrade the substrate in the presence of Ca^{2+}, although with less efficiency.

For the following experiments, these were the conditions used in the activity assays (20mM Tric-HCl pH 8, 50mM KCl, and 1mM $MgCl_2$) and also for the SPR experiments (in this case,

without Mg^{2+} and in the presence of EDTA to avoid substrate degradation).

Synechocystis sp. homologue displays RNase II-properties. After determining the optimal conditions for the activity buffer of the RNase II/R homologue of *Synechocystis* PCC6803, we analyzed the behaviour of the protein regarding the final end-product released using both single and double-stranded substrates as mentioned in Materials and Methods.

Both RNase II and RNase R of *E. coli* share some catalytic properties, however, they behave differently regarding the final product released and also in their ability to degrade double-stranded RNAs (10,13). While the *E. coli* RNase II releases a final end product of 4 nt and is sensitive to secondary structures, stalling 5 to 7nt before it reaches the double stranded region, RNase R degrades RNA releasing fragments of 2 nt of length and is able to overcame structured RNAs (10,13). We then tested how the recombinant protein from *Synechocystis* behaved regarding the degradation of two single-stranded substrates, Poly(A) and 16ss, and also using the double-stranded substrate 16-30ds. In order to compare *Synechocystis* RNase II/R homologue with *E. coli* RNase II and RNase R, the three proteins were tested at the same time. The activity of RNase II and RNase R was assayed in the conditions previously described (12,24,25). For the *Synechocystis* protein, the conditions used were the ones described above. The results obtained are represented in Figure 4.

It was already shown that *E. coli* RNase II and RNase R prefer poly(A) substrates (10,13). For that reason, this was one of the substrates that we used to test the activity of the *Synechocystis* protein from this family. We also decided to use the 16-mer RNA, which had a mixed composition of all ribonucleotides, in order to analyse if RNase II/R homologue from *Synechocystis* had some preference for Poly(A) substrates, similarly to what is observed for the *E. coli* counterparts. As already described, and as observed for both single-stranded substrates tested in this work, RNase II is able to degrade ssRNA substrates releasing a 4 nt fragment, while RNase R is able to proceed with catalysis until it reaches the 2 nt of length (Figure 4) (5). When we tested the recombinant protein from *Synechocystis* with the Poly(A) substrate, we were able to see that, with 50nM of protein, the final product released was a 5 nt fragment. However, when we used a higher protein concentration, 250nM, the protein was now able to release a 4 nt end-product (Figure 4). We also assayed this substrate with higher protein concentrations and no more cleavage events were observed (data not shown), confirming that the final end-product released is 4 nt, similarly to what happens with *E. coli* RNase II.

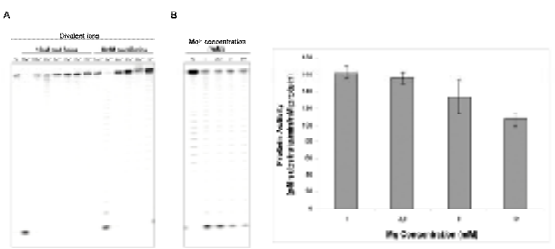

Figure 3. Divalent metal ion dependence of *Synechocystis* RNase II/R homologue. A. 10nM of recombinant protein were incubated with 10nM of Poly(A) at 37ºC for 5 and 60 minutes in a reaction buffer with different divalent metal ions. **B. A.** 5nM of recombinant protein were incubated with 10nM of Poly(A) at 37ºC for 5 minutes in a reaction buffer with different Mg^{2+}concentrations.**C.** Determination of the protein activity in the presence of different Mg^{2+} concentrations.

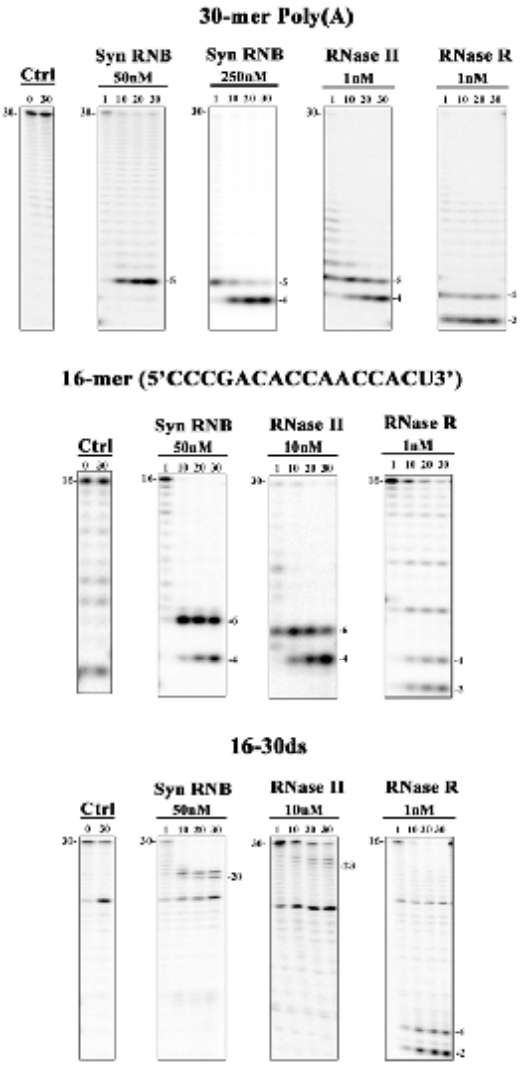

Figure 4. Exoribonucleolytic activity of *Synechocystis* protein: comparison with *E. coli* RNase II and RNase R. Activity assays were performed at 37ºC as described in Materials and Methods using three different substrates: 30-mer poly(A), the 16-mer and the double-stranded substrate 16-30ds, as referred. The concentration of proteins used is indicated in the figure. Samples were taken during the reaction at the time points indicated and reaction products were analyzed in a 20% polyacrylamide/7M urea gel. Control reactions with no enzyme added (*Ctrl*) were incubated at the maximum reaction time for each protein. Length of substrates and degradation products are labelled.

This behaviour was not observed when we tested the 16-mer substrate, since that 50nM of protein were sufficient to degrade the substrate until the 4 nt of length. We then determined the activity of the protein with both substrates as described in materials and methods. The results obtained showed that the protein had the same activity for both substrates (Figure 5). This indicates that, contrary to what happen with *E. coli* RNase II, which prefers poly(A) substrates (11,13), the RNase II/R homologue from *Synechocystis* does not have such preference. In fact, while in bacteria there is polyadenylation performed by

PAP, which originates homopolimeric tails, in cyanobacteria those tails are synthesized by PNPase and are heteropolymeric (1), which is in agreement with the results obtained regarding the activity of the protein. We also determined the dissociation constants by SPR using different single-stranded substrates, one of them constituted only by adenosines and the second with a random sequence. The results presented in Table 1 showed that the K_D values obtained for both single-stranded substrates are similar (3.9 ± 0.3 for the Poly(A) and 3.3 ± 0.5 for the 25ss), and the same was observed regarding the association (k_a) and dissociation (k_d) rates. Contrary, for ***E. coli*** RNase II and RNase R the K_D values previously obtained showed that these proteins have a increased affinity for Poly(A) substrates when compared to a random sequence (10,11,13).

The activity results presented above were obtained at 37ºC, which is the optimal activity for the ***E. coli*** enzymes. However, the ***Synechocystis*** PCC6803 cyanobacteria lives in freshwater and its optimal temperature for growth is around the 30ºC. For this reason, we compared the activity of the protein at 30ºC and 37ºC. As shown in Figure 5, the specific activity of the protein is the same at both temperatures, however, the degradation of the Poly(A) substrate is different at 30ºC (Figure 6). While at 37ºC we needed 250nM of protein to reach the final end-product of 4 nt, at 30ºC we were able to detect the 4 nt fragment with 50nM of protein (Figure 4 and Figure 6). Moreover, while at 37ºC we can observe the presence of high amounts of the intermediary fragment of 6 nt in the degradation of the 16-mer substrate, similarly to what is observed for RNase II (Figure 4), in the same conditions but at 30ºC the 6 nt fragment is no longer visible after 20 mins of reaction (Figure 6). These results indicate that the RNase II/R homologue from ***Synechocystis*** may have a higher affinity for small fragments at 30ºC, which can explain why it is able to reach the final end-product more rapidly when compared to the activity at 37ºC.

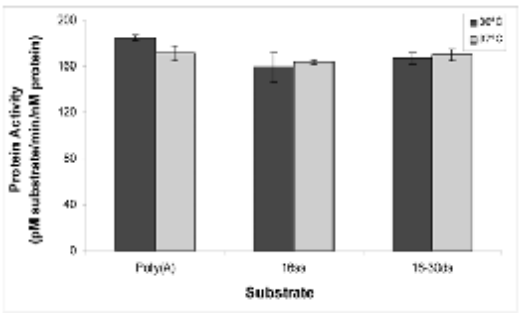

Figure 5. Determination of the activity of RNase II from *Synechocystis* at two different temperatures. The activity of the protein was determined at 30ºC and 37ºC using three different substrates: 30-mer poly(A), 16-mer and the double-stranded 16-30ds. All the activity assays were performed in triplicate.

Table 1: Kinetic parameters of RNase II-like protein from *Synechocystis sp.* The kinetic constants were determined by Surface Plasmon Resonance using Biacore 2000 with a 25-nt RNA oligomer (5'-Biotin-CCC GAC ACC AAC CAC UAA AAA AAA A-3') and 30nts PolyA as substrates.

	k_a (1/Ms)	k_d (1/s)	K_D (nM)
PolyA	3,0 ± 0,4 E03	1,9 ± 0,1 E-05	3,9 ± 0,3
25ss	3,7 ± 0,4 E03	1,1 ± 0,1 E-05	3,3 ± 0,5
16-25ds	2,4 ± 0,2 E05	1,4 ± 0,2 E-04	2,1 ± 0,1

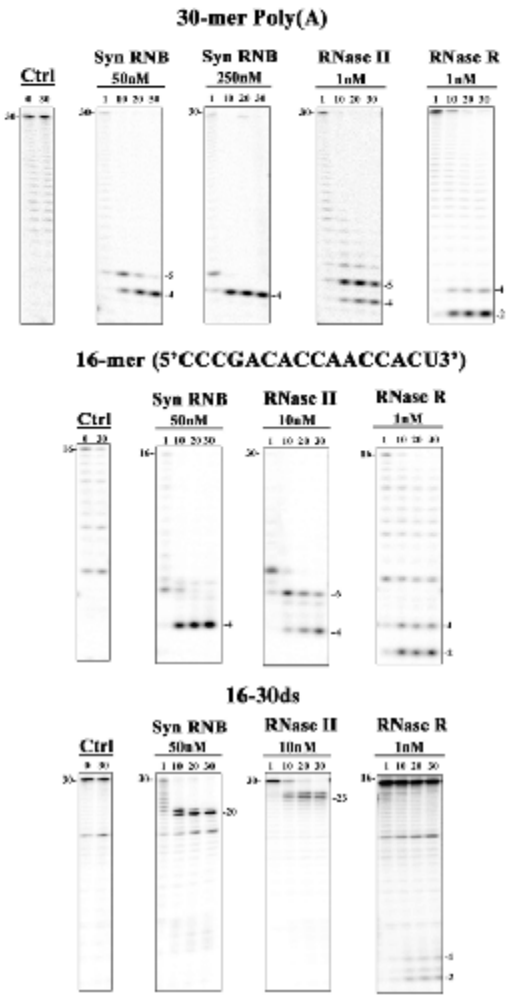

Figure 6. Exoribonucleolytic activity of *Synechocystis* protein: comparison with *E. coli* RNase II and RNase R. Activity assays were performed at 30ºC as described in Materials and Methods using three different substrates: 30-mer poly(A), the 16-mer and the double-stranded substrate 16-30ds, as referred. The concentration of proteins used is indicated in the figure. Samples were taken during the reaction at the time points indicated and reaction products were analyzed in a 20% polyacrylamide/7M urea gel. Control reactions with no enzyme added (*Ctrl*) were incubated at the maximum reaction time for each protein. Length of substrates and degradation products are labelled.

Finally, we went to test the activity of the protein against the double-stranded substrate, 16-30ds. ***E. coli*** RNase II is sensitive to secondary structures, and is not able to degrade this RNA, stalling 7 nt before it reaches the double-stranded region, releasing a 23 nt fragment (Figure 4) (30,31). Contrary, ***E. coli*** RNase R is able to overcome the secondary structures, releasing the typical 2 nt fragments (Figure 4) (32). When we tested the RNase II/R homologue from ***Synechocystis*** we could observe that it was not able to overcome secondary structures and stalled 4 nt before it reached the double-stranded region, releasing a fragment of 20 nt, which is shorter when compared to the one released by ***E. coli*** RNase II, which has 23 nt of length (Figure 4). The resolution of the crystal structure from ***E. coli*** RNase II showed us that the catalytic cavity of the protein is only

accessible to single stranded RNA due to the steric hindrance at its entrance caused by the RNA-binding domains (8). The *Synechocystis* homologue showed to be able to move closer to the double-stranded junction when compared to the *E. coli* protein, since that the final product released is shorter (20 nt vs. 23 nt, respectively). This may indicate that the RNA-binding domains may have a different rearrangement in this protein. In order to address this question, we modelled RNase II/R from *Synechocystis* and compared it with *E. coli* RNase II 3D structure (Figure 7). Both proteins seemed to have a similar overall structure arrangement, with the important residues for catalysis located in the same spatial position (Figure7). If we look closer to the RNA binding domains, it is possible to see that the CSD1 of RNase II/R from *Synechocystis* (Figure 7A) is quite different from the one from *E. coli* RNase II (Figure 7B). When we superimposed both structures, that difference is more notorious (Figure 7B). The CSD1 from *Synechocystis* protein is more distant from the S1 domain, which could result in a wider anchoring region which would allow the substrate to move nearer to the catalytic cavity, explaining why this protein is able to get closer to the double-stranded junction (Figure7). The activity of this protein was also determined with the 16-30ds and at both temperatures, 30ºC and 37ºC. Similarly to what was observed to the single-stranded substrates, the activity of the protein for the 16-30ds is the same as observed for the other substrates and does not change with temperature (Figure 5). Moreover, when we determined the dissociation constants for this substrate, the value is very similar to the ones obtained for the single-stranded substrates (Table 1). However, the protein associates and dissociates more rapidly to the double-stranded substrate when compared to the other two (Table 1, k_a and k_d values).

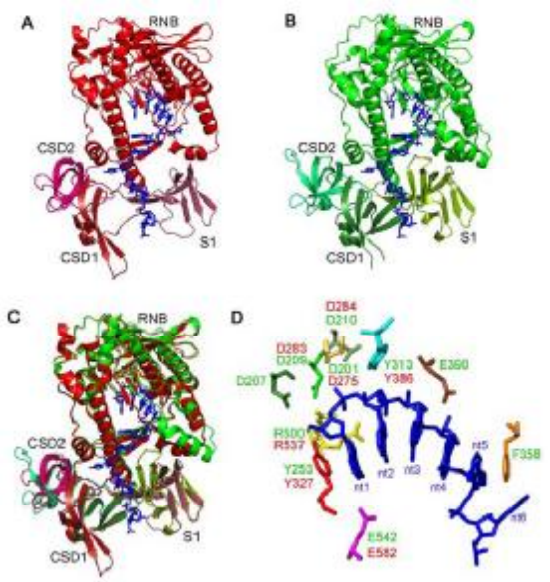

Figure 6. Modelling the RNase II protein from Synechocystis (A) Representation of the predictive 3D model from *Synechocystis* RNase II (red) (B) and *E. coli* RNase II crystal structure (green) (PDB 2IX0 and 2IX1), with the RNA molecule inside (blue). (C) Superposition of *E. coli* RNase II structure and *Synechocystis* RNase II model. (D) In the catalytic cavity, the residues important for the activity of *E. coli* RNase II are shown in green, while the ones from *Synechocystis* protein are indicated in red.

Together, these results showed us that the *Synechocystis* homologue behaved like an RNase II protein, since that the final product released was a 4 nt fragment for the single-stranded substrates and that the protein was shown to be sensitive to double-stranded substrates (Figure 4). However, contrary to what happens with *E. coli* RNB members, in *Synechocystis* RNase II does not prefer Poly(A) substrates. This may be related to the fact that there is no polyadenylation by a PAP enzyme and the tails are synthesized by PNPase and are heteropolymeric (1). This protein is the only member of the RNB-family present in *Synechocystis*. To date, when only a member of this family is described in an organism, it was shown to behave like RNase R. This was the case of *Mycoplasma genitalium* (23), *Legionella pneumophila* (15), and *Streptococcus pneumoniae* (22). *Synechocystis sp* is, in fact, the first organism where such observation was now shown not to be the case. Further studies are still necessary to clarify why *Synechocystis* evolved to have an RNase II and not an RNase R, similarly to what is observed in other organisms.

ACKNOWLEDGMENTS

Rute G. Matos was a recipient of a PhD fellowship funded by FCT- Fundação para a Ciência e a Tecnologia, Portugal. This work was supported by FCT-Fundação para a Ciência e a Tecnologia, Portugal.

REFERENCES

1.**Rott, R., G. Zipor, V. Portnoy, V. Liveanu, and G. Schuster.** 2003. RNA polyadenylation and degradation in Cyanobacteria are similar to the chloroplast but different from *Escherichia coli*. The Journal of biological chemistry *278*:15771-15777.

2.**Yehudai-Resheff, S., M. Hirsh, and G. Schuster.** 2001. Polynucleotide phosphorylase functions as both an exonuclease and a poly(A) polymerase in spinach chloroplasts. Molecular and cellular biology *21*:5408-5416.

3.**Lisitsky, I., P. Klaff, and G. Schuster.** 1996. Addition of destabilizing poly (A)-rich sequences to endonuclease cleavage sites during the degradation of chloroplast mRNA. Proceedings of the National Academy of Sciences of the United States of America *93*:13398-13403.

4.**Horie, Y., Y. Ito, M. Ono, N. Moriwaki, H. Kato, Y. Hamakubo, T. Amano, M. Wachi, et al.** 2007. Dark-induced mRNA instability involves RNase E/G-type endoribonuclease cleavage at the AU-box and SD sequences in cyanobacteria. Mol Genet Genomics *278*:331-346.

5.**Arraiano, C.M., J.M. Andrade, S. Domingues, I.B. Guinote, M. Malecki, R.G. Matos, R.N. Moreira, V. Pobre, et al.** 2010. The critical role of RNA processing and degradation in the control of gene expression. FEMS Microbiology Reviews *34*:883-923.

6.**Arraiano, C.M., R.G. Matos, and A. Barbas.** 2010. RNase II: The finer details of the *Modus operandi* of a molecular killer. RNA biology *7*.

7.**Cannistraro, V.J. and D. Kennell.** 1994. The processive reaction mechanism of ribonuclease II. Journal of molecular biology *243*:930-943.

8.**Frazão, C., C.E. McVey, M. Amblar, A. Barbas, C. Vonrhein, C.M. Arraiano, and M.A. Carrondo.** 2006. Unravelling the dynamics of RNA degradation by ribonuclease II and its RNA-bound complex. Nature *443*:110-114.

9.**Amblar, M., A. Barbas, A.M. Fialho, and C.M. Arraiano.** 2006. Characterization of the functional domains of Escherichia coli RNase II. Journal of molecular biology *360*:921-933.

10.**Matos, R.G., A. Barbas, and C.M. Arraiano.** 2009. RNase R mutants elucidate the catalysis of structured RNA: RNA-binding domains select the RNAs targeted for degradation. Biochem J *423*:291-301.

11.**Barbas, A., R.G. Matos, M. Amblar, E. Lopez-Viñas, P. Gomez-Puertas, and C.M. Arraiano.** 2008. New insights into the mechanism of RNA degradation by ribonuclease II: identification of the residue responsible for setting the RNase II end product. The Journal of biological chemistry *283*:13070-13076.

12.**Amblar, M. and C.M. Arraiano.** 2005. A single mutation in Escherichia coli ribonuclease II inactivates the enzyme without affecting RNA binding. FEBS J *272*:363-374.
13.**Barbas, A., R.G. Matos, M. Amblar, E. Lopez-Vinas, P. Gomez-Puertas, and C.M. Arraiano.** 2009. Determination of Key Residues for Catalysis and RNA Cleavage Specificity: one mutation turns RNase II into a "super-enzyme". The Journal of biological chemistry *284*:20486-20498.
14.**Awano, N., V. Rajagopal, M. Arbing, S. Patel, J. Hunt, M. Inouye, and S. Phadtare.** 2010. *Escherichia coli* RNase R has dual activities, helicase and RNase. Journal of bacteriology *192*:1344-1352.
15.**Charpentier, X., S.P. Faucher, S. Kalachikov, and H.A. Shuman.** 2008. Loss of RNase R induces competence development in *Legionella pneumophila*. Journal of bacteriology *190*:8126-8136.
16.**Dziembowski, A., E. Lorentzen, E. Conti, and B. Seraphin.** 2007. A single subunit, Dis3, is essentially responsible for yeast exosome core activity. Nature structural & molecular biology *14*:15-22.
17.**Matos, R.G., A. Barbas, P. Goméz-Puertas, and C.M. Arraiano.** 2011. Swapping the domains of exoribonucleases RNase II and RNase R: conferring upon RNase II the ability to degrade dsRNA. Proteins.
18.**Deutscher, M.P. and N.B. Reuven.** 1991. Enzymatic basis for hydrolytic versus phosphorolytic mRNA degradation in Escherichia coli and Bacillus subtilis. Proceedings of the National Academy of Sciences of the United States of America *88*:3277-3280.
19.**Cairrão, F., A. Cruz, H. Mori, and C.M. Arraiano.** 2003. Cold shock induction of RNase R and its role in the maturation of the quality control mediator SsrA/tmRNA. Molecular microbiology *50*:1349-1360.
20.**Cheng, Z.F. and M.P. Deutscher.** 2003. Quality control of ribosomal RNA mediated by polynucleotide phosphorylase and RNase R. Proceedings of the National Academy of Sciences of the United States of America *100*:6388-6393.
21.**Mohanty, B.K. and S.R. Kushner.** 2003. Genomic analysis in *Escherichia coli* demonstrates differential roles for polynucleotide phosphorylase and RNase II in mRNA abundance and decay. Molecular microbiology *50*:645-658.
22.**Domingues, S., R.G. Matos, F.P. Reis, A.M. Fialho, A. Barbas, and C.M. Arraiano.** 2009. Biochemical characterization of the RNase II family of exoribonucleases from the human pathogens *Salmonella typhimurium* and *Streptococcus pneumoniae*. Biochemistry *48*:11848-11857.
23.**Lalonde, M.S., Y. Zuo, J. Zhang, X. Gong, S. Wu, A. Malhotra, and Z. Li.** 2007. Exoribonuclease R in *Mycoplasma genitalium* can carry out both RNA processing and degradative functions and is sensitive to RNA ribose methylation. RNA (New York, N.Y *13*:1957-1968.
24.**Amblar, M., A. Barbas, P. Gomez-Puertas, and C.M. Arraiano.** 2007. The role of the S1 domain in exoribonucleolytic activity: substrate specificity and multimerization. RNA (New York, N.Y *13*:317-327.
25.**Arraiano, C.M., A. Barbas, and M. Amblar.** 2008. Characterizing ribonucleases *in vitro* examples of synergies between biochemical and structural analysis. Methods Enzymol *447*:131-160.
26.**Arnold, K., L. Bordoli, J. Kopp, and T. Schwede.** 2006. The SWISS-MODEL workspace: a web-based environment for protein structure homology modelling. Bioinformatics (Oxford, England) *22*:195-201.
27.**Kiefer, F., K. Arnold, M. Kunzli, L. Bordoli, and T. Schwede.** 2009. The SWISS-MODEL Repository and associated resources. Nucleic acids research *37*:D387-392.
28.**Schwede, T., J. Kopp, N. Guex, and M.C. Peitsch.** 2003. SWISS-MODEL: An automated protein homology-modeling server. Nucleic acids research *31*:3381-3385.
29.**DeLano, W.L.** 2002. The PyMOL Molecular Graphics System, 0.83 ed.. DeLano Scientific, San Carlos, CA..
30.**Cannistraro, V.J. and D. Kennell.** 1999. The reaction mechanism of ribonuclease II and its interaction with nucleic acid secondary structures. Biochimica et biophysica acta *1433*:170-187.
31.**Spickler, C. and G.A. Mackie.** 2000. Action of RNase II and polynucleotide phosphorylase against RNAs containing stem-loops of defined structure. Journal of bacteriology *182*:2422-2427.
32.**Cheng, Z.F. and M.P. Deutscher.** 2002. Purification and characterization of the *Escherichia coli* exoribonuclease RNase R. Comparison with RNase II. The Journal of biological chemistry *277*:21624-21629.

Appendix IV

Submitted manuscripts

12 - The *rnb* gene of *Synechocystis* PCC6803 encodes an RNA hydrolase displaying RNase II and not RNase R properties, by Rute G. Matos, Arsénio M. Fialho, Gadi Schuster and Cecília M. Arraiano

13 - The *H. volcanii* RNase R protein has a dual activity according to temperature, by Rute G. Matos, Paulino Goméz-Puertas and Cecília M. Arraiano

Nucleic Acids Research Advance Access published May 17, 2011

Nucleic Acids Research, 2011, 1–12
doi:10.1093/nar/gkr228

Identification of a DNA-binding site for the transcription factor Haa1, required for *Saccharomyces cerevisiae* response to acetic acid stress

Nuno P. Mira[1,2], Sílvia F. Henriques[1,2], Greg Keller[3], Miguel C. Teixeira[1,2], Rute G. Matos[4], Cecília M. Arraiano[4], Dennis R. Winge[3] and Isabel Sá-Correia[1,2,*]

[1]IBB, Instituto Biotecnologia e Bioengenharia, Center for Biological and Chemical Engineering, Instituto Superior Técnico, Avenida Rovisco Pais, 1049-001 Lisbon, Portugal, [2]Department of BIoengineering, Instituto Superior Técnico, Technical University of Lisbon, Avenida Rovisco Pais, 1049-001 Lisbon, Portugal, [3]Departments of Biochemistry and Medicine, University of Utah, Health Sciences Center, Salt Lake City, UT 84312, USA and [4]Instituto de Tecnologia Quimica e Biológica; Universidade Nova de Lisboa, 2781-901 Oeiras, Portugal

Received December 14, 2010; Revised March 29, 2011; Accepted March 30, 2011

ABSTRACT

The transcription factor Haa1 is the main player in reprogramming yeast genomic expression in response to acetic acid stress. Mapping of the promoter region of one of the Haa1-activated genes, *TPO3*, allowed the identification of an acetic acid responsive element (ACRE) to which Haa1 binds *in vivo*. The *in silico* analysis of the promoter regions of the genes of the Haa1-regulon led to the identification of an Haa1-responsive element (HRE) 5′-GNN(G/C)(A/C)(A/G)G(A/G/C)G-3′. Using surface plasmon resonance experiments and electrophoretic mobility shift assays it is demonstrated that Haa1 interacts with high affinity (K_D of 2 nM) with the HRE motif present in the ACRE region of *TPO3* promoter. No significant interaction was found between Haa1 and HRE motifs having adenine nucleotides at positions 6 and 8 (K_D of 396 and 6780 nM, respectively) suggesting that Haa1p does not recognize these motifs *in vivo*. A lower affinity of Haa1 toward HRE motifs having mutations in the guanine nucleotides at position 7 and 9 (K_D of 21 and 119 nM, respectively) was also observed. Altogether, the results obtained indicate that the minimal functional binding site of Haa1 is 5′-(G/C)(A/C)GG(G/C)G-3′. The Haa1-dependent transcriptional regulatory network active in yeast response to acetic acid stress is proposed.

INTRODUCTION

The *Saccharomyces cerevisiae* transcriptional activator Haa1 was first included into a family of fungal copper-regulated transcription factors, based on the identification of a putative copper-regulatory domain within its DNA-binding domain (DBD; 1). Besides Haa1, this family also includes the *S. cerevisiae* Ace1 and Mac1 transcription factors, *Candida glabrata* Amt1 and *Schizosaccharomyces pombe* Cuf1 (2). Unlike its homologs, the function of Haa1 is independent of the copper-status of the cell (1) suggesting that its physiological function is not related to copper homeostasis. A biological role for Haa1 in yeast tolerance to acetic and propionic acids was established in a previous study (3). The expression of the *HAA1* gene was shown to reduce the duration of the adaptation period of a yeast cell population suddenly exposed to toxic concentrations of these two short chain carboxylic acids, by decreasing the weak acid-induced loss of cell viability (3). More recently, the role of Haa1 in tolerance to lactic acid was also demonstrated (4). Acetic, propionic and lactic acids are widely used by food and beverage industries as preservative agents. However, the activity of spoilage yeasts and molds resistant to these weak acids seriously limits their usefulness, also bringing major economic losses (5). Acetic acid is also a byproduct of *S. cerevisiae* alcoholic fermentation and together with high concentrations of ethanol and other toxic metabolites, acetic acid may contribute to fermentation arrest and reduced ethanol productivity (5). This weak acid is also present in lignocellulosic hydrolysates, a highly interesting non-feedstock substrate in industrial biotechnology (6).

*To whom correspondence should be addressed. Tel: +351 218417682; Fax: +351 218489199; Email: isacorreia@ist.utl.pt

The molecular mechanisms underlying response and resistance to acetic acid and to other weak acids have been studied in *S. cerevisiae* to guide the design of more efficient preservation strategies and the engineering of more robust industrial strains to be used in processes in which yeast is explored as a cell factory and tolerance to acetic acid is required (5,7).

The transcriptional activation of 80% of the acetic acid-responsive genes is Haa1 dependent (8). This high percentage of direct or indirect Haa1 target genes points out this transcription factor as a key player in the control of yeast genomic expression program in response to acetic acid stress (8). The expression of a number of genes of the Haa1-regulon was found to confer yeast protection against acetic acid (8). Those having the more prominent effect were (i) *TPO2* and *TPO3*, encoding two plasma membrane transporters of the Major Facilitator Superfamily proposed to mediate the efflux of acetate from the cell interior during cultivation in the presence of acetic acid (3); (ii) *SAP30*, whose gene product is a subunit of the histone deacetylase Rpd3 complex, recently demonstrated to be involved in the regulation of yeast transcriptional response to environmental stress (9); and (iii) *HRK1*, which encodes a kinase belonging to a family of kinases involved in the post-translational regulation of plasma membrane transporters (10). The internal levels of acetic acid accumulated during growth of Δ*haa1* cells in the presence of the acid were higher than those registered in the parental strain (3), this being attributed to the reduced transcriptional activation of Haa1-target genes required for the reduction of the internal concentration of acetate (3,8). The objective of this work was the identification of the DNA motif used by Haa1 to activate the expression of acetic acid-responsive genes. The functional binding site of Haa1 is here described and the Haa1-dependent transcriptional regulatory network active in yeast response to acetic acid stress is proposed.

MATERIALS AND METHODS

Strains and growth media

Saccharomyces cerevisiae BY4741 (*MATa*, *his3Δ1*, *leu2Δ0*, *met15Δ0*, *ura3Δ0*), the deletion mutant BY4741_*Δhaa1* (*MATa*, *his3Δ1*, *leu2Δ0*, *met15Δ0*, *ura3Δ0*, *YPR008w::kanMX4*) and the *HAA1*-TAP strain (*MATa ade2 arg4 leu2-3,112 trp-289 ura3-52*) were all obtained from the Euroscarf collection. These yeast strains were batch-cultured, at 30°C, with orbital agitation (250 r.p.m.), in YPD growth medium (2% glucose, 2% bactopeptone and 1% yeast extract) or in minimal growth medium MM4 [contains, per liter, 1.7 g yeast nitrogen base without amino acids or NH_4^+, 20 g glucose, 2.65 g $(NH_4)_2SO_4$, 20 mg methionine, 20 mg histidine, 60 mg leucine and 20 mg uracil]. *Escherichia coli* BL21-CondonPlus(DE3)-RIL cells [genotype B F^- *ompT hsdS*(rB- mB-) dcm^+ Tet^r *gal* λ(DE3) *endA* Hte (*argU ileY leuW* Cam^r)] (Stratagene) were used for the over-expression of Haa1(DBD)-His_6 fusion protein.

Plasmids

A list of plasmids used in this study is available in Table 1. The construction of the *lacZ* fusion plasmid p*TPO3*::*lacZ* in the cloning vector pAJ152 was described before (3). Plasmids p*TPO3(-790)*::*lacZ*, p*TPO3(-590)*::*lacZ* and p*TPO3(-400)*::*lacZ* were constructed by cloning the 790, 590 and 400 bp DNA region upstream of *TPO3* start codon in the BamHI/HindIII sites of pAJ152 vector. p*ACRE-CYC1*::*lacZ* plasmid was constructed by cloning the acetic acid responsive element (ACRE) found in *TPO3* promoter (located between positions −790 to −590 upstream of its start codon) into the XhoI/XbaI sites of the pNB404 vector (11). Plasmid pACRE*-*CYC1*::*lacZ* was obtained by site-directed mutagenesis of the Haa1 responsive element (HRE) present in ACRE, using pACRE-*CYC1*::*lacZ* as template. Plasmid

Table 1. List of plasmids used in this study

Plasmid name	Description	Reference
p*TPO3*::*lacZ*	Expression fusion plasmid in which 1000 bp *TPO3* promoter were fused with *lacZ* coding sequence in pAJ152 basal vector	(3)
p*TPO3(-790)*::*lacZ*	Expression fusion plasmid in which 790 bp *TPO3* promoter were fused with *lacZ* coding sequence in pAJ152 basal vector	This study
p*TPO3(-590)*::*lacZ*	Expression fusion plasmid in which 590 bp *TPO3* promoter were fused with *lacZ* coding sequence in pAJ152 basal vector	This study
p*TPO3(-400)*::*lacZ*	Expression fusion plasmid in which 400 bp *TPO3* promoter were fused with *lacZ* coding sequence in pAJ152 basal vector	This study
pNB404	UAS-less vector containing the minimal promoter *CYC1* fused to *lacZ* coding sequence	(11)
pACRE-*CYC1*::*lacZ*	pNB404-derived vector that contains the ACRE region from *TPO3* promoter cloned upstream of minimal promoter *CYC1*;	This study
pACRE*-*CYC1*::*lacZ*	Vector derived from pACRE-*CYC1*::*lacZ* containing the HRE motif mutated	This study
pACRE (-740/-590) *CYC1*::*lacZ*	pNB404-based vector that contains the last 150 bp of the ACRE region found in *TPO3* promoter (between nucleotides −740 and −590) cloned upstream of minimal promoter *CYC1* and of *lacZ* coding sequence	This study
pACRE (-790/-690) *CYC1*::*lacZ*	pNB404-based vector that contains the first 100 bp of the ACRE region found in *TPO3* promoter (between nucleotides −790 and −690) cloned upstream of minimal promoter *CYC1* and of *lacZ* coding sequence	This study
pET23a(+)-*HAA1*	IPTG-inducible plasmid that drives the expression of Haa1 DNA-binding domain (N-terminal 123 residues) fused to a six histidine C-terminal tag	This study

pHaa1(DBD)::His_6 was obtained by cloning the DBD of Haa1 mapped to the N-terminal 123 residues of the protein (1), in the XhoI/BamHI sites of pET23a(+) expression vector (Novagen).

Determination of *TPO3* expression levels using *lacZ* fusion plasmids

The expression of the *lacZ* reporter gene produced in yeast transformants harboring the *lacZ* fusions with truncated regions of *TPO3* promoter was determined based on the quantification of β-galactosidase activity. Cells harboring the p*TPO3*::*lacZ*, p*TPO3(-790)*::*lacZ,* p*TPO3(-590)*::*lacZ* and p*TPO3(-400)*::*lacZ* plasmids were cultivated until mid-exponential phase (OD_{600nm} = 0.8 ± 0.05) in MM4 growth medium (at pH 4.0, using HCl as the acidulant) lacking uracil for plasmid maintenance. These cells were re-inoculated, at an OD_{600nm} of 0.2 ± 0.05, into this same basal medium either or not supplemented with acetic acid (60 mM). A stock solution of 5 M acetic acid (prepared in water and adjusted to pH 4.0 with NaOH) was used to supplement the growth medium. After 8 h of incubation in the presence or absence of acetic acid, cells were harvested by filtration, washed two times with water and the filters were kept at −20°C until further use. The determination of β-galactosidase activity produced from plasmids p*TPO3*::*lacZ*, p*TPO3(-790)*::*lacZ,* p*TPO3(-590)*::*lacZ* and p*TPO3(-400)*::*lacZ* in these cells was performed as described before (12). The assessment of the expression of *lacZ* gene (through β-galactosidase activity) in yeast cells harboring p*ACRE-CYC1*::*lacZ* or p*ACRE*-CYC1*::*lacZ* plasmids in the presence or absence of acetic acid stress (40 mM) was performed using the same protocol. Since the *CYC1* promoter is very weak and produces low levels of background expression of *lacZ* reporter gene (11), a lower concentration of acetic acid having a milder toxic effect on cell viability had to be used to assess β-galactosidase activity in yeast cells transformed with pNB404-based plasmids.

In vivo binding of Haa1 to *TPO3* promoter region in the presence or absence of acetic acid stress

In vivo binding of Haa1 to the promoter region of *TPO3* gene was assessed by chromatin immunoprecipitation (ChIP). For this, *HAA1*-TAP cells, which express Haa1 fused to a C-terminal tandem affinity purification (TAP) tag, were cultivated in YPD growth medium (adjusted at pH 4.0 with HCl) until mid-exponential phase (OD_{600nm} = 0.8 ± 0.05) and then re-inoculated in fresh YPD growth medium (at pH 4.0; used as control culture) or in this same basal medium supplemented with acetic acid (60 mM). The volume of inoculum used was calculated to obtain cell suspensions with an OD_{600nm} of 0.2 ± 0.05. After 30 min of cultivation in the presence or absence of acetic acid, 1% formaldehyde was added to both cultures and cells were left to grow for another 30 min. After that time, 125 mM glycine were added to both cellular suspensions for quenching and incubation proceeded for another 5 min. Cells were then harvested by centrifugation (8000 r.p.m., 5 min, 4°C, rotor JA20 Beckman), washed with Tris buffer (at pH 8.0) and frozen at −80°C until further use. DNA extraction and subsequent immunoprecipitation was performed as described before (13). Reversed cross-linked input and output DNAs were purified with polymerase chain reaction (PCR) purification columns (Qiagen). Two complementary oligonucleotides (I_1 5′-TTCTCTGTGCTTGG CGAGGGGTTTACTGGAGCCCAATC-3′ and I_2 3′-A AGAGACACGAACCGCTCCCCAAATGACCTCGG GTTAG-5′) were selected for the amplification of the ACRE region found in *TPO3* promoter using as templates the purified input and output DNAs collected. A DNA fragment within the *QDR3* promoter was used as a negative control since this gene is not regulated by Haa1 (our unpublished data).

Expression and purification of Haa1(DBD)-His_6 peptide in *E. coli*

Codon-optimized *E. coli* BL21 RIL cells (DE3, pLysS) (Stratagene) were transformed with plasmid p*HAA1*(*DBD*)::His_6 to yield expression of Haa1(DBD)-His_6 peptide. Transformants were cultivated at 37°C with orbital agitation (250 r.p.m.) in LB growth medium, supplemented with chloramphenicol (30 μg/ml) and ampicillin (150 μg/ml), until exponential phase (OD_{640nm} = 0.6 ± 0.05). At that point, 0.3 mM isopropyl β-D-1-thiogalactopyranoside (IPTG) were added to the culture to induce the expression of the Haa1(DBD)-His_6 fusion peptide and cells were left to grow for another 3 h. Cells were harvested by centrifugation (8000 r.p.m., 8 min, 4°C, rotor JA20 Beckman), washed with ice-cold distilled water and frozen at −80°C until further use. Crude protein extracts were obtained by sonication and subsequent centrifugation at 18 000*g* for 1 h at 4°C. The clarified supernatant was loaded into a His-trap column (GE Healthcare) previously equilibrated with 10 ml of ice-cold washing buffer [10 mM phosphate buffer (pH 7.4), 150 mM NaCl, 10 mM imidazole). Column washing was started with 5 ml of washing buffer and elution of the Haa1(DBD)-His_6 peptide was performed using a stepwise increasing gradient of imidazole concentration (in the range of 20–500 mM) in the wash buffer. The fractions containing the purified peptide were recovered, concentrated using Amicon ultracel filters (molecular weight cutoff of 10 kDa) (Millipore) and applied in a 75 Sephadex HR10-300 GL3-kDa–70-kDa column (GE Healthcare) for subsequent fast protein liquid chromatography (FPLC) purification. The fractions containing the purified protein were collected, concentrated and the protein concentration in each fraction was determined using Protein Assay Reagent (BioRad). Confirmation that the collected protein corresponded to the the Haa1(DBD)-His_6 peptide was performed by western-blot using an antibody against the histidine tag (acquired from Santa Cruz Biotech).

Electrophoretic mobility shift assays

The *in vitro* interaction of Haa1(DBD)-His_6 peptide with the HRE found in *TPO3* promoter was carried out by electrophoretic mobility shift assays (EMSAs). For this, 10 pmol of a 20-bp sequence of *TPO3* promoter that

spans the HRE motif (specifically from −770 to −790 bp of *TPO3* promoter) was radiolabeled at their 5′-terminus with [γ-^{32}P]-ATP using T4 phage kinase (Invitrogen). After labeling, 11 pmol of the complementary oligonucleotide were added to the suspension and the mixture was left at room temperature for 2 h to promote the annealing of both oligonucleotides. The oligoduplex obtained was purified with ProbeQuantG columns (GE Healthcare). The *in vitro* interaction assays were carried out in 20 µl of final volume using 10 fmol of the radiolabeled oligoduplex and a range of 0–25 ng of the purified Haa1(DBD)-His$_6$ peptide. The binding buffer used was 65 mM KCl, 10% glycerol, 10 mM Tris (pH 8.0), 0.025% Nonidet P40 and 20% bovine serum albumin. Binding reactions were left for 20 min at 30°C and then loaded on a 8-cm × 7-cm 6% acrylamide gels (pre-run at 100 V for 1 h). The gels were run at 11°C and 150 V until the bromophenol blue dye had migrated at least two-thirds of the way down the gel. The temperature of the electrophoresis was carried out at 11°C to prevent an eventual complex denaturation during the course of the electrophoresis as the result of the heating that could be generated during running of the samples in the acrylamide gel, a procedure that is been used before with success in the study of the interactions established between yeast transcription factors and their target genes (14). In other trials, the electrophoresis was run without temperature control, but this did not lead to an alteration of the results obtained. The signal obtained in the gels was acquired by laser-based imaging system using the Typhoon Trio equipment.

Measurement of dissociation constants of Haa1 HRE complexes by surface plasmon resonance

The DBD of Haa1, over-expressed and purified in *E. coli* using the protocol described above, was immobilized by the amine coupling procedure in flow cell 2 of the CM5 sensor chip (GE Healthcare) on a Biacore 2000 system (GE Healthcare), according to the manufacturer's instructions. Briefly, the surface was activated with a 1:1 mixture of 1-ethyl-3-(3-dimethyllaminopropyl) carbodiimide (EDC) and N-hydroxysuccinimide (NHS), injected during 5 min using a flow rate of 10 µl/min. Then, 5 µg/ml of Haa1 DBD were injected during 5 min at the same flow rate. After the injection of the ligand, ethanolamine was injected over the surface to deactivate it. The immobilization of the protein originated a response of 900 RU. On flow cell 1, no protein was immobilized and this cell was used as the control blank cell. Biosensor assays were run at 25°C in the same buffer used to carry out the EMSA assays. The sequences of the 10 DNA oligomers used in the analysis are provided in Supplementary Table 1. Nine of them correspond to the HRE motif and respective mutations and the last one is a random sequence, which was used as a negative control. The DNA oligomers were injected over flow cells 2–1 for 5 min at concentrations of 10, 25, 50, 100 and 200 nM using a flow rate of 20 µl/min. The dissociation was allowed to occur during 4 min in the running buffer. All experiments included triple injections of each oligomer concentration to determine the reproducibility of the signal. Bound oligomers were removed after each cycle with a 30-s wash with NaOH 50 mM. The effect of these washes with NaOH in Haa1 activity was assessed by performing five independent injections of one of the DNA oligos interspersed by a washing step. The replicas performed were almost coincident indicating that the binding partners were stable throughout the time required for the experiment and that the regeneration conditions were appropriate. After each cycle, the signal was stabilized during 1 min before a new oligomer injection. Data from flow cell 1 was used to correct for refractive index changes and nonspecific binding. Rate constants were calculated using the BIAEVALUATION 3.0 software package by fitting the sensograms obtained for each DNA oligomer to a 1:1 Langmuir binding model. A chi-square test was performed to estimate the reliability of the fitting and values below 10, considered by the manufacturer to be the maximum acceptable value for proper data fitting, were obtained for all the sensograms analyzed. K_D value was calculated as the ratio between k_d and k_a. Each DNA-oligomer assay was run at least three times each to determine the robustness of the data obtained. The values presented in Table 2 are the average of these three independent assays and the error presented corresponds to the associated standard deviation between these three experiments. To further confirm the results obtained, the interaction between Haa1 and the HRE motif present in *TPO3* promoter (considered the wild-type HRE) was performed by immobilizing the DNA oligomer from *TPO3* promoter that spans the HRE motif biotinylated at its 5′terminus in a streptavidin-coated chip (Biacore SA; General Healthcare). The Haa1 DBD peptide was then injected over it. On flow cell 1 no substrate was added so this could be used as the control blank cell and on flow cell 2 we immobilized the biotinylated DNA oligomer. The target substrate was captured on flow cell 2 by manually injecting 20 µl of a 500-nM solution of the substrate in reaction buffer at a 20 µl/min flow rate. The immobilization of the DNA sequence originated a response of 300 RU. The assays were run at 25°C in the buffer described above. The Haa1 DBD peptide was injected over flow cells 1 and 2 for 5 min at concentrations of 20, 25, 30, 35, 40 and 45 nM using a flow rate of 20 µl/min. The dissociation was allowed to occur for 4 min in the running buffer. All experiments included triple injections of each protein concentration to determine the reproducibility of the signal. Bound protein was removed with a 30-s wash with 2 M NaCl. After each cycle, the signal was stabilized during 1 min before a new protein injection. Data from flow cell 1 was used to correct for refractive index changes and nonspecific binding. The values of k_a, k_d and K_D were estimated using the same methodology as described above.

RESULTS

TPO3 promoter contains an upstream activating sequence necessary for Haa1 dependent *TPO3* transcriptional activation in response to acetic acid stress

The promoter region of *TPO3* gene was used to map the possible existence of one (or more) *cis*-acting regulatory

Table 2. Definition of the minimal functional Haa1-binding site

HRE motif	k_a (1/Ms) ($\times 10^4$)	k_d (1/s) ($\times 10^{-4}$)	K_D (nM)	Relative K_D
GGCGAGGGG	4.5 ± 0.3	1.1 ± 0.1	2.0 ± 0.2	1.0
AGCGAGGGG	7.6 ± 0.5	1.5 ± 0.2	1.9 ± 0.3	1.0
GGCCAGGGG	11.0 ± 1.0	4.9 ± 0.7	4.3 ± 0.3	2.2
GGCGCGGGG	7.1 ± 0.3	9.7 ± 0.5	13.6 ± 0.9	6.8
GGCGAAGGG	0.39 ± 0.02	13.0 ± 2.0	396.0 ± 51.1	198.0
GGCGAGAGG	3.9 ± 0.6	11.0 ± 2.0	21.4 ± 6.1	10.7
GGCGAGGCG	5.2 ± 0.3	21.0 ± 2.0	38.5 ± 4.5	19.3
GGCGAGGAG	0.33 ± 0.06	320.0 ± 30.0	6780.0 ± 865	3390.0
GGCGAGGGA	4.2 ± 0.2	54.0 ± 3.0	119.0 ± 3.6	59.5
Negative control	0.01 ± 0.002	130.0 ± 10.0	>10 000	>5000

The affinity of Haa1 to HRE motifs predicted from the degenerate consensus sequence obtained by *in silico* analysis of the promoter region of genes of the Haa1 regulon (shown in Figure 3) was compared by surface plasmon resonance. The association and dissociation rates (k_a and k_d) of complexes established between Haa1 and 37-bp DNA sequences harboring these motifs were obtained by fitting the sensograms to a Langmuir 1:1 model (Supplementary Figures S1A and S2), as detailed in 'Materials and Methods' section. The K_D values were calculated as the ratio between the dissociation and association constants. The error associated to this value is the standard deviation of three independent experiments that were carried out to study the interaction of Haa1 DBD peptide with each oligonucleotide. Relative K_D values were calculated relative to the value obtained for the HRE motif present in *TPO3* promoter (GGCGAGGGG) to which Haa1 was found to bind *in vivo* (Figure 1B). A random DNA sequence was used as a negative control.

element(s) that could be used by Haa1 as binding site(s). *TPO3* was selected with this objective among other genes regulated by Haa1 because it is a proposed direct Haa1 target gene (1) and it is induced in response to acetic acid in a Haa1-dependent manner (3,8). Moreover, a functional *TPO3*::*lacZ* fusion plasmid (p*TPO3*::*lacZ*), suitable for easy assessment of *TPO3* expression, was available (3). The acetic acid-induced transcriptional activation of *TPO3* was compared in cells carrying the p*TPO3*::*lacZ* plasmid (which contains the full-length *TPO3* promoter fused to *lacZ*) and in cells harboring plasmids p*TPO3(-790)*::*lacZ*, p*TPO3(-590)*::*lacZ* and p*TPO3(-400)*::*lacZ*, in which progressive 5′-truncations, of ~200 bp each, of *TPO3* promoter were performed (Figure 1A). In wild-type cells transformed with the p*TPO3*::*lacZ* plasmid the levels of *TPO3* expression where ~5-fold higher in acetic acid-stressed cells than in control cells (Figure 1A). However, in Δ*haa1* cells no significant increase in *TPO3* expression was found upon acetic acid challenge (Figure 1A) consistent with the described involvement of Haa1 in the activation of *TPO3* transcription under acetic acid stress (3,8). Elimination of the −790 to −590-bp portion of *TPO3* promoter abolished the Haa1-dependent transcriptional activation of this gene induced by acetic acid (Figure 1A), suggesting that this region contains an acetic acid responsive element (ACRE). ChIP analysis of the ACRE region within *TPO3* promoter (–590 to −790) confirms that Haa1 binds *in vivo* to this region under acetic acid stress as well as in unstressed yeast cells (Figure 1B).

ACRE confers an acetic-acid-responsiveness to the minimal promoter *CYC1*

To examine whether ACRE could regulate a heterologous reporter gene in an acetic acid-dependent-manner, this DNA region was cloned, in its natural orientation, in the UAS-less vector pNB404::*lacZ* (Figure 2). pNB404 is a UAS-less vector that contains only the minimal transcriptional and translational initiation sites from the *CYC1* gene, leading to a very low background expression of the reporter gene *lacZ* (11). Fusion of the ACRE sequence to *CYC1* promoter was sufficient to confer an acetic-acid-dependent regulation to *lacZ* expression, under the dependence of *HAA1* expression (Figure 2).

ACRE contains a DNA motif enriched in the promoter region of Haa1-regulated genes that is a functional binding site for Haa1

The results support the conclusion that the ACRE sequence found in *TPO3* promoter includes a functional binding site for Haa1, here designated HRE. To narrow down the ACRE to a binding site, truncated versions of this DNA element were cloned in the pNB404 vector and the acetic-acid-responsiveness of these constructs was compared with the one provided by a full-length ACRE sequence (Figure 2). The results obtained clearly show that the putative HRE is located between nucleotides −690 and −590 of *TPO3* promoter (Figure 2). To identify the HRE motif within this 100-bp region, the promoter regions (considered to be the 1000-bp upstream of start codon) of the 85 genes activated in response to acetic acid stress in a Haa1 dependent manner (8) were searched for enriched DNA motifs, using the AlignACE DNA motif finder (Aligns Nucleic Acid Conserved Elements; http://atlas.med.harvard.edu/) (15), using a strategy that is detailed in ref. 16. The algorithm identified a number of over-represented DNA motifs in the data set but only one of these motifs, 5′-GNN(G/C)(A/C)(A/G)G(G/C/A)G-3′, was within the 100-bp region of ACRE present in *TPO3* promoter presumed to harbor the HRE (Figure 3A). Reinforcing the idea that this motif is the functional binding site for Haa1, its mutation in *TPO3* promoter abrogated the Haa1-dependent acetic-acid-responsiveness of the pACRE-*CYC1*::*lacZ* construct (Figure 3B). To confirm that Haa1 interacts with the HRE motif identified in *TPO3* promoter an EMSA was carried out. For this, the Haa1 DBD was produced in *E. coli* and purified by immunoaffinity chromatography and FPLC. The

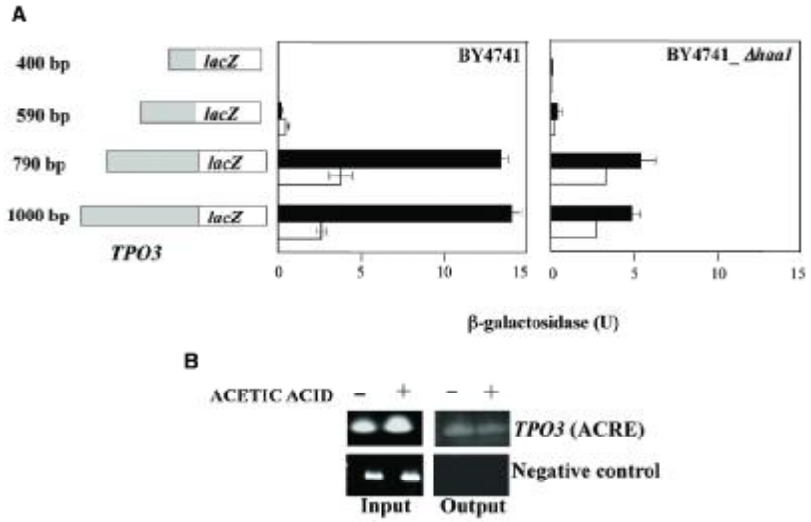

Figure 1. (**A**) Mapping of an upstream activating sequence underlying the Haa1 dependent activation of *TPO3* transcription under acetic acid stress. Progressive 5′ deletions, of ~200 bp each, of *TPO3* promoter were performed, according with the schematic representation shown, and the levels of β-galactosidase (U) produced from these truncated constructs were compared with those produced by a construct containing the full-length *TPO3* promoter (containing 1000 bp) in the absence (white bars) or presence of 60 mM acetic acid, at pH 4.0 (dark bars). Values are means of, at least, three independent experiments. (**B**) *In vivo* binding of Haa1 to ACRE region of *TPO3* promoter. Yeast cells expressing a Haa1–TAP fusion protein were cultivated for 30 min in the absence (–) or presence (+) of acetic acid and total DNA was extracted from these cells, immunoprecipitated with an anti-TAP antibody and purified (output). An aliquot of DNA not subjected to the immunoprecipitation step was used as a control (input). Oligonucleotides spanning the ACRE region of *TPO3* promoter were used to amplify the DNA signal in both extracts.

		BY4741		BY4741_*Δhaa1*	
	CYC1 promoter *lacZ*	- Acetic acid	+ Acetic acid	- Acetic acid	+ Acetic acid
pNB404 *CYC1 lacZ*		-	-	-	-
pACRE *CYC1 lacZ*	-790 -590	0.11±0.07	1.70±0.4	0.13±0.01	0.15±0.01
pACRE (-740/-590) *CYC1 lacZ*	-740 -590	0.10±0.01	2.30±0.06	0.08±0.02	0.10±0.01
pACRE (-790/-690) *CYC1 lacZ*	-790 -690	-	-	-	-

Figure 2. To narrow down the ACRE sequence into a smaller DNA fragment, overlapping fragments of this DNA sequence, depicted by horizontal dark bars, were cloned in front of *CYC1* minimal promoter and upstream of *lacZ* reporter gene. The levels of β-galactosidase produced by these constructs were compared with the level produced by a construct containing the full ACRE sequence in the presence or absence of acetic acid stress. The different plasmids were named according to the number of the initial nucleotide of *TPO3* promoter included in the constructs, as described in Table 1. β-Galactosidase activities represent the average of three independent experiments and (–) stands for a non-detectable activity.

interaction of this peptide with ACRE was tested using an oligonucleotide from *TPO3* promoter that spans the candidate motif. EMSA experiments confirmed the existence of a strong interaction between the Haa1(DBD)–His_6 peptide and the HRE motif (Figure 4). A similar result was obtained using a full-length Haa1 (data not shown).

Definition of HRE motifs that serve as functional binding sites for Haa1

The results described above point out the degenerate DNA motif 5′-GNN(G/C)(A/C)(A/G)G(G/C/A)G-3′ as the functional binding site of Haa1. Surface plasmon resonance (SPR) was used to estimate the kinetic constants (k_a, association rate constant; k_d, dissociation rate constant; and K_D, dissociation constant) of the formation of complexes established between Haa1 and those DNA motifs predicted by the degenerate HRE sequence. This information is considered essential, as it will allow the identification of those HRE motifs that serve as functional Haa1 binding sites, also providing an important insight into the identification of bases required for an efficient Haa1–DNA complex formation. The mutations of the HRE motif were created by site-directed mutagenesis of the motif present in *TPO3* promoter, 5′-GGCGAGGGG

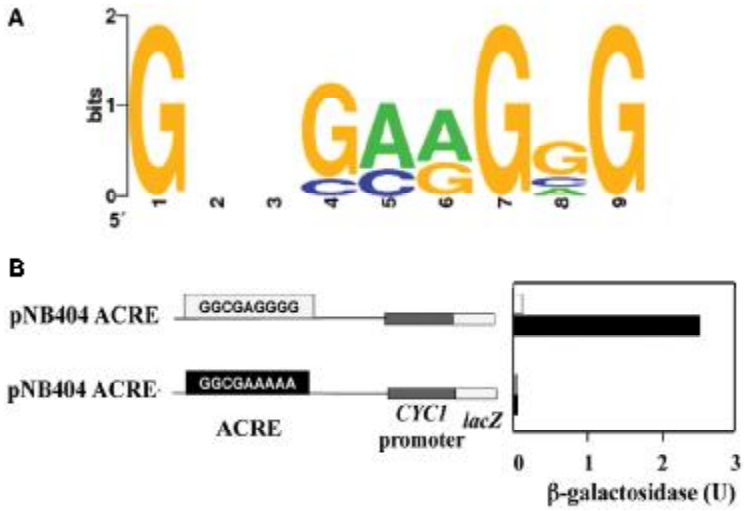

Figure 3. (**A**) Schematic representation of the DNA motif identified by the AlignAce algorithm as being enriched in the promoter region of the 85 genes activated by Haa1 in response to acetic acid stress (8). (**B**) Effect of the DNA motif identified by the referred bioinformatic analysis in the Haa1 dependent transcriptional activation of *TPO3* gene induced by acetic acid.

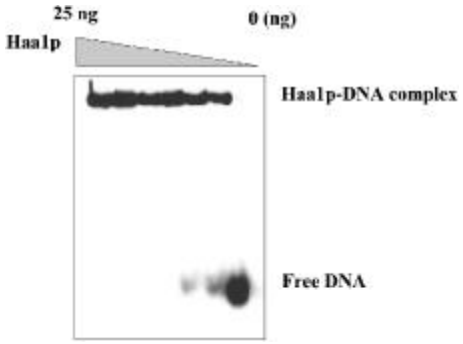

Figure 4. *In vitro* interaction of Haa1 with the HRE motif found in *TPO3* promoter sequence. Different amounts of the Haa1 DNA-binding domain, expressed in *E. coli* and purified by affinity chromatography and FPLC, were incubated for 20 min at 30°C with a ^{32}P-radiolabeled oligonucleotide from *TPO3* promoter containing the candidate Haa1 binding motif (GGCGAGGGG). The protein–DNA complexes were separated from free DNA probe by polyacrylamide gel electrophoresis and a representative result of the gels obtained is shown.

-3′ (considered to be the 'wild-type' HRE motif), since Haa1 was found in our study to establish a strong *in vitro* interaction with this DNA sequence (Figure 4). The sensograms obtained used to estimate the kinetic association and dissociation constants are shown in Supplementary Figures S1 and S2. Remarkably, among the HRE motifs tested the motif present in *TPO3* promoter was the one having the highest affinity to Haa1 (corresponding to the lowest K_D value obtained, 2 nM). By analyzing the k_a and k_d values we were also able to see that the Haa1–HRE complex associates rapidly and dissociates with a low velocity which is indicative of the formation of a stable complex (Table 2). To further confirm these results, the Haa1–HRE interaction was monitored using a reverse experimental strategy, that is, immobilizing the biotinylated oligo that contains the HRE motif in a streptavidin-coated chip and letting the peptide flow (Supplementary Figure S2). Expectedly, the values of the kinetic constants obtained, k_a $1.5 \times 10^5\,M^{-1}\,s^{-1}$ and k_d of $6.3 \times 10^{-4}\,s^{-1}$, are different but the resulting K_D value (4.3 nM) is close to the one that had been obtained using the protein has the immobilized ligand (which was 2.0 nM). A random DNA oligonucleotide was used as a negative control to test the specificity of the Haa1–HRE interaction. As expected, Haa1 had a highly impaired affinity for this DNA sequence, based on the low association rates (k_a of $1.1 \times 10^4\,M^{-1}\,s^{-1}$) and the high dissociation rates of the complex formed (k_d $1.3 \times 10^{-3}\,s^{-1}$) (Table 2). The affinity of Haa1 toward an HRE motif that harbors an adenine nucleotide at position 1 instead of a guanine was not affected (K_D of 1.9 nM, compared to 2 nM). Taking into account that k_a and k_d values are similar to the ones obtained for the 'wild-type' HRE motif, we may infer that the stability of the complex was not altered. This observation suggests that the capacity of Haa1 to recognize the HRE sequence is independent of the type of purine present at position 1. In fact, the first three nucleotides of the degenerate HRE motif should be dispensable

for Haa1 binding since no nucleotide conservation is found at positions 2 and 3 of this motif (Figure 3A). The replacement of the other conserved guanine nucleotides of the HRE motif at positions 7 and 9 for adenines had little effect on the Haa1–HRE association rate; however, these Haa1–'mutant HRE' complexes were less stable than a Haa1–'wild-type HRE', based on the higher complex dissociation rates obtained (Table 2). In particular, an almost 50-fold increase in dissociation rate was observed for the complex established between Haa1 and the GGCGAGGG**A** motif, suggesting that guanine nucleotide at position 9 is essential for efficient Haa1 binding. Consequently, HRE motifs with mutations in this position are unlikely to serve as functional Haa1 binding sites. Regarding the nucleotide degeneracy predicted at positions 4, 5 and 8 the results obtained demonstrate that although Haa1 has a lower affinity toward HRE motifs that differ from the one present in *TPO3* promoter, the values of the different kinetic parameters determined do not exclude the majority of the motifs tested as being functional binding sites (Table 2). The exceptions are the motifs having adenine nucleotide at position 8 (GGCGAGG**A**G) or at position 6 (GGCGA AGGG) which bind poorly to Haa1 (K_D of 6780 and 396 compared to 2.2 nM) (Table 2). Altogether, the results obtained with the SPR analysis indicate that the minimal functional Haa1 binding site is 5′-(G/C)(A/C)GG(G/C)G-3′.

Transcriptional regulatory network mediated by Haa1 in response to acetic acid stress

To reveal the transcriptional regulatory network governed by Haa1 under acetic acid stress we have searched the promoter region of the 85 genes whose expression is activated by Haa1 in response to acetic acid stress (8) for the HRE motif 5′-(G/C)(A/C)GG(G/C)G-3′. Approximately 55% of these Haa1-regulated genes harbor in their promoter region one or more copies of the minimal HRE motif suggesting that these are direct Haa1 targets (Figure 5A). Among these genes are *TPO3*, *TPO2, YPR157w* and *PHM8* (Figure 5A) which have been previously proposed to be directly regulated by Haa1 (1). In line with this, we have found that under acetic acid stress Haa1 binds *in vivo* to the promoter region of *TPO3* and *TPO2* genes (Figure 1B and our unpublished data). The effect of Haa1 in the transcriptional activation of genes that do not have a HRE motif is likely to be indirect and mediated by other transcription factors, whose expression is presumably regulated, directly or indirectly, by Haa1. Among the Haa1-activated genes under acetic acid stress that have a HRE motif in their promoter regions are *MSN4*, *FKH2* and *MCM1*, which encode three transcriptional activators (8). The genes presumed to be indirectly regulated by Haa1 were clustered with Msn4, Fkh2 and Mcm1, based on the existence of previous documented regulatory associations with these transcription factors, using the YEASTRACT database (17) (Figure 5B). Seven of the indirect Haa1 targets have documented regulatory associations with Msn4p, two with Fkh2p and two with Mcm1p (Figure 5B). However, for 19 Haa1 indirect targets it was not possible to find any association with these transcription factors (Figure 5B). Although the possibility exists that the description of Msn2-, Fkh2- and Mcm1-regulons is incomplete, this observation suggests the existence of additional transcription factor(s) contributing to the Haa1-dependent transcriptional regulatory network active under acetic acid stress (Figure 5B). Although not explicitly considered in the model, the combinatorial regulation of acetic-acid-responsive genes that are, directly or indirectly, regulated by Haa1, cannot of course be ignored.

DISCUSSION

In this study, it is demonstrated that the *S. cerevisae* transcription factor Haa1 requires the DNA sequence 5′-(G/C)(A/C)GG(G/C)G-3′ in the promoter region of acetic-acid-responsive genes to activate their expression. This DNA sequence, designated HRE, is the first functional binding site described for Haa1. Consistent with this result, Haa1 was found to interact with sequences harboring this HRE motif in a large-scale study carried out to identify the interactions occurring among a large number of yeast transcription factors and oligonucleotides containing evolutionary conserved sequences presumed to contain functional binding sites (14). Since the Haa1 DBD is highly homologous to Ace1 DBD it was thought that the two transcription factors could have similar DNA-binding sites (18), as found to occur with the Haa1 and Ace1 homologs Cuf1 and Amt1 (19,20). However, the Haa1-binding site here described does not resemble the Ace1 DNA target sequence. Other evidences also indicate that, *in vivo*, Haa1 and Ace1 bind to different DNA sequences, in specific, the over-expression of Haa1 in a mutant devoid of *ACE1* expression does not restore the expression of Ace1p target genes [(1) and our unpublished data] and no induction of Haa1-target genes is registered upon Ace1 overexpression in a Δ*haa1* background (our unpublished data). Consistent with these observations, no Ace1 binding site is found enriched in the promoter of Haa1-regulated genes and vice versa. Moreover, the sets of genes documented as being regulated by Ace1 and Haa1 do not overlap (17). It is likely that the Haa1 and Ace1 DBDs have a different structure, despite the homology of the amino acid sequence of these two peptides. The presence of a unique segment between residues 81 and 91 in Haa1 DBD could prevent the formation of a two-lobe structure similar to that of Ace1 (21). To bind DNA Ace1 requires the formation of a polycopper cluster within the DBD for stabilization of a functional conformer of the protein (18,21,22), thus activating Ace1p under copper-induced stress and maintaining an unstructured inactive form in the absence of copper stress (21,23). However, the activity of Haa1 is independent of the copper-status of the cell [(1) and our unpublished data] and the mutation of cysteine residues mediating copper binding in Ace1p does not reduce the ability of Haa1 to activate gene transcription (our unpublished data). These observations clearly indicate that the role played by copper in structuring Haa1 and Ace1 is

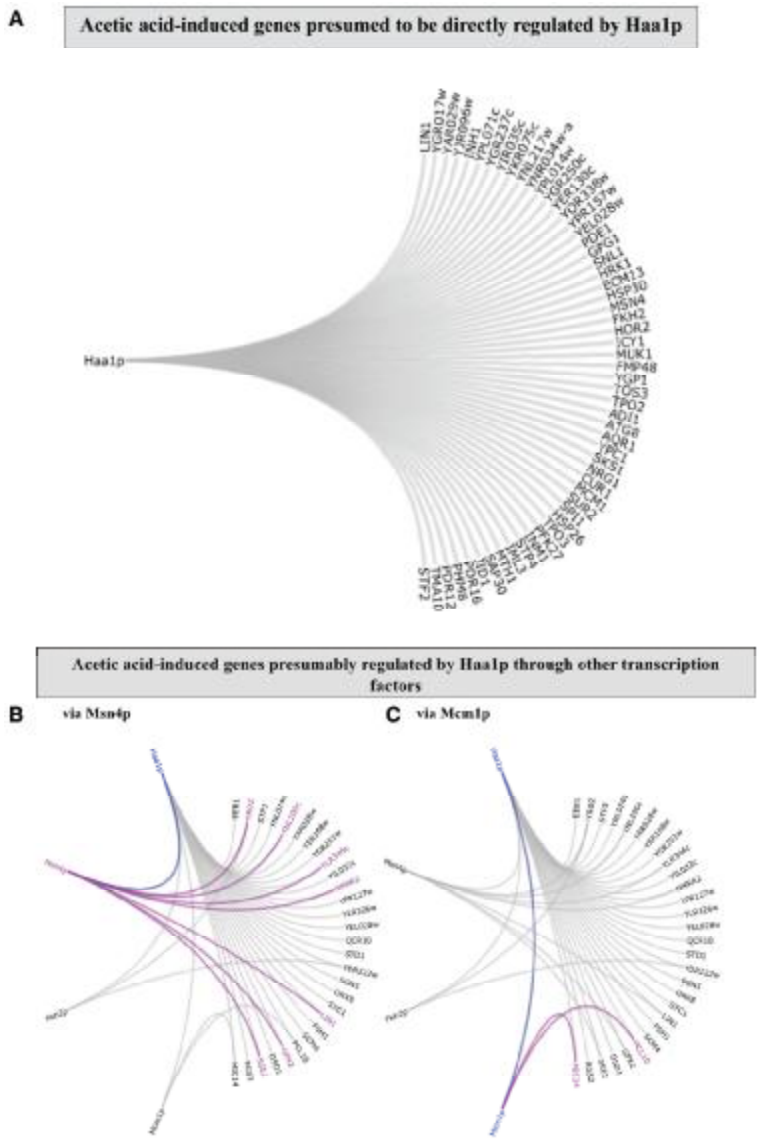

Figure 5. Putative Haa1 dependent transcriptional regulatory network active under acetic acid stress. The promoter region of the genes whose transcription was found to be activated by Haa1 in acetic acid-challenged cells was searched for the Haa1-binding motif (5′-(G/C)(A/C)GG(G/C)G-3′) using the YEASTRACT database. The genes that have at least one HRE motif in their promoter region, presumably the direct Haa1 target genes, are shown in (**A**). The documented targets of the Msn4p, Mcm1p or Fkh2p transcription factors were searched among the Haa1-activated genes that do not have a HRE motif in their promoter region (**B–D**). The non-direct Haa1-target genes which are also not documented targets of Msn4p, Fkh2p or Mcm1p were clustered under the putative regulation of an unidentified factor(s), X (**E**). All the transcriptional regulatory networks shown were built using the tools available in the YEASTRACT database (17).

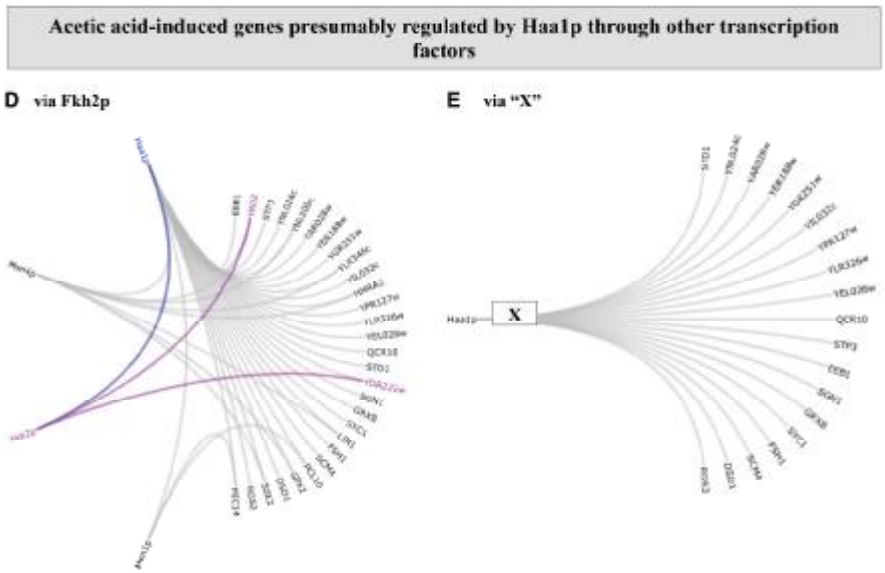

Figure 5. Continued.

different, although they do not exclude the possible stabilization of Haa1 DBD through the formation of a polycopper cluster.

One of the main differences between the Haa1 and Ace1 binding sites (5′-THNNGCTG-3′) is the absence in the HRE motif of a 5′-(A/T)-rich region which is essential for Ace1 binding and for binding of Cuf1 and Amt1 to their target DNA sequences (19–21,24). Ace1 was found to establish minor groove DNA contacts with this (A/T)-hook, through a RGRP motif (G = glycine; R = arginine; P = proline) present in its DBD (21,24,25), and strong major groove interactions with the guanine nucleotides of the GCTG core (18). A closer inspection of the promoter region of the Haa1 regulated genes harboring an HRE motif also shows that in 77% of the cases this motif is preceded by at least two adenine and/or thymine nucleotides. It is thus hypothesized that Haa1 may use these adenine or thymine nucleotides to promote minor groove contacts with HRE. Consistently, the RGRP motif is also present in Haa1 DBD between positions 36 and 39 and the mutation of arginine 38 abolishes the ability of Haa1 to induce gene expression and to bind the HRE motif (our unpublished data). Since the replacement of the conserved guanine nucleotides at positions 3 and 6 of the HRE motif (considered positions 6 and 9 in the degenerate HRE sequence) significantly destabilizes the Haa1–HRE complex, as assessed by the SPR analysis carried out, it is presumed that these nucleotides could mediate major groove contacts between Haa1 and the HRE motif.

It is interesting to note that no correlation was found between the number of HRE motifs having higher affinity for Haa1 in the promoter region of the Haa1-dependent genes and these genes' transcription. For example, the motif with the highest affinity to Haa1, 5′GAGGGG3′, is present in the promoter region of *TPO3*, *TPO2*, *STF2* and *AQR1* genes, whose transcriptional activation in response to acetic acid stress mediated by Haa1 range from 1.5-fold (for *AQR1*) to 18.7-fold (for *TPO2*) (8). This result suggests that other factors, besides DNA-binding affinity, are involved in the Haa1-dependent control of gene expression under acetic acid stress. Haa1 was found to bind to the promoter region of the *TPO3* gene independently of the presence of acetic acid in the growth medium (Figure 1B) and to be constitutively localized in the nucleus (our unpublished data). In the absence of acetic acid, no significant effect of *HAA1* expression in the yeast transcriptome was found, not even in the expression of genes activated in response to acetic acid stress in a Haa1-dependent manner, including *TPO3* (8). These observations suggest that Haa1 is apparently non-functional in unstressed yeast cells independently of its possible binding to the promoter region of target genes. The same behavior was described for War1 transcription factor, required for yeast adaptation and resistance to propionic and sorbic acids (26). War1 also binds to the promoter region of the *PDR12* gene but in the absence of these weak acids this transcription factor does not induce *PDR12* transcription (27,28). It is possible that the transactivation potential of Haa1 is enhanced under acetic acid stress leading to the increased recruitment of the transcriptional machinery to the promoter region of its target genes and, consequently, to their up-regulation, as demonstrated for Yap1 under benomyl stress (29) or

for War1 under propionic acid- and sorbic acid- induced stress (27). War1 activation was found to occur upon binding of sorbate and propionate anions (27), a mechanism also described for other xenobiotic compounds or cell metabolites and yeast transcription factors in particular for Pdr1p upon binding of ketoconazole (30), Leu3 upon binding of the intermediate of leucine biosynthesis α-isopropyl malate (31), Ppr1, upon binding of the pyrimidine biosynthesis intermediate dihydroorotic acid (32) and Lys14 upon binding of α-amino adipate semialdehyde (33). The possible interaction of Haa1 with acetate is an interesting possibility to explain the hypothesized activation mechanism of Haa1 under acetic acid stress.

A putative transcriptional regulatory network active under acetic acid stress and controlled by Haa1 is proposed in this work (Figure 5). Almost 55% of the genes whose transcription is upregulated under acetic acid stress in a Haa1-dependent manner are presumed to be primary targets of Haa1 as they harbour in their promoter at least one copy of the HRE motif. The effect of Haa1 in the expression of genes that do not have a HRE motif in their promoter is proposed to be mediated by Fkh2, Msn4 or Mcm1 transcription factors, whose transcription was found to be activated under acetic-acid-stress in a Haa1-dependent manner (Figure 5) (34). Msn4p, together with its close homolog Msn2p, mediates yeast transcriptional response to environmental stress (35), consistent with the classification of five (*YRO2*, *YNL200c*, *LIN1*, *GPX2* and *SSE2*) of the eight Haa1 indirect targets putatively co-regulated by Msn4 as stress-responsive genes, specifically (35). The transcription factor Fkh2p is involved in the regulation of genes related with the transition of G2/M phase and Mcm1 is involved in the regulation of genes related with cell mating type and pheromone response. Since a number of the putative indirect Haa1-target genes are not documented targets of Msn4, Fkh2 or Mcm1, the possible participation of an unidentified transcription factor (designated 'X') in the Haa1-mediated transcriptional regulatory network is anticipated, although no Haa1-dependent transcriptional activation of a gene encoding a transcription factor was detected (8). Interestingly, 10 out of the 19 genes clustered in the hypothetical 'X'-regulon are documented targets of Sfp1, a transcription factor involved in ribosome biogenesis in response to nutrient starvation and other stresses (36). Acetic acid stress was shown to induce a rapid degradation of ribosomal RNA (37) and a large set of genes involved in ribosome biogenesis were identified as determinants of resistance to acetic acid (34). However, the possible participation of Sfp1 in the control of the expression of the Haa1-regulated genes and/or the identification of other transcription factors that cooperate with Haa1 in the control of yeast genomic expression under acetic acid stress have to be proved. Nevertheless, results of the present study are an important contribution to the better understanding of the complexity of yeast transcriptional regulatory networks active under stress, in particular the one mediated by Haa1 in acetic-acid-challenged cells.

SUPPLEMENTARY DATA

Supplementary Data are available at NAR Online.

FUNDING

FEDER, Fundação para a Ciência e a Tecnologia (FCT) and PTDC Program (contracts PTDC/AGR-ALI/102608/2008, PTDC/EBB-EBI/108517/200 and ERA-IB/0002/2010, in the framework of the FP6 EraNet Programme on Industrial Biotechnology INTACT (Integral Engineering for Acetic Acid Tolerance in yeast); a post-doctoral grant to N.P.M. (SFRH/BPD/46982/2008) and a PhD grant to R.G.M. (SFRH/BD/36024/2007); and a grant from the National Institute of Health (contract ES03817 to D.R.W.). Funding for open access charge: Fundação Ciência e Tecnologia-PTDC program.

Conflict of interest statement. None declared.

REFERENCES

1. Keller,G., Ray,E., Brown,P.O. and Winge,D.R. (2001) Haa1, a protein homologous to the copper-regulated transcription factor Ace1, is a novel transcriptional activator. *J. Biol. Chem.*, **276**, 38697–38702.
2. Rutherford,J.C. and Bird,A.J. (2004) Metal-responsive transcription factors that regulate iron, zinc, and copper homeostasis in eukaryotic cells. *Eukaryot. Cell*, **3**, 1–13.
3. Fernandes,A.R., Mira,N.P., Vargas,R.C., Canelhas,I. and Sá-Correia,I. (2005) *Saccharomyces cerevisiae* adaptation to weak acids involves the transcription factor Haa1p and Haa1p-regulated genes. *Biochem. Biophys. Res. Commun.*, **337**, 95–103.
4. Abbott,D.A., Suir,E., van Maris,A.J.A. and Pronk,J.T. (2008) Physiological and transcriptional responses to high concentrations of lactic acid in anaerobic chemostat cultures of *Saccharomyces cerevisiae*. *Appl. Environ. Microbiol.*, **74**, 5769–5768.
5. Teixeira,M.C., Mira,N.P. and Sá-Correia,I. (2011) A genome-wide perspective on the response and tolerance to food-relevant stresses in *Saccharomyces cerevisiae*. *Curr. Opin. Biotechnol.*, **22**, 150–156.
6. Almeida,J.R., Modig,T., Petersson,A., Hähn-Hägerdal,B., Lidén,G. and Gorwa-Grauslund,M.F. (2007) Increased tolerance and conversion of inhibitors in lignocellulosic hydrolysates by *Saccharomyces cerevisiae*. *J Chem. Technol. Biotechnol.*, **82**, 340–349.
7. Mira,N.P., Teixeira,M.C. and Sá-Correia,I. (2010) Adaptation and tolerance to weak acid stress in *Saccharomyces cerevisiae*: a genome-wide view. *OMICS: J. Integr. Biol.*, **14**, 525–540.
8. Mira,N.P., Becker,J. and Sá-Correia,I. (2010) Genomic expression program involving the Haa1p-regulon in *Saccharomyces cerevisiae* response to acetic acid. *OMICS: J. Integr. Biol.*, **14**, 587–601.
9. Alejandro-Osorio,A.L., Huebert,D.J., Porcaro,D.T., Sonntag,M.E., Nillasithanukroh,S., Will,J.L. and Gasch,A.P. (2009) The histone deacetylase Rpd3p is required for transient changes in genomic expression in response to stress. *Genome Biol.*, **10**, R57.
10. Goossens,A., de la Fuente,N., Forment,J., Serrano,R. and Portillo,F. (2000) Regulation of yeast H+-ATPase by protein kinases belonging to a family dedicated to activation of plasma membrane transporters. *Mol. Cell. Biol.*, **20**, 7654–7661.
11. Bachhawat,N., Ouyang,Q. and Henry,S.A. (1995) Functional Characterization of an inositol-sensitive upstream activation sequence in yeast. *J. Biol. Chem.*, **270**, 25087–25095.
12. Broco,N., Tenreiro,S., Viegas,C.A. and Sá-Correia,I. (1999) *FLR1* gene (ORF YBR008c) is required for benomyl and methotrexate resistance in *Saccharomyces cerevisiae* and its benomyl-induced expression is dependent on pdr3 transcriptional regulator. *Yeast*, **15**, 1595–1608.

13. Keller,G., Bird,A. and Winge,D.R. (2005) Independent Metalloregulation of Ace1 and Mac1 in *Saccharomyces cerevisiae*. *Eukaryot. Cell*, **4**, 1863–1871.
14. Ho,S.W., Jona,G., Chen,C.T., Johnston,M. and Snyder,M. (2006) Linking DNA-binding proteins to their recognition sequences by using protein microarrays. *Proc. Natl Acad. Sci. USA*, **103**, 9940–9945.
15. Hughes,J.D., Estep,P.W., Tavazoie,S. and Church,G.M. (2000) Computational identification of *cis*-regulatory elements associated with groups of functionally related genes in *Saccharomyces cerevisiae*. *J. Mol. Biol.*, **296**, 1205–1214.
16. Mira,N.P., Teixeira,M.C. and Sá-Correia,I. (2011) Characterization of complex regulatory networks and identification of promoter regulatory elements in yeast: in silico and wet-lab approaches. *Methods in Molecular Biology - Transcriptional regulation: methods and protocols* (in press).
17. Teixeira,M.C., Monteiro,P., Jain,P., Tenreiro,S., Fernandes,A.R., Mira,N.P., Alenquer,M., Oliveira,A., Freitas,A.T. and Sá-Correia,I. (2006) The YEASTRACT database: a tool for the analysis of transcriptional regulatory associations in *Saccharomyces cerevisiae*. *Nucleic Acids Res.*, **34**, D446–D451.
18. Dobi,A., Dameron,C.T., Hu,S., Hamer,D. and Winge,D.R. (1995) Distinct regions of Cu(I)-ACE1 contact two spatially resolved DNA major groove sites. *J. Biol. Chem.*, **270**, 10171–10178.
19. Beaudoin,J. and Labbe,S. (2001) The fission yeast copper-sensing transcription factor Cuf1 regulates the copper transporter gene expression through an Ace1/Amt1-like recognition sequence. *J. Biol. Chem.*, **276**, 15472–15480.
20. Koch,K.A. and Thiele,D.J. (1996) Autoactivation by a *Candida glabrata* copper metalloregulatory transcription factor requires critical minor groove interactions. *Mol. Cell. Biol.*, **16**, 724–734.
21. Brown,K.R., Keller,G.L., Pickering,I.J., Harris,H.H., George,G.N. and Winge,D.R. (2002) Structures of the cuprous-thiolate clusters of the Mac1 and Ace1 transcriptional activators. *Biochemistry*, **41**, 6469–6476.
22. Huibregtse,J.M., Engelke,D.R. and Thiele,D.J. (1989) Copper-induced binding of cellular factors to yeast metallothionein upstream activation sequences. *Proc. Natl Acad. Sci. USA*, **86**, 65–69.
23. Gralla,E.B., Thiele,D.J., Silar,P. and Valentine,J.S. (1991) *ACE1*, a copper-dependent transcription factor, activates expression of the yeast copper, zinc superoxide dismutase gene. *Proc. Natl Acad. Sci. USA*, **88**, 8558–8562.
24. Turner,R.B., Smith,D.L., Zawrotny,M.E., Summers,M.F., Posewitz,M.C. and Winge,D.R. (1998) Solution structure of a zinc domain conserved in yeast copper-regulated transcription factors. *Nat. Struct. Mol. Biol.*, **5**, 551–555.
25. Jamison McDaniels,C.P., Jensen,L.T., Srinivasan,C., Winge,D.R. and Tullius,T.D. (1999) The yeast transcription factor Mac1 binds to DNA in a modular fashion. *J. Biol. Chem.*, **274**, 26962–26967.
26. Kren,A., Mamnun,Y.M., Bauer,B.E., Schuller,C., Wolfger,H., Hatzixanthis,K., Mollapour,M., Gregori,C., Piper,P. and Kuchler,K. (2003) War1p, a novel transcription factor controlling weak acid stress response in yeast. *Mol. Cell. Biol.*, **23**, 1775–1785.
27. Gregori,C., Schuller,C., Frohner,I.E., Ammerer,G. and Kuchler,K. (2008) Weak organic acids trigger conformational changes of the yeast transcription factor War1 in vivo to elicit stress adaptation. *J. Biol. Chem.*, **283**, 25752–25764.
28. Schuller,C., Mamnun,Y.M., Mollapour,M., Krapf,G., Schuster,M., Bauer,B.E., Piper,P.W. and Kuchler,K. (2004) Global phenotypic analysis and transcriptional profiling defines the weak acid stress response regulon in *Saccharomyces cerevisiae*. *Mol. Biol. Cell*, **15**, 706–720.
29. Lucau-Danila,A., Lelandais,G., Kozovska,Z., Tanty,V., Delaveau,T., Devaux,F. and Jacq,C. (2005) Early expression of yeast genes affected by chemical stress. *Mol. Cell. Biol.*, **25**, 1860–1868.
30. Thakur,J.K., Arthanari,H., Yang,F., Pan,S.J., Fan,X., Breger,J., Frueh,D.P., Gulshan,K., Li,D.K., Mylonakis,E. *et al.* (2008) A nuclear receptor-like pathway regulating multidrug resistance in fungi. *Nature*, **452**, 604–609.
31. Sze,J.Y., Woontner,M., Jaehning,J.A. and Kohlhaw,G.B. (1992) In vitro transcriptional activation by a metabolic intermediate: activation by Leu3 depends on alpha-isopropylmalate. *Science*, **258**, 1143–1145.
32. Flynn,P.J. and Reece,R.J. (1999) Activation of transcription by metabolic intermediates of the pyrimidine biosynthetic pathway. *Mol. Cell. Biol.*, **19**, 882–888.
33. El Alami,M., Feller,A., Pierard,A. and Dubois,E. (2002) The proper folding of a long C-terminal segment of the yeast Lys14p regulator is required for activation of LYS genes in response to the metabolic effector. *Mol. Microbiol.*, **43**, 1629–1639.
34. Mira,N.P., Palma,M., Guerreiro,J.F. and Sá-Correia,I. (2010) Genome-wide identification of *Saccharomyces cerevisiae* genes required for tolerance to acetic acid. *Microb. Cell. Fact.*, **9**, 79.
35. Gasch,A.P., Spellman,P.T., Kao,C.M., Carmel-Harel,O., Eisen,M.B., Storz,G., Botstein,D. and Brown,P.O. (2000) Genomic expression programs in the response of yeast cells to environmental changes. *Mol. Biol. Cell*, **11**, 4241–4257.
36. Marion,R.M., Regev,A., Segal,E., Barash,Y., Koller,D., Friedman,N. and O'Shea,E.K. (2004) Sfp1 is a stress- and nutrient-sensitive regulator of ribosomal protein gene expression. *Proc. Natl Acad. Sci. USA*, **101**, 14315–14322.
37. Mroczek,S. and Kufel,J. (2008) Apoptotic signals induce specific degradation of ribosomal RNA in yeast. *Nucleic Acids Res.*, **36**, 2874–2888.

J. Microbiol. Biotechnol. (2011), **21**(3), 243–251
doi: 10.4014/jmb.1009.09034
First published online 9 February 2011

JOURNAL OF MICROBIOLOGY AND BIOTECHNOLOGY

BolA Affects Cell Growth, and Binds to the Promoters of Penicillin-Binding Proteins 5 and 6 and Regulates Their Expression

Guinote, Inês Batista[1], Rute Gonçalves Matos[1], Patrick Freire[1,2], and Cecília Maria Arraiano[1]*

[1]*Instituto de Tecnologia Química e Biológica/Universidade Nova de Lisboa, Apartado 127, 2781-901 Oeiras, Portugal*
[2]*Laboratório Nacional de Investigação Veterinária - INRB, Estrada de Benfica 701, 1549-011 Lisboa, Portugal*

Received: September 27, 2010 / Revised: December 7, 2010 / Accepted: December 10, 2010

The gene *bolA* was discovered in the 80's, but unraveling its function in the cell has proven to be a complex task. The BolA protein has pleiotropic effects over cell physiology, altering growth and morphology, inducing biofilm formation, and regulating the balance of several membrane proteins. Recently, BolA was shown to be a transcription factor by repressing the expression of the *mreB* gene. The present report shows that BolA is a transcriptional regulator of the *dacA* and *dacC* genes, thus regulating both DD-carboxypeptidases PBP5 and PBP6 and thereby demonstrating the versatility of BolA as a cellular regulator. In this work, we also demonstrate that reduction of cell growth and survival can be connected to the overexpression of the *bolA* gene in different *E. coli* backgrounds, particularly in the exponential growth phase. The most interesting finding is that overproduction of BolA affects bacterial growth differently depending on whether the cells were inoculated directly from a plate culture or from an overnight batch culture. This strengthens the idea that BolA can be engaged in the coordination of genes that adapt the cell physiology in order to enhance cell adaptation and survival under stress conditions.

Keywords: BolA, DD-carboxypeptidase, transcriptional regulator, PBP

The BolA-like proteins are widely conserved from prokaryotes to eukaryotes. They seem to be involved in cell proliferation or cell-cycle regulation, although their molecular function is still a matter of debate. The 13.5 kDa *E. coli* BolA protein is encoded in the 10 min region of the genetic map, and is responsible for inducing spherical morphology in rod-shaped bacteria in the stationary phase, possibly in a FtsZ-dependent manner [3, 14]. The BolA protein contains a helix-turn-helix motif, that includes a putative DNA-binding domain, through which it can eventually interact with nucleic acids and regulate the expression of different genes [1].

The *bolA* gene is regulated by two promoters: a weak and constitutive promoter, *bolA2p*, and a main promoter, *bolA1p,* regulated by growth phase and/or growth rate. The expression from this "gearbox promoter" is driven by the σ^S sigma factor and shows an activity inversely dependent on growth rate [1–3]. The *bolA* gene was initially considered a stationary phase gene, but it was later shown that *bolA* can also be induced in the exponential phase in response to several stresses [19]. Ribonuclease III can act as a positive modulator of *bolA* [9]. BolA is suggested to be implicated in the tolerance to different environmental pressures since it is expressed under stress conditions, and leads to the reduction of the surface area of cells. Moreover, *bolA* was shown to be involved in the formation of biofilms, modulation of OmpF/OmpC balance, and control of the cell cycle [11, 13, 19, 23]. BolA may act as an inducer of cell wall biosynthetic enzymes, enhancing the expression of the mRNAs from the hydrolytic DD-carboxypeptidases penicillin-binding proteins PBP5 and PBP6 and the β-lactamase AmpC [1, 10, 20]. In fact, PBP5 overproduction, like *bolA* overexpression, has been reported to produce spherical cells [15]. The deletion of PBP5 produced an accumulation of muropeptides with pentapeptide side-chains and a reduction on the thickness of the peptidoglycan layer [20]. Additionally, PBP6 can change its protein levels, and it increases four times in the stationary phase [8].

Recently, BolA has been demonstrated to specifically interact with the *mreB* promoter and repress *mreB* transcription, leading to a reduction in protein levels and abnormal MreB polymerization [10]. The MreB protein, a structural homolog of actin, was revealed to be essential for

**Corresponding author*
Phone: +351 214469547; Fax: +351 214469549;
E-mail: cecilia@itqb.unl.pt

bacterial cell elongation and rod shape [12, 22]. Moreover, the absence of both PBP5 and PBP6 influences the cellular concentration of MreB in the stationary phase. These data support the existence of a concerted regulation between the peptidoglycan polymerization machinery and the morphology maintenance systems.

In this work, we have established that the high levels of BolA can be detrimental for cell morphology and viability, especially if present in the early phases of growth, where these protein levels are usually negligible. Even though too much BolA seems to be harmful, its homologs are evolutionary conserved, with the remarkable exception of Gram-positive bacteria, which include several species that can sporulate when adverse conditions occur. It thus seems tempting to speculate that this gene and the respective protein have been maintained along evolution to favor adaptation of cells to adverse conditions.

In this work, we also wanted to understand the role of BolA in the regulation of the PBP5 and PBP6 hydrolytic murein proteins. These two proteins are homologs, but they behave slightly differently within cells [17], as evaluated by the phenotypic differences in the single deletion mutants studied here. Part of the BolA function in the cell requires PBP5 or PBP6, since a double-deletion mutant showed different growth and morphologies in response to the increase in BolA levels [20]. When overexpressing BolA, the levels of PBP5 and PBP6 transcripts are increased. Here, we have shown by Surface Plasmon Resonance that BolA directly interacts with the operator region of both *dacA* (PBP5) and *dacC* (PBP6) promoters, thereby indicating a possible wider impact of BolA as a transcriptional regulator.

Methods

Bacterial Strains, Plasmids, and Genetic Manipulations

The strains used in this study are described in Table 1. When necessary, strains were transformed with plasmid pMAK580 [3] containing *bolA* under regulation of its own promoters. Transformations were carried out as previously described [18].

Media, Growth Conditions, and Viabilities

Luria broth (LB) and Luria agar (LA) were prepared as described previously [16]. When required, the media were supplemented with 0.4 mM thymine, 50 mg/ml chloramphenicol, and 50 mg/ml kanamycin (all from Sigma). Optical densities were measured in an Amersham Biosciences Ultrospec 500/1100pro spectrophotometer at 620 nm, using 10-mm light path cuvettes. The ODs were determined according to the Lambert–Beer law's limits of direct proportionality between OD and sample concentration (dilutions were made in LB so that density values would be read between 0.02 and 0.6); the phases of growth analyzed were determined according to growth curves. Batch cultures were launched in one of two ways: (i) directly from LA plate where colonies were grown 16–18 h at 37°C (the plates could be stored for at least one week at 4°C and the behavior was reproducible); (ii) from an overnight (16 h) liquid culture grown at 37°C and 100 rpm [the inoculi were diluted to an optical density of 0.08 measured at 620 nm (OD_{620})]. Cultures were grown aerobically at 37°C and 120 rpm. For evaluation of viability, the samples were processed in LB serial dilutions, and 100 μl was plated in LA. The number of colony forming units (CFU) was counted and viability was determined according to the equation: Number of dividing cells per ml = $CFU \times 10^{dilution} \times 1{,}000/100\ \mu l$.

Microscope Preparations

To observe the effect of BolA on cell morphology, planktonic cells were harvested from cultures growing in LB, at the time points corresponding to the log, early exponential, late exponential, early

Table 1. Strains used in this study.

Strains	Description	Reference or source	Observations
MG1693	thyA715	[4]	Background strain
CMA10	MG1693+*bolA*$^+$	[19]	Overexpressing *bolA* (after its own promoters) from pMAK580
ED3184	his supF	Kindly provided by Noreen Murray	Background strain for deletion mutants
JBS980	F–his supF recA dacA::Kanr	[21]	pbp5 deletion mutant based on ED3184 strain
JBS1001	F–his supF recA dacC	[7]	pbp6 deletion mutant based on ED3184 strain
JBS983	F–his supF recA dacC dacA::Kanr	[6]	pbp5 and pbp6 double-deletion mutant based on ED3184 strain
CMA15	JBS980+*bolA*$^+$	[20]	JBS980 overexpressing *bolA* from pMAK580
CMA16	JBS1001 + *bolA*$^+$	[20]	JBS1001 overexpressing *bolA* from pMAK580
CMA17	JBS983+*bolA*$^+$	[20]	JBS983 overexpressing *bolA* from pMAK580
CMA 18	ED3184+*bolA*$^+$	This study	ED3184 overexpressing *bolA* from pMAK580
CMA50	BL21 (DE3)+pPFA02	[10]	Novagen strain with plasmid overexpressing (His)6–BolA

stationary, and late stationary phases, according to the growth curves. Cells were fixed with 0.75% (v/v) formaldehyde and stored at 4°C. For the differential interference contrast (DIC) microscopy photographs, 20 µl of the samples were observed in slides coated with a thin 1.5% (w/v) agarose film, and enclosed with nr.1 cover glass. Images were obtained using a DMRA2 microscope (Leica) under Nomarski optics coupled to a CCD camera, with Metamorph software.

Overexpression and Purification of BolA Protein

The plasmid used for expression of BolA was a pET28a-derived pPFA02 [7] transformed into a Novagen *E. coli* BL21 (DE3) strain (Table 1). Cells were incubated at 37°C, in 250 ml of LB medium supplemented with 100 µg/ml ampicillin, to an OD_{620} of 0.5. Induction was performed with 0.5 mM IPTG during 60 min. Bacterial cells were pelleted by centrifugation at 6,500 rpm for 10 min and stored at −20°C.

Purification of BolA was performed by histidine affinity chromatography using HiTrap chelating HP columns (GE Healthcare) and an AKTA fast protein liquid chromatography system (GE Healthcare). Cells were resuspended in buffer A with 20 mM sodium phosphate (pH 7.4) and 50 mM NaCl and lysed using a French Press at 9,000 psi, in the presence of 0.1 mM phenylmethylsulfonyl fluoride (PMSF). The crude extracts were treated with Benzonase (Sigma) during 30 min and clarified by a 15 min centrifugation at 9,500 g. The clarified extracts were then added to a HiTrap Chelating Sepharose 1 ml column equilibrated in buffer A. Protein elution was achieved by a continuous imidazol gradient (until 100 mM) in the same buffer. The fractions containing purified protein were pooled together and buffer was exchanged to pure buffer A (without imidazol) using Amicon Ultra Centrifugal 10 kDa Filters (Millipore). Protein concentration was determined by spectrophotometry using a Nanodrop device and measuring the OD at 280 nm. Then 10 µl of purified protein fractions was applied to a 15% SDS−PAGE and visualized by Coomassie blue staining to assess protein purity (data not shown).

Surface Plasmon Resonance (SPR) Analysis

The SPR analysis was performed in a BIACORE 2000 instrument. Purified BolA protein was immobilized in a CM5 sensor chip by the amine coupling immobilization method according to the manufacturer's instructions (GE Healthcare). The same immobilization procedure was performed with the same molarity of BSA control protein in a reference flow cell, used to correct for refractive index changes and nonspecific binding. The PBP5 and PBP6 promoters were amplified by PCR using pbp5Fw 5'-GGGGTACCGCAACGTTTGCAAACCG AAG-3', pbp5Rev 5'-CCATCGATCTGAACTACGACATCCGTG-3', pbp6Fw 5'-GGGGTACCCAT ACTCACCCCTTTTCC-3', and pbp6Rev 5'-CCATCGATCCACCCGAGTATCCATTC-3' primers, respectively. As a positive control, the promoter sequence of the *mreBCD* operon was used and as a negative control we tested the *bolA* open reading frame (ORF) DNA encoding fragment as previously described [7]. We also used, as negative controls, the ORF from *mreB*, PBP5, PBP6, and RNase II. These regions were amplified by PCR using RTmreB 5'-ACTTGTCCATTGACCTGGGTACTG-3', RTmreB2 5'-GCCGCC GTGCATGTCGAT CATTTC-3', codingpbp5Fw 5'-CCGCTCGTATC ATGAAGCGCC-3', codingpbp5Rev 5'-CCGAAGAAGTTACCTTCCG GG-3', codingpbp6Fw 5'-CTCCTTCGTGGTCTTGC-3', codingpbp6Rev 5'-GATTAAGAGAACCAGCTGCCG-3', rnb_477 5'-GGCGATCG TTCTT TCTATGCAGAA-3', and Asp210Asn_Rev 5'- TAGCGAA GAGGGCGTTATCCATA TCTTCTG-3' [4]. The assays were run at 25°C in 20 mM sodium phosphate (pH 7.4), 1 mM dithiothreitol, and 500 mM NaCl buffer. The amplified DNA fragments were injected over the flow cells for 2.5 min at a minimum of 5 different concentrations between 6.4×10^{-5} and 5 nM using a flow rate of 20 µl/min. All experiments included triple injections of each sequence concentration to determine the reproducibility of the signal. Bound protein was removed with a 60 s wash with 50 mM NaOH. Equilibrium constants were determined using the BIA Evaluation 3.0 software package, according to the fitting model 1:1 Langmuir Binding, and χ^2 was the statistics used to measure the fitness of the model to the data.

RESULTS AND DISCUSSION

BolA Overexpression Impairs Cell Growth Rate

Bacterial growth rates after inoculation depend on the growth stage at time zero. If the culture is growth arrested, cell replication will be partially delayed as metabolism has to be restarted; if, on the contrary, the culture is in the exponential phase, the multiplication rate is maximal, and so there will be no lag phase. Regarding BolA expression, however, this situation is more prominent. In this case, the cells do not just have to resume or maintain growth, but it seems that they have to adapt to the levels of this protein in the cell.

In optimal growth conditions, BolA protein increases its levels when cells are entering into the stationary phase [1]. Therefore, if growth is initiated after an overnight suspension culture with BolA highly expressed, BolA will be present in high concentration in the cells diluted into new media. We wanted to study the role of differential BolA levels on starting cultures. Therefore, we have monitored the growth on two different backgrounds (MG1693 and ED3184), using cultures started after an overnight liquid growth (liq_MG1693, liq_ED3184), or cultures directly inoculated from the plate (pl_MG169, pl_ED3184). Comparisons were made for the same conditions using the strains transformed with the pMAK580 *bolA* overexpressing plasmid (respectively, CMA10 and CMA18). In the wild-type strains, the growth rate is not dependent on the starting culture (see pl_MG1693 *vs.*liq_MG1693, and pl_ED3184 *vs.* liq_ED3184, Fig. 1). Nevertheless, in the presence of additional copies of *bolA* due to the presence of pMAK580, a *bolA* overexpressing plasmid, serious changes in growth are observed depending on the inoculum [see pl_CMA10 (MG1693+$bolA^+$) *vs.* liq_CMA10 (MG1693+$bolA^+$) and pl_CMA18 (ED3184+$bolA^+$) *vs.* liq_CMA18 (ED3184+$bolA^+$)] (Fig. 1). For strains bearing the plasmid ($bolA^+$) growth is strongly impaired for cultures started from batch culture, when compared with the cultures directly inoculated from the plate. We have compared the levels of *bolA* mRNA levels in both starters and the results showed that the levels of *bolA* mRNA are about 2,3 times higher when the

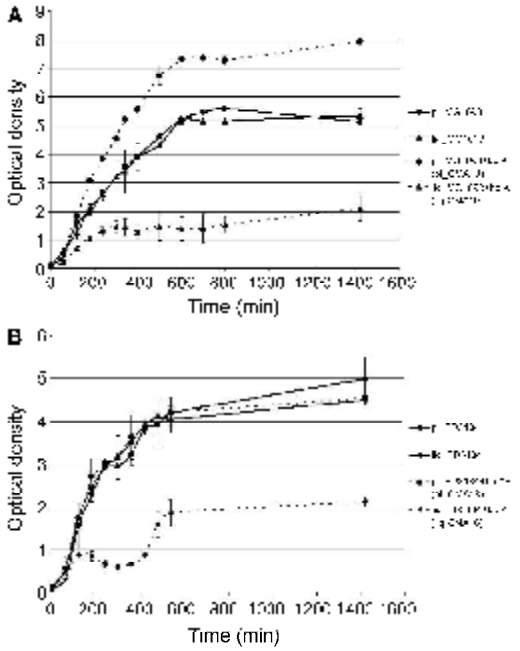

Fig. 1. Optical density measurements at 620 nm for determination of growth curves in LB media supplemented according to the strains, at 120 rpm, 37°C.
Average and standard deviations from a minimum of three independent repetitions are presented; prefix with starting OD: (pl_) for strains directly grown from plate and (liq_) after an overnight liquid growth. **A**. MG1693 and MG1693+*bolA*$^{+}$ (CMA10) strains; **B**. ED3184 and ED3184+*bolA*$^{+}$ (CMA18) strains.

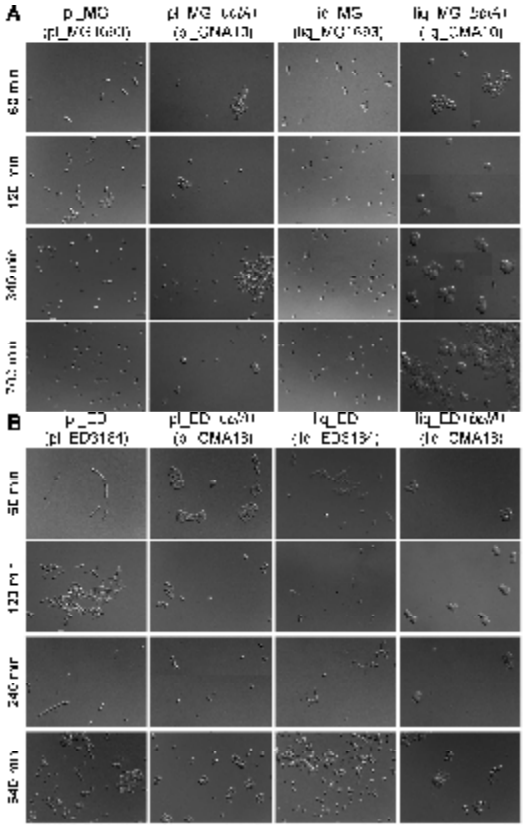

Fig. 2. Representative differential interference contrast (DIC) microscopy photographs overlaid in Photoshop to increase the amount of data presented.
DIC micrographs were obtained using a DMRA microscope (Leica) at time points 60, 120, 340, and 700 or 540 min of the growth curves. **A** MG1693 and CMA10 (MG1693+*bolA*$^{+}$) strains; **B**. ED3184 and CMA18 (ED3184+*bolA*$^{+}$) strains. The black bar represents 5 μm.

innoculum comes from an overnight liquid growth. In this case, cultures can only support growth until half of the maximum OD value reached when they are directly grown from plate (liq_CMA10 and liq_CMA18 *vs.* pl_CMA10 and pl_CMA18) (Fig. 1). This behavior is not reported for the strains without pMAK580 and occurs similarly in both MG1693 and ED3184 *E. coli* backgrounds (Fig. 1).

BolA Effect on Growth Rate is Correlated with Alterations in Bacterial Morphology

The changes in growth behavior were evaluated by microscopy analysis (Fig. 2). Similarly to what has been observed in the growth curves, cell morphology does not vary much according to the growth state of the inoculum for the wild-type strains: in MG1693 background, no differences can be distinguished (Fig. 2); and in the ED3184 strain, it is possible to see a mixed filament/rods population with a propensity for rods after an overnight liquid growth (Fig. 2). The strains carrying pMAK580 plasmid alter their morphologies from rods to spheres as advanced exponential phase is reached, when they start growth from an agar plate (pl_CMA10 and pl_CMA18) (Fig. 2). However, when they are started from a suspension culture (liq_CMA10 and liq_CMA18), cells present a spherical shape even in the beginning of the logarithmic phase. In this case, as long as cell division proceeds, the spherical morphologies evolve towards larger spheres that eventually bulge, or even burst (Fig. 2). This may be the reason for these strains to have a lower growth rate when compared with the others.

BolA Affects the PBP5 and PBP6 DD-Carboxypeptidases

After establishing how bacterial growth rates and patterns depend on the origin of the inocula, which revealed to be

particularly important for strains where BolA is more expressed, the effects of this protein over the *E. coli* DD-carboxypeptidases penicillin-binding proteins PBP5 and PBP6 were analyzed. For that purpose, strains derived from ED3184 wild type were used, namely single and double deletants for *dacA* (PBP5) and *dacC* (PBP6) genes, and those transformed with pMAK580 (see Table 1). Similarly to what had been observed for the background strains, the growth curves for the deletant mutants, with and without pMAK580, were completely superimposed when they were cultured from plated colonies (data not shown). Further analysis was performed in the conditions where strains presented pronounced phenotypic effects derived from BolA increased levels, and therefore starting after overnight batch cultures.

Initially, growth curves were performed for all the strains derived from ED3184, with and without pMAK580 plasmid for overexpression of BolA. The results show that the PBP deletants JBS980 (PBP5$^-$), JBS1001 (PBP6$^-$), and JBS983 (PBP5$^-$PBP6$^-$) follow a similar growth curve to their respective wild-type strain ED3184 (Fig. 3A). However, upon BolA overexpression, all strains except the double deletant have their growth strongly impaired, mainly in the early log phase, where optical density values remain constant or even decrease (see Fig. 3A). BolA is naturally expressed in the transition from the late exponential to the stationary phase [1], concomitantly with a multitude of metabolic and morphological changes in the cells [3, 10, 11, 20]. After a certain threshold, BolA might be toxic for cells. In that sense, most cells with increased BolA levels (in strains transformed with pMAK580, particularly after overnight growth) tend to have difficulties in recovering. The cultures present an adaptation period that can be considered as an "extreme" form of lag phase. In strain liq_ED3184+*bolA*$^+$ (liq_CMA18), while cells adapt to fresh media and restart a fast duplication stage (corresponding to the exponential phase of bacterial development), a significant increase in the cells sizes occurs (see Fig. 2B, liq_CMA18, times 60 to 120 min) increasing the OD unrelated to the changes in cell number. Those cells that significantly increase in size (the majority of the initial population inoculated) seem to become committed to lysis, and at about 240 min of growth we observe cells lysing or "bursting" (see Fig. 2B, liq_CMA18, 240 min). The transition between 120 and 240 min of the growth curve should correspond to the "explosion" of the majority of high dimensioned cells. At that time, a reduced number of smaller rod-shaped unsynchronized cells, already present at the inoculum, substitute the initial bacterial population already dividing at a fast rate, and that accounts for the subsequent increase in OD. All strains overexpressing BolA, with the exception of the double-deletion mutant, present a longer adaptation time to reach the exponential phase. In fact, the largest difference between growth

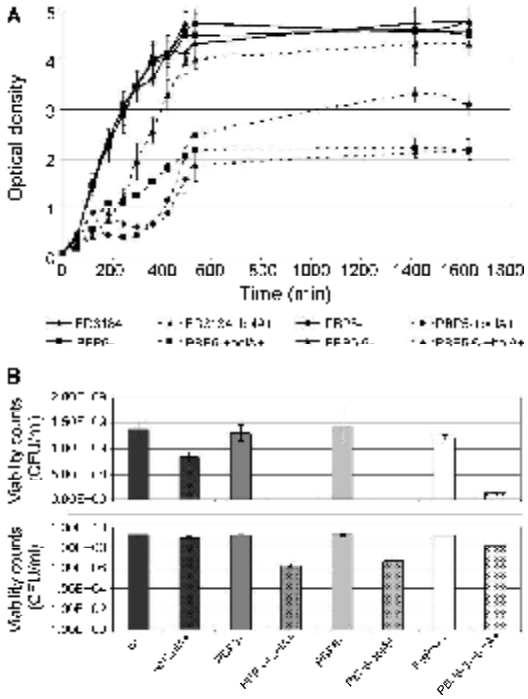

Fig. 3. Growth and viability analysis for evaluation of the role of BolA on PBP mutant strains (average and standard deviations from a minimum of three independent repetitions are presented). **A**. Optical density measurements at 620 nm for determination of growth curves in LB media supplemented according to the requirement of the respective strains, at 120 rpm, 37°C, after an overnight liquid growth. **B**. Viability analysis at 240 min, in decimal and logarithmic scales, according to Materials and Methods description.

curves with and without pMAK580 is not in the rate of multiplication, after the strains are already adapted to the new growth media. The rate is about the same for all, except the PBP6 single deletion strain overexpressing BolA. The latter multiplies about 2,7 times slower than all others. Differences in curves are mostly due to the time that the strains require to "adapt" BolA levels to new media conditions. In that sense, there is virtually no lag phase in cultures where pMAK580 is absent, and whereas the transformed background strain CMA18 takes the longest period to adjust (7 times more), the double mutant, along with the single PBP6 mutant overexpressing BolA, adapts faster (4 times faster than in the absence of the plasmid). It is possible that a partial substitution effect between PBPs might be happening, since the effects on growth due to BolA are apparently prevented in the simultaneous absence of both DD-carboxypeptidases. The data additionally suggest that PBP5 is a preferential target for BolA action. The strains where this protein is present

are more affected by BolA, not only in growth rate but also in the maximum OD reached by cultures: $OD_{620\,nm}$=2 for the PBP6 single mutant (where PBP5 is present) *versus* $OD_{620\,nm}$=3 for the PBP5 single deletant CMA15 and 4.5 for the double mutant CMA17, where both PBPs – and BolA targets – are absent. The double mutant CMA17, apart from an increased lag time, appears to grow quite similarly to the strains without the BolA overexpressing plasmid. A possible explanation could be that this lag period is independent from the effects of BolA over the PBPs, and instead related to regulation of *mreB* by BolA. In laboratory regular growth conditions, the MreB cytoskeleton protein should be continuously expressed until later stages of the growth curve, when its levels are reduced. Nevertheless, this protein is strongly inhibited by BolA, presenting reduced concentrations in cells whenever it is being expressed [10]. In this way, when cells should be ready to divide, their size is artificially reduced thus avoiding or delaying division. As a result, the fast growth phenotype and true exponential phase are concealed until BolA levels are reduced/washed out from cells, at about 240 min of growth, demonstrating a simple response of the division rate to the amount of MreB [10], directly dependent on the BolA levels (see Fig. 3A).

Convergent conclusions can be inferred from the examination of viabilities throughout growth, with the exception of the wild-type strain transformed with pMAK580 (CMA18) (Fig. 3B and 4). The CMA18 growth curve seems to be strongly impaired, but it is only slightly affected in actual viability counts (Fig. 3B). At 240 min of growth, viable colonies for strains transformed with pMAK580 increase about one order of magnitude from the $PBP5^-$ to the $PBP6^-$ strains, and the same happens between the PBP6 single mutant and the double mutant (that shows the minimal phenotype related to BolA, when comparing all the deletants). The PBP5 deletant with enhanced BolA expression reaches increased viable counts later on, after adaptation has occurred, giving the idea that this protein might not be naturally expressed at the early stationary phase. This can be clearly observed in the representative viability analysis of all strains along time (Fig. 4). The double mutant CMA17 is the one in which viability is less influenced by the increased BolA levels, whereas the viabilities for the single PBP6 mutant are the most affected, again suggesting that in the presence of PBP5 the cells are more sensitive to BolA levels. The detrimental effects of excess of BolA protein levels are particularly observed in fast cellular replication stages, coherently with the fact that this protein is naturally expressed in reduced growth rate conditions, such as in the stationary phase or upon stresses [1, 19]. These results further strengthen the idea that BolA may act as a regulator for both DD-carboxypeptidases. They also reinforce the observation that this regulation might be important for the phenotypes observed upon stationary phase or stress induction. It seems tempting to speculate that BolA has a preference for PBP5 as a target, since when this gene is deleted, the presence of pMAK580 has a reduced impact on growth impairment and cell counts remain higher.

Morphological evaluation of these strains by optical microscopy further substantiated that the double-deletion strain with pMAK580 is less sensitive to the BolA overproduction (Fig. 5). For the CMA17 strain, we can see that rods and even filaments are always present, and that even when some spheres appear they are not the dominant phenotype; however, in the other strains with the pMAK580 plasmid (CMA15, CMA16, and CMA18), the cells are essentially spherically shaped, changing in size and membrane integrity, as can be visualized through cells bulging and/or bursting (Fig. 5). Interestingly, when PBP5 is absent, the spheres seem to become larger than for the

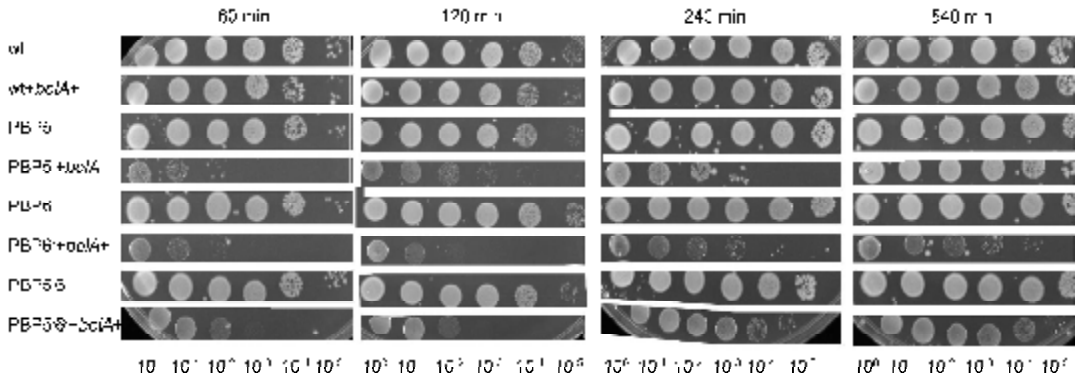

Fig. 4. Representative viability analysis for the time points 60, 120, 240, and 540 min, presented as 10-µl spots of serial dilutions (10^0 to 10^{-5}) from the cultures in LB media.

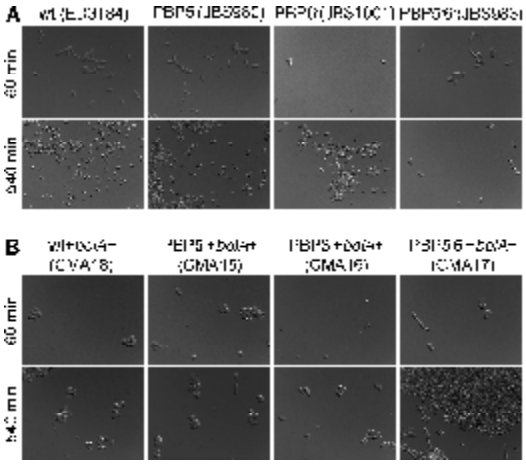

Fig. 5. Representative differential interference contrast microscopy photographs, obtained using a DMRA microscope (Leica), for the early exponential and early stationary phases of the all strains derived from ED3184 background (**A**) and the same strains transformed with *bolA*$^+$ (**B**).
The black bar represents 5 μm.

other single mutant, showing again that PBP5 and PBP6 are not equivalent targets for BolA.

BolA Interacts *In Vitro* with the Promoter Regions of *dacA* and *dacC*, Acting as a Positive Transcriptional Regulator for PBP5 and PBP6

Finally, we wanted to verify if the effect of BolA over the PBP5 and PBP6 proteins [1] and mRNA levels [17] is direct. It was previously determined that BolA directly interacts with *mreB* promoters *in vitro* [7]. In that system, BolA acts to repress *mreB* transcription and strongly reduces the *mreB* mRNA and protein levels. BolA upregulation of *dacA* and *dacC* mRNA levels has already been established [17]. By surface plasmon resonance, we measured the affinity of BolA protein to PBP5 and PBP6 promoters. As negative controls, we used DNA fragments amplified from the coding region of both PBPs (PBP5 ORF and PBP6 ORF) and also from a different gene, *rnb*, which encodes for the ribonuclease II (RNase II), an enzyme that degrades RNA molecules (RNase II ORF). As a positive control, we used the promoter region of *mreB*, previously demonstrated to have affinity for the BolA protein [10]. The results obtained are presented in Table 2. The dissociation constant value obtained for the *mreB* promoter in these new experiments corresponds to the one previously published (6.9 nM) [10]. The obtained data show that the BolA protein has slightly more affinity for *dacA* and *dacC* than for the *mreB* promoter (1.8 nM and 5.3 nM *vs*. 6.9 nM, respectively) (Table 2). In all cases, the affinity of BolA is significantly higher for the promoter regions than for the coding regions (120 nM and 102 nM, respectively). These results confirm that BolA behaves as a general transcriptional regulator. Furthermore, it can act either as a repressor of *mreB*, or as an activator of gene expression for production of PBP5 and PBP6. It is also possible to detect that BolA has more affinity for the PBP5 promoter when compared with the others (1.8 nM *vs*. 6.9 nM and 5.3 nM) (Table 2). According to the van´t Hoff equation, $\Delta G° = RT\ln K_D$, where R and T are the universal gas constant and absolute temperature, we determined the Gibbs free energy difference, $\Delta G°$. The values obtained are also reported in Table 2. The determination of the $\Delta G°$ informs us about the likelihood of complex formation. If $\Delta G°$ is negative, then we are in the presence of a spontaneous reaction. All the BolA protein–DNA interaction tests present a negative $\Delta G°$, which means that all these reactions are spontaneous and can occur *in vivo*. However, for the PBP5 promoter interaction, an even lower value is obtained when compared with the others (Table 2), meaning that the binding of BolA to the PBP5 promoter is much more probable. The binding to the coding regions PBP5 ORF, PBP6 ORF, and RNase II ORF, on the other hand, is not so favorable since they present the highest $\Delta G°$ values (Table 2). If we analyze the other equilibrium constants, we can see that the BolA protein interacts with the three promoters in a different way. The association rate constant (k_a) gives us

Table 2. BolA binding affinity for different promoter (Prom) and coding regions (ORF).

	k_a (1/Ms)	k_d (1/s)	K_D (nM)	χ^2	$\Delta G°$ (KJ/mol)
MreB Prom	1.1×10^{5}	7.4×10^{-4}	6.9	1.3	−46.6
PBP5 Prom	7.5×10^{4}	1.3×10^{-4}	1.8	0.8	−50.0
PBP5 ORF	8.4×10^{1}	1.0×10^{-5}	120	1.1	−39.5
PBP6 Prom	1.5×10^{3}	8.1×10^{-6}	5.3	1.7	−47.2
PBP6 ORF	9.8×10^{1}	9.9×10^{-6}	102	1.1	−39.9
RNase II Orf	2.8×10^{1}	1.0×10^{-5}	365	1.6	−36.8

Equilibrium constants (K_D) were determined by surface plasmon resonance using BIACORE2000 and according to the 1:1 Langmuir Binding Model. k_a is the association rate constant, k_d the dissociation rate constant, and K_D the equilibrium dissociation constant of the reaction. χ^2 was the statistics used to measure the fitness of the model to the data. $\Delta G°$ values were determined according to the van´t Hoff equation, $\Delta G° = RT\ln K_D$, where R and T are the universal gas constant and absolute temperature.

information about the kinetics of association, that is how fast the complex is formed, whereas the dissociation rate constant (k_d) relates to the dissociation kinetics or the velocity of complex dissociation. For the MreB promoter, the association is fast (k_a of 1.1×10^5 /M.s) and the dissociation is slow (k_d of 7.43×10^{-4} /s). For the PBP5 promoter, the association is not as fast as for the MreB promoter (k_a of 7.5×10^4 /M.s), but the dissociation is also slower (k_d of 1.3×10^{-4} /M.s) (Table 2) showing that the PBP5 promoter DNA–BolA complex is more stable than the MreB promoter DNA–BolA. However, for the PBP6 promoter, the results are quite different: the association of BolA to the promoter is really slow and the same is observed for the dissociation, which is much slower than the ones observed for the MreB or PBP5 promoters (Table 2). This behavior may indicate that the complex BolA–PBP6 promoter, once bound, can be even more stable when compared with the other complexes. For the coding regions tested, we can observe that the association is very slow, which reflects the poor affinity of BolA to these regions (Table 2).

Overall, the SPR experimental results confirm that BolA acts as a transcriptional regulator of *dacA*, *dacC*, and *mreB*. They particularly contribute to understanding why the single deletion mutants for the PBP5 and PBP6 proteins present such physiological differences in response to BolA accumulation, as reported in this work. An increase of the *dacA* (PBP5) and *dacC* (PBP6) mRNA levels had previously been observed when BolA was overexpressed [17], and therefore we can hypothesize that BolA is acting as an activator of *dacA* and *dacC*.

BolA is a protein whose levels strongly impact cellular growth rate, and the pattern of growth curves/ability to grow in rich LB media. The effects of overexpression of BolA result in aberrant cell morphologies, initially inducing formation of small spheres that then evolve into large spheres and aberrant morphologies. It was demonstrated that the phenotypes regarding the overexpression of *bolA* are much more prominent if the inoculum is taken from an overnight liquid culture, in which BolA has been considerably expressed and accumulated. It had been previously proposed that BolA might be related with the hydrolytic DD-carboxypeptidases penicillin-binding proteins PBP5 and PBP6. An increase of the *dacA* (PBP5) and *dacC* (PBP6) mRNA levels had previously been established [17], and a strain where the *bolA* gene was deleted seemed to show a decrease in PBP5 or PBP6 protein levels [1]. In this study, BolA was shown to be a more broad-range transcriptional regulator, directly interacting not only with the promoter region of *mreB* and reducing its expression levels, but also with the promoter regions of the genes that code for the murein cross-linking enzymes PBP5 and PBP6.

This work has opened new perspectives for the impact of BolA in bacterial growth and survival. Since BolA is able to target different genes as a transcriptional regulator, having the capacity of acting either as a repressor or as an activator, it is now important to determine to which other targets it can bind and regulate. Furthermore, it is also required to analyze how BolA regulation might connect with sigma factors and affect the global transcriptional machinery in stress conditions. This will allow us to determine to which extent BolA can modulate the cell and facilitate adaptation to less-than-optimal growth conditions.

Acknowledgments

We would like to thank Noreen Murray for all her kindness and continuous efforts to find and provide us the strain ED3184. I.B.G. and R.G.M. were recipients of Doctoral fellowships from FCT (Fundação para a Ciência e Tecnologia - Portugal). We thank FCT for funding this project and the Instituto Gulbenkian de Ciência for the access to their Cellular Imaging Unit, where all microscopy studies were performed.

References

1. Aldea, M., T. Garrido, C. Hernandez-Chico, M. Vicente, and S. R. Kushner. 1989. Induction of a growth-phase-dependent promoter triggers transcription of *bolA*, an *Escherichia coli* morphogene. *EMBO J.* **8:** 3923–3931.
2. Aldea, M., T. Garrido, J. Pla, and M. Vicente. 1990. Division genes in *Escherichia coli* are expressed coordinately to cell septum requirements by gearbox promoters. *EMBO J.* **9:** 3787–3794.
3. Aldea, M., C. Hernandez-Chico, A. G. de la Campa, S. R. Kushner, and M. Vicente. 1988. Identification, cloning, and expression of *bolA*, an ftsZ-dependent morphogene of *Escherichia coli*. *J. Bacteriol.* **170:** 5169–5176.
4. Bachmann, B. J. and K. B. Low. 1980. Linkage map of *Escherichia coli* K-12, edition 6. *Microbiol. Rev.* **44:** 1–56.
5. Barbas, A., R. G. Matos, M. Amblar, E. Lopez-Vinas, P. Gomez-Puertas, and C. M. Arraiano. 2008. New insights into the mechanism of RNA degradation by ribonuclease II: Identification of the residue responsible for setting the RNase II end product. *J. Biol. Chem.* **283:** 13070–13076.
6. Broome-Smith, J. K. 1985. Construction of a mutant of *Eschrichia coli* that has deletions of both the penicillin-binding protein 5 and 6 genes. *J. Gen. Microbiol*. **131:** 2115–2118.
7. Broome-Smith, J. K. and B. G. Spratt. 1982. Deletion of the penicillin-binding protein 6 gene of *Escherichia coli. J. Bacteriol*. **152:** 904–906.
8. Buchanan, C. E. and M. O. Sowell. 1982. Synthesis of penicillin-binding protein 6 by stationary-phase *Escherichia coli*. *J. Bacteriol.* **151:** 491–494.
9. Freire, P., J. D. Amaral, J. M. Santos, and C. M. Arraiano. 2006. Adaptation to carbon starvation: RNase III ensures normal

expression levels of bolA1p mRNA and sigma(S). *Biochimie* **88:** 341–346.

10. Freire, P., R. N. Moreira, and C. M. Arraiano. 2009. BolA inhibits cell elongation and regulates MreB expression levels. *J. Mol. Biol.* **385:** 1345–1351.
11. Freire, P., H. L. Vieira, A. R. Furtado, M. A. de Pedro, and C. M. Arraiano. 2006. Effect of the morphogene *bolA* on the permeability of the *Escherichia coli* outer membrane. *FEMS Microbiol. Lett.* **260:** 106–111.
12. Jones, L. J., R. Carballido-Lopez, and J. Errington. 2001. Control of cell shape in bacteria: Helical, actin-like filaments in *Bacillus subtilis*. *Cell* **104:** 913–922.
13. Kim, M. J., H. S. Kim, J. K. Lee, C. B. Lee, and S. D. Park. 2002. Regulation of septation and cytokinesis during resumption of cell division requires uvi31+, a UV-inducible gene of fission yeast. *Mol. Cells* **14:** 425–430.
14. Lange, R. and R. Hengge-Aronis. 1991. Growth phase-regulated expression of *bolA* and morphology of stationary-phase *Escherichia coli* cells are controlled by the novel sigma factor sigma S. *J. Bacteriol.* **173:** 4474–4481.
15. Markiewicz, Z., J. K. Broome-Smith, U. Schwarz, and B. G. Spratt. 1982. Spherical *E. coli* due to elevated levels of D-alanine carboxypeptidase. *Nature* **297:** 702–704.
16. Miller, J. H. 1972. *Experiments in Molecular Genetics*. Cold Spring Harbor Laboratory Press, Cold Spring Harbor, NY.
17. Nelson, D. E. and K. D. Young. 2001. Contributions of PBP 5 and DD-carboxypeptidase penicillin binding proteins to maintenance of cell shape in *Escherichia coli*. *J. Bacteriol.* **183:** 3055–3064.
18. Sambrook, J., T. Maniatis, and E. F. Fritsch. 1989. *Molecular Cloning: A Laboratory Manual*, 2nd Ed. Cold Spring Harbor Laboratory Press, Cold Spring Harbor, NY.
19. Santos, J. M., P. Freire, M. Vicente, and C. M. Arraiano. 1999. The stationary-phase morphogene *bolA* from *Escherichia coli* is induced by stress during early stages of growth. *Mol. Microbiol.* **32:** 789–798.
20. Santos, J. M., M. Lobo, A. P. Matos, M. A. De Pedro, and C. M. Arraiano. 2002. The gene *bolA* regulates *dacA* (PBP5), *dacC* (PBP6) and *ampC* (AmpC), promoting normal morphology in *Escherichia coli*. *Mol. Microbiol.* **45:** 1729–1740.
21. Spratt, B. G. 1980. Deletion of the penicillin-binding protein 5 gene of *Escherichia coli*. *J. Bacteriol*. **144:** 1190–1192.
22. van den Ent, F., L. A. Amos, and J. Lowe. 2001. Prokaryotic origin of the actin cytoskeleton. *Nature* **413:** 39–44.
23. Vieira, H. L., P. Freire, and C. M. Arraiano. 2004. Effect of *Escherichia coli* morphogene *bolA* on biofilms. *Appl. Environ. Microbiol.* **70:** 5682–5684.

Appendix III

Other papers published during this Doctoral work

10 - BolA Affects Cell Growth, and Binds to the Promoters of Penicillin-Binding Proteins 5 and 6 and Regulates Their Expression [Journal of Microbiology and Biotechnology 2011, 21(3): 243-251]

11 - Identification of a DNA binding site for the transcription factor Haa1p, required for *Saccharomyces cerevisiae* response to acetic acid stress [NAR 2011, 39(16):6896-6907]

Structure and Degradation Mechanisms of 3' to 5' Exoribonucleases

Rute G. Matos, Vânia Pobre, Filipa P. Reis, Michal Malecki, José M. Andrade and Cecília M. Arraiano

Instituto de Tecnologia Química e Biológica/Universidade Nova de Lisboa, Apartado 127, 2781-901 Oeiras, Portugal

Exoribonucleases are enzymes that cleave RNA molecules by removing terminal nucleotides from the 3' or 5' end of the RNA molecules. They are key factors in RNA metabolism and have a relevant role in the processing and degradation of all types of RNAs. The 3' to 5' exoribonucleases are divided into families, according to their sequence and structural characteristics. The PDX family contains phosphate dependent degradative enzymes, which can also perform the synthesis of RNA tails when phosphate is limiting. The RNB family contains hydrolytic enzymes with a similar domain organization. All proteins from this widespread family present the characteristic RNB domain, responsible for the 3' to 5' exoribonuclelolytic activity. In eukaryotes they can act alone or in a complex, the exosome, where they are the only active component. Finally, the DEDD family includes both RNA and DNA exonucleases and they present a similar mechanism of action. In this chapter, we will summarize the available information regarding the 3' to 5' exoribonucleases and discuss their importance for the RNA metabolism.

1. INTRODUCTION

The RNA levels in the cell depend on the efficiency of the transcription, and the rate of degradation. Although transcription is important to determine RNA steady state levels, the processing and degradation of RNA are also key factors in the regulation of gene expression.

Ribonucleases (RNases) are the enzymes that are able to process and degrade RNA. Moreover, they have a critical role in the maturation of ribosomal and transfer RNAs (Régnier and Arraiano 2000; Arraiano et al. 2010a). They are also involved in the quality control of all types of RNAs, allowing the recycling of the ribonucleotides in the cell (Li et al. 2002; Silva et al. 2011). RNases are present in all domains of life, and play a central role in the control of gene expression by determining the levels of functional RNAs in the cell (Régnier and Arraiano 2000; Arraiano and Maquat 2003; Parker and Song 2004). Many of the RNases in the cell are essential and others have overlapping functions (Régnier and Arraiano 2000). RNases can act alone or they can be part of RNA degradation complexes, namely the degradosome and the exosome. Ribonucleases can be divided into endoribonucleases (which cleave the RNA molecules internally) and exoribonucleases (which degrade the RNA by removing terminal nucleotides from the 3'end or the 5'end of the RNA molecules). In this chapter, we will focus on exoribonucleases, namely those which degrade the RNA from the 3' to the 5' end.

Exoribonucleases can act hydrolytically releasing nucleotide monophosphates, or phosphorolytically if they use inorganic phosphate to cleave the molecules releasing nucleotide diphosphates (Zuo and Deutscher 2001). The nucleotides released after the action of exoribonucleases are very important for turnover since they can be reutilized for the synthesis of new RNA molecules.

Exoribonucleases are involved in many RNA metabolic events, namely in RNA maturation and degradation (Andrade et al. 2009b). According to their sequence and structural characteristics, exoribonucleases can be divided into five families: RNB, PDX, DEDD, RRP4 and 5PX (the last two families do not have any representatives in bacteria) (Table 1). In this chapter we will summarize the available information about all families of exoribonucleases that degrade RNA from the 3' to the 5' end, and discuss the latest findings and their relevance in RNA metabolism.

2. PDX FAMILY

The PDX family of 3'-5' exoribonucleases includes PNPase, RNase PH from bacteria, and the core of the exosome in archaea and eukaryotes (Mian 1997; Zuo and Deutscher 2001; Pruijn 2005) (Fig. 1). These enzymes, contrary to the other exoribonucleases, are phosphate dependent enzymes, and release a dinucleotide as an end product of degradation. Beside their role as exoribonucleases the enzymes from this family can also catalyze other reactions like the addition of heteropolymeric tails to RNA substrates (Slomovic et al. 2008). In fact, the polymerization activity of PNPase was essential for the deciphering of the genetic code and this discovery led to the award of a Nobel Prize to Severo Ochoa in 1959 (Grunberg-Manago et al. 1955).

2.1. PNPase

PNPase is a multifunctional protein. Its main activity is the processive 3'-5' phosphorolytic degradation of single stranded RNA with a minimal 3' overhang of 7-10 unpaired ribonucleotides (Spickler and Mackie 2000). However, under conditions of low inorganic phosphate concentration, PNPase catalyzes the inverse reaction, i.e. polymerization of single-stranded RNA from nucleoside diphosphates (Littauer and Soreq 1982). Contrary to the homopolymeric poly(A) tails added by PAP I, the tails synthesized by PNPase are heteropolymeric, containing all four nucleotides (Slomovic et al. 2008). In spinach chloroplasts, cyanobacteria and Gram-positive bacteria, PNPase is suggested to be the main polyadenylating enzyme (Yehudai-Resheff et al. 2001; Rott et al. 2003; Sohlberg et al. 2003; Campos-Guillén et al. 2005). The archaeal exosome, which is very similar to PNPase (see below), has also been demonstrated to be responsible for the addition of heteropolymeric tails in *Sulfolobus* (Portnoy et al. 2005). PNPase also catalyzes the exchange reaction between the β-phosphate group of nucleoside diphosphates and free orthophosphate. More recently it was described that PNPase also regulates RNA translocation into mitochondria (Wang et al. 2010a).

PNPase can form complexes with other enzymes to easily degrade RNA. The main complex in which PNPase is involved is the degradosome. The degradosome is a large, multiprotein complex involved in RNA degradation. In *E. coli*, this multiprotein complex composed of the endoribonuclease RNase E, the 3'-5' exoribonuclease PNPase, the DEAD-box RNA helicase B (RhlB) and the glycolytic enzyme enolase

TABLE 1. Family of 3' to 5' Exoribonucleases

Family	*E. coli* members	Eukaryotic members	Catalytic mechanism	Comments
RNB	RNase II RNase R	Rrp44 (Dis3) Tazman	Hydrolytic	These enzymes are processive in the 3' to 5' direction; distributed in all domains of life
DEDD	RNase D	Rrp6	Hydrolytic	Proteins from this family are distributive in the 3' to 5' direction; some have DNase activity
	RNase T	-		
	Oligoribonuclease	Ynt20 (Rex2)		
	-	Pan2, ERI-1 Rex1, 3, 4		
PDX	PNPase	-	Phosphorolytic	The activity is processive in the 3' to 5' direction and phosphate dependent
	RNase PH	Rrp41-43, 45, 46 Mtr3		The activity is distributive in the 3' to 5' direction and phosphate dependent
		Csl4		

(Carpousis et al. 1994; Miczak et al. 1996; Py et al. 1996; Vanzo et al. 1998; Iost and Dreyfus 2006). RNase E provides the scaffold for the degradosome. Recent findings showed that *E. coli* PNPase and RNase E are present in the degradosome in an equimolar ratio (Nurmohamed et al. 2009). However, PNPase content can change in response to phosphosugar stress, temperature shock and growth stage (Beran and Simons 2001). In other organisms, the degradosome content might be different. In *Pseudomonas syringiae* PNPase is substituted by RNase R, and the DEAD-box helicase present in the degradosome is RhlE (Purusharth et al. 2005). PNPase can also exist as a $\alpha_3\beta_2$ complex where the β subunit has been identified as the helicase, RhlB (Lin and Lin-Chao 2005) and can form complexes with the host factor Hfq and PAP I (Mohanty et al. 2004).

X-ray crystal structures of *E. coli* and *Streptomyces antibioticus* PNPase reveal a homotrimeric subunit organization with a ring-like architecture (Fig. 1) (Symmons et al. 2000; Shi et al. 2008; Nurmohamed et al. 2009). Each monomer exhibits a five-domain arrangement: at the N-terminus two RNase PH domains (PH1 and PH2) are linked by an α-helical domain, and at the C-terminal end there are two RNA-binding domains (KH and S1) (Fig. 1a and b). The three monomers associate via trimerization interfaces of the core domains, forming a central channel, where catalysis occurs (Fig. 1c).

Structural and mutational analysis of *E. coli* and *S. antibioticus* PNPase and recent work on the spinach chloroplast and human PNPase (Sarkar et al. 2005) demonstrated that the catalytic site of PNPase is composed of structural elements of the first and second core domains (PH1 and PH2) (Symmons et al. 2000; Briani et al. 2007; Shi et al. 2008; Nurmohamed et al. 2009).

The all-α-helical domain was shown to be important for the catalytic activity of *E. coli* PNPase (Briani et al. 2007). This domain is highly dynamic and may affect the access of nucleoside diphosphates and phosphate to the active site. PNPase catalytic activity is dependent on a metal ion coordinated in the active site by the conserved residues D486, D492 and K494 (Nurmohamed et al. 2009). In *S. antibioticus* PNPase the metal used to identify the catalytic center was tungstate (a phosphate analogue) , which is coordinated to the T462 and S463 side chains (Symmons et al. 2000).

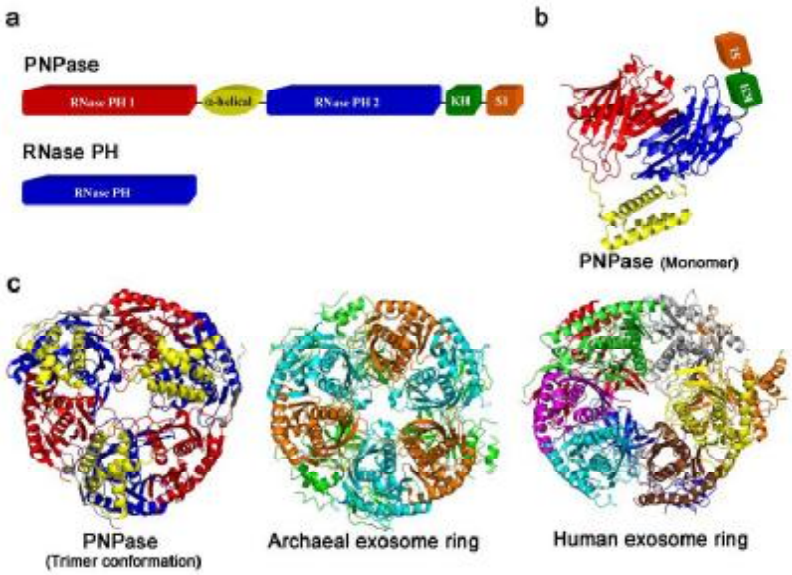

Figure 1. The PDX-family of enzymes. a. Linear representation of *E. coli* PNPase and RNase PH domains (note that the figures are not in scale). **b.** View of PNPase crystal structure in the monomer organization (PDB ID 3CDI - this PDB does not include the KH and S1 domains) (Shi et al. 2008). **c.** Comparison of PNPase trimer structure (PDB ID 3GCM - this PDB does not include the KH and S1 domains) (Nurmohamed et al. 2009) with the archaeal exosome ring from *Sulfolobus solfataricus* (Rrp41 is represented in light blue, Rrp42 in orange and Rrp4 in green; PDB ID 3L7Z) (Lu et al. 2010) and with the human exosome ring (Rrp4 is represented in orange, Rrp40 in red, Rrp41 in grey, Rrp42 in yellow, Rrp43 in light blue, Rrp45 in green, Rrp46 in magenta, Mtr3 in brown, and Csl4 in blue; PDB ID 2NN6) (Liu et al. 2006).

On the other hand, *E. coli* PNPase crystals were obtained in the presence of Mn^{2+}, since this ion can substitute Mg^{2+} to support catalysis and is more easily identified in the crystal structure. Interestingly, several mutations in the core region did not affect phosphorolytic or polymerase activities, but affected RNA binding. One example is the substitution of the conserved residue Gly454 by an aspartate in *E. coli* PNPase (Regonesi et al. 2006).

PNPase lacking either the S1 or KH domains retained phosphorolytic activity and still has some RNA binding capacity, but the truncated enzymes are much less active. Although PNPase lacking the S1 domain, KH domain, or both domains could still be assembled in the degradosome and their presence in the degradosome is vital at low temperature, the domains were shown to be essential to support growth in the cold. Nevertheless, the presence of both KH and S1 domains are required for proper RNA binding (Goverde et al. 1998; García-Mena et al. 1999; Zangrossi et al. 2000; Briani et al. 2007; Matus-Ortega et al. 2007; Shi et al. 2008). Shi and co-authors demonstrated that these RNA binding domains also have a major role in the formation of a more stable trimeric structure, and are essential for the constriction of the central channel (Shi et al. 2008). This is in agreement with a previous study where PNPase S1 domain was able to induce trimerization of an RNase II-PNPase chimeric protein (Amblar et al. 2007). Two constricted necks have been identified in the central channel (Symmons et al. 2000; Shi et al. 2008). Three arginine residues were identified in the PNPase neck region. The Arg102 and Arg103 residues are in the upper neck region close to the channel entrance and are involved in RNA binding. The third arginine residue (Arg106) is located in the lower neck region, closer to the active site, and apparently is involved in the processive RNA degradation (Shi et al. 2008). The upper neck and the crystal structure of the PNPase complexed with RNA support the hypothesis that the pathway followed by the RNA molecule is along the central pore in the direction to the active site (Symmons et al. 2000; Shi et al. 2008; Nurmohamed et al. 2009). The dynamic aperture of the central channel and the ability of its neighboring regions to undergo conformational changes, probably are the key aspects that allow PNPase to constrain and translocate the substrates in a processive mode of action (Nurmohamed et al. 2009).

PNPase is encoded by the *pnp* gene that is located downstream of the *rpsO* gene (encoding ribosomal protein S15) and is transcribed from two promoters (one upstream of the *rpsO* gene and another upstream of *pnp* gene. *pnp* expression is negatively autoregulated at the post-transcriptional level. This autoregulation only occurs after an initial cleavage by RNase III at the 5' end of the *pnp* message (Portier et al. 1987; Robert-Le Meur and Portier 1992; Jarrige et al. 2001; Carzaniga et al. 2009). PNPase levels are also affected by polyadenylation but not by Poly(A) polymerase (PAP I) itself (Jarrige et al. 2001). PNPase and RNase II are inter-regulated. In the absence of RNase II, PNPase levels are increased and PNPase overexpression leads to a decrease in RNase II activity (Zilhão et al. 1996a, 1996a). More recently it was shown that guanosine 5'-diphosphate 3'-diphosphate (ppGpp) inhibits *Nonomuraea sp.* and *Streptomyces* PNPase phosphorolytic and polymerization activities (Gatewood and Jones 2010; Siculella et al. 2010). In conclusion, PNPase has a complex regulation and its expression is finely controlled both at transcriptional and post-transcriptional levels (Andrade et al. 2009a).

PNPase does not seem to be indispensable to *E. coli* at optimal temperature, unless either RNase II or RNase R are also missing (Donovan and Kushner 1986; Cheng et al. 1998). However, PNPase is essential for *E. coli* growth at low temperatures (Luttinger et al. 1996; Piazza et al. 1996; Zangrossi et al. 2000). It was shown that overexpression of RNase II could complement cold shock function of PNPase (Awano et al. 2008).

PNPase has been implicated in the establishment of virulence in several pathogens, namely in *Salmonella*, *Dichelobacter nodosus*, *Dickeya dadantii*, *Yersinia*, *Campylobacter jejuni* and *Streptococcus pyogenes* (Arraiano et al. 2010a). However, PNPase role in virulence can be contradictory, while in some pathogens PNPase seems to act as a virulence repressor, in others PNPase is important for the establishment of virulence (Arraiano et al. 2010a).

2.2. RNase PH

RNase PH is encoded by the *rph* gene and is co-transcribed with pyrE, a gene necessary for pyrimidine synthesis which is located upstream of *rph* (Ost and Deutscher 1991). RNase PH is not essential for cell growth, unless RNase T or PNPase are also missing. In fact, the *rph* mutation only results in inviability in a strain already lacking RNases I, II, D, BN and T (Kelly et al. 1992). Contrary to PNPase, which is mainly involved in RNA degradation, RNase PH is involved in tRNA metabolism, namely in the processing of tRNA precursors (Deutscher et al. 1988; Kelly and Deutscher 1992a), and in ribosome metabolism (Zhou and Deutscher 1997; Redko and Condon 2010). RNase PH can act as a phosphorolytic ribonuclease (removing nucleotides following the CCA terminus of tRNA) or as a nucleotidyltransferase (adding nucleotides to the ends of RNA molecules) (Kelly and Deutscher 1992a; Wen et al. 2005; Bralley et al. 2006). RNase PH can also modify the 3' end of other small RNAs, including M1, 6 S, and 4.5 S RNA (Li et al. 1998).

The crystal structures of RNase PH from *Aquifex aeolicus*, *B. subtilis* and *Pseudomonas aeruginosa* have been determined. All the three proteins crystallized as a hexamer arranged as a trimer of dimers. The overall architecture of the three RNase PH is a βαβα fold, but the number of β-strands and α-helices are different between them (Ishii et al. 2003; Choi et al. 2004; Harlow et al. 2004). In the *A. aeolicus* RNase PH the phosphate-binding site consists of four residues, and is located at the bottom of a deep cleft, and it was proposed that the narrow entrance of this cleft can discriminate between single and double-strand RNA. Mutations of the conserved residues Arg86, Thr125 and Arg126 showed that these residues are very important for the phosphorolytic activity of the RNase PH. Based on structural and mutational analysis of the *A. aeolicus* RNase PH, Ishii and coworkers proposed that the RNase PH dimer only interacts with the tRNA acceptor stem, while the other parts of the tRNA remain unbound (Ishii et al. 2003). On the other hand, in the crystal structure of the *B. subtilis* RNase PH it was possible to identify a tRNA phosphate backbone binding region. The active binding site (Thr125, Arg126 and Gly123) for the *B. subtilis* RNase PH corresponds to the binding of the phosphate ion in the *A. aeolicus* RNase PH structure. Harlow and co-workers also identified three conserved arginine residues (Arg68, Arg73 and Arg76) as very important residues for the maintenance of the RNase PH hexameric structure (Harlow et al. 2004). The formation of the RNase PH hexameric ring is essential for the binding of precursor tRNA and also for the exoribonucleolytic activity (Choi et al. 2004).

2.3. The Exosome and the PDX family

The exosome is a multiprotein complex with a 3'-5' RNase activity that is involved in RNA degradation and processing. In Archaea, the exosome consists of two RNase PH subunits (Rrp41 and Rrp42) and two RNA binding

subunits (Rrp4 and Csl4) (Evguenieva-Hackenberg et al. 2003; Buttner et al. 2005). The crystal structure of the archaeal exosomes from the *Sulfolobus solfataricus*, *Archaeoglobus fulgidus* and *Pyrococcus abyssi* have been solved. These structures revealed a hexameric ring-like assembly formed by three Rrp41 and Rrp42 subunits. This hexameric ring is capped by a trimer of the RNA binding proteins Rrp4 and/or Csl4 (Buttner et al. 2005; Lorentzen et al. 2005) (Fig. 1c). Both Rrp41 and Rrp42 are involved in substrate binding, however only the Rrp41 has catalytic activity (Lorentzen et al. 2005). The archaeal exosome concomitantly binds three single-stranded RNA that enter the exosome catalytic site from the top side of the RNase PH ring. The narrow constriction of the central channel might be the reason why the exosome can degrade single-stranded RNA but stalls with the secondary structures (Bonneau et al. 2009). In addition to trapping and directing the substrate to the catalytic site, the exosome central channel also appears to have an important role in the RNA stabilization and processing. A model for the RNA processing by the archaeal exosome as been proposed, which is very similar to the one proposed for RNase II (Frazão et al. 2006). In this model, the single-stranded RNA binds to the RNA binding subunits and is then threaded to the catalytic site. After phosphorolytic cleavage the nucleoside diphosphate undergoes a structural arrangement and is released through a conserved side channel. At the same time, there is the entrance of a new inorganic phosphate. The final 4-5 nucleotide products are no longer capable of maintaining the interactions between the RNA and the RNA recognition cleft (formed at the interface of the Rrp41-Rrp42 subunits), so the translocation is no longer possible and the substrate is released.

The eukaryotic exosome is also formed by a six-subunit PH-domains ring, Rrp41, Rrp45, Rrp46, Rrp42, Rrp43, and Mtr3. However, and contrary to what happens in archaeal organisms, these proteins appear to lack catalytic activity. In fact, both yeast and human exosome cores do not present any catalytic activity (Liu et al. 2006; Dziembowski et al. 2007). In this case, the RNase PH homologues in Eukaryotes may have a role in substrate binding and recruitment.

3. RNB FAMILY

The RNB family of enzymes is present in all domains of life and exhibit the same modular organization (Fig. 2a). They processively degrade RNA in the 3' to the 5' direction. They have a hydrolytic activity, releasing 5'-nucleotide monophosphates (Mian 1997; Zuo and Deutscher 2001). ***E. coli*** RNase II is the prototype of this family of enzymes, which also comprises RNase R and the eukaryotic Rrp44/Dis3 (Table 1).

Members of this family play very important functions in the cell: they are essential for growth (Mitchell et al. 1997), they can be developmentally regulated (Cairrão et al. 2005), and mutations in its gene have been linked with abnormal chloroplast biogenesis (Bollenbach et al. 2005), mitotic control and cancer (Lim et al. 1997). They were also shown to be important for stress responses, RNA and protein quality control, and required for virulence in several organisms (Cheng et al. 1998; Cairrão et al. 2003; Cheng and Deutscher 2003, 2005; Andrade et al. 2006; Cairrão and Arraiano 2006; Purusharth et al. 2007; Charpentier et al. 2008; Erova et al. 2008).

In eukaryotes, RNase II homologues can act independently or can be associated in multiprotein complexes, like the exosome, a complex of exoribonucleases crucial for the maintenance of the correct levels of RNAs in the cell (van Hoof and Parker 1999).

3.1. RNase II

E. coli RNase II is the prototype of this family of enzymes. This 72kDa protein encoded by gene *rnb* is the major hydrolytic enzyme, responsible for 90% of the exoribonucleolytic activity in crude extracts (Deutscher and Reuven 1991). RNase II is expressed from two different promoters, P1 and P2, which implies a differential regulation of the *rnb* gene at the level of transcription (Zilhão et al. 1996b). This protein is also regulated at post-transcriptional levels (Cairrão et al. 2001). Other ribonucleases, such as RNase III, RNase E and PNPase, are involved in the modulation of RNase II levels (Zilhão et al. 1995; Zilhão et al. 1996a), and it was also shown that there is a post-translational regulation of RNase II levels conferred by the *gmr* gene (Gene Modulating RNase II), which is located downstream of the *rnb* gene (Cairrão et al. 2001).

RNase II is a hydrolytic enzyme which processively degrades RNA in the 3' to 5' direction releasing 5' monophosphates, and the final product released is a 4 nt fragment. The activity of this protein is sequence independent but sensitive to secondary structures (RNase II stalls around seven nucleotides before it reaches the double stranded region) (Fig. 2e) (Spickler and Mackie 2000).Ten nucleotides is the minimum of length of the RNA molecule needed for the processivity of the enzyme. For fragments less than 10 nt, the activity of RNase II becomes distributive (Cannistraro and Kennell 1994). Although being specific for RNA, RNase II is able to bind to DNA molecules without being able to cleave them. It seems that the DNA oligonucleotides can act an inhibitors of RNase II action since they bind its specific binding site (Cannistraro and Kennell 1994).

RNase II activity does not depend on the RNA sequence, however, it has a marked preference for poly(A) substrates. Polyadenylation is responsible for the control of mRNA stability in several organisms. The poly(A) tails are synthesized by poly(A) polymerase I (PAP I) to target RNAs to be degraded by exoribonucleases. Since RNase II has preference for poly(A) substrates, it will rapidly degrade these tails. The degradation process proceeds until a secondary structure, such as a Rho independent terminator is found. By rapidly degrading these Poly(A) tails, RNase II can impede the binding of other exoribonucleases to the RNA molecule, since no overhang is left to allow the binding of other ribonucleases, thus preventing the RNA degradation. With this behaviour, RNase II is acting paradoxically by protecting some messages (Marujo et al. 2000; Andrade et al. 2009b). By sequence analysis, it was proposed that RNase II has a modular organization, with three conserved domains: a CSD at the N-terminal region, a central catalytic RNB domain, and a C-terminal S1 domain (Andrade et al. 2009b; Arraiano et al. 2010a; Arraiano et al. 2010b) (Fig. 2a). The RNB domain is well conserved and it is exclusive to RNase II-like proteins. It contains four highly conserved motifs (I to VI) with several invariant amino acids (Mian 1997). The function of each domain was determined and it was shown that the RNB domain is responsible for the catalytic activity, whereas CSD and S1 domains are responsible for the binding to RNA (Amblar et al. 2006). The resolution of the crystal structure of RNase II (the first of an RNB-family member) revealed the existence of four domains instead of the three previously proposed: two N-terminal CSD, the central RNB domain and the S1 domain at the C-terminal region (Frazão et al. 2006). Moreover, it was possible to see that the RNB domain presents an unprecedented fold which is characteristic of this family.

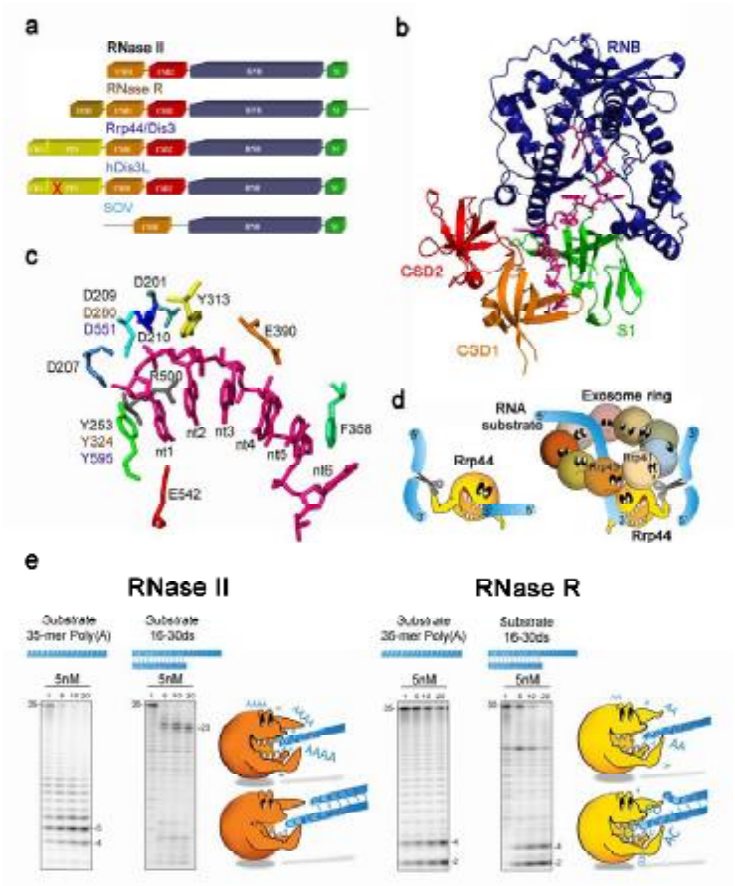

Figure 2. The RNase II-family of enzymes. a. Schematic representation of RNB-family members, which share a similar modular organization (note that the figures are not in scale). **b.** RNase II 3D structure shows that it is comprised of two N-terminal Cold Shock Domains (CSD1 in orange and CSD 2 in red), a central RNB domain (in blue) and a C-terminal S1 domain (in green); the RNA molecule is also represented (in pink) (PDB ID 2IX0 and 2IX1) (Frazão et al. 2006). **c.** In the catalytic cavity, several conserved residues interact with the RNA molecule (Frazão et al. 2006) Residues from *E. coli* RNase II are written in black, from *E. coli* RNase R in brown and yeast Rrp44/Dis3 in dark blue. **d.** The Rrp44 protein is the only active subunit in the yeast exosome and has both exo and endonucleolytic activity (Dziembowski et al. 2007; Schaeffer et al. 2009). This protein can act as a member of the exosome and it is also possible that it may act alone. **e.** Comparing the catalysis of *E. coli* RNase II and RNase R with different substrates. RNase II releases a 4 nt fragment as end-product when degrading single-stranded substrates. For structured substrates, the product released by RNase II has an overhang of 4-7 nt before the duplex. RNase R is able to degrade both single and double-stranded substrates releasing a 2 nt fragment as end-product.

The RNA-binding domains (CSD1, CSD2 and S1) are grouped together on one side of the structure, while the active site is on the other side of the molecule (Frazão et al. 2006) (Fig. 2b).

An RNase II mutant found in nature (D209N) was previously described and it was showed to encode an inactive protein still able to bind to RNA (Amblar and Arraiano 2005). The structure of this mutant was also solved, and the crystallization proceeded with a RNA molecule that was inside. This allowed the co-crystalization of the RNA molecule inside the protein, which was very important since enabled the visualization of RNA-protein contacts, and explains the mode of action (Frazão et al. 2006). The RNA contacts RNase II at two different and non-contiguous regions, which act synergistically to provide a processive degradation: the anchoring region, constituted by the three RNA-binding domains, and the catalytic region, which is buried inside the catalytic domain and is flanked by the four RNase II conserved motifs (Frazão et al. 2006). The shortest RNA substrate that is able to contact both anchor and catalytic regions is a 10 nt fragment. In fact, this is the minimum size necessary for the enzyme to be processive. For shorter RNA fragments, fewer contacts with the protein are established and the enzyme becomes distributive (Frazão et al. 2006). The access to the catalytic pocket is restricted to ssRNA due to the steric hindrance at its entrance and explains why RNase II is not able to cleave double stranded substrates (Spickler and Mackie 2000; Frazão et al. 2006). The first five nucleotides counting from the 3' end are stacked between the two aromatic residues Tyr253 e Phe358 (Fig. 2c), which helped us to understand why 4 nt is the final end product released by RNase II: when the RNA molecule is shorter than five nucleotides, the stacking no longer occurs, and the molecule is released (Frazão et al. 2006). A mutational analysis identified residue Tyr253 as responsible for setting the final end-product in RNase II. The substitution of this residue by an alanine changed the RNase II product from 4 to 10 nt and it was also shown to be crucial for the RNA binding at the 3'-end (Barbas et al. 2008; Arraiano et al. 2010b; Matos et al. 2010). The active site of RNase II has four highly conserved aspartic acids in positions 201, 207, 209, and 210 and an arginine in position 500 (Fig. 2c), which were postulated to assist in catalysis, namely by fixing the RNA molecule correctly. It was shown that the four aspartates are not equivalent in their function, with Asp209 being the only one essential for catalysis (Barbas et al. 2008; Arraiano et al. 2010b). The same result was obtained with other members of this family (Dziembowski et al. 2007; Matos et al. 2009). The Arg500 was also proved to have a crucial role in RNA degradation (Barbas et al. 2009; Arraiano et al. 2010b). The residue Glu542 is in close proximity with the leaving nucleotide (Fig. 2c), and it was proposed that it helped to release the last nucleotide after cleavage. However, its substitution in *E. coli* RNase II by an alanine led to a mutant which is 110-fold more active and with a 20-fold higher RNA affinity when compared to the wild type protein (Barbas et al. 2009; Matos et al. 2010). This mutant protein constructed was described as an RNase II "Super-Enzyme". This result showed that, in fact, Glu542 slows down

the activity of the protein (Barbas et al. 2009; Arraiano et al. 2010b). As mentioned previously, RNase II is able to bind to DNA but it cannot cleave it. The resolution of RNase II structure allowed to see the interaction between Tyr313 and Asp201 and the O2' ribose oxygen of the second ribose and Glu390 with the O2' ribose oxygen of the fourth ribose (Frazão et al. 2006) (Fig. 2c). It was also demonstrated that RNase II has a strict requirement for a ribose at the second and/or the fourth nucleotide from the 3'-end of the molecule (Barbas et al. 2009; Arraiano et al. 2010b). Moreover, these contacts are responsible for the RNA specificity (Barbas et al. 2009).

3.2. RNase R

RNase R-like enzymes have a wide impact in RNA metabolism in many different organisms. RNase II stalls when reaching near a duplex, and PNPase needs association with a helicase to overcome such structures. However, RNase R has the remarkable feature of degrading double-stranded RNAs. The substrate list for RNase R includes defective tRNAs (Li et al. 2002) or rRNA (Cheng and Deutscher 2003) as well as mRNAs with REP-containing sequences (Cheng and Deutscher 2005) or small RNAs like the stable SsrA/tmRNA (Cairrão et al. 2003). Degradation of a RNA duplex occurs provided there is a single stranded 3' overhang of at least 7 nts (Vincent and Deutscher 2006) and RNase R was shown to be a key enzyme involved in the degradation of polyadenylated RNA (Andrade et al. 2009a).

The activity of RNase R is modulated according to environmental stimuli and its protein levels are upregulated under several stresses, namely stationary-phase of growth and in cold-shock (Andrade et al. 2006; Cairrão and Arraiano 2006). RNase R was shown to be involved in the degradation of the *ompA* transcript specifically in the stationary phase of growth, while no effect is detected in exponentially growing cells (Andrade et al. 2006). ***E. coli*** RNase R deficient colonies are smaller especially in the cold (Cairrão et al. 2003) and this enzyme is even essential for survival at low temperatures in pathogenic strains like ***Pseudomonas syringae*** (Purusharth et al. 2005) or ***Aeromonas hydrophila*** (Erova et al. 2008). In addition to its role in stress response, RNase R has also been implicated in virulence mechanisms (Tobe et al. 1992; Lalonde et al. 2007; Erova et al. 2008; Tsao et al. 2009). The stress-induction of RNase R levels can in fact be highly advantageous, enabling pathogens to adapt to environmental challenges imposed prior and during the infection process. Accordingly, most RNase R-deficient bacteria have been shown to be less virulent than the wild type strains. How this is achieved is still unclear but it has been suggested that RNase R may control the export of proteins involved in virulence mechanisms (Tobe et al. 1992). A common trait of pathogenic RNase R mutants seems to be impaired motility (Erova et al. 2008; Tsao et al. 2009). RNase R also affects other cellular processes, like the development of competence in ***Legionella pneumophila*** (Charpentier et al. 2008) or the expression of apoptosis genes in ***Helicobacter pylori*** (Tsao et al. 2009). This is probably related to critical RNA degradation pathways mediated by RNase R.

Currently, the structure of RNase R remains unknown, which represents a major drawback in understanding RNase R mechanism of action. Most of the knowledge on RNase R structure is inferred from the available structures of its close counterparts, RNase II and Rrp44. RNase R follows the typical modular organization found on RNase II-family members: a RNB catalytic domain flanked by RNA binding domains (CSD1 and CSD2 located at the N-terminus and a C-terminal S1 domain). Furthermore, additional features are exclusively found in the RNase R sequence, namely a predicted nucleic acid binding motif (Helix-turn-Helix) at the N-terminal and a highly basic extended region after the S1 domain (Fig. 2a). All these regions must combine in a way that makes RNase R unique amongst exoribonucleases.

The majority of the residues interacting with the 3' end of the RNA are conserved throughout the RNase II-family of exoribonucleases, suggesting a similar mechanism for hydrolysis (Barbas et al. 2008; Bonneau et al. 2009). Structural differences might help explaining the divergence in substrate recognition between the members of RNase II-family. Despite the biochemical similarities many uncertainties remain concerning the pathway followed to effect the degradation of structured substrates.

A three-dimensional model of RNase R has been proposed based on the structure of its paralogue RNase II (Barbas et al. 2008). Mutational analysis identified the highly conserved acid residues located in the active center responsible for catalysis: D272, D278 and D280 (Matos et al. 2009; Awano et al. 2010). As in the other members of the RNase II-family, these highly conserved Aspartates are involved in coordination of divalent metal ions (preferably Mg^{2+}) essential to catalysis. In particular, the RNase R D280N mutant showed no exonucleolytic activity although RNA binding was not affected, analogous to what was reported with the D209N mutant in RNase II (Amblar and Arraiano 2005; Matos et al. 2009; Awano et al. 2010). The highly conserved Tyrosine Y324 was found to be responsible for setting the final end-product of RNase R. Mutation Y342A altered the final end product from 2 to 5 nucleotides, probably due to loose packing of the 3'-terminal nucleotides in the catalytic cavity (Matos et al. 2009). Overall, the structural model of RNase R when compared to RNase II and Rrp44 structures identified the critical residues located in similar catalytic environments (Barbas et al. 2008). However, mutagenic studies revealed that despite all similarities, the catalytic channel is not alike between these enzymes. RNase R was shown to bind RNA more tightly within its catalytic channel than does RNase II. The amino acid residue Arg572 located in the nuclease domain channel strongly affects RNase R catalytic properties. Mutation to a Lysine (the equivalent residue found in RNase II) greatly impaired RNase R activity on structured RNAs (Vincent and Deutscher 2009a). Surprisingly, just the nuclease domain of RNase R (but not the one from RNase II) without accessory domains is able to degrade a double-stranded RNA (Matos et al. 2009; Vincent and Deutscher 2009b). A truncated form of RNase R expressing only the RNB domain degrades a blunt dsRNA (Fig. 3) although with a low level of activity when compared to wild-type protein. However, the presence of the auxiliary domains for substrate binding completely inhibits this activity, probably by "blocking" the entrance of dsRNA into the catalytic channel (Fig. 3). In the presence of CSD1, CSD2 and S1 domains, a short 3' unpaired overhang is required to allow the degradation of dsRNA (Fig. 3). Available data indicates that RNA binding domains actually discriminate the substrates that can be targeted by RNase R, favoring the selection of RNA molecules tagged with a 3' linear tail (Matos et al. 2009). Remarkably, RNA binding domains may have an intrinsic ability to help to unwind the double-stranded RNA molecules. As an additional probe of the resourceful enzyme that RNase R is, it has been suggested that it can function both as an exoribonuclease as well as an RNA "helicase" (Awano et al. 2010). RNase R intrinsic "helicase" unwinding

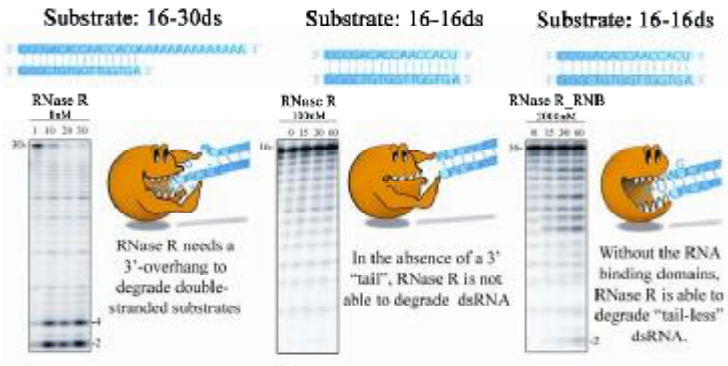

Figure 3. Degradation of double-stranded substrates by *E. coli* RNase R. RNase R needs a 3' single-stranded overhang to degrade double-stranded substrates. In the absence of the RNA binding domains, the protein can degrade "tail-less" RNAs.

activity is dependent on RNA-binding regions (namely on CDS2). In vitro studies showed that exonuclease and "helicase" activities are distinct and independent being located in separate domains. Like CsdA and other DEAD-box RNA helicases, RNase R was shown to be more active at unwinding short (10-bp) rather than longer RNA duplexes. Not surprisingly, only a double stranded RNA with a 3' linear overhang was shown to be a suitable substrate for RNase R helicase action. Moreover, the additional motifs exclusively found in RNase R may expand the known functions of the anchor domains (Zuo et al. 2006; Andrade et al. 2009b). The helix-turn-helix predicted in the N-terminus is a potential nucleic acid binding motif although there are no experimental evidence yet of this role. The extended region found in the C-terminal end contains a positively charged surface patch formed by basic arginine and lysine residues. This suggests a possible role in nucleic acid binding through electrostatic interactions. These potential extra protein:RNA interactions might contribute to "melting" of secondary RNA structures, and help to explain the impressive RNase R mode of action. However, this is quite speculative at the moment. In fact it was proven that these "extra" domains in RNase R are not there merely for cosmetic purposes; the basic region in the C-terminal region was found to control the stability of RNase R through interactions with components of the *trans*-translation machinery. RNase R is an unstable protein but is highly stabilized if SmpB and/or tmRNA are prevented from interacting with the C-terminal region of RNase R (Liang and Deutscher 2010). It is still not clear how binding of SmpB and tmRNA to RNase R leads to its destabilization. Possible structural changes of the complex might help explaining these observations. More recently, it was also shown that the C-terminal lysine-rich region is necessary for the recruitment of RNase R to stalled ribosomes and to the selective decay of defective transcripts (Ge et al. 2010). It was also shown that the S1 domain from RNase R, namely the C-terminal region, is involved in the degradation of structured substrates in an RNase II context, probably by helping to unwind the substrate (Matos et al. 2011).

A definitive model for RNA degradation by RNase R is still open, and it seems clear that only the resolution of RNase R structure will answer the many questions about its remarkable mode of action.

3.3. Rrp44 (Dis3)

Rrp44, a member of the RNB family of enzymes, degrades RNA hydrolytically from 3' to 5' in a processive manner to a final product of 3 to 5 nucleotides. In addition to single stranded RNA, Rrp44 is able to degrade secondary structures provided that it has a 3' end overhang with at least 4 nucleotides (Dziembowski et al. 2007; Bonneau et al. 2009).

In addition to the domains described for RNase II and RNase R, Rrp44 contains in the N-terminus a region with three conserved cysteines (CR3 region) and a highly conserved pilT N-terminal (PIN) domain with endonucleolytic activity (Cairrão et al. 2005; Lebreton et al. 2008; Schaeffer et al. 2009; Schneider et al. 2009). The two active sites responsible for both exo and endonucleolytic activity coordinate to degrade and process exosome substrates.

In *Saccharomyces cerevisiae*, the crystallographic structure of a single aminoacid mutant (D551N) of Rrp44ΔPIN in complex with RNA was determined (Bonneau et al. 2009). Although, while in the RNase II D209N mutant the RNA molecule was fortuitously co-crystalized with the protein, in this case, the RNA fragment was forced to be co-crystallized. This mutant contains a point mutation (D551N) within the active site that allows RNA binding but prevents the exoribonucleolytic cleavage (Dziembowski et al. 2007; Schneider et al. 2007). This mutation is equivalent to D209N in RNase II which impairs the coordination of one of the two magnesium ion essential for catalysis (Amblar and Arraiano 2005; Frazão et al. 2006). Similarly to RNase II, the amino-terminal region starts with a α-helix followed by the two consecutive cold-shock domains (CSD1 and 2). At the carboxy terminus, there is a third RNA-binding domain with a typical S1 RNA-binding fold. Between the two CSD and the S1 domain, the RNB catalytic domain is centered around a core that is reminiscent of RNase H and is surrounded by several α-helices. The superposition of Rrp44 and RNase II showed that 85 % of the residues of the RNB domain and more than 70 % of the three OB-fold domains superpose in their α-carbon positions. Besides the structural conservation in all domains, there is a difference concerning the relative orientation of the binding domains, with implications on the route of RNA access to the catalytic site. In Rrp44, the RNA is threaded to the catalytic site by binding the CSD1 and the RNB domains, while in RNase II, the RNA is threaded by binding S1 and CSD2 domains. It was suggested that these different routes are responsible for the difference in RNA-unwinding properties and activity on structured RNA substrates between RNase II and Rrp44 enzymes (Bonneau et al. 2009). The crystal structure of the Rrp44 PIN domain was elucidated in a ternary complex constituted by Rrp44 and two other exosome proteins (Rrp41 and Rrp45). The final model includes residues 36–231 of the Rrp44 PIN domain and residues 253–1001 of the Rrp44 RNase II-like region (Bonneau et al. 2009). This domain folds in a twisted parallel β□-sheet, surrounded by helices, with the catalytic site in the C-terminus ends of the β strands (Malet et al. 2010).

Rrp44 is the only active component of the yeast cytoplasmic exosome (Liu et al. 2006; Dziembowski et al.

2007; Schneider et al. 2007). Electron microscopic analysis of the *S. cerevisiae* exosome showed that Rrp44 binds to the bottom of the exosome PH ring through the interaction of the PIN domain and Rrp41, and the RNase II-like region contacts with Rrp41, Rrp43 and Rrp45 (see Fig. 2d) (Wang et al. 2007). The crystal structure of the ternary complex Rrp44-Rrp41-Rrp45 confirmed this finding and gave more details about the interaction between Rrp44 and the core exosome (Bonneau et al. 2009). The N-terminus of the PIN domain wraps around Rrp41, and the RNase II-like region of Rrp44 contacts both Rrp41-Rrp45 and the PIN domain. Biochemical results showed that the interaction between the PIN domain and Rrp41 is the strongest between Rrp44 and the exosome. These interactions seem to be conserved in other species.

Structural and biochemical data showed that the PIN domain faces the solvent rather than the exosome core and can be accessed from solvent without passing through the central channel of the core exosome. According to the structure, the exoribonuclease site of Rrp44 is also in principle accessible from solvent. However, a conformational change at residues 696–719 of the RNB domain inhibits this entrance, and seems to be stabilized by the binding of Rrp44 to the exosome core. This finding, together with nuclease and RNase protection assays indicate that a path where the 3'-end of the RNA is threaded through the central channel of the core exosome until the exoribonucleolytic site of Rrp44 is favored. However, there is no evidence in vivo that supports this model (Bonneau et al. 2009).

Usually cells present a single Rrp44 ortholog, however there are cases where two or more orthologues of Rrp44 exist. In *S. cerevisiae* the unique Rrp44 is present in the nucleus and the cytoplasm (Houseley et al. 2006). In humans, there are two Rrp44 homologues, hDIS3 and hDIS3L, which interact with the exosome and display processive exonuclease activity (Staals et al. 2010; Tomecki et al. 2010). hDIS3 mainly localizes in the nucleoplasm, has endonucleolytic activity, and complements lower levels of yeast Rrp44, while hDIS3L is strictly cytoplasmic and has no endonucleolytic activity, probably due to several mutations in the PINc domain (Tomecki et al. 2010) (Fig. 2a). Recently, a protein that contains the RNase II like region, without one or more of the CSD domains, but lacks the PIN domain was identified in *Arabidopsis thaliana* (Zhang et al. 2010) (Fig. 2a). This protein, named suppressor of varicose (SOV), is a major cytoplasmic protein with mRNA decay activity in vivo. Like RNase II like proteins, it was proposed to have 3' to 5' exoribonuclease activity, but the absence of the PIN domain suggests that it is not one of the components of the exosome. SOV-like proteins have been conserved in distant lineages, namely in *Mus musculus*, *Drosophila melanogaster*, *Oryza sativa*, *Selaginella moellendorffii* and *Caenorhabditis elegans*.

In *Drosophila*, the Rrp44/Dis3 homologue was characterized and named Tazman. It was shown to be more similar to RNase R and Rrp44 than to RNase II, and, similarly to Rrp44, it has an N-terminal PINc domain and a CR3 region (Cairrão et al. 2005). This N-terminal region is sufficient for the endoribonucleolytic activity and also contributes to the interaction with the exosome and with protein localization (Mamolen et al. 2010). This protein was also shown to be differentially expressed during the *Drosophila* life cycle, suggesting that it may play an important role in the modulation of RNA levels important for development (Cairrão et al. 2005).

4. DEDD FAMILY

This family of enzymes includes both RNA and DNA exonucleases. These proteins have a characteristic core with four invariant acidic amino acids (which are responsible for the designation of this family) and other conserved residues which are distributed in three distinct sequence motifs. In motif III, the presence of a tyrosine or histidine led to the division of this family into two subgroups, DEDDy and DEDDh, respectively. All proteins of this family share a common mechanism of action which involves two metal ions (Zuo and Deutscher 2001).

4.1. Oligoribonuclease

Pioneering work identified Oligoribonuclease as the "finishing enzyme" in RNA metabolism. The degradative activity of other exoRNases result in final RNA fragments ranging from 2-5nts whose accumulation could be deleterious to the cell. Oligoribonuclease acts at the final steps of RNA degradation, converting the small oligoribonucleotides to mononucleotides (Ghosh and Deutscher 1999).

Oligoribonuclease (OligoRNase/Orn) is a 3'-5' RNase member of the DnaQ-like/DEDD exonuclease superfamily. It shows the typical DnaQ-fold containing five-stranded β-sheets flanked by α-helices (Fig. 4). The DnaQ-like exonuclease domain contains three well conserved ExoI, ExoII and ExoIII sequence motifs clustered around the active site. Like all members of this family, Orn contains four highly conserved acidic residues (DEDD) in the active center. These amino acids are proposed to be essential for binding divalent metal ions and thus for catalytic activity (Steitz and Steitz 1993). In addition to these invariant residues, Orn has other conserved residues with particular importance of a histidine in the ExoIII motif. Such a feature places Orn in the DEDDh subgroup, which includes both DNA- (like the ε subunit of DNA polymerase III) and RNA-processing enzymes (like RNase T).

Only a preliminary X-ray crystal study of *E. coli* Oligoribonuclease was published (PDB 1YTA) (Fiedler et al. 2004), although a more refined structure is available in the PDB database (PDB 2IGI). A more detailed structural work concerning Orn was done with the plant pathogen *Xanthomonas campestris*, which oligoribonuclease XC847 shares a 52.6% identity with *E. coli* Orn (Chin et al. 2006). A general catalytic mechanism for Oligoribonuclease was proposed involving all four conserved acidic residues and the conserved histidine, present at a highly flexible loop in the ExoIII motif. All DEDD family exonucleases share common active site geometry with the four acidic side chains coordinating two divalent cations (preferably Mn^{2+} for *E. coli* Orn).

Oligoribonuclease functions as a homodimeric enzyme (Zhang et al. 1998). The dimeric architecture of Oligoribonuclease is very similar to the arrangement seen in RNase T (Fig. 4). The two DEDD domains appear to complement each other with single monomer providing a substrate binding surface leading into the catalytic center of the other monomer (Zuo et al. 2005). The resulting DEDD cavity is long enough to accommodate three to four nucleotides (Zuo et al. 2007). Destabilization of the dimer conformation can alter protein activity and possibly cause its inactivation. Oligoribonuclease is a processive enzyme and nuclease activity is inversely proportional to the length of the single-stranded substrate with a 5-mer oligoribonucleotide being a preferable substrate. Orn is insensitive to 5' RNA phosphorylation state but the molecule must have a free 3'-OH end (Datta and Niyogi 1975). Although Orn is a single-stranded specific exonuclease with strong affinity to small (2-5nts) RNA fragments it has been reported that higher

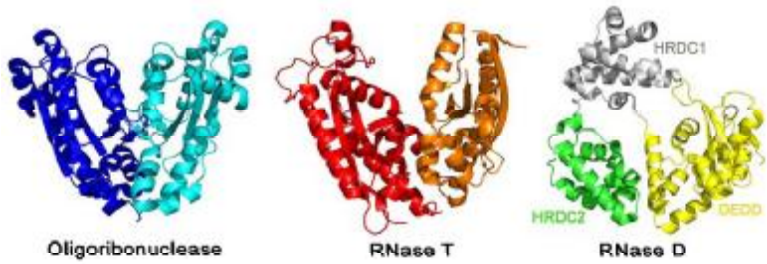

Figure 4. Comparison of the structures of the three members of the DEDD family from *E. coli*: oligoribonuclease (PDB ID 2IGI) (Fiedler et al to be published), RNase T (PDB ID 2IS3) (Zuo et al. 2007) and RNase D (PDB ID 1YT3) (Zuo et al. 2005).

concentrations of the enzyme can degrade short DNA oligos (Mechold et al. 2006). Interestingly, the overall architecture of XC847 is quite similar to 3'-5' DNases.

Oligoribonucleases are found in the Proteobacteria (β and γ divisions) and *Actinomycetes* in bacterial genomes and have not been detected in archaea, although are present in all eukaryotes (Zuo and Deutscher 2001). Oligoribonucleases are inhibited by the nucleotide 3'-phosphoadenosine-5' phosphate (pAp) that is generated in both prokaryotes and eukaryotes during the process of sulfur assimilation (Mechold et al. 2006). *E. coli* Oligoribonuclease is encoded by the *orn* gene and is the only essential exoRNase required for cell viability in this organism (Ghosh and Deutscher 1999). *Bacillus subtilis* lacks an Orn homologue (Mechold et al. 2006). However, *B. subtilis* has at least two functional analogues of Orn, termed nanoRNases NrnA and NrnB that can complement *in vivo* a defective *E. coli orn* mutant. The preferred substrate of these enzymes is a 3-mer instead of 5-mer RNA (Fang et al. 2009). Most likely, additional Nrn-like enzymes are present in *B. subtilis* genome as a double *nrn*A *nrn*B mutant is viable.

Homologues of bacterial oligoribonuclease are found in many eukaryotes (Zhang et al. 1998). Yeast homologue Ynt20/Rex2 is localized in mitochondria whereas its function there remains unclear (Hanekamp and Thorsness 1999). It was also reported to function in the nucleus, namely in the processing of some stable and small RNAs (van Hoof et al. 2000). The human homologue was proposed to exist in two isoforms that arise from alternatively spliced transcripts, one of them, Sfnα, contains mitochondrial targeting sequence, while the other protein, referred as Sfn, was shown to be oligoribonuclease in vitro and, in contrast to the bacterial enzyme, is able to digest both DNA and RNA substrates (Nguyen et al. 2000)

4.2. RNase D

RNase D is a 40kDa protein encoded by the *rnd* gene. As a member of DEDD family of enzymes, it requires divalent metal ions for its activity and has a high degree of substrate specificity (Cudny et al. 1981). This enzyme was initially discovered through its action on "denatured" and damaged tRNAs but it also acts on tRNA precursors with extra 30 residues following the CCA sequence, 5S rRNA and other small-structured RNAs but not ssRNA (Cudny and Deutscher 1980; Zhang and Deutscher 1988b). RNase D is not an essential protein for the cell however, is crucial for viability when RNase II, BN, T, and PH are absent, which may indicate that is a backup enzyme when the principal ribonucleases are missing (Kelly and Deutscher 1992b). RNase D overexpression seems to be deleterious for the cell (Zhang and Deutscher 1988a). In the cell, the *rnd* expression may be limited because: the chromosomal gene uses UUG as the initiation codon; it has an abnormally high level of rare codons; its expression is negatively regulated at the translational level by the initiation codon (Zhang and Deutscher 1989).

The resolution of the RNase D crystal structure showed that this protein has one C-terminal DEDD catalytic domain and two HRDC domains at the N-terminal region. The interactions between HRDC2 and DEDD are responsible for bringing the three domains into a funnel-shaped ring structure, which is very flexible, and suggests a processive activity (Fig. 4). The DEDD domain forms a closed, very compact structure on one side, and an open pocket on the other side. The putative active site of RNase D (formed by the DEDD residues) is located inside the open pocket, which is surrounded by three flexible loops. RNase D is not able to degrade short oligonucleotides, possibly due to their weak binding at the active center (Zuo et al. 2005).

RNase D homologues have been found in many bacterial organisms. In some genomes, it is possible to find more than one close homologue. In archeal genomes it was not possible to find any RNase D homologue, while in Eukaryotes there is, at least, one RNase D homologue, named Rrp6 (Zuo and Deutscher 2001).

In contrast to the situation in the Archaea, in yeast and human cells the exosome ring proteins do not have phosphorolytic activity and the only active subunits of the complex are the two ring connected nucleases Rrp44 and Rrp6 (Liu et al. 2006; Dziembowski et al. 2007). Rrp6 structure of the yeast enzyme was solved showing similarity of nuclease domain to RNase D (Midtgaard et al. 2006) with the presence of one HRDC domain. Rrp6 is a distributive single-strand specific RNA nuclease. Recently it was shown that the TRAMP complex accelerates the rate of RNA degradation by yeast Rrp6 in vitro. TRAMP is a complex which contains a polymerase, a helicase, and zinc knuckle proteins that add poly(A) tails to eukaryotic RNA substrates, targeting them to degradation (Callahan and Butler 2010). In yeast, Rrp6 plays a role in nuclear mRNA surveillance and in the degradation of rRNA maturation by-products or intergenic transcripts (Houseley et al. 2006). It is also involved in the final step in processing several non-coding RNAs (Allmang et al. 1999).

The intracellular localization of Rrp6 in eukaryotes is intriguing. In yeast cells this nuclease is strictly nuclear; in human cells hRrp6 can be found in both the nucleus (where seems to be enriched in nucleoli), and in the cytoplasm. In plants, it was shown that there are three different Rrp6-like proteins, which are localized in nucleus, nucleolus and cytoplasm, respectively. Each of them seems to serve some specific and unique function (Lange et al. 2008). Nuclear Rrp6 co-purifies with exosome complex, however, Rrp6 was shown to have functions that are independent from the exosome. It will be interesting to determine whether cytoplasmatic Rrp6 also helps in exosome substrate degradation, or is a independent enzyme with specific functions.

4.3. RNase T

RNase T, also a member of the DEDD superfamily of RNases, is a single-strand-specific exoribonuclease which also has DNA exonuclease activity (Viswanathan et al. 1998). It has a distributive activity, which depends on the presence of divalent metal ions, such as Mg^{2+} or Mn^{2+}, and an unusual base specificity, discriminating against pyrimidines and, particularly, C residues. This sequence specificity is determined by the last four nucleotides at the 3' end (Deutscher and Marlor 1985; Zuo and Deutscher 2002a, b). When compared to other ribonucleases, RNase T is the only enzyme capable of removing nucleotides near the duplex structure without unwinding the substrate, generating blunt-ended RNAs. RNase T is involved in the final step of maturation of many stable RNAs (Li and Deutscher 1995, 1996; Li et al. 1998): it is essential for the maturation of the 3' ends of 5S and 23S rRNA genes (Li and Deutscher 1995; Li et al. 1999), and it is also involved in the end turnover of tRNAs (Deutscher and Marlor 1985).

In order to be functional, RNase T needs to form a dimer, both in vivo and in vitro (Li et al. 1996). Mutational analysis identified three NBS (nucleic acid binding sequence) segments important for substrate binding (Zuo and Deutscher 2002a). The resolution of crystal structure of RNase T from both *E. coli* and *Pseudomonas aeruginosa* show that the protein has an oligoribonuclease-like homodimer architecture (Fig. 4) (Zuo et al. 2007). The two monomers face in opposite directions, i. e., the NBS segment from one monomer is located in the vicinity of the DEDD active center pocket of the other monomer. This arrangement allows the binding of the RNA molecule from one monomer to be close to the active site of the other, and also helps us to explain why the enzyme requires the formation of the homodimer in order to be active (Zuo et al. 2007). Despite its critical role in RNA metabolism, RNase T orthologues are only found in the division of Proteobacteria (Zuo and Deutscher 2001).

4.4. Deadenylases

In eukaryotic cells,deadenylation is the first step that precedes messenger degradation. Poly(A) tails are important not only in controlling the stability of the transcripts, but also in RNA processing, translation or nuclear export processes. Deadenylation is performed by poly(A) specific 3'-5' RNA exonucleases.

In yeast, two different protein complexes were recognized to be involved in RNA deadenylation: Ccr4-Caf1 and Pan2-Pan3 (Tucker et al. 2001; Yamashita et al. 2005). Ccr4-Caf1 (or Ccr4-NOT) contains at least ten interacting proteins, among them Ccr4 and Caf1(Pop2) are the poly(A)-specific nucleases. Caf1 is the nuclease classified in the DEDD family, although the characteristic motif in this enzyme is replaced by SEDQ sequence (Thore et al. 2003). However, the human orthologs of Caf1 contain the conserved catalytic DEDD motif. The other nuclease in the complex-Crr4 represents a DNase-I like family of two metal ion dependent nucleases. The crystal structure of the catalytic domain of the human homologue of Ccr4-CNOT6L gave some insights into its poly(A) specificity and catalytic mechanism (Wang et al. 2010b). Ccr4 is suggested to be the main deadenylase in yeast Ccr4-Caf1 complex, but both nucleases of the complex seems to be involved in RNA degradation (Schwede et al. 2008).

The active subunit of the Pan2-Pan3 deadenylation complex is Pan2, a DEDD family nuclease, while the protein in the second complex, Pan3, stimulates the nuclease activity (Brown et al. 1996). In yeast, the CCr4-Caf1 complex seems to be the main deadenylation factor, however, in mammalian cells, both complexes Ccr4-Caf1 and Pan2-Pan3 work sequentially in degradation of poly(A) tails with initial shortening by Pan2-Pan3 and subsequent degradation by Ccr4-Caf1 (Yamashita et al. 2005)

Many eukaryotes contain also a third poly(A) specific nuclease, named PARN. The PARN nuclease domain contains the characteristic DEDD motif and is structurally similar to Caf1. Moreover, PARN contains an RNA recognition motif (RRM) and an R3H domain. In addition to its nuclease activity, PARN is also a cap binding protein and the interaction with RNA cap stimulates the RNase activity of the enzyme. PARN is a dimeric protein and its crystal structure, together with cap and with poly(A) RNA, showed that cap binding causes conformational changes, suggesting the existence of a open and closed form of the active site (Wu et al. 2005).

Other yeast nucleases from the DEDD nuclease family are Rex1, Rex3, Rex4. The two first were proved to be involved in RNA processing events. Homologues of these proteins can also be found in other eukaryotes, including humans (van Hoof et al. 2000).

The ERI-1 exoribonuclease also belongs to this family of enzymes. The enzyme of *Caenorhabditis elegans* and *Schizosaccharomyces pombe* where it negatively regulates the RNA interference pathway, probably by degrading dsRNAs. In both organisms, Eri-1 also takes part in the processing of 3' end of 5.8S rRNA (Kennedy et al. 2004; Gabel and Ruvkun 2008). In humans, the homologue of Eri-1 is known to be involved in the metabolism of histone mRNA but its exact role in this and other processes in mammalian cells still remains to be elucidated (Yang et al. 2009).

5. CONCLUDING REMARKS

To maintain the correct RNA levels in the cell, RNA metabolism must be tightly controlled. One of the factors involved are ribonucleases, which will determine the degradation pathway for each RNA molecule. Exoribonucleases play an important role in the mechanism of RNA degradation, and they behave differently regarding RNA recognition and degradation. While some RNases are important for RNA degradation, others are specialized in the processing and maturation of some types of RNA. The determination of crystal structures of these enzymes has allowed investigators to better understand their mechanism of action and further our knowledge of RNA metabolism. It is also possible to verify that the similarities between prokaryotes and eukaryotes are much higher than initially expected.

6. ACKNOWLEDGEMENTS

We thank Miguel Luís for graphical assistance in Figures 2 and 3.

7. REFERENCES

Allmang C, Kufel J, Chanfreau G, Mitchell P, Petfalski E, Tollervey D (1999) Functions of the exosome in rRNA, snoRNA and snRNA synthesis. EMBO J 18:5399-5410

Amblar M, Arraiano CM (2005) A single mutation in *Escherichia coli* ribonuclease II inactivates the enzyme without affecting RNA binding. FEBS J 272:363-374

Amblar M, Barbas A, Fialho AM, Arraiano CM (2006) Characterization of the functional domains of *Escherichia coli* RNase II. J Mol Biol 360:921-933

Amblar M, Barbas A, Goméz-Puertas P, Arraiano CM (2007) The role of the S1 domain in exoribonucleolytic activity: substrate specificity and multimerization. RNA 13:317-327

Andrade JM, Cairrão F, Arraiano CM (2006) RNase R affects gene expression in stationary phase: regulation of *ompA*. Mol Microbiol 60:219-228

Andrade JM, Hajnsdorf E, Régnier P, Arraiano CM (2009a). The poly(A)-dependent degradation pathway of *rpsO* mRNA is primarily mediated by RNase R. RNA 15:316-326

Andrade JM, Pobre V, Silva IJ, Domingues S, Arraiano CM (2009b) The role of 3'-5' exoribonucleases in RNA degradation. Prog Mol Biol Transl Sci 85:187-229

Arraiano CM, Andrade JM, Domingues S, Guinote IB, Malecki M, Matos RG, Moreira RN, Pobre V, Reis FP, Saramago M, Silva IJ, Viegas SC (2010a) The critical role of RNA processing and degradation in the control of gene expression. FEMS Microbiol Rev 34:883-923

Arraiano CM, Maquat LE (2003) Post-transcriptional control of gene expression: effectors of mRNA decay. Mol Microbiol 49:267-276

Arraiano CM, Matos RG, Barbas A, (2010b) RNase II: the finer details of the *Modus operandi* of a molecular killer. RNA Biol 7:276-281

Awano N, Inouye M, Phadtare S (2008) RNase activity of polynucleotide phosphorylase is critical at low temperature in *Escherichia coli* and is complemented by RNase II. J Bacteriol 190:5924-5933

Awano N, Rajagopal V, Arbing M, Patel S, Hunt J, Inouye M, Phadtare S (2010) *Escherichia coli* RNase R has dual activities, helicase and RNase. J Bacteriol 192:1344-1352

Barbas A, Matos RG, Amblar M, Lopez-Viñas E, Goméz-Puertas P, Arraiano CM (2008) New insights into the mechanism of RNA degradation by ribonuclease II: identification of the residue responsible for setting the RNase II end product. J Biol Chem 283:13070-13076

Barbas A, Matos RG, Amblar M, Lopez-Viñas E, Goméz-Puertas P, Arraiano CM (2009) Determination of key residues for catalysis and RNA cleavage specificity: one mutation turns RNase II into a "super-enzyme". J Biol Chem 284:20486-20498

Beran RK, Simons RW (2001) Cold-temperature induction of *Escherichia coli* polynucleotide phosphorylase occurs by reversal of its autoregulation. Mol Microbiol 39:112-125

Bollenbach TJ, Lange H, Gutierrez R, Erhardt M, Stern DB, Gagliardi D (2005) RNR1, a 3'-5' exoribonuclease belonging to the RNR superfamily, catalyzes 3' maturation of chloroplast ribosomal RNAs in *Arabidopsis thaliana*. Nucleic Acids Res 33:2751-2763

Bonneau F, Basquin J, Ebert J, Lorentzen E, Conti E (2009) The yeast exosome functions as a macromolecular cage to channel RNA substrates for degradation. Cell 139:547-559

Bralley P, Gust B, Chang S, Chater KF, Jones GH (2006) RNA 3'-tail synthesis in Streptomyces: in vitro and in vivo activities of RNase PH, the SCO3896 gene product and polynucleotide phosphorylase. Microbiology 152:627-636

Briani F, Del Favero M, Capizzuto R, Consonni C, Zangrossi S, Greco C, De Gioia L, Tortora P, Dehò G (2007) Genetic analysis of polynucleotide phosphorylase structure and functions. Biochimie 89:145-157

Brown CE, Tarun SZ Jr, Boeck R, Sachs AB (1996) PAN3 encodes a subunit of the Pab1p-dependent poly(A) nuclease in *Saccharomyces cerevisiae*. Mol Cell Biol 16:5744-5753

Buttner K, Wenig K, Hopfner KP (2005) Structural framework for the mechanism of archaeal exosomes in RNA processing. Mol Cell 20:461-471

Cairrão F, Arraiano CM (2006) The role of endoribonucleases in the regulation of RNase R. Biochem Biophys Res Commun 343:731-737

Cairrão F, Arraiano CM, Newbury S (2005) *Drosophila* gene tazman, an orthologue of the yeast exosome component Rrp44p/Dis3, is differentially expressed during development. Dev Dyn 232:733-737

Cairrão F, Chora A, Zilhão R, Carpousis AJ, Arraiano CM (2001) RNase II levels change according to the growth conditions: characterization of *gmr*, a new *Escherichia coli* gene involved in the modulation of RNase II. Mol Microbiol 39:1550-1561

Cairrão F, Cruz A, Mori H, Arraiano CM (2003) Cold shock induction of RNase R and its role in the maturation of the quality control mediator SsrA/tmRNA. Mol Microbiol 50:1349-1360

Callahan KP, Butler JS (2010) TRAMP complex enhances RNA degradation by the nuclear exosome component Rrp6. J Biol Chem 285:3540-3547

Campos-Guillén J, Bralley P, Jones GH, Bechhofer DH, Olmedo-Alvarez G (2005) Addition of poly(A) and heteropolymeric 3' ends in *Bacillus subtilis* wild-type and polynucleotide phosphorylase-deficient strains. J Bacteriol 187:4698-4706

Cannistraro VJ, Kennell D (1994) The processive reaction mechanism of ribonuclease II. J Mol Biol 243:930-943

Carpousis AJ, Van Houwe G, Ehretsmann C, Krisch HM (1994) Copurification of *E. coli* RNaase E and PNPase: evidence for a specific association between two enzymes important in RNA processing and degradation. Cell 76:889-900

Carzaniga T, Briani F, Zangrossi S, Merlino G, Marchi P, Dehò G (2009) Autogenous regulation of *Escherichia coli* polynucleotide phosphorylase expression revisited. J Bacteriol 191:1738-1748

Charpentier X, Faucher SP, Kalachikov S, Shuman HA (2008) Loss of RNase R induces competence development in *Legionella pneumophila*. J Bacteriol 190:8126-8136

Cheng ZF, Deutscher MP (2003) Quality control of ribosomal RNA mediated by polynucleotide phosphorylase and RNase R. Proc. Natl. Acad. Sci USA 100:6388-6393

Cheng ZF, Deutscher MP (2005) An important role for RNase R in mRNA decay. Mol Cell 17:313-318

Cheng ZF, Zuo Y, Li Z, Rudd KE, Deutscher MP (1998) The *vacB* gene required for virulence in *Shigella flexneri* and *Escherichia coli* encodes the exoribonuclease RNase R. J Biol Chem 273:14077-14080

Chin KH, Yang CY, Chou CC, Wang AH, Chou SH (2006) The crystal structure of XC847 from *Xanthomonas campestris*: a 3'-5' oligoribonuclease of DnaQ fold family with a novel opposingly shifted helix. Proteins 65:1036-1040

Choi JM, Park EY, Kim JH, Chang SK, Cho Y (2004) Probing the functional importance of the hexameric ring structure of RNase PH. J Biol Chem 279:755-764

Cudny H, Deutscher MP (1980) Apparent involvement of ribonuclease D in the 3' processing of tRNA precursors. Proc Natl Acad Sci USA 77:837-841

Cudny H, Zaniewski R, Deutscher MP (1981) *Escherichia coli* RNase D. Catalytic properties and substrate specificity. J Biol Chem 256:5633-5637

Datta AK, Niyogi K (1975) A novel oligoribonuclease of *Escherichia coli*. II. Mechanism of action. J Biol Chem 250:7313-7319

Deutscher MP, Marlor CW (1985) Purification and characterization of *Escherichia coli* RNase T. J Biol Chem 260:7067-7071

Deutscher MP, Marshall GT, Cudny H (1988) RNase PH: an *Escherichia coli* phosphate-dependent nuclease distinct from polynucleotide phosphorylase. Proc Natl Acad Sci USA 85:4710-4714

Deutscher MP, Reuven NB (1991) Enzymatic basis for hydrolytic versus phosphorolytic mRNA degradation in *Escherichia coli* and *Bacillus subtilis*. Proc Natl Acad Sci USA 88:3277-3280

Donovan WP, Kushner SR (1986) Polynucleotide phosphorylase and ribonuclease II are required for cell viability and mRNA turnover in *Escherichia coli* K-12. Proc Natl Acad Sci USA 83:120-124

Dziembowski A, Lorentzen E, Conti E, Seraphin B (2007) A single subunit, Dis3, is essentially responsible for yeast exosome core activity. Nat Struct Mol Biol 14:15-22.

Erova TE, Kosykh VG, Fadl AA, Sha J, Horneman AJ, Chopra AK (2008) Cold shock exoribonuclease R (VacB) is involved in *Aeromonas hydrophila* pathogenesis. J Bacteriol 190:3467-3474

Evguenieva-Hackenberg E, Walter P, Hochleitner E, Lottspeich F, Klug G (2003) An exosome-like complex in *Sulfolobus solfataricus*. EMBO Rep 4:889-893

Fang M, Zeisberg WM, Condon C, Ogryzko V, Danchin A, Mechold U (2009) Degradation of nanoRNA is performed by multiple redundant RNases in *Bacillus subtilis*. Nat Struct Mol Biol 37:5114-5125

Fiedler TJ, Vincent HA, Zuo Y, Gavrialov O, Malhotra A (2004) Purification and crystallization of *Escherichia coli* oligoribonuclease. Acta Crystallogr D Biol Crystallogr 60:736-739

Frazão C, McVey CE, Amblar M, Barbas A, Vonrhein C, Arraiano CM, Carrondo MA (2006) Unravelling the dynamics of RNA degradation by ribonuclease II and its RNA-bound complex. Nature 443:110-114

Gabel HW, Ruvkun G (2008) The exonuclease ERI-1 has a conserved dual role in 5.8S rRNA processing and RNAi. Nat Struct Mol Biol 15:531-533

García-Mena J, Das A, Sánchez-Trujillo A, Portier C, Montañez C (1999) A novel mutation in the KH domain of polynucleotide phosphorylase affects autoregulation and mRNA decay in *Escherichia coli*. Mol Microbiol 33:235-248

Gatewood ML, Jones GH (2010) (p)ppGpp inhibits polynucleotide phosphorylase from streptomyces but not from *Escherichia coli* and increases the stability of bulk mRNA in *Streptomyces coelicolor*. J Bacteriol 192:4275-4280

Ge Z, Mehta P, Richards J, Karzai AW (2010) Non-stop mRNA decay initiates at the ribosome. Mol Microbiol 78:1159-1170

Ghosh S, Deutscher MP (1999) Oligoribonuclease is an essential component of the mRNA decay pathway. Proc Natl Acad Sci USA 96:4372-4377

Goverde RL, Huis in't Veld JH, Kusters JG, Mooi FR (1998) The psychrotrophic bacterium *Yersinia enterocolitica* requires expression of *pnp*, the gene for polynucleotide phosphorylase, for growth at low temperature (5 degrees C). Mol Microbiol 28:555-569

Grunberg-Manago M, Oritz PJ, Ochoa S (1955) Enzymatic synthesis of nucleic acid-like polynucleotides. Science 122:907-910

Hanekamp T, Thorsness PE (1999) YNT20, a bypass suppressor of yme1 yme2, encodes a putative 3'-5' exonuclease localized in mitochondria of *Saccharomyces cerevisiae*. Curr Genet 34:438-448

Harlow LS, Kadziola A, Jensen KF, Larsen S (2004) Crystal structure of the phosphorolytic exoribonuclease RNase PH from *Bacillus subtilis* and implications for its quaternary structure and tRNA binding. Protein Sci 13:668-677

Houseley J, LaCava J, Tollervey D (2006) RNA-quality control by the exosome. Nature Rev 7:529-539

Iost I, Dreyfus M (2006) DEAD-box RNA helicases in *Escherichia coli*. Nucleic Acids Res. 34:4189-4197

Ishii R, Nureki O, Yokoyama S (2003) Crystal structure of the tRNA processing enzyme RNase PH from *Aquifex aeolicus*. J Biol Chem 278:32397-32404

Jarrige AC, Mathy N, Portier C (2001). PNPase autocontrols its expression by degrading a double-stranded structure in the *pnp* mRNA leader. EMBO J 20:6845-6855

Kelly KO, Deutscher MP (1992a) Characterization of *Escherichia coli* RNase PH. J Biol Chem 267:17153-17158

Kelly KO, Deutscher MP (1992b) The presence of only one of five exoribonucleases is sufficient to support the growth of *Escherichia coli*. J Bacteriol 174:6682-6684

Kelly KO, Reuven NB, Li Z, Deutscher MP (1992). RNase PH is essential for tRNA processing and viability in RNase-deficient *Escherichia coli* cells. J Biol Chem 267:16015-16018

Kennedy S, Wang D, Ruvkun G (2004) A conserved siRNA-degrading RNase negatively regulates RNA interference in *C. elegans*. Nature 427:645-649

Lalonde MS, Zuo Y, Zhang J, Gong X, Wu S, Malhotra A, Li Z (2007) Exoribonuclease R in *Mycoplasma genitalium* can carry out both RNA processing and degradative functions and is sensitive to RNA ribose methylation. RNA 13:1957-1968

Lange H, Holec S, Cognat V, Pieuchot L, Le Ret M, Canaday J, Gagliardi D (2008) Degradation of a polyadenylated rRNA maturation by-product involves one of the three RRP6-like proteins in *Arabidopsis thaliana*. Mol Cell Biol 28:3038-3044

Lebreton A, Tomecki R, Dziembowski A, Seraphin B (2008) Endonucleolytic RNA cleavage by a eukaryotic exosome. Nature 456:993-996

Li Z, Deutscher MP (1995) The tRNA processing enzyme RNase T is essential for maturation of 5S RNA. Proc Natl Acad Sci USA 92:6883-6886

Li Z, Deutscher MP (1996) Maturation pathways for *E. coli* tRNA precursors: a random multienzyme process in vivo. Cell 86:503-512

Li Z, Pandit S, Deutscher MP (1998) 3' exoribonucleolytic trimming is a common feature of the maturation of small, stable RNAs in *Escherichia coli*. Proc Natl Acad Sci USA 95:2856-2861

Li Z, Pandit S, Deutscher MP (1999) Maturation of 23S ribosomal RNA requires the exoribonuclease RNase T. RNA 5:139-146

Li Z, Reimers S, Pandit S, Deutscher MP (2002) RNA quality control: degradation of defective transfer RNA. EMBO J 21:1132-1138

Li Z, Zhan L, Deutscher MP (1996) *Escherichia coli* RNase T functions in vivo as a dimer dependent on cysteine 168. J Biol Chem 271:1133-1137

Liang W, Deutscher MP (2010) A novel mechanism for ribonuclease regulation: transfer-messenger RNA (tmRNA) and its associated protein SmpB regulate the stability of RNase R. J Biol Chem 285:29054-29058

Lim J, Kuroki T, Ozaki K, Kohsaki H, Yamori T, Tsuruo T, Nakamori S, Imaoka S, Endo M, Nakamura Y (1997) Isolation of murine and human homologues of the fission-yeast dis3+ gene encoding a mitotic-control protein and its overexpression in cancer cells with progressive phenotype. Cancer Res 57:921-925

Lin PH, Lin-Chao S (2005) RhlB helicase rather than enolase is the beta-subunit of the *Escherichia coli* polynucleotide phosphorylase (PNPase)-exoribonucleolytic complex. Proc Natl Acad Sci USA 102:16590-16595

Littauer YZ, Soreq H (1982) Polynucleotide Phosphorylase. Academic Press, New York

Liu Q, Greimann JC, Lima CD (2006) Reconstitution, activities, and structure of the eukaryotic RNA exosome. Cell 127:1223-1237

Lorentzen E, Walter P, Fribourg S, Evguenieva-Hackenberg E, Klug G, Conti E (2005) The archaeal exosome core is a hexameric ring structure with three catalytic subunits. Nat Struct Mol Biol 12:575-581

Lu C, Ding F, Ke A (2010) Crystal structure of the *S. solfataricus* archaeal exosome reveals conformational flexibility in the RNA-binding ring. PloS One 5:e8739.

Luttinger A, Hahn J, Dubnau D (1996) Polynucleotide phosphorylase is necessary for competence development in *Bacillus subtilis*. Mol Microbiol 19:343-356

Malet H, Topf M, Clare DK, Ebert J, Bonneau F, Basquin J, Drazkowska K, Tomecki R, Dziembowski A, Conti E, Saibil HR, Lorentzen E (2010) RNA channelling by the eukaryotic exosome. EMBO Rep 11:936-942

Mamolen M, Smith A, Andrulis ED (2010) *Drosophila melanogaster* Dis3 N-terminal domains are required for ribonuclease activities, nuclear localization and exosome interactions. Nucleic Acids Res 38:5507-5517

Marujo PE, Hajnsdorf E, Le Derout J, Andrade R, Arraiano CM, Régnier P (2000) RNase II removes the oligo(A) tails that destabilize the *rpsO* mRNA of *Escherichia coli*. RNA 6:1185-1193

Matos RG, Barbas A, Arraiano CM (2009) RNase R mutants elucidate the catalysis of structured RNA: RNA-binding domains select the RNAs targeted for degradation. Biochem J 423:291-301

Matos RG, Barbas A, Arraiano CM (2010) Comparison of EMSA and SPR for the characterization of RNA-RNase II complexes. Protein J 29:394-397

Matos RG, Barbas A, Goméz-Puertas P, Arraiano CM, 2011. Swapping the domains of exoribonucleases RNase II and RNase R: conferring upon RNase II the ability to degrade ds RNA. PROTEINS Accepted

Matus-Ortega ME, Regonesi ME, Pina-Escobedo A, Tortora P, Dehò G, García-Mena J (2007) The KH and S1 domains of *Escherichia coli* polynucleotide phosphorylase are necessary for autoregulation and growth at low temperature. Biochim Biophys Acta 1769:194-203

Mechold U, Ogryzko V, Ngo S, Danchin A (2006) Oligoribonuclease is a common downstream target of lithium-induced pAp accumulation in *Escherichia coli* and human cells. Nucleic Acids Res 34:2364-2373

Mian IS (1997) Comparative sequence analysis of ribonucleases HII, III, II PH and D. Nucleic Acids Res 25:3187-3195

Miczak A, Kaberdin VR, Wei CL, Lin-Chao S (1996) Proteins associated with RNase E in a multicomponent ribonucleolytic complex. Proc Natl Acad Sci USA 93:3865-3869

Midtgaard SF, Assenholt J, Jonstrup AT, Van LB, Jensen TH, Brodersen DE (2006) Structure of the nuclear exosome component Rrp6p reveals an interplay between the active site and the HRDC domain. Proc Natl Acad Sci USA 103:11898-11903

Mitchell P, Petfalski E, Shevchenko A, Mann M, Tollervey D (1997) The exosome: a conserved eukaryotic RNA processing complex containing multiple 3'-->5' exoribonucleases. Cell 91:457-466

Mohanty BK, Maples VF, Kushner SR (2004) The Sm-like protein Hfq regulates polyadenylation dependent mRNA decay in *Escherichia coli*. Mol Microbiol 54:905-920

Nguyen LH, Erzberger JP, Root J, Wilson DM 3rd (2000) The human homolog of *Escherichia coli* Orn degrades small single-stranded RNA and DNA oligomers. J Biol Chem 275:25900-25906

Nurmohamed S, Vaidialingam B, Callaghan AJ, Luisi BF (2009) Crystal structure of *Escherichia coli* polynucleotide phosphorylase core bound to RNase E, RNA and manganese: implications for catalytic mechanism and RNA degradosome assembly. J Mol Biol 389:17-33

Ost KA, Deutscher MP (1991) *Escherichia coli orf*E (upstream of *pyr*E) encodes RNase PH. J Bacteriol 173:5589-5591

Parker R, Song H (2004) The enzymes and control of eukaryotic mRNA turnover. Nat Struct Mol Biol 11:121-127

Piazza F, Zappone M, Sana M, Briani F, Dehò G (1996) Polynucleotide phosphorylase of *Escherichia coli* is required for the establishment of bacteriophage P4 immunity. J Bacteriol 178:5513-5521

Portier C, Dondon L, Grunberg-Manago M, Régnier P (1987) The first step in the functional inactivation of the *Escherichia coli* polynucleotide phosphorylase messenger is a ribonuclease III processing at the 5' end. EMBO J 6:2165-2170

Portnoy V, Evguenieva-Hackenberg E, Klein F, Walter P, Lorentzen E, Klug G, Schuster G (2005) RNA polyadenylation in Archaea: not observed in *Haloferax* while the exosome polynucleotidylates RNA in *Sulfolobus*. EMBO Rep 6:1188-1193

Pruijn GJ (2005) Doughnuts dealing with RNA. Nat Struct Mol Biol 12:562-564

Purusharth RI, Klein F, Sulthana S, Jager S, Jagannadham MV, Evguenieva-Hackenberg E, Ray MK, Klug G (2005) Exoribonuclease R interacts with endoribonuclease E and an RNA helicase in the psychrotrophic bacterium *Pseudomonas syringae Lz4W*. J Biol Chem 280:14572-14578

Purusharth RI, Madhuri B, Ray MK (2007) Exoribonuclease R in *Pseudomonas syringae* is essential for growth at low temperature and plays a novel role in the 3' end processing of 16 and 5 S ribosomal RNA. J Biol Chem 282:16267-16277

Py B, Higgins CF, Krisch HM, Carpousis AJ (1996) A DEAD-box RNA helicase in the *Escherichia coli* RNA degradosome. Nature 381:169-172

Redko Y, Condon C (2010) Maturation of 23S rRNA in *Bacillus subtilis* in the absence of Mini-III. J Bacteriol 192:356-359

Régnier P, Arraiano CM (2000) Degradation of mRNA in bacteria: emergence of ubiquitous features. Bioessays 22:235-244

Regonesi ME, Del Favero M, Basilico F, Briani F, Benazzi L, Tortora P, Mauri P, Dehò G (2006) Analysis of the *Escherichia coli* RNA degradosome composition by a proteomic approach. Biochimie 88:151-161

Robert-Le Meur M, Portier C (1992) *E.coli* polynucleotide phosphorylase expression is autoregulated through an RNase III-dependent mechanism. EMBO J. 11:2633-2641

Rott R, Zipor G, Portnoy V, Liveanu V, Schuster G (2003) RNA polyadenylation and degradation in cyanobacteria are similar to the chloroplast but different from *Escherichia coli*. J Biol Chem 278:15771-15777

Sarkar D, Park ES, Emdad L, Randolph A, Valerie K, Fisher PB (2005) Defining the domains of human polynucleotide phosphorylase (hPNPaseOLD-35) mediating cellular senescence. Mol Cell Biol 25:7333-7343

Schaeffer D, Tsanova B, Barbas A, Reis FP, Dastidar EG, Sanchez-Rotunno M, Arraiano CM, van Hoof A (2009) The exosome contains domains with specific endoribonuclease, exoribonuclease and cytoplasmic mRNA decay activities. Nat Struct Mol Biol 16:56-62

Schneider C, Anderson JT, Tollervey D (2007) The exosome subunit Rrp44 plays a direct role in RNA substrate recognition. Mol Cell 27:324-331

Schneider C, Leung E, Brown J, Tollervey D (2009) The N-terminal PIN domain of the exosome subunit Rrp44 harbors endonuclease activity and tethers Rrp44 to the yeast core exosome. Nucleic Acids Res 37:1127-1140

Schwede A, Ellis L, Luther J, Carrington M, Stoecklin G, Clayton C (2008) A role for Caf1 in mRNA deadenylation and decay in trypanosomes and human cells. Nucleic Acids Res 36:3374-3388

Shi Z, Yang WZ, Lin-Chao S, Chak KF, Yuan HS (2008) Crystal structure of *Escherichia coli* PNPase: central channel residues are involved in processive RNA degradation. RNA 14:2361-2371

Siculella L, Damiano F, di Summa R, Tredici SM, Alduina R, Gnoni GV, Alifano P (2010) Guanosine 5'-diphosphate 3'-diphosphate (ppGpp) as a negative modulator of polynucleotide phosphorylase activity in a 'rare' actinomycete. Mol Microbiol 77:716-729

Silva IJ, Saramago M, Dressaire C, Domingues S, Viegas SC, Arraiano CM (2011) Importance and key events of prokaryotic RNA decay: the ultimate fate of an RNA molecule. WIREs RNA *Accepted*

Slomovic S, Portnoy V, Yehudai-Resheff S, Bronshtein E, Schuster G (2008) Polynucleotide phosphorylase and the archaeal exosome as poly(A)-polymerases. Biochim Biophys Acta 1779:247-255

Sohlberg B, Huang J, Cohen SN (2003) The *Streptomyces coelicolor* polynucleotide phosphorylase homologue, and not the putative poly(A) polymerase, can polyadenylate RNA. J Bacteriol 185:7273-7278

Spickler C, Mackie GA (2000) Action of RNase II and polynucleotide phosphorylase against RNAs containing stem-loops of defined structure. J. Bacteriol 182:2422-2427

Staals RH, Bronkhorst AW, Schilders G, Slomovic S, Schuster G, Heck AJ, Raijmakers R, Pruijn GJ (2010) Dis3-like 1: a novel exoribonuclease associated with the human exosome. EMBO J 29:2358-2367

Steitz TA, Steitz JA (1993) A general two-metal-ion mechanism for catalytic RNA. Proc Natl Acad Sci 90:6498-6502

Symmons MF, Jones GH, Luisi BF (2000) A duplicated fold is the structural basis for polynucleotide phosphorylase catalytic activity, processivity, and regulation. Structure 8:1215-1226

Thore S, Mauxion F, Seraphin B, Suck D (2003) X-ray structure and activity of the yeast Pop2 protein: a nuclease subunit of the mRNA deadenylase complex. EMBO Rep 4:1150-1155

Tobe T, Sasakawa C, Okada N, Honma Y, Yoshikawa M (1992) *vacB*, a novel chromosomal gene required for expression of virulence genes on the large plasmid of *Shigella flexneri*. J Bacteriol 174:6359-6367

Tomecki R, Kristiansen MS, Lykke-Andersen S, Chlebowski A, Larsen KM, Szczesny RJ, Drazkowska K, Pastula A, Andersen JS, Stepien PP, Dziembowski A, Jensen TH (2010) The human core exosome interacts with differentially localized processive RNases: hDIS3 and hDIS3L. EMBO Journal 29:2342-2357

Tsao MY, Lin TL, Hsieh PF, Wang JT (2009) The 3'-to-5' exoribonuclease (encoded by HP1248) of *Helicobacter pylori* regulates motility and apoptosis-inducing genes. J Bacteriol 191:2691-2702

Tucker M, Valencia-Sanchez MA, Staples RR, Chen J, Denis CL, Parker R (2001) The transcription factor associated Ccr4 and Caf1 proteins are components of the major cytoplasmic mRNA deadenylase in *Saccharomyces cerevisiae*. Cell 104:377-386

van Hoof A, Lennertz P, Parker R (2000) Three conserved members of the RNase D family have unique and overlapping functions in the processing of 5S, 5.8S, U4, U5, RNase MRP and RNase P RNAs in yeast. EMBO J 19:1357-1365

van Hoof A, Parker R (1999) The exosome: a proteasome for RNA? Cell 99:347-350

Vanzo NF, Li YS, Py B, Blum E, Higgins CF, Raynal LC, Krisch HM, Carpousis AJ (1998) Ribonuclease E organizes the protein interactions in the *Escherichia coli* RNA degradosome. Genes Dev 12:2770-2781

Vincent HA, Deutscher MP (2006) Substrate recognition and catalysis by the exoribonuclease RNase R. J Biol Chem 281:29769-29775

Vincent HA, Deutscher MP (2009a) Insights into how RNase R degrades structured RNA: analysis of the nuclease domain. J Mol Biol 387:570-583

Vincent HA, Deutscher MP (2009b) The roles of individual domains of RNase R in substrate binding and exoribonuclease activity. The nuclease domain is sufficient for digestion of structured RNA. J Biol Chem 284:486-494

Viswanathan M, Dower KW, Lovett ST (1998) Identification of a potent DNase activity associated with RNase T of *Escherichia coli*. J Biol Chem 273:35126-35131

Wang G, Chen HW, Oktay Y, Zhang J, Allen EL, Smith GM, Fan KC, Hong JS, French SW, McCaffery JM, Lightowlers RN, Morse HC 3rd, Koehler CM, Teitell MA (2010a) PNPase regulates RNA import into mitochondria. Cell 142:456-467

Wang H, Morita M, Yang X, Suzuki T, Yang W, Wang J, Ito K, Wang Q, Zhao C, Bartlam M, Yamamoto T, Rao Z (2010b) Crystal

structure of the human CNOT6L nuclease domain reveals strict poly(A) substrate specificity. EMBO J 29: 2566-2576

Wang HW, Wang J, Ding F, Callahan K, Bratkowski J, Butler JS, Nogles E, Ke A (2007) Architecture of the yeast Rrp44-exosome complex suggests routes of RNA recruitment for 3´end processing. Proc Nat Acad Sci USA 104:16844-16849

Wen T, Oussenko IA, Pellegrini O, Bechhofer DH, Condon C (2005) Ribonuclease PH plays a major role in the exonucleolytic maturation of CCA-containing tRNA precursors in *Bacillus subtilis*. Nucleic Acids Research 33:3636-3643

Wu M, Reuter M, Lilie H, Liu Y, Wahle E, Song H (2005) Structural insight into poly(A) binding and catalytic mechanism of human PARN. EMBO J 24:4082-4093

Yamashita,A, Chang TC, Yamashita Y, Zhu W, Zhong Z, Chen CY, Shyu AB (2005) Concerted action of poly(A) nucleases and decapping enzyme in mammalian mRNA turnover. Nat Struct Mol Biol 12:1054-1063

Yang XC, Torres MP, Marzluff WF, Dominski Z (2009) Three proteins of the U7-specific Sm ring function as the molecular ruler to determine the site of 3'-end processing in mammalian histone pre-mRNA. Mol Cell Biol 29:4045-4056

Yehudai-Resheff S, Hirsh M, Schuster G (2001) Polynucleotide phosphorylase functions as both an exonuclease and a poly(A) polymerase in spinach chloroplasts. Mol Cell Biol 21:5408-5416

Zangrossi S, Briani F, Ghisotti D, Regonesi ME, Tortora P, Dehò G (2000) Transcriptional and post-transcriptional control of polynucleotide phosphorylase during cold acclimation in *Escherichia coli*. Mol Microbiol 36:1470-1480

Zhang JR, Deutscher MP (1988a) Cloning, characterization, and effects of overexpression of the *Escherichia coli rnd* gene encoding RNase D. J Bacteriol 170:522-527

Zhang JR, Deutscher MP (1988b) Transfer RNA is a substrate for RNase D in vivo. J Biol Chem 263:17909-17912

Zhang JR, Deutscher MP (1989) Analysis of the upstream region of the *Escherichia coli rnd* gene encoding RNase D. Evidence for translational regulation of a putative tRNA processing enzyme. J Biol Chem 264:18228-18233

Zhang W, Murphy C, Sieburth LE (2010) Conserved RNase II domain protein functions in cytoplasmic mRNA decay and suppresses *Arabidopsis* decapping mutant phenotypes. Proc Natl Acad Sci USA 107:15981-15985

Zhang X, Zhu L, Deutscher MP (1998) Oligoribonuclease is encoded by a highly conserved gene in the 3'-5' exonuclease superfamily. J Bacteriol 180:2779-2781

Zhou Z, Deutscher MP (1997) An essential function for the phosphate-dependent exoribonucleases RNase PH and polynucleotide phosphorylase. J Bacteriol 179:4391-4395

Zilhão R, Cairrão F, Régnier P, Arraiano CM (1996ª) PNPase modulates RNase II expression in *Escherichia coli*: implications for mRNA decay and cell metabolism. Mol Microbiol 20:1033-1042

Zilhão R, Cairrão F, Régnier P, Arraiano CM (1996a) PNPase modulates RNase II expression in *Escherichia coli*: implications for mRNA decay and cell metabolism. Mol Microbiol 20:1033-1042

Zilhão R, Plumbridge J, Hajnsdorf E, Régnier P, Arraiano CM (1996b) *Escherichia coli* RNase II: characterization of the promoters involved in the transcription of *rnb*. Microbiology 142:367-375

Zilhão R, Régnier P, Arraiano CM (1995) The role of endonucleases in the expression of ribonuclease II in *Escherichia coli*. FEMS Microbiol Lett 130:237-244

Zuo Y, Deutscher MP (2001) Exoribonuclease superfamilies: structural analysis and phylogenetic distribution. Nucleic Acids Res 29:1017-1026

Zuo Y, Deutscher MP (2002a) Mechanism of action of RNase T. I. Identification of residues required for catalysis, substrate binding, and dimerization. J Biol Chem 277:50155-50159

Zuo Y, Deutscher MP (2002b) Mechanism of action of RNase T. II. A structural and functional model of the enzyme. J Biol Chem 277:50160-50164

Zuo Y, Vincent HA, Zhang J, Wang Y, Deutscher MP, Malhotra A (2006) Structural basis for processivity and single-strand specificity of RNase II. Mol Cell 24:149-156

Zuo Y, Wang Y, Malhotra A (2005) Crystal structure of *Escherichia coli* RNase D, an exoribonuclease involved in structured RNA processing. Structure 13:973-984

Zuo Y, Zheng H, Wang Y, Chruszcz M, Cymborowski M, Skarina T, Savchenko A, Malhotra A, Minor W (2007) Crystal structure of RNase T, an exoribonuclease involved in tRNA maturation and end turnover. Structure 15:417-428

Appendix II

Book chapters

9 - Structure and degradation mechanisms of 3' to 5' exoribonucleases [Ribonucleases, Nucleic Acids and Molecular Biology (Springer). Edited by Professor Allen Nicholson. 2011. 26: 193-222.

PROTEINS
STRUCTURE ■ FUNCTION ■ BIOINFORMATICS

Swapping the domains of exoribonucleases RNase II and RNase R: Conferring upon RNase II the ability to degrade ds RNA

Rute Gonçalves Matos,[1] Ana Barbas,[1] Paulino Gómez-Puertas,[2] and Cecília Maria Arraiano[1]*

[1] Instituto de Tecnologia Química e Biológica/Universidade Nova de Lisboa, Apartado 127, 2781-901 Oeiras, Portugal
[2] Centro de Biología Molecular "Severo Ochoa" (CSIC-UAM). Cantoblanco, 28049 Madrid, Spain

ABSTRACT

RNase II and RNase R are the two *E. coli* exoribonucleases that belong to the RNase II super family of enzymes. They degrade RNA hydrolytically in the 3′ to 5′ direction in a processive and sequence independent manner. However, while RNase R is capable of degrading structured RNAs, the RNase II activity is impaired by dsRNAs. The final end-product of these two enzymes is also different, being 4 nt for RNase II and 2 nt for RNase R. RNase II and RNase R share structural properties, including 60% of amino acid sequence similarity and have a similar modular domain organization: two N-terminal cold shock domains (CSD1 and CSD2), one central RNB catalytic domain, and one C-terminal S1 domain. We have constructed hybrid proteins by swapping the domains between RNase II and RNase R to determine which are the responsible for the differences observed between RNase R and RNase II. The results obtained show that the S1 and RNB domains from RNase R in an RNase II context allow the degradation of double-stranded substrates and the appearance of the 2 nt long end-product. Moreover, the degradation of structured RNAs becomes tail-independent when the RNB domain from RNase R is no longer associated with the RNA binding domains (CSD and S1) of the genuine protein. Finally, we show that the RNase R C-terminal Lysine-rich region is involved in the degradation of double-stranded substrates in an RNase II context, probably by unwinding the substrate before it enters into the catalytic cavity.

Proteins 2011; 79:1853–1867.

Key words: ribonuclease; RNA; exosome; RNA degradation; protein domains; protein structure; RNA metabolism; protein modeling.

INTRODUCTION

RNase II and RNase R are the two *Escherichia coli* exoribonucleases that belong to the RNase II super family of enzymes. RNase II is the prototype of this family of exoribonucleases, and RNase II/R homologues are present in all domains of life.[1–5] The other member of the RNase II family, RNase R, has been shown to be required for virulence and is involved in mRNA degradation, and RNA and protein quality control.[5–10] In the nucleus and the cytoplasm of eukaryotic cells, the RNase II homologue—Rrp44/Dis3 is part of the exosome, an essential multiprotein complex of exoribonucleases, involved in processing, turnover, and quality control of different types of RNAs.[3] Most importantly, this enzyme was reported to be the only catalytically active nuclease in the yeast core exosome,[11] and studies have shown that this protein has a dual function since it comprises both an exo and an endoribonucleolytic activity.[5,12,13]

RNase II and RNase R share catalytic properties: they both processively degrade RNA hydrolytically in the 3′ to 5′ direction releasing 5′-nucleosite monophosphates. Both enzymes share structural properties, including 60% aminoacid sequence similarity, and 29% protein sequence identity.[14] Their activity is sequence independent but while RNase II is sensitive to secondary structures, RNase R is capable of degrading highly structured RNAs.[7,10,14,15] In fact, recent studies have shown that the RNB domain of RNase R is the one responsible for the degradation of double-stranded substrates.[16,17] It is known that RNase R needs a 3′- single-stranded overhang of at least five nucleotides in length to be able to attach to the substrate and proceed to the degradation of the structured RNA molecules.[18] However, it was recently shown that the CSDs and S1 domains are those responsible for the selective degradation of double-stranded substrates that contain a 3′ single-stranded overhang of five or more nucleotides.[16] Another difference between these two *E. coli* enzymes is that the final degradation product of RNase II is a 4 nucleotide fragment, whereas the end-product of RNase R is a 2 nucleotide fragment.[15,19,20] The same differences have been observed in *Salmonella*, which also has both RNase

Additional Supporting Information may be found in the online version of this article.
Grant sponsor: FCT-Fundação para a Ciência e a Tecnologia, Portugal
*Correspondence to: Cecilia M. Arraiano, Instituto de Tecnologia Química e Biológica / Universidade Nova de Lisboa, Apartado 127, 2781-901 Oeiras, Portugal. E-mail: cecilia@itqb.unl.pt.
Received 2 November 2010; Revised 5 January 2011; Accepted 28 January 2011
Published online 10 February 2011 in Wiley Online Library (wileyonlinelibrary.com).
DOI: 10.1002/prot.23010

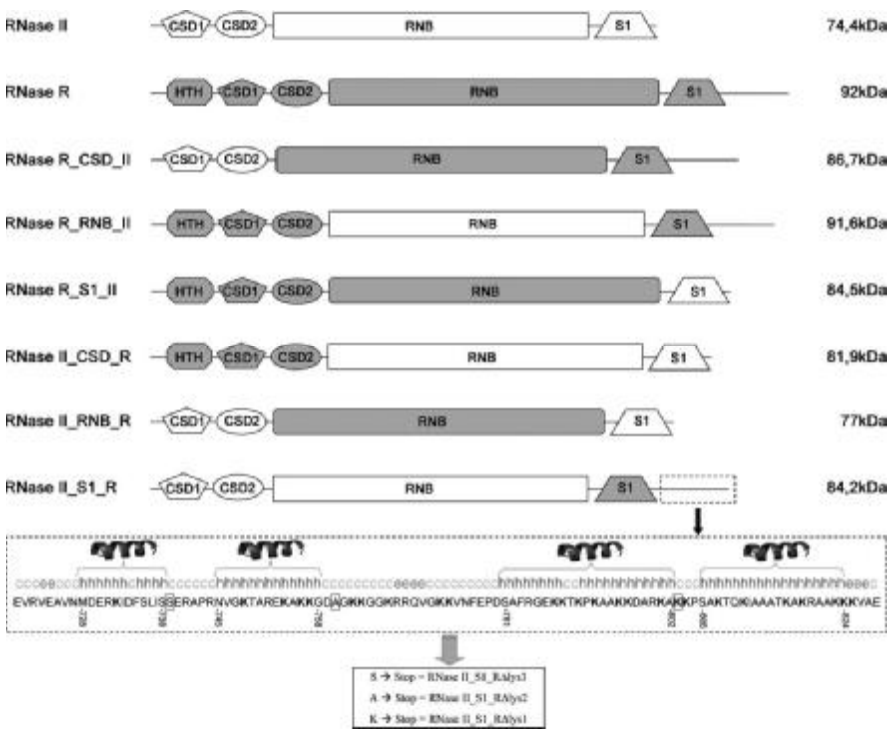

Figure 1

Linear representation of the domains of wild type RNase II, RNase R and its derivatives proteins. The lysine-rich tail of the S1 domain from RNase R is highlighted, and the protein structure is represented. The aminoacids that were substituted by stop codons to construct the proteins RNase II_S1_RΔLys1, RNase II_S1_RΔLys2, and RNase II_S1_RΔLys3 are boxed. On the top of the protein structure is the secondary structure prediction using the GOR 4 method of NPS@ as described in Experimental Procedures. h stands for alpha helix, e stands for extended strand and c stands for random coil.

II and RNase R like proteins.[21] In *Streptococcus pneumoniae*, only one member of this family of enzymes is present. Its characterization showed that it behaves like RNase R, since it is able to degrade double-stranded substrates releasing a 2 nt fragment as its end-product.[21]

RNase II is a protein encoded by gene *rnb* with 72KDa. In *E. coli*, this protein is the major hydrolytic enzyme that is responsible for 90% of the exoribonucleolytic activity in crude extracts.[22] RNase II expression is differentially regulated at the transcriptional and post-transcriptional levels and the protein can be regulated by the environmental conditions.[23–26] The determination of the 3D structure of *E. coli* RNase II showed that RNase II consists of 4 domains: two N-terminal cold shock domains (CSD1 and CSD2), one central RNB catalytic domain, and one C-terminal S1 domain[27,28] (Fig. 1). The final degradation product of RNase II is 4 nt. The structure of the RNA bound complex showed that there is a tight packing of the five 3′-terminal nucleotides in the catalytic cavity, and the RNA "clamping" is mediated by the aromatic residues Tyr253 and Phe358.[27] Subsequently, it was demonstrated that Tyr253 is the residue responsible for setting the end-product of RNase II.[26,29] It was also demonstrated that Tyr-313 and Glu390 are important for the discrimination of cleavage of RNA versus DNA.[16,26,30] During the determination of key residues for catalysis, we have recently discovered that the substitution of the Glu-542 by alanine lead to a 110-fold increase in the exoribonucleolytic activity and 20-fold in RNA binding, turning RNase II into a "super-enzyme."[26,30,31]

RNase R is a 92KDa protein encoded by the *rnr* gene that is involved in the degradation of different types of RNAs such as rRNAs, small RNAs and mRNAs. It was shown that RNase R has *in vivo* affinity for polyadenylated RNA and can be a key enzyme involved in poly(A) metabolism.[32] It is a cold shock protein that is regulated

Table I
Plasmids Used in this Study

Plasmid	Relevant characteristic	Reference
pFCT6.1	gene *rnb* cloned into pET15b, Amp^R	Cairrão *et al.*,[23]
pABA-RNR	gene *rnr* cloned into pET15b, Amp^R	Amblar *et al.*,[19]
pFCT_SpeI514	pFCT6.1 with a SpeI restriction site in position 514 of *rnb* gene	This work
pFCT_SmaI1729	pFCT6.1 with a *Sma*I restriction site in position 1729 of *rnb* gene	This work
pFCT_SpeI514_SmaI1729	pFCT_SpeI514 with a *Sma*I restriction site in position 1729 of *rnb* gene	This work
pABA-RNR_SpeI547	pABA-RNR with a *Spe*I restriction site in position 547 of *rnr* gene	This work
pABA-RNR_SmaI1924	pABA-RNR with a SmaI restriction site in position 1924 of *rnr* gene	This work
pABA-RNR_SpeI547_SmaI1924	pABA-RNR_SpeI547 with a *Sma*I restriction site in position 1924 of *rnr* gene	This work
pFCT_CSD_R	Expresses RNase II with HTH, CSD1 and CSD2 domains from RNase R	This work
pFCT_RNB_R	Expresses RNase II with RNB domain from RNase R	This work
pFCT_S1_R	Expresses RNase II with S1 domain from RNase R	This work
pABA-RNR_CSD_II	Expresses RNase R with CSD1 and CSD2 domains from RNase II	This work
pABA-RNR_RNB_II	Expresses RNase R with RNB domain from RNase II	This work
pABA-RNR_S1_II	Expresses RNase R with S1 domain from RNase II	This work
pFCT_S1_R_ΔLys1	Expresses RNase II with S1 domain from RNase R without the last 26 aa	This work
pFCT_S1_R_ ΔLys2	Expresses RNase II with S1 domain from RNase R without the last 67 aa	This work
pFCT_S1_R_ ΔLys3	Expresses RNase II with S1 domain from RNase R without the last 87 aa	This work

at the transcriptional and post-transcriptional levels.[8,9] The activity of RNase R is modulated according the growth conditions of the cell[23] and its levels increase in stationary phase and under other stress conditions.[7,9,10] It has been shown that this protein is also involved in pathogenesis in different microorganisms.[6,33–35] The structural model of *E. coli* RNase R protein has been constructed based on the RNase II structure. It clearly indicates that these enzymes share a common three-dimensional arrangement, with all the critical residues for exoribonucleolytic activity located in equivalent spatial positions.[29] In fact, recent studies have shown that like in RNase II D209N mutant, Asp280 in RNase R is important for the activity of the enzyme but not for the RNA binding. Also it has been described that Tyr324 is also the conserved residue responsible for setting the final end product in RNase R, comparable with what is observed with RNase II.[16]

The aim of this work was to determine if the catalytical differences observed between RNase II and RNase R could be assigned directly to one of the domains. As such, we wanted to investigate which domain could be accounted for the setting of the different end-products (4 nt for RNase II and 2 nt for RNase R), and which domain could be responsible for the discrimination between single- and double-stranded RNA cleavage. For that, we constructed a set of six different hybrid proteins by swapping the cold shock domains, the catalytic domains, and the S1 domains between RNase II and RNase R (Fig. 1). The results presented here show that in fact the RNB domain from RNase R is the one responsible for the degradation of double-stranded substrates. However and more interestingly, our data shows that the C-terminal region from RNase R has a very important role in the degradation of double-stranded substrates. We show that this domain might contribute to the unwinding of the secondary structures, and this can explain why RNase R is capable of degrading RNA structured substrates.

MATERIALS AND METHODS

Materials

Restriction enzymes, T4 DNA ligase, Pfu DNA polymerase and T4 Polynucleotide Kinase were purchased from Fermentas. Unlabeled oligonucleotide primers were synthesized by STAB Vida, Portugal.

Strains

The *E. coli* strains used were DH5α (F′ fhuA2 Δ(argF-lacZ)U169 phoA glnV44 Φ80 Δ(lacZ)M15 gyrA96 recA1 relA1 endA1 thi-1 hsdR17a)[36] for cloning experiments and BL21(DE3) (F^- $r_B{}^-$ $m_B{}^-$ gal ompT (int::P_{lacUV5} T7 gen1 imm21 nin5)[37] for protein expression.

Construction of hybrid proteins

The hybrid proteins were constructed by swapping the N-terminal region (corresponding to the Cold Shock Domains), the catalytic domain RNB or the C-terminal region (S1 domain) between $(His)_6$-RNase II and $(His)_6$-RNase R, thus obtaining the following six proteins: RNase II_CSD_R, RNase II_RNB_R, RNase II_S1_R, RNase R_CSD_II, RNase R_RNB_II, and RNase R_S1_II (Fig. 1).

For this purpose, the *Spe*I and *Sma*I restriction sites were introduced into the pFCT6.1 plasmid (Table I) at the 514 nt and 1729 nt positions respectively and in the pABA-RNR plasmid (Table I) at the 547 nt and 1924 nt positions respectively by overlapping PCR. The mutagenic primers used were pFCT¬_SpeI514_Fw, pFCT_SpeI514_Rev, pFCT_SmaI1729_Fw, pFCT_SmaI1729_Rev, RNR_SpeI547_Fw, RNR_SpeI547_Rev, RNR_SmaI1924_

Table II
Primers used in this Study

Primer	Sequence (5′ – 3′)[ab]	Purpose
pFCT_SpeI514_Fw	CACAATACATCACT**AG**TGGTGACG	Introduces SpeI restriction site into pFCT6.1 at the position 514
pFCT_SpeI514_Rev	CGTCACC**CT**AGTGATGTATTGTG	Introduces SpeI restriction site into pFCT6.1 at the position 514
pFCT_SmaI1729_Fw	CCTGAAAGACAAA**C**CCGGGACCGACACCCG	Introduces SmaI restriction site into pFCT6.1 at the position 1729
pFCT_SmaI1729_Rev	CGGGTGTCGGTCCCGG**G**TTTGTCTTTCAGG	Introduces SmaI restriction site into pFCT6.1 at the position 1729
RNR_SpeI547_Fw	GTCGAAGTGCTGGGC**CT**AG**T**ATGGGCACC	Introduces SpeI restriction site into pABA-RNR at the position 547
RNR_SpeI547_Rev	GGTGCCCATA**CTAGT**GCCCAGCACTTCGAC	Introduces SpeI restriction site into pABA-RNR at the position 547
RNR_SmaI1924_Fw	GTGTGACTTCATG**C**CCG**GG**CAGGTAGG	Introduces SmaI restriction site into pABA-RNR at the position 1924
RNR_SmaI1924_Rev	CCTACCTG**CC**CGGGCATGAAGTCACAC	Introduces SmaI restriction site into pABA-RNR at the position 1924
Δlys1_Fw	TTTAGCCTGATCTCC**TAA**GAACGCGCACCG	Introduces stop codon into pFCT_S1_R at the position 2172
Δlys1_Rev	CGGTGCGCGTTC**TTA**GGAGATCAGGCTAAA	Introduces stop codon into pFCT_S1_R at the position 2172
Δlys2_Fw	GAAAAAAGGCGAT**TA**AGGTAAAAAAGGCGG	Introduces stop codon into pFCT_S1_R at the position 2049
Δlys2_Rev	CCGCCTTTTTTACCT**TA**ATCGCCTTTTTTC	Introduces stop codon into pFCT_S1_R at the position 2049
Δlys3_Fw	GCGAGAAAAGCG**T**AAAAGCCATCGG	Introduces stop codon into pFCT_S1_R at the position 1989
Δlys3_Rev	CCGATGGCTTTT**A**CGCTTTTCTCGC	Introduces stop codon into pFCT_S1_R at the position 1989

Bases underlined indicate restriction sites.
Bases in bold indicate aminoacid changes.

Fw, and RNR_SmaI1924_Rev (Table II). To construct the hybrid proteins RNase II_RNB_R and RNase R_RNB_II, the resulting plasmids pFCT_SpeI514_SmaI1729 and pABA-RNR_SpeI547_SmaI1924 (Table II) were digested with *Spe*I and *Sma*I, obtaining degradation products of 6195 bps and 1216 bps for pFCT_SpeI514_SmaI1729 and 7005 bps and 1270 bps for pABA-RNR_SpeI547_SmaI1924. The restriction fragment with 1216 bps resultant of the restriction of pFCT_SpeI514_SmaI1729 was ligated to the restriction fragment of 7005 bps resultant of the digestion of pABA-RNR_SpeI547_SmaI1924, originating the hybrid protein RNase R_RNB_II. The restriction fragment with 6195 bps resultant of the restriction of pFCT_SpeI514_SmaI1729 was ligated to the restriction fragment of 1270 bps resultant of the digestion of pABA-RNR_SpeI547_SmaI1924, originating the hybrid protein RNase II_RNB_R.

To construct the hybrid proteins RNase II_CSD_R and RNase R_CSD_II, the plasmids with the insertion of *Spe*I restriction site only, pFCT_SpeI514 and pABA-RNR_SpeI547 (Table I) were digested with *Spe*I and *Xba*I (the restriction enzyme *Xba*I cleaves the pET15b plasmid upstream the insertion of the *rnb* or *rnr* genes), obtaining degradation products of 6860 bps and 551 bps for pFCT_SpeI514 and 7529 bps and 746 bps for pABA-RNR_SpeI547. The restriction fragment with 551 bps resultant of the restriction of pFCT_SpeI514 was ligated to the restriction fragment of 7529 bps resultant of the digestion of pABA-RNR_SpeI547, originating the hybrid protein RNase R_CSD_II. The restriction fragment with 6860 bps resultant of the restriction of pFCT_SpeI514 was ligated to the restriction fragment of 746 bps resultant of the digestion of pABA-RNR_SpeI547, originating the hybrid protein RNase II_CSD_R.

To construct the hybrid proteins RNase II_S1_R and RNase R_S1_II, the plasmids with the insertion of *Sma*I restriction site only, pFCT_SmaI1729 and pABA-RNR_SmaI1924 (Table I) were digested with *Sma*I and *Hind*III (the restriction enzyme *Hind*III cleaves the pET15b plasmid downstream the insertion of the *rnb* or *rnr* genes), obtaining degradation products of 7076 bps and 335 bps for pFCT_SmaI1729 and 7325 bps and 950 bps for pABA-RNR_SmaI1924. The restriction fragment with 335 bps resultant of the restriction of pFCT_SmaI1729 was ligated to the restriction fragment of 7325 bps resultant of the digestion of pABA-RNR_SmaI1924, originating the hybrid protein RNase R_S1_II. The restriction fragment with 7076 bps resultant of the restriction of pFCT_SmaI1729 was ligated to the restriction fragment of 950 bps resultant of the digestion of pABA-RNR_SmaI1924, originating the hybrid protein RNase II_S1_R.

The Δlys mutations in the RNase II_S1_R_Δlys1, RNase II_S1_R_Δlys2, and RNase II_S1_R_Δlys3 proteins were introduced into the pFCT_S1_R (Table I) by PCR overlapping. The primers used in the constructions were Δlys1_Fw, Δlys1_Rev, Δlys2_Fw, Δlys2_Rev, Δlys3_Fw, and Δlys3_Rev (Table II).

Overexpression and purification of wild type and hybrid proteins

The plasmid used for expression of wild-type *E. coli* histidine-tagged RNase II protein was pFCT6.1 plasmid (Table I). The plasmid used for expression of wild-type *E. coli* histidine-tagged RNase R protein was pABA-RNR (Table I).

All plasmids were transformed into BL21(DE3) *E. coli* strain (Novagen) to allow the expression of the recombinant proteins. Cells were grown at 30°C in 100 mL LB medium supplemented with 150 μg/mL ampicillin to an OD_{600} of 1.5. Then, they were transferred to 18°C for 30 min and then induced by addition of 0.5 m*M* IPTG; induction proceeded for 20 hours at 18°C. Cell cultures were pelleted by centrifugation at 6000 rpms for 15 min and stored at −80°C.

Purification of all proteins was performed by histidine affinity chromatography using HiTrap Chelating HP columns (GE Healthcare) and AKTA HLPC system (GE Healthcare) following the protocol previously described.[15,38] Protein concentration was determined by spectrophotometry using a Nanodrop device and measuring the OD at 280nm. Finally 50% (v/v) glycerol was added to the final fractions prior storage at −20°C. 0.5 µg of each purified protein was applied in an 8% SDS-PAGE and visualized by Coomassie blue staining (data not shown) to assess protein purity.

Activity assays

Exoribonucleolytic activity was assayed using three different RNA oligoribonucleotides as substrates.[15,38] The 30mer oligoribonucleotide (5′-CCCGACACCAACCACUAAAAAAAAA AAAAA-3′), the 16mer oligoribonucleotide (5′-CCCGACACCAACCACU-3′) and the poly(A) chain of 35 nt were labelled at its 5′-end with [γ-^{32}ATP] and T4 polynucleotide kinase. The RNA oligomers were then purified using Microcon YM-3 Centrifugal Filter Devices (Millipore) to remove the nonincorporated nucleotide. The labelled 30mer and 16mer oligoribonucleotides were hybridized to the complementary 16mer oligodeoxyribonucleotide (5′AGT GGT TGG TGT CGG G 3′), thus obtaining the corresponding double stranded substrate 16–30ds and 16-16ds, respectively. The hybridization was performed in a 1:1 (mol:mol) ratio in the Tris component of the activity by 5 min of incubation at 68°C followed by 45 min at 37°C. The exoribonucleolytic reactions were carried out in a final volume of 10 µl containing 30 nm of substrate, 20 m*M* Tris-HCl pH 8, 100 m*M* KCl, 1 m*M* $MgCl_2$, and 1 m*M* DTT. The amount of each enzyme added to the reaction was adjusted to obtain linear conditions and is indicated in the respective figures. Reactions were started by the addition of the enzyme and incubated at 37°C. Samples were withdrawn at the time points indicated in the figures, and the reaction was stopped by adding formamide-containing dye supplemented with 10 m*M* EDTA. Reaction products were resolved in a 20% polyacrylamide/7 *M* urea and analyzed by autoradiography. The exoribonucleolytic activity of the enzymes was determined by measuring and quantifying the disappearance of the substrate in several distinct experiments in which the protein concentration was adjusted in order that, under those conditions, less than 25% of substrate was degraded. Each value obtained represents the mean of these independent assays.

Surface plasmon resonance analysis—BIACORE

Surface Plasmon Resonance analysis was developed for the study of the interaction between RNases and RNA molecules as previously described.[38] Biacore SA chips were obtained from Biacore Inc. (GE Healthcare). The Flow cells of the SA streptavidin sensor chip were coated with a low concentration of the following substrates. On flow cell 1, no substrate was added so this cell could be used as the control blank cell. On flow cell 2, a 5′ biotinylated 25-nucleotide RNA oligomer (5′-CCC GAC ACC AAC CAC UAA AAA AAA A-3′) was added to allow the study of the protein interaction with a single-stranded RNA molecule. On flow cell 3, a 5′ biotinylated 30-mer PolyA substrate. The target substrates were captured on flow cells 2 and 3 by manually injecting 20 µl of a 500 nm solution of the substrates in 1 *M* NaCl at a 10 µl/min flow rate, as described in previous reports.[31,38,39] The biosensor assay was run at 4°C in the buffer with 20 m*M* Tris-HCl pH8, 100 m*M* KCl, 1 m*M* DTT and 25 m*M* EDTA. The proteins were injected over flow cells 1, 2, and 3 for 2 min at concentrations of 10, 20, 30, 40, and 50 n*M* using a flow rate of 20µl/min. All experiments included triple injections of each protein concentration to determine the reproducibility of the signal and control injections to assess the stability of the RNA surface during the experiment. Bound protein was removed with a 60-s wash with 2 *M* NaCl, which did not damage the substrate surface. Data from flow cell 1 were used to correct for refractive index changes and nonspecific binding. Rate constants and equilibrium constants were calculated using the BIA EVALUATION 3.0 software package, according to the fitting model 1:1 Languimir Binding. Obtained and fitted data are represented in Supporting Information Figure 1.

Secondary structure prediction of the lysine-rich tail of RNase R, protein modeling and multiple sequence alignment

To predict the secondary structure of the Lysine-rich tail of RNase R, we used the NPS@ server (Network Protein Sequence Analysis)[40] with the GOR4 method[41] (http://npsa-pbil.ibcp.fr).

Structural model of the *E. coli* RNase R protein as well as RNase II_S1_R and RNase R_RNB_II constructions were performed by standard comparative modeling methods and the software DeepView,[42] using the crystal structures of wild-type RNase II and the RNase II D209N mutant complexed with a 13-nucleotide poly(A) RNA as templates (PDB codes: 2IX1 and 2IX0[27]). To optimize geometries, models were energy minimized using the GROMOS 43B1 force field implemented in DeepView,[42] using 500 steps of steepest descent minimization followed by 500 steps of conjugate-gradient minimization. Sequence identity between RNase II and modeled RNase R was 26%, with a Blast e-value of 3.3×10^{-43}. The quality of the model was checked using the analysis programs (Anolea, Gromos and Verify3D) provided by the SWISS-MODEL server (http://swissmodel.expasy.org/[43–45]).

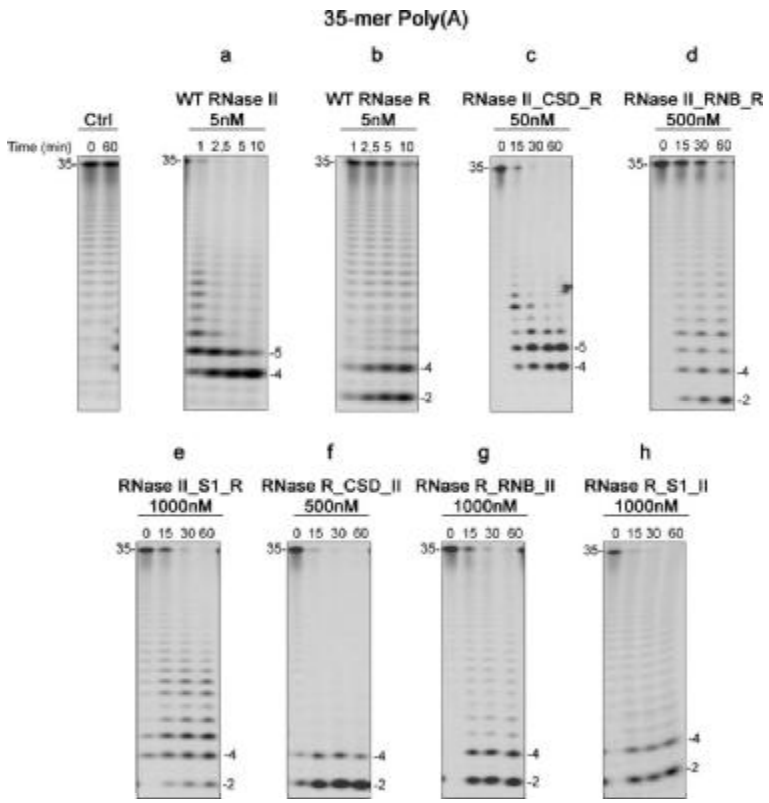

Figure 2

Exoribonuclease activity with a 35ss Poly(A) substrate: comparison of wild-type with hybrid enzymes. Activity assays were performed as described under Materials and Methods using a poly(A) chain of 35 nt. The proteins used and their respective concentrations are shown. The wild-type enzymes were used as control. Samples were taken during the reaction at the time points indicated, and reaction products were analyzed in a 20% polyacrylamide/7 *M* urea gel. Control reactions with no enzyme added (*Ctrl*) were incubated at the maximum reaction time for each protein. Length of substrates and degradation products are indicated in the figure.

Structures were manipulated using the Swiss-PDB viewer and were rendered using Pymol.[46]

Homologous sequences belonging to the to RNase II family of proteins in protein databases were obtained using Blast,[47] and they were aligned using ClustalW[48] and T-COFFEE[49] algorithms.

RESULTS

Characterizing the exoribonucleolytic activity of the hybrid proteins using poly(A) substrate

RNase II and RNase R are members of the same family of exoribonucleases and therefore share catalytic and structural properties. However, they behave differently regarding the final end-product released: while RNase II releases a 4 nt fragment as its end-product, RNase R releases a mixture of 2 nt and 4 nt fragments, but 2 nt is the predominant product [Fig. 2(a, b)].[15,19,20] The mechanism of RNase II has been elucidated and the size of the final product released depends on the aromatic residues Tyr-253 and Phe-358. that "clamp" the RNA.[27,29] In RNase R, Phe-429 is located in the position immediately downstream of the equivalent residue of Phe-358 in RNase II.[29] This residue may allow a partial "clamp" of the RNA and a 4 nt end-product is released. However, other oligoribonucleotides may still bind to the catalytic cavity and are able to be degraded up to the final 2 nt fragment.[16] Since these two enzymes

Table III
Exoribonucleolytic Activity of Wild Type and Hybrid Proteins

Protein	Protein Activity (pmol subst/nmol prot/min)
wt RNase II	299.4 ± 36.0
RNase II_CSD_R	0.5 ± 0.05
RNase II_RNB_R	0.05 ± 0.002
RNase II_S1_R	0.04 ± 0.001
RNase II _S1_R_ΔLys1	0.01 ± 0.001
RNase II _S1_R_ΔLys2	0.01 ± 0.001
RNase II _S1_R_ΔLys3	0.01 ± 0.001
RNase II D209N	<0.0001[29]
wt RNase R	130.8 ± 6.3
RNase R_CSD_II	0.04 ± 0.001
RNase R_RNB_II	0.02 ± 0.001
RNase R_S1_II	0.08 ± 0.002
RNase R D280N	<0.0001[16]

Exoribonucleolytic activity was assayed using a 35 nt poly(A) chain as substrate. Activity assays were performed in triplicate as described in Experimental Procedures.

also share a common 3D arrangement and have the same domain organization,[29] we were interested in studying which domain(s) would be responsible for these differences. For this purpose, we exchanged the domains between RNase II and RNase R and constructed six hybrid proteins. In the designation chosen, the first word represents the protein that "received" the other domain as explained in Figure 1. The constructed proteins are: RNase II_CSD_R, which consists of RNase II with the two cold shock domains and the helix turn helix region from RNase R; RNase II_RNB_R, which consists of RNase II with the RNB domain of RNase R; RNase II_S1_R that is RNase II with the S1 and basic region from RNase R; RNase R_CSD_II, in which the CSDs from RNase II substitute those of RNase R; RNase R_RNB_II, which consists of RNase R with the RNB from RNase II; and finally, RNase R_S1_II, in which the S1 domain from RNase II substitutes the S1 domain from RNase R (Fig. 1).

We started to analyze the protein activity by using a single-stranded poly(A) substrate. This substrate was chosen to determine the activity of the proteins, since it has been shown that RNase II family members reflect a marked preference for poly(A) substrates.[16,30] To determine the activity of the hybrid proteins, we tested several different protein concentrations, and performed the calculations in triplicate using the values where less than 25% of the substrate was degraded. The results obtained are presented in Table III and the units of activity refer to the pmol of substrate which is degraded by 1 n*M* of protein in 1 min. When compared with their wild type counterparts, we can see that the six engineered proteins have a reduced activity (Table III). The decrease in the activity of the hybrid proteins ranges from 600-fold (RNase II_CSD_R protein) to 7000-fold (RNase II_S1_R protein). However, when compared with the inactive mutants RNase II D209N and RNase R D280N (Table III), we can safely say that, although bearing a low activity, these proteins are still able to degrade RNA substrates. Since we are working with engineered proteins that do not exist in nature, we also need to consider the possibility that only a fraction of the hybrid proteins adopt a catalytically active conformation. In this case, the determination of the activity could be underestimated. Another objective of this work was to identify the end-product of each of these engineered proteins. To do so, we tested different conditions to ensure that all the enzymes had reached their end-product. As a consequence, we had to use higher protein concentrations for the hybrid proteins than those used for both RNase II and RNase R. Figures 2–5 show the representative assays from the several ones performed that we believe better illustrate the results obtained.

In RNase II_CSD_R, when we changed the CSDs of RNase II by the ones from RNase R we observed that the protein behaved like RNase II [Fig. 2(c)]. However, when we changed the RNB or S1 domains of RNase II by the equivalents of RNase R (as is the case in the RNase II_RNB_R and RNase II_S1_R proteins), we were able to see that the final product changed to 2 nt [Fig. 2(d, e)]. For RNase II_S1_R protein, it was possible to observe that the majority of the product released was a 4 nt fragment and only a small portion of substrate was able to be degraded until the 2 nt of length, contrary to what happened for RNase R [Fig. 2(e)]. Thus, we can conclude that the S1 and RNB domains from RNase R are each sufficient to allow RNase II to behave like RNase R, and generate the 2 nt end-product.

When we changed the RNase R domains by the ones in RNase II (RNase R_CSD_II, RNase R_RNB_II and RNase R_S1_II proteins), we observed that the final end-product released was always a 2 nt [Fig. 2(f–h)]. These results indicate that the RNB domain of RNase R is responsible for setting the final end-product. However, when the RNB domain of RNase II was inserted into RNase R (RNase R_RNB_II), the final product was not altered as expected, which suggested to us that the RNA binding domains of RNase R are also involved, probably by inducing a different conformation of the protein.

The hybrid proteins prefer poly(A) substrates

To see if the binding ability was affected in the hybrid proteins, we determined the dissociation constants by SPR using two different single-stranded substrates, a 25-nt RNA oligomer and a 30 nt poly(A) oligomer and compared them with the wild type enzymes (Table IV). In all the cases, and for all the proteins, the affinity constants determined using the 30 nt poly(A) substrate were always lower when compared with those detected using the other ssRNA substrate. This was expected, and indicates that, like in the cases of wild-type RNase II and

Table IV
RNA Binding Affinity of the Hybrid Proteins

Protein	K_D (nM) 25-mer	K_D (nM) PolyA
wt RNase II	6.5 ± 0.4	1.3 ± 0.4
RNase II_CSD_R	16.0 ± 0.4	4.3 ± 0.3
RNase II_RNB_R	7.0 ± 0.9	2.0 ± 0.3
RNase II_S1_R	3.2 ± 0.5	1.3 ± 0.1
wt RNase R	3.2 ± 0.4	1.2 ± 0.1
RNase R_CSD_II	8.6 ± 0.7	5.1 ± 0.1
RNase R_RNB_II	5.4 ± 0.6	4.4 ± 0.1
RNase R_S1_II	10.1 ± 1.4	3.2 ± 0.2

The dissociation constants (K_D) were determined by Surface Plasmon resonance using BIACORE 2000 with a 25 nt RNA oligomer (5′-Biotin-CCC GAC ACC AAC CAC UAA AAA AAA A-3′) and a 30 nt poly(A) RNA oligomer.

RNase R, the hybrid proteins constructed reflect their preference for poly(A) type substrates. However, in the case of RNase R_RNB_II and RNase R_S1_R that preference is not so marked (Table IV).

The results obtained also showed that, for almost all proteins, the affinity is slightly reduced for both substrates when compared with the wild type enzymes (Table IV). These differences are not significant, however, they can help us explain the reduction in the activity of the hybrid proteins, since the affinity of a protein is not always correlated with its activity. For example, the RNase II_D209N and RNase R_D280N mutants were inactive but the RNA affinity was not altered.[16,29,50]

Degradation of double-stranded substrates by hybrid proteins

To study which domains could be responsible for the differences regarding the ability to cleave double-stranded substrates, we tested the hybrid proteins against a 16–30ds substrate, that consists of a 30-mer ribonucleotide hybridized with a complementary 16-mer oligonucleotide, as described in Experimental Procedures. To detect the ribonucleolytic activity with this substrate, we tested several different concentrations of the various proteins to find the optimal conditions. In our assays, the hybrid proteins were active with double stranded substrates when using as little as 10 nm of protein. However, in such conditions it was difficult to determine which was the real final product released and if, in fact, the protein was degrading the substrate. For this reason, in Figure 3 the protein concentrations used in the assays are extremely high.

The results showed that when RNase II has the N-terminal region of RNase R (RNase II_CSD_R) the hybrid protein behaved like RNase II since it was not able to degrade double-stranded substrates. However, the protein was capable to degrade a few more nucleotides than RNase II, releasing a 20 nt fragment instead of the usual 23 nt fragment [Fig. 3(a, c)]. RNase II_RNB_R protein was able to cleave the 16–30ds substrate just like RNase R [Fig. 3(d)]. It was previously described that RNase R needs a 3′-single-stranded overhang of at least 7 nucleotides of length to attach to the substrate and proceed with the degradation[18] and it is not able to cleave a substrate in the absence of a 3′-end tail [Fig. 4(a)]. However, the hybrid protein RNase II_RNB_R did not present this requirement since it was able to degrade double-stranded substrates in the absence of a 3′-overhang [Fig. 4(c)], even though only a small percentage of the 16–16ds substrate was degraded. This fact confirms that, as previously demonstrated,[16] the RNB domain from RNase R is the one responsible for the degradation of double-stranded substrates. The substitution of only one RNase R binding domain (CSD or S1 domains) eliminates the requirement of a 3′ single-stranded overhang for the degradation of dsRNA substrates. Surprisingly, the RNase II_S1_R protein was also able to cleave double-stranded substrates releasing a fragment with 2 nt of length [Fig. 3(e)]. Nevertheless, for this protein the requirement for a 3′-overhang was essential since it was not able to cleave the perfect double-stranded substrate [Fig. 4(d)]. This suggests that the catalytic cavity of the protein is only accessible to single-stranded substrates, similarly to that which occurs with RNase II.[27] This implies that the RNA is entering into the catalytic cavity in a single-stranded form, which means that the substrate is being unwound before its entry. Thus, the domain responsible for this action must be the S1 domain from RNase R.

RNase R_CSD_II, RNase R_RNB_II and RNase R_S1_II proteins were able to cleave the double-stranded substrates similar to RNase R [Fig. 3(f–h)]. When the RNB domain of RNase R was substituted by the one of RNase II (RNase R_RNB_II), the protein was still able to cleave the double-stranded substrate [Fig. 3(g)]. In this case, the requirement for a 3′-overhang was also verified, since the protein was not able to degrade the 16–16ds substrate [Fig. 4(f)]. This suggests that the RNB domain from RNase R is not the only one responsible for the degradation of structured RNA.

In our work, we showed that the simple substitution of the RNB domain in RNase II for that of RNase R lead to the construction of a protein that was active against double-stranded substrates. The RNB domain does not seem to be acting alone in this process, because when switching the S1 domain from RNase II for the S1 domain from RNase R, the respective protein is also able to cleave double-stranded substrates (Fig. 3). However, it seems that the RNB and S1 domains may act differently against structured RNAs when they are in an RNase II context. While RNase R S1 domain requires a 3′single-stranded overhang to bind to the substrate and degrade it, the RNB domain from RNase R is able to bind and degrade structured RNAs in the absence of a tail, as previously demonstrated.[16] The results obtained led us to

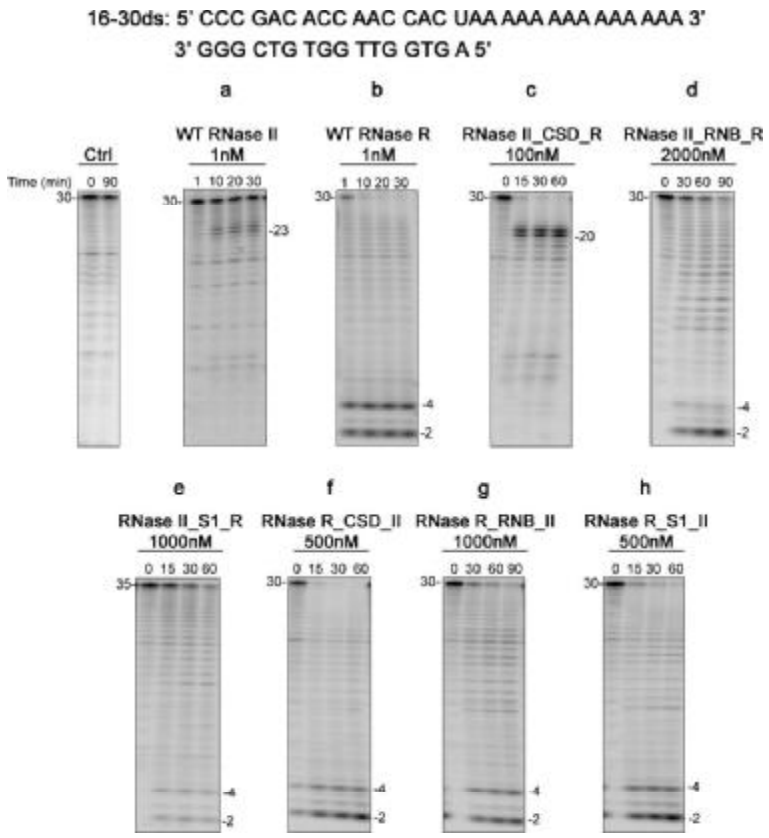

Figure 3

Exoribonuclease activity with 16–30ds substrate: comparison of wild-type with hybrid enzymes. Activity assays were performed as described under Material and Methods using a 30-mer oligoribonucleotide hybridized to the complementary 16mer oligodeoxyribonucleotide, thus obtaining the corresponding double stranded substrate 16–30ds. The proteins used and their respective concentrations are shown. The wild-type enzymes were used as control. Samples were taken during the reaction at the time points indicated, and reaction products were analyzed in a 20% polyacrylamide/7 *M* urea gel. Control reactions with no enzyme added (*Ctrl*) were incubated at the maximum reaction time for each protein. Length of substrates and degradation products are indicated in the figure.

further analyze the role of the C-terminal region of RNase R in the mechanism of degradation of double-stranded substrates.

Unravelling the role of the lysine-rich tail of RNase R

Since the S1 domain from RNase R is allowing the cleavage of double-stranded substrates, we wanted to discriminate which region could be conferring that property. By comparing the C-terminal region of both RNase II and RNase R proteins, it is possible to observe that, apart from the S1 domain, RNase R has an extra lysine-rich tail (Fig. 1). To understand the role of this region in RNA degradation, we predicted its secondary structure in the Network Protein Sequence Analysis as described in Experimental Procedures. The results predicted showed that this region is formed by four alpha-helices: the first (from the C-terminal end) comprises the last 22 aa of the protein, the second is formed by the aa 781 to 802, the third comprises aa 745 to 758 and the forth, which is smaller when compared with the others, is constituted by aa 728 to 738 (note that this numbering refers to RNase R and not to the hybrid protein, as indicated in the figure) (Fig. 1). To investigate the contribution of the three major alpha-helices in the degradation of double-stranded substrates, we

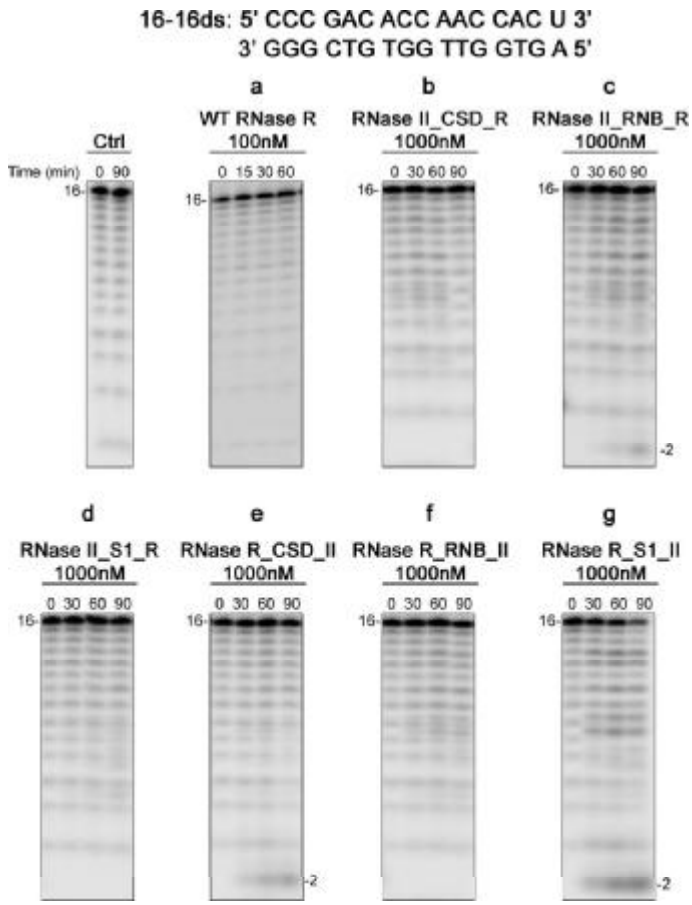

Figure 4

Exoribonuclease activity with 16–30ds substrate: comparison of wild-type with hybrid enzymes. Activity assays were performed as described under Material and Methods using a 16-mer oligoribonucleotide hybridized to the complementary 16mer oligodeoxyribonucleotide, thus obtaining the corresponding double stranded substrate 16–16ds. The proteins used and their respective concentrations are shown. The wild-type enzymes were used as control. Samples were taken during the reaction at the time points indicated, and reaction products were analyzed in a 20% polyacrylamide/7 *M* urea gel. Control reactions with no enzyme added (*Ctrl*) were incubated at the maximum reaction time for each protein. Length of substrates and degradation products are indicated in the figure.

introduced three stop codons into the hybrid protein RNase II_S1_R as indicated in Figure 1, thus obtaining the three proteins, RNase II_S1_RΔlys1, RNase II_S1_RΔlys2 and RNase II_S1_RΔlys3, which lack one, two or three alpha-helices, respectively. The determination of the role of the C-terminal region of the S1 domain from RNase R in the degradation of double-stranded substrates was performed in an RNase II context, using the hybrid protein RNase II_S1_R. The mutations were introduced in this protein and not in RNase R wt because the RNB domain of RNase R by itself is able to degrade double-stranded substrates[16] and this characteristic could bias the results obtained. The proteins were then analyzed regarding their activity against single- and double-stranded substrates and RNA affinity.

We also determined the exoribonucleolytic activity of these three proteins, and we could observe that the activity is 4-fold reduced when we compare with RNase II_S1_R (Table III). This indicates that the Lysine-rich tail is also contributing for the activity of RNase II_S1_R

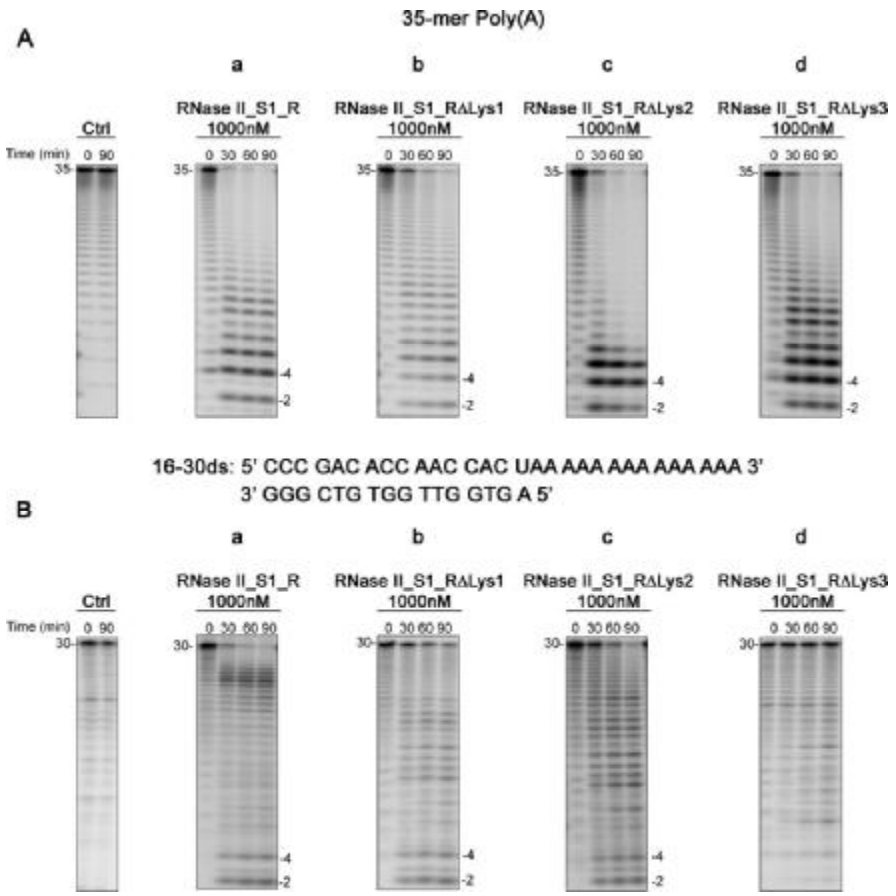

Figure 5

Exoribonuclease activity of RNase II_S1_R and ΔLys mutants. Activity assays were performed as described under Materials and Methods using a poly(A) chain of 35 nt (A), and a 30-mer oligoribonucleotide hybridized to the complementary 16mer oligodeoxyribonucleotide, thus obtaining the corresponding double stranded substrate 16–30ds (B). The proteins used and their respective concentrations are shown. The wild-type enzyme was used as control. Samples were taken during the reaction at the time points indicated, and reaction products were analyzed in a 20% polyacrylamide/7 *M* urea gel. Control reactions with no enzyme added (*Ctrl*) were incubated at the maximum reaction time for each protein. Length of substrates and degradation products are indicated in the figure.

protein. When the substrate used was the single-stranded one, the results obtained were similar to those obtained for the RNase II_S1_R hybrid protein, since all the three proteins tested released a 2 nt fragment as end-product [Fig. 5(A)]. When we tested the double stranded-substrate 16–30ds, we could observe some differences between these proteins. As already mentioned, the RNase II_S1_R is able to cleave double-stranded substrates. The same behaviour is observed when the first and second alpha helices are absent (in RNase II_S1_R_Δlys1 and RNase II_S1_R_Δlys2 proteins) [Fig. 5B(b, c)]. However, when we removed all three helices, the protein RNase II_S1_R_Δlys3 was not able to degrade the substrate tested [Fig. 5B(d)]. These results indicate that the Lysine-rich region can be involved in the degradation of double-stranded substrates in RNase R. We also measured the RNA affinity of these proteins with the two different substrates tested previously and compared the data with the values obtained with the RNase II_S1_R protein (Table V). For both substrates used it was possible to see that the K_D value raised slightly when the helices were removed. In the case of the 25ss substrate, the hybrid

Table V
RNA Binding Affinity of the Δlys Hybrid Proteins

Protein	K_D (nM) 25-mer	K_D (nM) PolyA
RNase II_S1_R	3.2 ± 0.5	1.3 ± 0.1
RNase II _S1_RΔLys1	4.2 ± 0.4	1.4 ± 0.3
RNase II _S1_RΔLys2	5.5 ± 0.9	1.4 ± 0.1
RNase II _S1_RΔLys3	6.9 ± 0.2	2.4 ± 0.3

The dissociation constants (K_D) were determined by Surface Plasmon resonance using BIACORE 2000 with a 25 nt RNA oligomer (5′-Biotin-CCC GAC ACC AAC CAC UAA AAA AAA A-3′) and a 30 nt poly(A) RNA oligomer.

protein II_S1_R presented a K_D value that was equivalent to the one presented by RNase R, which was 3.2 nm for both proteins (Table V). When the three helices were absent, the K_D value presented by the II_S1_R_Δlys3 protein became closer to the one presented by RNase II wt (6.9 ± 0.2 and 6.5 ± 0.4 nm, respectively). The results obtained indicate that the lysine rich tail from RNase R is also responsible for a higher affinity for some RNA substrates.

DISCUSSION

To understand which domains are responsible for the differences observed between RNase II and RNase R regarding the RNA degradation, we switched domains between them and analyzed the activity of the six hybrid proteins against single- and double-stranded substrates.

When we used a single-stranded substrate, we observed that the presence of the RNB domain from RNase R in RNase II changed the final product from 4 to a mixture of 4 and 2 nt [Fig. 2(d)]. This result clearly indicates that it is in the RNB domain of both proteins that resides the difference regarding the releasing of the final product after cleavage. However, when the RNB domain from RNase II was inserted into RNase R, the end-product was not altered to 4 nt as expected by the previous result [Fig. 2(g)]. One possible explanation for this could be the fact that the differences in both RNB domains can not be related with the amino acid sequence but with the conformation that the protein acquires when it is folded. In the RNase R_RNB_II protein, the presence of the CSD and S1 domains of RNase R can lead to a subtle conformational rearrangement of the catalytic cavity in the RNB domains of RNase II. To elucidate this question, we modelled both proteins and compared them with RNase II structure[27] and RNase R model[29] [Fig. 6(a)]. In fact, by comparing the four models, it is possible to see that all proteins share an almost identical structure. If we analyze in more detail the catalytic cavity of all proteins, no dramatic changes are observed (data not shown). So, it appears that the differences observed in the activity of these enzymes are not due to changes in the overall protein structure. A suitable explanation could be the different nature of the residues located in S1 domain in close contact to RNA [Fig. 6(b–d), purple residues]. In RNase II, the residues in S1 domain which are in close contact with the RNA molecule are Ser572, Gly574, Phe588, Pro590, Pro592, Phe593, Arg632, Thr635, and Ser637 as indicated in Figure 5B. In the protein RNase II_S1_R, the residues from the S1 domain from RNase R that contact the RNA molecule are different (Thr655, Phe657, Leu671, His673, Ser675, Ser676, Asn714, Glu717, Lys719), that implies differences in the properties of the relationship between RNA and S1 [Fig. 6(c)]. When compared with other proteins of the family, the nature of RNA-contacting residues is, as expected, more conserved among members of the same sub-family (RNase II sub-family versus RNase R sub-family) and, to some extent, different between these sub-families [Fig. 6(d)]. Moreover, when comparing the interactions between the RNB and the S1 domains of RNase II [Fig. 6(b)] and the RNB of RNase II with the S1 from RNase R [Fig. 6(c)], it is possible to observe differences regarding the residues involved in the contact of the S1 domain with the RNB. While in S1 domain from RNase II the residues in contact with the RNB domain are Arg577, Arg579, Asn583, Glu606, Lys619, Val620, and Thr621, in the RNase II_S1_R protein we can see that Phe660, Arg662,Leu666, Ile668, Gln689, Arg701, Leu702, and Gly703 are the ones involved in this interaction [Fig. 6(b–d)]. The residues responsible for the domain-domain interactions in the S1 domain are conserved between sub-families but not conserved in RNase II and RNase R [Fig. 6(d)]. The different nature of the residues in S1 domain that contact to the same residues in RNB domain (as this domain is conserved both in RNase II and RNase II_S1_R proteins) could be responsible for changes in the relative position of S1 domain from RNase in the overall structure of the RNase II_S1_R protein [Fig. 6(c)]. It could not be discarded that the alterations in the interactions of the RNB and S1 domains in this hybrid protein may induce a subtle conformational change in some residues near the catalytic cavity. These modifications may result in a higher affinity for RNA in the catalytic cavity, and a fraction of the 4 nt fragments can still bind to the protein and be cleaved until they reach the 2 nt of length.

When we determined the K_D values of the hybrid proteins we observed that with the poly(A) substrate the affinity was reduced when compared with the 25-mer. This indicates that, like for wild-type RNase II and RNase R, the hybrid proteins also reflect their marked preference for poly(A) type substrates.

Regarding the degradation of the double-stranded substrate, five of the six hybrid proteins tested were able to overcome the secondary structures and degrade the substrates totally. It was previously described that the RNB domain from RNase R is able, by itself, to degrade double-stranded substrates.[16,17] So, it was not a surprise to see that when we switched the RNB domain from RNase

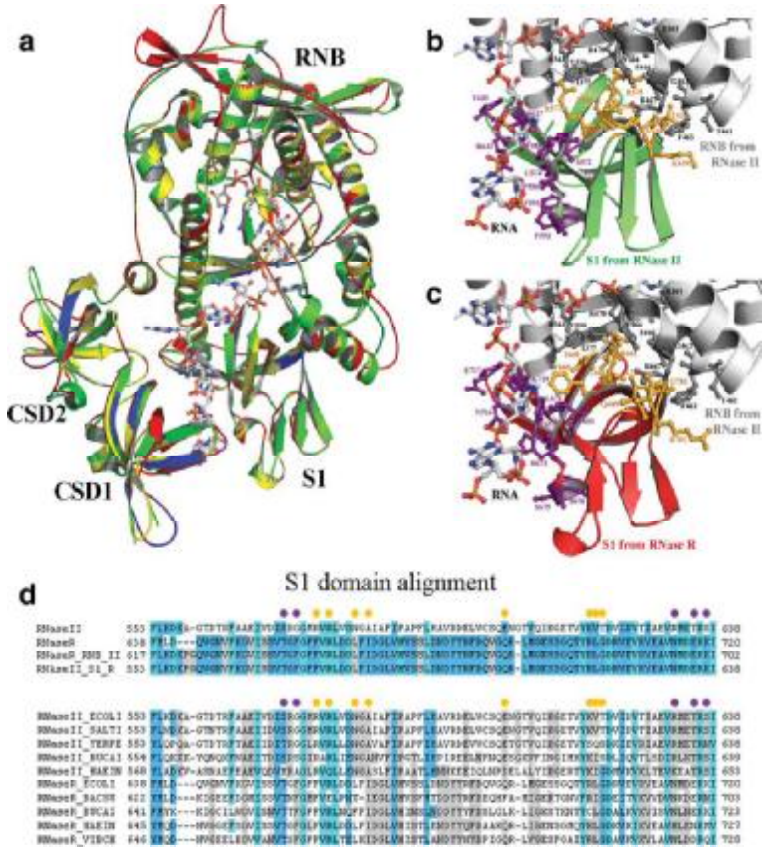

Figure 6

Modelling the hybrid proteins RNase II_S1_R and RNase R_RNB_II. (**a**) Representation of RNase II structure (green) and the predictive 3D models of the *E. coli* RNase R (red), RNase II_S1_R (yellow) and RNase R_RNB_II (blue) proteins (**b**) Residues of S1 domain from RNase II (green cartoon, residues in purple) in close contact to RNA: Ser572, Gly574, Phe588, Pro590, Pro592, Phe593, Arg632, Thr635 and Ser637; Residues of S1 domain from RNase II (residues in orange—Arg577, Arg579, Asn583, Glul606, Lys619, Val620 and Thr621) in close contact to RNB domain from RNase II (residues in dark grey—Arg361, Tyr364, Ile377, Thr461, Gly462, Phe463, Ser466, Arg467, Arg470, Arg543, and Tyr550). (**c**) Residues of S1 domain from RNase R (red cartoon, residues in purple) in close contact to RNA: Thr655, Phe657, Leu671, His673, Ser675, Ser676, Asn714, Glu717 and Lys719); Residues of S1 domain from RNase R (residues in orange—Phe660, Arg662, Leu666, Ile668, Gln689, Arg701, Leu702 and Gly703) in close contact to RNB domain from RNase II (residues in dark grey—Arg361, Tyr364, Ile377, Thr461, Gly462, Phe463, Ser466, Arg467, Arg470, Arg543, and Tyr550). (**d**) Top: structure alignment of the S1 domain of RNase II, RNase R and the constructed polypeptides RNase R_RNB_II and RNaseII_S1_R. Bottom: alignment of the S1 domain of RNase II and RNase R from different bacteria (*Escherichia coli* –ECOLI-, *Salmonella typhimurium* –SALTI-, *Yersinia pestis* –YERPE-, *Buchnera aphidicola* -BUCAI-, *Haemophilus influenzae* –HAEIN-, *Bacillus subtilis* –BACSU- *and Vibrio cholerae* –VIBCH-). Sequences from *E. coli* are included in both alignments for comparison purposes. Multiple alignments are coloured according to conservation. Position of some important residues is highlighted: purple dots—residues in S1 domain contacting RNA molecule; orange dots—residues in S1 domain contacting RNB domain.

II for the one from RNase R, the resultant protein was able to cleave double-stranded substrates. The same was valid for the hybrid proteins where the RNB of RNase R is present (RNase R_CSD_II and RNase R_S1_II). We also observed that the requirement of a single-stranded 3′ overhang to degrade dsRNA is a property resulting from the association of the RNB domain with the CSD and S1 RNA binding domains of RNase R.

The most intriguing result was obtained with the RNase II_S1_R and RNase R_RNB_II proteins. In both cases, the RNB from RNase R is not present and the proteins are still able to overcome secondary structures (Fig.

3). The common element between these proteins is the S1 domain from RNase R, thus this domain has to be the one responsible for the behaviour observed for these proteins. Moreover, the degradation of structured RNA molecules by the S1 domain implies the existence of a 3′-single-stranded overhang for cleavage to occur. In fact, in the C-terminal region of RNase R there is a lysine-rich region positioned after the S1 domain, and this feature is absent in S1 from RNase II (Fig. 1). Recently it was shown that the Lysine-rich region of RNase R is important for recruitment of stalled ribosomes and for the selection of defective transcripts to be degraded.[51] If we analyze other proteins from the RNase II-family of enzymes, we can see that this Lysine-rich tail is only present in RNase R-like proteins, which led us to hypothesize that it could be also involved in the degradation of structured RNAs. The results obtained confirm that, in an RNase II context, the lysine-rich region is important for the degradation of double-stranded substrates. Our results are in agreement with recent findings that show that RNase R could have some helicase activity which is conferred by the binding domains.[52] Our experiments indicate that the helicase activity could be of the responsibility of the S1 domain of RNase R, namely of the lysine-rich tail in the C-terminus of the protein, which can be responsible for the unwinding of the substrate. Moreover, we showed that this activity is intrinsic to RNase R, since this protein was able to degrade double-stranded substrates in the absence of ATP, in contrast to other helicases.

With this work we intended to unravel the different modes of action between the two major *E. coli* exoribonucleases, RNase II and RNase R, namely we aimed to explain their different behaviours. With the lack of the 3D structure of RNase R, only biochemical and modelling studies can help disclose the differences between these two homologue enzymes, belonging to the same RNase II family of proteins. In this report we show that both S1 and RNB domains from RNase R, in separate, allow the appearance of the characteristic 2 nt end-product and the degradation of double-stranded substrates. Finally, we demonstrated that the degradation of structured RNAs is tail-independent when the catalytic domain from RNase R is no longer associated with the RNA binding domains from RNase R.

As such, the results obtained in this report can be extrapolated for the comprehension of the mode of action of other members of the RNase II family. Moreover, this work represents a major breakthrough in the distinction between these two so close but yet so different exoribonucleases.

ACKNOWLEDGMENTS

We thank Prof. Arsénio M. Fialho for the critical reading, and Miguel Luís for helping with the images. We also thank Biomol-Informatics SL <www.biomol-informatics.com> for bioinformatics advising. R. G. Matos was a recipient of a PhD fellowship and A. Barbas was a recipient of a Post Doctoral fellowship, both of them funded by FCT- Fundação para a Ciência e a Tecnologia, Portugal.

REFERENCES

1. Grossman D, van Hoof A. RNase II structure completes group portrait of 3′ exoribonucleases. Nat Struct Mol Biol 2006;13:760–761.
2. Mian IS. Comparative sequence analysis of ribonucleases HII, III, II PH and D. Nucleic Acids Res 1997;25:3187–3195.
3. Mitchell P, Petfalski E, Shevchenko A, Mann M, Tollervey D. The exosome: a conserved eukaryotic RNA processing complex containing multiple 3′—>5′ exoribonucleases. Cell 1997;91:457–466.
4. Zuo Y, Deutscher MP. Exoribonuclease superfamilies: structural analysis and phylogenetic distribution. Nucleic Acids Res 2001;29:1017–1026.
5. Arraiano CM, Andrade JM, Domingues S, Guinote IB, Malecki M, Matos RG, Moreira RN, Pobre V, Reis FP, Saramago M, Silva IJ, Viegas SC. The critical role of RNA processing and degradation in the control of gene expression. FEMS Microbiol Rev 2010;34:883–923.
6. Cheng ZF, Zuo Y, Li Z, Rudd KE, Deutscher MP. The vacB gene required for virulence in Shigella flexneri and Escherichia coli encodes the exoribonuclease RNase R. J Biol Chem 1998;273:14077–14080.
7. Cheng ZF, Deutscher MP. An important role for RNase R in mRNA decay. Mol Cell 2005;17:313–318.
8. Cairrão F, Arraiano CM. The role of endoribonucleases in the regulation of RNase R. Biochem Biophys Res Commun 2006;343:731–737.
9. Cairrão F, Cruz A, Mori H, Arraiano CM. Cold shock induction of RNase R and its role in the maturation of the quality control mediator SsrA/tmRNA. Mol Microbiol 2003;50:1349–1360.
10. Andrade JM, Cairrão F, Arraiano CM. RNase R affects gene expression in stationary phase: regulation of ompA. Mol Microbiol 2006;60:219–228.
11. Dziembowski A, Lorentzen E, Conti E, Seraphin B. A single subunit, Dis3, is essentially responsible for yeast exosome core activity. Nat Struct Mol Biol 2007;14:15–22.
12. Schaeffer D, Tsanova B, Barbas A, Reis FP, Dastidar EG, Sanchez-Rotunno M, Arraiano CM, van Hoof A. The exosome contains domains with specific endoribonuclease, exoribonuclease and cytoplasmic mRNA decay activities. Nat Struct Mol Biol 2009;16:56–62.
13. Lebreton A, Tomecki R, Dziembowski A, Seraphin B. Endonucleolytic RNA cleavage by a eukaryotic exosome. Nature 2008;456:993–996.
14. Cheng ZF, Deutscher MP. Purification and characterization of the Escherichia coli exoribonuclease RNase R. Comparison with RNase II. J Biol Chem 2002;277:21624–21629.
15. Amblar M, Barbas A, Fialho AM, Arraiano CM. Characterization of the functional domains of Escherichia coli RNase II. J Mol Biol 2006;360:921–933.
16. Matos RG, Barbas A, Arraiano CM. RNase R mutants elucidate the catalysis of structured RNA: RNA-binding domains select the RNAs targeted for degradation. Biochem J 2009;423:291–301.
17. Vincent HA, Deutscher MP. The roles of individual domains of RNase R in substrate binding and exoribonuclease activity: the nuclease domain is sufficient for digestion of structured RNA. J Biol Chem 2009;284:486–494.
18. Vincent HA, Deutscher MP. Substrate recognition and catalysis by the exoribonuclease RNase R. J Biol Chem 2006;281:29769–29775.
19. Amblar M, Barbas A, Gomez-Puertas P, Arraiano CM. The role of the S1 domain in exoribonucleolytic activity: substrate specificity and multimerization. RNA 2007;13:317–327.

20. Cannistraro VJ, Kennell D. The processive reaction mechanism of ribonuclease II. J Mol Biol 1994;243:930–943.
21. Domingues S, Matos RG, Reis FP, Fialho AM, Barbas A, Arraiano CM. Biochemical characterization of the RNase II family of exoribonucleases from the human pathogens Salmonella typhimurium and Streptococcus pneumoniae. Biochemistry 2009;48:11848–11857.
22. Deutscher MP, Reuven NB. Enzymatic basis for hydrolytic versus phosphorolytic mRNA degradation in Escherichia coli and Bacillus subtilis. Proc Natl Acad Sci USA 1991;88:3277–3280.
23. Cairrão F, Chora A, Zilhao R, Carpousis AJ, Arraiano CM. RNase II levels change according to the growth conditions: characterization of gmr, a new Escherichia coli gene involved in the modulation of RNase II. Mol Microbiol 2001;39:1550–1561.
24. Zilhão R, Cairrão F, Régnier P, Arraiano CM. PNPase modulates RNase II expression in Escherichia coli: implications for mRNA decay and cell metabolism. Mol Microbiol 1996;20:1033–1042.
25. Zilhão R, Camelo L, Arraiano CM. DNA sequencing and expression of the gene rnb encoding Escherichia coli ribonuclease II. Mol Microbiol 1993;8:43–51.
26. Arraiano CM, Matos RG, Barbas A. RNase II: the finer details of the *Modus Operandi* of a molecular killer. RNA Biol 2010;7:276–278.
27. Frazão C, McVey CE, Amblar M, Barbas A, Vonrhein C, Arraiano CM, Carrondo MA. Unravelling the dynamics of RNA degradation by ribonuclease II and its RNA-bound complex. Nature 2006;443:110–114.
28. Zuo Y, Vincent HA, Zhang J, Wang Y, Deutscher MP, Malhotra A. Structural basis for processivity and single-strand specificity of RNase II. Mol Cell 2006;24:149–156.
29. Barbas A, Matos RG, Amblar M, Lopez-Viñas E, Gomez-Puertas P, Arraiano CM. New insights into the mechanism of RNA degradation by ribonuclease II: identification of the residue responsible for setting the RNase II end product. J Biol Chem 2008;283:13070–13076.
30. Barbas A, Matos RG, Amblar M, Lopez-Vinas E, Gomez-Puertas P, Arraiano CM. Determination of key residues for catalysis and RNA cleavage specificity: one mutation turns RNase II into a "super-enzyme." J Biol Chem 2009;284:20486–20498.
31. Matos RG, Barbas A, Arraiano CM. Comparison of EMSA and SPR for the characterization of RNA-RNase II complexes. Protein J 2010;29:394–397.
32. Andrade JM, Hajnsdorf E, Regnier P, Arraiano CM. The poly(A)-dependent degradation pathway of rpsO mRNA is primarily mediated by RNase R. RNA 2009;15:316–326.
33. Erova TE, Kosykh VG, Fadl AA, Sha J, Horneman AJ, Chopra AK. Cold shock exoribonuclease R (VacB) is involved in Aeromonas hydrophila pathogenesis. J Bacteriol 2008;190:3467–3474.
34. Tobe T, Sasakawa C, Okada N, Honma Y, Yoshikawa M. vacB, a novel chromosomal gene required for expression of virulence genes on the large plasmid of Shigella flexneri. J Bacteriol 1992;174:6359–6367.
35. Tsao MY, Lin TL, Hsieh PF, Wang JT. The 3′-to-5′ exoribonuclease (encoded by HP1248) of Helicobacter pylori regulates motility and apoptosis-inducing genes. J Bacteriol 2009;191:2691–2702.
36. Taylor RG, Walker DC, McInnes RR. E. coli host strains significantly affect the quality of small scale plasmid DNA preparations used for sequencing. Nucleic Acids Res 1993;21:1677–1678.
37. Studier FW, Moffatt BA. Use of bacteriophage T7 RNA polymerase to direct selective high-level expression of cloned genes. J Mol Biol 1986;189:113–130.
38. Arraiano CM, Barbas A, Amblar M. Characterizing ribonucleases in vitro examples of synergies between biochemical and structural analysis. Methods Enzymol 2008;447:131–160.
39. Park S, Myszka DG, Yu M, Littler SJ, Laird-Offringa IA. HuD RNA recognition motifs play distinct roles in the formation of a stable complex with AU-rich RNA. Mol Cell Biol 2000;20:4765–4772.
40. Combet C, Blanchet C, Geourjon C, Deleage G. NPS@: network protein sequence analysis. Trends Biochem Sci 2000;25:147–150.
41. Garnier J, Gibrat JF, Robson B. GOR method for predicting protein secondary structure from amino acid sequence. Methods Enzymol 1996;266:540–553.
42. Guex N, Peitsch MC. SWISS-MODEL and the Swiss-PdbViewer: an environment for comparative protein modeling. Electrophoresis 1997;18:2714–2723.
43. Kiefer F, Arnold K, Kunzli M, Bordoli L, Schwede T. The SWISS-MODEL repository and associated resources. Nucleic Acids Res 2009;37(Database issue):D387–D392.
44. Arnold K, Bordoli L, Kopp J, Schwede T. The SWISS-MODEL workspace: a web-based environment for protein structure homology modelling. Bioinformatics 2006;22:195–201.
45. Schwede T, Kopp J, Guex N, Peitsch MC. SWISS-MODEL: an automated protein homology-modeling server. Nucleic Acids Res 2003;31:3381–3385.
46. DeLano WL. The PyMOL molecular graphics system, 0.83 ed. San Carlos, CA: DeLano Scientific; 2002.
47. Altschul SF, Madden TL, Schaffer AA, Zhang J, Zhang Z, Miller W, Lipman DJ. Gapped BLAST and PSI-BLAST: a new generation of protein database search programs. Nucleic Acids Res 1997;25:3389–3402.
48. Thompson JD, Higgins DG, Gibson TJ. CLUSTAL W: improving the sensitivity of progressive multiple sequence alignment through sequence weighting, position-specific gap penalties and weight matrix choice. Nucleic Acids Res 1994;22:4673–4680.
49. Notredame C, Higgins DG, Heringa J. T-Coffee: a novel method for fast and accurate multiple sequence alignment. J Mol Biol 2000;302:205–217.
50. Amblar M, Arraiano CM. A single mutation in Escherichia coli ribonuclease II inactivates the enzyme without affecting RNA binding. FEBS J 2005;272:363–374.
51. Ge Z, Mehta P, Richards J, Karzai AW. Non-stop mRNA decay initiates at the ribosome. Mol Microbiol 2010;78:1159–1170.
52. Awano N, Rajagopal V, Arbing M, Patel S, Hunt J, Inouye M, Phadtare S. *Escherichia coli* RNase R has dual activities, helicase and ribonuclease. J Bacteriol 2010;192:1344–1352.

FEMS MICROBIOLOGY REVIEWS

REVIEW ARTICLE

The critical role of RNA processing and degradation in the control of gene expression

Cecília M. Arraiano, José M. Andrade, Susana Domingues, Inês B. Guinote, Michal Malecki, Rute G. Matos, Ricardo N. Moreira, Vânia Pobre, Filipa P. Reis, Margarida Saramago, Inês J. Silva & Sandra C. Viegas

Instituto de Tecnologia Química e Biológica, Universidade Nova de Lisboa, Apartado, Oeiras, Portugal

Correspondence: Cecília M. Arraiano, Instituto de Tecnologia Química e Biológica, Universidade Nova de Lisboa, Apartado 127, 2781-901 Oeiras, Portugal. Tel.: +351 214 469 547; fax: +351 214 469 549; e-mail: cecilia@itqb.unl.pt

Received 30 April 2010; revised 18 June 2010; accepted 20 June 2010.
Final version published online July 2010.

DOI:10.1111/j.1574-6976.2010.00242.x

Editor: William Margolin

Keywords
RNases; RNA; post-transcriptional control of gene expression.

Abstract

The continuous degradation and synthesis of prokaryotic mRNAs not only give rise to the metabolic changes that are required as cells grow and divide but also rapid adaptation to new environmental conditions. In bacteria, RNAs can be degraded by mechanisms that act independently, but in parallel, and that target different sites with different efficiencies. The accessibility of sites for degradation depends on several factors, including RNA higher-order structure, protection by translating ribosomes and polyadenylation status. Furthermore, RNA degradation mechanisms have shown to be determinant for the post-transcriptional control of gene expression. RNases mediate the processing, decay and quality control of RNA. RNases can be divided into endonucleases that cleave the RNA internally or exonucleases that cleave the RNA from one of the extremities. Just in *Escherichia coli* there are $>$ 20 different RNases. RNase E is a single-strand-specific endonuclease critical for mRNA decay in *E. coli*. The enzyme interacts with the exonuclease polynucleotide phosphorylase (PNPase), enolase and RNA helicase B (RhlB) to form the degradosome. However, in *Bacillus subtilis*, this enzyme is absent, but it has other main endonucleases such as RNase J1 and RNase III. RNase III cleaves double-stranded RNA and family members are involved in RNA interference in eukaryotes. RNase II family members are ubiquitous exonucleases, and in eukaryotes, they can act as the catalytic subunit of the exosome. RNases act in different pathways to execute the maturation of rRNAs and tRNAs, and intervene in the decay of many different mRNAs and small noncoding RNAs. In general, RNases act as a global regulatory network extremely important for the regulation of RNA levels.

Introduction

General outline

Many cellular mechanisms cannot be fully understood without a profound knowledge of the RNA metabolism. Protein production depends not only on the levels of mRNAs but also on other RNA species. The translation of mRNAs is mediated by tRNAs and rRNAs and functional RNAs also intervene in the regulation of gene expression. Synergies between the structure and function of RNAs contribute towards orchestrating their fundamental role in cell viability.

Bacterial mRNAs are rapidly degraded and this allows the microorganisms to rapidly adapt to changing environments. Even though transcription is quite important to determine steady-state levels, increasingly it is being established that the role of post-transcriptional control is critical in the regulation of gene expression. Analyzing RNA degradation in prokaryotes has been particularly difficult not only due to the coupling of transcription, translation and mRNA degradation but also because most mRNAs undergo a rapid exponential decay with an average of 1.3 min at 37 °C. The rRNAs and tRNAs are usually more stable, but in order to be functionally active, they have to be processed to the mature form. It has been shown that the levels of small noncoding RNAs (sRNAs) are also highly dependent on post-transcriptional events. The knowledge collected makes it clear how far our understanding of RNA degradation has come in the last few years and how much remains to be discovered about this important genetic regulatory process. Applications of this knowledge in medicine and biotechnology are underway.

RNases are the enzymes that intervene in the processing, degradation and quality control of all types of RNAs. A limited number of RNases can exert a determinant level of control acting as a global regulatory network, monitoring and adapting the RNA levels to the cell needs. Many of them are essential, but others exhibit a functional overlap and are interchangeable. RNases can act alone or they can cooperate in RNA degradation complexes. During RNA degradation, they do not only act as 'molecular killers' eliminating RNA species. RNases act according to the requirements of growth in adaptation to the environment; they play an extremely important role in contributing to the recycling of ribonucleotides, and also carry out surveillance, destroying aberrant RNAs that would produce detrimental proteins.

Individual RNA species differ widely with respect to their stability. The rate of turnover has no relation to the length of the gene, the segments that decay more rapidly can be anywhere in the mRNA and the stability of the gene transcripts seems to be regulated by determinants localized to specific mRNA segments. Secondary structure features can also influence the degradation by RNases.

Several factors can intervene in the decay mechanism: the sequence/structure of RNAs can act as stabilizer or destabilizer elements to specific RNases; the presence of ribosomes during active translation can hide some RNA loci that are vulnerable to RNases; poly(A) stretches are the preferred substrate for several RNases – therefore, the addition of poly(A) tails can modulate the stability of full-length transcripts and degradation intermediates and accelerate the decay of defective stable RNAs; *trans*-acting factors can bind to the RNAs and expose or hide RNA sites that are preferential targets for RNases – for instance, the host factor Hfq is known to bind sRNAs and affect their turnover; and other factors such as helicases can act in *trans* and contribute to RNA degradation because they unwind RNA structures and can change their accessibility to RNases.

In this review, we will focus on RNA processing and degradation in *Escherichia coli*, but we will also provide comparative examples from many other microorganisms. Namely, we will include the description of enzymes that exist in *Bacillus subtilis* and are absent in *E. coli*, we will provide examples from archaea and we will also include a section that makes a parallel to what happens in yeast.

We will start by describing most of the known RNases, characterizing their structure and function and the regulation of their expression. They will be divided into endonucleases, which cleave the RNA internally, and exonucleases, which cleave the RNA from one of the extremities. After the characterization of RNases, we will focus on their protein complexes involved in decay mechanisms. Then we will focus on the 'RNases in action'. Examples will be provided regarding the processing and degradation of RNAs. We will describe the maturation of rRNAs and tRNAs, and characterize the decay of many different mRNAs and sRNAs. Finally, we will compare with what is known in eukaryotic microorganisms, namely yeast. A small degree of overlap is unavoidable between sections on related topics. This allows for each section to be read and understood as an independent unit.

This review is intended to be an exhaustive and updated overview of what is known on RNAs, RNases and the post-transcriptional control of gene expression in microorganisms. It is expected that it can be used as a reference to put in perspective the critical role of RNA processing and degradation as a major global regulatory network.

Endonucleases

RNase E

RNase E, encoded by the *rne* gene, was first identified by a temperature-sensitive mutation (*rne-3071*) (Apirion & Lassar, 1978) and was initially described as an activity required for the processing of the *E. coli* 9S rRNA gene (Ghora & Apirion, 1978). The *ams* (altered mRNA stability) locus was also identified by a temperature-sensitive mutation (*ams-1*) (Ono & Kuwano, 1980) and was shown to play an important role in *E. coli* RNA turnover (Ono & Kuwano, 1979). The combination of the Ams and RNase II ts-alleles plus deficiency in polynucleotide phosphorylase (PNPase) was shown to substantially increase the half-life of bulk mRNA, and specific messengers were highly stabilized in the *ams-1 rnb-500 pnp-7* mutant (Arraiano *et al.*, 1988). Later, it was shown that these two previously identified genes, *rne* and *ams*, were actually different mutant alleles of the same gene encoding RNase E (Mudd *et al.*, 1990; Babitzke & Kushner, 1991; Melefors & von Gabain, 1991; Taraseviciene *et al.*, 1991). This important endonuclease is essential for cell growth, and the inactivation of temperature-sensitive mutants impedes processing and prolongs the lifetime of bulk mRNA (Apirion & Lassar, 1978; Ono & Kuwano, 1979; Arraiano *et al.*, 1988; Mudd *et al.*, 1990; Babitzke & Kushner, 1991; Melefors & von Gabain, 1991; Taraseviciene *et al.*, 1991). It has been reported that RNase E plays a central role in the processing of precursors of the 5S rRNA gene (Apirion & Lassar, 1978; Misra & Apirion, 1979), the 16S rRNA gene (Li *et al.*, 1999b), tRNAs (Ow & Kushner, 2002), transfer mRNA (tmRNA) (Lin-Chao *et al.*, 1999) and the M1 RNA component of the RNase P ribozyme (Lundberg & Altman, 1995; Ko *et al.*, 2008). Homologues of RNase E have been identified in > 50 bacteria, archaea and plants (Lee & Cohen, 2003).

Escherichia coli RNase E is a 1061-residue enzyme composed of two distinct functional regions (Fig. 1a). The amino-terminal half forms the catalytic domain (residues 1–529) and is relatively conserved among prokaryotes (Marcaida *et al.*, 2006). The carboxy-terminal half of RNase

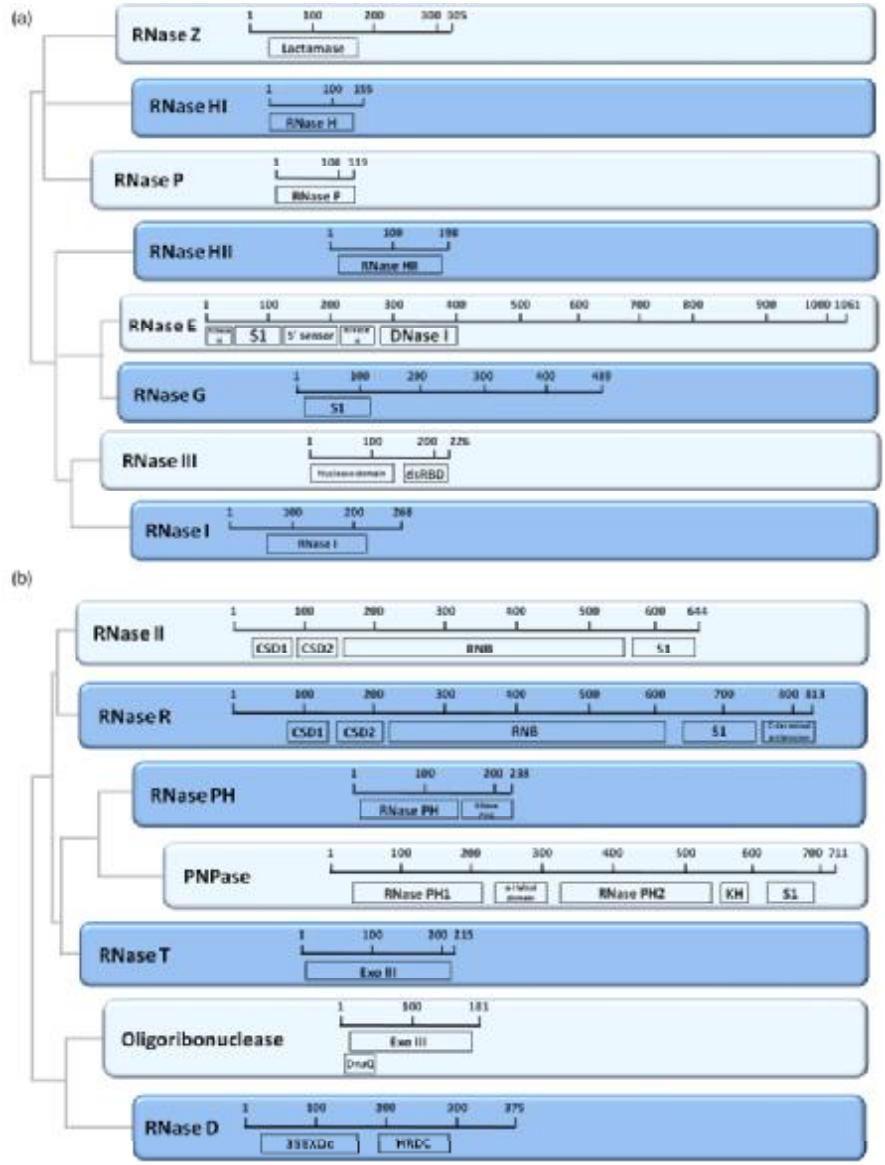

Fig. 1. Representative dendrograms of the endoribonucleases (a) and exoribonucleases (b) of *Escherichia coli*. This representation was based on the amino acid sequence of each enzyme, after a multiple alignment using the CLUSTAL program (Thompson *et al*., 1997). Near each enzyme is the length (number of amino acids) and architecture, emphasizing the domains of each enzyme. This representation was made based on the CDART program (Geer *et al.*, 2002). These dendrograms were adapted from Barbas *et al.* (2006).

E (residues 530–1061) is a noncatalytic region, largely unstructured and poorly conserved (Callaghan *et al.*, 2004). Segment A is located between residues 565 and 582 and is responsible for binding of RNase E to the inner cytoplasmic membrane (Khemici *et al.*, 2008). Residues 601–700 form an arginine-rich segment that binds RNA *in vitro* and that is

believed to enhance the activity of RNase E in mRNA degradation *in vivo* (Lopez *et al.*, 1999; Ow *et al.*, 2000). Residues 701–1061 form a scaffold for interactions between RNase E and the other major components of the degradosome, a protein complex involved in mRNA decay (see Complexes of RNases) (Kaberdin *et al.*, 1998; Vanzo *et al.*, 1998).

The first crystal structure for a member of the RNase E family has been determined at 2.9 Å, and it reveals that the catalytic domain of RNase E forms a homotetramer with a molecular mass of roughly 260 kDa, organized as a dimer of dimers (Callaghan *et al.*, 2005a). Each protomer is composed of two globular portions: the 'large' and 'small' domains. The 'large' domain can be divided into four subdomains that closely resemble established folds. One is related to the RNase H endoribonuclease family, but is inactive. In this subdomain an S1 domain is embedded and has a fold that participates in the recognition of the 5′ terminus of RNA (5′-sensor). The rest of the large domain is similar to the repetitive structural element within the endodeoxyribonuclease DNase I. In isolation, each protomer appears elongated, with a large domain comprising the subdomains (S1, 5′-sensor, RNase H and DNase I), an elongated linker region (Zn-link) and then the small domain. The dimer–dimer interface is formed by the small domains. At the junction point, there is a zinc-binding site (Callaghan *et al.*, 2005a, b). The arrangement of the domains within each dimer resembles the blades and handles of an open pair of scissors.

Escherichia coli RNase E is a single-stranded, nonspecific endonuclease with a preference for cleaving A/U-rich sequences (Mackie, 1992; McDowall *et al.*, 1995). *In vitro* experiments have shown that purified *E. coli* RNase E prefers to cleave RNAs that are monophosphorylated at the 5′ end (Mackie, 1998). Recently, it was shown that RNA pyrophosphohydrolase (RppH) converts the 5′ terminus of primary transcripts from a triphosphate to a monophosphate (Celesnik *et al.*, 2007; Deana *et al.*, 2008). However, some structured substrates can be cleaved independent of its state of phosphorylation by RNase E even if the 5′ end forms a secondary structure (Baker & Mackie, 2003; Hankins *et al.*, 2007). This indicates that while the 5′-monophosphate-dependent pathway makes a significant contribution to mRNA degradation (Mackie, 1998, 2000), there is another pathway of initial substrate recognition by RNase E termed 'bypass' or 'internal entry' (Baker & Mackie, 2003; Kime *et al.*, 2009).

The crystal structure explains some features of the protein and suggests a mechanism of RNA recognition and cleavage. A pocket is formed between the 5′-sensor and the RNase H subdomains and can bind a monophosphate group at a 5′ end (Callaghan *et al.*, 2005a). The catalytic site is physically separated from the 5′-sensing site. It contains conserved residues on the surface of the DNase I subdomain of RNase E and coordinate a magnesium ion implicated in catalysis. A 'mouse-trap' model for communication between the 5′-sensing pocket and the site of catalysis has been suggested: S1- and 5′-sensing domains move together as one body to clamp down the substrate (Koslover *et al.*, 2008). This conformational change suggests a mechanism of RNA recognition and catalysis that explains the enzyme's preference for substrates with a 5′-monophosphate over a 5′-triphosphate and 5′-hydroxyl RNA. Substantial flexibility was also observed at one of the dimer–dimer interfaces, a deformation that may be essential to accommodate structured RNA for processing by internal entry.

The cellular level and activity of RNase E are subject to complex regulation. First, the enzyme concentration in the cell is regulated by a feedback loop in which RNase E modulates the decay of its own mRNA, maintaining the level of the enzyme within a narrow range (Mudd & Higgins, 1993; Jain & Belasco, 1995; Diwa *et al.*, 2000; Sousa *et al.*, 2001; Ow *et al.*, 2002). Second, the efficiency of RNase E cleavage depends on the structure of the substrates and the accessibility of putative cleavage sites. A 5′-monophosphate in substrate RNAs serves as an allosteric activator of RNase E activity (Mackie, 1998; Jiang & Belasco, 2004). Third, interactions of mRNA targets with Hfq and sRNAs play an important role in the cleavage of certain mRNAs by RNase E (Wagner *et al.*, 2002). Fourth, the activity of RNase E is globally affected by protein inhibitors, namely the L4 ribosomal protein, RraA and RraB (the regulator of RNase activity A and B, respectively) that interact with RNase E and inhibit RNase E endonucleolytic cleavages of a selective group of transcripts (Lee *et al.*, 2003; Gao *et al.*, 2006). Fifth, the membrane localization of RNase E and its association with the bacterial cytoskeleton may affect its function through various mechanisms (Liou *et al.*, 2001; Khemici *et al.*, 2008; Taghbalout & Rothfield, 2008).

Some variants of RNase E can be found in *Alphaproteobacteria*, *Synechocystis* spp. and in the high G+C Gram-positive bacteria (Condon & Putzer, 2002). In *Rhodobacter capsulatus*, RNase E is the enzyme responsible for the majority of the endonucleolytic cleavages. *Rhodobacter capsulatus* RNase E (118 kDa) has a conserved N-terminal region (Jäger *et al.*, 2001) and a C-terminal portion, probably involved in the scaffold of degradosome assembly. It was purified in two different complexes: one where it is associated with a helicase and an unidentified protein and the other, which was coupled with a helicase, Rho and an unidentified protein (Jäger *et al.*, 2001). Moreover, in *R. capsulatus*, this enzyme is involved in the endonucleolytic processing and stabilization of *cspA* mRNA (Jäger *et al.*, 2004). Similar to *R. capsulatus*, *Pseudomonas syringae*, a psychrophilic bacterium, also has an RNase E that is associated with RNase R and the DEAD-box helicase RhlE in a degradosome (see Complexes of RNases) (Purusharth *et al.*, 2005).

RNase G

Escherichia coli RNase G was initially identified by its role in chromosome segregation and cell division (Okada *et al.*, 1994). Overproduction of this protein led to morphological changes in which the bacteria formed anucleated chained cells containing long axial filaments, justifying its former name, *cafA* (cytoplasmic axial filament) (Okada *et al.*, 1994). RNase G was subsequently shown to exhibit endonuclease activity both *in vivo* (Li *et al.*, 1999b; Wachi *et al.*, 1999; Umitsuki *et al.*, 2001) and *in vitro* (Jiang *et al.*, 2000; Tock *et al.*, 2000). RNase G is a paralogue of RNase E (McDowall *et al.*, 1993), belonging to the RNase E/G family, and is also involved in the degradation and processing of RNA (Carpousis *et al.*, 2009).

A strong resemblance has been identified between RNase G and the amino-terminal portion of *E. coli* RNase E, sharing a high level of sequence identity (35%) and similarity (50%) (McDowall *et al.*, 1993) (Fig. 1a). Purified RNase G has *in vitro* properties similar to RNase E and both enzymes are required for a two-step sequential reaction of 5′ maturation of the 16S rRNA gene (Li *et al.*, 1999b; Wachi *et al.*, 1999). Their activity is 5′ end dependent and both RNases attack substrates in A+U-rich regions (Jiang *et al.*, 2000; Tock *et al.*, 2000). Moreover, residues of RNase E that can contact a 5′-monophosphorylated end and coordinate the catalytic magnesium ion are conserved in RNase G (McDowall *et al.*, 1993; Callaghan *et al.*, 2005a). RNase G seems to have a higher preference for 5′-monophosphorylated substrates than RNase E (Tock *et al.*, 2000) and the precise cleavage sites of RNase E and RNase G are not strictly conserved (Li *et al.*, 1999b; Tock *et al.*, 2000). The 5′-monophosphate end, which stimulates RNase G, is generated by RppH (Deana *et al.*, 2008) or by other endonucleases (Lee *et al.*, 2002).

Whereas cells lacking RNase E are normally nonviable (Apirion & Lassar, 1978; Ono & Kuwano, 1979), RNase G is dispensable for viability (Li *et al.*, 1999b; Wachi *et al.*, 1999) and is present in lower abundance (Lee *et al.*, 2002). Some functional homology between RNase G and RNase E was suggested by the observations that RNase G expression can confer viability to the *rne* deletion mutant strain (Lee *et al.*, 2002). However, at intracellular physiological levels, RNase G cannot complement RNase E mutations (Lee *et al.*, 2002; Ow *et al.*, 2003). Recently, single amino acid changes in the predicted RNase H domain of RNase G led to complementation of RNase E deletion mutants, suggesting that this region of the two proteins may help distinguish their *in vivo* biological activities (Chung *et al.*, 2010). However, these RNase G mutant proteins do not fully substitute RNase E in mRNA decay and tRNA processing (Chung *et al.*, 2010).

Microarray data showed that RNase G controls the level of transcripts associated with sugar metabolism centered on glycolysis (*adhE*, *pgi*, *glk*, *nagB*, *acs*, *eno*, *tpiA*) (Lee *et al.*, 2002), and it has been shown that strains defective in RNase G produce increased levels of pyruvic acid (Sakai *et al.*, 2007). These results suggest that RNase G is involved in the regulation of central metabolism.

RNase III

RNase III was originally identified by Robertson *et al.* (1968) in extracts of *E. coli* as the first specific double-stranded RNA (dsRNAs) endoribonuclease. Members of the RNase III family are widely distributed among prokaryotic and eukaryotic organisms, sharing structural and functional features (Lamontagne *et al.*, 2001) (Fig. 1a). However, until now, homologues of RNase III have not been found in the genomes of archaea (Condon & Putzer, 2002). All enzymes of this family are hydrolytic and have a specificity for dsRNAs, generating 5′-monophosphate and 3′-hydroxyl termini with a two-base overhang at the 3′ end (Meng & Nicholson, 2008). The RNase III family comprises four classes, according to their polypeptide structure. The class I is the simplest, containing an endonuclease domain (NucD), characterized in several bacteria by the presence of a highly conserved amino acid stretch NERLEFLGDS, and a dsRNA-binding domain (dsRBD) (Blaszczyk *et al.*, 2001). The class II is exemplified by the *Drosophila melanogaster* Drosha protein, which contains a long N-terminal extension, followed by two NucD and a single dsRBD. The class III is represented by Dicer, which has an N-terminal helicase/ATPase domain, followed by a domain of unknown function (DUF283), a centrally positioned Piwi Argonaute Zwille (PAZ) domain and a C-terminal configuration like Drosha, consisting of two NucD and one dsRBD (Drider & Condon, 2004; MacRae & Doudna, 2007). Finally, the class IV is only represented, to date, by the Mini-RNase III of *B. subtilis*, which is constituted by a single NucD domain (Redko *et al.*, 2008).

The class I members of the RNase III family are ubiquitously found in bacteria, bacteriophages and some fungi (MacRae & Doudna, 2007). *Escherichia coli* RNase III has served as the prototypical member of the family. In this model microorganism, RNase III is encoded by the *rnc* gene, and is active as a 52 kDa homodimer (Li & Nicholson, 1996). Each monomer contains a C-terminal dsRBD, located in the last 74 amino acids, which is responsible for substrate recognition and adopts a tertiary fold with the characteristic α_1-β_1-β_2-β_3-α_2 structure that is conserved throughout the RNase III family (Blaszczyk *et al.*, 2001). Additionally, each monomer contains an N-terminal NucD. When the two monomers are combined (RNase III homodimer), they form a single processing center in the subunit interface, in which each monomer contributes to the hydrolysis of one RNA strand of the duplex substrate. Ji and

colleagues (Blaszczyk *et al.*, 2004; Gan *et al.*, 2006) resolved the structure of the hyperthermophilic bacteria *Aquifex aeolicus* RNase III and the data have revealed two functional forms of dsRNA binding by RNase III: a catalytic form, functioning as a dsRNA-processing enzyme, cleaving both natural and synthetic dsRNA, and a noncatalytic form, in which RNase III plays the role of a dsRNA-binding protein (without cleaving). The latter activity is in agreement with previous studies in which this enzyme binds certain substrates in order to influence gene expression, affecting RNA structures (Court, 1993; Oppenheim *et al.*, 1993; Dasgupta *et al.*, 1998; Calin-Jageman & Nicholson, 2003). Furthermore, magnesium (Mg^{2+}) is the preferred cofactor. Recent data are indicative that each active site contains two divalent cations during substrate hydrolysis (Meng & Nicholson, 2008).

The RNase III substrate selection consists of a combination of structural determinants and sequence elements referred to as reactivity epitopes, such as the helix length, the strength of base-pairing or the occurrence of specific nucleotide pairs (termed proximal and distal boxes) located at defined positions related to the cleavage site. In addition, there are also two classes of double-helical elements that can function as negative determinants, which can either inhibit the recognition of this endoribonuclease or suppress the cleavage (without affecting recognition) (Zhang & Nicholson, 1997; Pertzev & Nicholson, 2006b).

RNase III in *E. coli* is not essential; however, it was observed that mutants for this endoribonuclease have a slow-growth phenotype (Nicholson, 1999). This enzyme was initially identified due to its role in the maturation of tRNA precursors and rRNA. Regarding the maturation of rRNA, RNase III is involved in the processing of 16S and 23S from a 30S rRNA gene precursor (Babitzke *et al.*, 1993). In *Salmonella* and other members of *Alphaproteobacteria*, RNase III is also responsible for the cleavage of the intervening sequences (IVS) found in their 23S rRNA gene (Evguenieva-Hackenberg & Klug, 2000), and is also involved in the decay of several mRNA species (Condon & Putzer, 2002; Calin-Jageman & Nicholson, 2003). For example, in *E. coli*, this enzyme participates in the first step of the decay of *pnp* mRNA (Régnier & Portier, 1986), the gene encoding PNPase, downregulating its synthesis (Régnier & Grunberg-Manago, 1990; Robert-Le Meur & Portier, 1992; Jarrige *et al.*, 2001). Interestingly, this endoribonuclease also has the ability to regulate its own synthesis with a specific cleavage near the 5′ end of its own mRNA that removes a stem loop, which acts as a degradation barrier (Bardwell *et al.*, 1989; Matsunaga *et al.*, 1996).

RNase III participates as a stress response modulator, controlling the steady-state levels of genes involved in cellular adaptation to stress (Santos *et al.*, 1997; Freire *et al.*, 2006; Sim *et al.*, 2010). It was seen in *Salmonella typhimurium* that RNase III regulates the levels of the sRNA MicA (Viegas *et al.*, 2007), a main regulator of the abundant outer membrane protein OmpA that plays an important structural role in the cell and is involved in pathogenesis (Guillier *et al.*, 2006). The enzyme is also involved in the decay of sRNA/mRNA complexes upon translational silencing (Vogel *et al.*, 2004; Afonyushkin *et al.*, 2005; Huntzinger *et al.*, 2005; Kaberdin & Blasi, 2006). In this way, cleavage by RNase III within the sRNA/mRNA duplex and the resulting subsequent decay of the mRNA intermediate by the *E. coli* RNA decay machinery could resemble the RNA interference (RNAi) in the eukaryotic cells (Agrawal *et al.*, 2003). RNAi is an evolutionarily conserved phenomenon that functions as a safeguard for the maintenance of genomic integrity. This phenomenon allows the selective post-transcriptional downregulation of target genes in the cells, in which RNase III-like enzymes dictate the degradation of dsRNA molecules (Jagannath & Wood, 2007; Ma *et al.*, 2007; Jinek & Doudna, 2009). Accordingly, the RNase III family has been associated with gene expression regulation, potential antivirus agents and tumor suppressors (Lamontagne *et al.*, 2001).

Bs-RNase III is a homologue of *E. coli* RNase III in *B. subtilis*. It is a 28-kDa protein (Mitra & Bechhofer, 1994), encoded by the *rncS* gene (Mitra & Bechhofer, 1994; Herskovitz & Bechhofer, 2000). In contrast to *E. coli* and *Staphylococcus aureus*, where the RNase III gene can be deleted without loss of viability, in *B. subtilis* and in the yeast, *Saccharomyces cerevisiae* and *Schizosaccharomyces pombe*, this enzyme is essential (Huntzinger *et al.*, 2005). Although the local environment of the site of Bs-RNase III cleavage appears to be very similar to that of *E. coli* RNase III, there are important differences in their substrate specificity (Mitra & Bechhofer, 1994; Wang & Bechhofer, 1997). Some of the substrates for this enzyme are the 30S ribosomal precursor RNA (Wang & Bechhofer, 1997) and the small cytoplasmic RNA (scRNA) (Oguro *et al.*, 1998; Yao *et al.*, 2007). More recently, another RNase III-like protein was identified in *B. subtilis* called Mini-III, reported to be involved in 23S rRNA gene maturation (Redko *et al.*, 2008). Interestingly, like Bs-RNaseIII, Mini-III does not seem to have endogenous mRNA substrates (Bechhofer, 2009). In *Lactococcus lactis*, RNase III is encoded by the *rnc* gene and plays a determinant role in the control of *citQRP* mRNA stability (Drider *et al.*, 1998, 1999). Complementation assays performed in *E. coli* showed that *L. lactis* RNase III can process *E. coli* rRNAs and regulate the levels of PNPase mRNA, substituting the endogenous RNase III (Amblar *et al.*, 2004).

Taken together, the functional and evolutionary conservation of the RNase III family in bacteria and higher organisms is indicative of their biological relevance in RNA maturation and degradation. Despite the fact that RNase E is

considered the major RNase that catalyzes the initial rate-determining cleavage of several transcripts, the RNase III family of enzymes has emerged as one of the most important groups of endoribonucleases in the control of RNA stability (Jaskiewicz & Filipowicz, 2008).

RNase H

Both RNase III and RNase H are representatives of components of the RNAi machinery and both are Mg^{2+}-dependent hydrolytic endoribonucleases. The analysis of the crystal structure of *E. coli* RNase H (Yang *et al.*, 1990) revealed the stepwise participation of two magnesium atoms in the enzyme mechanism (Nowotny & Yang, 2006).

RNases H are enzymes that cleave the RNA of RNA/DNA hybrids that are formed during replication and repair, preventing aberrant chromosome replication (for a review, see Condon & Putzer, 2002; Worrall & Luisi, 2007; Tadokoro & Kanaya, 2009). It is a ubiquitous enzyme distributed among all domains of life, and three different RNase H enzymes have been identified (HI, HII and HIII) (Ohtani *et al.*, 1999). In *E. coli*, 95% of RNase H activity is provided by RNase HI (widely distributed in *Proteobacteria*) and the remainder by RNase HII (Fig. 1a). In *B. subtilis*, RNase H activity is mostly provided by RNase HII and HIII. RNase H activity is essential to both bacteria. Thus, the inactivation of one of the *rnh* genes, but not both, is tolerated in these two organisms (Itaya *et al.*, 1999; Ohtani *et al.*, 1999).

RNase HII is widely distributed in bacteria and archaea, while RNase HIII is only present in a limited number of bacteria (Ohtani *et al.*, 1999). Proteins similar to HI and HII (named H1 and H2, respectively) can also be found in eukaryotes, but are larger and more complex than their prokaryotic counterparts (see Cerritelli & Crouch, 2009 for a review). The RNase H domain was also described in retroviruses (RNase HI), where it is associated with a reverse transcriptase (Davies *et al.*, 1991; Mian, 1997).

The PIWI domain of the eukaryotic Argonaute proteins, involved in RNA silencing, is structurally similar to the RNase H domain and conserves the residues necessary for RNase H endonucleolytic activity (Song *et al.*, 2004; Kitamura *et al.*, 2010). The eukaryotic Ago proteins showing endonuclease activity (slicer) can digest one RNA strand of the RNA/RNA hybrid. In contrast, the few prokaryotic Ago proteins known show a higher affinity for RNA/DNA hybrids. Very recently, it was reported for the first time that *Pyrococcus furiosus* RNase HII (*pf*-RNase HII) can digest an RNA/RNA hybrid in the presence of Mn^{2+} (Kitamura *et al.*, 2010).

RNase P

RNase P is a ribozyme considered to be a vestige from the 'RNA world'. It was discovered by Sidney Altman, almost 40 years ago (Robertson *et al.*, 1972), and for this, he received the Nobel Prize in Chemistry in 1989. This ancestral protein is a quasi-universal endoribonuclease found in all three domains of life: Bacteria, Eukarya (and eukaryotic organelles) and Archaea. RNase P is best known for universally catalyzing the endonucleolytic cleavage of the extra nucleotides in the 5′ end of the pre-tRNAs to generate the mature tRNAs (for a recent review by Sidney Altman, see Liu & Altman, 2009).

This ribozyme appears to have adapted to modern cellular life by adding protein to the RNA catalytic core. The bacterial version is the most simple, with a single RNA [350–400 nucleotide (nt), encoded by the *rpnB* gene] and a single small protein subunit (approximately 15 kDa, encoded by the *rpnA* gene) (Fig. 1a), both essential for cell viability (Shiraishi & Shimura, 1986; Kirsebom *et al.*, 1988; Baer *et al.*, 1989). In archaea and eukaryotes, the RNA subunit is bound by multiple proteins (at least four and nine proteins, respectively) with no relationship with their bacterial counterpart (Hall & Brown, 2002).

Five distinct structural classes of RNase P RNAs have been defined, based on the RNA secondary structure. In bacteria, two distinct types predominate: the A type (for ancestral), represented by *E. coli* RNase P RNA, and the B type (for *Bacillus*), confined to the low G+C Gram-positive bacteria (Chen *et al.*, 1998; Massire *et al.*, 1998; Smith *et al.*, 2007). Although evolution retained the catalysis function associated with the RNA subunit, the protein(s) play vital supporting roles. The higher protein : RNA mass ratio in the archaeal and eukaryal holoenzymes reflects a recruitment of protein cofactors during evolution, broadening the substrate spectrum in the more complex cellular environments (Liu & Altman, 1994).

In the bacterium *A. aeolicus*, candidate genes for *rpnA* and *rpnB* could not be identified (Willkomm *et al.*, 2002; Lombo & Kaberdin, 2008). However, recent work has demonstrated the existence of an RNase P-like activity in this hyperthermophilic bacterium (Marszalkowski *et al.*, 2008). The universality of RNase P is also challenged in the archaeon *Nanoarchaeum equitans* in which tRNAs are transcribed as primary 5′ mature tRNAs, and therefore, RNase P activity has been dispensed (Randau *et al.*, 2008). In eukaryotes, a different exception occurs. Human mitochondria and higher plant chloroplasts possess a protein-only version of the enzyme, known as 'Proteinaceous RNase P', which lacks the RNA subunit (Holzmann *et al.*, 2008; Gobert *et al.*, 2010). In this case, RNase P enzymes seem to have lost the RNA component during evolution.

Despite less efficiently than with tRNAs, RNase P has been shown to cleave other substrates, both *in vivo* and *in vitro*. Namely, the *E. coli* enzyme processes two other important stable RNA substrates involved in protein synthesis: the tmRNA (Gimple & Schon, 2001) and 4.5S RNA (Bothwell

et al., 1976; Peck-Miller & Altman, 1991). Other substrates include phage-induced regulatory RNAs (Hartmann *et al.*, 1995), sRNA duplex substrates and snoRNAs (Ko & Altman, 2007; Yang & Altman, 2007), riboswitches (Altman *et al.*, 2005; Seif & Altman, 2008) and intergenic regions of polycistronic operon mRNAs (Alifano *et al.*, 1994; Li & Altman, 2003).

Catalysis by RNase P RNA is hydrolytic and absolutely dependent on divalent metal ions (Mg^{2+} or Mn^{2+}) (Smith *et al.*, 1992; Kirsebom & Trobro, 2009). Its turnover rate is slow compared with other enzymes, what may reflect a specialization for cleavage-site selectivity and recognition of several different substrates rather than for rapid catalysis. This would explain the complex nature of this ancient ribozyme.

RNase Z

RNase Z is a conserved endonuclease that belongs to the β-lactamase superfamily of metal-dependent hydrolases (Fig. 1a). Genes encoding RNase Z homologues were identified in all three domains of life (Minagawa *et al.*, 2004; de la Sierra-Gallay *et al.*, 2005). The enzyme is mainly responsible for the 3′ end maturation of tRNAs.

Mature tRNAs all bear a CCA sequence at the end of the acceptor stem that is essential for aminoacylation and interaction with the ribosome. Two main modes for 3′ tRNA processing have been described: (1) a one-step maturation involving direct endonucleolytic cleavage by RNase Z at the 3′ end (CCA less tRNAs). The cleavage occurs after the discriminator base (the unpaired nucleotide immediately upstream the CCA motif) (Nashimoto, 1997; Pellegrini *et al.*, 2003) and provides the substrate for subsequent CCA addition by tRNA nucleotidyltransferase to generate the mature tRNA (Deutscher, 1990; Nashimoto, 1997; Schiffer *et al.*, 2002); and (2) multistep maturation involving endo- and exonucleases (e.g. in *E. coli* where all genes have the CCA encoded). Hence, the presence or not of the universal 3′-terminal CCA sequence in the tRNA primary transcript is the key determinant for the 3′-tRNA processing pathway (Deutscher, 1990; Schiffer *et al.*, 2002). In organisms such as *B. subtilis*, both types of 3′-tRNA processing may occur (see the section below on processing).

While the RNase Z gene is essential in *B. subtilis* for cell viability (Schilling *et al.*, 2004), in *E. coli*, mutants lacking RNase Z have no obvious growth phenotype (Schilling *et al.*, 2004). The *E. coli* RNase Z, also known as the ElaC protein, was initially identified as a zinc phosphodiesterase, ZiPD (Vogel *et al.*, 2002; Schilling *et al.*, 2004). It had been identified several years before as RNase BN, initially thought to be a cobalt-activated RNase with exonuclease activity (Asha *et al.*, 1983). The enzyme was required for the maturation of tRNA precursors encoded by phage T4. However, the gene encoding RNase BN (*rbn*) was originally misidentified, and was only recently shown to be the *elaC* gene, known to encode RNase Z (Ezraty *et al.*, 2005). Therefore, the *E. coli* enzyme is still called RNase BN occasionally. Other denominations include tRNase Z, 3′-tRNase and 3′-pre-tRNase.

The enzyme is a zinc-dependent metallo-hydrolase, and like RNase P, recognizes the tRNA structure in precursor molecules (Pellegrini *et al.*, 2003). RNase Z crystal structures have revealed that the enzyme forms a dimer of metallo-β-lactamase domains and has a characteristic domain, named a flexible arm or an exosite, which protrudes from the metallo-β-lactamase core and is involved in tRNA binding (de la Sierra-Gallay *et al.*, 2005). In the case of *Thermotoga maritima*, the structure of the flexible arm of the enzyme is different from those of homologue enzymes and may explain why, in this bacterium, tRNase Z exceptionally cleaves precisely after the CCA sequence (at 3′) and not after the discriminator base (Ishii *et al.*, 2005).

The intriguing presence of an RNase Z homologue in some members of the *Gammaproteobacteria*, such as *E. coli* and *Salmonella* spp., even though its action is not needed for tRNA maturation, has led to a search for other potential substrates for RNase Z. Surprising results were obtained when the *rnz* mutation was combined with a mutation in RNase E. The lack of both enzymes resulted in a drastic increase in the half-live compared with the absence of either enzyme alone (Perwez & Kushner, 2006a). These authors also observed that *E. coli* RNase Z was able to cleave *rpsT* mRNA *in vitro* at locations distinct from those obtained with RNase E. The enzyme is also capable of cleaving unstructured RNA substrates (Shibata *et al.*, 2006).

Deutscher and coworkers proposed that the *E. coli* enzyme (RNase BN) may differ in certain respects from the RNase Z homologues in other organisms; namely, it can have a dual exo- and an endoribonuclease activity (Dutta & Deutscher, 2009, 2010). This dual activity was also seen in RNase J from *B. subtilis*, another member of the zinc-dependent metallo-β-lactamases family (see the section on Other endonucleases) (Mathy *et al.*, 2007).

Other endonucleases

Several other endonucleases have been described not only in *E. coli* but also in other microorganisms. Below, we will briefly mention some of their main characteristics.

RNase I is a broad-specificity endoribonuclease, very active, present in the periplasmic space of *E. coli*. The enzyme belongs to the T2 superfamily of RNases, whose members are widely distributed throughout nature (Irie, 1997; Condon & Putzer, 2002) (Fig. 1a). Although RNase I activity is easily detected, its function in cell metabolism has never been clarified, because RNase I-deficient mutants are viable and do not affect global mRNA degradation (Zhu

et al., 1990). The enzyme can cleave RNA between every residue to yield mononucleotides and its activity is not inhibited in the presence of EDTA. It was proposed to be implicated in the scavenging of ribonucleotides from the extracellular environment (Condon & Putzer, 2002).

There are reports of other broad-specificity endoribonucleases that are RNase I related, namely, RNase I* (Cannistraro & Kennell, 1991) and RNase M (Cannistraro & Kennell, 1989). However, their existence was never confirmed and seems to consist merely of different manifestations of RNase I (Subbarayan & Deutscher, 2001).

Escherichia coli RNase LS is an RNase that, despite playing a minor role in noninfected bacteria (reviewed in Uzan, 2009), seems to constitute an important cellular defense mechanism against bacteriophage invasion (Otsuka & Yonesaki, 2005). Namely, bacteriophage T4 uses a combination of host- and phage-encoded enzymes to degrade its mRNAs in a stage-dependent manner. Phage T4 encodes RegB, a sequence-specific endoribonuclease (Sanson & Uzan, 1995; Uzan, 2001) that inactivates T4 early transcripts shortly after infection. The middle and late T4 mRNAs are protected from degradation by the viral factor Dmd. In T4-phages defective for the *dmd* gene, RNase LS (for late-gene silencing in T4) cleaves these T4 mRNAs, inhibiting phage multiplication. Therefore, this endonuclease acts as an antagonist of T4 phage replication and Dmd is required for overcoming the host's RNase LS defense role.

Escherichia coli also encodes for a large number of suicide or toxin genes. Their expression is toxic to their host cells, causing growth arrest and eventual cell death. For example, *E. coli* RelE and MazF are two different families of bacterial toxins that inhibit translation by specific endonucleolytic mRNA cleavage (Pedersen *et al.*, 2003; Neubauer *et al.*, 2009; Yamaguchi & Inouye, 2009).

In *B. subtilis*, it was shown that the majority of the ribonucleolytic activity is phosphorolytic. However, several studies showed that PNPase is not responsible for the initial step in RNA decay in *B. subtilis*, but is a secondary enzyme that acts after the decay has been initiated by other RNases (Bechhofer, 2009). Recently, two proteins (RNase J1 and RNase J2) with cleavage activity equivalent to *E. coli* RNase E were purified in this organism (Even *et al.*, 2005). Moreover, these enzymes share many other characteristics with RNase E, which may be related to their similar endonucleolytic activities (Bechhofer, 2009). RNase J1 and J2 are around 61 kDa and have both endonucleolytic and 5′–3′ exonucleolytic activity, which is sensitive to the 5′ phosphorylation state of the substrate. These enzymes were the first described 5′–3′ exonucleases in bacteria (Mathy *et al.*, 2007), the J1 activity being twofold higher than J2 (Mathy *et al.*, 2010) (see also under the topic Exonucleases the section on RNase J1/J2). Furthermore, RNase J1 is essential, while RNase J2 is not (Even *et al.*, 2005).

RNase J1 plays a major role in RNA stability (Mader *et al.*, 2008) and maturation. It functions as a 5′–3′ exoribonuclease in the maturation of 16S rRNA gene and in regulating the mRNA stability of the stationary-phase insecticidal protein transcript *cryIIIA* (Mathy *et al.*, 2007; Deikus *et al.*, 2008). RNase J1 is also responsible for increasing the stability of the downstream fragments that result from the endonucleolytic cleavage of *thrS* and *thrZ* mRNAs (Even *et al.*, 2005). A recent study using a bacterial two-hybrid system showed that PNPase, RNase J1 and two glycolytic enzymes can interact with RNase Y and potentially form a degradosome-like complex (Commichau *et al.*, 2009) (see Complexes of RNases). Moreover, it was shown recently that RNase J1 and J2 in wild-type cells are mostly in a complex. While the individual enzymes have similar endonucleolytic cleavage activities and specificities, as a complex, they behave synergistically to alter cleavage site preference and to increase cleavage efficiency at specific sites (Mathy *et al.*, 2010).

RNase J1 homologues are widely distributed in several other bacteria and archaea (Even *et al.*, 2005). The enzyme is a member of the β-CASP subfamily of zinc-dependent metallo-β-lactamases. The enzyme is composed of three domains: an N-terminal β-lactamase domain, a β-CASP and a C-terminal domain necessary for the enzyme activity. A binding pocket coordinating the phosphate and base moieties of the nucleotide in the surrounding area of the catalytic center provides a basis for the 5′-monophosphate-dependent 5′–3′ exoribonuclease activity (de la Sierra-Gallay *et al.*, 2008). The endonucleolytic activity of the enzyme is not dependent of 5′-monophosphate. For the initiation of endonuclease cleavage, RNase J1 either binds to the 5′ end or directly to the internal site of the mRNA. The upstream product is rapidly degraded by the 3′–5′ exonuclease activity of PNPase. The downstream RNA fragment with the 5′-monophosphate end can be a target of new RNase J1 endonuclease cleavage or processive 5′–3′ exonucleolytic decay from the 5′ end (Bechhofer, 2009). It was also shown that RNase J1 requires a single-stranded 5′ end with AU-rich regions to allow the exoribonucleolytic activity (Mathy *et al.*, 2007). This was observed in *infC* leader RNA (Choonee *et al.*, 2007), *trp* leader RNA (Deikus *et al.*, 2008) and the RNA species called scRNA (Yao *et al.*, 2007).

Similar to what happens with *B. subtilis*, we can find RNase J1 and J2 also in *Streptococcus pyogenes*. While in *B. subtilis* only RNase J1 is an essential protein, in *S. pyogenes*, both proteins are essential for growth. In this bacterium, RNases J1 and J2 were also seen to affect the decay of several mRNAs (Bugrysheva & Scott, 2009).

Another endonuclease sensitive to the 5′ end phosphorylation state of the substrate was discovered recently. RNase Y is involved in the initiation of turnover of *B. subtilis* *S*-adenosylmethionine-dependent riboswitches (Shahbabian

et al., 2009), which controls the expression of 11 transcriptional units (Winkler & Breaker, 2005; Henkin, 2008). The enzyme has a major function in the initiation of mRNA degradation in this organism, affecting mRNA stability > 30% in an RNase J1/J2 double-mutant strain. RNase Y orthologues are present in about 40% of the eubacteria; however, this enzyme is absent from archaea and eukaryotic organisms, with the exception of *Drosophila willistoni* (Shahbabian *et al.*, 2009).

Other endonucleases are described in *B. subtilis* such as RNase M5, RNase Z (see the above section on RNase Z), RNase Bsn and RNase P (see the above section on RNase P). However, neither RNase M5 nor RNase Z appears to have mRNA targets in *B. subtilis* (Condon *et al.*, 2002). RNase M5's major role is the maturation of the 5S rRNA gene (Sogin & Pace, 1974) and can only be found in low G+C Gram-positive bacteria (Condon *et al.*, 2001). Bsn is an extracellular nuclease, apparently with no sequence specificity. It can cleave RNA endonucleolytically to yield 5′-phosphorylated oligonucleotides. The enzyme is found in some members of low G+C Gram-positive bacteria (Nakamura *et al.*, 1992).

Barnase is a guanyl-specific extracellular RNase. Although it is found in many of the *Bacilli*, it is not present in *B. subtilis*. Orthologues of *Bacillus amyloliquefaciens* Barnase and its inhibitor Barstar are also found in *Clostridium acetobutylicum* and the Gram-positive *Yersinia pestis*. It appears that some organisms have lost their copy of the Barnase gene because it was no longer required for a selective advantage. Alternatively, they acquired the resistance gene because other organisms sharing the same niche produced Barnase (Belitsky *et al.*, 1997).

Besides the well-known endonucleases, there are some DNA-binding proteins in archaea with RNase endonucleolytic activity; however, the physiological relevance of these proteins with respect to RNA metabolism is not clear (Evguenieva-Hackenberg & Klug, 2009). The attempts to purify novel RNase activities from archaea resulted in the isolation of very different proteins. Two proteins with RNase activity were purified from *Sulfolobus solfataricus* (called p1 and p2). It was shown that divalent cations are not required for their activity, and they were capable of cleaving yeast tRNA (Fusi *et al.*, 1993; Shehi *et al.*, 2001). Another 9-kDa protein, called SaRD, whose RNase activity is not affected in the presence of different divalent cations, was purified from *Sulfolobus acidocaldarius* (Kulms *et al.*, 1995). Furthermore, two different dehydrogenases were identified in the same organism, with RNase III-like properties and cleavage patterns dependent on $MgCl_2$: an aspartate-semialdehyde dehydrogenase and acyl-CoA dehydrogenase (Evguenieva-Hackenberg *et al.*, 2002). A homologue of the eukaryotic initiation factor 5A (eIF-5A) called archaeal initiation factor 5A (aIF-5A), from *Halobacterium salinarum*, was also described as an RNase with activity in low salt concentrations without addition of $MgCl_2$ (Wagner & Klug, 2007). It was shown that aIF5A efficiently binds structured RNA containing certain motifs and that the interaction is hypusine dependent (Xu *et al.*, 2004).

Exonucleases

PNPase

PNPase belongs to the PDX family of exoribonucleases, which also includes RNase PH from bacteria, and the core of the exosome in archaea and eukaryotes (Mian, 1997; Zuo & Deutscher, 2001; Pruijn, 2005) (Fig. 1b). In 1959, Severo Ochoa received the Nobel Prize for his studies on the polymerase activity of this enzyme, being the first to synthesize RNA outside the cell. This was a major contribution towards deciphering the genetic code. PNPase is also involved in global mRNA decay, being widely conserved from bacteria to plants and metazoans (Zuo & Deutscher, 2001; Bermúdez-Cruz *et al.*, 2005).

PNPase is encoded by the *pnp* gene and is transcribed from two promoters (Portier & Regnier, 1984). *pnp* expression is negatively autoregulated at the post-transcriptional level by the concerted action of PNPase and RNase III (Portier *et al.*, 1987; Robert-Le Meur & Portier, 1992, 1994; Jarrige *et al.*, 2001; Carzaniga *et al.*, 2009). This autoregulation can be disrupted by ribosomal protein S1, which binds to the *pnp* mRNA 5′-UTR (Briani *et al.*, 2008). In an RNase III-deficient strain, there is a 10-fold increase in the PNPase levels (Portier *et al.*, 1987). PNPase levels are also affected by polyadenylation. It is likely that polyadenylated transcripts titrate out the amount of PNPase available to carry out normal autoregulation (Mohanty & Kushner, 2002). PNPase and RNase II are cross-regulated (Zilhão *et al.*, 1996a). In the absence of RNase II, PNPase levels are increased and PNPase overexpression leads to a decrease in RNase II activity (Zilhão *et al.*, 1996a).

PNPase does not seem to be indispensable to *E. coli* at optimal temperature, unless either RNase II or RNase R is also missing (Donovan & Kushner, 1986; Cheng *et al.*, 1998). However, PNPase is essential for *E. coli* growth at low temperatures (Luttinger *et al.*, 1996; Piazza *et al.*, 1996; Zangrossi *et al.*, 2000) and certain mutations of the RNA-binding domains have been shown to confer a cold-sensitive phenotype (García-Mena *et al.*, 1999; Briani *et al.*, 2007; Matus-Ortega *et al.*, 2007). Higher levels of RNase II allow lower levels of PNPase, and in fact, overexpression of RNase II could complement the cold-shock function of PNPase (Zilhão *et al.*, 1996a; Awano *et al.*, 2008). PNPase was also shown to be involved in the long-term survival of *Campylobacter jejuni* at temperatures > 10 °C (Haddad *et al.*, 2009). In *E. coli*, cold-temperature induction of *pnp* expression occurs at post-transcriptional levels including the reversal of

pnp autoregulation (Zangrossi *et al.*, 2000; Beran & Simons, 2001; Mathy *et al.*, 2001).

PNPase processively catalyzes the 3′–5′ phosphorolytic degradation of RNA, releasing nucleoside 5′-diphosphates. Although the degrading activity of *E. coli* PNPase is known to be blocked by dsRNA structures (Spickler & Mackie, 2000), PNPase can form complexes with other proteins, allowing it to degrade through extensive structured RNA. The main multiprotein complex that integrates PNPase is the degradosome (see the Complexes of RNases). To degrade certain dsRNAs, PNPase can form a complex ($\alpha_3\beta_2$) with RNA helicase B (RhlB) (Liou *et al.*, 2002; Lin & Lin-Chao, 2005). PNPase also forms complexes with Hfq and PAP I (Mohanty *et al.*, 2004). The enzyme was reported to degrade a stem-loop without the assistance of RhlB, but this could be related to the low thermodynamic stability of the stem-loop (Mohanty & Kushner, 2010). In the Gram-negative bacteria *Thermus thermophilus*, the PNPase homologue (Tth PNPase) was shown to have phosphorolytic activity at the optimal temperature of 65 °C. Surprisingly, it is able to completely degrade RNAs with very stable intramolecular secondary structures (Falaleeva *et al.*, 2008).

A minimal 3′ overhang of 7–10 unpaired ribonucleotides is required for an RNA molecule to be bound by PNPase (Py *et al.*, 1996; Cheng & Deutscher, 2005), and the action of the enzyme on folded RNAs is known to be stimulated by 3′ polyadenylation (Xu & Cohen, 1995; Py *et al.*, 1996; Carpousis *et al.*, 1999; Spickler & Mackie, 2000). PNPase is also able to catalyze the polymerization of RNA from nucleoside diphosphates at a low inorganic phosphate (Pi) concentration (Godefroy, 1970; Littauer & Soreq, 1982; Sulewski *et al.*, 1989). *In vivo*, PNPase is essentially devoted to the processive degradation of RNA, but is also responsible for adding the heteropolymeric tails observed in *E. coli* mutants devoid of the main polyadenylating enzyme PAP I (Mohanty & Kushner, 2000b; Slomovic *et al.*, 2008). In exponentially growing *E. coli*, $>$ 90% of the transcripts are polyadenylated and Rho-dependent transcription terminators were suggested to be modified by the polymerase activity of PNPase (Mohanty & Kushner, 2006). In spinach chloroplasts, *Cyanobacteria* and *Streptomyces coelicolor*, PNPase seems to be the main tail polymerizing enzyme (Yehudai-Resheff *et al.*, 2001; Rott *et al.*, 2003; Sohlberg *et al.*, 2003). PNPase-dependent RNA tailing and degradation are believed to occur mainly at low ATP concentrations, because ATP has been shown to inhibit both activities (Del Favero *et al.*, 2008). Recently, it was shown that *B. subtilis* PNPase, in the presence of Mn^{2+} and low levels of Pi, is also able to degrade ssDNA, while in the presence of Mg^{2+} and higher amounts of Pi, it degrades RNA. This suggests that PNPase degradation of RNA and ssDNA occurs by mutually exclusive mechanisms (Cardenas *et al.*, 2009). Because of the ability of PNPase to carry out several distinct activities, the enzyme can be considered as a multifunctional protein. It is a pleiotropic regulator, involved in a number of different pathways of RNA degradation. Indeed, it is the only exoribonuclease in *Streptomyces* and is an essential enzyme in these organisms (Bralley & Jones, 2003; Bralley *et al.*, 2006). In *E. coli*, PNPase is now believed to play a greater role in mRNA degradation than previously thought and its inactivation increases the steady-state levels of many transcripts (Deutscher & Reuven, 1991; Mohanty & Kushner, 2003). The enzyme was also reported to play an important role in protecting *E. coli* cells under oxidative stress (Wu *et al.*, 2009). In *B. subtilis*, the RNA decay is primarily phosphorolytic and this major activity is attributed to the PNPase, which is the principal 3′–5′ exoribonuclease in this organism. The deletion of PNPase in *B. subtilis* causes a number of phenotypes such as competence deficiency, cold and tetracycline sensitivity, and filamentous growth (Hahn *et al.*, 1996; Luttinger *et al.*, 1996; Wang & Bechhofer, 1996).

X-ray crystal structures of *E. coli* and *Streptomyces antibioticus* PNPase reveal a homotrimeric subunit organization with a ring-like architecture (Symmons *et al.*, 2000; Shi *et al.*, 2008; Nurmohamed *et al.*, 2009). Each monomer exhibits a five-domain arrangement: at the N-terminus, two RNase PH domains (PH1 and PH2) are linked by an α-helical domain; two RNA-binding domains, KH and S1, are found in the C-terminal end. In the quaternary structure, the KH and S1 domains are found together in one face of the trimer, while the active site is found in the opposite side.

PNPase mutants lacking either the S1 or the KH domain retain phosphorolytic activity (Jarrige *et al.*, 2002; Stickney *et al.*, 2005; Matus-Ortega *et al.*, 2007). However, the presence of both KH and S1 domains is required for a proper binding (Matus-Ortega *et al.*, 2007), and their absence was proposed to affect product release and enzyme cycling, leading to a decreased turnover number (Stickney *et al.*, 2005). The crystal structure of a KH/S1 deletion mutant, along with biochemical and biophysical data, strongly suggests that these domains are involved not only in RNA binding but also contribute to the formation of a more stable trimeric structure (Shi *et al.*, 2008). Indeed, a previous study has shown that the S1 domain from PNPase was able to induce trimerization of a chimeric RNase II containing PNPase S1 (Amblar *et al.*, 2007).

The association of the three subunits encloses a central channel. A properly constricted channel and the conserved basic residues located in the neck region have been shown to play critical roles in trapping RNA for processive degradation (Shi *et al.*, 2008). Two constricted points have been identified in the channel, and the structure of PNPase in complex with RNA clearly indicates that the pathway followed by the RNA molecule is along the central pore in the direction of the active site (Symmons *et al.*, 2000; Shi *et al.*, 2008; Nurmohamed *et al.*, 2009). The ability of the

aperture at the central channel and its neighboring regions to undergo conformational changes is likely to be a key aspect of the dynamic translocation of RNA by PNPase (Nurmohamed *et al.*, 2009).

The catalytic site of PNPase is composed of structural elements of both PH1 and PH2 core domains, and several mutations introduced into the PNPase core abolish or drastically decrease all catalytic activities of the enzyme (Jarrige *et al.*, 2002; Briani *et al.*, 2007). However, other mutations in the core region were analyzed that do not affect phosphorolytic or polymerase activities, but rather RNA binding is severely impaired (Regonesi *et al.*, 2004). *Streptomyces antibioticus* PNPase catalytic center has been identified using tungstate (a phosphate analogue), which is coordinated by T462 and S463 (Symmons *et al.*, 2000). *Escherichia coli* PNPase crystals obtained in the presence of Mn^{2+} (which can substitute for Mg^{2+} to support catalysis) showed that the metal is coordinated by the conserved residues D486, D492 and K494 (Nurmohamed *et al.*, 2009). Indeed, the substitution of D492 abolished both phosphorolysis and polymerization activities (Jarrige *et al.*, 2002).

PNPase has been described to play a role in the establishment of virulence in several pathogens. In *Salmonella*, PNPase activity decreases the expression of genes from the pathogenicity islands SPI 1 (containing genes for invasion) and SPI 2 (containing genes for intracellular growth) (Clements *et al.*, 2002). Similarly, in *Dichelobacter nodosus*, PNPase acts as a virulence repressor in benign strains by decreasing twitching motility (Palanisamy *et al.*, 2009). In contrast, in *Yersinia*, PNPase modulates the type three secretion system (TTSS) by affecting the steady-state levels of TTSS transcripts and controlling the secretion rate (Rosenzweig *et al.*, 2005, 2007). This is probably the reason why the *pnp* deletion results in a less virulent strain in a mouse model (Rosenzweig *et al.*, 2007). In *C. jejuni* PNPase is involved in motility (Haddad *et al.*, 2009). Finally, in *S. pyogenes*, PNPase activity is rate-limiting for the decay of *sagA* and *sda*, which code for the important virulence factors streptolysin S and streptodornase (a DNase), respectively (Barnett *et al.*, 2007).

RNase II

Escherichia coli RNase II is the prototype of the RNase II family of enzymes (Mian, 1997; Mitchell *et al.*, 1997; Zuo & Deutscher, 2001; Frazão *et al.*, 2006; Grossman & van Hoof, 2006) (Fig. 1b). RNase II-like proteins are widespread among the three domains of life, and in eukaryotes, they are the catalytic component of the exosome (Liu *et al.*, 2006b; Dziembowski *et al.*, 2007).

RNase II is encoded by the *rnb* gene that can be transcribed from two promoters P1 and P2 and terminates in a Rho-independent terminator 10 nucleotides downstream of the *rnb* stop codon (Zilhão *et al.*, 1993, 1995a, 1996b). PNPase regulates RNase II expression by degrading the *rnb* mRNA (Zilhão *et al.*, 1996a). RNase III and RNase E endonucleases are also involved in the control of RNase II expression at the post-transcriptional level. RNase III does not affect *rnb* mRNA directly, but affects PNPase levels, and RNase E is directly involved in the *rnb* mRNA degradation (Zilhão *et al.*, 1995b).

The protein stability of RNase II is known to be post-translationally regulated and its levels are adjusted according to the growth conditions. *gmr* (gene modulating RNase II) is located downstream of *rnb* and the related protein is involved in the modulation of the stability of RNase II (Cairrão *et al.*, 2001). Gmr has a PAS domain that can act as an environmental sensor detecting changes in growth conditions.

Escherichia coli RNase II is a sequence-independent hydrolytic exoribonuclease that processively degrades RNA in the 3′–5′ direction, yielding 5′-nucleoside monophosphates. However, the processive degradation of an RNA molecule by RNase II is easily blocked by secondary structures, and the enzyme is known to stall around seven nucleotides before it reaches a double-stranded region (Cannistraro & Kennell, 1999; Spickler & Mackie, 2000). In *E. coli*, RNase II is the major hydrolytic enzyme and participates in the terminal stages of mRNA degradation (Deutscher & Reuven, 1991). However, the enzyme is not essential for *E. coli* growth unless PNPase is also missing (Donovan & Kushner, 1986; Zilhão *et al.*, 1996a). Although RNase II-degrading activity is sequence independent, the most reactive substrate is the homopolymer poly(A). Because the presence of a poly(A) tail is often needed for the RNA degradative process, the rapid degradation of polyadenylated stretches by RNase II can paradoxically protect some RNAs by impairing the access of other exoribonucleases (Hajnsdorf *et al.*, 1994; Pepe *et al.*, 1994; Coburn & Mackie, 1996a; Marujo *et al.*, 2000; Mohanty & Kushner, 2000a; Folichon *et al.*, 2005). Indeed, in the absence of RNase II, a large number (31%) of *E. coli* mRNAs are decreased, especially ribosomal protein genes, suggesting a major function for this enzyme in the protection of specific mRNAs through poly(A) tail removal (Mohanty & Kushner, 2003).

The structure of *E. coli* RNase II and its RNA-bound complex was determined (Frazão *et al.*, 2006) (Fig. 2a). This was the first structure of an exoribonuclease from the RNase II family that has been resolved (Frazão *et al.*, 2006). The overall X-ray crystallographic structure of the wild-type enzyme (Frazão *et al.*, 2006; Zuo *et al.*, 2006) revealed four domains, as predicted previously by Amblar *et al.* (2006) (see Figs 1b and 2a). Three RNA-binding domains have been identified: two cold-shock domains (CSD1 and CSD2) in the N-terminal region and an S1 RNA-binding domain at

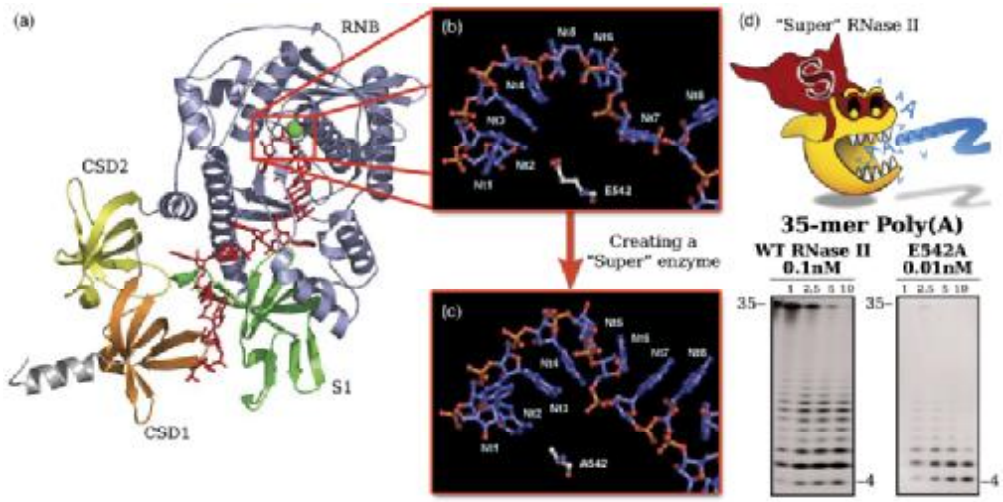

Fig. 2. The making of a 'super-enzyme'. (a) RNase II is composed of two N-terminal cold shock domains (CSD1 in orange and CSD2 in yellow), a central catalytic domain (RNB in gray), a C-terminal S1 domain (in green). (b) Zooming the catalytic cavity of RNase II. (c) Modelling the E542A mutant with the Poly(A) RNA strand in the RNB domain. Substitution in position 542 of the negatively charged glutamic side-chain for the smaller neutral methyl group of alanine could reduce significantly both electrostatic and steric surfaces in the RNA-binding interface. (d) Exoribonuclease activity with the Poly(A) substrate: comparison of wild-type and E542A proteins. It is possible to see that we need to use higher concentrations of RNase II when compared with the E542A mutant, which is 110-fold more active when compared with the wild type (Barbas *et al.*, 2009. ©The American Society for Biochemistry and Molecular Biology).

the C-terminus. The catalytic site resides in the central RNB domain, whose structure has shown an unprecedented fold characteristic of this family. This domain contains four highly conserved sequence motifs (I–IV) with several invariant carboxylate residues (Mian, 1997). The RNA-binding domains (CSD1, CSD2 and S1) are grouped together on one side of the structure, while the active site is on the other side of the molecule (Frazão *et al.*, 2006).

Elimination of the N-terminal CSD1 resulted in an increase in the RNA-binding affinity of the enzyme for poly(A), suggesting that this domain may play a role in controlling the movement of the enzyme on the poly(A) chain (Amblar *et al.*, 2006; Arraiano *et al.*, 2008). Interestingly, without all the RNA-binding domains, the enzyme is still able to degrade RNA, although with much less efficiency than the wild-type enzyme (Matos *et al.*, 2009; Vincent & Deutscher, 2009).

The structure of the RNA-bound enzyme revealed that the RNA fragment interacts with the protein at two non-contiguous regions: the 'anchor' and catalytic regions (Cannistraro & Kennell, 1994; Frazão *et al.*, 2006) (Fig. 2a). Nucleotides 1–5, at the 5′ end of the 13-mer RNA fragment, are located in the 'anchor' region in a deep cleft between the two CSDs and the S1 domain. The final nucleotides 9–13 are located in a cavity deep within the RNB domain, stacked and 'clamped' between the conserved residues Phe358 and Tyr253. A 10-nucleotide fragment is the shortest RNA able to retain contacts with both the anchor and the catalytic regions. This explains why RNase II is processive on long RNA molecules, but becomes distributive on substrates shorter than 10–15 nucleotides. When the RNA molecule is shorter than five nucleotides, the required packing of the bases can no longer occur, preventing the translocation of the RNA, and a final end product of four nucleotides is released (Frazão *et al.*, 2006). Tyr-253 has been identified as the residue responsible for setting the RNase II end product, and its substitution was shown to alter the smallest end product of degradation from 4 to 10 nucleotides (Barbas *et al.*, 2008). This mutation has been proposed to cause loosening of the RNA substrate at the catalytic site and, as a consequence, binding at the anchor region would be essential to keep the RNA attached to the protein and allow cleavage. Molecules shorter than 10 nucleotides are too small to be simultaneously bound at both sites, meaning that they would have to be degraded in a distributive manner (Barbas *et al.*, 2008).

The access to the catalytic pocket is restricted to single-stranded RNA by steric hindrance, which explains the inability of RNase II to degrade dsRNA. DNA is not a substrate because there is a specific interaction between the protein and the ribose rings of nucleotides that directly contact the enzyme (Frazão *et al.*, 2006). Residues Tyr-313

and Glu-390 have been demonstrated to be responsible for the discrimination of the cleavage of RNA vs. DNA (Barbas *et al.*, 2009).

Several residues in the catalytic region are important for catalysis (Amblar & Arraiano, 2005; Frazão *et al.*, 2006). Asp-201 and Asp-210 substitution led to a significant loss of RNase II activity, and Arg-500 has also been shown to be crucial for RNA cleavage (Frazão *et al.*, 2006; Barbas *et al.*, 2008, 2009). However, Asp-209 is the only essential residue for RNA degradation (Barbas *et al.*, 2008). The conserved residue Glu-542 has been proposed to facilitate the elimination of the exiting nucleotide upon phosphodiester cleavage (Frazão *et al.*, 2006). Interestingly, its substitution by alanine rendered the mutant RNase II much more active than the wild type and significantly increased the RNA-binding ability (Fig. 2b–d). Three-dimensional modelling of the mutant enzyme indicated that the substitution induced a subtle conformational change in the RNB domain. This resulted in a reorganization of the RNA-binding interface that transformed the RNase II into the so-called 'super-enzyme', an enzyme with extraordinary catalysis and binding abilities. When compared with the wild-type RNase II, the 'super-enzyme' exhibits $>$ 100-fold increase in the exoribonucleolytic activity (Fig. 2d) and about a 20-fold increase in the RNA-binding affinity (Barbas *et al.*, 2009).

RNase R

RNase R encoded by the *rnr* gene (previously *vacB*) is a 3′–5′ hydrolytic exoribonuclease from the RNase II family of exoribonucleases (Cheng & Deutscher, 2002; Vincent & Deutscher, 2006). The *rnr* gene is second in an operon, together with *nsrR* (a transcriptional regulator), *rlm*B (rRNA methyltransferase) and *yjfI* (unknown function). Transcription is driven from a putative σ^{70} promoter upstream of *nsrR* (Cheng *et al.*, 1998; Cairrão *et al.*, 2003). *rnr* mRNAs are post-transcriptionally regulated by RNase E, although RNase G may also participate (Cairrão & Arraiano, 2006). RNase R is a processive and sequence-independent enzyme, with a wide impact on RNA metabolism (Cairrão *et al.*, 2003; Cheng & Deutscher, 2005; Oussenko *et al.*, 2005; Andrade *et al.*, 2006, 2009a; Purusharth *et al.*, 2007). It is unique among the RNA-degradative exonucleases present in *E. coli* as it can easily degrade highly structured RNAs (Cheng & Deutscher, 2002, 2003; Awano *et al.*, 2010). RNase R is able to degrade an RNA duplex, provided there is a single-stranded 3′ overhang (Cheng & Deutscher, 2002; Vincent & Deutscher, 2006). In fact, RNase R was shown to be a key enzyme involved in the degradation of polyadenylated RNA (Andrade *et al.*, 2009a).

RNase R shows a modular organization of RNA-binding domains (CSD1 and CSD2 located at the N-terminus and a C-terminal S1 domain) flanking the central catalytic RNB domain, typically found on RNase II-family members (Fig. 1b). A three-dimensional model of RNase R has been proposed based on the structure of its paralogue RNase II (Barbas *et al.*, 2008). Mutational analysis identified important residues located in the active center: D272, D278 and D280 (Matos *et al.*, 2009). A D280N mutant showed no exonucleolytic activity, similarly to what was reported with the D209N mutant in RNase II (Amblar & Arraiano, 2005; Matos *et al.*, 2009; Awano *et al.*, 2010). RNase R degradation is processive, and unlike RNase II, the final end product of digestion is a dinucleotide. Tyrosine Y324 was found to be responsible for setting the final end product of RNase R (Matos *et al.*, 2009).

RNase R was shown to bind RNA more tightly within its catalytic channel than does RNAase II (Matos *et al.*, 2009; Vincent & Deutscher, 2009). Surprisingly, a mutant expressing only the nuclease domain (RNB) is able to degrade a perfect dsRNA (Matos *et al.*, 2009). Paradoxically, the presence of the RNA-binding domains (CDS1, CDS2 and S1) requires the presence of a short tail in order to degrade dsRNA (Matos *et al.*, 2009). The RNA-binding domains 'block' the entrance of dsRNA into the catalytic channel. Accordingly, it was proposed that RNA-binding domains actually discriminate the substrates that can be processed by RNase R, favoring the selection of RNA molecules harboring a 3′ linear tail. It has been suggested that RNase R can function both as an exoribonuclease as well as an RNA 'helicase' (Awano *et al.*, 2010). RNase R intrinsic 'helicase' unwinding activity is dependent on RNA-binding regions (S1, CDS1, and most importantly, CDS2). The dsRNA must have a 3′ linear overhang in order to become a suitable substrate for RNase R helicase activity. Altogether, RNA-binding domains of RNase R seem to be responsible for the selection of RNA substrates harboring a 3′ linear region, which can be provided by polyadenylation (Andrade *et al.*, 2009a; Matos *et al.*, 2009). Clearly, only the resolution of the RNase R structure will allow a full understanding of its remarkable modes of action.

RNase R is critical in RNA quality control, namely in the degradation of defective tRNAs (Vincent & Deutscher, 2006; Awano *et al.*, 2010) and rRNA (Cheng & Deutscher, 2003). Together with PNPase, RNase R eliminates aberrant fragments of the 16S and 23S rRNA genes, whose accumulation potentially affects ribosome maturation and assembly. Furthermore, the importance of RNase R in the accuracy of gene expression is broadened with its role in protein quality control. In the absence of RNase R, the small stable SsrA/tmRNA is not processed properly, leading to defects in *trans*-translation and significant errors in protein tagging for proteolysis (Cairrão *et al.*, 2003). RNase R has also emerged as an important novel contributor to mRNA degradation. The absence of both RNase R and PNPase results in the strong accumulation of REP-containing mRNA sequences (Cheng & Deutscher, 2005). However, the presence of only

one of these exoribonucleases is sufficient to remove such transcripts, revealing again a functional overlap between these two enzymes. Remarkably, RNase R was also shown to degrade the *ompA* transcript in a growth-phase-specific manner (Andrade *et al.*, 2006). In the stationary phase of growth, the single inactivation of RNase R results in the accumulation of *ompA* mRNA and this correlated with increasing intracellular levels of OmpA protein. This work revealed a role for RNase R in the control of gene expression that could not be replaced by any of the other exoribonucleases (Andrade *et al.*, 2006).

The activity of RNase R is modulated according to the growth conditions of the cell and responds to environmental stimuli. RNase R seems to be a general stress-induced protein, whose levels are increased under several stresses, namely in cold shock, and the stationary phase of growth (Cairrão *et al.*, 2003; Andrade *et al.*, 2006). RNase R-like enzymes are widespread in most sequenced genomes. Although most of the knowledge on this protein came from work in *E. coli*, many RNase R from other bacterial species have been identified. Notably, RNase R has also been implicated in the establishment of virulence in a growing number of pathogens.

In *Shigella flexneri*, RNase R was shown to be required for the expression of the invasion factors IpaB, IpaC, IpaD and VirG (Tobe *et al.*, 1992). The disruption of the VacB gene in other *Shigella* spp. and enteroinvasive *E. coli* resulted in the reduced expression of virulence phenotypes (Tobe *et al.*, 1992). In *Legionella pneumophila* RNase R is the only hydrolytic exoribonuclease present. This protein is not essential for growth at optimal temperature; however, it is important for growth and viability at low temperatures and induces the competence (Charpentier *et al.*, 2008). To date, only one exoribonuclease, RNase R (MgR), was identified in *Mycoplasma genitalium*, where it is an essential protein (Hutchison *et al.*, 1999). MgR shares some properties of both *E. coli* RNase R and RNase II and can carry out a broad range of RNA processing and degradative functions (Lalonde *et al.*, 2007). Similar to what happens in *E. coli*, RNase R from *Aeromonas hydrophila* is also a cold-shock protein essential for viability at lower temperatures and its absence leads to a reduction in *A. hydrophila* motility (Erova *et al.*, 2008). The infection of mouse cells with Δ*rnr* strains shows that the virulence is attenuated, confirming the role of this enzyme in the pathogenesis of this organism (Erova *et al.*, 2008). In *Streptococcus pneumoniae*, there is a unique homologue of the RNase II family of enzymes that was shown to be a RNase R-like protein (Domingues *et al.*, 2009). RNase R from *Salmonella* showed a reduction in its activity and the ability to bind to RNA when compared with *E. coli* RNase R (Domingues *et al.*, 2009). Proteins isolated from different strains regarding their virulence ability (virulent vs. nonvirulent) are different regarding their activity and RNA affinity (Domingues *et al.*, 2009). Further studies are still necessary to confirm whether the differences observed in RNase R protein are responsible for the virulence of these strains.

In *P. syringae*, RNase R is the exoribonuclease present in the degradosome as opposed to most other systems, where PNPase is part of such complexes (Purusharth *et al.*, 2005) (see Complexes of RNases). Like in *E. coli*, RNase R is also particularly important at low temperatures, because inactivation of the *rnr* gene inhibits the growth of both *Pseudomonas putida* (Reva *et al.*, 2006) and *P. syringae* (Purusharth *et al.*, 2007) at 4 °C. In *P. syringae*, RNase R is involved in 3′ end maturation of the 16S and 5S rRNA genes and in tmRNA turnover (Purusharth *et al.*, 2007). Genomic studies revealed that *P. putida* RNase R plays an important role in mRNA turnover because its absence led to the accumulation of several mRNAs (Fonseca *et al.*, 2008). On the other hand, RNase R (previously YvaJ) from *B. subtilis* was suggested not to play a critical role in RNA degradation; however, it may play a role in mRNA turnover when polyadenylation at the 3′ end occurs (Oussenko *et al.*, 2005). Moreover, *B. subtilis* RNase R was shown to be important for the quality control of tRNAs (Campos-Guillen *et al.*, 2010).

Overall, RNase R-deficient bacteria have been shown to be less virulent than the wild-type parental strains. However, how this is achieved is still not completely clear. This is probably related to critical RNA degradation pathways. The fact that RNase R was found to be key in the degradation of sRNAs, namely the virulence regulator SsrA/tmRNA, paves the way to broaden its role in pathogenesis. It has also been suggested that RNase R may control the export of proteins involved in virulence mechanisms. Altogether, the available data suggest that bacterial RNase R may be attractive as a potential therapeutic agent, but clearly more studies are required.

Oligoribonuclease

The end products resulting from the degradation of previously described RNases constitute a severe problem to the cell viability, because these enzymes release RNA fragments of 2–5 nucleotides in length whose accumulation may be deleterious (Ghosh & Deutscher, 1999). Oligoribonuclease is the enzyme that degrades these short oligoribonucleotides (Stevens & Niyogi, 1967; Niyogi & Datta, 1975). From the known exoribonuclease genes in *E. coli* the oligoribonuclease gene, *orn*, is the only one required for cell viability (Ghosh & Deutscher, 1999).

Oligoribonuclease belongs to the DEDD family of exoribonucleases (Zuo & Deutscher, 2001), and is a homodimeric (α2) enzyme (Zhang *et al.*, 1998) that produces mononucleotides and requires the presence of divalent cations (Mn^{2+}) (Niyogi & Datta, 1975) (Fig. 1b). The hydrolysis is

processive in the 3′–5′ direction; this enzyme has a higher affinity to 5-mer oligoribonucleotides and the reaction rate decreases with increasing chain length (Datta & Niyogi, 1975). This enzyme requires a free 3′-OH end and is not sensitive to the 5′-phosphorylation state of the RNA (Datta & Niyogi, 1975). Only the preliminary X-ray characterization of the *E. coli* oligoribonuclease structure has been reported (Fiedler *et al.*, 2004). It was shown recently that Orn can degrade short DNA oligos, like its human homologue Sfn, but this degradation requires higher enzyme concentrations than the RNA-directed activity (Mechold *et al.*, 2006).

Bacillus subtilis does not have an oligoribonuclease (Orn) homologue. However, a functional analogue of Orn was identified in this organism that was named YtqI (NrnA). Surprisingly, this protein *in vitro* can degrade not only short oligonucleotides (with a preference for 3-mer) but also 3′-phosphoadenosine 5′-phosphate (pAp). This suggests the existence of a closer link between sulfur and RNA metabolism in *B. subtilis* (Mechold *et al.*, 2007). More recently, a second nanoRNase was discovered and named YngD (NrnB). This protein is a member of the DHH/DHHA1 protein family of phosphoesterases, and degrades nanoRNA 5-mers *in vitro* similar to oligoribonuclease from *E. coli* (Fang *et al.*, 2009).

In *Streptomyces griseus* and *S. coelicolor*, the gene *ornA* encodes the oligoribonuclease protein. It is transcribed from two promoters: one that is developmentally regulated and the other that is a constitutive promoter (Ohnishi *et al.*, 2000). Unlike *E. coli*, in which oligoribonuclease is an essential enzyme, if the *ornA* gene is deleted, the cells are viable, but not able to form aerial hyphae (Ohnishi *et al.*, 2000). It was also shown that the degradation of RNA oligomers by oligoribonuclease is critical for the completion of the life cycle (Sello & Buttner, 2008).

In RNA metabolism, oligoribonuclease acts as the 'finishing enzyme' to degrade oligoribonucleotides of two to five nucleotides in length to mononucleotides in a wide range of organisms.

RNase J1/J2

Recently, the discovery of RNase J1 and J2 shed new light on the mechanism of RNA degradation in *B. subtilis*. These enzymes were the first to be demonstrated to have bacterial 5′–3′ exoribonucleolytic activity (Mathy *et al.*, 2007). Moreover, two different activities can be observed for these enzymes, because they can act both as endo- and as exoribonucleases (Even *et al.*, 2005). RNases J1 and J2 had already been described under endoribonucleases (see the above section on Other endonucleases). RNase J1 is an essential protein (Even *et al.*, 2005) and its exoribonucleolytic activity depends on the phosphorylation state at the 5′ end, with a preference for monophosphate substrates (Mathy *et al.*, 2007). It was also shown that RNase J1 requires a single-stranded 5′ end to allow the exoribonucleolytic activity (Mathy *et al.*, 2007). It also functions as a 5′–3′ exoribonuclease in the maturation of the 16S rRNA gene and in regulating the mRNA stability of the *Bacillus thuringiensis* stationary-phase insecticidal protein transcript *cryIIIA* and the *trp* leader sequence (Mathy *et al.*, 2007; Deikus *et al.*, 2008). There are indications that RNase J1 plays an important role both in the maturation or degradation of specific RNAs and in governing global mRNA stability (Mader *et al.*, 2008). Interestingly, RNase J homologues are not present in *Gammaproteobacteria* such as *E. coli*, but are widely distributed in other bacteria and in archaea (Even *et al.*, 2005; Mathy *et al.*, 2007).

Other 3′–5′ exonucleases

In *E. coli*, besides the exoribonucleases mentioned above, three others are present in the cell: RNase PH, RNase D and RNase T.

RNase PH belongs to the same family of PNPase, the PDX family of exoribonucleases (see Fig. 1b). It is encoded by the *rph* gene and cotranscribed with pyrE, a gene necessary for pyrimidine synthesis that is located upstream of *rph* (Ost & Deutscher, 1991). However, while PNPase has an important function in mRNA degradation, RNase PH is involved in tRNA metabolism, namely in the processing of tRNA precursors (Deutscher *et al.*, 1988; Kelly *et al.*, 1992). RNase PH can act as a phosphorolytic RNase by removing nucleotides following the CCA terminus of tRNA and also as a nucleotidyltransferase by adding nucleotides to the ends of RNA molecules (Jensen *et al.*, 1992; Kelly & Deutscher, 1992). RNase PH can also cleave off the 3′ end of other sRNAs, including M1, 6S and 4.5S RNA (Li *et al.*, 1998). Deletion of the *rph* gene has no effect on the growth or the viability of the cells. However, the combination of this deletion with RNase T or PNPase deletions affects growth. These data suggest that RNase PH has overlapping functions *in vivo* with both RNase T and PNPase (Kelly *et al.*, 1992). In *B. subtilis*, there are two pathways for tRNA maturation and RNase PH seems to be the most important for the maturation of tRNA precursors with CCA motifs, while RNase Z is responsible for the processing of CCA-less tRNA precursors (Wen *et al.*, 2005). The crystal structure of *B. subtilis* RNase PH has been determined with a medium resolution and it can be superimposed to the second core domain structure of PNPase. Similar to what happens with RNase PH from *A. aeolicus* and *Pseudomonas aeruginosa*, the protein crystallizes as a hexamer arranged as a trimer of dimers and the substrate interacts with the dimer (Ishii *et al.*, 2003; Choi *et al.*, 2004; Harlow *et al.*, 2004). However, the hexameric ring formation is essential for the binding of precursor tRNA and also for exoribonucleolytic activity (Choi *et al.*,

2004). In *Streptomyces*, an RNase PH-like enzyme encoded by the *SCO2904* gene was identified. Similar to PNPase, this can polyadenylate the 3′ end of RNA *in vitro*; however, *in vivo* studies showed that RNase PH may not be involved in the synthesis or the maintenance of poly(A) tails in *S. coelicolor* (Bralley *et al.*, 2006). In *Streptomyces*, all essential tRNA genes must encode the CCA end and the RNase PH must be required to induce maturation of the 3′ end of these tRNAs (Bralley *et al.*, 2006) (see also below the section on processing).

RNase D is a 3′–5′ hydrolytic exoribonuclease from the DEDD superfamily, which contains both DNA and RNA exonucleases (Zuo & Deutscher, 2001) (Fig. 1b). As a member of this family, it has three conserved motifs. In motif III, the presence of a tyrosine or histidine led to the division of this family into two subgroups, DEDDy and DEDDh, with RNase D belonging to the first one (Zuo & Deutscher, 2001). RNase D requires divalent metal ions for its activity and has a high degree of substrate specificity; its substrates include denatured and damaged tRNAs, as well as tRNA precursors with extra 3′ residues following the CCA sequence, but not ssRNA (Cudny & Deutscher, 1980; Cudny *et al.*, 1981; Zhang & Deutscher, 1988b) (see also below the section on processing). RNase D overexpression seems to be deleterious for the cell (Zhang & Deutscher, 1988a). The chromosomal gene uses UUG as the initiation codon and has an abnormally high level of rare codons, which could limit the levels of endogenous protein (Kane, 1995). Moreover, it was shown that RNase D expression is negatively regulated at the translational level by the initiation codon (Zhang & Deutscher, 1989). The crystal structure of RNase D shows that this protein has one DEDD catalytic domain and two HRDC domains with a funnel-shaped ring architecture that could be important to define the exoribonucleolytic activity of RNase D, which may be processive (Zuo *et al.*, 2005). RNase D homologues have been found in many organisms, except archaea, and, in some genomes, it is possible to find more than one homologue (Zuo & Deutscher, 2001).

RNase T is a 3′–5′ exoribonuclease that belongs to the DEDD superfamily of RNases and to the DEDDh subgroup (Zuo & Deutscher, 2001) (Fig. 1b). It is a single-strand-specific exonuclease and the activity is dependent on the presence of divalent metal ions, such as Mg^{2+} or Mn^{2+} (Deutscher & Marlor, 1985; Zuo & Deutscher, 2002). Besides the ability to cleave RNA molecules, RNase T also has DNA exonuclease activity (Viswanathan *et al.*, 1998). RNase T has a distributive activity and an unusual base specificity, discriminating against pyrimidines and, particularly, C residues (Zuo & Deutscher, 2002). This sequence specificity is largely determined by the last four nucleotides at the 3′ end (Zuo & Deutscher, 2002). It is involved in the final step of maturation of many stable RNAs and seems to be the most important RNase with that function (Li & Deutscher, 1995, 1996; Li *et al.*, 1998). In fact, it was shown that RNase T is essential for the maturation of the 3′ ends of 5S and 23S rRNA genes (Li & Deutscher, 1995; Li *et al.*, 1999a), and it is also involved in the end turnover of tRNAs (Deutscher *et al.*, 1985). The crystal structures of RNase T from both *E. coli* and *P. aeruginosa* show that the protein adopts an oligoribonuclease-like homodimer architecture, which was shown to be required for its activity (Li *et al.*, 1996; Zuo *et al.*, 2007). The two monomers are facing opposite ends, which means that the active site of one monomer is facing the binding site of the other. This arrangement allows the binding of the RNA molecule from one monomer to be close to the active site of the other one (Zuo *et al.*, 2007). Despite its critical role in RNA metabolism, RNase T orthologues are just found in a small group of bacteria, the *Gamma* division of *Proteobacteria* (Zuo & Deutscher, 2001).

Both *E. coli* and *Salmonella* belong to the *Enterobacteriaceae* family. A recent work showed that the two hydrolytic enzymes present in *E. coli*, RNase II and RNase R, are also found in *Salmonella* and behave quite similarly in terms of their the ability to degrade structured substrates and the final product that is released. However, the proteins from *Salmonella* showed a reduction in their activity and an ability to bind to RNA when compared with the *E. coli* enzymes (Domingues *et al.*, 2009).

In *B. subtilis*, besides the proteins mentioned above, we can find other RNase, YhaM. This protein has been implicated in DNA replication (is able to degrade ssDNA), and *in vitro* studies showed that is also able to cleave RNA into the 3′–5′ direction in a Mn^{2+}-dependent manner. However, the *in vivo* function of YhaM in RNA metabolism remains to be determined (Noirot-Gros *et al.*, 2002; Oussenko *et al.*, 2002). Sequence homologues of YhaM were found only in Gram-positive bacteria (Oussenko *et al.*, 2002).

Cyanobacteria are prokaryotes organisms that may be related to the ancestor of chloroplasts. In the genome of *Synechocystis*, it is possible to find genes that have a high homology to RNase E, PNPase, RNase II/R and PAP, the most important proteins involved in mRNA degradation and polyadenylation (Rott *et al.*, 2003). However, the product of the putative PAP gene has nucleotidyltransferase and not PAP activity, and the reaction of polyadenylation in *Synechocystis* is performed by PNPase, which originates heterogeneous poly(A)-rich tails, like it occurs in chloroplasts. These tails are found in the amino acid coding region, the 5′ and 3′ untranslated regions of mRNAs, in rRNA and the single intron located at the tRNAfmet (Rott *et al.*, 2003). PNPase is an essential protein for this organism because the deletion of this gene causes lethality. The same is observed when the gene for RNase II/R is disrupted (Rott *et al.*, 2003). There is no degradosome complex in cyanobacteria (see Complexes of RNases).

Complexes of RNases

RNA-degrading machines

The degradosome is a large multiprotein complex involved in RNA degradation. It is believed to act as a general RNA decay machine in which the components of the degradosome cooperate during the decay of many RNAs. The complex formation contributes to the coordination of the endoribonucleolytic cleavage with the exoribonucleolytic degradation (Py *et al.*, 1994, 1996; Miczak *et al.*, 1996; Vanzo *et al.*, 1998).

In *E. coli*, this multiprotein complex is formed by RNA degradation enzymes RNase E and the exonuclease PNPase, as well as the ATP-dependent RhlB and the glycolytic enzyme enolase (Py *et al.*, 1994; Miczak *et al.*, 1996; Vanzo *et al.*, 1998). RNase E provides the organizing scaffold for the degradosome, through its carboxy-terminal half. In the carboxy-terminal half, four segments were found to show a tendency to form a secondary structure (Callaghan *et al.*, 2004), namely A, B, C and D. Segment A localizes the degradosome to the inner cytoplasmic membrane (Khemici *et al.*, 2008). RhlB binds a 69-residue conserved segment downstream of segment B, a coiled coil that may engage RNA (Chandran *et al.*, 2007; Worrall *et al.*, 2008b). Segment C is the enolase-binding site (Chandran & Luisi, 2006), and segment D interacts with PNPase (Callaghan *et al.*, 2004).

Under normal growth conditions, crystallographic and biophysical measurements indicate that one enolase dimer and one helicase protomer interact with one RNase E monomer (Chandran & Luisi, 2006; Chandran *et al.*, 2007; Worrall *et al.*, 2008a). Findings for the stoichiometry of PNPase with the isolated recognition site from RNase E (Callaghan *et al.*, 2004), and recent crystallographic analysis of the *E. coli* PNPase/RNase E complex reveal an equimolar ratio (Nurmohamed *et al.*, 2009). In principle, three RNase E tetramers and four PNPase trimers could form a self-closing assembly composed of 12 protomers, satisfying all possible binding sites. The ideal composition of such an assembly is 12 : 12 : 24 : 12 (RNase E : PNPase : enolase : RhlB) (Marcaida *et al.*, 2006).

The group of minor components that bind to the degradosome to affect its composition and modulate its enzymatic activity includes polyphosphate kinase, poly(A) polymerase, ribosomal proteins and the molecular chaperones DnaK and GroEL (Miczak *et al.*, 1996; Butland *et al.*, 2005; Morita *et al.*, 2005; Regonesi *et al.*, 2006) and other DEAD-box helicases (SrmB, RhlE and CsdA) that may bind to sites outside the RhlB recognition region (Khemici & Carpousis, 2004). Another potential interaction may occur between the degradosome and the cytoskeleton protein MinD (a membrane-localized bacterial cytoskeletal protein), which may account for the apparent association of the degradosome with the cytoskeleton (Taghbalout & Rothfield, 2007).

The composition of the degradosome can also undergo changes depending on the conditions of growth or stress (Khemici *et al.*, 2004; Prud'homme-Genereux *et al.*, 2004; Morita *et al.*, 2005; Gao *et al.*, 2006). A different complex containing RNase E, Hfq and SgrS, a small regulatory RNA, is formed under conditions of phosphosugar stress (Morita *et al.*, 2005). The formation of the complex with Hfq and SgrS requires the same region of RNase E that is necessary for the formation of the canonical RNA degradosome, and evidence suggests that the degradosome is remodelled as a consequence of the new interaction. There is evidence that RNase E can form a 'cold-shock' RNA degradosome in which the helicase RhlB is replaced by CsdA, another DEAD-box RNA helicase (Khemici *et al.*, 2004; Prud'homme-Genereux *et al.*, 2004). The compositional changes in the degradosome following cold exposure may account, in part, for changes in mRNA stability associated with cold shock response. The PNPase content of the degradosome can change in response to phosphosugar stress, temperature shock and the growth stage (Beran & Simons, 2001; Liou *et al.*, 2001). Surprisingly, RNase E from *P. syringae* interacts with the hydrolytic exoribonuclease RNase R instead of PNPase and with another DEAD-box helicase, RhlE (Purusharth *et al.*, 2005).

Degradosome composition and function may also be modulated through its interactions with the RNase E inhibitory proteins RraA and RraB, which interact with the C-terminal half of RNase E, thereby altering the composition of the degradosome, namely the amount of PNPase, RhlB and enolase bound to RNase E. RraB expression gave rise to degradosomes that contained the noncanonical components DnaK and CsdA.

The global effects of mutations in degradosome constituents on mRNA levels have been evaluated using microarrays (Bernstein *et al.*, 2004). This work reported that the functions of all degradosome constituents are necessary for normal mRNA turnover and that assembled degradosome components work in concert to regulate the transcripts of some *E. coli* metabolic pathways, but not others. This suggests the existence of structural features or biochemical factors that distinguish among different classes of mRNAs targeted for degradation.

Archaea are microscopic, single-celled organisms with no nucleus, no mitochondria and no chloroplasts. Regarding mRNA, they are more similar to bacteria than to eukaryotes: mRNA does not have introns, it is polycistronic, is not modified and does not have long stabilizing poly(A) tails at the 3′ end (Brown & Coleman, 1975; Brown & Reeve, 1986). However, in *Sulfolobus* and *Methanothermobacter*, the existence of an archaeal exosome with characteristics of the eukaryotic exosome was demonstrated (Evguenieva-Hackenberg *et al.*, 2003; Farhoud *et al.*, 2005). The exosome is a multiprotein complex involved in the maintenance of the

correct levels of mRNA in eukaryotic cells (van Hoof & Parker, 1999) (see also below the section on RNA degradation on eukaryotic microorganisms). The exosome of the archaeon *S. solfataricus* is a protein complex with a dual function: it is an RNA-tailing and RNA-degrading enzyme because it has both phosphorolytic and polyadenylating activity (Lorentzen *et al.*, 2005; Portnoy *et al.*, 2005). It is formed by a hexameric ring consisting of three dimers of the orthologues of Rrp41 and Rrp42, and is responsible for phosphorolytic RNA degradation (Lorentzen *et al.*, 2005). It is able to synthesize heteropolymeric RNA tails, and, generally, RNA synthesis by the hexameric ring is more efficient than RNA phosphorolysis (Evguenieva-Hackenberg *et al.*, 2008). The Rrp41 orthologue contains the active site; however, the ring structure is necessary for the activity of the complex (Lorentzen *et al.*, 2005). On the top of the ring there are three polypeptides with RNA-binding domains that are orthologues of Rrp4 (which contains S1 and KH domains) and/or Csl4 (which contains S1 and Zn-ribbon domains) (Buttner *et al.*, 2005; Lorentzen *et al.*, 2007). Recently, the structure of the *S. solfataricus* exosome was resolved (Lu *et al.*, 2010). The structure showed that the RNA-binding ring is flexible, which may be important for the unwinding of secondary structures (Lu *et al.*, 2010). The structure of the archaeal nine-subunit exosome is very similar to the one present in Eukarya and to PNPase (Lorentzen *et al.*, 2005, 2007; Liu *et al.*, 2006b). However, the archaeal exosome contains at least one additional subunit with an unknown function, a protein designated DnaG (Evguenieva-Hackenberg *et al.*, 2003), which can participate in 5S rRNA gene maturation. The *S. solfataricus* exosome is able to degrade synthetic and natural RNA efficiently, which is in accordance with its proposed role as a major complex of 3′ to 5′ exoribonucleases in the cell. Moreover, the genome of *S. solfataricus* does not contain genes for other predicted 3′–5′ exoribonucleases. In the absence of triphosphate at the 5′ end, the mRNA degradation can also occur in the 5′–3′ direction (Hasenohrl *et al.*, 2008). In this case, the degradation is probably performed by the RNase J1/J2 homologue, which is identical to the Mbl-like RNase (Koonin *et al.*, 2001).

However, in halophilic and many methanogenic archaea genomes, it is not possible to find the orthologues of exosomal subunits, which indicates that the mechanism for RNA degradation may be different in these archaea (Koonin *et al.*, 2001). Moreover, in archaea without an exosome, there is no post-transcriptional modification of the RNA molecules, and no tails are added to RNAs (Portnoy *et al.*, 2005; Portnoy & Schuster, 2006). In halophilic archaea, there is an RNase R-like protein that is not found in methanogenic archaea (Portnoy & Schuster, 2006). Like in *Mycoplasma*, these archaea also have a minimal genome, and, for this reason, the RNase R homologue may be the only enzyme responsible for the exoribonucleolytic activity, because both exosome and PNPase are absent (Zuo & Deutscher, 2001). *Haloferax volcanii* is a representative halophilic archaeon. It was shown that RNase R is required for viability in *H. volcanni*, and therefore, plays an important role in the mechanism of RNA degradation independent of polyadenylation (Portnoy *et al.*, 2005; Portnoy & Schuster, 2006).

The RNases in action

Processing and degradation of RNAs

Processing of RNAs

All rRNA and tRNA species are transcribed as precursor molecules that further undergo a series of modifications to achieve the mature molecules (Deutscher, 2009). Here, we will focus on the importance of RNases in the processing events during the maturation of rRNA and tRNA effectors. We will also refer to their role in the quality control of these processes.

In prokaryotes, the 70S ribosomes are constituted of two subunits: 30S and 50S particles. The smaller subunit comprises a 16S rRNA molecule and 21 proteins, and the larger subunit comprises a 23S and a 5S rRNA molecules plus 33 proteins. rRNAs are transcribed as precursor molecules that are processed and modified while assembly is occurring. In *E. coli*, there are seven rRNA operons comprising the three rRNA molecules always displayed in the same order: the 16S gene at the 5′ end, followed by the 23S, and finally by the 5S rRNA gene at the 3′ end (Deutscher, 2009). During transcription, RNase III cleaves double-stranded structures in the pre-rRNAs, releasing the fragments that will be subsequently cleaved to generate the 16S, 23S and 5S rRNA genes (Robertson *et al*., 1968; Gegenheimer & Apirion, 1975).

RNase E further reduces the extra 115 nt from the 17S rRNA gene (16S rRNA gene precursor) to 66 at the 5′ end, resulting in a 16.3S intermediate. Finally, RNase G (also termed RNase M16) converts the 5′ end to the mature molecule (Hayes & Vasseur, 1976; Dahlberg *et al.*, 1978; Li *et al.*, 1999b). In *B. subtilis*, the 5′–3′ exoribonuclease RNase J1 is involved in rRNA processing (Even *et al.*, 2005; Britton *et al.*, 2007; de la Sierra-Gallay *et al.*, 2008). The 3′ maturation enzyme remains to be characterized both in *E. coli* and in *B. subtilis*. In *P. syringae* the 3′–5′ exonuclease RNase R seems to be acting to directly induce the maturation of the 3′ terminus of the 16S rRNA gene (Cheng & Deutscher, 2002, 2005; Deutscher, 2006, 2009; Purusharth *et al.*, 2007).

The *E. coli* 23S rRNA gene precursor is released, harboring three or seven 5′ and seven to nine 3′ extra residues. The 3′ maturation requires RNase T for completion (Li *et al.*, 1999a). In *B. subtilis* the RNase III family Mini-III dimeric enzyme is responsible for the simultaneous maturation of both 5′ and 3′ sides of the double-stranded stalk that flanks

the mature 23S rRNA gene (Olmedo & Guzman, 2008; Redko *et al.*, 2008). *Salmonella* constitutes an interesting case where RNase III removes IVS in a way that the mature rRNA molecule results from two fragments (Burgin *et al.*, 1990).

The *E. coli* 5S rRNA gene derives from a 9S precursor, which is endonucleolytically cleaved by RNase E, releasing an intermediate molecule with three additional nucleotides at both ends (Ghora & Apirion, 1978; Misra & Apirion, 1979). The 5′ maturation is still uncharacterized, while RNase T is again responsible for removing (at least) the least two 3′ residues (Li & Deutscher, 1995). *Bacillus subtilis* almost repeats the mechanism of maturation of the 23S for the 5S rRNA gene, but in this case, RNase M5 cleaves the double-stranded region, simultaneously inducing the maturation of the 5′ and 3′ ends (Sogin *et al.*, 1977).

rRNA degradation takes place whenever errors (e.g. improper structure conformations, or misordered addition of proteins) occur and also in response to stress conditions (Deutscher, 2009). Quality control mechanisms occur at levels that are almost negligible in fast-growing cells, but are nevertheless essential as they avoid the accumulation of defective ribosomes. RNase LS may participate in the 23S rRNA gene degradation; PNPase, together with an RNA helicase or RNase R, may also be involved, because they are the only ones that can degrade structured RNAs. In addition to these, any process that leads to damaged cell membranes induces drastic RNA degradation, because it promotes the release of the nonspecific endoribonuclease RNase I from the periplasm into the cells (Cheng & Deutscher, 2005; Otsuka & Yonesaki, 2005; Deutscher, 2009).

tRNAs are vital adaptors for the decoding of the genome into proteins, and contribute up to 20% of the total RNA in the cell (Dittmar *et al.*, 2004; Hartmann *et al.*, 2009). Both *E. coli* K12 and *B. subtilis* bear 86 tRNA genes in their genome, many of them associated into operons (Fournier & Ozeki, 1985; Inokuchi & Yamao, 1995; Dittmar *et al.*, 2004). Introns are rarely found and are present only in the anticodon loop of some tRNAs in bacteria, but occur extensively in archaea (Vogel & Hess, 2001; Marck & Grosjean, 2002, 2003). Two endoribonucleases mainly process the pre-tRNAs: RNase P, which almost universally generates 5′ mature ends (Evans *et al.*, 2006; Randau *et al.*, 2008), and RNase Z, which cleaves the CCA-less pre-tRNAs (see the sections on RNase P and RNase Z for details on these enzymes). All tRNA molecules must have a CCA signal at their 3′ end to allow aminoacylation by the tRNA nucleotidyltransferase. That can be achieved, either by removing all extra nucleotides, when it is already present in the sequence, or cutting after the discriminator nucleotide (Li & Deutscher, 1995; Hartmann *et al.*, 2009). The CCA motif varies from absent in eukarya to being present in all genes of *E. coli*, about 2/3 of the *B. subtilis* pre-tRNAs, and from 0% to 100% in archaea (Hartmann *et al.*, 2009). Two main modes of 3′ maturation have been described so far: a one-step endonucleolytic cleavage by the universally conserved RNase Z homodimer (Dutta & Deutscher, 2009) and a multistep process involving both endo- and exonucleases (Li *et al.*, 1998; Hartmann *et al.*, 2009).

For instance, in *E. coli* where all genes encode the CCA sequence, maturation usually begins with an RNase E cut at the 3′ end (eventually aided by PNPase or RNase II), followed by 5′ processing by RNase P, and a final 3′ exonucleolytic trimming to expose the CCA sequence. The trimming reaction is carried out by RNase II, RNase D, or more effectively, RNase T or RNase PH (Li & Deutscher, 2002; Ow & Kushner, 2002).

Even though RNase Z is not essential for *E. coli*, it is encoded in its genome and has been shown to be able to shut down growth when overexpressed (Takaku & Nashimoto, 2008).

In *B. subtilis* all the CCA-less tRNAs are processed by the RNase Z and all the CCA-containing tRNAs are envisaged to follow a multistep maturation pathway, although the endonuclease responsible for the first step has not yet been found (Pellegrini *et al.*, 2003). RNase PH is the main exo involved in the trimming process (Wen *et al.*, 2005).

tRNAs have several constraints because they must be sufficiently similar to be processed, and able to fit within the ribosome, but must be sufficiently different to ensure correct loading with specific amino acids and recognize exclusively the codon(s) for their anticodon sequence (Hopper *et al.*, 2010). Modifications are of absolute importance for folding stabilization avoiding rapid decay, fidelity and efficiency of aminoacylation and/or proper binding to the ribosomes (Hou & Perona, 2010; Phizicky & Alfonzo, 2010). Indeed, about 100 modifications have been described for tRNAs so far (Czerwoniec *et al.*, 2009; Hopper *et al.*, 2010). Although tRNAs are stable, they have quality control mechanisms for eliminating defective species, and it seems at least partially dependent on polyadenylation by poly(A) polymerase (and removal by polynucleotide phosphorylase). RNase R has also been shown to participate in tRNA quality control mechanisms in a *B. subtilis* conditional CCA mutant strain. In this sense, flawed stable RNA molecules would behave like unstable RNAs being rapidly degraded by similar mechanisms (Li *et al.*, 2002; Campos-Guillen *et al.*, 2010).

tmRNA is a hybrid/bifunctional RNA molecule that shares the characteristics of both tRNA structural folds involving the 3′ and 5′ ends (Hayes & Keiler, 2010) – and mRNA – bearing a sequence that encodes for an ORF, consisting of a peptide signal for proteolytic degradation, ended with UAA termination codons. The tmRNA maturation is similar to the mechanism described above regarding tRNA processing. However, it was shown that RNase R is quite important for the maturation of the 3′ end of the

tmRNA, even more relevantly under cold-shock conditions (Cairrão *et al.*, 2003). SmpB is a small basic protein that binds to tmRNA with a high affinity and specificity (Karzai *et al.*, 1999; Dulebohn *et al.*, 2006), and specifically recognizes paused ribosomes near the 3′ end of truncated mRNAs (Janssen & Hayes, 2009). This RNA-binding protein is a regulator for the tmRNA-based quality control system in the cells, because it can prevent tmRNA degradation by RNase R (Hong *et al.*, 2005).

RNA degradation mechanisms

The same RNA molecule can be degraded by different pathways depending on the stress conditions or the growth phase. Thus, the degradation pathways are not universal. However, the interplay between the different factors involved in RNA decay emphasizes the role of RNases in the degradation of multiple substrates (Fig. 3).

In this section, we illustrate various examples of the relevant mechanisms of mRNAs and sRNAs degradation mainly in *E. coli*, but we also refer to examples from *B. subtilis*.

pyrF-orfF

The dicistronic transcript from *pyrF-orfF* contains *pyrF*, encoding orotidine-5′-monophosphatase decarboxylase, and an ORF (*orfF*) encoding a polypeptide of unknown function (Donovan & Kushner, 1983; Jensen *et al.*, 1984; Turnbough *et al.*, 1987). The full-length transcript is rapidly cleaved into a series of breakdown products, and at least 18 endonucleolytic cleavage sites have been mapped throughout the full-length mRNA (Arraiano *et al.*, 1997). Moreover, it seems that the *pyrF-orfF* transcript may be degraded by more than one enzymatic pathway depending on where the initial cleavage occurs. Therefore, some fragments seem to be degraded in a 5′–3′ direction, while other degradation products are processively cleaved in a 3′–5′ direction. The results obtained by Arraiano *et al.* (1997) provided, for the first time, support to the hypothesis that multiple decay pathways are involved in the decay of a single transcript. It thus seems reasonable to assume that *in vivo* there are a variety of ways in which a particular mRNA can be degraded. Which pathway is used may be related to the particular context in which one or more of the decay-mediating factors has access to the mRNA.

trxA

The *E. coli trxA* gene, which encodes for thioredoxin, is transcribed as a monocistronic message of 493 nucleotides. In the study of the *trxA* decay multiple mutant strains were constructed deficient in RNase E (*rne* – previously known as *ams*), PNPase (*pnp*) and RNase II (*rnb*) (Arraiano *et al.*, 1988). Northern and S1 analysis showed that full-length transcripts are initially processed by endonucleolytic cleavages (Arraiano *et al.*, 1993). The complete degradation of the initially cleaved transcripts occurs through progression of endonucleolytic steps in the 3′–5′ direction, followed by exonucleolytic degradation by RNase II and PNPase. This was the first report of a progression of endonucleolytic cleavages in a 3′–5′ direction during the degradation of a full-length transcript.

rpsO

The *rpsO* gene encodes for the *E. coli* ribosomal protein S15. The degradation of *rpsO* mRNA is accomplished by several independent pathways, including the RNase E-dependent endonucleolytic pathway and a pathway that requires the polyadenylation of transcripts (Braun *et al.*, 1996). The stability of the *rpsO* transcript is mainly controlled by RNase E. After RNase E cleavage, the mRNA lacking the 3′-terminal RNA secondary structure becomes an ideal substrate for PNPase (Braun *et al.*, 1996). When the primary pathway of decay mediated by RNase E is inactive, the exoribonucleolytic poly(A)-dependent degradation of *rpsO* mRNA is stimulated (Hajnsdorf *et al.*, 1995; Marujo *et al.*, 2003; Folichon *et al.*, 2005). It was shown that RNase R is the main enzyme involved in the poly(A)-dependent degradation of the *rpsO* mRNA (Andrade *et al.*, 2009a) and that RNase II protects the full-length *rpsO* mRNA from degradation by removing the poly(A) tails (Marujo *et al.*, 2000). Elongated *rpsO* transcripts harboring poly(A) tails of increased length are specifically recognized by RNase R and strongly accumulate in the absence of this exonuclease. Because this enzyme is able to degrade dsRNAs, the 3′ oligo(A)-extension may stimulate the binding of RNase R, allowing the complete degradation of the *rpsO* mRNA. The RNA chaperone Hfq can protect the *rpsO* mRNA from exonucleolytic degradation by PNPase and RNase II, and from cleavage by RNase E (Folichon *et al.*, 2003). Moreover, it was shown recently that in the absence of this chaperone, stabilization of *rpsO* mRNA occurs, with a concomitant decrease in its level, indicating that the change in the mRNA levels in the *hfq* mutant does not result from the modification of RNA stability, but probably from changes in transcriptional activity (Le Derout *et al.*, 2010).

rpsT

The *rpsT* gene encodes the *E. coli* ribosomal protein S20. This gene is transcribed from two promoters (P1 and P2) and terminates at a Rho-independent terminator, yielding two monocistronic mRNA species: P1 (447 nt) and P2 (356 nt) (Mackie & Parsons, 1983). The first step of the *rpsT* decay is carried out by RNase E and there are several lines of evidence indicating that this step is independent of polyadenylation (Mackie, 1991; Coburn & Mackie, 1996b, 1998). However,

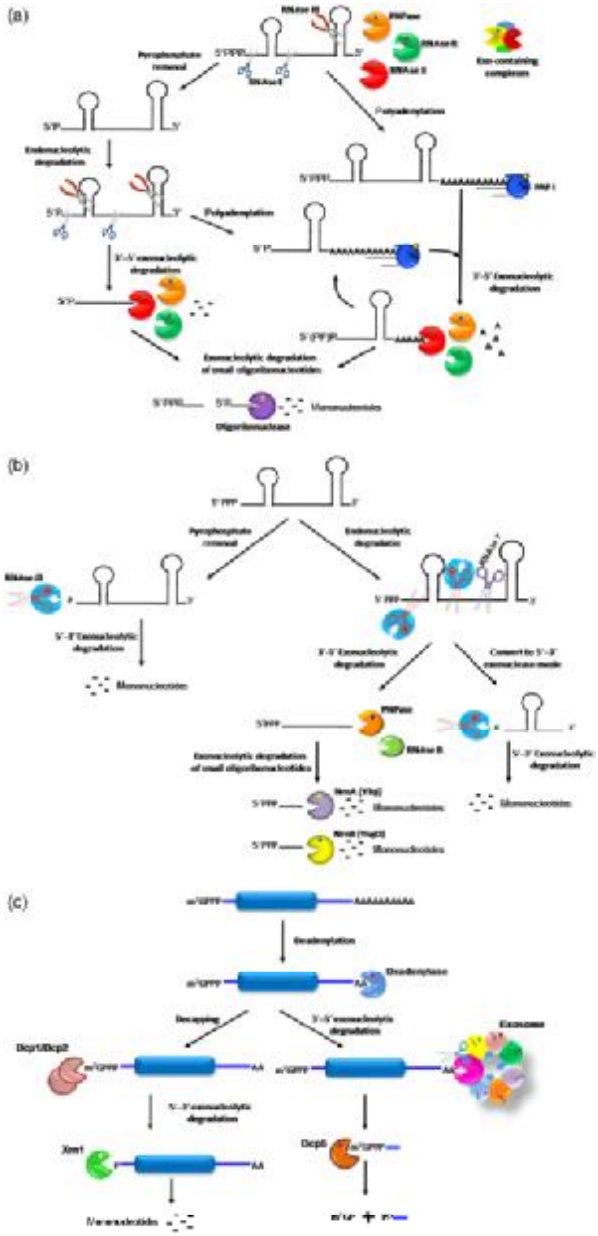

Fig. 3. Mechanisms of decay. (a) Model of RNA degradation pathways in *Escherichia coli*. The decay of the majority of transcripts starts with an endoribonucleolytic cleavage by RNase E. This endoribonuclease prefers a monophosphorylated 5′ end, but not in a strict way, and several RNAs escaping this rule have been described (Kime *et al.*, 2009). RNase III is another enzyme responsible for the initial endoribonucleolytic cleavage of structured RNAs. However, unlike RNase E (that only cleaves single-stranded RNAs), RNase III cleaves dsRNAs. After endoribonucleolytic cleavages, the linear transcripts are rapidly degraded by the 3′–5′ degradative exoribonucleases, RNase II, RNase R and PNPase. RNase R, unlike RNase II and PNPase, is efficient against highly structured RNAs. PNPase, in association with other proteins, namely RNA helicases, can also unwind RNA duplexes. A minor pathway in the cell is the exoribonucleolytic degradation of full-length transcripts. Poly(A) polymerase (PAP I) adds a poly(A) tail to the short 3′ overhang. These tails provide a 'toe-hold' to which exoribonucleases can bind. Cycles of polyadenylation and exoribonucleolytic digestion can overcome RNA secondary structures. The small oligoribonucleotides (two to five nucleotides) released by exoribonucleases are finally degraded to mononucleotides by oligoribonuclease (Andrade *et al.*, 2009b). (b) Model of RNA degradation pathways in *Bacillus subtilis*. In *B. subtilis*, the main enzyme responsible for RNA decay is RNase J1. RNase J1 has both an endoribonucleolytic and a 5′–3′ exoribonucleolytic activity (Mathy *et al.*, 2007). RNase J2 has endoribonucleolytic cleavage activities and specificities similar to RNase J1 and normally they form a complex. RNAs can be degraded from the 5′ end by the 5′–3′ exoribonuclease activity of RNase J1, or first, they can be endonucleolytically cleaved by RNase J1 or by RNase Y (Shahbabian *et al.*, 2009). The products from this endoribonucleolytic cleavage can then be degraded by the 3′–5′ exoribonucleases, PNPase and RNase R, or by the 5′–3′ exoribonuclease activity of RNase J1 (Bechhofer, 2009). The small oligoribonucleotides released by the 3′–5′ exoribonucleases are finally degraded to mononucleotides by the NrnA (YTqI) or the NrnB (YngD) enzymes (Fang *et al.*, 2009). (c) Model of RNA degradation in eukaryotes. In yeast, the mRNA decay is initiated with the shortening of the poly(A) tail at the 3′ end (deadenylation). After deadenylation, there are two possible degradation pathways for the transcripts. One is the removal of the 5′ cap structure of the transcripts by the Dcp1p/Dcp2p decapping complex, leaving the RNA molecule accessible to the Xrn1 5′–3′ exoribonuclease, which rapidly degrades the uncapped RNA. The other pathway is the 3′–5′ exoribonucleolytic degradation by the exosome, a multiprotein complex in which the Rrp44 is the only active RNase (Houseley & Tollervey, 2009). Recently, it was demonstrated that Rrp44 can degrade RNA in both an exo- and an endoribonucleolytic manner (Schaeffer *et al.*, 2009). The capped oligonucleotides produced from the exosome RNA decay are hydrolyzed by the DcpS scavenger decapping enzyme (Liu & Kiledjian, 2006a).

PAP I, PNPase, ATP and phosphate are necessary to catalyze the degradation of the smaller intermediates generated by RNase E cleavage (Coburn & Mackie, 1998). On the other hand, RNase II inhibits PNPase-mediated degradation of transcripts by removing the poly(A) tails added by PAP I. The same had also been observed with *rpsO* (Coburn & Mackie,

1998; Marujo *et al.*, 2000). Therefore, RNase II paradoxically protects these RNAs from degradation by PNPase.

malEF

The polycistronic malEFG operon of *E. coli* encodes three proteins involved in the transport of maltodextrins. The *malEF* intercistronic region contains two REP sequences (Newbury *et al.*, 1987) that protect the transcript from 3′–5′ exonucleolytic degradation (Higgins *et al.*, 1988). RNase R and PNPase are shown to play a major role in the degradation of the sRNA fragments resulting from the RNase E cleavage (Khemici & Carpousis, 2004; Cheng & Deutscher, 2005). PNPase degradation of the *malEF* transcript is only accomplished in the presence of RNase E and RhlB, indicating that the degradosome complex participates in this degradation (Stickney *et al.*, 2005). RhlB unwinds the folded RNA and passes it to PNPase (Coburn *et al.*, 1999; Khemici & Carpousis, 2004). Polyadenylation of the *malEF* REP sequences by PAP I seems to be a crucial factor in the degradation of these sequences because they accumulate to high levels in *pcn*B mutants (Khemici & Carpousis, 2004).

ompA

The *ompA* gene is transcribed as a monocistronic mRNA and encodes the major protein of *E. coli* outer membrane OmpA (von Gabain *et al.*, 1983). It was demonstrated previously that *ompA* stability is growth rate dependent and that shorter generation times in the exponential phase corresponded to longer *ompA* mRNA half-lives (Nilsson *et al.*, 1984). The degradation of this mRNA is initiated by an RNase E cleavage in the 5′ UTR stem-loops (Melefors & von Gabain, 1988; Arnold *et al.*, 1998). Then, exonucleolytic degradation and polyadenylation seem to account for the elimination of breakdown products (O'Hara *et al.*, 1995; Mohanty & Kushner, 1999; Andrade *et al.*, 2006). The presence of only one of the exoribonucleases (RNase II, RNase R or PNPase) may be sufficient to remove most of the decay intermediates (Cheng & Deutscher, 2005). Furthermore, the exonucleolytic activity on the full-length *ompA* transcript was shown to be growth phase regulated (Andrade *et al.*, 2006). The sRNA MicA, first known as SraD, is the principal post-transcriptional regulator of the *ompA* expression (Rasmussen *et al.*, 2005; Udekwu *et al.*, 2005). This antisense sRNA, when present in high levels, blocks ribosome binding at the *ompA* mRNA translation start site and subsequently destabilizes this mRNA. Moreover, the MicA-mediated decay of *ompA* mRNA depends on Hfq (Rasmussen *et al.*, 2005; Udekwu *et al.*, 2005). Therefore, the levels of *ompA* are also dependent on the levels of MicA. Because OmpA is one of the main outer membrane proteins in *E. coli*, it is fundamental to have a strict regulation in order to maintain the homeostasis of the cell.

pac

Penicillin amidase, encoded by the *pac* gene, is an important enzyme for industry because it is used in the production of semi-synthetic penicillins. The degradation of this mRNA seems to be initiated by an endonucleolytic cleavage because the most remarkable stabilization of the *E. coli pac* mRNA was obtained in the RNase E mutant. RNase III seems to play no role in the degradation of this transcript. The RNase E cleavage is followed by the exonucleolytic degradation by RNase II, RNase R and/or PNPase. Single deletions of any of these exoribonucleases were unable to stabilize this mRNA most probably because of their redundant effect (Viegas *et al.*, 2005).

trp

In the last few years, the degradation of the *B. subtilis* tryptophan operon, *trp*, has been studied in detail. This operon was used recently for the study of the cleavage specificity of the RNase J1 endonuclease (Deikus & Bechhofer, 2009). The *trp* operon is regulated at the level of transcription termination (Babitzke & Gollnick, 2001; Henkin & Yanofsky, 2002), which is controlled by binding of the *trp* RNA-binding attenuation protein (TRAP) to the *trp* leader RNA. When the supply of intracellular tryptophan is low, the *trp* operon genes are transcribed from a constitutive promoter and more tryptophan is generated. When the intracellular supply of tryptophan is sufficient, the TRAP protein complex binds to a specific region of the *trp* leader sequence. This binding results in the formation of a stem-loop structure that induces transcription termination, generating a 140 nt *trp* leader RNA.

The degradation of this *trp* leader RNA is initiated by an RNase J1 endonucleolytic cleavage at a single-stranded AU-rich region upstream of the 3′ transcription terminator (Deikus *et al.*, 2008). This cleavage is followed by a 5′–3′ degradation of the downstream fragment by the exonucleolytic activity of the RNase J1 (Deikus *et al.*, 2008) and a 3′–5′ degradation of the upstream fragment by PNPase (Deikus *et al.*, 2004). The PNPase action is essential for the efficient release and recycling of TRAP (Deikus *et al.*, 2004).

sRNAs

RNases also play a very important role in the regulation of sRNAs. These RNAs have received considerable attention over the past decade because they can be crucial for the post-transcriptional control of gene expression (Storz *et al.*, 2004; Viegas & Arraiano, 2008). In order to understand the action of these sRNAs, it is fundamental to study the processing and turnover of these molecules.

sRNA MicA and RybB are stationary-phase regulators and belong to the group of sRNAs that control outer membrane permeability. RybB controls the expression of outer membrane proteins OmpC and OmpW (Guillier

et al., 2006; Johansen *et al.*, 2006) and MicA controls the expression of OmpA (Rasmussen *et al.*, 2005; Udekwu *et al.*, 2005). In *E. coli*, MicA and RybB are destabilized by PNPase in the stationary phase (Andrade & Arraiano, 2008). Moreover, PNPase can degrade MicA in a degradosome-independent manner. Polyadenylation of MicA by PAP I appears not to be essential for PNPase action on this sRNA. The 3′ exoribonucleases RNase II and RNase R appear not to be required for the degradation of MicA.

In *S. typhimurium*, the sRNAs MicA, SraL, CsrB and CsrC are also mainly degraded by PNPase in the late stationary phase. In the case of CsrB and CsrC, the absence of this exoribonuclease also induced a change in degradation patterns with the accumulation of several decay intermediates (Viegas *et al.*, 2007).

The antisense RNA CopA inhibits the replication of plasmid R1 by binding to the target region, CopT, that is located within the *repA* mRNA. This binding blocks the synthesis of the replication initiator protein RepA (Stougaard *et al.*, 1981; Givskov & Molin, 1984). The decay of CopA is initiated by an endonucleolytic cleavage by RNase E, followed by the addition of a poly(A) tail. The poly(A) tails facilitate degradation by PNPase and RNase II (Söderbom *et al.*, 1997). Both PNPase and RNase II were able to degrade the processed transcript (Söderbom & Wagner, 1998).

ColE1 RNAI is the copy number regulator of the plasmid ColE1 (Lin-Chao & Cohen, 1991). PNPase, PAP I, RNase E and RNase III have been demonstrated to play roles in ColE1 RNAI decay (Lin-Chao & Cohen, 1991; Xu *et al.*, 1993; Xu & Cohen, 1995; Binnie *et al.*, 1999). Two degradation pathways have been suggested for this RNA (Binnie *et al.*, 1999). The primary pathway starts with RNase E cleavage, followed by PAP I polyadenylation and PNPase-mediated degradation. The second mechanism begins with the polyadenylation of RNAI, followed by RNase III cleavage and a subsequent exonucleolytic attack. In the absence of RNase E, RNase III and PAP I, the antisense RNAI continues to disappear, showing that yet other enzymes are able to catalyze its decay.

The replication of the ColE2 plasmid requires a plasmid-coded initiator protein, Rep. ColE2 RNAI controls *rep* expression by the blockage of translation (Takechi *et al.*, 1994). ColE2 RNAI degradation starts with RNase E cleavage at the 5′ end. PAP I polyadenylates the 3′ ends of degradation intermediates and both RNase II and PNPase act in further exoribonucleolytic degradation (Nishio & Itoh, 2008). Because PNPase and RNase II prefer a single-stranded 'toe-hold' to bind the 3′ end of the mRNA, PAP I generates a binding site for these exoribonucleases by adding a poly(A) tail to the 3′ end of the mRNA. Thus, cycles of polyadenylation and exoribonucleolytic attack contribute towards the correct degradation of the mRNA after the initial cleavage.

The *hok*/*sok* system mediates plasmid R1 stabilization by killing plasmid-free cells. Sok antisense RNA inhibits the translation of the *hok* mRNA, a toxic protein mRNA (Gerdes *et al.*, 1990). As Sok RNA is highly unstable, the pool of free Sok RNA decays rapidly in plasmid-free cells. The decay of Sok RNA leads to Hok protein synthesis and killing of the plasmid-free cells (Dam Mikkelsen & Gerdes, 1997). Like in the other antisense RNAs described previously, the initial step of Sok RNA decay is performed by RNase E in the single-stranded 5′ end. RNase E cleavage products are rapidly degraded from their 3′ ends by PNPase using a PAP I-dependent mechanism. Sok RNA, as well as CopA, is destabilized when RNase II is absent.

RNA degradation in eukaryotes

Because this publication has focused mainly on RNA degradation in prokaryotes, it was not the purpose of this chapter to provide a complete overview of RNA metabolism in eukaryotic cells but only pinpoints some interesting links between the systems. For a more comprehensive overview of the RNA degradation pathways in eukaryotes, readers can refer to publications focused on eukaryotes (Doma & Parker, 2007; Amaral *et al.*, 2008; Rougemaille *et al.*, 2008; Shyu *et al.*, 2008; Houseley & Tollervey, 2009; Moore & Proudfoot, 2009).

RNA degradation in eukaryotes is much more complex and involves more factors than those in prokaryotes (Houseley & Tollervey, 2009). The eukaryotic cell is divided into two main parts: the nucleus and the cytoplasm, and RNA degradation is important in both compartments. Compartmentalization causes considerable change in mRNA's fate; eukaryotic RNAs have to survive in the cell much longer than prokaryotic messengers, and the molecule synthesized in the nucleolus has to be transported to the cytoplasm for protein production. In the nucleus, aberrant transcripts are selectively degraded; RNases also act in multiple processing steps and remove the processing byproducts and a myriad of noncoding cryptic transcripts. The balance between the rate of transcription and RNA degradation regulates messenger levels. In the cytoplasm, the transcripts are translated to the proteins; therefore, in this compartment, it is very important to check the translational abilities of RNAs and remove incorrect molecules that can cause the production of aberrant proteins (Doma & Parker, 2007). In the cytoplasm, differences in the degradation rate can influence protein expression. A set of factors can affect the lifetime of the transcript including RNA-binding proteins that bind to the RNAs, and sRNAs that can drive transcripts to degradation or cause translational silencing (siRNA and miRNA) (Eulálio *et al.*, 2008; Carthew & Sontheimer, 2009).

It has been considered that in eukaryotes, the RNA degradation is mainly exonucleolytic (Fig. 3), while in prokaryotes, endonucleases have a significant impact on degradation process. In the best-studied model – yeast *S. cerevisiae* – the main enzymes involved in the degradation are exoribonucleases. Degradation in the 5′–3′ direction is performed by the Xrn1 protein in the cytoplasm and the Rat1 enzyme in the nucleus (Fritz *et al.*, 2004; Meyer *et al.*, 2004). The main yeast 3′–5′ hydrolytic exonuclease is Rrp44/(Dis3) from the RNase II family. In the nucleus, there is also another 3′–5′ exonuclease: Rrp6. Rrp44 interacts with the nine-protein ring-shapes complex to generate a ribonucleolytically active exosome, where Rrp44 is the only active RNase (Liu *et al.*, 2006b; Dziembowski *et al.*, 2007). The exosome ring is homologous to the archaeal complex with phosphorolytic nuclease activity and to the bacterial PNPase (Lorentzen *et al.*, 2007). Surprisingly, this huge protein machine lost its phosphorolytic activity in the evolution and in most eukaryotes can induce RNA degradation only when cooperating with the active component Rrp44 (Dziembowski *et al.*, 2007). Recent structural studies showed that even if the Rrp44 protein by itself is able to degrade RNA, it seems that the substrates that are delivered to this nuclease first have to pass the channel in the exosome ring structure (Bonneau *et al.*, 2009).

Research performed in the last few years proved that involvement of endonuclease activity in the RNA degradation process in eukaryotes was underestimated. Among the other examples (Huntzinger *et al.*, 2008; Eberle *et al.*, 2009), the most evident was the discovery of the endonucleolytic activity of the exosome complex; this activity is carried by the PIN domain localized in the N-terminal part of the Rrp44 protein. Rrp44, the only active component of the yeast exosome, can degrade RNA in both an exo- and an endonucleolytic manner. Because the homologues of Rrp44 from other eukaryotes also have PIN domains, it seems that endonucleolytic activity is the common feature in its RNA degradation (Lebreton *et al.*, 2008; Schaeffer *et al.*, 2009).

For a long time, the function of polyadenylation in the RNA degradation process was considered as one of the most striking differences between the eukaryotic and the prokaryotic RNA metabolism. In the eukaryotes, long poly(A) tails added by the poly(A) polymerase to the 3′ end of newly created transcripts have been considered as RNA-stabilizing elements while in the prokaryotic cell polyadenylation leads to transcript degradation. Surprisingly, it was discovered that in eukaryotes, polyadenylation can also drive RNAs to decay. The TRAMP complex composed of poly(A) polymerase, helicase and an RNA-binding protein is able to add short poly(A) tails to the aberrant transcripts, targeting them to induce rapid degradation (LaCava *et al.*, 2005). This showed that the poly(A)-dependent RNA degradation mechanism active in prokaryotes is still present in eukaryotic cells.

Last discoveries in the field of RNA degradation in eukaryotes showed that we can find much more similarities to prokaryotic systems than was previously expected. The degradation pathways in eukaryotes are obviously more complex and different in many aspects, but at the same time, many mechanisms are very similar. We can find homologues of prokaryotic enzymes that serve important functions in eukaryotic systems such as bacterial RNase II and RNase R homologue Rrp44, RNase D homologue Rrp6, the exosome ring that is structurally very similar to PNPase and others. Moreover, we can find strikingly similar mechanisms even if they are performed by factors without obvious homology. A key example is the prokaryotic antiviral defense system CRISPR, which resembles the eukaryotic RNAi mechanism (Hale *et al.*, 2009). Another example is the 5′–3′ direction exoribonucleolytic degradation pathway, which is very important in eukaryotic RNA metabolism. In the last few years, it became clear that, in spite of earlier beliefs, this pathway in prokaryotes also exists, but enzymes that are involved are not homologues of the eukaryotic ones (Mathy *et al.*, 2007). This and many other examples clearly show that evolution has led to the development of similar solutions regarding degradation mechanisms.

Eukaryotic organelles are structures of endosymbiotic prokaryotic origin; they possess their own usually reduced genome, which is expressed and transcribed, and RNAs are processed and degraded. The expression of proteins encoded in the organellar genome is, in most cases, crucial for energy management in eukaryotic cells. Many questions still remain about the RNA degradation pathways in organelles, mostly because they seem to be different in different organisms and so it is hard to find the general rules that can be applied to all systems. Nonetheless, RNA metabolic pathways in the organelles retained some characteristics of the prokaryotic ancestors. RNA degradation in chloroplasts seems to be most similar to prokaryotic process. In the higher plant genomes, we can find sequences of homologues of bacterial nucleases RNase E and RNase J that are localized in chloroplasts (Lange *et al.*, 2009). The degradation process, similar to that in bacteria, starts with endonucleolytic cleavage and is then accelerated by polyadenylation and exonucleolytic degradation by PNPase. There is also an RNase R homologue that was shown to play a role in rRNA processing (Bollenbach *et al.*, 2005).

RNA degradation pathways in the mitochondria seem to be more divergent in different organisms. Interestingly, and in contrast to the situation in chloroplasts, degradation pathways in the mitochondria are supposed to be mostly exonucleolytic. In plants, the main player seems to be PNPase, which degrades polyadenylated RNA molecules in the mitochondria (Holec *et al.*, 2006). In contrast, in yeast *S. cerevisiae*, there is no mitochondrial PNPase; instead, the main degrading machinery is the mitochondrial

degradosome complex (mtEXO), which digests RNA in the 3′–5′ direction and is composed of the homologue of RNase II-Dis3 protein and the conserved RNA DEAD-box helicase Suv3 (Dziembowski *et al.*, 2003; Malecki *et al.*, 2007). Additionally, it was suggested that there is one more potential enzyme Pet127 that can degrade RNA in the 5′–3′ direction (Fekete *et al.*, 2008). Surprisingly, there is no polyadenylaton in yeast mitochondria; instead, stabilizing functions are served by the proteins that bind to the 3′ and 5′ untranslated ends of the RNA molecules. Degradation of transcripts in human mitochondria is not well characterized. Although the data on this topic are not consistent, it seems that a homologue of bacterial PNPase is present in the mitochondria, and it was found recently that it can form a complex with the human homologue of Suv3 helicase. Suv3 is involved in RNA degradation and removal of aberrant and cryptic transcripts; the exact function of this protein is still not clear (Szczesny *et al.*, 2010). Transcripts in human mitochondria are stably polyadenylated, which, in contrast to the situation in plant mitochondria, suggests a stabilization role for poly(A) tails (Tomecki *et al.*, 2004). On the other hand, scientists also discovered polyadenylated degradation byproducts, which suggests that polyadenylation can trigger or aid transcripts' degradation; therefore, it seems that polyadenylation in human mitochondria can serve both functions (Slomovic *et al.*, 2005; Szczesny *et al.*, 2010).

Concluding remarks

Maintenance of optimal levels of RNAs at any time and under any circumstance is an extremely difficult task to achieve and requires great coordination among all the factors involved in this control. It is also assumed that there is a cross-talk between transcription and degradation to maintain the balance that is best for the survival of microorganisms. There are several examples where this is obvious, and when a specific message is more transcribed, it is also more stabilized, and vice versa.

Transcripts can have a different half-life under different growth conditions to rapidly carry out the necessary changes and adjust to adequate RNA levels. The same RNA can have a 'preferred' decay pathway, but there are examples where there are alternative degradation pathways for the same transcript, depending on which enzyme cleaves first. After cleavage, the RNA breakdown product(s) can have a distinct half-life depending on sequence and structure. Therefore, the structural characteristics of RNA stability and instability predetermine the 'fate' of an RNA, but the environment and the consequent levels and nature of the degradative enzymes will also play a determinant role in its turnover. For instance, the mRNAs expressed in heterologous systems can have a very different half-life than if they are expressed in their own microorganism. The directionality of the decay process depends on the transcript analyzed. Once we characterize the enzymes from one microorganism, we can design strategies to stabilize RNAs. Mutants have been instrumental in characterizing degradation pathways and in changing the turnover of specific transcripts, especially because a limited number of RNases intervene in the maturation and degradation of RNAs.

There are fundamental principles that govern RNA decay in all organisms. Evolution has resulted in similar functions performed by different enzymes. For instance, in *E. coli*, RNase E is one of the major endonucleases, but this enzyme is absent in *B. subtilis*. In *B. subtilis*, RNase J1 seems to take over the same function, and this enzyme is not present in *E. coli*. RNase J1 has been shown to have both endo and 5′–3′ exo activities. In yeast, 5′–3′ decay is prominent, and Rrp44/Dis3, an RNase II family enzyme, has dual endo and 3′–5′ exo activities, being an example of an optimized 'RNA degradation machine'. Sometimes, RNases also combine into complexes to speed up the decay process or confer specificity to certain targets.

It is fascinating to know that RNases themselves are strictly regulated proteins and have mechanisms to adapt them to the environment and to the levels of the other RNases. For instance, RNase R is highly increased under cold shock; the levels of PNPase and RNase II are inter-regulated and the level of RNase E is autoregulated.

Recent studies demonstrate that, between prokaryotic and eukaryotic systems, the RNA degradation mechanisms have much more similarities than expected. The mechanism of RNAi in eukaryotes has shown the power of RNA degradation mechanisms involving RNases. It is now obvious that the modulation of RNA levels and their respective proteins can be rapidly achieved. In prokaryotes, it was already known that antisense RNAs could be quite important for the control of gene expression. Moreover, the recently discovered CRISP RNAs (Karginov & Hannon, 2010), which can be considered a bacterial RNAi mechanism, have lent an extra level of complexity to the study of RNAs and bacterial RNA degradation mechanisms. It is very stimulating to work in a field of research still full of surprises! This is a thorough review, but in a few years, we are sure that there will be much more to say!

It is our hope that this review conveys some of the current excitement in research on RNA and serves as a source of inspiration for scientists entering this field.

Acknowledgements

This work was supported by grants from FCT, Portugal. We thank Clementine Dressaire for critically reading this manuscript and Miguel Luís for the graphic assistance in Fig. 2.

References

Afonyushkin T, Vecerek B, Moll I, Blasi U & Kaberdin VR (2005) Both RNase E and RNase III control the stability of *sodB* mRNA upon translational inhibition by the small regulatory RNA RyhB. *Nucleic Acids Res* **33**: 1678–1689.

Agrawal N, Dasaradhi PV, Mohmmed A, Malhotra P, Bhatnagar RK & Mukherjee SK (2003) RNA interference: biology, mechanism, and applications. *Microbiol Mol Biol R* **67**: 657–685.

Alifano P, Rivellini F, Piscitelli C, Arraiano CM, Bruni CB & Carlomagno MS (1994) Ribonuclease E provides substrates for ribonuclease P-dependent processing of a polycistronic mRNA. *Gene Dev* **8**: 3021–3031.

Altman S, Wesolowski D, Guerrier-Takada C & Li Y (2005) RNase P cleaves transient structures in some riboswitches. *P Natl Acad Sci USA* **102**: 11284–11289.

Amaral PP, Dinger ME, Mercer TR & Mattick JS (2008) The eukaryotic genome as an RNA machine. *Science* **319**: 1787–1789.

Amblar M & Arraiano CM (2005) A single mutation in *Escherichia coli* ribonuclease II inactivates the enzyme without affecting RNA binding. *FEBS J* **272**: 363–374.

Amblar M, Viegas SC, Lopez P & Arraiano CM (2004) Homologous and heterologous expression of RNase III from *Lactococcus lactis*. *Biochem Bioph Res Co* **323**: 884–890.

Amblar M, Barbas A, Fialho AM & Arraiano CM (2006) Characterization of the functional domains of *Escherichia coli* RNase II. *J Mol Biol* **360**: 921–933.

Amblar M, Barbas A, Gomez-Puertas P & Arraiano CM (2007) The role of the S1 domain in exoribonucleolytic activity: substrate specificity and multimerization. *RNA* **13**: 317–327.

Andrade JM & Arraiano CM (2008) PNPase is a key player in the regulation of small RNAs that control the expression of outer membrane proteins. *RNA* **14**: 543–551.

Andrade JM, Cairrao F & Arraiano CM (2006) RNase R affects gene expression in stationary phase: regulation of *ompA*. *Mol Microbiol* **60**: 219–228.

Andrade JM, Hajnsdorf E, Régnier P & Arraiano CM (2009a) The poly(A)-dependent degradation pathway of *rpsO* mRNA is primarily mediated by RNase R. *RNA* **15**: 316–326.

Andrade JM, Pobre V, Silva IJ, Domingues S & Arraiano CM (2009b) The role of 3′–5′ exoribonucleases in RNA degradation. *Prog Mol Biol Transl Sci* **85**: 187–229.

Apirion D & Lassar AB (1978) A conditional lethal mutant of *Escherichia coli* which affects the processing of ribosomal RNA. *J Biol Chem* **253**: 1738–1742.

Arnold TE, Yu J & Belasco JG (1998) mRNA stabilization by the *ompA* 5′ untranslated region: two protective elements hinder distinct pathways for mRNA degradation. *RNA* **4**: 319–330.

Arraiano C, Yancey SD & Kushner SR (1993) Identification of endonucleolytic cleavage sites involved in decay of *Escherichia coli trx*A mRNA. *J Bacteriol* **175**: 1043–1052.

Arraiano CM, Yancey SD & Kushner SR (1988) Stabilization of discrete mRNA breakdown products in *ams pnp rnb* multiple mutants of *Escherichia coli* K-12. *J Bacteriol* **170**: 4625–4633.

Arraiano CM, Cruz AA & Kushner SR (1997) Analysis of the *in vivo* decay of the *Escherichia coli* dicistronic *pyr*F-*orf*F transcript: evidence for multiple degradation pathways. *J Mol Biol* **268**: 261–272.

Arraiano CM, Barbas A & Amblar M (2008) Characterizing ribonucleases *in vitro* examples of synergies between biochemical and structural analysis. *Method Enzymol* **447**: 131–160.

Asha PK, Blouin RT, Zaniewski R & Deutscher MP (1983) Ribonuclease BN: identification and partial characterization of a new tRNA processing enzyme. *P Natl Acad Sci USA* **80**: 3301–3304.

Awano N, Inouye M & Phadtare S (2008) RNase activity of polynucleotide phosphorylase is critical at low temperature in *Escherichia coli* and is complemented by RNase II. *J Bacteriol* **190**: 5924–5933.

Awano N, Rajagopal V, Arbing M, Patel S, Hunt J, Inouye M & Phadtare S (2010) *Escherichia coli* RNase R has dual activities, helicase and RNase. *J Bacteriol* **192**: 1344–1352.

Babitzke P & Gollnick P (2001) Posttranscription initiation control of tryptophan metabolism in *Bacillus subtilis* by the *trp* RNA-binding attenuation protein (TRAP), anti-TRAP, and RNA structure. *J Bacteriol* **183**: 5795–5802.

Babitzke P & Kushner SR (1991) The Ams (altered mRNA stability) protein and ribonuclease E are encoded by the same structural gene of *Escherichia coli*. *P Natl Acad Sci USA* **88**: 1–5.

Babitzke P, Granger L, Olszewski J & Kushner SR (1993) Analysis of mRNA decay and rRNA processing in *Escherichia coli* multiple mutants carrying a deletion in RNase III. *J Bacteriol* **175**: 229–239.

Baer MF, Wesolowski D & Altman S (1989) Characterization *in vitro* of the defect in a temperature-sensitive mutant of the protein subunit of RNase P from *Escherichia coli*. *J Bacteriol* **171**: 6862–6866.

Baker KE & Mackie GA (2003) Ectopic RNase E sites promote bypass of 5′-end-dependent mRNA decay in *Escherichia coli*. *Mol Microbiol* **47**: 75–88.

Barbas A, Andrade JM, Fialho AM & Arraiano CM (2006) Ribonucleases e controlo pós-transcripcional da expressão génica. *O Mundo do RNA – Novos Desafios e Perspectivas Futuras* (Arraiano CM & Fialho AM, eds), pp. 119–139. Lidel Edições Técnicas, Lisbon, Portugal.

Barbas A, Matos RG, Amblar M, Lopez-Vinas E, Gomez-Puertas P & Arraiano CM (2008) New insights into the mechanism of RNA degradation by ribonuclease II: identification of the residue responsible for setting the RNase II end-product. *J Biol Chem* **283**: 13070–13076.

Barbas A, Matos RG, Amblar M, Lopez-Vinas E, Gomez-Puertas P & Arraiano CM (2009) Determination of key residues for catalysis and RNA cleavage specificity: one mutation turns RNase II into a 'SUPER-ENZYME'. *J Biol Chem* **284**: 20486–20498.

Bardwell JC, Régnier P, Chen SM, Nakamura Y, Grunberg-Manago M & Court DL (1989) Autoregulation of RNase III operon by mRNA processing. *EMBO J* **8**: 3401–3407.

Barnett TC, Bugrysheva JV & Scott JR (2007) Role of mRNA stability in growth phase regulation of gene expression in the group A *Streptococcus*. *J Bacteriol* **189**: 1866–1873.

Bechhofer DH (2009) Messenger RNA decay and maturation in *Bacillus subtilis*. *Prog Mol Biol Transl Sci* **85**: 231–273.

Belitsky BR, Gustafsson MC, Sonenshein AL & Von Wachenfeldt C (1997) An lrp-like gene of *Bacillus subtilis* involved in branched-chain amino acid transport. *J Bacteriol* **179**: 5448–5457.

Beran RK & Simons RW (2001) Cold-temperature induction of *Escherichia coli* polynucleotide phosphorylase occurs by reversal of its autoregulation. *Mol Microbiol* **39**: 112–125.

Bermúdez-Cruz RM, Fernandez-Ramírez F, Kameyama-Kawabe L & Montañez C (2005) Conserved domains in polynucleotide phosphorylase among eubacteria. *Biochimie* **87**: 737–745.

Bernstein JA, Lin PH, Cohen SN & Lin-Chao S (2004) Global analysis of *Escherichia coli* RNA degradosome function using DNA microarrays. *P Natl Acad Sci USA* **101**: 2758–2763.

Binnie U, Wong K, McAteer S & Masters M (1999) Absence of RNase III alters the pathway by which RNAI, the antisense inhibitor of ColE1 replication, decays. *Microbiology* **145**: 3089–3100.

Blaszczyk J, Tropea JE, Bubunenko M, Routzahn KM, Waugh DS, Court DL & Ji X (2001) Crystallographic and modeling studies of RNase III suggest a mechanism for double-stranded RNA cleavage. *Structure* **9**: 1225–1236.

Blaszczyk J, Gan J, Tropea JE, Court DL, Waugh DS & Ji X (2004) Noncatalytic assembly of ribonuclease III with double-stranded RNA. *Structure* **12**: 457–466.

Bollenbach TJ, Lange H, Gutierrez R, Erhardt M, Stern DB & Gagliardi D (2005) RNR1, a 3′–5′ exoribonuclease belonging to the RNR superfamily, catalyzes 3′ maturation of chloroplast ribosomal RNAs in *Arabidopsis thaliana*. *Nucleic Acids Res* **33**: 2751–2763.

Bonneau F, Basquin J, Ebert J, Lorentzen E & Conti E (2009) The yeast exosome functions as a macromolecular cage to channel RNA substrates for degradation. *Cell* **139**: 547–559.

Bothwell AL, Garber RL & Altman S (1976) Nucleotide sequence and *in vitro* processing of a precursor molecule to *Escherichia coli* 4.5 S RNA. *J Biol Chem* **251**: 7709–7716.

Bralley P & Jones GH (2003) Overexpression of the polynucleotide phosphorylase gene (pnp) of *Streptomyces antibioticus* affects mRNA stability and poly(A) tail length but not ppGpp levels. *Microbiology* **149**: 2173–2182.

Bralley P, Gust B, Chang S, Chater KF & Jones GH (2006) RNA 3′-tail synthesis in *Streptomyces*: *in vitro* and *in vivo* activities of RNase PH, the SCO3896 gene product and polynucleotide phosphorylase. *Microbiology* **152**: 627–636.

Braun F, Hajnsdorf E & Régnier P (1996) Polynucleotide phosphorylase is required for the rapid degradation of the RNase E-processed *rps*O mRNA of *Escherichia coli* devoid of its 3′ hairpin. *Mol Microbiol* **19**: 997–1005.

Briani F, Del Favero M, Capizzuto R *et al.* (2007) Genetic analysis of polynucleotide phosphorylase structure and functions. *Biochimie* **89**: 145–157.

Briani F, Curti S, Rossi F, Carzaniga T, Mauri P & Dehò G (2008) Polynucleotide phosphorylase hinders mRNA degradation upon ribosomal protein S1 overexpression in *Escherichia coli*. *RNA* **14**: 2417–2429.

Britton RA, Wen T, Schaefer L *et al.* (2007) Maturation of the 5′ end of *Bacillus subtilis* 16S rRNA by the essential ribonuclease YkqC/RNase J1. *Mol Microbiol* **63**: 127–138.

Brown JW & Reeve JN (1986) Polyadenylated RNA isolated from the archaebacterium *Halobacterium halobium*. *J Bacteriol* **166**: 686–688.

Brown S & Coleman G (1975) Messenger ribonucleic acid content of *Bacillus amyloliquefaciens* throughout its growth cycle compared with *Bacillus subtilis* 168. *J Mol Biol* **96**: 345–352.

Bugrysheva JV & Scott JR (2009) The ribonucleases J1 and J2 are essential for growth and have independent roles in mRNA decay in *Streptococcus pyogenes*. *Mol Microbiol* **75**: 731–743.

Burgin AB, Parodos K, Lane DJ & Pace NR (1990) The excision of intervening sequences from *Salmonella* 23S ribosomal RNA. *Cell* **60**: 405–414.

Butland G, Peregrin-Alvarez JM, Li J *et al.* (2005) Interaction network containing conserved and essential protein complexes in *Escherichia coli*. *Nature* **433**: 531–537.

Buttner K, Wenig K & Hopfner KP (2005) Structural framework for the mechanism of archaeal exosomes in RNA processing. *Mol Cell* **20**: 461–471.

Cairrão F & Arraiano CM (2006) The role of endoribonucleases in the regulation of RNase R. *Biochem Bioph Res Co* **343**: 731–737.

Cairrão F, Chora A, Zilhão R, Carpousis AJ & Arraiano CM (2001) RNase II levels change according to the growth conditions: characterization of *gmr*, a new *Escherichia coli* gene involved in the modulation of RNase II. *Mol Microbiol* **39**: 1550–1561.

Cairrão F, Cruz A, Mori H & Arraiano CM (2003) Cold shock induction of RNase R and its role in the maturation of the quality control mediator SsrA/tmRNA. *Mol Microbiol* **50**: 1349–1360.

Calin-Jageman I & Nicholson AW (2003) RNA structure-dependent uncoupling of substrate recognition and cleavage by *Escherichia coli* ribonuclease III. *Nucleic Acids Res* **31**: 2381–2392.

Callaghan AJ, Aurikko JP, Ilag LL *et al.* (2004) Studies of the RNA degradosome-organizing domain of the *Escherichia coli* ribonuclease RNase E. *J Mol Biol* **340**: 965–979.

Callaghan AJ, Marcaida MJ, Stead JA, McDowall KJ, Scott WG & Luisi BF (2005a) Structure of *Escherichia coli* RNase E catalytic domain and implications for RNA turnover. *Nature* **437**: 1187–1191.

Callaghan AJ, Redko Y, Murphy LM *et al.* (2005b) 'Zn-link': a metal-sharing interface that organizes the quaternary structure and catalytic site of the endoribonuclease, RNase E. *Biochemistry* **44**: 4667–4675.

Campos-Guillen J, Arvizu-Gomez JL, Jones GH & Olmedo-Alvarez G (2010) Characterization of tRNACys processing in a conditional *Bacillus subtilis* CCase mutant reveals the

participation of RNase R in its quality control. *Microbiology* **156**: 2102–2111.
Cannistraro VJ & Kennell D (1989) Purification and characterization of ribonuclease M and mRNA degradation in *Escherichia coli*. *Eur J Biochem* **181**: 363–370.
Cannistraro VJ & Kennell D (1991) RNase I*, a form of RNase I, and mRNA degradation in *Escherichia coli*. *J Bacteriol* **173**: 4653–4659.
Cannistraro VJ & Kennell D (1994) The processive reaction mechanism of ribonuclease II. *J Mol Biol* **243**: 930–943.
Cannistraro VJ & Kennell D (1999) The reaction mechanism of ribonuclease II and its interaction with nucleic acid secondary structures. *Biochim Biophys Acta* **1433**: 170–187.
Cardenas PP, Carrasco B, Sanchez H, Deikus G, Bechhofer DH & Alonso JC (2009) *Bacillus subtilis* polynucleotide phosphorylase 3′-to-5′ DNase activity is involved in DNA repair. *Nucleic Acids Res* **37**: 4157–4169.
Carpousis AJ, Vanzo NF & Raynal LC (1999) mRNA degradation. A tale of poly(A) and multiprotein machines. *Trends Genet* **15**: 24–28.
Carpousis AJ, Luisi BF & McDowall KJ (2009) Endonucleolytic initiation of mRNA decay in *Escherichia coli*. *Prog Mol Biol Transl Sci* **85**: 91–135.
Carthew RW & Sontheimer EJ (2009) Origins and mechanisms of miRNAs and siRNAs. *Cell* **136**: 642–655.
Carzaniga T, Briani F, Zangrossi S, Merlino G, Marchi P & Dehò G (2009) Autogenous regulation of *Escherichia coli* polynucleotide phosphorylase expression revisited. *J Bacteriol* **191**: 1738–1748.
Celesnik H, Deana A & Belasco JG (2007) Initiation of RNA decay in *Escherichia coli* by 5′ pyrophosphate removal. *Mol Cell* **27**: 79–90.
Cerritelli SM & Crouch RJ (2009) Ribonuclease H: the enzymes in eukaryotes. *FEBS J* **276**: 1494–1505.
Chandran V & Luisi BF (2006) Recognition of enolase in the *Escherichia coli* RNA degradosome. *J Mol Biol* **358**: 8–15.
Chandran V, Poljak L, Vanzo NF *et al.* (2007) Recognition and cooperation between the ATP-dependent RNA helicase RhlB and ribonuclease RNase E. *J Mol Biol* **367**: 113–132.
Charpentier X, Faucher SP, Kalachikov S & Shuman HA (2008) Loss of RNase R induces competence development in *Legionella pneumophila*. *J Bacteriol* **190**: 8126–8136.
Chen JL, Nolan JM, Harris ME & Pace NR (1998) Comparative photocross-linking analysis of the tertiary structures of *Escherichia coli* and *Bacillus subtilis* RNase P RNAs. *EMBO J* **17**: 1515–1525.
Cheng ZF & Deutscher MP (2002) Purification and characterization of the *Escherichia coli* exoribonuclease RNase R. Comparison with RNase II. *J Biol Chem* **277**: 21624–21629.
Cheng ZF & Deutscher MP (2003) Quality control of ribosomal RNA mediated by polynucleotide phosphorylase and RNase R. *P Natl Acad Sci USA* **100**: 6388–6393.
Cheng ZF & Deutscher MP (2005) An important role for RNase R in mRNA decay. *Mol Cell* **17**: 313–318.
Cheng ZF, Zuo Y, Li Z, Rudd KE & Deutscher MP (1998) The *vacB* gene required for virulence in *Shigella flexneri* and *Escherichia coli* encodes the exoribonuclease RNase R. *J Biol Chem* **273**: 14077–14080.
Choi JM, Park EY, Kim JH, Chang SK & Cho Y (2004) Probing the functional importance of the hexameric ring structure of RNase PH. *J Biol Chem* **279**: 755–764.
Choonee N, Even S, Zig L & Putzer H (2007) Ribosomal protein L20 controls expression of the *Bacillus subtilis infC* operon via a transcription attenuation mechanism. *Nucleic Acids Res* **35**: 1578–1588.
Chung DH, Min Z, Wang BC & Kushner SR (2010) Single amino acid changes in the predicted RNase H domain of *Escherichia coli* RNase G lead to complementation of RNase E deletion mutants. *RNA* **16**: 1371–1385.
Clements MO, Eriksson S, Thompson A, Lucchini S, Hinton JC, Normark S & Rhen M (2002) Polynucleotide phosphorylase is a global regulator of virulence and persistency in *Salmonella enterica*. *P Natl Acad Sci USA* **99**: 8784–8789.
Coburn GA & Mackie GA (1996a) Overexpression, purification, and properties of *Escherichia coli* ribonuclease II. *J Biol Chem* **271**: 1048–1053.
Coburn GA & Mackie GA (1996b) Differential sensitivities of portions of the mRNA for ribosomal protein S20 to 3′-exonucleases dependent on oligoadenylation and RNA secondary structure. *J Biol Chem* **271**: 15776–15781.
Coburn GA & Mackie GA (1998) Reconstitution of the degradation of the mRNA for ribosomal protein S20 with purified enzymes. *J Mol Biol* **279**: 1061–1074.
Coburn GA, Miao X, Briant DJ & Mackie GA (1999) Reconstitution of a minimal RNA degradosome demonstrates functional coordination between a 3′ exonuclease and a DEAD-box RNA helicase. *Gene Dev* **13**: 2594–2603.
Commichau FM, Rothe FM, Herzberg C *et al.* (2009) Novel activities of glycolytic enzymes in *Bacillus subtilis*: interactions with essential proteins involved in mRNA processing. *Mol Cell Proteomics* **8**: 1350–1360.
Condon C & Putzer H (2002) The phylogenetic distribution of bacterial ribonucleases. *Nucleic Acids Res* **30**: 5339–5346.
Condon C, Brechemier-Baey D, Beltchev B, Grunberg-Manago M & Putzer H (2001) Identification of the gene encoding the 5S ribosomal RNA maturase in *Bacillus subtilis*: mature 5S rRNA is dispensable for ribosome function. *RNA* **7**: 242–253.
Condon C, Rourera J, Brechemier-Baey D & Putzer H (2002) Ribonuclease M5 has few, if any, mRNA substrates in *Bacillus subtilis*. *J Bacteriol* **184**: 2845–2849.
Court DL (1993) RNA processing and degradation by RNase III. *Control of Messenger RNA Stability* (Belasco GJ & Brawerman G, ed), pp. 71–116. Academic Press, New York.
Cudny H & Deutscher MP (1980) Apparent involvement of ribonuclease D in the 3′ processing of tRNA precursors. *P Natl Acad Sci USA* **77**: 837–841.
Cudny H, Zaniewski R & Deutscher MP (1981) *Escherichia coli* RNase D. Catalytic properties and substrate specificity. *J Biol Chem* **256**: 5633–5637.

Czerwoniec A, Dunin-Horkawicz S, Purta E *et al.* (2009) MODOMICS: a database of RNA modification pathways. 2008 update. *Nucleic Acids Res* **37**: D118–D121.

Dahlberg AE, Dahlberg JE, Lund E *et al.* (1978) Processing of the 5′ end of *Escherichia coli* 16S ribosomal RNA. *P Natl Acad Sci USA* **75**: 3598–3602.

Dam Mikkelsen N & Gerdes K (1997) Sok antisense RNA from plasmid R1 is functionally inactivated by RNase E and polyadenylated by poly(A) polymerase I. *Mol Microbiol* **26**: 311–320.

Dasgupta S, Fernandez L, Kameyama L, Inada T, Nakamura Y, Pappas A & Court DL (1998) Genetic uncoupling of the dsRNA-binding and RNA cleavage activities of the *Escherichia coli* endoribonuclease RNase III – the effect of dsRNA binding on gene expression. *Mol Microbiol* **28**: 629–640.

Datta AK & Niyogi K (1975) A novel oligoribonuclease of *Escherichia coli*. II. Mechanism of action. *J Biol Chem* **250**: 7313–7319.

Davies JF II, Hostomska Z, Hostomsky Z, Jordan SR & Matthews DA (1991) Crystal structure of the ribonuclease H domain of HIV-1 reverse transcriptase. *Science* **252**: 88–95.

Deana A, Celesnik H & Belasco JG (2008) The bacterial enzyme RppH triggers messenger RNA degradation by 5′ pyrophosphate removal. *Nature* **451**: 355–358.

Deikus G & Bechhofer DH (2009) *Bacillus subtilis trp* Leader RNA: RNase J1 endonuclease cleavage specificity and PNPase processing. *J Biol Chem* **284**: 26394–26401.

Deikus G, Babitzke P & Bechhofer DH (2004) Recycling of a regulatory protein by degradation of the RNA to which it binds. *P Natl Acad Sci USA* **101**: 2747–2751.

Deikus G, Condon C & Bechhofer DH (2008) Role of *Bacillus subtilis* RNase J1 endonuclease and 5′-exonuclease activities in *trp* leader RNA turnover. *J Biol Chem* **283**: 17158–17167.

de la Sierra-Gallay IL, Pellegrini O & Condon C (2005) Structural basis for substrate binding, cleavage and allostery in the tRNA maturase RNase Z. *Nature* **433**: 657–661.

de la Sierra-Gallay IL, Zig L, Jamalli A & Putzer H (2008) Structural insights into the dual activity of RNase J. *Nat Struct Mol Biol* **15**: 206–212.

Del Favero M, Mazzantini E, Briani F, Zangrossi S, Tortora P & Dehò G (2008) Regulation of *Escherichia coli* polynucleotide phosphorylase by ATP. *J Biol Chem* **283**: 27355–27359.

Deutscher MP (1990) Ribonucleases, tRNA nucleotidyltransferase, and the 3′ processing of tRNA. *Prog Nucleic Acid Re* **39**: 209–240.

Deutscher MP (2006) Degradation of RNA in bacteria: comparison of mRNA and stable RNA. *Nucleic Acids Res* **34**: 659–666.

Deutscher MP (2009) Maturation and degradation of ribosomal RNA in bacteria. *Prog Mol Biol Transl Sci* **85**: 369–391.

Deutscher MP & Marlor CW (1985) Purification and characterization of *Escherichia coli* RNase T. *J Biol Chem* **260**: 7067–7071.

Deutscher MP & Reuven NB (1991) Enzymatic basis for hydrolytic versus phosphorolytic mRNA degradation in *Escherichia coli* and *Bacillus subtilis*. *P Natl Acad Sci USA* **88**: 3277–3280.

Deutscher MP, Marlor CW & Zaniewski R (1985) RNase T is responsible for the end-turnover of tRNA in *Escherichia coli*. *P Natl Acad Sci USA* **82**: 6427–6430.

Deutscher MP, Marshall GT & Cudny H (1988) RNase PH: an *Escherichia coli* phosphate-dependent nuclease distinct from polynucleotide phosphorylase. *P Natl Acad Sci USA* **85**: 4710–4714.

Dittmar KA, Mobley EM, Radek AJ & Pan T (2004) Exploring the regulation of tRNA distribution on the genomic scale. *J Mol Biol* **337**: 31–47.

Diwa A, Bricker AL, Jain C & Belasco JG (2000) An evolutionarily conserved RNA stem-loop functions as a sensor that directs feedback regulation of RNase E gene expression. *Gene Dev* **14**: 1249–1260.

Doma MK & Parker R (2007) RNA quality control in eukaryotes. *Cell* **131**: 660–668.

Domingues S, Matos RG, Reis FP, Fialho AM, Barbas A & Arraiano CM (2009) Biochemical characterization of the RNase II family of exoribonucleases from the human pathogens *Salmonella typhimurium* and *Streptococcus pneumoniae*. *Biochemistry* **48**: 11848–11857.

Donovan WP & Kushner SR (1983) Cloning and physical analysis of the *pyr*F gene (coding for orotidine-5′-phosphate decarboxylase) from *Escherichia coli* K-12. *Gene* **25**: 39–48.

Donovan WP & Kushner SR (1986) Polynucleotide phosphorylase and ribonuclease II are required for cell viability and mRNA turnover in *Escherichia coli* K-12. *P Natl Acad Sci USA* **83**: 120–124.

Drider D & Condon C (2004) The continuing story of endoribonuclease III. *J Mol Microb Biotech* **8**: 195–200.

Drider D, Santos JM, Arraiano CM & Lopez P (1998) RNA processing is involved in the post-transcriptional control of the citQRP operon from *Lactococcus lactis* biovar *diacetylactis*. *Mol Gen Genet* **258**: 9–15.

Drider D, Garcia-Quintans N, Santos JM, Arraiano CM & Lopez P (1999) A comparative analysis of the citrate permease P mRNA stability in *Lactococcus lactis* biovar diacetylactis and *Escherichia coli*. *FEMS Microbiol Lett* **172**: 115–122.

Dulebohn DP, Cho HJ & Karzai AW (2006) Role of conserved surface amino acids in binding of SmpB protein to SsrA RNA. *J Biol Chem* **281**: 28536–28545.

Dutta T & Deutscher MP (2009) Catalytic properties of RNase BN/RNase Z from *Escherichia coli*: RNase BN is both an exo- and endoribonuclease. *J Biol Chem* **284**: 15425–15431.

Dutta T & Deutscher MP (2010) Mode of action of RNase BN/RNase Z on tRNA precursors: RNase BN does not remove the CCA sequence from tRNA. *J Biol Chem*, in press.

Dziembowski A, Piwowarski J, Hoser R *et al.* (2003) The yeast mitochondrial degradosome. Its composition, interplay between RNA helicase and RNase activities and the role in mitochondrial RNA metabolism. *J Biol Chem* **278**: 1603–1611.

Dziembowski A, Lorentzen E, Conti E & Seraphin B (2007) A single subunit, Dis3, is essentially responsible for yeast exosome core activity. *Nat Struct Mol Biol* **14**: 15–22.

Eberle AB, Lykke-Andersen S, Muhlemann O & Jensen TH (2009) SMG6 promotes endonucleolytic cleavage of nonsense mRNA in human cells. *Nat Struct Mol Biol* **16**: 49–55.

Erova TE, Kosykh VG, Fadl AA, Sha J, Horneman AJ & Chopra AK (2008) Cold shock exoribonuclease R (VacB) is involved in *Aeromonas hydrophila* pathogenesis. *J Bacteriol* **190**: 3467–3474.

Eulálio A, Huntzinger E & Izaurralde E (2008) Getting to the root of miRNA-mediated gene silencing. *Cell* **132**: 9–14.

Evans D, Marquez SM & Pace NR (2006) RNase P: interface of the RNA and protein worlds. *Trends Biochem Sci* **31**: 333–341.

Even S, Pellegrini O, Zig L, Labas V, Vinh J, Brechemmier-Baey D & Putzer H (2005) Ribonucleases J1 and J2: two novel endoribonucleases in *B. subtilis* with functional homology to *E. coli* RNase E. *Nucleic Acids Res* **33**: 2141–2152.

Evguenieva-Hackenberg E & Klug G (2000) RNase III processing of intervening sequences found in helix 9 of 23S rRNA in the alpha subclass of Proteobacteria. *J Bacteriol* **182**: 4719–4729.

Evguenieva-Hackenberg E & Klug G (2009) RNA degradation in Archaea and Gram-negative bacteria different from *Escherichia coli*. *Prog Mol Biol Transl Sci* **85**: 275–317.

Evguenieva-Hackenberg E, Schiltz E & Klug G (2002) Dehydrogenases from all three domains of life cleave RNA. *J Biol Chem* **277**: 46145–46150.

Evguenieva-Hackenberg E, Walter P, Hochleitner E, Lottspeich F & Klug G (2003) An exosome-like complex in *Sulfolobus solfataricus*. *EMBO Rep* **4**: 889–893.

Evguenieva-Hackenberg E, Roppelt V, Finsterseifer P & Klug G (2008) Rrp4 and Csl4 are needed for efficient degradation but not for polyadenylation of synthetic and natural RNA by the archaeal exosome. *Biochemistry* **47**: 13158–13168.

Ezraty B, Dahlgren B & Deutscher MP (2005) The RNase Z homologue encoded by *Escherichia coli elaC* gene is RNase BN. *J Biol Chem* **280**: 16542–16545.

Falaleeva MV, Chetverina HV, Ugarov VI, Uzlova EA & Chetverin AB (2008) Factors influencing RNA degradation by *Thermus thermophilus* polynucleotide phosphorylase. *FEBS J* **275**: 2214–2226.

Fang M, Zeisberg WM, Condon C, Ogryzko V, Danchin A & Mechold U (2009) Degradation of nanoRNA is performed by multiple redundant RNases in *Bacillus subtilis*. *Nucleic Acids Res* **37**: 5114–5125.

Farhoud MH, Wessels HJ, Steenbakkers PJ *et al*. (2005) Protein complexes in the archaeon *Methanothermobacter thermautotrophicus* analyzed by blue native/SDS-PAGE and mass spectrometry. *Mol Cell Proteomics* **4**: 1653–1663.

Fekete Z, Ellis TP, Schonauer MS & Dieckmann CL (2008) Pet127 governs a $5' \rightarrow 3'$-exonuclease important in maturation of apocytochrome b mRNA in *Saccharomyces cerevisiae*. *J Biol Chem* **283**: 3767–3772.

Fiedler TJ, Vincent HA, Zuo Y, Gavrialov O & Malhotra A (2004) Purification and crystallization of *Escherichia coli* oligoribonuclease. *Acta Crystallogr D* **60**: 736–739.

Folichon M, Arluison V, Pellegrini O, Huntzinger E, Régnier P & Hajnsdorf E (2003) The poly(A) binding protein Hfq protects RNA from RNase E and exoribonucleolytic degradation. *Nucleic Acids Res* **31**: 7302–7310.

Folichon M, Marujo PE, Arluison V, Le Derout J, Pellegrini O, Hajnsdorf E & Régnier P (2005) Fate of mRNA extremities generated by intrinsic termination: detailed analysis of reactions catalyzed by ribonuclease II and poly(A) polymerase. *Biochimie* **87**: 819–826.

Fonseca P, Moreno R & Rojo F (2008) Genomic analysis of the role of RNase R in the turnover of *Pseudomonas putida* mRNAs. *J Bacteriol* **190**: 6258–6263.

Fournier MJ & Ozeki H (1985) Structure and organization of the transfer ribonucleic acid genes of *Escherichia coli* K-12. *Microbiol Rev* **49**: 379–397.

Frazão C, McVey CE, Amblar M, Barbas A, Vonrhein C, Arraiano CM & Carrondo MA (2006) Unravelling the dynamics of RNA degradation by ribonuclease II and its RNA-bound complex. *Nature* **443**: 110–114.

Freire P, Amaral JD, Santos JM & Arraiano CM (2006) Adaptation to carbon starvation: RNase III ensures normal expression levels of bolA1p mRNA and sigma(S). *Biochimie* **88**: 341–346.

Fritz DT, Bergman N, Kilpatrick WJ, Wilusz CJ & Wilusz J (2004) Messenger RNA decay in mammalian cells: the exonuclease perspective. *Cell Biochem Biophys* **41**: 265–278.

Fusi P, Tedeschi G, Aliverti A, Ronchi S, Tortora P & Guerritore A (1993) Ribonucleases from the extreme thermophilic archaebacterium *S. solfataricus*. *Eur J Biochem* **211**: 305–310.

Gan J, Tropea JE, Austin BP, Court DL, Waugh DS & Ji X (2006) Structural insight into the mechanism of double-stranded RNA processing by ribonuclease III. *Cell* **124**: 355–366.

Gao J, Lee K, Zhao M *et al*. (2006) Differential modulation of *E. coli* mRNA abundance by inhibitory proteins that alter the composition of the degradosome. *Mol Microbiol* **61**: 394–406.

García-Mena J, Das A, Sánchez-Trujillo A, Portier C & Montanez C (1999) A novel mutation in the KH domain of polynucleotide phosphorylase affects autoregulation and mRNA decay in *Escherichia coli*. *Mol Microbiol* **33**: 235–248.

Geer LY, Domrachev M, Lipman DJ & Bryant SH (2002) CDART: protein homology by domain architecture. *Genome Res* **12**: 1619–1623.

Gegenheimer P & Apirion D (1975) *Escherichia coli* ribosomal ribonucleic acids are not cut from an intact precursor molecule. *J Biol Chem* **250**: 2407–2409.

Gerdes K, Thisted T & Martinussen J (1990) Mechanism of post-segregational killing by the *hok/sok* system of plasmid R1: *sok* antisense RNA regulates formation of a *hok* mRNA species correlated with killing of plasmid-free cells. *Mol Microbiol* **4**: 1807–1818.

Ghora BK & Apirion D (1978) Structural analysis and *in vitro* processing to p5 rRNA of a 9S RNA molecule isolated from an *rne* mutant of *E. coli*. *Cell* **15**: 1055–1066.

Ghosh S & Deutscher MP (1999) Oligoribonuclease is an essential component of the mRNA decay pathway. *P Natl Acad Sci USA* **96**: 4372–4377.

Gimple O & Schon A (2001) *In vitro* and *in vivo* processing of cyanelle tmRNA by RNase P. *Biol Chem* **382**: 1421–1429.

Givskov M & Molin S (1984) Copy mutants of plasmid R1: effects of base pair substitutions in the *cop*A gene on the replication control system. *Mol Gen Genet* **194**: 286–292.

Gobert A, Gutmann B, Taschner A *et al.* (2010) A single *Arabidopsis* organellar protein has RNase P activity. *Nat Struct Mol Biol* **17**: 740–744.

Godefroy T (1970) Kinetics of polymerization and phosphorolysis reactions of *Escherichia coli* polynucleotide phosphorylase. Evidence for multiple binding of polynucleotide in phosphorolysis. *Eur J Biochem* **14**: 222–231.

Grossman D & van Hoof A (2006) RNase II structure completes group portrait of 3′ exoribonucleases. *Nat Struct Mol Biol* **13**: 760–761.

Guillier M, Gottesman S & Storz G (2006) Modulating the outer membrane with small RNAs. *Gene Dev* **20**: 2338–2348.

Haddad N, Burns CM, Bolla JM, Prévost H, Federighi M, Drider D & Cappelier JM (2009) Long-term survival of *Campylobacter jejuni* at low temperatures is dependent on polynucleotide phosphorylase activity. *Appl Environ Microb* **75**: 7310–7318.

Hahn J, Luttinger A & Dubnau D (1996) Regulatory inputs for the synthesis of ComK, the competence transcription factor of *Bacillus subtilis*. *Mol Microbiol* **21**: 763–775.

Hajnsdorf E, Steier O, Coscoy L, Teysset L & Régnier P (1994) Roles of RNase E, RNase II and PNPase in the degradation of the *rpsO* transcripts of *Escherichia coli*: stabilizing function of RNase II and evidence for efficient degradation in an *ams pnp rnb* mutant. *EMBO J* **13**: 3368–3377.

Hajnsdorf E, Braun F, Haugel-Nielsen J & Régnier P (1995) Polyadenylylation destabilizes the *rps*O mRNA of *Escherichia coli*. *P Natl Acad Sci USA* **92**: 3973–3977.

Hale CR, Zhao P, Olson S *et al.* (2009) RNA-guided RNA cleavage by a CRISPR RNA–Cas protein complex. *Cell* **139**: 945–956.

Hall TA & Brown JW (2002) Archaeal RNase P has multiple protein subunits homologous to eukaryotic nuclear RNase P proteins. *RNA* **8**: 296–306.

Hankins JS, Zappavigna C, Prud'homme-Genereux A & Mackie GA (2007) Role of RNA structure and susceptibility to RNase E in regulation of a cold shock mRNA, cspA mRNA. *J Bacteriol* **189**: 4353–4358.

Harlow LS, Kadziola A, Jensen KF & Larsen S (2004) Crystal structure of the phosphorolytic exoribonuclease RNase PH from *Bacillus subtilis* and implications for its quaternary structure and tRNA binding. *Protein Sci* **13**: 668–677.

Hartmann RK, Heinrich J, Schlegl J & Schuster H (1995) Precursor of C4 antisense RNA of bacteriophages P1 and P7 is a substrate for RNase P of *Escherichia coli*. *P Natl Acad Sci USA* **92**: 5822–5826.

Hartmann RK, Gossringer M, Spath B, Fischer S & Marchfelder A (2009) The making of tRNAs and more – RNase P and tRNase Z. *Prog Mol Biol Transl Sci* **85**: 319–368.

Hasenohrl D, Lombo T, Kaberdin V, Londei P & Blasi U (2008) Translation initiation factor a/eIF2(-gamma) counteracts 5′ to 3′ mRNA decay in the archaeon *Sulfolobus solfataricus*. *P Natl Acad Sci USA* **105**: 2146–2150.

Hayes CS & Keiler KC (2010) Beyond ribosome rescue: tmRNA and co-translational processes. *FEBS Lett* **584**: 413–419.

Hayes F & Vasseur M (1976) Processing of the 17-S *Escherichia coli* precursor RNA in the 27-S pre-ribosomal particle. *Eur J Biochem* **61**: 433–442.

Henkin TM (2008) Riboswitch RNAs: using RNA to sense cellular metabolism. *Gene Dev* **22**: 3383–3390.

Henkin TM & Yanofsky C (2002) Regulation by transcription attenuation in bacteria: how RNA provides instructions for transcription termination/antitermination decisions. *Bioessays* **24**: 700–707.

Herskovitz MA & Bechhofer DH (2000) Endoribonuclease RNase III is essential in *Bacillus subtilis*. *Mol Microbiol* **38**: 1027–1033.

Higgins CF, McLaren RS & Newbury SF (1988) Repetitive extragenic palindromic sequences, mRNA stability and gene expression: evolution by gene conversion? A review. *Gene* **72**: 3–14.

Holec S, Lange H, Kuhn K, Alioua M, Borner T & Gagliardi D (2006) Relaxed transcription in *Arabidopsis* mitochondria is counterbalanced by RNA stability control mediated by polyadenylation and polynucleotide phosphorylase. *Mol Cell Biol* **26**: 2869–2876.

Holzmann J, Frank P, Loffler E, Bennett KL, Gerner C & Rossmanith W (2008) RNase P without RNA: identification and functional reconstitution of the human mitochondrial tRNA processing enzyme. *Cell* **135**: 462–474.

Hong SJ, Tran QA & Keiler KC (2005) Cell cycle-regulated degradation of tmRNA is controlled by RNase R and SmpB. *Mol Microbiol* **57**: 565–575.

Hopper AK, Pai DA & Engelke DR (2010) Cellular dynamics of tRNAs and their genes. *FEBS Lett* **584**: 310–317.

Hou YM & Perona JJ (2010) Stereochemical mechanisms of tRNA methyltransferases. *FEBS Lett* **584**: 278–286.

Houseley J & Tollervey D (2009) The many pathways of RNA degradation. *Cell* **136**: 763–776.

Huntzinger E, Boisset S, Saveanu C *et al.* (2005) *Staphylococcus aureus* RNAIII and the endoribonuclease III coordinately regulate *spa* gene expression. *EMBO J* **24**: 824–835.

Huntzinger E, Kashima I, Fauser M, Sauliere J & Izaurralde E (2008) SMG6 is the catalytic endonuclease that cleaves mRNAs containing nonsense codons in metazoan. *RNA* **14**: 2609–2617.

Hutchison CA, Peterson SN, Gill SR *et al.* (1999) Global transposon mutagenesis and a minimal *Mycoplasma* genome. *Science* **286**: 2165–2169.

Inokuchi H & Yamao F (1995) Structure and expression of prokaryotic tRNA genes. *tRNA: Structure, Biosynthesis, and Function* (Söll D & RajBhandary UL, eds), pp. 17–30. ASM Press, Washington, DC.

Irie M (1997) RNase T1/RNase T2 family RNases. *Ribonucleases: Structure and Functions* (D'Allessio GRJ, ed), pp. 101–124. Academic Press, San Diego, CA.

Ishii R, Nureki O & Yokoyama S (2003) Crystal structure of the tRNA processing enzyme RNase PH from *Aquifex aeolicus*. *J Biol Chem* **278**: 32397–32404.

Ishii R, Minagawa A, Takaku H, Takagi M, Nashimoto M & Yokoyama S (2005) Crystal structure of the tRNA 3′ processing endoribonuclease tRNase Z from *Thermotoga maritima*. *J Biol Chem* **280**: 14138–14144.

Itaya M, Omori A, Kanaya S, Crouch RJ, Tanaka T & Kondo K (1999) Isolation of RNase H genes that are essential for growth of *Bacillus subtilis* 168. *J Bacteriol* **181**: 2118–2123.

Jagannath A & Wood M (2007) RNA interference based gene therapy for neurological disease. *Brief Funct Genomic Proteomic* **6**: 40–49.

Jäger S, Fuhrmann O, Heck C, Hebermehl M, Schiltz E, Rauhut R & Klug G (2001) An mRNA degrading complex in *Rhodobacter capsulatus*. *Nucleic Acids Res* **29**: 4581–4588.

Jäger S, Evguenieva-Hackenberg E & Klug G (2004) Temperature-dependent processing of the *cspA* mRNA in *Rhodobacter capsulatus*. *Microbiology* **150**: 687–695.

Jain C & Belasco JG (1995) Autoregulation of RNase E synthesis in *Escherichia coli*. *Nucleic Acids Symp Ser* **33**: 85–88.

Janssen BD & Hayes CS (2009) Kinetics of paused ribosome recycling in *Escherichia coli*. *J Mol Biol* **394**: 251–267.

Jarrige A, Brechemier-Baey D, Mathy N, Duche O & Portier C (2002) Mutational analysis of polynucleotide phosphorylase from *Escherichia coli*. *J Mol Biol* **321**: 397–409.

Jarrige AC, Mathy N & Portier C (2001) PNPase autocontrols its expression by degrading a double-stranded structure in the *pnp* mRNA leader. *EMBO J* **20**: 6845–6855.

Jaskiewicz L & Filipowicz W (2008) Role of Dicer in posttranscriptional RNA silencing. *Curr Top Microbiol* **320**: 77–97.

Jensen KF, Larsen JN, Schack L & Sivertsen A (1984) Studies on the structure and expression of *Escherichia coli pyr*C, *pyr*D, and *pyr*F using the cloned genes. *Eur J Biochem* **140**: 343–352.

Jensen KF, Andersen JT & Poulsen P (1992) Overexpression and rapid purification of the *orfE/rph* gene product, RNase PH of *Escherichia coli*. *J Biol Chem* **267**: 17147–17152.

Jiang X & Belasco JG (2004) Catalytic activation of multimeric RNase E and RNase G by 5′-monophosphorylated RNA. *P Natl Acad Sci USA* **101**: 9211–9216.

Jiang X, Diwa A & Belasco JG (2000) Regions of RNase E important for 5′-end-dependent RNA cleavage and autoregulated synthesis. *J Bacteriol* **182**: 2468–2475.

Jinek M & Doudna JA (2009) A three-dimensional view of the molecular machinery of RNA interference. *Nature* **457**: 405–412.

Johansen J, Rasmussen AA, Overgaard M & Valentin-Hansen P (2006) Conserved small non-coding RNAs that belong to the sigmaE regulon: role in down-regulation of outer membrane proteins. *J Mol Biol* **364**: 1–8.

Kaberdin VR & Blasi U (2006) Translation initiation and the fate of bacterial mRNAs. *FEMS Microbiol Rev* **30**: 967–979.

Kaberdin VR, Miczak A, Jakobsen JS, Lin-Chao S, McDowall KJ & von Gabain A (1998) The endoribonucleolytic N-terminal half of *Escherichia coli* RNase E is evolutionarily conserved in *Synechocystis* sp. and other bacteria but not the C-terminal half, which is sufficient for degradosome assembly. *P Natl Acad Sci USA* **95**: 11637–11642.

Kane JF (1995) Effects of rare codon clusters on high-level expression of heterologous proteins in *Escherichia coli*. *Curr Opin Biotech* **6**: 494–500.

Karginov FV & Hannon GJ (2010) The CRISPR system: small RNA-guided defense in bacteria and archaea. *Mol Cell* **37**: 7–19.

Karzai AW, Susskind MM & Sauer RT (1999) SmpB, a unique RNA-binding protein essential for the peptide-tagging activity of SsrA (tmRNA). *EMBO J* **18**: 3793–3799.

Kelly KO & Deutscher MP (1992) Characterization of *Escherichia coli* RNase PH. *J Biol Chem* **267**: 17153–17158.

Kelly KO, Reuven NB, Li Z & Deutscher MP (1992) RNase PH is essential for tRNA processing and viability in RNase-deficient *Escherichia coli* cells. *J Biol Chem* **267**: 16015–16018.

Khemici V & Carpousis AJ (2004) The RNA degradosome and poly(A) polymerase of *Escherichia coli* are required *in vivo* for the degradation of small mRNA decay intermediates containing REP-stabilizers. *Mol Microbiol* **51**: 777–790.

Khemici V, Toesca I, Poljak L, Vanzo NF & Carpousis AJ (2004) The RNase E of *Escherichia coli* has at least two binding sites for DEAD-box RNA helicases: functional replacement of RhlB by RhlE. *Mol Microbiol* **54**: 1422–1430.

Khemici V, Poljak L, Luisi BF & Carpousis AJ (2008) The RNase E of *Escherichia coli* is a membrane-binding protein. *Mol Microbiol* **70**: 799–813.

Kime L, Jourdan SS, Stead JA, Hidalgo-Sastre A & McDowall KJ (2009) Rapid cleavage of RNA by RNase E in the absence of 5′-monophosphate stimulation. *Mol Microbiol* **76**: 590–604.

Kirsebom LA & Trobro S (2009) RNase P RNA-mediated cleavage. *IUBMB Life* **61**: 189–200.

Kirsebom LA, Baer MF & Altman S (1988) Differential effects of mutations in the protein and RNA moieties of RNase P on the efficiency of suppression by various tRNA suppressors. *J Mol Biol* **204**: 879–888.

Kitamura S, Fujishima K, Sato A, Tsuchiya D, Tomita M & Kanai A (2010) Characterization of RNase HII substrate recognition using RNase HII-Argonaute chimeric enzymes from *Pyrococcus furiosus*. *Biochem J* **426**: 337–344.

Ko JH & Altman S (2007) OLE RNA, an RNA motif that is highly conserved in several extremophilic bacteria, is a substrate for and can be regulated by RNase P RNA. *P Natl Acad Sci USA* **104**: 7815–7820.

Ko JH, Han K, Kim Y *et al.* (2008) Dual function of RNase E for control of M1 RNA biosynthesis in *Escherichia coli*. *Biochemistry* **47**: 762–770.

Koonin EV, Wolf YI & Aravind L (2001) Prediction of the archaeal exosome and its connections with the proteasome and the translation and transcription machineries by a comparative-genomic approach. *Genome Res* **11**: 240–252.

Koslover DJ, Callaghan AJ, Marcaida MJ, Garman EF, Martick M, Scott WG & Luisi BF (2008) The crystal structure of the *Escherichia coli* RNase E apoprotein and a mechanism for RNA degradation. *Structure* **16**: 1238–1244.

Kulms D, Schafer G & Hahn U (1995) SaRD, a new protein isolated from the extremophile archaeon *Sulfolobus acidocaldarius*, is a thermostable ribonuclease with DNA-binding properties. *Biochem Bioph Res Co* **214**: 646–652.

LaCava J, Houseley J, Saveanu C, Petfalski E, Thompson E, Jacquier A & Tollervey D (2005) RNA degradation by the exosome is promoted by a nuclear polyadenylation complex. *Cell* **121**: 713–724.

Lalonde MS, Zuo Y, Zhang J, Gong X, Wu S, Malhotra A & Li Z (2007) Exoribonuclease R in *Mycoplasma genitalium* can carry out both RNA processing and degradative functions and is sensitive to RNA ribose methylation. *RNA* **13**: 1957–1968.

Lamontagne B, Larose S, Boulanger J & Elela SA (2001) The RNase III family: a conserved structure and expanding functions in eukaryotic dsRNA metabolism. *Curr Issues Mol Biol* **3**: 71–78.

Lange H, Sement FM, Canaday J & Gagliardi D (2009) Polyadenylation-assisted RNA degradation processes in plants. *Trends Plant Sci* **14**: 497–504.

Lebreton A, Tomecki R, Dziembowski A & Seraphin B (2008) Endonucleolytic RNA cleavage by a eukaryotic exosome. *Nature* **456**: 993–996.

Le Derout J, Boni IV, Régnier P & Hajnsdorf E (2010) Hfq affects mRNA levels independently of degradation. *BMC Mol Biol* **11**: 17.

Lee K & Cohen SN (2003) A *Streptomyces coelicolor* functional orthologue of *Escherichia coli* RNase E shows shuffling of catalytic and PNPase-binding domains. *Mol Microbiol* **48**: 349–360.

Lee K, Bernstein JA & Cohen SN (2002) RNase G complementation of *rne* null mutation identifies functional interrelationships with RNase E in *Escherichia coli*. *Mol Microbiol* **43**: 1445–1456.

Lee K, Zhan X, Gao J *et al.* (2003) RraA. A protein inhibitor of RNase E activity that globally modulates RNA abundance in *E. coli*. *Cell* **114**: 623–634.

Li H & Nicholson AW (1996) Defining the enzyme binding domain of a ribonuclease III processing signal. Ethylation interference and hydroxyl radical footprinting using catalytically inactive RNase III mutants. *EMBO J* **15**: 1421–1433.

Li Y & Altman S (2003) A specific endoribonuclease, RNase P, affects gene expression of polycistronic operon mRNAs. *P Natl Acad Sci USA* **100**: 13213–13218.

Li Z & Deutscher MP (1995) The tRNA processing enzyme RNase T is essential for maturation of 5S RNA. *P Natl Acad Sci USA* **92**: 6883–6886.

Li Z & Deutscher MP (1996) Maturation pathways for *E. coli* tRNA precursors: a random multienzyme process *in vivo*. *Cell* **86**: 503–512.

Li Z & Deutscher MP (2002) RNase E plays an essential role in the maturation of *Escherichia coli* tRNA precursors. *RNA* **8**: 97–109.

Li Z, Zhan L & Deutscher MP (1996) *Escherichia coli* RNase T functions *in vivo* as a dimer dependent on cysteine 168. *J Biol Chem* **271**: 1133–1137.

Li Z, Pandit S & Deutscher MP (1998) 3′ Exoribonucleolytic trimming is a common feature of the maturation of small, stable RNAs in *Escherichia coli*. *P Natl Acad Sci USA* **95**: 2856–2861.

Li Z, Pandit S & Deutscher MP (1999a) Maturation of 23S ribosomal RNA requires the exoribonuclease RNase T. *RNA* **5**: 139–146.

Li Z, Pandit S & Deutscher MP (1999b) RNase G (CafA protein) and RNase E are both required for the 5′ maturation of 16S ribosomal RNA. *EMBO J* **18**: 2878–2885.

Li Z, Reimers S, Pandit S & Deutscher MP (2002) RNA quality control: degradation of defective transfer RNA. *EMBO J* **21**: 1132–1138.

Lin-Chao S & Cohen SN (1991) The rate of processing and degradation of antisense RNAI regulates the replication of ColE1-type plasmids *in vivo*. *Cell* **65**: 1233–1242.

Lin-Chao S, Wei CL & Lin YT (1999) RNase E is required for the maturation of SsrA RNA and normal SsrA RNA peptide-tagging activity. *P Natl Acad Sci USA* **96**: 12406–12411.

Lin PH & Lin-Chao S (2005) RhlB helicase rather than enolase is the beta-subunit of the *Escherichia coli* polynucleotide phosphorylase (PNPase)-exoribonucleolytic complex. *P Natl Acad Sci USA* **102**: 16590–16595.

Liou GG, Jane WN, Cohen SN, Lin NS & Lin-Chao S (2001) RNA degradosomes exist *in vivo* in *Escherichia coli* as multicomponent complexes associated with the cytoplasmic membrane via the N-terminal region of ribonuclease E. *P Natl Acad Sci USA* **98**: 63–68.

Liou GG, Chang HY, Lin CS & Lin-Chao S (2002) DEAD box RhlB RNA helicase physically associates with exoribonuclease PNPase to degrade double-stranded RNA independent of the degradosome-assembling region of RNase E. *J Biol Chem* **277**: 41157–41162.

Littauer YZ & Soreq H (1982) *Polynucleotide Phosphorylase*. Academic Press, New York.

Liu F & Altman S (1994) Differential evolution of substrates for an RNA enzyme in the presence and absence of its protein cofactor. *Cell* **77**: 1093–1100.

Liu F & Altman S (2009) *Ribonuclease P*. Springer-Verlag, New York.

Liu H & Kiledjian M (2006a) Decapping the message: a beginning or an end. *Biochem Soc T* **34**: 35–38.

Liu Q, Greimann JC & Lima CD (2006b) Reconstitution, activities, and structure of the eukaryotic RNA exosome. *Cell* **127**: 1223–1237.

Lombo TB & Kaberdin VR (2008) RNA processing in *Aquifex aeolicus* involves RNase E/G and an RNase P-like activity. *Biochem Bioph Res Co* **366**: 457–463.

Lopez PJ, Marchand I, Joyce SA & Dreyfus M (1999) The C-terminal half of RNase E, which organizes the *Escherichia coli* degradosome, participates in mRNA degradation but not rRNA processing *in vivo*. *Mol Microbiol* **33**: 188–199.

Lorentzen E, Walter P, Fribourg S, Evguenieva-Hackenberg E, Klug G & Conti E (2005) The archaeal exosome core is a hexameric ring structure with three catalytic subunits. *Nat Struct Mol Biol* **12**: 575–581.

Lorentzen E, Dziembowski A, Lindner D, Seraphin B & Conti E (2007) RNA channelling by the archaeal exosome. *EMBO Rep* **8**: 470–476.

Lu C, Ding F & Ke A (2010) Crystal structure of the *S. solfataricus* archaeal exosome reveals conformational flexibility in the RNA-binding ring. *PLoS One* **5**: e8739.

Lundberg U & Altman S (1995) Processing of the precursor to the catalytic RNA subunit of RNase P from *Escherichia coli*. *RNA* **1**: 327–334.

Luttinger A, Hahn J & Dubnau D (1996) Polynucleotide phosphorylase is necessary for competence development in *Bacillus subtilis*. *Mol Microbiol* **19**: 343–356.

Ma Y, Chan CY & He ML (2007) RNA interference and antiviral therapy. *World J Gastroentero* **13**: 5169–5179.

Mackie GA (1991) Specific endonucleolytic cleavage of the mRNA for ribosomal protein S20 of *Escherichia coli* requires the product of the *ams* gene *in vivo* and *in vitro*. *J Bacteriol* **173**: 2488–2497.

Mackie GA (1992) Secondary structure of the mRNA for ribosomal protein S20. Implications for cleavage by ribonuclease E. *J Biol Chem* **267**: 1054–1061.

Mackie GA (1998) Ribonuclease E is a 5′-end-dependent endonuclease. *Nature* **395**: 720–723.

Mackie GA (2000) Stabilization of circular rpsT mRNA demonstrates the 5′-end dependence of RNase E action *in vivo*. *J Biol Chem* **275**: 25069–25072.

Mackie GA & Parsons GD (1983) Tandem promoters in the gene for ribosomal protein S20. *J Biol Chem* **258**: 7840–7846.

MacRae IJ & Doudna JA (2007) Ribonuclease revisited: structural insights into ribonuclease III family enzymes. *Curr Opin Struc Biol* **17**: 138–145.

Mader U, Zig L, Kretschmer J, Homuth G & Putzer H (2008) mRNA processing by RNases J1 and J2 affects *Bacillus subtilis* gene expression on a global scale. *Mol Microbiol* **70**: 183–196.

Malecki M, Jedrzejczak R, Stepien PP & Golik P (2007) *In vitro* reconstitution and characterization of the yeast mitochondrial degradosome complex unravels tight functional interdependence. *J Mol Biol* **372**: 23–36.

Marcaida MJ, DePristo MA, Chandran V, Carpousis AJ & Luisi BF (2006) The RNA degradosome: life in the fast lane of adaptive molecular evolution. *Trends Biochem Sci* **31**: 359–365.

Marck C & Grosjean H (2002) tRNomics: analysis of tRNA genes from 50 genomes of Eukarya, Archaea, and Bacteria reveals anticodon-sparing strategies and domain-specific features. *RNA* **8**: 1189–1232.

Marck C & Grosjean H (2003) Identification of BHB splicing motifs in intron-containing tRNAs from 18 archaea: evolutionary implications. *RNA* **9**: 1516–1531.

Marszalkowski M, Willkomm DK & Hartmann RK (2008) 5′-End maturation of tRNA in *Aquifex aeolicus*. *Biol Chem* **389**: 395–403.

Marujo PE, Hajnsdorf E, Le Derout J, Andrade R, Arraiano CM & Régnier P (2000) RNase II removes the oligo(A) tails that destabilize the *rps*O mRNA of *Escherichia coli*. *RNA* **6**: 1185–1193.

Marujo PE, Braun F, Haugel-Nielsen J, Le Derout J, Arraiano CM & Régnier P (2003) Inactivation of the decay pathway initiated at an internal site by RNase E promotes poly(A)-dependent degradation of the *rps*O mRNA in *Escherichia coli*. *Mol Microbiol* **50**: 1283–1294.

Massire C, Jaeger L & Westhof E (1998) Derivation of the three-dimensional architecture of bacterial ribonuclease P RNAs from comparative sequence analysis. *J Mol Biol* **279**: 773–793.

Mathy N, Jarrige AC, Robert-Le Meur M & Portier C (2001) Increased expression of *Escherichia coli* polynucleotide phosphorylase at low temperatures is linked to a decrease in the efficiency of autocontrol. *J Bacteriol* **183**: 3848–3854.

Mathy N, Benard L, Pellegrini O, Daou R, Wen T & Condon C (2007) 5′-to-3′ exoribonuclease activity in bacteria: role of RNase J1 in rRNA maturation and 5′ stability of mRNA. *Cell* **129**: 681–692.

Mathy N, Hebert A, Mervelet P *et al*. (2010) *Bacillus subtilis* ribonucleases J1 and J2 form a complex with altered enzyme behaviour. *Mol Microbiol* **75**: 489–498.

Matos RG, Barbas A & Arraiano CM (2009) RNase R mutants elucidate the catalysis of structured RNA: RNA-binding domains select the RNAs targeted for degradation. *Biochem J* **423**: 291–301.

Matsunaga J, Simons EL & Simons RW (1996) RNase III autoregulation: structure and function of *rncO*, the posttranscriptional 'operator'. *RNA* **2**: 1228–1240.

Matus-Ortega ME, Regonesi ME, Pina-Escobedo A, Tortora P, Dehò G & García-Mena J (2007) The KH and S1 domains of *Escherichia coli* polynucleotide phosphorylase are necessary for autoregulation and growth at low temperature. *Biochim Biophys Acta* **1769**: 194–203.

McDowall KJ, Hernandez RG, Lin-Chao S & Cohen SN (1993) The *ams-1* and *rne-3071* temperature-sensitive mutations in the *ams* gene are in close proximity to each other and cause substitutions within a domain that resembles a product of the *Escherichia coli mre* locus. *J Bacteriol* **175**: 4245–4249.

McDowall KJ, Kaberdin VR, Wu SW, Cohen SN & Lin-Chao S (1995) Site-specific RNase E cleavage of oligonucleotides and inhibition by stem-loops. *Nature* **374**: 287–290.

Mechold U, Ogryzko V, Ngo S & Danchin A (2006) Oligoribonuclease is a common downstream target of lithium-

induced pAp accumulation in *Escherichia coli* and human cells. *Nucleic Acids Res* **34**: 2364–2373.

Mechold U, Fang G, Ngo S, Ogryzko V & Danchin A (2007) YtqI from *Bacillus subtilis* has both oligoribonuclease and pAp-phosphatase activity. *Nucleic Acids Res* **35**: 4552–4561.

Melefors O & von Gabain A (1988) Site-specific endonucleolytic cleavages and the regulation of stability of *E. coli omp*A mRNA. *Cell* **52**: 893–901.

Melefors O & von Gabain A (1991) Genetic studies of cleavage-initiated mRNA decay and processing of ribosomal 9S RNA show that the *Escherichia coli ams* and *rne* loci are the same. *Mol Microbiol* **5**: 857–864.

Meng W & Nicholson AW (2008) Heterodimer-based analysis of subunit and domain contributions to double-stranded RNA processing by *Escherichia coli* RNase III *in vitro*. *Biochem J* **410**: 39–48.

Meyer S, Temme C & Wahle E (2004) Messenger RNA turnover in eukaryotes: pathways and enzymes. *Crit Rev Biochem Mol* **39**: 197–216.

Mian IS (1997) Comparative sequence analysis of ribonucleases HII, III, II PH and D. *Nucleic Acids Res* **25**: 3187–3195.

Miczak A, Kaberdin VR, Wei CL & Lin-Chao S (1996) Proteins associated with RNase E in a multicomponent ribonucleolytic complex. *P Natl Acad Sci USA* **93**: 3865–3869.

Minagawa A, Takaku H, Takagi M & Nashimoto M (2004) A novel endonucleolytic mechanism to generate the CCA 3′ termini of tRNA molecules in *Thermotoga maritima*. *J Biol Chem* **279**: 15688–15697.

Misra TK & Apirion D (1979) RNase E, an RNA processing enzyme from *Escherichia coli*. *J Biol Chem* **254**: 11154–11159.

Mitchell P, Petfalski E, Shevchenko A, Mann M & Tollervey D (1997) The exosome: a conserved eukaryotic RNA processing complex containing multiple 3′ → 5′ exoribonucleases. *Cell* **91**: 457–466.

Mitra S & Bechhofer DH (1994) Substrate specificity of an RNase III-like activity from *Bacillus subtilis*. *J Biol Chem* **269**: 31450–31456.

Mohanty BK & Kushner SR (1999) Analysis of the function of *Escherichia coli* poly(A) polymerase I in RNA metabolism. *Mol Microbiol* **34**: 1094–1108.

Mohanty BK & Kushner SR (2000a) Polynucleotide phosphorylase, RNase II and RNase E play different roles in the *in vivo* modulation of polyadenylation in *Escherichia coli*. *Mol Microbiol* **36**: 982–994.

Mohanty BK & Kushner SR (2000b) Polynucleotide phosphorylase functions both as a 3′ right-arrow 5′ exonuclease and a poly(A) polymerase in *Escherichia coli*. *P Natl Acad Sci USA* **97**: 11966–11971.

Mohanty BK & Kushner SR (2002) Polyadenylation of *Escherichia coli* transcripts plays an integral role in regulating intracellular levels of polynucleotide phosphorylase and RNase E. *Mol Microbiol* **45**: 1315–1324.

Mohanty BK & Kushner SR (2003) Genomic analysis in *Escherichia coli* demonstrates differential roles for polynucleotide phosphorylase and RNase II in mRNA abundance and decay. *Mol Microbiol* **50**: 645–658.

Mohanty BK & Kushner SR (2006) The majority of *Escherichia coli* mRNAs undergo post-transcriptional modification in exponentially growing cells. *Nucleic Acids Res* **34**: 5695–5704.

Mohanty BK & Kushner SR (2010) Processing of the *Escherichia coli leuX* tRNA transcript, encoding tRNALeu5, requires either the 3′ → 5′ exoribonuclease polynucleotide phosphorylase or RNase P to remove the Rho-independent transcription terminator. *Nucleic Acids Res* **38**: 597–607.

Mohanty BK, Maples VF & Kushner SR (2004) The Sm-like protein Hfq regulates polyadenylation dependent mRNA decay in *Escherichia coli*. *Mol Microbiol* **54**: 905–920.

Moore MJ & Proudfoot NJ (2009) Pre-mRNA processing reaches back to transcription and ahead to translation. *Cell* **136**: 688–700.

Morita T, Maki K & Aiba H (2005) RNase E-based ribonucleoprotein complexes: mechanical basis of mRNA destabilization mediated by bacterial noncoding RNAs. *Gene Dev* **19**: 2176–2186.

Mudd EA & Higgins CF (1993) *Escherichia coli* endoribonuclease RNase E: autoregulation of expression and site-specific cleavage of mRNA. *Mol Microbiol* **9**: 557–568.

Mudd EA, Krisch HM & Higgins CF (1990) RNase E, an endoribonuclease, has a general role in the chemical decay of *Escherichia coli* mRNA: evidence that *rne* and *ams* are the same genetic locus. *Mol Microbiol* **4**: 2127–2135.

Nakamura A, Koide Y, Miyazaki H, Kitamura A, Masaki H, Beppu T & Uozumi T (1992) Gene cloning and characterization of a novel extracellular ribonuclease of *Bacillus subtilis*. *Eur J Biochem* **209**: 121–127.

Nashimoto M (1997) Distribution of both lengths and 5′ terminal nucleotides of mammalian pre-tRNA 3′ trailers reflects properties of 3′ processing endoribonuclease. *Nucleic Acids Res* **25**: 1148–1154.

Neubauer C, Gao Y-G, Andersen KR *et al*. (2009) The structural basis for mRNA recognition and cleavage by the ribosome-dependent endonuclease RelE. *Cell* **139**: 1084–1095.

Newbury SF, Smith NH & Higgins CF (1987) Differential mRNA stability controls relative gene expression within a polycistronic operon. *Cell* **51**: 1131–1143.

Nicholson AW (1999) Function, mechanism and regulation of bacterial ribonucleases. *FEMS Microbiol Rev* **23**: 371–390.

Nilsson G, Belasco JG, Cohen SN & von Gabain A (1984) Growth-rate dependent regulation of mRNA stability in *Escherichia coli*. *Nature* **312**: 75–77.

Nishio SY & Itoh T (2008) The effects of RNA degradation enzymes on antisense RNAI controlling ColE2 plasmid copy number. *Plasmid* **60**: 174–180.

Niyogi SK & Datta AK (1975) A novel oligoribonuclease of *Escherichia coli*. Isolation and properties. *J Biol Chem* **250**: 7307–7312.

Noirot-Gros MF, Dervyn E, Wu LJ, Mervelet P, Errington J, Ehrlich SD & Noirot P (2002) An expanded view of bacterial DNA replication. *P Natl Acad Sci USA* **99**: 8342–8347.

Nowotny M & Yang W (2006) Stepwise analyses of metal ions in RNase H catalysis from substrate destabilization to product release. *EMBO J* **25**: 1924–1933.

Nurmohamed S, Vaidialingam B, Callaghan AJ & Luisi BF (2009) Crystal structure of *Escherichia coli* polynucleotide phosphorylase core bound to RNase E, RNA and manganese: implications for catalytic mechanism and RNA degradosome assembly. *J Mol Biol* **389**: 17–33.

O'Hara EB, Chekanova JA, Ingle CA, Kushner ZR, Peters E & Kushner SR (1995) Polyadenylylation helps regulate mRNA decay in *Escherichia coli*. *P Natl Acad Sci USA* **92**: 1807–1811.

Oguro A, Kakeshita H, Nakamura K, Yamane K, Wang W & Bechhofer DH (1998) *Bacillus subtilis* RNase III cleaves both 5′- and 3′-sites of the small cytoplasmic RNA precursor. *J Biol Chem* **273**: 19542–19547.

Ohnishi Y, Nishiyama Y, Sato R, Kameyama S & Horinouchi S (2000) An oligoribonuclease gene in *Streptomyces griseus*. *J Bacteriol* **182**: 4647–4653.

Ohtani N, Haruki M, Morikawa M, Crouch RJ, Itaya M & Kanaya S (1999) Identification of the genes encoding Mn^{2+}-dependent RNase HII and Mg^{2+}-dependent RNase HIII from *Bacillus subtilis*: classification of RNases H into three families. *Biochemistry* **38**: 605–618.

Okada Y, Wachi M, Hirata A, Suzuki K, Nagai K & Matsuhashi M (1994) Cytoplasmic axial filaments in *Escherichia coli* cells: possible function in the mechanism of chromosome segregation and cell division. *J Bacteriol* **176**: 917–922.

Olmedo G & Guzman P (2008) Mini-III, a fourth class of RNase III catalyses maturation of the *Bacillus subtilis* 23S ribosomal RNA. *Mol Microbiol* **68**: 1073–1076.

Ono M & Kuwano M (1979) A conditional lethal mutation in an *Escherichia coli* strain with a longer chemical lifetime of messenger RNA. *J Mol Biol* **129**: 343–357.

Ono M & Kuwano M (1980) Chromosomal location of a gene for chemical longevity of messenger ribonucleic acid in a temperature-sensitive mutant of *Escherichia coli*. *J Bacteriol* **142**: 325–326.

Oppenheim AB, Kornitzer D, Altuvia S & Court DL (1993) Posttranscriptional control of the lysogenic pathway in bacteriophage lambda. *Prog Nucleic Acid Re* **46**: 37–49.

Ost KA & Deutscher MP (1991) *Escherichia coli orfE* (upstream of *pyrE*) encodes RNase PH. *J Bacteriol* **173**: 5589–5591.

Otsuka Y & Yonesaki T (2005) A novel endoribonuclease, RNase LS, in *Escherichia coli*. *Genetics* **169**: 13–20.

Oussenko IA, Sanchez R & Bechhofer DH (2002) *Bacillus subtilis* YhaM, a member of a new family of 3′-to-5′ exonucleases in gram-positive bacteria. *J Bacteriol* **184**: 6250–6259.

Oussenko IA, Abe T, Ujiie H, Muto A & Bechhofer DH (2005) Participation of 3′-to-5′ exoribonucleases in the turnover of *Bacillus subtilis* mRNA. *J Bacteriol* **187**: 2758–2767.

Ow MC & Kushner SR (2002) Initiation of tRNA maturation by RNase E is essential for cell viability in *E. coli*. *Gene Dev* **16**: 1102–1115.

Ow MC, Liu Q & Kushner SR (2000) Analysis of mRNA decay and rRNA processing in *Escherichia coli* in the absence of RNase E-based degradosome assembly. *Mol Microbiol* **38**: 854–866.

Ow MC, Liu Q, Mohanty BK, Andrew ME, Maples VF & Kushner SR (2002) RNase E levels in *Escherichia coli* are controlled by a complex regulatory system that involves transcription of the *rne* gene from three promoters. *Mol Microbiol* **43**: 159–171.

Ow MC, Perwez T & Kushner SR (2003) RNase G of *Escherichia coli* exhibits only limited functional overlap with its essential homologue, RNase E. *Mol Microbiol* **49**: 607–622.

Palanisamy SK, Fletcher C, Tanjung L, Katz ME & Cheetham BF (2009) Deletion of the C-terminus of polynucleotide phosphorylase increases twitching motility, a virulence characteristic of the anaerobic bacterial pathogen *Dichelobacter nodosus*. *FEMS Microbiol Lett* **302**: 39–45.

Peck-Miller KA & Altman S (1991) Kinetics of the processing of the precursor to 4.5 S RNA, a naturally occurring substrate for RNase P from *Escherichia coli*. *J Mol Biol* **221**: 1–5.

Pedersen K, Zavialov AV, Pavlov MY, Elf J, Gerdes K & Ehrenberg M (2003) The bacterial toxin RelE displays codon-specific cleavage of mRNAs in the ribosomal A site. *Cell* **112**: 131–140.

Pellegrini O, Nezzar J, Marchfelder A, Putzer H & Condon C (2003) Endonucleolytic processing of CCA-less tRNA precursors by RNase Z in *Bacillus subtilis*. *EMBO J* **22**: 4534–4543.

Pepe CM, Maslesa-Galic S & Simons RW (1994) Decay of the IS10 antisense RNA by 3′ exoribonucleases: evidence that RNase II stabilizes RNA-OUT against PNPase attack. *Mol Microbiol* **13**: 1133–1142.

Pertzev AV & Nicholson AW (2006b) Characterization of RNA sequence determinants and antideterminants of processing reactivity for a minimal substrate of *Escherichia coli* ribonuclease III. *Nucleic Acids Res* **34**: 3708–3721.

Perwez T & Kushner SR (2006a) RNase Z in *Escherichia coli* plays a significant role in mRNA decay. *Mol Microbiol* **60**: 723–737.

Phizicky EM & Alfonzo JD (2010) Do all modifications benefit all tRNAs? *FEBS Lett* **584**: 265–271.

Piazza F, Zappone M, Sana M, Briani F & Dehò G (1996) Polynucleotide phosphorylase of *Escherichia coli* is required for the establishment of bacteriophage P4 immunity. *J Bacteriol* **178**: 5513–5521.

Portier C & Regnier P (1984) Expression of the *rpsO* and *pnp* genes: structural analysis of a DNA fragment carrying their control regions. *Nucleic Acids Res* **12**: 6091–6102.

Portier C, Dondon L, Grunberg-Manago M & Régnier P (1987) The first step in the functional inactivation of the *Escherichia coli* polynucleotide phosphorylase messenger is a ribonuclease III processing at the 5′ end. *EMBO J* **6**: 2165–2170.

Portnoy V & Schuster G (2006) RNA polyadenylation and degradation in different Archaea; roles of the exosome and RNase R. *Nucleic Acids Res* **34**: 5923–5931.

Portnoy V, Evguenieva-Hackenberg E, Klein F, Walter P, Lorentzen E, Klug G & Schuster G (2005) RNA polyadenylation in Archaea: not observed in *Haloferax* while the exosome polynucleotidylates RNA in *Sulfolobus*. *EMBO Rep* **6**: 1188–1193.

Prud'homme-Genereux A, Beran RK, Iost I, Ramey CS, Mackie GA & Simons RW (2004) Physical and functional interactions among RNase E, polynucleotide phosphorylase and the cold-shock protein, CsdA: evidence for a 'cold shock degradosome'. *Mol Microbiol* **54**: 1409–1421.

Pruijn GJ (2005) Doughnuts dealing with RNA. *Nat Struct Mol Biol* **12**: 562–564.

Purusharth RI, Klein F, Sulthana S *et al.* (2005) Exoribonuclease R interacts with endoribonuclease E and an RNA helicase in the psychrotrophic bacterium *Pseudomonas syringae* Lz4W. *J Biol Chem* **280**: 14572–14578.

Purusharth RI, Madhuri B & Ray MK (2007) Exoribonuclease R in *Pseudomonas syringae* is essential for growth at low temperature and plays a novel role in the 3′ end processing of 16 and 5 S ribosomal RNA. *J Biol Chem* **282**: 16267–16277.

Py B, Causton H, Mudd EA & Higgins CF (1994) A protein complex mediating mRNA degradation in *Escherichia coli*. *Mol Microbiol* **14**: 717–729.

Py B, Higgins CF, Krisch HM & Carpousis AJ (1996) A DEAD-box RNA helicase in the *Escherichia coli* RNA degradosome. *Nature* **381**: 169–172.

Randau L, Schroder I & Soll D (2008) Life without RNase P. *Nature* **453**: 120–123.

Rasmussen AA, Eriksen M, Gilany K, Udesen C, Franch T, Petersen C & Valentin-Hansen P (2005) Regulation of *omp*A mRNA stability: the role of a small regulatory RNA in growth phase-dependent control. *Mol Microbiol* **58**: 1421–1429.

Redko Y, Bechhofer DH & Condon C (2008) Mini-III, an unusual member of the RNase III family of enzymes, catalyses 23S ribosomal RNA maturation in *B. subtilis*. *Mol Microbiol* **68**: 1096–1106.

Régnier P & Grunberg-Manago M (1990) RNase III cleavages in non-coding leaders of *Escherichia coli* transcripts control mRNA stability and genetic expression. *Biochimie* **72**: 825–834.

Régnier P & Portier C (1986) Initiation, attenuation and RNase III processing of transcripts from the *Escherichia coli* operon encoding ribosomal protein S15 and polynucleotide phosphorylase. *J Mol Biol* **187**: 23–32.

Regonesi ME, Briani F, Ghetta A, Zangrossi S, Ghisotti D, Tortora P & Deho G (2004) A mutation in polynucleotide phosphorylase from *Escherichia coli* impairing RNA binding and degradosome stability. *Nucleic Acids Res* **32**: 1006–1017.

Regonesi ME, Del Favero M, Basilico F *et al.* (2006) Analysis of the *Escherichia coli* RNA degradosome composition by a proteomic approach. *Biochimie* **88**: 151–161.

Reva ON, Weinel C, Weinel M, Bohm K, Stjepandic D, Hoheisel JD & Tummler B (2006) Functional genomics of stress response in *Pseudomonas putida* KT2440. *J Bacteriol* **188**: 4079–4092.

Robert-Le Meur M & Portier C (1992) *E.coli* polynucleotide phosphorylase expression is autoregulated through an RNase III-dependent mechanism. *EMBO J* **11**: 2633–2641.

Robert-Le Meur M & Portier C (1994) Polynucleotide phosphorylase of *Escherichia coli* induces the degradation of its RNase III processed messenger by preventing its translation. *Nucleic Acids Res* **22**: 397–403.

Robertson HD, Webster RE & Zinder ND (1968) Purification and properties of ribonuclease III from *Escherichia coli*. *J Biol Chem* **243**: 82–91.

Robertson HD, Altman S & Smith JD (1972) Purification and properties of a specific *Escherichia coli* ribonuclease which cleaves a tyrosine transfer ribonucleic acid precursor. *J Biol Chem* **247**: 5243–5251.

Rosenzweig JA, Weltman G, Plano GV & Schesser K (2005) Modulation of *Yersinia* type three secretion system by the S1 domain of polynucleotide phosphorylase. *J Biol Chem* **280**: 156–163.

Rosenzweig JA, Chromy B, Echeverry A *et al.* (2007) Polynucleotide phosphorylase independently controls virulence factor expression levels and export in *Yersinia* spp. *FEMS Microbiol Lett* **270**: 255–264.

Rott R, Zipor G, Portnoy V, Liveanu V & Schuster G (2003) RNA polyadenylation and degradation in cyanobacteria are similar to the chloroplast but different from *Escherichia coli*. *J Biol Chem* **278**: 15771–15777.

Rougemaille M, Villa T, Gudipati RK & Libri D (2008) mRNA journey to the cytoplasm: attire required. *Biol Cell* **100**: 327–342.

Sakai T, Nakamura N, Umitsuki G, Nagai K & Wachi M (2007) Increased production of pyruvic acid by *Escherichia coli* RNase G mutants in combination with *cra* mutations. *Appl Microbiol Biot* **76**: 183–192.

Sanson B & Uzan M (1995) Post-transcriptional controls in bacteriophage T4: roles of the sequence-specific endoribonuclease RegB. *FEMS Microbiol Rev* **17**: 141–150.

Santos JM, Drider D, Marujo PE, Lopez P & Arraiano CM (1997) Determinant role of *E. coli* RNase III in the decay of both specific and heterologous mRNAs. *FEMS Microbiol Lett* **157**: 31–38.

Schaeffer D, Tsanova B, Barbas A *et al.* (2009) The exosome contains domains with specific endoribonuclease, exoribonuclease and cytoplasmic mRNA decay activities. *Nat Struct Mol Biol* **16**: 56–62.

Schiffer S, Rosch S & Marchfelder A (2002) Assigning a function to a conserved group of proteins: the tRNA 3′-processing enzymes. *EMBO J* **21**: 2769–2777.

Schilling O, Ruggeberg S, Vogel A *et al.* (2004) Characterization of an *Escherichia coli elaC* deletion mutant. *Biochem Bioph Res Co* **320**: 1365–1373.

Seif E & Altman S (2008) RNase P cleaves the adenine riboswitch and stabilizes *pbuE* mRNA in *Bacillus subtilis*. *RNA* **14**: 1237–1243.

Sello JK & Buttner MJ (2008) The oligoribonuclease gene in *Streptomyces coelicolor* is not transcriptionally or translationally coupled to *adp*A, a key *bld*A target. *FEMS Microbiol Lett* **286**: 60–65.

Shahbabian K, Jamalli A, Zig L & Putzer H (2009) RNase Y, a novel endoribonuclease, initiates riboswitch turnover in *Bacillus subtilis*. *EMBO J* **28**: 3523–3533.

Shehi E, Serina S, Fumagalli G *et al*. (2001) The Sso7d DNA-binding protein from *Sulfolobus solfataricus* has ribonuclease activity. *FEBS Lett* **497**: 131–136.

Shi Z, Yang WZ, Lin-Chao S, Chak KF & Yuan HS (2008) Crystal structure of *Escherichia coli* PNPase: central channel residues are involved in processive RNA degradation. *RNA* **14**: 2361–2371.

Shibata HS, Minagawa A, Takaku H, Takagi M & Nashimoto M (2006) Unstructured RNA is a substrate for tRNase Z. *Biochemistry* **45**: 5486–5492.

Shiraishi H & Shimura Y (1986) Mutations affecting two distinct functions of the RNA component of RNase P. *EMBO J* **5**: 3673–3679.

Shyu AB, Wilkinson MF & van Hoof A (2008) Messenger RNA regulation: to translate or to degrade. *EMBO J* **27**: 471–481.

Sim SH, Yeom JH, Shin C *et al*. (2010) *Escherichia coli* ribonuclease III activity is downregulated by osmotic stress: consequences for the degradation of *bdm* mRNA in biofilm formation. *Mol Microbiol* **75**: 413–425.

Slomovic S, Laufer D, Geiger D & Schuster G (2005) Polyadenylation and degradation of human mitochondrial RNA: the prokaryotic past leaves its mark. *Mol Cell Biol* **25**: 6427–6435.

Slomovic S, Portnoy V, Yehudai-Resheff S, Bronshtein E & Schuster G (2008) Polynucleotide phosphorylase and the archaeal exosome as poly(A)-polymerases. *Biochim Biophys Acta* **1779**: 247–255.

Smith D, Burgin AB, Haas ES & Pace NR (1992) Influence of metal ions on the ribonuclease P reaction. Distinguishing substrate binding from catalysis. *J Biol Chem* **267**: 2429–2436.

Smith JK, Hsieh J & Fierke CA (2007) Importance of RNA–protein interactions in bacterial ribonuclease P structure and catalysis. *Biopolymers* **87**: 329–338.

Söderbom F & Wagner EG (1998) Degradation pathway of *Cop*A, the antisense RNA that controls replication of plasmid R1. *Microbiology* **144**: 1907–1917.

Söderbom F, Binnie U, Masters M & Wagner EG (1997) Regulation of plasmid R1 replication: PcnB and RNase E expedite the decay of the antisense RNA, *Cop*A. *Mol Microbiol* **26**: 493–504.

Sogin ML & Pace NR (1974) *In vitro* maturation of precursors of 5S ribosomal RNA from *Bacillus subtilis*. *Nature* **252**: 598–600.

Sogin ML, Pace B & Pace NR (1977) Partial purification and properties of a ribosomal RNA maturation endonuclease from *Bacillus subtilis*. *J Biol Chem* **252**: 1350–1357.

Sohlberg B, Huang J & Cohen SN (2003) The *Streptomyces coelicolor* polynucleotide phosphorylase homologue, and not the putative poly(A) polymerase, can polyadenylate RNA. *J Bacteriol* **185**: 7273–7278.

Song JJ, Smith SK, Hannon GJ & Joshua-Tor L (2004) Crystal structure of Argonaute and its implications for RISC slicer activity. *Science* **305**: 1434–1437.

Sousa S, Marchand I & Dreyfus M (2001) Autoregulation allows *Escherichia coli* RNase E to adjust continuously its synthesis to that of its substrates. *Mol Microbiol* **42**: 867–878.

Spickler C & Mackie GA (2000) Action of RNase II and polynucleotide phosphorylase against RNAs containing stem-loops of defined structure. *J Bacteriol* **182**: 2422–2427.

Stevens A & Niyogi SK (1967) Hydrolysis of oligoribonucleotides by an enzyme fraction from *Escherichia coli*. *Biochem Bioph Res Co* **29**: 550–555.

Stickney LM, Hankins JS, Miao X & Mackie GA (2005) Function of the conserved S1 and KH domains in polynucleotide phosphorylase. *J Bacteriol* **187**: 7214–7221.

Storz G, Opdyke JA & Zhang A (2004) Controlling mRNA stability and translation with small, noncoding RNAs. *Curr Opin Microbiol* **7**: 140–144.

Stougaard P, Molin S & Nordström K (1981) RNAs involved in copy-number control and incompatibility of plasmid R1. *P Natl Acad Sci USA* **78**: 6008–6012.

Subbarayan PR & Deutscher MP (2001) *Escherichia coli* RNase M is a multiply altered form of RNase I. *RNA* **7**: 1702–1707.

Sulewski M, Marchese-Ragona SP, Johnson KA & Benkovic SJ (1989) Mechanism of polynucleotide phosphorylase. *Biochemistry* **28**: 5855–5864.

Symmons MF, Jones GH & Luisi BF (2000) A duplicated fold is the structural basis for polynucleotide phosphorylase catalytic activity, processivity, and regulation. *Structure* **8**: 1215–1226.

Szczesny RJ, Borowski LS, Brzezniak LK, Dmochowska A, Gewartowski K, Bartnik E & Stepien PP (2010) Human mitochondrial RNA turnover caught in flagranti: involvement of hSuv3p helicase in RNA surveillance. *Nucleic Acids Res* **38**: 279–298.

Tadokoro T & Kanaya S (2009) Ribonuclease H: molecular diversities, substrate binding domains, and catalytic mechanism of the prokaryotic enzymes. *FEBS J* **276**: 1482–1493.

Taghbalout A & Rothfield L (2007) RNaseE and the other constituents of the RNA degradosome are components of the bacterial cytoskeleton. *P Natl Acad Sci USA* **104**: 1667–1672.

Taghbalout A & Rothfield L (2008) RNaseE and RNA helicase B play central roles in the cytoskeletal organization of the RNA degradosome. *J Biol Chem* **283**: 13850–13855.

Takaku H & Nashimoto M (2008) *Escherichia coli* tRNase Z can shut down growth probably by removing amino acids from aminoacyl-tRNAs. *Genes Cells* **13**: 1087–1097.

Takechi S, Yasueda H & Itoh T (1994) Control of ColE2 plasmid replication: regulation of Rep expression by a plasmid-coded antisense RNA. *Mol Gen Genet* **244**: 49–56.

Taraseviciene L, Miczak A & Apirion D (1991) The gene specifying RNase E (*rne*) and a gene affecting mRNA stability (*ams*) are the same gene. *Mol Microbiol* **5**: 851–855.

Thompson JD, Gibson TJ, Plewniak F, Jeanmougin F & Higgins DG (1997) The CLUSTAL_X windows interface: flexible strategies for multiple sequence alignment aided by quality analysis tools. *Nucleic Acids Res* **25**: 4876–4882.

Tobe T, Sasakawa C, Okada N, Honma Y & Yoshikawa M (1992) *vacB*, a novel chromosomal gene required for expression of virulence genes on the large plasmid of *Shigella flexneri*. *J Bacteriol* **174**: 6359–6367.

Tock MR, Walsh AP, Carroll G & McDowall KJ (2000) The CafA protein required for the 5′-maturation of 16 S rRNA is a 5′-end-dependent ribonuclease that has context-dependent broad sequence specificity. *J Biol Chem* **275**: 8726–8732.

Tomecki R, Dmochowska A, Gewartowski K, Dziembowski A & Stepien PP (2004) Identification of a novel human nuclear-encoded mitochondrial poly(A) polymerase. *Nucleic Acids Res* **32**: 6001–6014.

Turnbough CL Jr, Kerr KH, Funderburg WR, Donahue JP & Powell FE (1987) Nucleotide sequence and characterization of the *pyr*F operon of *Escherichia coli* K12. *J Biol Chem* **262**: 10239–10245.

Udekwu KI, Darfeuille F, Vögel J, Reimegard J, Holmqvist E & Wagner EG (2005) Hfq-dependent regulation of OmpA synthesis is mediated by an antisense RNA. *Gene Dev* **19**: 2355–2366.

Umitsuki G, Wachi M, Takada A, Hikichi T & Nagai K (2001) Involvement of RNase G in *in vivo* mRNA metabolism in *Escherichia coli*. *Genes Cells* **6**: 403–410.

Uzan M (2001) Bacteriophage T4 RegB endoribonuclease. *Method Enzymol* **342**: 467–480.

Uzan M (2009) RNA processing and decay in bacteriophage T4. *Prog Mol Biol Transl Sci* **85**: 43–89.

van Hoof A & Parker R (1999) The exosome: a proteasome for RNA? *Cell* **99**: 347–350.

Vanzo NF, Li YS, Py B *et al*. (1998) Ribonuclease E organizes the protein interactions in the *Escherichia coli* RNA degradosome. *Gene Dev* **12**: 2770–2781.

Viegas SC & Arraiano CM (2008) Regulating the regulators: How ribonucleases dictate the rules in the control of small non-coding RNAs. *RNA Biol* **5**: 230–243.

Viegas SC, Schmidt D, Kasche V, Arraiano CM & Ignatova Z (2005) Effect of the increased stability of the penicillin amidase mRNA on the protein expression levels. *FEBS Lett* **579**: 5069–5073.

Viegas SC, Pfeiffer V, Sittka A, Silva IJ, Vogel J & Arraiano CM (2007) Characterization of the role of ribonucleases in *Salmonella* small RNA decay. *Nucleic Acids Res* **35**: 7651–7664.

Vincent HA & Deutscher MP (2006) Substrate recognition and catalysis by the exoribonuclease RNase R. *J Biol Chem* **281**: 29769–29775.

Vincent HA & Deutscher MP (2009) The roles of individual domains of RNase R in substrate binding and exoribonuclease activity. The nuclease domain is sufficient for digestion of structured RNA. *J Biol Chem* **284**: 486–494.

Viswanathan M, Dower KW & Lovett ST (1998) Identification of a potent DNase activity associated with RNase T of *Escherichia coli*. *J Biol Chem* **273**: 35126–35131.

Vogel A, Schilling O, Niecke M, Bettmer J & Meyer-Klaucke W (2002) ElaC encodes a novel binuclear zinc phosphodiesterase. *J Biol Chem* **277**: 29078–29085.

Vogel J & Hess WR (2001) Complete 5′ and 3′ end maturation of group II intron-containing tRNA precursors. *RNA* **7**: 285–292.

Vogel J, Argaman L, Wagner EG & Altuvia S (2004) The small RNA IstR inhibits synthesis of an SOS-induced toxic peptide. *Curr Biol* **14**: 2271–2276.

von Gabain A, Belasco JG, Schottel JL, Chang AC & Cohen SN (1983) Decay of mRNA in *Escherichia coli*: investigation of the fate of specific segments of transcripts. *P Natl Acad Sci USA* **80**: 653–657.

Wachi M, Umitsuki G, Shimizu M, Takada A & Nagai K (1999) *Escherichia coli cafA* gene encodes a novel RNase, designated as RNase G, involved in processing of the 5′ end of 16S rRNA. *Biochem Bioph Res Co* **259**: 483–488.

Wagner EG, Altuvia S & Romby P (2002) Antisense RNAs in bacteria and their genetic elements. *Adv Genet* **46**: 361–398.

Wagner S & Klug G (2007) An archaeal protein with homology to the eukaryotic translation initiation factor 5A shows ribonucleolytic activity. *J Biol Chem* **282**: 13966–13976.

Wang W & Bechhofer DH (1996) Properties of a *Bacillus subtilis* polynucleotide phosphorylase deletion strain. *J Bacteriol* **178**: 2375–2382.

Wang W & Bechhofer DH (1997) *Bacillus subtilis* RNase III gene: cloning, function of the gene in *Escherichia coli*, and construction of *Bacillus subtilis* strains with altered *rnc* loci. *J Bacteriol* **179**: 7379–7385.

Wen T, Oussenko IA, Pellegrini O, Bechhofer DH & Condon C (2005) Ribonuclease PH plays a major role in the exonucleolytic maturation of CCA-containing tRNA precursors in *Bacillus subtilis*. *Nucleic Acids Res* **33**: 3636–3643.

Willkomm DK, Feltens R & Hartmann RK (2002) tRNA maturation in *Aquifex aeolicus*. *Biochimie* **84**: 713–722.

Winkler WC & Breaker RR (2005) Regulation of bacterial gene expression by riboswitches. *Annu Rev Microbiol* **59**: 487–517.

Worrall JA & Luisi BF (2007) Information available at cut rates: structure and mechanism of ribonucleases. *Curr Opin Struc Biol* **17**: 128–137.

Worrall JA, Gorna M, Crump NT *et al*. (2008a) Reconstitution and analysis of the multienzyme *Escherichia coli* RNA degradosome. *J Mol Biol* **382**: 870–883.

Worrall JA, Howe FS, McKay AR, Robinson CV & Luisi BF (2008b) Allosteric activation of the ATPase activity of the *Escherichia coli* RhlB RNA helicase. *J Biol Chem* **283**: 5567–5576.

Wu J, Jiang Z, Liu M, Gong X, Wu S, Burns CM & Li Z (2009) Polynucleotide phosphorylase protects *Escherichia coli* against oxidative stress. *Biochemistry* **48**: 2012–2020.

Xu A, Jao DL & Chen KY (2004) Identification of mRNA that binds to eukaryotic initiation factor 5A by affinity co-purification and differential display. *Biochem J* **384**: 585–590.

Xu F & Cohen SN (1995) RNA degradation in *Escherichia coli* regulated by 3′ adenylation and 5′ phosphorylation. *Nature* **374**: 180–183.

Xu F, Lin-Chao S & Cohen SN (1993) The *Escherichia coli pcn*B gene promotes adenylylation of antisense RNAI of ColE1-type plasmids *in vivo* and degradation of RNAI decay intermediates. *P Natl Acad Sci USA* **90**: 6756–6760.

Yamaguchi Y & Inouye M (2009) mRNA interferases, sequence-specific endoribonucleases from the toxin-antitoxin systems. *Prog Mol Biol Transl Sci* **85**: 467–500.

Yang L & Altman S (2007) A noncoding RNA in *Saccharomyces cerevisiae* is an RNase P substrate. *RNA* **13**: 682–690.

Yang W, Hendrickson WA, Crouch RJ & Satow Y (1990) Structure of ribonuclease H phased at 2 Å resolution by MAD analysis of the selenomethionyl protein. *Science* **249**: 1398–1405.

Yao S, Blaustein JB & Bechhofer DH (2007) Processing of *Bacillus subtilis* small cytoplasmic RNA: evidence for an additional endonuclease cleavage site. *Nucleic Acids Res* **35**: 4464–4473.

Yehudai-Resheff S, Hirsh M & Schuster G (2001) Polynucleotide phosphorylase functions as both an exonuclease and a poly(A) polymerase in spinach chloroplasts. *Mol Cell Biol* **21**: 5408–5416.

Zangrossi S, Briani F, Ghisotti D, Regonesi ME, Tortora P & Dehò G (2000) Transcriptional and post-transcriptional control of polynucleotide phosphorylase during cold acclimation in *Escherichia coli*. *Mol Microbiol* **36**: 1470–1480.

Zhang JR & Deutscher MP (1988a) Cloning, characterization, and effects of overexpression of the *Escherichia coli rnd* gene encoding RNase D. *J Bacteriol* **170**: 522–527.

Zhang JR & Deutscher MP (1988b) Transfer RNA is a substrate for RNase D *in vivo*. *J Biol Chem* **263**: 17909–17912.

Zhang JR & Deutscher MP (1989) Analysis of the upstream region of the *Escherichia coli rnd* gene encoding RNase D. Evidence for translational regulation of a putative tRNA processing enzyme. *J Biol Chem* **264**: 18228–18233.

Zhang K & Nicholson AW (1997) Regulation of ribonuclease III processing by double-helical sequence antideterminants. *P Natl Acad Sci USA* **94**: 13437–13441.

Zhang X, Zhu L & Deutscher MP (1998) Oligoribonuclease is encoded by a highly conserved gene in the 3′-5′ exonuclease superfamily. *J Bacteriol* **180**: 2779–2781.

Zhu LQ, Gangopadhyay T, Padmanabha KP & Deutscher MP (1990) *Escherichia coli rna* gene encoding RNase I: cloning, overexpression, subcellular distribution of the enzyme, and use of an *rna* deletion to identify additional RNases. *J Bacteriol* **172**: 3146–3151.

Zilhão R, Camelo L & Arraiano CM (1993) DNA sequencing and expression of the gene *rnb* encoding *Escherichia coli* ribonuclease II. *Mol Microbiol* **8**: 43–51.

Zilhão R, Caillet J, Regnier P & Arraiano CM (1995a) Precise physical mapping of the *Escherichia coli rnb* gene, encoding ribonuclease II. *Mol Gen Genet* **248**: 242–246.

Zilhão R, Régnier P & Arraiano CM (1995b) The role of endonucleases in the expression of ribonuclease II in *Escherichia coli*. *FEMS Microbiol Lett* **130**: 237–244.

Zilhão R, Cairrão F, Régnier P & Arraiano CM (1996a) PNPase modulates RNase II expression in *Escherichia coli*: implications for mRNA decay and cell metabolism. *Mol Microbiol* **20**: 1033–1042.

Zilhão R, Plumbridge J, Hajnsdorf E, Regnier P & Arraiano CM (1996b) *Escherichia coli* RNase II: characterization of the promoters involved in the transcription of *rnb*. *Microbiology* **142**: 367–375.

Zuo Y & Deutscher MP (2001) Exoribonuclease superfamilies: structural analysis and phylogenetic distribution. *Nucleic Acids Res* **29**: 1017–1026.

Zuo Y & Deutscher MP (2002) The physiological role of RNase T can be explained by its unusual substrate specificity. *J Biol Chem* **277**: 29654–29661.

Zuo Y, Wang Y & Malhotra A (2005) Crystal structure of *Escherichia coli* RNase D, an exoribonuclease involved in structured RNA processing. *Structure* **13**: 973–984.

Zuo Y, Vincent HA, Zhang J, Wang Y, Deutscher MP & Malhotra A (2006) Structural basis for processivity and single-strand specificity of RNase II. *Mol Cell* **24**: 149–156.

Zuo Y, Zheng H, Wang Y *et al.* (2007) Crystal structure of RNase T, an exoribonuclease involved in tRNA maturation and end turnover. *Structure* **15**: 417–428.

Protein J (2010) 29:394–397
DOI 10.1007/s10930-010-9265-1

Comparison of EMSA and SPR for the Characterization of RNA–RNase II Complexes

Rute G. Matos · Ana Barbas · Cecília M. Arraiano

Published online: 30 June 2010

Abstract RNases are enzymes that process and degrade RNA molecules. As such, the study of the interactions between these enzymes and RNA molecules is essential in order to better understand their mechanism of action. In this report, our aim was to use *E. coli* RNase II as a model to compare two different techniques for the characterization and interpretation of the stability of RNA–protein complexes: Surface Plasmon Resonance and Electrophoretic Mobility Shift Assay.

Keywords RNase II · RNA binding · RNA degradation · Ribonucleases · RNA–protein complexes · EMSA · SPR · Dissociation constant

Abbreviations

RNase	Ribonuclease
EMSA	Electrophoretic mobility shift assay
SPR	Surface plasmon resonance
EDTA	Ethylenediamine tetraacetic acid
K_D	Dissociation constant
CSD	Cold Shock domain
DTT	Dithiothreitol
BSA	Bovine serum albumin
k_a	Association rate constant
k_d	Dissociation rate constant

R. G. Matos · A. Barbas · C. M. Arraiano (✉)
Instituto de Tecnologia Química e Biológica, Universidade Nova de Lisboa, Apartado 127, 2781-901 Oeiras, Portugal
e-mail: cecilia@itqb.unl.pt

Ribonucleases (RNases) are enzymes present in all domains of life. They process and degrade RNA, playing a central role in the control of the RNA metabolism [5, 9–11]. One of the most important ribonucleases is RNase II, an exoribonuclease widely distributed which processively degrades RNA from the 3′-end releasing 5′-nucleotide monophosphates [3, 12]. It is formed by two N-terminal CSD domains and a C-terminal S1 domain, the three of them involved in RNA binding, and a central RNB domain responsible for the catalytic activity [2, 8]. RNase II has been subject of an intensive characterization regarding its activity and ability to bind RNA. Different techniques have been developed to study and determine the affinity of this protein to RNA. The most commonly used techniques include the Filter Binding Assays [2, 4] and the Electrophoretic Mobility Shift Assays (EMSA) [1, 4]. However, these methods are laborious, require a radioactive labeled RNA and the determination of the dissociation constants is most of the times based on an indirect method. Moreover, the stability of the RNA–protein complexes may interfere in the determination of the K_D values, since more unstable complexes can be underestimated.

We have characterized the RNA binding capability of wild type RNase II and of 16 RNase II mutants by Surface Plasmon Resonance (SPR). In this report, we compare the results obtained using two distinct techniques: SPR and EMSA, for the same proteins using the exact same substrate. Taking into account that the activity of RNase II is dependent of a Mg^{2+} ion, the determination of the binding ability of this protein requires the complete abolishment of its ribonucleolytic activity. For that purpose, the EMSA and SPR reactions were performed in a buffer containing a saturating concentration of EDTA, a chelating agent that sequesters the Mg^{2+}, thus avoiding RNA degradation by RNase II and the mutant proteins.

The proteins used in this work were previously characterized [6, 7]. The EMSAs were performed with a 35-mer Poly(A) RNA as substrate. Briefly, the substrate was first labelled at the 5′-end using [γ-32ATP] and T4 polynucleotide kinase. The substrate was then purified with Microcon YM-3 Centrifugal Filter Devices (Millipore) to remove the non-incorporated nucleotides. Binding reactions were performed in 10 µl of volume containing 20 mM Tris–HCl pH8, 100 mM KCl, 1 mM DTT, 0.5 µg/µl BSA and 25 mM EDTA, 1 fmol of substrate and increasing concentration of enzyme. Mixtures containing increasing concentration of each enzyme were incubated for 10 min at 37 °C and then subjected to UV crosslinking (600 mJ, 10 min, 254 nm). The samples were analyzed in a 10% nondenaturing polyacrylamide gel, and the RNA–protein complexes were detected by using the PhosphorImager system from Molecular Dynamics. The results obtained are present in Fig. 1. RNA–protein complexes were quantified by using the Image Quant Software (Molecular Dynamics). The values obtained for the RNA–protein complexes and protein concentrations were plotted. The K_D was measured as the concentration of the protein at which half of the target RNA is bound. The values obtained are presented in Table 1. For SPR analysis we used the BIACORE 2000 instrument and the Biacore SA chips from GE Healthcare. The biotinylated RNA was immobilized in flow cell 2 by manually injecting 20 µl of a 500 nM solution at a 20 µl/min flow rate. No RNA was captured on flow cell 1, so it could be used as reference. The biosensor assay was run at 4 °C in a buffer composed of 20 mM Tris–HCl pH8, 100 mM KCl, 1 mM DTT and 25 mM EDTA (the presence of EDTA in the buffers used in both techniques is very important for the inactivation of the activity of this exoribonuclease in order to avoid RNA degradation). The proteins were injected over flow cells 1 and 2 for 2.5 min at concentrations of 10, 20, 30, 40 and 50 nM using a flow rate of 20 µl/min. All experiments included triple injections of each protein concentration to determine the reproducibility of the signal. Bound protein was removed with a 60 s wash with 2 M NaCl. Data from flow cell 1 were used to correct for refractive index changes and nonspecific binding. Rate and equilibrium constants were calculated using the BIA EVALUATION 3.0 software package, according to the fitting model 1:1 Languimir Binding (Table 1).

According to the van′t Hoff equation: $\Delta G^\circ = RT\ln K_D$, where R and T are the universal gas constant and absolute temperature, we determined the Gibbs free energy

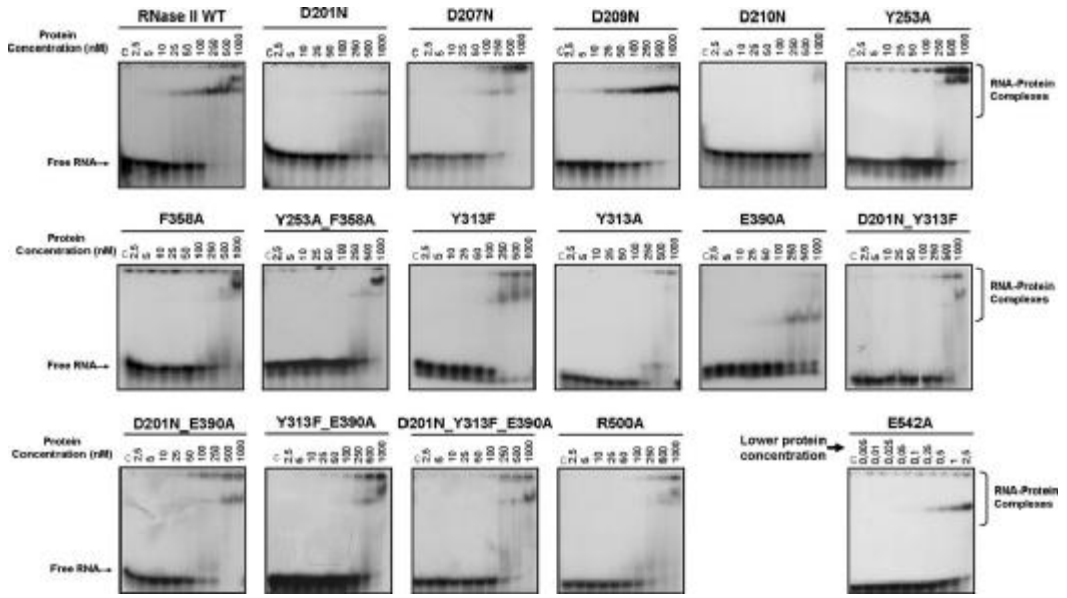

Fig. 1 Electrophoretic mobility shift assay (EMSA) of wild type RNase II and mutant proteins with a Poly(A) substrate. The 35-mer poly(A) RNA was incubated with the proteins under the conditions described. The enzyme concentration used was the same for all mutants except for E542A where much less concentration was necessary. We have indicated in the figure the respective protein concentration. A control reaction without enzyme added was performed in all experiments (*C*). Binding reactions were applied on a 10% non-denaturing PAA gel. The mobility of free and complexed substrate was detected using the PhosphorImager system from Molecular Dynamics

Table 1 Kinetic analysis of RNase II wt and mutant proteins

Protein	SPR data				EMSA data
	k_a (1/Ms)	k_d (1/s)	K_D (nM)	$\Delta G°$ (KJ/mol)	K_D (nM)
WT	$3.3 \pm 0.3 \times 10^5$	$4.4 \pm 0.4 \times 10^{-4}$	1.3 ± 0.4	−47,15	46.7 ± 3.8
D201N	$1.2 \pm 0.05 \times 10^6$	$1.3 \pm 0.1 \times 10^{-3}$	1.1 ± 0.1	−47,53	>1,000
D207N	$1.1 \pm 0.3 \times 10^3$	$2.7 \pm 0.4 \times 10^{-6}$	3.6 ± 0.3	−44,80	88.6 ± 2.8
D209N	$1.2 \pm 0.1 \times 10^5$	$1.5 \pm 0.1 \times 10^{-4}$	1.2 ± 0.2	−47,33	76.6 ± 1.9
D210N	$4.5 \pm 0.3 \times 10^5$	$1.6 \pm 0.08 \times 10^{-3}$	3.0 ± 0.4	−45,22	>1,000
Y253A	$9.9 \pm 0.6 \times 10^2$	$5.9 \pm 0.7 \times 10^{-6}$	5.9 ± 0.8	−43,66	101.3 ± 5.2
F358A	$4.2 \pm 0.2 \times 10^5$	$3.6 \pm 0.08 \times 10^{-3}$	8.7 ± 0.4	−42,77	650.7 ± 1.0
Y253A_F358A	$2.3 \pm 0.3 \times 10^2$	$5.2 \pm 0.6 \times 10^{-8}$	1.1 ± 0.2	−47,53	744.0 ± 15.9
Y313F	$4.3 \pm 0.3 \times 10^2$	$1.8 \pm 0.07 \times 10^{-6}$	4.4 ± 0.1	−44,34	171.3 ± 10.0
Y313A	$1.1 \pm 0.2 \times 10^3$	$4.5 \pm 0.2 \times 10^{-6}$	4.2 ± 0.7	−44,45	471.3 ± 31.8
E390A	$1.6 \pm 0.3 \times 10^{-1}$	$3.0 \pm 0.3 \times 10^{-10}$	2.3 ± 0.4	−45,83	>1,000
D201N_Y313F	$1.8 \pm 0.1 \times 10^3$	$7.9 \pm 0.6 \times 10^{-6}$	4.4 ± 0.6	−44,34	468.9 ± 36.8
D201N_E390A	$5.1 \pm 0.3 \times 10^3$	$8.0 \pm 0.5 \times 10^{-6}$	1.6 ± 0.1	−46,67	348.4 ± 14.6
Y313F_E390A	$1.0 \pm 0.1 \times 10^3$	$5.9 \pm 0.4 \times 10^{-6}$	6.0 ± 0.7	−43,62	486.5 ± 26.1
D201N_Y313F_E390A	$7.1 \pm 0.8 \times 10^2$	$7.5 \pm 0.5 \times 10^{-6}$	12.0 ± 2.9	−42,03	442.7 ± 6.8
R500A	$8.0 \pm 0.7 \times 10^5$	$2.6 \pm 0.2 \times 10^{-3}$	3.3 ± 0.6	−45,00	$250.4 \pm 21,2$
E542A	$1.7 \pm 0.4 \times 10^7$	$7.0 \pm 0.6 \times 10^{-2}$	0.06 ± 0.005	−54,24	1.03 ± 0.04

The kinetic constants were determined by EMSA and by Surface Plasmon Resonance using BIACORE 2000 with a 30-mer Poly(A) RNA. k_a is the association rate constant, k_d the dissociation rate constant, and K_D the equilibrium dissociation constant of the reaction. The Gibbs free energy difference, $\Delta G°$ was determined according to the van′t Hoff equation: $\Delta G° = RT\ln K_D$, where R and T are the universal gas constant and absolute temperature

difference, $\Delta G°$, which is a measure of likelihood of complex formation. When the value is negative, it means that the reaction is spontaneous. For all the mutants tested, we observed that the value obtained is negative, confirming that the association between the different RNases and RNA is a spontaneous reaction. Moreover, for the mutant E542A, which has a higher affinity for RNA (Table 1; Fig. 1), the $\Delta G°$ value is much lower when compared to the others, confirming that the binding of this mutant to RNA is much more favourable when compared to the wild type and the other mutants.

By comparing the results obtained by EMSA, it is possible to see that the wild type enzyme is able to form very stable complexes. These are only detectable when the protein is present in concentrations over 5 nM (Fig. 1). The same result is observed for the D209N mutant, which was shown to be an inactive protein. This confirms that the protein is still able to bind to RNA efficiently, as previously demonstrated with different and more structured RNA substrates [1]. When we determined the K_D values for both proteins by quantifying the amount of RNA bound, we obtained a value of 46.7 ± 3.8 nM for the wild type protein and 76.6 ± 1.90 nM for the D209N mutant (Table 1, right column). This confirms that both proteins have a similar affinity for RNA. Moreover, the K_D values obtained for the Poly(A) substrate determined in this study were reduced when compared to the ones obtained with other substrates [1]. This confirms the preference of these enzymes for Poly(A) substrates [6, 7]. Also, for the E542A mutant it is possible to see the formation of a highly stable complex. Moreover, lower protein concentrations are needed to detect these stable complexes (Fig. 1). The K_D value calculated for this mutant was 1.03 ± 0.04 nM (Table 1, right column), confirming that this enzyme binds to RNA more efficiently when compared to the wild type enzyme. All the other mutant proteins tested appear to bind to RNA less efficiently when compared to the wild type enzyme (Fig. 1). The same conclusions can be reached by looking to the K_D values determined (Table 1, right column). However, for these last mutants, we can observe the existence of a smear rather than a clear band upon RNA binding. This fact supports the idea of the formation of less stable RNA–protein complexes that dissociate during running (Fig. 1). If the dissociation of the complexes is happening during gel running, the results obtained for these mutants are being underestimated with this technique.

The K_D values determined by SPR show us that most of the enzymes present a similar affinity for RNA when compared to the wild type (Table 1), while with EMSA the differences seem to be greater (Fig. 1). Moreover, the data extracted from the SPR analysis can give us more information about the kinetics of association and dissociation of

the complexes (k_a and k_d). k_a values of 10^5 or higher signify that the association of formation of the complexes is fast. When the values are lower, the association of the protein to the RNA is slow. Regarding the k_d values, if they range between 10^{-1} and 10^{-3} this indicates that the protein complex dissociates faster than the ones in which the values presented are lower than 10^{-4}. Moreover, slow dissociation kinetics implies that the complexes formed are more stable than the ones with faster dissociation kinetics. For example, RNase II wt and D209N have fast association kinetics ($3.3 \pm 0.3 \times 10^5$ and $1.2 \pm 0.1 \times 10^5$ M^{-1} s^{-1}) and slow dissociation kinetics ($4.4 \pm 0.4 \times 10^{-4}$ and $1.5 \pm 0.1 \times 10^{-4}$ s^{-1}), thus presenting more stable complexes as clearly detected by EMSA (Fig. 1). However, in the presence of both slow association and dissociation kinetics, the observation of stable complexes may not be possible. This is explained since the time spent for the complex to associate plus the duration of the running of the gel, may induce the complex dissociation (like in the case of Y313F mutant). When the RNA–protein interactions are characterized by fast association kinetics followed also by fast dissociation kinetics, the complexes are usually more unstable, since their half life is very short. This is the case of F358A mutant, for example (Table 1; Fig. 1). The most surprisingly result, however, was obtained with the E542A mutant, which associates and dissociates faster than all the others (Table 1) and is also able to form very stable complexes (Fig. 1). Nevertheless, this behaviour agrees with the extraordinary catalysis and turnover rate that was observed with this mutant, which is 110-fold more active than the wild type [6].

Although the results obtained with both techniques are different, they are not contradictory, since they give different types of information: while in SPR we can observe and measure the association and dissociation of the complex (k_a and k_d values), and Gibbs free energy difference, in EMSA analysis we are observing intact complexes that need to be highly stable in order to be detected by electrophoresis. Taking all the considerations together, we can say that the SPR analysis is more reliable and sensible to perform a comparison between a wild type protein and its mutants. Moreover, it is a much faster technique and less laborious making it possible to extract more information from the data obtained. Taking into account the aim of our study, which was the study of the effect of protein mutations in binding ability, we believe that the best option is to use the SPR technique, since one might not know if we are in the presence of stable or unstable complexes. Moreover, it provides more kinetic data when compared to EMSA, allowing us to better understand the kinetics of the binding and of the mode of action of the protein.

References

1. Amblar M, Arraiano CM (2005) FEBS J 272:363–374
2. Amblar M, Barbas A, Fialho AM, Arraiano CM (2006) J Mol Biol 360:921–933
3. Andrade JM, Pobre V, Silva IJ, Domingues S, Arraiano CM (2009) Prog Mol Biol Transl Sci 85:187–229
4. Arraiano CM, Barbas A, Amblar M (2008) Methods Enzymol 447:131–160
5. Arraiano CM, Maquat LE (2003) Mol Microbiol 49:267–276
6. Barbas A, Matos RG, Amblar M, Lopez-Vinas E, Gomez-Puertas P, Arraiano CM (2009) J Biol Chem 284:20486–20498
7. Barbas A, Matos RG, Amblar M, Lopez-Viñas E, Gomez-Puertas P, Arraiano CM (2008) J Biol Chem 283:13070–13076
8. Frazão C, McVey CE, Amblar M, Barbas A, Vonrhein C, Arraiano CM, Carrondo MA (2006) Nature 443:110–114
9. Nicholson AW (1999) FEMS Microbiol Rev 23:371–390
10. Parker R, Song H (2004) Nat Struct Mol Biol 11:121–127
11. Régnier P, Arraiano CM (2000) Bioessays 22:235–244
12. Zuo Y, Deutscher MP (2001) Nucleic Acids Res 29:1017–1026

RNA Biology 7:3, 276-281; May/June 2010; © 2010 Landes Bioscience

RNase II

The finer details of the Modus operandi of a molecular killer

Cecilia M. Arraiano,* Rute G. Matos and Ana Barbas
Instituto de Tecnologia Química e Biológica; Universidade Nova de Lisboa; Oeiras, Portugal

The RNase II family of enzymes is ubiquitous and has crucial roles in the processing, degradation and quality control of all types of RNA. These exoribonucleases processively degrade RNA from the 3'-end releasing 5'-nucleotide monophosphates. In prokaryotes, RNase II and RNase R have two N-terminal CSD and one C-terminal S1 domain involved in RNA binding, and a central catalytic RNB domain. In eukaryotes, Rrp44p/Dis3, is a RNase II-like protein with similar modular organization, that is the only catalytically active nuclease in the exosome, a complex crucial for RNA metabolism. Here we review recent progresses in the understanding of the degradation mechanism of RNase II, based on mutational analysis and their characterization regarding catalysis and RNA affinity. We have given particular emphasis on *E. coli* RNase II but the synergies between the functional and structural studies have shown that our findings have implications in the understanding the similar mode of action of other RNase II family members.

Key words: ribonuclease, RNase II, RNase R, *Escherichia coli*, RNA degradation, exosome

Abbreviations: RNases, ribonucleases; 3D, three-dimensional; CSD, cold shock domain; RNB, RNase II catalytic domain; EM, electron microscopy

Submitted: 02/04/10

Accepted: 02/09/10

Previously published online: www.landesbioscience.com/journals/rnabiology/article/11490

*Correspondence to: Cecília M. Arraiano; Email: cecilia@itqb.unl.pt

RNA degradation plays a fundamental role in all biological processes. Ribonucleases (RNases) are ubiquitous and play a central role in the control of the RNA metabolism. They process and degrade RNA, and are the main factors responsible for the determination of the functional mRNA levels in the cell.[1-5] Most RNases have been implicated in the processing of stable ribosomal RNAs (rRNA) or transfer RNAs (tRNA).[2] RNases can be involved in quality control mechanisms and play an important part in the recycling of the ribonucleotides in the cell.[6] The ribonucleases can be broadly classified as endoribonucleases (which cleave on internal RNA sequences) or exoribonucleases (remove nucleotides from either the 5' end or 3' end of the RNA molecule).

The enzymes of the RNase II-family of exoribonucleases are present in all domains of life, and processively degrade RNA in the 3' to 5' direction with a hydrolytic activity releasing 5'-nucleotide monophosphates.[7-10] RNase II is often essential for growth,[8] can be developmentally regulated,[11] and mutations in its gene have been linked with abnormal chloroplast biogenesis,[12] mitotic control and cancer[13] (**Fig. 1**). RNase R, a member of the RNase II-family of enzymes, has been shown to be important for stress responses, RNA and protein quality control, and it is required for virulence in several microorganims[14-20] (**Fig. 1**). Enzymes of this family are involved in poly(A) dependent RNA degradation mechanism[21,22] (**Fig. 1**). In eukaryotes RNase II-like enzymes can act independently or can be associated in multiprotein complexes like the exosome—a complex of exoribonucleases crucial for RNA metabolism.[8,22,23] The exosome is involved in the maturation and turnover of RNA,[8] RNA interference[24] and surveillance pathways that recognize and degrade aberrant RNAs.[22,25,26] Rrp44/Dis3, a RNase II-family member, is the only catalytically active nuclease in the yeast core exosome[27,28] (**Fig. 1**). We have recently discovered that Rrp44 includes a PINc domain that confers endonucleolytic activity to the enzyme.[29] Accordingly, this enzyme acts not only as

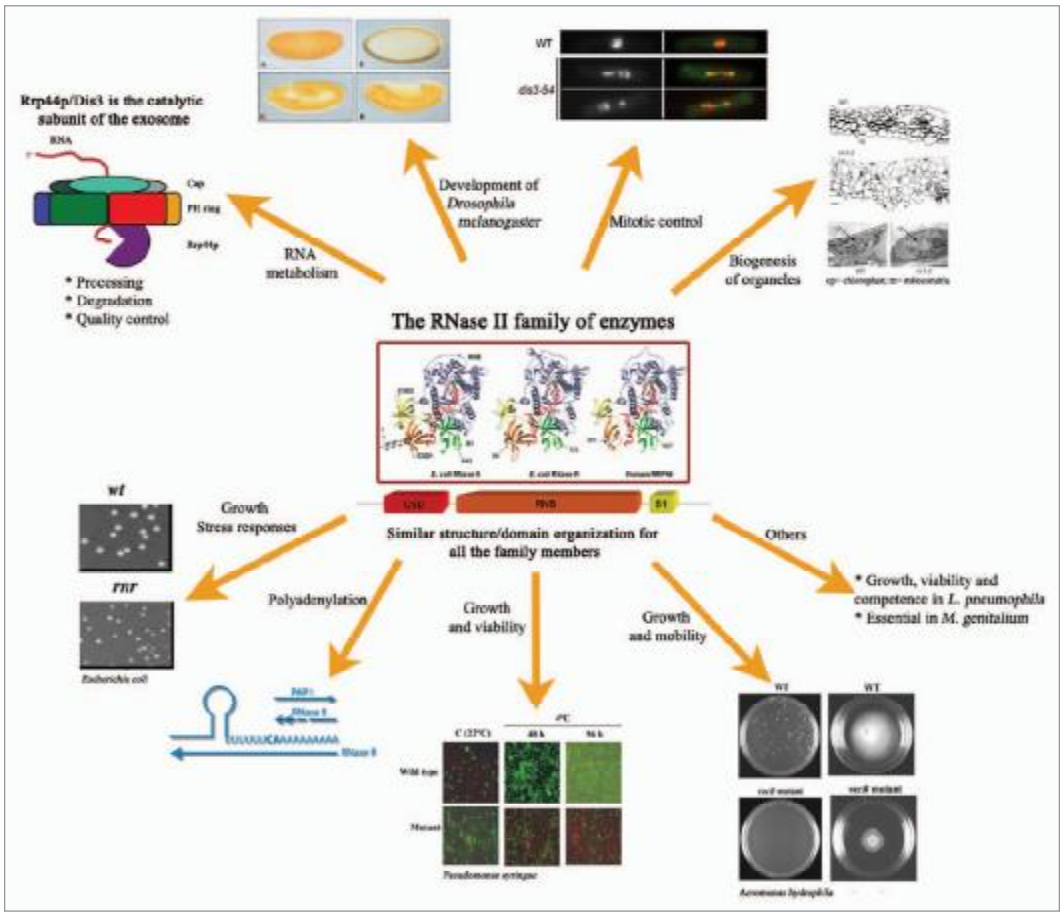

Figure 1. The multiple roles of RNase II-family of enzymes. RNase II-family of enzymes is ubiquitous, share the same modular organization and many of its members are crucial in RNA metabolism. In Eucaryotes, RNase II-like enzymes (Rrp44/Dis3) are the only catalytic subunit of the exosome, a crucial protein complex involved in processing, degradation and quality control (adapted from Schaeffer et al. 2009); Tazman is the RNase II *Drosophila melanogaster* homologue that is differentially expressed during development (adapted and reprinted from Cairrão et al. 2005 with permission of Wiley Interscience publishing); RNase II-like enzymes can also be involved in mitotic control (adapted and reprinted from Murakami et al. 2007 with permission of Public Library of Science) and in the biogenesis of chloroplasts (adapted and reprinted from Bollenbach et al. 2005 with permission of Oxford University Press). In Prokaryotes, RNase II and RNase R have been shown to be involved in Poly(A)-mediated RNA degradation mechanisms (adapted from Andrade et al. 2009); in *E. coli* RNase R is involved in growth and stress responses (Adapted and reprinted from Cairrão et al. 2003 with permission of Wiley Blackwell publishing), in growth and viability in *P. syringae* (this research was originally published in *The Journal of Biological Chemistry* by Purushart et al. 2007; 282:16267–77. © the American Society for Biochemistry and Molecular Biology), in growth and motility of *A. hydrophila* (adapted and reprinted from Erova et al. 2008 with the permission of the American Society for microbiology), in growth and competence of *L. pneumophila* (Charpentier et al. 2008).

an exonuclease but is also able to cleave the RNA internally.[29-31]

E. coli RNase II is the prototype of the RNase II-family of enzymes. This 72 KDa protein encoded by gene *rnb* is the major hydrolytic enzyme, responsible for 90% of the exoribonucleolytic activity in crude extracts.[32] RNase II activity is sequence independent but it is sensitive to secondary structures. RNase II expression is controlled at transcriptional and posttranscriptional levels,[31,32] and can also be regulated at the level of protein stability.[33] Also, the RNase II levels can change with different environmental conditions.[33]

Determination and Analysis of the RNase II Structure

We have determined the structure of *E. coli* RNase II and its RNA-bound complex.[34] This was a major breakthrough, since it was the first member of RNase II family whose structure was solved. Biochemical

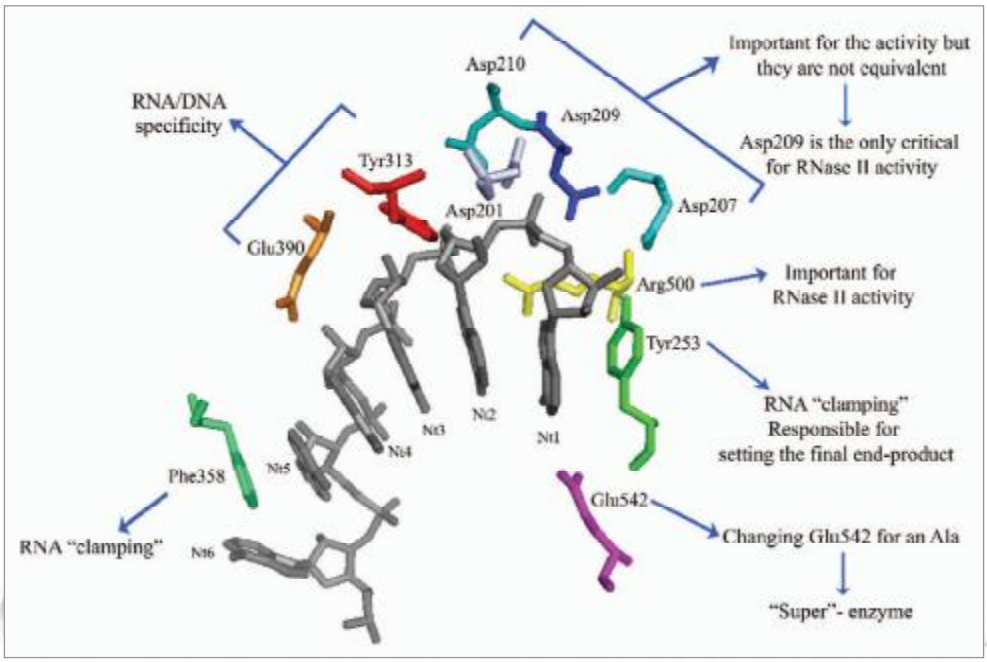

Figure 2. Zooming into the catalytic cavity of RNase II: critical residues in the mechanism of RNA degradation. The last five nucleotides of the 3'-end of the RNA molecule are stacked between the aromatic residues Tyr253 and Phe358. The conserved aspartates 201, 207, 209 and 210 and arginine 500 are located in the active site of RNase II. The last nucleotide establishes contacts with glutamate in position 542, while Tyr313 and Glu390 contact with nucleotides 2 and 4 being the responsible for the RNA/DNA specificity. Figure was constructed with Pymol© (DeLano Scientific LLC, San Carlos, CA) (PDB code 2IX0) (Frazão et al., 2006).

and structural analysis of RNase II led us to propose a 3D model explaining the dynamics of RNase II-mediated degradation. With these important structural features we could extrapolate to other members of this family.

RNase II has four domains: two N-terminal cold shock domains (CSD1 and CSD2) involved in RNA binding and recognition, one central RNB catalytic domain, and one C-terminal S1 domain, also responsible for the binding to the substrate.[34-36] The structural data, together with the biochemical analysis, gave new insights into the mechanisms of catalysis, translocation and processivity of this important RNA-degrading enzyme. Structural studies on eukaryotic enzymes have shown that *E. coli* RNase II is, in fact, a good model for the study of proteins of this family.[28,37-40]

The RNA contacts RNase II at two different and non-contiguous regions which act synergistically to provide a processive degradation: the anchoring region (formed by the three RNA binding domains) and the catalytic region (buried inside the catalytic domain).[34,41] The shortest RNA substrate able to retain contacts with these two regions is a 10-nucleotide fragment and in fact this is the minimum size necessary to maintain the processivity of the enzyme.[34,37,41] The catalytic region forms a cavity that is only accessible to single stranded RNA, where the last five nucleotides at the 3'-end of the RNA molecule are stacked and "clamped" between the aromatic residues Tyr-253 and Phe-358 (**Fig. 2**). It was postulated that the RNA degradation by RNase II involves one Mg^{2+} ion, four highly conserved aspartic acids (201, 207, 209 and 210), and the recruitment of a second Mg^{2+} for catalysis. The analysis of RNase II-RNA bound complex structure also allowed us to understand the RNA specificity of the enzyme.[34]

In order to determine the role of the residues involved in RNase II RNA degradation mechanism several mutants were constructed and analyzed regarding their exoribonucleolytic activity and RNA affinity. The results obtained substantially improved the model for RNA degradation, and can be applied to better understand the decay mechanisms for all RNase II family members that have revealed a similar mode of action, including those present in the exosome.

Aspartate Residues Present in the Active Site have Different Roles in Catalysis

As mentioned above, in the active site of RNase II there are four highly conserved aspartic acids in positions 201, 207, 209 and 210 (**Fig. 2**). It has been postulated that they are important to position the RNA molecule correctly and promote

the nucleophilic attack of the phosphodiester bond.[34,42] It was shown previously that the single substitution of Asp209 by Asn in RNase II (mutant D209N) is responsible for the total loss of RNase II activity without affecting RNA binding ability.[42] Similar mutations in RNase R from *E. coli* and *Legionella pneumophila* and in yeast Rrp44p also showed that this residue is important for the activity of the enzyme but not for the RNA binding.[27-29,43,44] To go further in the comprehension of the role of the other three aspartates, the residues were changed into asparagines. The results obtained showed that mutants D201N and D210N presented a significant loss of activity; one of the coordinations of the Mg^{2+} ion was abolished, thus destabilizing the cation at the active site and impairing the reaction.[37] The role of Asp-207 does not seem to be so critical for catalysis when compared with the other mutants, since with this alteration the protein retains 12% of its activity.[37] After modulating the wild-type protein, it was possible to see that the Asp207 residue is displaced to a far position from the Mg^{2+} ion when compared to the other aspartates, which explains the fact that this residue is not so critical for the activity of the enzyme.[37] When the RNA binding was analyzed, the values were not so different from those of the wild-type enzyme, suggesting that the aspartates are not directly involved in the RNA binding.[37]

The modeling of *E. coli* RNase R and human Rrp44 proteins revealed that the four aspartic residues have spatial positions equivalent to those in RNase II.[37] Therefore, similar catalytic roles for these residues can be proposed for other RNase II-like enzymes.

Arg500 is Important for RNase II Activity but not for RNA Binding Ability

In the active site of RNase II there is another highly conserved residue, Arg500 (**Fig. 2**). This residue was postulated to assist in catalysis by fixing the phosphodiester bond at the cleavage position and enhancing the susceptibility of the leaving phosphorous atom to a nucleophilic attack.[34] In fact, Arg500 is very important for the activity of the enzyme, since its substitution by an alanine practically lead to the inactivation of the enzyme, although it was still able to bind to RNA efficiently.[45] These results support the essential role of Arg500 in assisting catalysis.

Tyr253 is Responsible for Setting the Final End-Product

In the active site of RNase II, the final five nucleotides from the 3'-end are stacked and "clamped" between the aromatic residues Tyr253 and Phe358,[34] (**Fig. 2**). The role of these residues in RNA degradation was also determined by mutating them into alanines. Based on the crystal structure of the protein, it would be expected that RNase II loses its activity if the RNA "clamping" is perturbed. However, the presence of an alanine in position 253 only reduced the activity of the protein in ~4-fold.[37] Tyr253 is very important for the maintenance of the RNA "clamping", since that it remains firmly stacked to the outgoing nucleotide. In its absence, there must be other residues located in close vicinity to Tyr253 that can contact with the RNA molecule allowing cleavage to occur. But the most surprising result was that the final product released by the mutant protein Y253A was a 10 nt fragment instead of the usual 4 nts.[37] The 3D model of RNase II revealed that 10 nt is the minimum length necessary to the RNA molecule to be able to contact with both the anchoring and the catalytic regions.[34] When the RNA is shorter than that, it will only establish interactions with the catalytic region, and RNase II becomes distributive. The absence of Tyr253 in the mutant Y253A may cause the loosening of the substrate in the catalytic region, suggesting that the binding to the anchoring region is essential to retain the RNA molecule attached to the protein. For this reason, this mutant is only able to degrade RNA fragments until they reach 10 nts of length. Tyr253 residue is also very important for the binding at the 3'-end of the RNA substrate, as showed by the RNA affinity of this mutant that is ~6-fold higher when compared to the wild type.[37] A similar result was obtained when the equivalent residue was changed in *E. coli* RNase R.[44]

When the other residue responsible for the RNA "clamping", Phe358, was mutated into an alanine, the mutant protein was unexpectedly 2-fold more active than wild type enzyme. It was also possible to observe, together with the usual 4 nts product, a 5 nts fragment. This result suggested that Phe358 may function as a "propeller" by helping to push the last nucleotide towards the catalytic site.[37]

These results clearly indicate that Tyr253 and Phe358 have different functions in RNA degradation mechanism: Tyr253 is the one responsible for setting the final end-product, mediating stabilization of the outgoing nucleotide at the 3'-end during catalysis, while Phe358 plays a more accessory role in the maintenance of the proper RNA conformation.[37]

The Making of a "Super"-Enzyme

In RNase II, Glu542 is in close proximity to the leaving nucleotide (**Fig. 2**). It was postulated that this residue was responsible for the nucleotide elimination after the cleavage event, thus allowing the degradation process to continue.[34] In order to confirm the role of this residue in the degradation mechanism, it was changed into an alanine. Surprisingly, this alteration in RNase II rendered a protein that was 110-fold more active when compared to the wild type and the E542A protein can bind RNA more tightly than the wild-type enzyme.[45] Moreover, the kinetic data suggests that this mutant not only has a much higher affinity for the poly(A) RNA substrate but also presents a much higher catalytic rate, confirming its role in the catalytic event.[45] The computational model for this mutant showed that there are subtle conformational changes in the RNB domain itself that are responsible for a reorganization of the RNA binding interface. This allows the mutant enzyme to have more RNA bases in a stable stacked conformation, which explains the increased ability to bind to RNA. This also can be favoring the RNA translocation after the cleavage event leading to higher degradation efficiency.[45]

The consequences of having a recombinant RNase II with an outstanding

catalytic efficiency will be evaluated by in vivo RNA degradation studies. Furthermore, we also need to consider its potential for several biotechnological applications.

Why RNase II is Specific for RNA

It was previously described that the presence of a ribose between positions 2 through 5 from the 3'-end of the RNA substrate is required for cleavage to occur.[41] In the RNase II crystal structure, the residues Tyr313 and Asp201 are interacting with the O2' ribose oxygen of the second ribose and Glu390 with the O2' ribose oxygen of the fourth ribose[34] (**Fig. 2**). By mutational analysis we have recently shown that RNase II has a strict requirement for a ribose in the second and/or the fourth nucleotides from the 3'-end of the molecule and not in other positions.[45] Moreover, these contacts are necessary and sufficient for cleavage to occur, and therefore, they seem to be responsible for the RNA specificity versus DNA in RNase II.[45]

RNA-Binding Domains Select the RNAs Targeted for Degradation

All the members of RNase II family share a similar domain organization, with the presence of CSD, S1 and RNB domains (**Fig. 1**), with the first two involved in RNA binding and the RNB in the catalytic activity.[36,44,46] Recently, it was shown that the RNA-binding domains are the ones responsible for the selection of which RNA should be degraded in the cell, picking just the ones that are tagged with a tail. RNase R, the other member of this family in *E. coli*, is able to degrade double stranded substrates only when there is an overhang of seven or more nucleotides. In the absence of the RNA-binding domains, RNase R is able to degrade the double stranded substrates without the need of a tail.[44]

Final Remarks

Since Rrp44p/Dis3 is the only catalytically active nuclease in the exosome,[27] understanding the degradation mechanism of this RNase II homolog will have a large impact in future studies of the exosome. Moreover, it has been shown that the yeast and human exosomes have the same minimum length of RNA substrate and the same final end-product as *E. coli* RNase II.[22,36,47] The EM reconstruction[38] and crystal structure[39] of yeast Dis3/Rrp44 showed that *E. coli* RNase II is a good study model, since the atomic models of *E. coli* RNase II could be easily fitted into the body region of Dis3/Rrp44. Also, yeast Rrp44/Dis3 has a similar linear arrangement of domains in the sequence when compared to *E. coli* RNase II. Both proteins share a high degree of identity being their conservation the highest at the active site. This suggests that these two exoribonucleases share a similar hydrolytic mechanism.[29] As such, the results obtained on *E. coli* RNase II mutants can therefore be extrapolated for the comprehension of the mode of action of other members of the RNase II family.

However, when we think we are obtaining significant insights into the modus operandi of these "molecular killers", this family is still full of surprises. The latest breakthrough was the finding that eukaryotic RNase II-like enzymes have an extra domain that enables them to also act as an endonuclease.[29-31] Like a Swiss army knife, new tools are being added to optimize the performance of this degrading machine. More and more we need to "zoom" into the detail of RNase II ribonucleolytic activity, but it looks like many surprises are yet to come.

References

1. Nicholson AW. Function, mechanism and regulation of bacterial ribonucleases. FEMS Microbiol Rev 1999; 23:1-5.
2. Régnier P, Arraiano CM. Degradation of mRNA in bacteria: emergence of ubiquitous features. Bioessays 2000; 22:235-44.
3. Arraiano CM, Maquat LE. Post-transcriptional control of gene expression: effectors of mRNA decay. Mol Microbiol 2003; 49:267-76.
4. Parker R, Song H. The enzymes and control of eukaryotic mRNA turnover. Nat Struct Mol Biol 2004; 11:121-7.
5. Andrade JM, Pobre V, Silva IJ, Domingues S, Arraiano CM. The role of 3'-5' exoribonucleases in RNA degradation. Prog Mol Biol Transl Sci 2009; 85:187-229.
6. Deutscher MP. Promiscuous exoribonucleases of *Escherichia coli*. J Bacteriol 1993; 175:4577-83.
7. Zuo Y, Deutscher MP. Exoribonuclease superfamilies: structural analysis and phylogenetic distribution. Nucleic acids research 2001; 29:1017-26.
8. Mitchell P, Petfalski E, Shevchenko A, Mann M, Tollervey D. The exosome: a conserved eukaryotic RNA processing complex containing multiple 3'→5' exoribonucleases. Cell 1997; 91:457-66.
9. Grossman D, van Hoof A. RNase II structure completes group portrait of 3' exoribonucleases. Nat Struct Mol Biol 2006; 13:760-1.
10. Mian IS. Comparative sequence analysis of ribonucleases HII III, II PH and D. Nucleic Acids Res 1997; 25:3187-95.
11. Cairrao F, Arraiano C, Newbury S. Drosophila gene tazman, an orthologue of the yeast exosome component Rrp44p/Dis3, is differentially expressed during development. Dev Dyn 2005; 232:733-7.
12. Bollenbach TJ, Lange H, Gutierrez R, Erhardt M, Stern DB, Gagliardi D. RNR1, a 3'-5' exoribonuclease belonging to the RNR superfamily, catalyzes 3' maturation of chloroplast ribosomal RNAs in *Arabidopsis thaliana*. Nucleic Acids Res 2005; 33:2751-63.
13. Lim J, Kuroki T, Ozaki K, Kohsaki H, Yamori T, Tsuruo T, et al. Isolation of murine and human homologues of the fission-yeast dis3$^+$ gene encoding a mitotic-control protein and its overexpression in cancer cells with progressive phenotype. Cancer Res 1997; 57:921-5.
14. Cheng ZF, Zuo Y, Li Z, Rudd KE, Deutscher MP. The vacB gene required for virulence in *Shigella flexneri* and *Escherichia coli* encodes the exoribonuclease RNase R. J Biol Chem 1998; 273:14077-80.
15. Cheng ZF, Deutscher MP. An important role for RNase R in mRNA decay. Molecular Cell 2005; 17:313-8.
16. Cairrão F, Arraiano CM. The role of endoribonucleases in the regulation of RNase R. Biochem Biophys Res Commun 2006; 343:731-7.
17. Cairrão F, Cruz A, Mori H, Arraiano CM. Cold shock induction of RNase R and its role in the maturation of the quality control mediator SsrA/tmRNA. Mol Microbiol 2003; 50:1349-60.
18. Andrade JM, Cairrão F, Arraiano CM. RNase R affects gene expression in stationary phase: regulation of ompA. Mol Microbiol 2006; 60:219-28.
19. Cheng ZF, Deutscher MP. Quality control of ribosomal RNA mediated by polynucleotide phosphorylase and RNase R. Proc Natl Acad Sci USA 2003; 100:6388-93.
20. Erova TE, Kosykh VG, Fadl AA, Sha J, Horneman AJ, Chopra AK. Cold shock exoribonuclease R (VacB) is involved in *Aeromonas hydrophila* pathogenesis. J Bacteriol 2008; 190:3467-74.
21. Andrade JM, Hajnsdorf E, Regnier P, Arraiano CM. The poly(A)-dependent degradation pathway of rpsO mRNA is primarily mediated by RNase R. RNA (New York, NY) 2009.
22. LaCava J, Houseley J, Saveanu C, Petfalski E, Thompson E, Jacquier A, Tollervey D. RNA degradation by the exosome is promoted by a nuclear polyadenylation complex. Cell 2005; 121:713-24.
23. Houseley J, Tollervey D. The many pathways of RNA degradation. Cell 2009; 136:763-76.
24. Orban TI, Izaurralde E. Decay of mRNAs targeted by RISC requires XRN1, the Ski complex, and the exosome. RNA 2005; 11:459-69.
25. Lejeune F, Li X, Maquat LE. Nonsense-mediated mRNA decay in mammalian cells involves decapping, deadenylating and exonucleolytic activities. Molecular Cell 2003; 12:675-87.
26. van Hoof A, Frischmeyer PA, Dietz HC, Parker R. Exosome-mediated recognition and degradation of mRNAs lacking a termination codon. Science 2002; 295:2262-4.
27. Dziembowski A, Lorentzen E, Conti E, Seraphin B. A single subunit, Dis3, is essentially responsible for yeast exosome core activity. Nat Struct Mol Biol 2007; 14:15-22.
28. Schneider C, Anderson JT, Tollervey D. The exosome subunit Rrp44 plays a direct role in RNA substrate recognition. Molecular Cell 2007; 27:324-31.

29. Schaeffer D, Tsanova B, Barbas A, Reis FP, Dastidar EG, Sanchez-Rotunno M, et al. The exosome contains domains with specific endoribonuclease, exoribonuclease and cytoplasmic mRNA decay activities. Nat Struct Mol Biol 2009; 16:56-62.
30. Lebreton A, Tomecki R, Dziembowski A, Seraphin B. Endonucleolytic RNA cleavage by a eukaryotic exosome. Nature 2008; 456:993-6.
31. Schneider C, Leung E, Brown J, Tollervey D. The N-terminal PIN domain of the exosome subunit Rrp44 harbors endonuclease activity and tethers Rrp44 to the yeast core exosome. Nucleic Acids Res 2009; 37:1127-40.
32. Deutscher MP, Reuven NB. Enzymatic basis for hydrolytic versus phosphorolytic mRNA degradation in *Escherichia coli* and *Bacillus subtilis*. Proc Natl Acad Sci USA 1991; 88:3277-80.
33. Cairrão F, Chora A, Zilhao R, Carpousis AJ, Arraiano CM. RNase II levels change according to the growth conditions: characterization of gmr, a new *Escherichia coli* gene involved in the modulation of RNase II. Mol Microbiol 2001; 39:1550-61.
34. Frazão C, McVey CE, Amblar M, Barbas A, Vonrhein C, Arraiano CM, Carrondo MA. Unravelling the dynamics of RNA degradation by ribonuclease II and its RNA-bound complex. Nature 2006; 443:110-4.
35. Zuo Y, Vincent HA, Zhang J, Wang Y, Deutscher MP, Malhotra A. Structural basis for processivity and single-strand specificity of RNase II. Molecular Cell 2006; 24:149-56.
36. Amblar M, Barbas A, Fialho AM, Arraiano CM. Characterization of the functional domains of *Escherichia coli* RNase II. J Mol Biol 2006; 360:921-33.
37. Barbas A, Matos RG, Amblar M, Lopez-Viñas E, Gomez-Puertas P, Arraiano CM. New insights into the mechanism of RNA degradation by ribonuclease II: identification of the residue responsible for setting the RNase II end product. J Biol Chem 2008; 283:13070-6.
38. Wang HW, Wang J, Ding F, Callahan K, Bratkowski MA, Butler JS, et al. Architecture of the yeast Rrp44 exosome complex suggests routes of RNA recruitment for 3' end processing. Proc Natl Acad Sci USA 2007; 104:16844-9.
39. Bonneau F, Basquin J, Ebert J, Lorentzen E, Conti E. The yeast exosome functions as a macromolecular cage to channel RNA substrates for degradation. Cell 2009; 139:547-59.
40. Domingues S, Matos RG, Reis FP, Fialho AM, Barbas A, Arraiano CM. Biochemical characterization of the RNase II family of exoribonucleases from the human pathogens *Salmonella typhimurium* and *Streptococcus pneumoniae*. Biochemistry 2009; 48:11848-57.
41. Cannistraro VJ, Kennell D. The processive reaction mechanism of ribonuclease II. J Mol Biol 1994; 243:930-43.
42. Amblar M, Arraiano CM. A single mutation in *Escherichia coli* ribonuclease II inactivates the enzyme without affecting RNA binding. FEBS J 2005; 272:363-74.
43. Charpentier X, Faucher SP, Kalachikov S, Shuman HA. Loss of RNase R induces competence development in *Legionella pneumophila*. J Bacteriol 2008; 190:8126-36.
44. Matos RG, Barbas A, Arraiano CM. RNase R mutants elucidate the catalysis of structured RNA: RNA-binding domains select the RNAs targeted for degradation. Biochem J 2009; 423:291-301.
45. Barbas A, Matos RG, Amblar M, Lopez-Vinas E, Gomez-Puertas P, Arraiano CM. Determination of Key Residues for Catalysis and RNA Cleavage Specificity: one mutation turns RNase II into a "super-enzyme". J Biol Chem 2009; 284:20486-98.
46. Vincent HA, Deutscher MP. The Roles of Individual Domains of RNase R in Substrate Binding and Exoribonuclease Activity: The nuclease domain is sufficient for digestion of structured RNA. J Biol Chem 2009; 284:486-94.
47. Liu Q, Greimann JC, Lima CD. Reconstitution, activities and structure of the eukaryotic RNA exosome. Cell 2006; 127:1223-37.

11848 *Biochemistry* **2009,** *48,* 11848–11857
DOI: 10.1021/bi901105n

BIOCHEMISTRY
including biophysical chemistry & molecular biology
Article

Biochemical Characterization of the RNase II Family of Exoribonucleases from the Human Pathogens *Salmonella typhimurium* and *Streptococcus pneumoniae*[†]

Susana Domingues,[‡] Rute G. Matos,[‡] Filipa P. Reis,[‡] Arsénio M. Fialho,[§] Ana Barbas,[‡] and Cecília M. Arraiano*[,‡]

[‡]*Instituto de Tecnologia Química e Biológica/Universidade Nova de Lisboa, Apartado 127, 2781-901 Oeiras, Portugal, and* [§]*Institute for Biotechnology and Bioengineering Centre for Biological and Chemical Engineering/Instituto Superior Técnico, Lisboa, Portugal*

Received June 30, 2009; Revised Manuscript Received October 2, 2009

ABSTRACT: Maturation, turnover, and quality control of RNA are performed by many different classes of ribonucleases. *Escherichia coli* RNase II is the prototype of the RNase II family of ribonucleases, a ubiquitous family of hydrolytic, processive 3′ → 5′ exonucleases crucial in RNA metabolism. RNase R is a member of this family that is modulated in response to stress and has been implicated in virulence. In this work, RNase II-like proteins were characterized in the human pathogens *Salmonella typhimurium* and *Streptococcus pneumoniae*. By sequence analysis, only one member of the RNase II family was identified in *S. pneumoniae*, while both RNase II and RNase R were found in *Sa. typhimurium*. These enzymes were cloned, expressed, purified, and characterized with regard to their biochemical features and modular architecture. The specificity of substrates and the final products generated by the enzymes were clearly demonstrated. *Sa. typhimurium* RNase II and RNase R behaved essentially as their respective *E. coli* counterparts. We have shown that the only hydrolytic RNase found in *S. pneumoniae* was able to degrade structured RNAs as is the case with *E. coli* RNase R. Our results further showed that there are differences with regard to the activity and ability to bind RNA from enzymes belonging to two distinct pneumococcal strains, and this may be related to a single amino acid substitution in the catalytic domain. Since ribonucleases have not been previously characterized in *S. pneumoniae* or *Sa. typhimurium*, this work provides an important first step in the understanding of post-transcriptional control in these pathogens.

RNA metabolism plays an essential role in the control of gene expression, and several distinct ribonucleases are involved in the degradation, processing, turnover, and quality control of RNA. *Escherichia coli* RNase II and RNase R are representatives of the RNase II family of exoribonucleases, a widespread class of enzymes that have a key function in RNA metabolism and are present in prokaryotes and eukaryotes (*1*−*3*). *E. coli* RNase II and RNase R exhibit similar catalytic and structural properties: they both degrade RNA hydrolytically in the 3′ → 5′ direction in a processive and sequence-independent manner. However, while RNase R is capable of degrading highly structured RNA, the RNase II activity is impaired by the presence of secondary structures (reviewed in ref *3*).

E. coli RNase II, a monomer of approximately 73 kDa encoded by the *rnb* gene, is the prototype of this family. In this bacterium, RNase II is the major hydrolytic enzyme (*4*). However, because of its strong affinity for the homopolymer poly(A), it can rapidly degrade some polyadenylated stretches necessary for degradation by other exoribonucleases, and paradoxically, it can act as a protector of full-length RNAs (*5*, *6*). The enzyme is tightly regulated at the transcriptional and post-transcriptional levels, and its amount changes with growth conditions (*7*, *8*). Determination of the 3D[1] structure of *E. coli* RNase II showed that RNase II consists of four domains: two N-terminal cold shock domains (CSD1 and CSD2), one central RNB catalytic domain, and one C-terminal S1 domain (*9*, *10*) (Figure 1). The biochemical and structural data allowed an understanding of the RNA degradation mechanism of this family of enzymes (*9*).

RNase R is an ∼92 kDa protein encoded by the *rnr* gene and shares an identical domain organization and three-dimensional arrangement with RNase II (*11*). RNase R was initially described as a secondary exoribonuclease only responsible for the residual hydrolytic activity in *E. coli*. However, orthologues of RNase R are found in most bacteria, and recent studies have demonstrated that, in fact, this enzyme is implicated in the processing and degradation of different types of RNA, such as tRNA, rRNA, mRNA, and small RNAs (sRNA) (*12*−*14*). RNase R is also involved in RNA quality control, being responsible for the degradation of defective tRNA as well as the elimination of aberrant rRNA (*14*−*16*). The ability of RNase R to act on highly structured RNA molecules, like the small RNAs, leads to important physiological consequences. It has been reported that the correct maturation of *tm*RNA, a small RNA involved in the quality control of proteins, requires the action of this protein (*13*). All these features indicate a more specific role of RNase R in RNA metabolism. Moreover, RNase R has been shown to be

[†]S.D. and A.B. were recipients of postdoctoral fellowships and R.G. M. and F.P.R. recipients of Ph.D. fellowships, all of them funded by FCT-Fundação para a Ciência e a Tecnologia, Portugal. The work at the ITQB was supported by FCT.

*To whom correspondence should be addressed: Instituto de Tecnologia Química e Biológica/Universidade Nova de Lisboa, Apartado 127, 2781-901 Oeiras, Portugal. Phone: +351 214469547. Fax: +351 214411277. E-mail: cecilia@itqb.unl.pt.

[1]Abbreviations: CSD, cold shock domain; RNB, RNase II catalytic domain; Amp, ampicillin; Tet, tetracycline; LB, Luria Broth; IPTG, isopropyl β-D-thiogalactoside; DTT, dithiothreitol; PMSF, phenylmethanesulfonyl fluoride, EDTA, ethylenediaminetetraacetic acid; NCBI, National Center for Biotechnology Information; HTH, helix−turn−helix; 3D, three-dimensional.

 Published on Web 10/28/2009

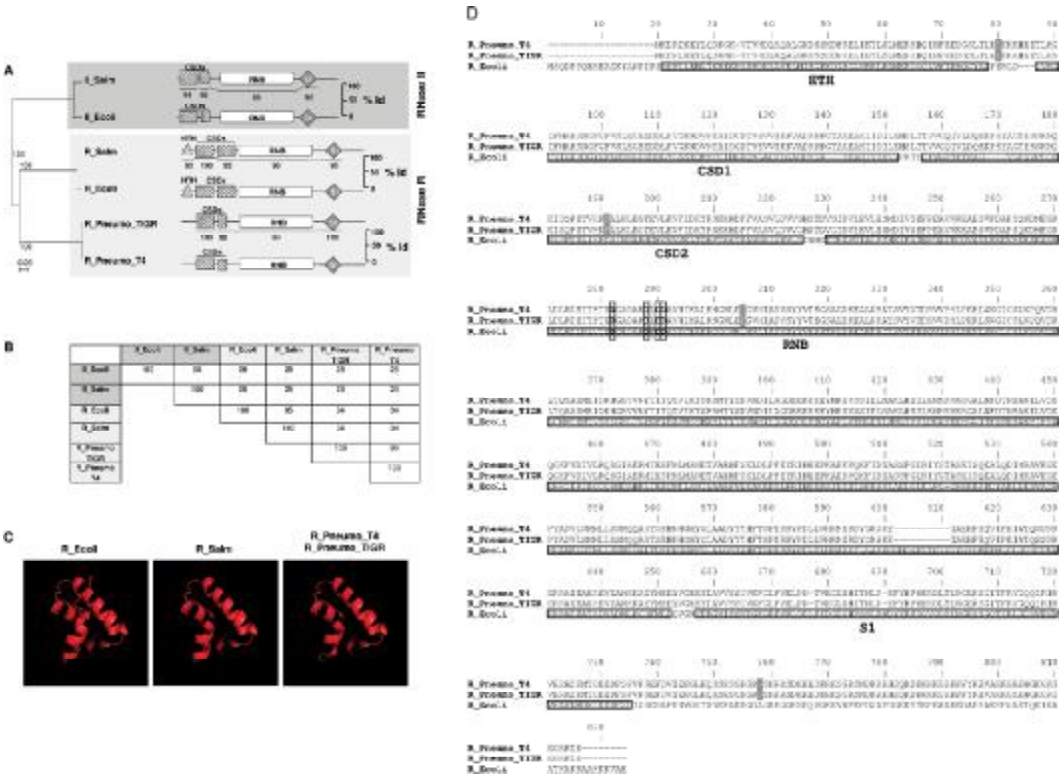

FIGURE 1: Bioinformatic analysis of proteins from the RNase II family. (A) Phylogenetic tree of the six hydrolytic enzymes, organized in two distinct groups. One group includes RNase II-like proteins (II_Ecoli and II_Salm) and the other group RNase R-like proteins (R_Ecoli R_Salm, R_Pneumo_TIGR, and R_Pneumo_T4). The values adjacent to a node indicate the percentage of 500 bootstrap trees that contain the node. The RNase R group has two branches differentiating *Salmonella typhimurium* and *E. coli* RNase R from those of *Streptococcus pneumoniae*. A schematic representation of the modular architecture of each protein produced using Pfam is shown. All the enzymes present two cold shock domains (CSD) at the N-terminus, S1 at the carboxy end and the RNB catalytic domain spanning the middle region of the proteins. An additional helix−turn−helix (HTH) motif was found in the N-terminal end of R_Ecoli and R-Salm. The amino acid identity between the domains of the enzymes of each group is also indicated. (B) Total amino acid identity among the six members of the RNase II family of exoribonucleases being studied. (C) Homology-based 3D models of the N-terminal spanning residues of the RNase R-like enzymes: R_Ecoli (amino acids 18−78), R_salm (amino acids 23−78), and R_Pneumo_T4 and R_Pneumo_TIGR (amino acids 4−58). Because of the perfect homology between R_Pneumo_T4 and R_Pneumo_TIGR in this region, only one model is shown. (D) Sequence alignment of R_Pneumo_T4, R_Pneumo_TIGR, and R_Ecoli. The alignment was prepared with ClustalW (*38*). The domains identified in R_Ecoli (HTH, CSD1, CSD2, RNB, and S1) are denoted. The four different amino acids between R_Pneumo_T4 and R_Pneumo_TIGR are highlighted in gray. The aspartate residues proposed to compose the active site are boxed (*11*).

modulated in response to different stress conditions (*12*, *13*, *17*−*21*). Previous studies have shown that RNase R is a cold shock protein, and other stress conditions were also able to induce RNase R (*13*). RNase R protein levels were shown to increase in the stationary phase (*7*, *12*, *22*).

Since the infection process exposes pathogens to numerous stress conditions (e.g., temperature shifts, pH changes, and nutritional deprivation), adaptation of bacteria to stress is a crucial step in the virulence process. Not surprisingly, RNase R has been involved in the modulation of the expression of virulence in a number of pathogenic organisms such as *Aeromonas hydrophyla*, *Shigella flexneri*, *Burkholderia* spp., and *Helicobacter pylori* (*20*, *23*−*25*). In *Legionella pneumophila*, an opportunistic pathogen of human macrophages that can cause a severe and mortal disease, RNase R is the only hydrolytic exoribonuclease, and its loss has a significant impact in *L. pneumophila* growth and viability at low temperatures (*18*). In *Mycoplasma genitalium*, a human pathogen linked to urethritis and other sexually transmitted diseases, RNase R has been the only exoribonuclease identified, being an essential enzyme in this organism (*26*−*28*).

Streptococcus pneumoniae is a human pathogen that is the major cause of pneumonia, septicemia, meningitis, and otitis. It is also one of the principal causes of septicemia in HIV-infected individuals. Collectively, these diseases result in millions of deaths worldwide each year. The currently available vaccine is only partially effective, and multiple drug-resistant strains of this pathogen have emerged in recent years (*29*). For this reason, great effort to understand the mechanisms of pathogenesis is being spent to identify new targets for vaccines and novel drugs.

Salmonella infections are a serious medical and veterinary problem worldwide. Meat and eggs contaminated with *Salmonella enterica* sv. *typhimurium* (*Salmonella typhimurium*) are common fonts of acute gastroenteritis in humans (*15*). Salmonellosis constitutes a health problem, especially for fecal

contamination of water resources, and new strategies for prevention and control are necessary. The understanding of *Salmonella* cellular control mechanisms may lead to identification of novel targets for therapeutic intervention.

Since it has been shown that exoribonucleases are involved in virulence and practically nothing is known about RNases in *S. pneumoniae* or *Sa. typhimurium*, the characterization of the biochemical properties of the exoribonucleases in these organisms may be useful for further understanding the virulence mechanisms. To achieve this purpose, we performed a search of the available genomic sequences of *Sa. typhimurium* and *S. pneumoniae*. Two homologues of the RNase II family of proteins were indentified in *Sa. typhimurium*, while only one member of this family was found in *S. pneumoniae* (Figure 1). Both hydrolytic enzymes from *Sa. typhimurium* and the RNase R-like enzyme from two different *S. pneumoniae* strains were cloned, overexpressed, purified, and characterized with regard to their RNA binding ability and exonucleolytic activity. The results clearly show the specificity of substrates and the end products generated by each enzyme. In agreement with the in silico analysis, *Sa. typhimurium* contains both hydrolytic enzymes, RNase II and RNase R, while the only enzyme present in *S. pneumoniae* behaves like RNase R. Interestingly, *Sa. typhimurium* RNase II can approach the double-stranded region more closely than the *E. coli* homologue. Besides RNase R, *S. pneumoniae* also contains a PNPase-like exoribonuclease. To the best of our knowledge, this is the first time that an RNase R from a Gram-positive bacterium with this genetic background has been studied. Our results further show that a single amino acid substitution may be responsible for the different biochemical properties exhibited by the two pneumococcal RNase R-like proteins studied.

EXPERIMENTAL PROCEDURES

Materials. Restriction enzymes, T4 DNA ligase, and T4 polynucleotide kinase were purchased from New England Biolabs, and Pfu DNA polymerase was from Fermentas. Unlabeled oligonucleotide primers were synthesized by STAB Vida. The sequence of the *rnr* gene from *S. pneumoniae* strain T4, a derivative of *S. pneumoniae* R6 (*30*), was determined on double-stranded DNA using the appropriate primers. This sequence was deposited in GenBank (accession number FJ999997). The sequence of the *rnr* gene from *S. pneumoniae* TIGR4 was confirmed on double-stranded DNA with the appropriate primers.

Bacterial Strains and Growth Conditions. The following *E. coli* strains were used: DH5α [fhuA2 Δ(argF-lacZ)U169 phoA glnV44 Φ80 Δ(lacZ)M15 gyrA96 recA1 relA1 endA1 thi-1 hsdR17 (*31*)] and NovaBlue (endA1 hsdR17 supE44 thi-1 recA1 gyrA86 relA1 lac [F′ $proA^+B^+$ $lacI^q$ lacZΔM15::Tn10]) (Novagene) for cloning experiments and BL21(DE3) [F^- r_B^- m_B^- gal ompT (int::P_{lacUV5} T7 gen1 imm21 nin5) (*32*)] for expression of the enzymes. *E. coli* BL21(DE3) strains expressing *E. coli* RNase II and *E. coli* RNase R have been previously described (*33*, *34*).

E. coli was cultivated in Luria Broth (LB) medium at 37 °C, except when specified differently. When required, this medium was supplemented with 200 μg/mL ampicillin (Amp), 15 μg/mL tetracycline (Tet), and 0.4% glucose.

Construction of Recombinant Proteins. All genes encoding the proteins in this study were cloned into the pET-15b vector (Novagen) under the control of the φ10 T7 promoter, allowing the expression of His_6-tagged fusion proteins. The primers used for the construction of the recombinant proteins are listed in Table 1. *Pfu* DNA polymerase (Fermentas) was used in PCRs (polymerase chain reactions). *Sa. typhimurium* SL1344 *rnr* (also known as *vacB*) and *rnb* genes were amplified from genomic DNA supplied by S. Viegas (*35*) using primers smd007/smd008 and smd005/smd006, respectively. The genes encoding the hydrolytic RNase from *S. pneumoniae* T4 and TIGR4 strains were amplified from genomic DNA kindly supplied by P. Lopez (CIB-CSIC, Madrid, Spain) using primers rnrNde and rnrBam. The amplified fragments were cloned into the NdeI/BamHI site of pET-15b except the *rnb* PCR product, which was cloned into the EcoRI/XhoI site of the same plasmid. *Sa. typhimurium* genes were first cloned into *E. coli* DH5α, while the plasmid containing the *rnr* genes derived from *S. pneumoniae* was transformed into *E. coli* Novablue and selected in LB medium supplemented with Tet and glucose, besides Amp. The plasmids were subsequently transformed into *E. coli* strain BL21(DE3) (Novagen) to allow the expression of the recombinant proteins. As a negative control used in all the following experiments, pET-15b (without insert) was also transformed into BL21(DE3). All constructs were confirmed by DNA sequencing at STAB Vida (Oeiras, Portugal).

Table 1: Primer Sequences Used in This Study[a]

primer	sequence (5′−3′)
smd005	ggaattccatATGTTTCAGGACAACCCGC
smd006	cgcggatccGTGGTTACGCTGCCGGTCGG
smd007	ggaatctcgagATGTCACAAGATCCTTTCC
smd008	ccggaattcGCTCACTCTGCCGCTTTTTTC
rnrNde	ggaattccatATGAAAGATAGAATAAAAGAATATTTAC
rnrBam	cgcggatccTACGATTGTATAGTCGTGGCGTGCC

[a]Lowercase letters indicate restriction sites.

Overexpression and Purification of RNase II-like Proteins. Recombinant proteins were expressed and purified following the strategy previously described for the purification of *E. coli* RNase II and RNase R (*33*, *34*, *36*). Briefly, *E. coli* BL21(DE3) containing the recombinant plasmid of interest was grown at 37 °C in 200 mL of LB medium supplemented with 200 μg/mL Amp to an optical density at 600 nm (OD_{600}) of ≈0.5. Protein expression was then induced by addition of 1 mM IPTG for 3 h at 37 °C. Cells were harvested by centrifugation and stored at −80 °C.

Purification of all proteins was performed by histidine affinity chromatography using HisTrap Chelating HP columns (GE Healthcare) and an AKTA HPLC system (GE Healthcare) following the protocol previously described (*33*, *36*). Briefly, frozen cells were thawed and resuspended on 6 mL of buffer A [20 mM Tris-HCl, 0.5 M NaCl, 1 mM DTT, and 5 mM imidazole (pH 8)]. Cell suspensions were lysed using a French press at 9000 psi in the presence of 0.1 mM PMSF. The crude extracts were treated with Benzonase (Sigma) to degrade the nucleic acids and clarified by a 30 min centrifugation at 10000*g*. The clarified extracts were then loaded into a HisTrap Chelating Sepharose 1 mL column equilibrated in buffer A. Protein elution was achieved with a continuous imidazole gradient (from 20 to 500 mM) in buffer A.

Eluted protein was buffer exchanged with buffer C [20 mM Tris-HCl, 250 mM NaCl, and 1 mM DTT (pH 8)] and concentrated by centrifugation at 4 °C with Amicon Ultra Centrifugal

Filter Devices (Millipore) with a molecular mass cutoff of 50 kDa. Protein concentrations were determined by spectrophotometry using a NanoDrop 1000 instrument (Alfagene), and 50% (v/v) glycerol was added to the final fractions prior to storage at −20 °C. The purity of the enzymes was analyzed by sodium dodecyl sulfate−polyacrylamide gel electrophoresis (SDS−PAGE) and revealed ~90% homogeneity (supplementary data).

The strategy described above was followed for the control strain [*E. coli* BL21(DE3) containing pET-15b without an insert]. The obtained protein extract was used as a negative control in all the experiments performed with the recombinant proteins.

Western Immunoblotting. His-tagged recombinant proteins were analyzed by Western immunoblotting. For this purpose, purified proteins were separated by SDS−PAGE and transferred to a nitrocellulose membrane (Hybond ECL, GE Healthcare) by electroblotting using the Trans-Blot SD semidry electrophoretic system (Bio-Rad). Membranes were probed with a 1:3000 dilution of anti-His antibodies (GE Healthcare). ECL anti-mouse IgG-conjugated horseradish peroxidase (from sheep) was used as the secondary reagent in a 1:5000 dilution. Immunodetection was conducted via a chemiluminescence reaction using Amersham ECL Western Blotting Detection Reagents (GE Healthcare).

Activity Assays. Exoribonucleolytic activity was assayed using oligoribonucleotides as substrates. The 30-mer (5′-CCCGACACCAACCACUAAAAAAAAAAAAAA-3′) and 35-mer poly(A) oligoribonucleotides were labeled at their 5′-ends with [γ-^{32}P]ATP with T4 polynucleotide kinase. The labeled 30-mer ribonucleotide was hybridized to the complementary 16-mer deoxyribonucleotide (5′-AGTGGTTGGTGTCGGG-3′), thus yielding the corresponding double-stranded substrates (16−30ds) (*36*). The hybridization was performed in a 1:1 (molar) ratio in the Tris component of the activity buffer by incubation for 5 min at 68 °C followed by 45 min at room temperature. The exoribonucleolytic reactions were performed in a final volume of 12.5 μL containing the same activity buffer as previously described (*37*). In all cases, 30 nM single-stranded (nonhybridized) or double-stranded (hybridized) oligonucleotide substrates were used, and the amount of each enzyme was adjusted to achieve linear kinetics. Reactions were started by the addition of the enzyme and mixtures incubated at 37 °C. Samples were withdrawn at the times indicated in the figures, and the reaction was stopped via addition of formamide-containing dye supplemented with 10 mM EDTA. Reaction products were resolved in a 20% polyacrylamide/7 M urea gel and analyzed by autoradiography. The exoribonucleolytic activity of the enzymes was determined by measuring and quantifying the disappearance of the substrate in several distinct experiments, and each value obtained represents the mean of three independent assays. The relative activity for all proteins was standardized for a 1 min reaction per 1 nmol of protein. The specific activity of each enzyme is given as picomoles of substrate oligoribonucleotide consumed per minute per nanomole of protein at 37 °C. For quantification, the amount of purified enzyme used was selected to ensure that less than 25% of the substrate was degraded. The results obtained are listed in Table 2.

Surface Plasmon Resonance Analysis (*Biacore*). Biacore SA chips were obtained from Biacore Inc. (GE Healthcare). The flow cells of the SA streptavidin sensor chip were coated with a low concentration of the RNA substrate. On flow cell 1, no substrate was added so this cell could be used as the control blank cell. On flow cell 2, a 5′-biotinylated 25-nucleotide RNA oligomer (5′-CCCGACACCAACCACUAAAAAAAAA-3′) was added to allow the study of the interaction of the protein with a single-stranded RNA molecule. On flow cell 3, a 5′-biotinylated 30-nucleotide poly(A) oligomer was added to allow the study of the interaction of the protein with a single-stranded RNA molecule composed only of adenosines. The target RNA substrates were captured on the respective flow cells by 20 μL triple injections of a 500 nM solution of the target RNA in 1 M NaCl at a flow rate of 10 μL/min, as described in previous reports (*11*, *38*). The biosensor assay was conducted at 4 °C in a buffer composed of 20 mM Tris-HCl (pH 8), 100 mM KCl, 1 mM DTT, and 25 mM EDTA. The proteins were injected over flow cells 1−3 for 2 min at concentrations of 10, 20, 30, 40, and 50 nM using a flow rate of 20 μL/min. All experiments included triple injections of each protein concentration to determine the reproducibility of the signal and control injections to assess the stability of the RNA surface during the experiment. Bound protein was removed with a 60 s wash with 2 M NaCl, which did not damage the substrate surface. Data from flow cell 1 were used to correct for refractive index changes and nonspecific binding. To ensure that during SPR analysis the exoribonucleolytic activity of the proteins studied was completely blocked, we conducted these experiments in a buffer with a 2.5-fold higher concentration of EDTA [25 mM instead of the usual 10 mM used in RNA binding assays (*33*)]. Under these conditions, we can be sure that EDTA saturation was obtained and that there is no degradation of the RNA substrate by the enzymes. Rate constants and equilibrium constants were calculated using BIA EVALUATION version 3.0, according to the 1:1 Langmuir binding fitting model. The dissociation constants (K_D) obtained are listed in Table 3.

Multiple-Sequence Alignment, Phylogenetic Tree Construction, Domain Architecture Analysis, and 3D Homology Modeling. Sequence similarity searches were performed using BLAST 2.0 at the NCBI. Multiple-sequence alignments of the six-RNase II family of exoribonucleases were conducted using CLUSTAL X 1.83 with default parameters (*39*). The resulting alignment was used to calculate the distance matrix by the Tree-puzzle method (*40*). The phylogenetic tree was constructed by the Neighbor-Joining method (*41*) and supported by 500 bootstrap steps (*42*). The amino acid sequences of the exoribonucleases under study were searched in the Pfam A (http://pfam.sanger.ac.uk/) (*43*) database for the annotation of domains and their arrangements. The 3D models for the proteins in study were determined using standard homology modeling methods based on the multiple-sequence alignment of the family members. The model structures were built using the Phyre webserver [http://www.sbg.bio.ic.ac.uk/phyre (*44*)]. 3D models for the RNase II family members were based on the crystal structures of wild-type RNase II and the RNase II D209N mutant complexed with a 13-nucleotide poly(A) RNA [Protein Data Bank (PDB) entries 2IX1 and 2IX0 (*9*)]. Because of the lack of the N-terminal HTH motif in these crystal structures, the 3D models of the additional N-terminal region of RNase R-like proteins were based on the crystal structure of PDB entry 1mkm (*45*). Structure figures were generated with Pymol (*46*).

RESULTS

RNase II-like Enzymes from Salmonella and Streptococcus. RNases have been involved in the virulence mechanisms of several pathogenic organisms (*18*, *20*, *24*, *47*, *48*), and an improved understanding of the biochemical mode of action of these proteins may be important for further studies on virulence.

Table 2: Exoribonucleolytic Activities of Proteins from the RNase II Family[a]

protein	protein activity (pmol min^{-1} $nmol^{-1}$)
II_Ecoli	299.4 ± 36.0
R_Ecoli	130.8 ± 6.3
II_Salm	87.5 ± 2.1
R_Salm	72.8 ± 7.3
R_Pneumo_T4	3.4 ± 0.03
R_Pneumo_TIGR	7.5 ± 0.02

[a]Exoribonucleolytic activity was assayed using a 35-nucleotide poly(A) chain as a substrate. Activity assays were performed in triplicate as described in Experimental Procedures. Each value represents the number of picomoles of substrate oligoribonucleotide consumed per minute per nanomole of protein.

Table 3: RNA Binding Affinities of Proteins from the RNase II Family[a]

protein	25-mer ssRNA K_D (nM)	poly(A) ssRNA K_D (nM)
pET15b	ND[b]	ND[b]
II_Ecoli	6.5 ± 0.4	1.3 ± 0.4
R_Ecoli	3.2 ± 0.4	1.2 ± 0.1
II_Salm	12.0 ± 2.0	3.7 ± 0.1
R_Salm	19.7 ± 1.6	7.0 ± 0.6
R_Pneumo_T4	16.9 ± 1.6	5.7 ± 0.7
R_Pneumo_TIGR	9.6 ± 0.6	3.3 ± 0.2

[a]The dissociation constants (K_D) were determined by surface plasmon resonance using a Biacore 2000 instrument with a 25-nucleotide RNA oligomer (5′-biotin-CCC GAC ACC AAC CAC UAA AAA AAA A-3′) and a 30-nucleotide poly(A) RNA oligomer (5′-biotin-AAA AAA AAA AAA AAA AAA AAA AAA A-3′). [b]Not detected (no binding affinity detected for this negative control).

Hence, we decided to characterize the members of the RNase II family of enzymes of *Sa. typhimurium* and *S. pneumoniae*, two clinically important human pathogens.

Results of the phylogenetic analysis of the RNase II family of enzymes of *Sa. typhimurium* and *S. pneumoniae* are shown in Figure 1. The phylogenetic tree reveals that these enzymes form two distinct groups that clearly separate the *E. coli* enzymes RNase II and RNase R. Although the enzymes share the same domain architecture, the level of sequence identity is very low between proteins from different groups (Figure 1B). Interestingly, besides the domains previously described for the RNase II family of proteins (two CSD, one RNB, and one S1), a search in the Pfam database identified a helix−turn−helix (HTH) motif in the N-terminus of the two enteric RNase R-like proteins. However, when a more thorough analysis was conducted, by recurring to homology-based 3D modeling using only the N-terminal spanning amino acids of the enzymes, the same domain was detected in both RNase R-like proteins of *S. pneumoniae* (Figure 1C). Interestingly, this motif seems to be highly conserved among RNase R-like enzymes and may assist in RNA binding. The HTH domain is found in many proteins that regulate gene expression and has been described as a major structural motif capable of binding nucleic acids (*49*). Although the HTH motif has typically been associated with DNA binding, it has also been reported in RNA-binding proteins (*50*, *51*).

Both *E. coli* and *Sa. typhimurium* belong to the Enterobacteriaceae family, and as such, the presence of two hydrolytic RNases in the *Sa. typhimurium* genome is not surprising. One of the *Sa. typhimurium* proteins studied in this report is found jointly with *E. coli* RNase II, while the other is grouped together with *E. coli* RNase R. When the genome of *S. pneumoniae* was analyzed, only one hydrolytic RNase could be found. This enzyme falls in the RNase R cluster together with *E. coli* and *Sa. typhimurium* RNase R (Figure 1A). Although the comparison of the protein domains shows that the level of amino acid identity is very high among the enzymes of the same group, this value decreases significantly (to <40%) when the entire sequence of the proteins is compared (Figure 1B). Therefore, in the phylogenetic tree, *E. coli* and *Salmonella* RNase R are found together in the same cluster while the pneumococcal orthologues form an independent cluster.

This analysis indicates that *Sa. typhimurium* contains both hydrolytic enzymes, an RNase II-like and an RNase R-like enzyme, while the only enzyme present in *S. pneumoniae* is an RNase R-like form. Via comparison of the RNase R sequence of *S. pneumoniae* TIGR4 with that of *S. pneumoniae* T4, four different amino acids were detected (Figure 1D). Thus, we decided to characterize both proteins, since it could be interesting to study the biochemical mode of action of two enzymes presenting small amino acid differences. The choice of these two strains was also based on the fact that TIGR4 is highly virulent, while T4 is a nonvirulent strain.

The hydrolytic enzymes found in *Sa. typhimurium* and *S. pneumoniae* carrying an N-terminal His tag were purified by affinity chromatography and characterized in vitro and their biochemical properties compared to those of their *E. coli* homologues. The purity and homogeneity of the purified proteins were evaluated by SDS−PAGE, and all the purified proteins were immunodetected with an anti-His antibody (data not shown). Interestingly, when using *E. coli* RNase II antibodies, not only the purified *E. coli* RNase II but also, although with lower intensity, all the other enzymes of the RNase II family were detected (data not shown). The same was observed with *E. coli* RNase R specific antibodies. These data reinforce the structural resemblance between the proteins belonging to this family (*9*, *11*).

Exoribonuclease Activity. The behavior of the purified proteins with regard to their exoribonuclease activity against different RNA substrates was studied and compared to that of the *E. coli* homologue enzymes (*11*, *33*, *34*, *52*). Activity assays were performed using two RNA molecules as substrates, a single-stranded 35-mer poly(A) and a double-stranded RNA substrate, 16−30ds.

It is known that *E. coli* RNase II is able to degrade single-stranded substrates until it reaches a four-nucleotide fragment as an end product, while RNase R is able to degrade a few more nucleotides, releasing a final product of two nucleotides (*34*). When we analyzed the exoribonucleolytic activity of the homologous proteins from *Sa. typhimurium* and *S. pneumoniae* using a 35-nucleotide poly(A) RNA substrate, we observed that *Sa. typhimurium* RNase II (II_Salm) behaves like *E. coli* RNase II (II_Ecoli), since its final end product also contains four nucleotides, while all the other proteins behave like *E. coli* RNase R (R_Ecoli), rendering a two-nucleotide fragment as the final product (Figure 2A).

However, there are some differences with regard to the exoribonucleolytic activity. While II_Ecoli presents an activity of 299.4 ± 36.0 pmol min^{-1} $nmol^{-1}$, its homologue II_Salm has an activity that is ~3.5-fold lower, 87.5 ± 2.1 pmol min^{-1} $nmol^{-1}$ (Table 2). The variation is not so significant between the activities of R_Ecoli and R_Salm, with R_Ecoli being only 2-fold more active than its R_Salm homologue [130.8 ± 6.3 and 72.8 ± 7.3 pmol min^{-1} $nmol^{-1}$, respectively (Table 2)]. When the activity of

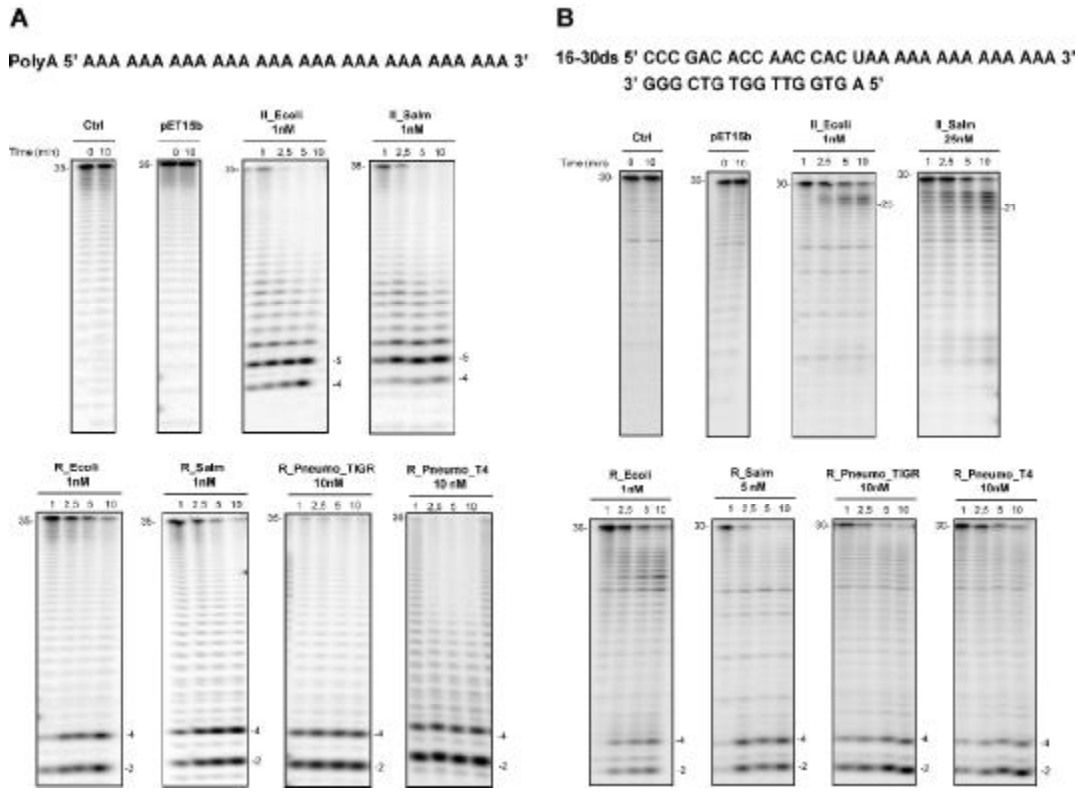

FIGURE 2: Exoribonuclease activity of RNase II homologues. The quantity of enzyme used in each reaction is specified on top. Samples were taken at the indicated time points. Reaction products were analyzed in a denaturing 20% polyacrylamide gel with 7 M urea. Control reaction mixtures with no enzyme added (Ctrl) were incubated at the maximum reaction time for each protein. In all the experiments, pET15b indicates the negative control, corresponding to the addition of the protein extract obtained under the same conditions, from a strain carrying only the expression vector (pET-15b). Lengths of substrates and degradation products are indicated. (A) 30 nM 30-nucleotide poly(A) molecule used as the substrate and (B) 30 nM 16−30ds molecule used as the substrate.

the enzymes from *S. pneumoniae* (R_Pneumo_TIGR and R_Pneumo_T4) is compared, the difference is more pronounced, with R_Ecoli being 17-fold more active than R_Pneumo_TIGR and 40-fold more active than R_Pneumo_T4 (Table 2).

Besides the divergence with regard to the final end product of the reaction, another distinguishing feature between RNase II and RNase R resides in their ability to degrade structured RNA. While RNase R is capable of overcoming the secondary structures, RNase II stalls seven to nine nucleotides before it reaches the double-stranded region (*9*, *33*). Thus, to test the ability of these enzymes to digest through secondary structures, we performed activity assays using a double-stranded substrate with an additional 14-nucleotide single-stranded extension at the 3′-end (16−30ds). Previous results have shown that *E. coli* RNase II is able to catalyze the rapid shortening of the 3′-single-stranded portion of this 16−30ds substrate, generating 23−25-nucleotide fragments as final products (*33*). II_Salm, as expected, displayed the same behavior as II_Ecoli by being unable to proceed through the secondary structure. However, an interesting result is that II_Salm gives rise to fragments of 21−23 nucleotides, slightly shorter than those from II_Ecoli, indicating that this protein can move closer to the double-stranded region of the substrate (Figure 2B).

E. coli RNase R is known to be capable of degrading the 16−30ds substrate to near completion, releasing a final end product of two nucleotides (*33*). In agreement with our prediction, all the RNase R-like proteins were able to degrade the 16−30ds substrate close to completion, leaving the characteristic two-nucleotide end product (Figure 2B). This confirms their ability to efficiently degrade an extensive region of double-stranded RNA.

These results show that the only member of the RNase II family found in both strains of *S. pneumoniae* analyzed has an activity similar to that of RNase R. Indeed, RNase R has been shown to be the only hydrolytic enzyme, and even the only exoribonuclease present in several organisms (*3*).

RNA Binding Ability. We were also interested in characterizing the proteins regarding their RNA binding ability. For that, the dissociation constants (K_D) were determined by surface plasmon resonance analysis (SPR) using Biacore 2000, and the data are presented in Table 3. The analysis of the results obtained showed that all the proteins studied in this work exhibit K_D values in the same range for both substrates tested [a 25-nucleotide RNA oligomer and a 30-nucleotide poly(A) RNA]. II_Ecoli presented a K_D value of 6.5 ± 0.4 nM (*11*), while R_Ecoli exhibited 2 times more affinity for the 25-nucleotide RNA

oligomer [3.2 ± 0.4 nM (Table 3)]. Such a difference was not as pronounced when the substrate analyzed was a 30-nucleotide poly(A) RNA (1.3 ± 0.4 and 1.2 ± 0.1 nM for II_Ecoli and R_Ecoli, respectively). This may be explained since this type of substrate has been described as the preferred substrate for RNase II (*53*).

The results obtained for the 25-nucleotide RNA oligomer showed that the II_Salm protein had a 2-fold reduction in the RNA affinity (6.5 ± 0.4 nM) when compared to that of the *E. coli* homologue (12.0 ± 2.0 nM) (Table 3). R_Salm was the protein that exhibited the lowest affinity for the 25-nucleotide ssRNA substrate with a K_D value of 19.7 ± 1.6 nM. With regard to the *S. pneumoniae* RNases, both proteins presented a slight reduction in their RNA binding ability, with a small increase in their K_D values when compared to R_Ecoli (16.9 ± 1.6 and 9.6 ± 0.6 nM for R_Pneumo_T4 and R_Pneumo_TIGR, respectively) (Table 3).

When the RNA binding ability was analyzed with the poly(A) substrate, the overall behavior was maintained. Contrary to what happens in *E. coli*, in *Sa. typhimurium* the II_Salm protein had a higher RNA affinity with a 2-fold reduction in the K_D value (3.7 ± 0.1 nM) when compared to that of R_Salm (7.0 ± 0.6 nM) (Table 3), suggesting that poly(A) might not be the preferred substrate of II_Salm. R_Pneumo_T4 and R_Pneumo_TIGR presented the following dissociation constants for the analysis of the poly(A) substrate: 5.7 ± 0.7 and 3.3 ± 0.2 nM, respectively. Once again, the tendency was kept among the *S. pneumoniae* proteins with R_Pneumo_TIGR being the one that exhibits the higher RNA−protein affinity of the two tested.

DISCUSSION

Some exoribonucleases have been described as being involved in the modulation of the expression of virulence in a number of pathogenic organisms (*20*, *24*, *25*). Since not much is known about RNases in *S. pneumoniae* or *Sa. typhimurium*, two widespread human pathogens, we focused our study on the biochemical characterization of the RNase II family of proteins present in these microorganisms.

In our initial analysis, we searched for homologues of the RNase II family of proteins in the genomic sequences of *Sa. typhimurium* and *S. pneumoniae* and sequenced the corresponding region of nonvirulent *S. pneumoniae* strain T4. We were able to identify two homologues of the RNase II family of proteins in *Sa. typhimurium*, while only one member of this family was found in *S. pneumoniae*.

Biochemical characterization of the identified proteins showed that one of the two hydrolytic enzymes found in *Sa. typhimurium* behaves like RNase II and the other like RNase R, which agrees with the prediction made by sequence comparison. However, in *S. pneumoniae*, the only hydrolytic enzyme present in both strains behaves like RNase R, since it is able to degrade structured RNAs and the shortest product released is two nucleotides in length.

Interestingly, our results showed that the products generated by II_Salm with the 16−30ds substrate were slightly smaller in size than those of II_Ecoli, suggesting that this protein can more closely approach the double-stranded region. A similar result had previously been reported with an RNase II mutant lacking an N-terminal CSD domain (*33*), and the explanation given to this behavior was based on the fact that the absence of one RNA-binding domain in this protein would result in less steric hindrance, allowing the RNA substrate to move closer to the catalytic pocket. Similarly, in II_Salm, there may be a different rearrangement in the RNA binding domains that could result in a wider anchoring region. This would allow the substrate to move nearer to the catalytic cavity, even though the double-stranded moiety would impede further degradation. Another explanation could be a slight difference in their catalytic cavities, and this could account for the 88% level of amino acid identity of the RNB domains of both enzymes (Figure 1A). To gain further insight in the analysis of the results, homology-based 3D models were generated for all the proteins under study (Figure 3). The models clearly indicate that these four enzymes share a common 3D arrangement, being all the critical residues for exoribonucleolytic activity (*11*, *54*) located in equivalent spatial positions. Superimposition of the II_Ecoli crystal structure with the generated II_Salm 3D model did not reveal significant conformational changes (data not shown) that could confirm any of the hypotheses stated above. However, slight structural differences may account for the observed results. In contrast to II_Ecoli, our results indicate that poly(A) RNA may not be the preferred substrate of II_Salm. This raises the question of the role of II_Salm in digesting poly(A) tails in vivo and the consequent protection of full-length RNAs, suggesting a different RNA metabolism in *Salmonella*.

The hydrolytic enzymes from the two *S. pneumoniae* strains exhibited the same behavior with regard to the pattern of degradation of the RNA substrates studied. However, the R_Pneumo_TIGR enzyme from the virulent strain is ~50% more active than that from the nonvirulent strain. Moreover, this protein also exhibited a higher RNA affinity. These two factors can be related since a higher affinity for an RNA substrate may increase the activity of the enzyme. There is a close relation between the ability of the proteins to bind to the substrate and its processivity. In the case of exoribonucleases, the enzymes need to bind well enough to attach themselves to the RNA but not bind so strongly that they impede the translocation of the RNA. The variation between the pneumococcal enzymes might be linked with the different amino acids identified in the two enzymes (see Figure 1D). According to the 3D models, the first different amino acid between R_Pneumo_TIGR and R_Pneumo_T4 falls into the variable region before the first CSD of the enzymes, and the last is located after the S1 domain. Hence, these two amino acids most probably do not account for the observed variation in the activity and binding between the two enzymes. One of the substitutions (serine in T4, proline in TIGR4) is placed inside the CSD2 domain. This change may be related to the different binding ability displayed by the two proteins. However, the most interesting difference falls inside the RNB catalytic domain. In II_Ecoli, the active site contains four conserved aspartic acid residues. Four aspartate residues in R_Ecoli are also predicted to be involved in the coordination of the Mg^{2+} ion, which is essential for catalysis (*9*). In the active site, in the vicinity of the four conserved aspartate residues, a leucine (L285) in T4 is replaced with a phenylalanine (F285) in TIGR4. Although leucine is usually conserved in this position, the replacement with an aromatic amino acid may confer R_Pneumo_TIGR the ability to bind RNA more tightly and enhance its exoribonucleolytic activity. In fact, the RNB domain of RNase R is known to bind to RNA more tightly than the RNB domain of RNase II, and the exoribonucleolytic activity is less dependent on the

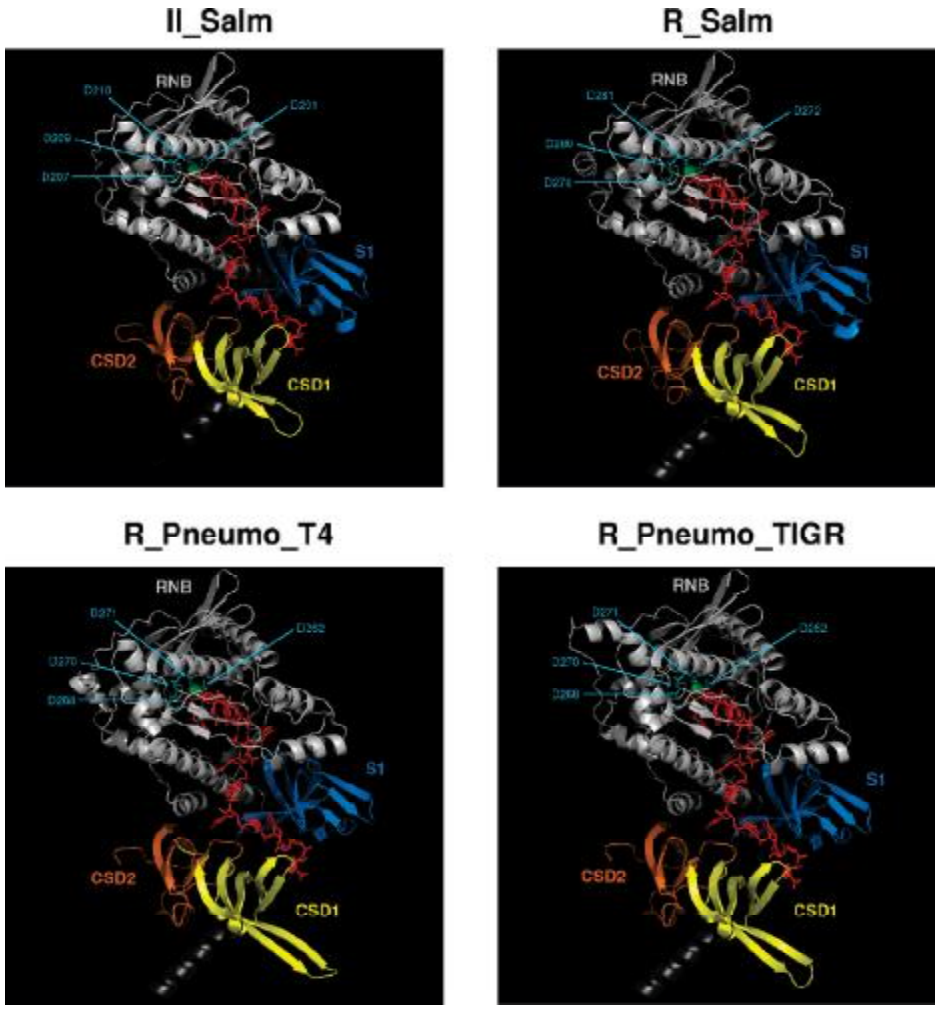

FIGURE 3: Predictive 3D models of the *E. coli* RNase II orthologues: II_Salm (amino acids 3−644), R_Salm (amino acids 65−726), R_Pneumo_T4 (amino acids 44−705), and R_Pneumo_TIGR (amino acids 44−705). A view of the cartoons from the 3D models showing domains CSD1 (yellow), CSD2 (orange), RNB (light gray), and S1 (blue) is presented. The RNA molecule (red) and the Mg^{2+} ion (green) were superimposed in all the models. The position of all equivalent residues of the catalytic site of the RNase II enzyme is indicated in all proteins. The regions excluded from the models were due to the lack of an appropriately aligned template structure.

presence of the CSDs and S1 domain (*52*, *55*). According to the analysis of the 3D models (Figure 4), although this amino acid does not seem to contact the RNA molecule directly, the spatial arrangement of the aromatic side chain of F285 may induce subtle conformational changes in the helix below that could account for the observed differences between the two enzymes. This helix corresponds to helix α8, known to contact the RNA molecule in the *E. coli* RNase II crystal structure (*9*). Thus, the substitution of this amino acid alone may be responsible for the different biochemical properties exhibited by R_Pneumo_TIGR.

This was the first time that ribonucleases of the RNase II family of *Sa. typhimurium* and *S. pneumoniae* were biochemically characterized, bringing new insights into the RNA metabolism of these two human pathogens of clinical importance. Although there are a number of genes involved in virulence, the characterization of the biochemical mode of action of proteins that might be involved in the expression of genes related to pathogenicity may be helpful for the understanding of the virulence mechanisms.

ACKNOWLEDGMENT

We thank Colin McVey for helpful advice and discussions on Phyre-Server and Pymol. We also thank Paulino Gomez-Puertas for the *E. coli* RNase R 3D model. Genomic DNA from *S. pneumoniae* strains TIGR4 and T4 was kindly supplied by Paloma Lopez, and *Sa. typhimurium* DNA was gently provided by Sandra Viegas. We acknowledge Paloma Lopez for the critical reading of the manuscript.

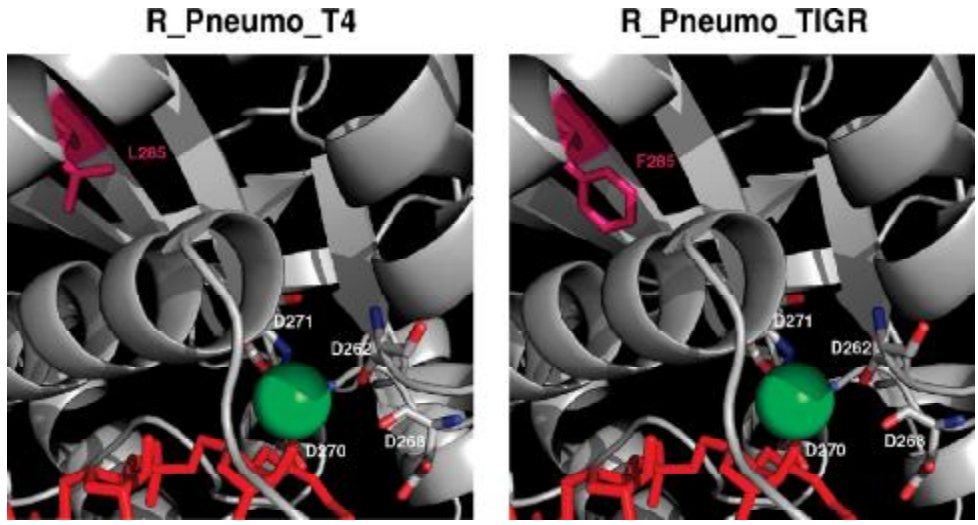

FIGURE 4: Magnified views of the proposed catalytic regions of the R_Pneumo_T4 and R_Pneumo_TIGR enzymes. The four aspartate residues involved in the coordination of the Mg^{2+} ion (green) are indicated, and the superimposed RNA molecule is colored red. L285 (pink) in R_Pneumo_T4 is replaced with F285 (pink) in R_Pneumo_TIGR.

SUPPORTING INFORMATION AVAILABLE

SDS−PAGE analysis of the purified proteins. This material is available free of charge via the Internet at http://pubs.acs.org.

REFERENCES

1. Mian, I. S. (1997) Comparative sequence analysis of ribonucleases HII, III, II, PH and D. *Nucleic Acids Res. 25*, 3187–3195.
2. Zuo, Y., and Deutscher, M. P. (2001) Survey and Summary. Exoribonuclease superfamilies: Structural analysis and phylogenetic distribution. *Nucleic Acids Res. 209*, 1017–1026.
3. Andrade, J. M., Pobre, V., Silva, I. J., Domingues, S., and Arraiano, C. M. (2009) The role of 3′-5′ exoribonucleases in RNA degradation. *Prog. Nucleic Acid Res. Mol. Biol. 85*, 187–229.
4. Deutscher, M. P., and Reuven, N. B. (1991) Enzymatic basis for hydrolytic versus phosphorolytic mRNA degradation in *Escherichia coli* and *Bacillus subtilis*. *Proc. Natl. Acad. Sci. U.S.A. 88*, 3277–3280.
5. Marujo, P. E., Hajnsdorf, E., Le Derout, J., Arraiano, C. M., and Régnier, P. (2000) RNase II removes the oligo(A) tails that destabilize the rpsO mRNA of *Escherichia coli*. *RNA 6*, 1185–1193.
6. Mohanty, B. K., and Kushner, S. R. (2000) Polynucleotide phosphorylase, RNase II and RNase E play different roles in the *in vivo* modulation of polyadenylation in *Escherichia coli*. *Mol. Microbiol. 36*, 982–994.
7. Cairrão, F., Chora, A., Zilhão, R., Carpousis, J., and Arraiano, C. M. (2001) RNase II levels change according to the growth conditions: Characterization of *gmr*, a new *Escherichia coli* gene involved in the modulation of RNase II. *Mol. Microbiol. 276*, 19172–19181.
8. Zilhão, R., Cairrão, F., Régnier, P., and Arraiano, C. M. (1996) PNPase modulates RNase II expression in *Escherichia coli*: Implications for mRNA decay and cell metabolism. *Mol. Microbiol. 20*, 1033–1042.
9. Frazão, C., McVey, C. E., Amblar, M., Barbas, A., Vonrhein, C., Arraiano, C. M., and Carrondo, M. A. (2006) Unravelling the dynamics of RNA degradation by ribonuclease II and its RNA-bound complex. *Nature 443*, 110–114.
10. Zuo, Y., Vincent, H. A., Zhang, J., Wang, Y., Deutscher, M. P., and Malhotra, A. (2006) Structural basis for processivity and single-strand specificity of RNase II. *Mol. Cell 24*, 149–156.
11. Barbas, A., Matos, R. G., Amblar, M., Lopez-Vinas, E., Gomez-Puertas, P., and Arraiano, C. M. (2008) New Insights into the Mechanism of RNA Degradation by Ribonuclease II: Identification of the residue responsible for setting the RNase II end-product. *J. Biol. Chem. 283*, 13070–13076.
12. Andrade, J. M., Cairrão, F., and Arraiano, C. M. (2006) RNase R affects gene expression in stationary phase: Regulation of *omp*A. *Mol. Microbiol. 60*, 219–228.
13. Cairrão, F., Cruz, A., Mori, H., and Arraiano, C. M. (2003) Cold shock induction of RNase R and its role in the maturation of the quality control mediator SsrA/tmRNA. *Mol. Microbiol. 50*, 1349–1360.
14. Cheng, Z. F., and Deutscher, M. P. (2003) Quality control of ribosomal RNA mediated by polynucleotide phosphorylase and RNase R. *Proc. Natl. Acad. Sci. U.S.A. 100*, 6388–6393.
15. Mahan, M. J., Slauch, J. M., and Mekalanos, J. J. (1996) Environmental regulation of virulence gene expression in *Escherichia, Salmonella and Shigella spp*. In E. coli and Salmonella: Cell and Molecular Biology , 2nd ed., pp 2803−2815, American Society for Microbiology Press, Washington, DC.
16. Li, Z., Reimers, S., Pandit, S., and Deutscher, M. P. (2002) RNA quality control: Degradation of defective transfer RNA. *EMBO J. 21*, 1132–1138.
17. Chen, C., and Deutscher, M. P. (2005) Elevation of RNase R in response to multiple stress conditions. *J. Biol. Chem. 280*, 34393–34396.
18. Charpentier, X., Faucher, S. P., Kalachikov, S., and Shuman, H. A. (2008) Loss of RNase R induces competence development in Legionella pneumophila. *J. Bacteriol. 190*, 8126–8136.
19. Purusharth, R. I., Klein, F., Sulthana, S., Jager, S., Jagannadham, M. V., Evguenieva-Hackenberg, E., Ray, M. K., and Klug, G. (2005) Exoribonuclease R interacts with endoribonuclease E and an RNA helicase in the psychrotrophic bacterium *Pseudomonas syringae* Lz4W. *J. Biol. Chem. 280*, 14572–14578.
20. Erova, T. E., Kosykh, V. G., Fadl, A. A., Sha, J., Horneman, A. J., and Chopra, A. K. (2008) Cold shock exoribonuclease R (VacB) is involved in *Aeromonas hydrophila* pathogenesis. *J. Bacteriol. 190*, 3467–3474.
21. Reva, O. N., Weinel, C., Weinel, M., Bohm, K., Stjepandic, D., Hoheisel, J. D., and Tummler, B. (2006) Functional genomics of stress response in *Pseudomonas putida* KT2440. *J. Bacteriol. 188*, 4079–4092.
22. Cheng, Z. F., and Deutscher, M. P. (2005) An important role for RNase R in mRNA decay. *Mol. Cell 17*, 313–318.
23. Cheng, Z. F., Zuo, Y., Li, Z., Rudd, K. E., and Deutscher, M. P. (1998) The *vac*B gene required for virulence in *Shigella flexneri* and *Escherichia coli* encodes the exoribonuclease RNase R. *J. Biol. Chem. 273*, 14077–14080.
24. Tobe, T., Sasakawa, C., Okada, N., Honma, Y., and Yoshikawa, M. (1992) *vac*B, a novel chromosomal gene required for expression of virulence genes on the large plasmid of *Shigella flexneri*. *J. Bacteriol. 174*, 6359–6367.

25. Tsao, M. Y., Lin, T. L., Hsieh, P. F., and Wang, J. T. (2009) The 3′-to-5′ exoribonuclease (HP1248) of *Helicobacter pylori* regulates motility and apoptosis-inducing genes. *J. Bacteriol. 191*, 2691–2702.
26. Lalonde, M. S., Zuo, Y., Zhang, J., Gong, X., Wu, S., Malhotra, A., and Li, Z. (2007) Exoribonuclease R in *Mycoplasma genitalium* can carry out both RNA processing and degradative functions and is sensitive to RNA ribose methylation. *RNA 13*, 1957–1968.
27. Zuo, Y., and Deutscher, M. P. (2001) Exoribonuclease superfamilies: Structural analysis and phylogenetic distribution. *Nucleic Acids Res. 29*, 1017–1026.
28. Hutchison, C. A., Peterson, S. N., Gill, S. R., Cline, R. T., White, O., Fraser, C. M., Smith, H. O., and Venter, J. C. (1999) Global transposon mutagenesis and a minimal *Mycoplasma* genome. *Science 286*, 2165–2169.
29. Tomasz, A. (1999) New faces of an old pathogen: Emergence and spread of multidrug-resistant *Streptococcus pneumoniae*. *Am. J. Med. 107*, 55S–62S.
30. Hoskins, J., Alborn, W. E. Jr., Arnold, J., Blaszczak, L. C., Burgett, S., DeHoff, B. S., Estrem, S. T., Fritz, L., Fu, D. J., Fuller, W., Geringer, C., Gilmour, R., Glass, J. S., Khoja, H., Kraft, A. R., Lagace, R. E., LeBlanc, D. J., Lee, L. N., Lefkowitz, E. J., Lu, J., Matsushima, P., McAhren, S. M., McHenney, M., McLeaster, K., Mundy, C. W., Nicas, T. I., Norris, F. H., O'Gara, M., Peery, R. B., Robertson, G. T., Rockey, P., Sun, P. M., Winkler, M. E., Yang, Y., Young-Bellido, M., Zhao, G., Zook, C. A., Baltz, R. H., Jaskunas, S. R., Rosteck, P. R.Jr., Skatrud, P. L., and Glass, J. I. (2001) Genome of the bacterium *Streptococcus pneumoniae* strain R6. *J. Bacteriol. 183*, 5709–5717.
31. Taylor, R. G., Walker, D. C., and McInnes, R. R. (1993) *E. coli* host strains significantly affect the quality of small scale plasmid DNA preparations used for sequencing. *Nucleic Acids Res. 21*, 1677–1678.
32. Studier, F. W., and Moffatt, B. A. (1986) Selective expression of cloned genes directed by T7 RNA polymease. *J. Mol. Biol. 189*, 113–130.
33. Amblar, M., Barbas, A., Fialho, A. M., and Arraiano, C. M. (2006) Characterization of the Functional Domains of *Escherichia coli* RNase II. *J. Mol. Biol. 360*, 921–933.
34. Amblar, M., Barbas, A., Gomez-Puertas, P., and Arraiano, C. M. (2007) The role of the S1 domain in exoribonucleolytic activity: Substrate specificity and multimerization. *RNA 13*, 317–327.
35. Viegas, S. C., Pfeiffer, V., Sittka, A., Silva, I. J., Vogel, J., and Arraiano, C. M. (2007) Characterization of the role of ribonucleases in *Salmonella* small RNA decay. *Nucleic Acids Res. 35*, 7651–7664.
36. Arraiano, C. M., Barbas, A., and Amblar, M. (2008) Characterizing Ribonucleases *in vitro*: Examples of Synergies between Biochemical and Structural Analysis. *Methods Enzymol. 447*, 131–160.
37. Amblar, M., and Arraiano, C. M. (2005) A single mutation in *Escherichia coli* ribonuclease II inactivates the enzyme without affecting RNA binding. *FEBS J. 272*, 363–374.
38. Park, S., Myszka, D. G., Yu, M., Littler, S. J., and Laird-Offringa, I. A. (2000) HuD RNA recognition motifs play distinct roles in the formation of a stable complex with AU-rich RNA. *Mol. Cell. Biol. 20*, 4765–4772.
39. Higgins, D. G., and Sharp, P. M. (1988) CLUSTAL: A package for performing multiple sequence alignment on a microcomputer. *Gene 73*, 237–244.
40. Schmidt, H. A., Strimmer, K., Vingron, M., and von Haeseler, A. (2002) TREE-PUZZLE: Maximum likelihood phylogenetic analysis using quartets and parallel computing. *Bioinformatics 18*, 502–504.
41. Saitou, N., and Nei, M. (1987) The neighbor-joining method: A new method for reconstructing phylogenetic trees. *Mol. Biol. Evol. 4*, 406–425.
42. Felsenstein, J. (1985) Confidence limits on phylogenies: An approach using the bootstrap. *Evolution 39*, 783–791.
43. Finn, R. D., Tate, J., Mistry, J., Coggill, P. C., Sammut, S. J., Hotz, H. R., Ceric, G., Forslund, K., Eddy, S. R., Sonnhammer, E. L., and Bateman, A. (2008) The Pfam protein families database. *Nucleic Acids Res. 36*, D281–D288.
44. Kelley, L. A., and Sternberg, M. J. (2009) Protein structure prediction on the Web: A case study using the Phyre server. *Nat. Protoc. 4*, 363–371.
45. Zhang, R. G., Kim, Y., Skarina, T., Beasley, S., Laskowski, R., Arrowsmith, C., Edwards, A., Joachimiak, A., and Savchenko, A. (2002) Crystal structure of *Thermotoga maritima* 0065, a member of the IclR transcriptional factor family. *J. Biol. Chem. 277*, 19183–19190.
46. DeLano, W. L. (2002) The PyMOL Molecular Graphics System , 0.83 ed., DeLano Scientific, San Carlos, CA.
47. Ygberg, S. E., Clements, M. O., Rytkonen, A., Thompson, A., Holden, D. W., Hinton, J. C., and Rhen, M. (2006) Polynucleotide phosphorylase negatively controls spv virulence gene expression in *Salmonella enterica*. *Infect. Immun. 74*, 1243–1254.
48. Miyoshi, A., Rosinha, G. M., Camargo, I. L., Trant, C. M., Cardoso, F. C., Azevedo, V., and Oliveira, S. C. (2007) The role of the vacB gene in the pathogenesis of *Brucella abortus*. *Microbes Infect. 9*, 375–381.
49. Brennan, R. G., and Matthews, B. W. (1989) The helix-turn-helix DNA binding motif. *J. Biol. Chem. 264*, 1903–1906.
50. Liu, W., Seto, J., Sibille, E., and Toth, M. (2003) The RNA binding domain of Jerky consists of tandemly arranged helix-turn-helix/homeodomain-like motifs and binds specific sets of mRNAs. *Mol. Cell. Biol. 23*, 4083–4093.
51. Hosaka, H., Nakagawa, A., Tanaka, I., Harada, N., Sano, K., Kimura, M., Yao, M., and Wakatsuki, S. (1997) Ribosomal protein S7: A new RNA-binding motif with structural similarities to a DNA architectural factor. *Structure 5*, 1199–1208.
52. Matos, R. G., Barbas, A., and Arraiano, C. M. (2009) RNase R mutants elucidate the catalysis of structured RNA: RNA-binding domains select the RNAs targeted for degradation. *Biochem. J. 423*, 291–301.
53. Coburn, G. A., and Mackie, G. A. (1996) Overexpression, purification and properties of *Escherichia coli* ribonuclease II. *J. Biol. Chem. 271*, 1048–1053.
54. Barbas, A., Matos, R. G., Amblar, M., Lopez-Vinas, E., Gomez-Puertas, P., and Arraiano, C. M. (2009) Determination of key residues for catalysis and RNA-cleavage specificity: One mutation turns RNase II into a "super"-enzyme. *J. Biol. Chem. 284*, 20486–20498.
55. Vincent, H. A., and Deutscher, M. P. (2009) The roles of individual domains of RNase R in substrate binding and exoribonuclease activity. The nuclease domain is sufficient for digestion of structured RNA. *J. Biol. Chem. 284*, 486–494.

BJ www.biochemj.org

Biochem. J. (2009) **423**, 291–301 (Printed in Great Britain) doi:10.1042/BJ20090839

RNase R mutants elucidate the catalysis of structured RNA: RNA-binding domains select the RNAs targeted for degradation

Rute Gonçalves MATOS, Ana BARBAS and Cecília Maria ARRAIANO[1]

Instituto de Tecnologia Química e Biológica/Universidade Nova de Lisboa, Apartado 127, 2781-901 Oeiras, Portugal

The RNase II superfamily is a ubiquitous family of exoribonucleases that are essential for RNA metabolism. RNase II and RNase R degrade RNA in the $3' \rightarrow 5'$ direction in a processive and sequence-independent manner. However, although RNase R is capable of degrading highly structured RNAs, the RNase II activity is impaired by the presence of secondary structures. RNase II and RNase R share structural properties and have a similar modular domain organization. The eukaryotic RNase II homologue, Rrp44/Dis3, is the catalytic subunit of the exosome, one of the most important protein complexes involved in the maintenance of the correct levels of cellular RNAs. In the present study, we constructed truncated RNase II and RNase R proteins and point mutants and characterized them regarding their exoribonucleolytic activity and RNA-binding ability. We report that Asp^{280} is crucial for RNase R activity without affecting RNA binding. When Tyr^{324} was changed to alanine, the final product changed from 2 to 5 nt in length, showing that this residue is responsible for setting the end-product. We have shown that the RNB domain of RNase II has catalytic activity. The most striking result is that the RNase R RNB domain itself degrades double-stranded substrates even in the absence of a 3′-overhang. Moreover, we have demonstrated for the first time that the substrate recognition of RNase R depends on the RNA-binding domains that target the degradation of RNAs that are 'tagged' by a 3′-tail. These results can have important implications for the study of poly(A)-dependent RNA degradation mechanisms.

Key words: exosome, ribonuclease, RNA degradation, RNase II, RNase R, structured RNA.

INTRODUCTION

Escherichia coli RNase II is the prototype of the RNase II superfamily of exoribonucleases. Homologues of RNase II/R are present in all domains of life [1–4]. RNase R is a member of this family that is involved in mRNA degradation, in RNA and protein quality control and has been shown to be required for virulence [5–9]. In the nucleus and cytoplasm of eukaryotic cells, the RNase II homologue Rrp44/Dis3 is a subunit of the exosome, an essential multiprotein complex involved in the processing, turnover and quality control of different types of RNA [3]. Rrp44/Dis3 is the only catalytically active nuclease in the yeast core exosome [10], and it was shown recently that it has both exo- and endoribonuclease activities [11,12].

RNase II and RNase R share catalytic properties: they both degrade RNA processively, in the $3' \rightarrow 5'$ direction releasing 5′-nucleotide monophosphates. These enzymes also share structural properties, including 60 % sequence homology [13]. Their activity is sequence-independent, but whereas RNase II is sensitive to secondary structures, RNase R is capable of degrading highly structured RNA [6,9,13,14]. Another difference is that the final degradation product of RNase II is a 4 nt fragment, whereas the end-product of RNase R is a 2 nt fragment [14–16].

RNase R is a 92 kDa protein encoded by the *rnr* gene. It is involved in the degradation of different types of RNA, such as rRNA, sRNA (small non-coding RNA) and mRNA. It was shown that RNase R has *in vivo* affinity for polyadenylated RNA and that it can be a key enzyme involved in poly(A) metabolism [17]. RNase R is the only known $3' \rightarrow 5'$ exoribonuclease able to degrade double-stranded RNA without the aid of helicase activity [18]. It is a cold-shock protein that is regulated transcriptionally and post-transcriptionally [7,8]. The activity of RNase R is modulated according to the growth conditions of the cell [19], and its levels increase in stationary phase and under stress conditions [6,8,9]. It has been shown that this protein is also involved in pathogenesis in different micro-organisms [5,20–22].

RNase II is a 72 kDa protein encoded by the *rnb* gene. In *E. coli*, this protein is the major hydrolytic enzyme that is responsible for 90 % of the exoribonucleolytic activity in crude extracts [23]. RNase II expression is differentially regulated at the transcriptional and post-transcriptional levels, and the protein can be regulated by the environmental conditions [19,24,25]. The determination of the three-dimensional structure of *E. coli* RNase II showed that RNase II consists of four domains: two N-terminal CSDs (cold-shock domains) (CSD1 and CSD2), one central RNB catalytic domain, and one C-terminal S1 domain [26,27] (Figure 1). Structural and biochemical analysis helped to explain the activity of the enzyme and led to the proposal of a model for RNA degradation by RNase II. RNA contacts RNase II in two different and non-contiguous regions: the anchoring and the catalytic regions [16,26]. The shortest RNA substrate able to retain contacts with these two regions is a 10 nt fragment, and it was known that this was the minimum size necessary to maintain the processivity of the enzyme [16,26,28]. It was demonstrated that Tyr^{313} and Glu^{390} are important to the discrimination of cleavage of RNA compared with DNA [29]. During the determination of key residues for catalysis, we have recently discovered that the substitution of alanine for Glu^{542} leads to a 100-fold increase in the exoribonucleolytic activity, turning RNase II into a 'super-enzyme' [29].

The structure of the RNA-bound complex led to the explanation of why a 4 nt fragment is the final degradation product for RNase II [26]. This is a result of the tight packing of the five 3′-terminal nucleotides in the catalytic cavity, mediated by

Abbreviations used: CSD, cold-shock domain; DTT, dithiothreitol; HTH, helix–turn–helix; SPR, surface plasmon resonance.

[1] To whom correspondence should be addressed (email cecilia@itqb.unl.pt).

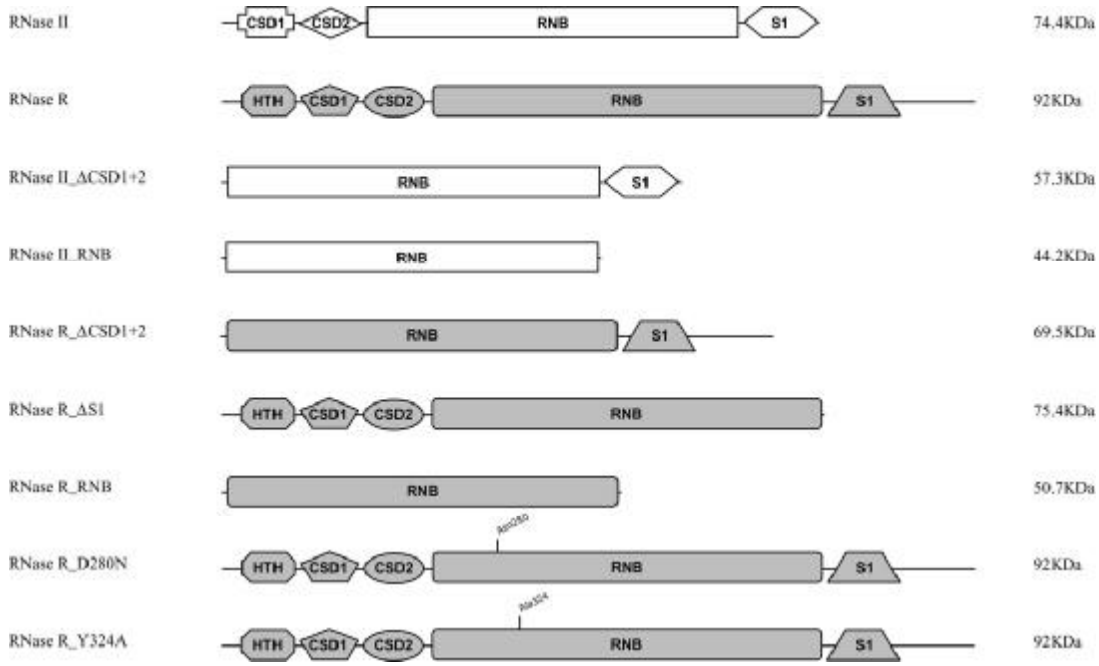

Figure 1 Linear representation of the domains of wild-type RNase II, RNase R and its derivative proteins

the aromatic residues Tyr[253] and Phe[358] [26]. It was reported that the highly conserved Tyr[253] is the residue responsible for setting the end-product of RNase II and it is extremely important for the maintenance of the 'RNA clamping' in the catalytic site of RNase II [28].

The structural model of *E. coli* RNase R protein was constructed on the basis of the RNase II structure; the two enzymes share a common three-dimensional arrangement, with all the critical residues for exoribonucleolytic activity being located in equivalent spatial positions [28]. By comparing the protein models, it was noteworthy that these two proteins have a common arrangement of the clamping tyrosine residue, but, in contrast, the presence of Phe[358] is exclusive to RNase II. RNase R protein presents a phenylalanine residue in the immediate downstream position (Phe[429]), perhaps with a similar functionality in fixing the RNA. The differences in the equivalent Phe[358] in RNase II and RNase R could explain their differences in regard to RNA degradation [28].

It was also shown that the conserved Asp[209] is directly involved in RNA cleavage by RNase II. This is the only critical aspartate residue for RNase II activity [28,30], and its replacement by asparagine was responsible for the total loss of protein activity without affecting its RNA-binding ability [30]. Moreover, a similar mutation in the yeast RNase II homologue Rrp44/Dis3 (D551N) totally abolished activity without reducing substrate binding. This mutation was also responsible for a very strong growth defect, suggesting that the phenotype of this mutant is very important for yeast physiology [10,31].

In the present study, we constructed and analysed the equivalent mutants to Y253A and D209N of *E. coli* RNase II in RNase R, Y324A and D280N respectively. Our aim was to confirm their importance in the activity of the enzymes of the RNase II family. We observed that the D280N mutant has no activity, but is still able to bind RNA efficiently, which confirms the importance of this aspartate residue in catalysis. When Tyr[324] was changed into an alanine, we verified that the final product of RNase R changed from 2 to 5 nt, confirming the importance of this residue in setting the final end-product in this family of enzymes.

Furthermore, we constructed a set of truncated proteins of RNase R lacking CSDs and/or S1 domains in order to understand the contribution of each domain (Figure 1). We analysed the activity and the binding ability of the truncated proteins using different substrates and observed that the RNB domain of RNase R alone is capable of degrading RNA molecules. In addition, we show that this domain is sufficient for the degradation of structured substrates, and that is also able to bind to RNA, although with less efficiency when compared with the wild-type protein. We also observed that the CSDs and S1 domains are responsible for the binding of the proteins to the substrate and that they are crucial for the recognition of which substrates are targeted to be degraded. In the absence of both of these domains, the protein is capable of degrading perfect double-stranded RNAs that lack the 3′-end overhang. To date, it had always been reported that the existence of a 3′-end overhang of at least 5 nt in length for RNase R was essential for catalysis to occur; in the present study, we have unravelled why.

EXPERIMENTAL

Restriction enzymes, T4 DNA ligase, Pfu DNA polymerase and T4 polynucleotide kinase were purchased from Fermentas.

Table 1 Plasmids used in the present study

Plasmid	Relevant characteristic	Reference
pFCT6.1	gene *rnb* cloned into pET15b, Amp^R	[19]
pABA-RNR	gene *rnr* cloned into pET15b, Amp^R	[15]
pABA-RNR_D280N	Expresses RNase R with a D280N mutation	The present study
pABA-RNR_Y324A	Expresses RNase R with a Y324A mutation	The present study
pFCT_XhoI521	pFCT6.1 with a XhoI restriction site in position 521 of *rnb* gene	The present study
pABA-RNR_NdeI549	pABA-RNR with a NdeI restriction site in position 549 of *rnr* gene	The present study
pFCT_CSD1+2	Expresses RNase II lacking CSD1 and CSD2	The present study
pFCT_RNB	Expresses RNase II lacking CSD1, CSD2 and S1 domains	The present study
pABA-RNR_ΔCSD1+2	Expresses RNase R lacking HTH, CSD1 and CSD2	The present study
pABA-RNR_ΔS1	Expresses RNase R lacking an S1 domain	The present study
pABA-RNR_RNB	Expresses RNase R lacking HTH, CSD1, CSD2 and the S1 domain	The present study

Unlabelled oligonucleotide primers were synthesized by STAB VIDA.

Strains

The *E. coli* strains used were DH5α [F′ *fhuA2* Δ(*argF-lacZ*)*U169 phoA glnV44* Φ*80* Δ(*lacZ*)*M15 gyrA96 recA1 relA1 endA1 thi-1 hsdR17*a] [32] for cloning experiments and BL21(DE3) [F^- r_B^- m_B^- *gal ompT* (*int*::P_{lacUV5} *T7 gen1 imm21 nin5*)] [33] for expression and purification of enzymes.

Construction of RNase R mutants by PCR overlapping

The point mutations D280N and Y324A were introduced into pABA-RNR (Table 1) by PCR overlapping. The primers used in the construction of RNase R mutants were Asp280Asn_Fw, Asp280Asn_Rev, Tyr324Ala_Fw and Tyr324Ala_Rev (Table 2).

All mutant constructs were confirmed by DNA sequencing at STAB VIDA.

Construction of truncated proteins

The truncated proteins were constructed by removing different regions of *rnb* and *rnr* genes in pFCT6.1 and pABA-RNR plasmids (Table 1). An XhoI restriction site was introduced into pFCT6.1 in the position 512 by overlapping PCR using the primers pFCT_XhoI512_Fw and pFCT_XhoI521_Rev (Table 2) originating the pFCT_XhoI521 plasmid. The natural occurrence of an XhoI recognition site at position 69 allowed us to construct pFCT_ΔCSDs by digesting the plasmid pFCT_XhoI521 with XhoI (producing degradation products of 6955 and 456 bp, with the latter corresponding to CSD1 and CSD2 of RNase II) and circularizing the fragment of 6955 bp. The protein RNase II_RNB was constructed by introduction of a stop codon (TAA) at position 1735 in the plasmid pFCT_ΔCSDs using the primers RNB_Stop1735_Fw and RNB_Stop1735_Rev (Table 2).

In the pABA-RNR plasmid (Table 1) an NdeI restriction site was introduced at position 549 by overlapping PCR using the primers RNR_NdeI549_Fw and RNR_NdeI549_Rev (Table 2) creating the pABA-RNR_NdeI549 plasmid. The natural occurrence of an NdeI recognition site at position 60 allowed us to construct pABA-RNR_ΔCSDs by digesting the plasmid pABA-RNR_NdeI549 with NdeI [producing degradation products of 7624 and 651 bp, with the latter corresponding to HTH (helix–turn–helix), CSD1 and CSD2 of RNase R] and circularizing the fragment of 7624 bp. The proteins RNR_ΔS1 and pABA-RNR_RNB were constructed by introduction of a stop codon (TAA) at position 1927 in the plasmids pABA-RNR and pABA-RNR_ΔCSDs respectively, using the primers RNR_Stop1927_Fw and RNR_Stop1927_Rev (Table 2).

Overexpression and purification of wild-type RNase II and RNase II mutants

The plasmid used for expression of wild-type *E. coli* His_6-tagged RNase II protein was pFCT6.1 plasmid [19] (Table 1). This plasmid contains the *rnb* gene cloned into pET-15b vector (Novagen) under the control of ϕ10 promoter, allowing the expression of the His_6-tagged RNase II fusion protein. The plasmid used for expression of wild-type *E. coli* His_6-tagged RNase R protein was pABA-RNR plasmid [15] (Table 1) that contains the *rnr* gene cloned into pET-15b vector (Novagen) under the control of ϕ10 promoter, allowing the expression of the His_6-tagged RNase R fusion protein.

All plasmids were transformed into BL21(DE3) *E. coli* strain (Novagen) to allow the expression of the recombinant proteins. Cells were grown at 30°C in 100 ml of LB (Luria–Bertani) medium supplemented with 150 μg/ml ampicillin to a D_{600} of 1.5. Then, they were transferred to 18°C for 30 min and then induced by addition of 0.5 mM IPTG (isopropyl β-D-thiogalactoside); induction proceeded for 20 h at 18°C. Cell cultures were pelleted by centrifugation at 8500 ***g*** for 15 min and stored at −80°C.

Purification of all proteins was performed by histidine-affinity chromatography using HiTrap Chelating HP columns

Table 2 Primers used in the present study

Bases underlined indicate restriction endonuclease sites. Bases in bold indicate amino acid changes

Primer	Sequence (5′ → 3′)	Purpose
Asp280Asn_Fw	CGCCCGGGACTTT**A**ACGATGC	Introduces D280N mutation into pABA-RNR
Asp280Asn_Rev	GCATCGT**T**AAAGTCCCGGGCG	Introduces D280N mutation into pABA-RNR
Tyr324Ala_Fw	CCGTGGGACGTCGGTG**GC**CTTCCCTTCGC	Introduces Y324A mutation into pABA-RNR
Tyr324Ala_Rev	GCGAAGGGAAG**GC**CACCGACGTCCCACGG	Introduces Y324A mutation into pABA-RNR
pFCT_XhoI512_Fw	CATCACTTTTGGT**CT**CGA**G**CACTTTGTACCGT	Introduces XhoI restriction site into pFCT6.1 at position 512
pFCT_XhoI521_Rev	ACGGTACAAAGTG**CT**CG**AG**ACCAAAAGTGATG	Introduces XhoI restriction site into pFCT6.1 at position 512
RNB_Stop1735_Fw	GCCGGG**TAA**GACACGCGTTTCGC	Introduces stop codon into pFCT6.1 at position 1735
RNB_Stop1735_Rev	GCGAAACGCGTGTC**TTA**CCCGGC	Introduces stop codon into pFCT6.1 at position 1735
RNR_NdeI549_Fw	GTCGAAGTGCTGGGCGAC**C**ATATGGGCACC	Introduces NdeI restriction site into pABA-RNR at position 549
RNR_NdeI549_Rev	GGTGCC**C**ATATG**G**GTCGCCCAGCACTTCGAC	Introduces NdeI restriction site into pABA-RNR at position 549
RNR_Stop1927_Fw	GTGTGACTTCATGCTCGACCAG**TA**AGG	Introduces stop codon into pABA-RNR at position 1927
RNR_Stop1927_Rev	CCT**TA**CTGGTCGAGCATGAAGTCACAC	Introduces stop codon into pABA-RNR at position 1927

(GE Healthcare) and ÄKTA HLPC system (GE Healthcare) following the protocol described previously [14,34]. Briefly, cell suspensions were lysed using a French press at 9000 psi (1 psi = 6.9 kPa) in the presence of 0.1 mM PMSF. The crude extracts were treated with Benzonase (Sigma) to degrade the nucleic acids and clarified by a 30 min of centrifugation at 10000 ***g***. The clarified extracts were then added to a 1 ml HiTrap Chelating Sepharose column equilibrated in buffer A (20 mM Tris/HCl and 0.5 M NaCl, pH 8) plus 20 mM imidazole and 2 mM 2-mercaptoethanol. Protein elution was achieved by a continuous imidazole gradient (from 20 to 500 mM) in buffer A. The fractions containing the purified protein were pooled and buffer-exchanged to buffer B (20 mM Tris/HCl, pH 8, 100 mM KCl and 2 mM 2-mercaptoethanol) using a 5 ml desalting column (GE Healthcare). Eluted proteins were concentrated by centrifugation at 7000 ***g*** for 15 min at 15 °C with Amicon Ultra Centrifugal Filter Devices of 30000 Da molecular-mass cut-off (Millipore). Protein concentration was determined by spectrophotometry and 50 % (v/v) glycerol was added to the final fractions before storage at − 20 °C. A 0.5 μg sample of each purified protein was separated by SDS/PAGE (8 % gel) and visualized by Coomassie Blue staining (results not shown).

Activity assays

Exoribonucleolytic activity was assayed using three different RNA oligoribonucleotides as substrates [14,34]. The 30-mer oligoribonucleotide (5′-CCCGACACCAACCACUAAAAAAA-AAAAAAA-3′), the 16-mer oligoribonucleotide (5′-CCCGACA-CCAACCACU-3′) and the poly(A) chain of 35 nt were labelled at its 5′-end with [γ-^{32}P]ATP and T4 polynucleotide kinase. The RNA oligomers were then purified using Microcon YM-3 Centrifugal Filter Devices (Millipore) to remove the non-incorporated nucleotides. The labelled 30-mer and 16-mer oligoribonucleotides were hybridized to the complementary 16-mer oligodeoxiribonucleotide (5′-AGTGGTTGGTGTCGGG-3′), thus obtaining the corresponding double-stranded substrate, 16–30ds and 16–16ds respectively. The hybridization was performed in a 1:1 (mol/mol) ratio, with the substrate prepared in 20 mM Tris, by 5 min of incubation at 68 °C followed by 45 min at 37 °C. The exoribonucleolytic reactions were carried out in a final volume of 10 μl containing 30 nM substrate, 20 mM Tris/HCl (pH 8), 100 mM KCl, 1 mM $MgCl_2$ and 1 mM DTT (dithiothreitol). The amount of each enzyme added to the reaction is indicated in the respective Figures. Reactions were started by the addition of the enzyme and the mixtures incubated at 37 °C. Samples were withdrawn at the time points indicated in the Figures, and the reaction was stopped by adding formamide-containing dye supplemented with 10 mM EDTA. Reaction products were resolved in a 20 % polyacrylamide/7 M urea gel and analysed by autoradiography. The exoribonucleolytic activity of the enzymes was determined by measuring and quantifying the disappearance of the substrate in several distinct experiments in which the protein concentration was adjusted in order that, under those conditions, less than 25 % of substrate was degraded. Each value obtained represents the mean for these independent assays. The exoribonucleolytic activity of the wild-type enzymes was taken as 100 %.

SPR (surface plasmon resonance) analysis

Biacore SA chips were obtained from Biacore (GE Healthcare). The flow cells of the SA (streptavidin) sensorchip were coated with a low concentration of the following substrates. On flow cell 1, no substrate was added so this cell could be used as the control blank cell. On flow cell 2, a 5′-biotinylated 25-mer RNA oligomer (5′-CCCGACACCAACCACUAAAAAAAAA-3′) was added, and on flow cell 3, we added a 5′-biotinylated 30-mer poly(A) oligomer to allow the study of the protein interaction with different single-stranded RNA substrates. The target substrates were captured on flow cells 2 and 3 by manually injecting 20 μl of a 500 nM solution of the substrates in 1 M NaCl at a 10 μl/min flow rate, as described previously [28,29,34,35]. The biosensor assay was run at 4 °C in the buffer with 20 mM Tris/HCl (pH 8), 100 mM KCl, 1 mM DTT and 25 mM EDTA. The proteins were injected over flow cells 1, 2 and 3 for 2 min at concentrations of 10, 20, 30, 40 and 50 nM using a flow rate of 20 μl/min. All experiments included triple injections of each protein concentration to determine the reproducibility of the signal and control injections to assess the stability of the RNA surface during the experiment. Bound protein was removed with a 60 s wash with 2 M NaCl, which did not damage the substrate surface. Data from flow cell 1 were used to correct for refractive index changes and non-specific binding. Rate constants and equilibrium constants were calculated using the BIA EVALUATION 3.0 software package, according to the 1:1 Langmuir binding fitting model.

Multiple sequence alignment

Homologous sequences belonging to the to RNase II family of proteins in protein databases were obtained using BLAST [36] and they were aligned using ClustalW [37] and T-Coffee [38] algorithms.

RESULTS AND DISCUSSION

Asp^{280} is crucial for RNase R activity without affecting RNA-binding ability

The active site of RNase II has four conserved aspartate residues that are the responsible for positioning the RNA substrate correctly in order to promote the nucleophilic attack of the phosphodiester bond [26]. Previous studies have shown that, in this protein, Asp^{209} is a crucial residue for the catalytic activity without affecting RNA binding [30] and that this aspartate residue is the only one that is essential for the activity of RNase II [28]. Since this is a highly conserved residue in this family of enzymes (see Supplementary Figure S1 at http://www.BiochemJ.org/bj/423/bj4230291add.htm), we also mutated the correspondent amino acid in RNase R, Asp^{280}, to better understand the reaction mechanism of this exoribonuclease. For that, we introduced the point mutation D280N into the pABA-RNR [15], and overexpressed and purified the respective protein. The exoribonucleolytic activity of this mutant protein was analysed and compared with the wild-type enzyme by performing activity assays using different types of RNA substrates.

Wild-type RNase R is able to degrade single- and double-stranded RNA substrates releasing a 2 nt fragment as the shortest final end-product in both cases (Figure 2). In fact, the final end-product is a mixture of a 2 and 4 nt fragments (Figure 2). The structure of RNase II showed that, in the catalytic pocket, 5 nt of RNA were clamped between the aromatic residues Tyr^{253} and Phe^{358} [26]. Tyr^{253} is highly conserved and equivalent residues are present in all RNase II family members (see Supplementary Figure S1). However, in RNase R, the equivalent residue to Phe^{358} does not exist and that could be a possible explanation for the differences regarding the final end-product [28]. In RNase R, there is a phenylalanine residue (Phe^{429}) in the position immediately downstream of the equivalent residue (Phe^{358}) in RNase II (see Supplementary Figure S1). It is possible that some RNA fragments are still partially ‘clamped’ and therefore they

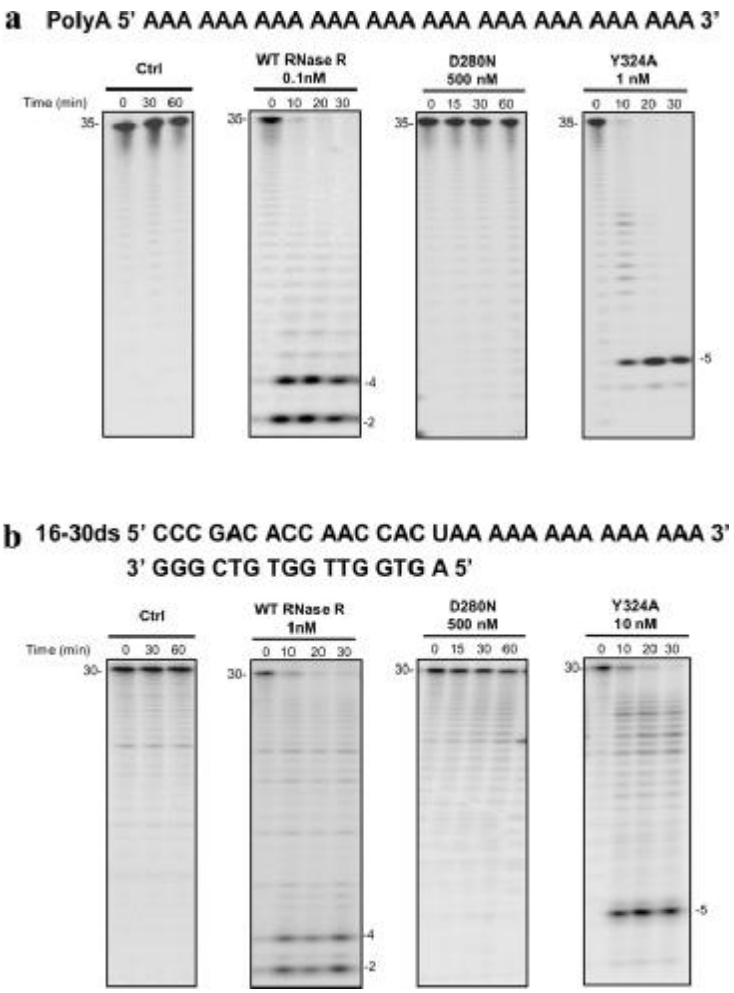

Figure 2 Exoribonuclease activity of RNase R wild-type and point mutant enzymes

Activity assays were performed as described in the Experimental section using a poly(A) chain of 35 nt (**a**) or a 30-mer oligoribonucleotide hybridized to the complementary 16-mer oligodeoxyribonucleotide, thus obtaining the corresponding double-stranded substrate 16–30ds (**b**). The wild-type enzyme (WT RNase R) was used for comparison. Samples were taken during the reaction at the time points indicated and reaction products were analysed in a 20% polyacrylamide/7 M urea gel. Control reactions with no enzyme added (Ctrl) were incubated at the maximum reaction time for each protein. Lengths of substrates and degradation products are indicated (in nt).

are released when they reach 4 nt. Others bind the catalytic cavity more efficiently and are able to be degraded up to a 2 nt fragment. This issue will be clarified when the RNase R crystal structure is solved. When the D280N mutant of RNase R was tested with both single- and double-stranded substrates, no activity was found (Figure 2), similarly to what happened with RNase II_D209N mutant [28,30]. Furthermore, we determined the exoribonucleolytic activity of wild-type RNase R and D280N mutant enzymes. Our results are consistent and confirm those obtained with the activity assays, i.e. the activity of D280N mutant is highly diminished when compared with the wild-type enzyme (Table 3). To determine the involvement of this residue in RNA binding, we calculated the dissociation constants of the wild-type and mutant proteins by SPR using two different RNA substrates, a 25-mer and a poly(A) oligomer. We observed that the binding ability of the protein is not affected by the presence of this mutation, since the D280N mutant presented a K_d value very similar to that of the wild-type RNase R protein with both substrates tested: 2.2 ± 0.3 nM with 25-mer and 1.3 ± 0.2 nM with poly(A) for D280N compared with 3.2 ± 0.4 nM with 25-mer and 1.2 ± 0.1 nM with poly(A) for RNase R (Table 4). These results confirm that, similarly to what happens with RNase II, this aspartate residue is indeed essential for the activity of RNase R without affecting RNA binding.

Table 3 Exoribonucleolytic activity of wild-type RNase R and point mutant enzymes

Exoribonucleolytic activity was assayed using a 35 nt poly(A) chain as substrate. Activity assays were performed in triplicate as described in the Experimental section

Enzyme	Enzyme activity (pmol · min^{-1} · $nmol^{-1}$)	Relative activity (%)
Wild-type RNase R	130.8 ± 6.3	100
D280N mutant	≪0.01	≪0.01
Y324A mutant	3.3 ± 0.2	2.5

Table 4 RNA-binding affinity of wild-type RNase R and point mutant enzymes

The dissociation constants (K_d) were determined by SPR using Biacore 2000 with a 25-nt RNA oligomer (5′-biotin-CCCGACACCAACCACUAAAAAAAAA-3′) and 30 nt poly(A) as substrates as described in the Experimental section

Enzyme	K_d 25-mer	Relative K_d 25-mer	K_d poly(A)	Relative K_d poly(A)
Wild-type RNase R	3.2 ± 0.4	1.0	1.2 ± 0.1	1.0
D280N mutant	2.2 ± 0.3	0.7	1.3 ± 0.2	1.1
Y324A mutant	20.4 ± 1.4	6.4	6.7 ± 0.3	5.6

In RNase R, the four aspartate residues in the active centre are located at positions 272, 278, 280 and 281, and, like Asp^{209} in RNase II, the equivalent Asp^{280} in RNase R may well be the only critical aspartate in this protein. Recent studies have shown that a mutation in Asp^{278} impairs RNase R activity, but the D278N mutant still retains 4 % of activity [39]. Moreover, we can say that this residue plays a crucial role in the activity of all the proteins of this family, since a mutation in the equivalent residue in RNase R of *Legionella pneumophila*, Asp^{283}, also led to the loss the exoribonucleolytic activity of the enzyme [40].

Tyr^{324} is responsible for setting the final end-product in RNase R

In RNase II, the RNA molecule is stacked and clamped between two aromatic residues, Tyr^{253} and Phe^{358} [26], and it was shown previously that Tyr^{253} is important for setting the final end-product of 4 nt. In the Y253A mutant, the final product released was a 10 nt fragment, which is the minimum length necessary for the RNA molecules to establish contacts between the catalytic and the anchoring regions simultaneously [28]. In RNase R, the equivalent tyrosine is at position 324 (see Supplementary Figure S1), and, in the present study, we wanted to see whether this residue also played such an important role in the mechanism of RNA degradation. For that purpose, we introduced the point mutation Y324A into the pABA-RNR plasmid [15] and purified the respective protein. The exoribonucleolytic activity was analysed with different RNA substrates and compared with the wild-type. As shown in Figure 2(a), the mutant Y324A is capable of degrading the poly(A) substrate, rendering a final product of 5 nt instead of the usual 2 nt observed for the wild-type. The same behaviour is observed when we used the double-stranded 16–30ds substrate (Figure 2b). After this last cleavage event, the resultant 5 nt fragment is no longer capable of establishing the necessary contacts with the protein in order achieve the cleavage of the substrate and is released. As such, and similarly to what was shown with Tyr^{253} in RNase II, using the Y324A mutant [28], the corresponding residue in RNase R, Tyr^{324}, is also responsible for the establishment of the final end-product of this protein. When we measured the activity of Y324A, we observed that it retains only 2.5 % of activity when compared with the wild-type (3.3 ± 0.2 and 130.8 ± 6.3 pmol · min^{-1} · $nmol^{-1}$ respectively) (Table 3), whereas, in RNase II, the equivalent mutation retained approx. 25 % of activity [28]. However, when we compared the dissociation constants (K_d values) obtained by SPR, the mutant presented a ∼6-fold reduction for both substrates tested (Table 4), a similar result to the one obtained for the Y253A mutant in RNase II [28]. These results suggest that the tyrosine residue in RNase R is also important for the binding of the RNA molecule at the 3′-end, but has a much more important function in the activity of the enzyme than in RNase II. This could be due to the fact that the second residue involved in the RNA clamping in RNase II, Phe^{358}, has no equivalent in RNase R, which can confer on Tyr^{324} a more important function in RNA clamping.

The RNB domain of RNase II has catalytic activity and is able to bind to RNA

When the *E. coli* RNase II structure was solved, it was possible to see that it is composed of four domains instead of the three initially proposed. This protein is formed by two CSDs at the N-terminal region, a central catalytic RNB domain and a S1 domain at the C-terminal region [26]. Before the RNase II structure was known, previous studies were performed with truncated RNase II proteins, where the ΔCSD and RNB mutants included the regions that corresponded to the CSD2 [14]. In the present study, we constructed the genuine ΔCSD1+2 and RNB mutants lacking both CSD1/CSD2 and CSD1/CSD2/S1 domains respectively (Figure 1). We then induced and purified the truncated RNase II proteins and performed activity assays using different substrates.

When we analysed the two truncated RNase II proteins regarding their ability to degrade the single-stranded poly(A) substrate, we observed that, like wild-type RNase II, both RNase II_ΔCSD1+2 and RNase II_RNB were able to degrade the substrate until it reaches 4 nt as a final end-product (Figure 3a). However, the activity of these truncated RNase II proteins is very diminished when compared with the wild-type enzyme, with RNase II_ΔCSD1+2 retaining only 0.03 % of the enzyme's activity and RNase II_RNB less than 0.01 % (Table 5). Taking into account that the two CSDs and S1 are the domains responsible for the RNA binding [14,26], we can clearly say that the loss of activity observed in these mutants is caused by the decrease in their ability to bind to the RNA molecule. The determination of the K_d values showed that these mutants are able to bind to RNA molecules less efficiently than the wild-type enzyme for both substrates tested. While RNase II presents a K_d value of 6.5 ± 0.4 and 1.3 ± 0.4 nM for the 25-mer and poly(A) substrate respectively [29], the absence of both CSDs causes a 4-fold increase in the K_d value, with RNase II_ΔCSD1+2 presenting K_d values of 24.1 ± 2.9 and 5.2 ± 0.6 nM for the 25-mer and poly(A) substrates respectively (Table 6). The absence of all of the RNA-binding domains of the protein is responsible for a more pronounced reduction in RNA affinity, with the RNase II_RNB protein presenting almost a 10-fold reduction in the K_d values when compared with the wild-type enzyme (Table 6).

When we analysed the activity using a double-stranded substrate, 16–30ds, we verified that RNase II_ΔCSD1+2 is able to degrade a few more nucleotides than the wild-type enzyme, releasing fragments of 20–22 nt compared with the 23–25 nt released by RNase II (Figure 3b). This suggests that this mutant can get closer to the double-stranded region, maybe because the absence of both domains results in less steric hindrance, and allows the better entrance of double-stranded molecules into the catalytic cavity. A similar result was obtained with the mutant lacking only the CSD1 [14]. However, when we

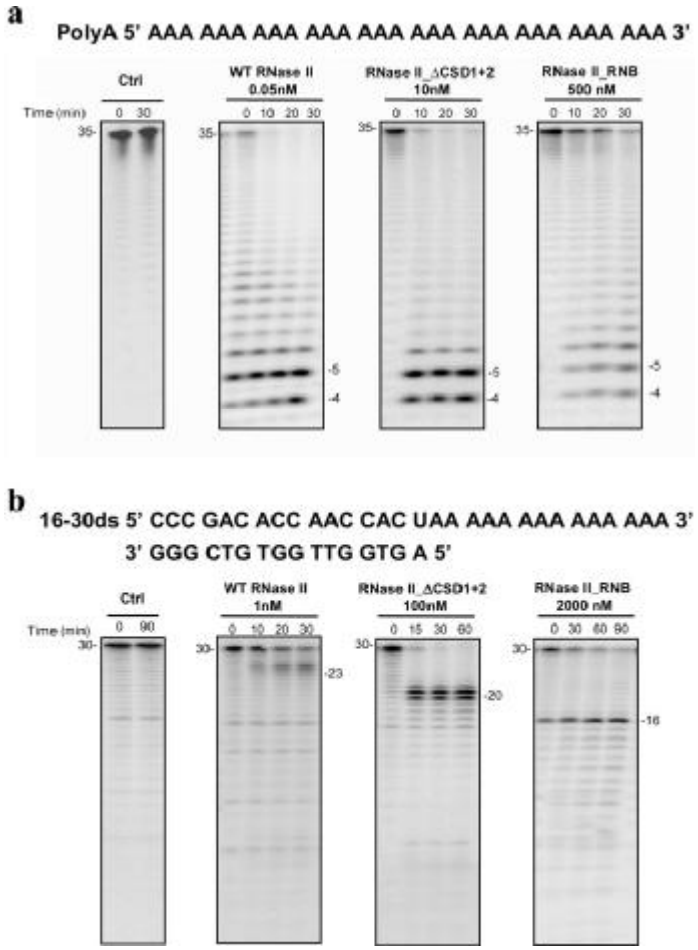

Figure 3 Exoribonuclease activity of wild-type and truncated RNase II enzymes

Activity assays were performed as described in the Experimental section using a poly(A) chain of 35 nt (**a**) or a 30-mer oligoribonucleotide hybridized to the complementary 16-mer oligodeoxyribonucleotide, thus obtaining the corresponding double-stranded substrate 16–30ds (**b**). The wild-type enzyme (WT RNase II) was used for comparison. Other details were as in Figure 2. Ctrl, control.

Table 5 Exoribonucleolytic activity of wild-type and truncated RNase II

Exoribonucleolytic activity was assayed using a 35 nt poly(A) chain as substrate. Activity assays were performed in triplicate as described in the Experimental section

Enzyme	Enzyme activity (pmol · min^{-1} · nmol^{-1})	Relative activity (%)
Wild-type RNase II	299.4 ± 36.0	100
RNase II_ΔCSD1+2	0.1 ± 0.01	0.03
RNase II_RNB	≪0.01	≪0.01

Table 6 RNA-binding affinity of wild-type and truncated RNase II

The dissociation constants (K_d) were determined by SPR using Biacore 2000 with a 25 nt RNA oligomer (5′-biotin-CCCGACACCAACCACUAAAAAAAAA-3′) and 30 nt poly(A) as substrates as described in the Experimental section

Enzyme	K_d 25-mer	Relative K_d 25-mer	K_d poly(A)	Relative K_d poly(A)
Wild-type RNase II	6.5 ± 0.4	1.0	1.3 ± 0.4	1.0
RNase II_ΔCSD1+2	24.1 ± 2.9	3.7	5.2 ± 0.6	4.0
RNase II_RNB	59.9 ± 6.0	9.2	11.7 ± 2.1	9.0

tested the same substrate with the RNase II_RNB mutant, we observed that it was capable of degrading all of the single-stranded 3′-overhang of the substrate. The reaction stopped when RNase II_RNB mutant reached the single-strand/double-strand junction and released a 16 nt blunt-ended fragment (Figure 3b). It is possible to see that the band that corresponds to the 16 nt fragment is to a small extent present in all reactions, even in

Table 7 Exoribonucleolytic activity of wild-type and truncated RNase R

Exoribonucleolytic activity was assayed using a 35 nt poly(A) chain as substrate. Activity assays were performed in triplicate as described in the Experimental section.

Enzyme	Enzyme activity (pmol · min^{-1} · nmol^{-1})	Relative activity (%)
Wild-type RNase R	130.8 ± 6.3	100
RNase R_ΔCSD1+2	0.2 ± 0.04	0.1
RNase R_ΔS1	0.02 ± 0.002	0.02
RNase R_RNB	≪0.01	≪0.01

Table 8 RNA-binding affinity of wild-type and truncated RNase R

The dissociation constants (K_d) were determined by SPR using Biacore 2000 with a 25 nt RNA oligomer (5′-biotin-CCCGACACCAACCACUAAAAAAAAA-3′) and 30 nt poly(A) as substrates as described in the Experimental section

Enzyme	K_d 25-mer	Relative K_d 25-mer	K_d poly(A)	Relative K_d poly(A)
Wild-type RNase R	3.2 ± 0.4	1.0	1.2 ± 0.1	1.0
RNase R_ΔCSD1+2	9.6 ± 1.4	3.0	3.1 ± 0.1	2.6
RNase R_ΔS1	5.4 ± 0.3	1.7	2.1 ± 0.2	1.8
RNase R_RNB	20.7 ± 2.8	6.5	7.4 ± 0.4	6.2

the control. However, since the intensity of the bands is clearly more pronounced in the RNase II_RNB mutant, and no other products are observed, this indicates that the substrate is being degraded. As such, we can say that the 16 nt product is the final one that is being released by the mutant. Previous studies have shown that wild-type RNase II has more difficulty in degrading the nucleotides adjacent to the double-stranded region [39]. Our results confirm that the RNA-binding channel formed by the CSDs and S1 domains in RNase II could be the initial barrier for the degradation of double-stranded substrates [14]. In fact, removal of the RNA-binding domains does allow RNase II to proceed further and the RNase II_RNB mutant protein is able to degrade all the way up to the double-stranded region.

The cleavage of double-stranded RNA is a property of the RNB domain of RNase R

The structural model of *E. coli* RNase R indicates that this protein shares a common three-dimensional arrangement with *E. coli* RNase II and both enzymes have the same domain organization [28]. However, RNase R has an additional HTH domain at the N-terminal region and a basic region after the S1 domain (Figure 1). It is already known that the CSDs and S1 domains of RNase II are involved in RNA binding and that RNB domain is responsible for the catalytic activity of the enzyme [14]. This modular domain organization has also been postulated for RNase R and the domains predicted to have the same function [28]. In order to confirm this hypothesis, we constructed truncated RNase R proteins which lack both CSDs and HTH and/or S1 domains as described in Figure 1.

In order to see the contribution of each domain to the activity and binding of the enzyme, we performed activity assays with a 35-mer poly(A) substrate, calculated the exoribonucleolytic activity and determined the K_d values.

RNase R is able to degrade single-stranded substrates, releasing a 2 nt fragment as the final end-product of the reaction [15] (Figure 4a). The same behaviour is observed for all the truncated proteins, RNase R_ΔCSD1+2, RNase R_ΔS1 and RNase R_RNB (Figure 4a). However, when we compared the activity of the different enzymes with the wild-type, it was possible to verify that all the truncated proteins analysed presented a significant decrease in their activity (Table 7). The absence of both CSDs in RNase R_ΔCSD1+2 protein causes a decrease of the activity of the enzyme more than 1000-fold, from 130.8 ± 6.3 to 0.2 ± 0.04 pmol · min^{-1} · nmol^{-1}. This reduction is more pronounced when the S1 domain is absent, with RNase R_ΔS1 presenting an activity of 0.02 ± 0.002 pmol · min^{-1} · nmol^{-1}. When only the RNB domain is present, the activity of the enzyme decreases more than 10000-fold, to values lower than 0.01 pmol · min^{-1} · nmol^{-1}. These results show that both the CSDs and the S1 domain are important for the activity of the enzyme, with the S1 domain having a more important role.

Since it is postulated that CSDs and the S1 domain are involved in RNA binding, the decrease in the activity observed in the truncated proteins can be due to a decrease in RNA-binding ability. To confirm this hypothesis, we determined the K_d values of each protein by SPR using two different substrates. In fact, all of the truncated proteins showed a decrease in their K_d values when compared with the wild-type enzyme for both substrates tested (Table 8). By analysing the K_d values obtained for the truncated proteins, it is possible to see that the CSDs are more important for the RNA binding when compared with the S1 domain. This is illustrated by the fact that the RNase R_ΔCSD1+2 protein presented a 3-fold reduction in its binding ability, whereas the absence of S1 domain was responsible for only a 2-fold reduction (Table 8). When the three domains are absent, the reduction in the ability to bind RNA molecules is much more significant, with RNase R_RNB protein presenting a K_d value of 20.7 ± 2.8 nM for the 25-mer substrate and 7.4 ± 0.4 nM for the poly(A) substrate, values that are approx. 6-fold higher than those described for RNase R (Table 8). In RNase R_ΔS1 protein, the reduction in the activity is more pronounced than that verified for the RNase R_ΔCSD1+2 (Table 7), whereas the dissociation constants obtained for both substrates tested are just 2-fold higher for this protein when compared with wild-type compared with 3-fold higher for the RNase R_ΔCSD1+2 protein. This result led us to conclude that the CSDs and the S1 domains have different roles in RNA binding. The CSDs must be more important for the recruitment of the substrate, whereas the S1 domain might help in the orientation and stabilization of the substrate in the catalytic cavity. It is interesting that the RNB domain is able to bind to RNA, although with a 6-fold decrease when compared with the wild-type. This also helps to explain the residual activity found in the RNase R_RNB protein.

As referred to above, RNase R is able to degrade the double-stranded substrate 16–30ds, releasing a final product of 2 nt (Figure 4b) [15]. When the truncated RNase R proteins were analysed with the same substrate, we verified that all of them were able to degrade it, releasing the characteristic 2 nt fragment (Figure 4b).

RNase R RNA-binding domains discriminate which RNA molecules will be targeted for degradation

It has been suggested that RNase R needs a single-stranded 3′-overhang at least 5 nt in length in order to degrade structured RNA molecules [41]. Then, cleavage occurs at the single-stranded 3′-overhang and proceeds processively in the 5′-direction, degrading the secondary structure [41,42]. To verify which domains are responsible for the 3′-overhang requirement in RNase R, we performed activity assays with the truncated RNase R proteins using a 16–16ds substrate (which lacks a 3′-overhang). As expected, wild-type RNase R is not able to degrade the blunt-ended substrate that was tested (Figure 4c). Previous reports

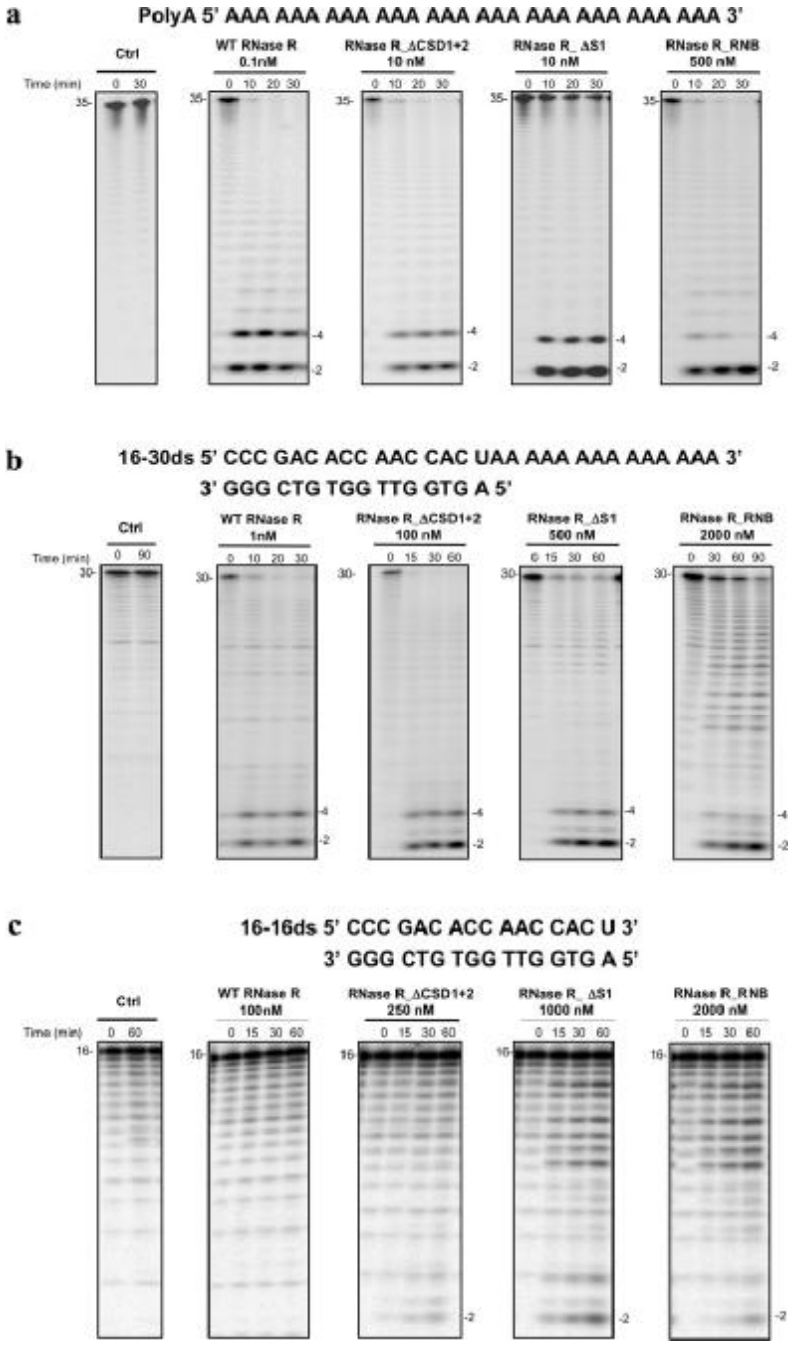

Figure 4 Exoribonuclease activity of wild-type and truncated RNase R enzymes

Activity assays were performed as described in the Experimental section using a poly(A) chain of 35 nt (**a**), a 30-mer oligoribonucleotide hybridized to the complementary 16-mer oligodeoxyribonucleotide, thus obtaining the corresponding double-stranded substrate 16–30ds (**b**) or a 16-mer oligoribonucleotide hybridized to the complementary 16-mer oligodeoxyribonucleotide, thus obtaining the corresponding double-stranded substrate 16–16ds (**c**). The wild-type enzyme (WT RNase R) was used as control. Other details were as in Figure 2. Ctrl, control.

have also shown that the enzyme is not capable of degrading other blunt-ended substrates, even using more extreme reaction conditions (i.e. higher concentrations of enzyme and longer incubation periods) [41]. Surprisingly, the absence of CSDs and/or the S1 domain resulted in the ability to degrade the 16–16ds substrate as shown in Figure 4(c). These results show that the binding domains (CSD1, CSD2 and S1) are blocking the entrance of the double-stranded substrates into the catalytic channel. In their absence, the substrate is free to enter into the catalytic cavity and cleavage can occur.

Together, these results show that the RNB domain of RNase R is sufficient for the activity of the enzyme. This domain is also capable of binding to RNA substrates, although with less efficiency, and this explains its decreased activity. The decrease in RNA affinity upon deletion of either the CSDs or the S1 domain confirms that these regions indeed function as RNA-binding domains. They are also responsible for the selective degradation of double-stranded substrates that contain a single-stranded 3′-overhang of five or more nucleotides. In fact, in both prokaryotes and eukaryotes, the RNAs targeted for degradation usually contain a short poly(A) tail [43]. In the case of RNase R, the presence of the binding domains is important for the degradation of only structured RNA molecules that have an overhang of at least 5 nt in length. This suggests that this protein is capable of degrading RNA molecules only when they are targeted to that purpose. As such, the discrimination of which molecules are targeted for decay is made by the CSD1, CSD2 and S1 domains.

In conclusion, the results of the present study provide an important breakthrough in the understanding of the RNase R mechanism of action. We have identified Tyr^{324} as being responsible for setting the final end-product as 5 nt, instead of the usual 2 nt observed for the wild-type RNase R. This residue is fully conserved in all domains of life and was proved to have the same function in RNase II. We have also shown that Asp^{280}, present in the RNase R active site, is crucial for the activity of the enzyme, but not for RNA binding.

We have demonstrated that RNB domains of RNase II and RNase R are able to degrade RNA, even in the absence of the RNA-binding domains. The most striking result is that, in contrast with the existing literature, the RNB domain of RNase R is sufficient for the degradation of double-stranded substrates even in the absence of a 3′-overhang. The RNA-binding domains present in the wild-type RNase R prevent the degradation of blunt double-stranded RNA molecules. The discrimination of which molecules will be susceptible to degradation by RNase R is made by CSD1, CSD2 and the S1 domains that target the degradation of RNAs that are 'tagged' by a 3′-tail. These results can have important implications for the study of poly(A)-dependent degradation mechanisms.

AUTHOR CONTRIBUTION

Rute G. Matos performed most of the experimental work, Ana Barbas contributed to the planning and execution of some experiments, and Cecília M. Arraiano co-ordinated the work described.

ACKNOWLEDGEMENT

We thank Miguel Luís for helping with the images.

FUNDING

R. G. M. was a recipient of a Ph.D. fellowship and A. B. was a recipient of a postdoctoral fellowship, both of them funded by FCT-Fundação para a Ciência e a Tecnologia, Portugal. This work was supported by FCT-Fundação para a Ciência e a Tecnologia, Portugal.

REFERENCES

1 Grossman, D. and van Hoof, A. (2006) RNase II structure completes group portrait of 3′ exoribonucleases. Nat. Struct. Mol. Biol. **13**, 760–761
2 Mian, I. S. (1997) Comparative sequence analysis of ribonucleases HII, III, II PH and D. Nucleic Acids Res. **25**, 3187–3195
3 Mitchell, P., Petfalski, E., Shevchenko, A., Mann, M. and Tollervey, D. (1997) The exosome: a conserved eukaryotic RNA processing complex containing multiple 3′ → 5′ exoribonucleases. Cell **91**, 457–466
4 Zuo, Y. and Deutscher, M. P. (2001) Exoribonuclease superfamilies: structural analysis and phylogenetic distribution. Nucleic Acids Res. **29**, 1017–1026
5 Cheng, Z. F., Zuo, Y., Li, Z., Rudd, K. E. and Deutscher, M. P. (1998) The vacB gene required for virulence in *Shigella flexneri* and *Escherichia coli* encodes the exoribonuclease RNase R. J. Biol. Chem. **273**, 14077–14080
6 Cheng, Z. F. and Deutscher, M. P. (2005) An important role for RNase R in mRNA decay. Mol. Cell **17**, 313–318
7 Cairrão, F. and Arraiano, C. M. (2006) The role of endoribonucleases in the regulation of RNase R. Biochem. Biophys. Res. Commun. **343**, 731–737
8 Cairrão, F., Cruz, A., Mori, H. and Arraiano, C. M. (2003) Cold shock induction of RNase R and its role in the maturation of the quality control mediator SsrA/tmRNA. Mol. Microbiol. **50**, 1349–1360
9 Andrade, J. M., Cairrão, F. and Arraiano, C. M. (2006) RNase R affects gene expression in stationary phase: regulation of *ompA*. Mol. Microbiol. **60**, 219–228
10 Dziembowski, A., Lorentzen, E., Conti, E. and Seraphin, B. (2007) A single subunit, Dis3, is essentially responsible for yeast exosome core activity. Nat. Struct. Mol. Biol. **14**, 15–22
11 Lebreton, A., Tomecki, R., Dziembowski, A. and Seraphin, B. (2008) Endonucleolytic RNA cleavage by a eukaryotic exosome. Nature **456**, 993–996
12 Schaeffer, D., Tsanova, B., Barbas, A., Reis, F. P., Dastidar, E. G., Sanchez-Rotunno, M., Arraiano, C. M. and van Hoof, A. (2009) The exosome contains domains with specific endoribonuclease, exoribonuclease and cytoplasmic mRNA decay activities. Nat. Struct. Mol. Biol. **16**, 56–62
13 Cheng, Z. F. and Deutscher, M. P. (2002) Purification and characterization of the *Escherichia coli* exoribonuclease RNase R: comparison with RNase II. J. Biol. Chem. **277**, 21624–21629
14 Amblar, M., Barbas, A., Fialho, A. M. and Arraiano, C. M. (2006) Characterization of the functional domains of *Escherichia coli* RNase II. J. Mol. Biol. **360**, 921–933
15 Amblar, M., Barbas, A., Gomez-Puertas, P. and Arraiano, C. M. (2007) The role of the S1 domain in exoribonucleolytic activity: substrate specificity and multimerization. RNA **13**, 317–327
16 Cannistraro, V. J. and Kennell, D. (1994) The processive reaction mechanism of ribonuclease II. J. Mol. Biol. **243**, 930–943
17 Andrade, J. M., Hajnsdorf, E., Regnier, P. and Arraiano, C. M. (2008) The poly(A)-dependent degradation pathway of *rpsO* mRNA is primarily mediated by RNase R. RNA **15**, 316–326
18 Andrade, J. M., Pobre, V., Silva, I. J., Domingues, S. and Arraiano, C. M. (2009) The role of 3′-5′ exoribonucleases in RNA degradation. Prog. Mol. Biol. Transl. Sci. **85**, 187–229
19 Cairrão, F., Chora, A., Zilhao, R., Carpousis, A. J. and Arraiano, C. M. (2001) RNase II levels change according to the growth conditions: characterization of *grr*, a new *Escherichia coli* gene involved in the modulation of RNase II. Mol. Microbiol. **39**, 1550–1561
20 Erova, T. E., Kosykh, V. G., Fadl, A. A., Sha, J., Horneman, A. J. and Chopra, A. K. (2008) Cold shock exoribonuclease R (VacB) is involved in *Aeromonas hydrophila* pathogenesis. J. Bacteriol. **190**, 3467–3474
21 Tobe, T., Sasakawa, C., Okada, N., Honma, Y. and Yoshikawa, M. (1992) *vacB*, a novel chromosomal gene required for expression of virulence genes on the large plasmid of *Shigella flexneri*. J. Bacteriol. **174**, 6359–6367
22 Tsao, M. Y., Lin, T. L., Hsieh, P. F. and Wang, J. T. (2009) The 3′-to-5′ exoribonuclease (encoded by HP1248) of *Helicobacter pylori* regulates motility and apoptosis-inducing genes. J. Bacteriol. **191**, 2691–2702
23 Deutscher, M. P. and Reuven, N. B. (1991) Enzymatic basis for hydrolytic versus phosphorolytic mRNA degradation in *Escherichia coli* and *Bacillus subtilis*. Proc. Natl. Acad. Sci. U.S.A. **88**, 3277–3280
24 Zilhão, R., Cairrão, F., Régnier, P. and Arraiano, C. M. (1996) PNPase modulates RNase II expression in *Escherichia coli*: implications for mRNA decay and cell metabolism. Mol. Microbiol. **20**, 1033–1042
25 Zilhão, R., Camelo, L. and Arraiano, C. M. (1993) DNA sequencing and expression of the gene rnb encoding *Escherichia coli* ribonuclease II. Mol. Microbiol. **8**, 43–51
26 Frazão, C., McVey, C. E., Amblar, M., Barbas, A., Vonrhein, C., Arraiano, C. M. and Carrondo, M. A. (2006) Unravelling the dynamics of RNA degradation by ribonuclease II and its RNA-bound complex. Nature **443**, 110–114

27 Zuo, Y., Vincent, H. A., Zhang, J., Wang, Y., Deutscher, M. P. and Malhotra, A. (2006) Structural basis for processivity and single-strand specificity of RNase II. Mol. Cell **24**, 149–156
28 Barbas, A., Matos, R. G., Amblar, M., Lopez-Viñas, E., Gomez-Puertas, P. and Arraiano, C. M. (2008) New insights into the mechanism of RNA degradation by ribonuclease II: identification of the residue responsible for setting the RNase II end product. J. Biol. Chem. **283**, 13070–13076
29 Barbas, A., Matos, R. G., Amblar, M., Lopez-Viñas, E., Gomez-Puertas, P. and Arraiano, C. M. (2009) Determination of key residues for catalysis and RNA-cleavage specificity: one mutation turns RNase II into a "super"-enzyme. J. Biol. Chem. **284**, 20486–20498
30 Amblar, M. and Arraiano, C. M. (2005) A single mutation in *Escherichia coli* ribonuclease II inactivates the enzyme without affecting RNA binding. FEBS J. **272**, 363–374
31 Schneider, C., Anderson, J. T. and Tollervey, D. (2007) The exosome subunit Rrp44 plays a direct role in RNA substrate recognition. Mol. Cell **27**, 324–331
32 Taylor, R. G., Walker, D. C. and McInnes, R. R. (1993) *E. coli* host strains significantly affect the quality of small scale plasmid DNA preparations used for sequencing. Nucleic Acids Res. **21**, 1677–1678
33 Studier, F. W. and Moffatt, B. A. (1986) Use of bacteriophage T7 RNA polymerase to direct selective high-level expression of cloned genes. J. Mol. Biol. **189**, 113–130
34 Arraiano, C. M., Barbas, A. and Amblar, M. (2008) Characterizing ribonucleases *in vitro*: examples of synergies between biochemical and structural analysis. Methods Enzymol. **447**, 131–160
35 Park, S., Myszka, D. G., Yu, M., Littler, S. J. and Laird-Offringa, I. A. (2000) HuD RNA recognition motifs play distinct roles in the formation of a stable complex with AU-rich RNA. Mol. Cell. Biol. **20**, 4765–4772
36 Altschul, S. F., Madden, T. L., Schaffer, A. A., Zhang, J., Zhang, Z., Miller, W. and Lipman, D. J. (1997) Gapped BLAST and PSI-BLAST: a new generation of protein database search programs. Nucleic Acids Res. **25**, 3389–3402
37 Thompson, J. D., Higgins, D. G. and Gibson, T. J. (1994) CLUSTAL W: improving the sensitivity of progressive multiple sequence alignment through sequence weighting, position-specific gap penalties and weight matrix choice. Nucleic Acids Res. **22**, 4673–4680
38 Notredame, C., Higgins, D. G. and Heringa, J. (2000) T-Coffee: a novel method for fast and accurate multiple sequence alignment. J. Mol. Biol. **302**, 205–217
39 Vincent, H. A. and Deutscher, M. P. (2009) The roles of individual domains of RNase R in substrate binding and exoribonuclease activity: the nuclease domain is sufficient for digestion of structured RNA. J. Biol. Chem. **284**, 486–494
40 Charpentier, X., Faucher, S. P., Kalachikov, S. and Shuman, H. A. (2008) Loss of RNase R induces competence development in *Legionella pneumophila*. J. Bacteriol. **190**, 8126–8136
41 Vincent, H. A. and Deutscher, M. P. (2006) Substrate recognition and catalysis by the exoribonuclease RNase R. J. Biol. Chem. **281**, 29769–29775
42 Worrall, J. A. R. and Luisi, B. F. (2007) Information available at cut rates: structure and mechanism of ribonucleases. Curr. Opin. Struct. Biol. **17**, 128–137
43 Houseley, J., LaCava, J. and Tollervey, D. (2006) RNA-quality control by the exosome. Nat. Rev. **7**, 529–539

Received 10 June 2009/14 July 2009; accepted 27 July 2009
Published as BJ Immediate Publication 27 July 2009, doi:10.1042/BJ20090839

Biochem. J. (2009) **423**, 291–301 (Printed in Great Britain) doi:10.1042/BJ20090839

Online data

SUPPLEMENTARY ONLINE DATA

RNase R mutants elucidate the catalysis of structured RNA: RNA-binding domains select the RNAs targeted for degradation

Rute Gonçalves MATOS, Ana BARBAS and Cecília Maria ARRAIANO[1]

Instituto de Tecnologia Química e Biológica/Universidade Nova de Lisboa, Apartado 127, 2781-901 Oeiras, Portugal

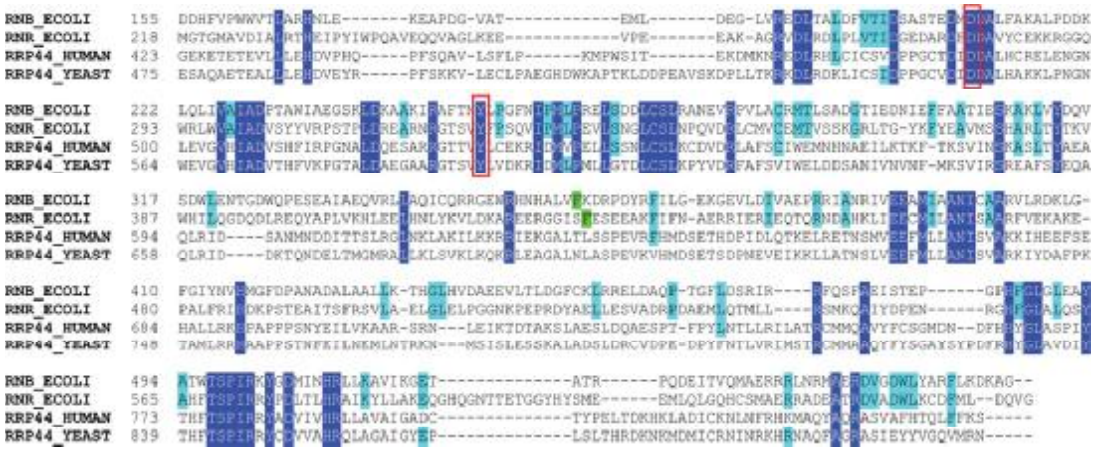

Figure S1 Sequence alignment of RNB domains from RNase II, RNase R, human Rrp44 and yeast Rrp44

Residues highlighted in dark blue are fully conserved in all domains of life and residues highlighted in light blue are conserved in prokaryotes. The aspartate and tyrosine residues studied are boxed in red. Phe[358] from RNase II and Phe[429] from RNase R are highlighted in green.

Received 10 June 2009/14 July 2009; accepted 27 July 2009
Published as BJ Immediate Publication 27 July 2009, doi:10.1042/BJ20090839

[1] To whom correspondence should be addressed (email cecilia@itqb.unl.pt).

THE JOURNAL OF BIOLOGICAL CHEMISTRY VOL. 284, NO. 31, pp. 20486–20498, July 31, 2009

Determination of Key Residues for Catalysis and RNA Cleavage Specificity

ONE MUTATION TURNS RNase II INTO A "SUPER-ENZYME"[*] [S]

Received for publication, November 14, 2008, and in revised form, May 13, 2009 Published, JBC Papers in Press, May 19, 2009, DOI 10.1074/jbc.M109.020693

Ana Barbas[‡1,2], **Rute G. Matos**[‡1,3], **Mónica Amblar**[§], **Eduardo López-Viñas**[¶‖], **Paulino Gomez-Puertas**[‖], **and Cecília M. Arraiano**[‡4]

From the [‡]*Instituto de Tecnologia Química e Biológica/Universidade Nova de Lisboa, 2781-901 Oeiras, Portugal, the* [§]*Centro Nacional de Microbiología, Instituto de Salud Carlos III, 28029 Madrid, Spain, the* [¶]*CIBER "Fisiopatología de la Obesidad y la Nutrición" (CB06/03), Instituto de Salud Carlos III, 28029 Madrid, Spain, and the* [‖]*Centro de Biologia Molecular "Severo Ochoa," 28049 Madrid, Spain*

RNase II is the prototype of a ubiquitous family of enzymes that are crucial for RNA metabolism. In *Escherichia coli* this protein is a single-stranded-specific 3′-exoribonuclease with a modular organization of four functional domains. In eukaryotes, the RNase II homologue Rrp44 (also known as Dis3) is the catalytic subunit of the exosome, an exoribonuclease complex essential for RNA processing and decay. In this work we have performed a functional characterization of several highly conserved residues located in the RNase II catalytic domain to address their precise role in the RNase II activity. We have constructed a number of RNase II mutants and compared their activity and RNA binding to the wild type using different single- or double-stranded substrates. The results presented in this study substantially improve the RNase II model for RNA degradation. We have identified the residues that are responsible for the discrimination of cleavage of RNA *versus* DNA. We also show that the Arg-500 residue present in the RNase II active site is crucial for activity but not for RNA binding. The most prominent finding presented is the extraordinary catalysis observed in the E542A mutant that turns RNase II into a "super-enzyme."

Exoribonuclease II (RNase II)[5] is one of the major exoribonucleases involved in the degradation of RNA (1). This protein degrades RNA hydrolytically in the 3′ to 5′ direction, releasing 5′-nucleotide monophosphates in a processive manner. Its activity is sequence independent but sensitive to secondary structures, and poly(A) is the preferential substrate for this enzyme (2–6). In *Escherichia coli* RNase II is responsible for 90% of the hydrolytic activity in crude extracts (7). Moreover, its expression is differentially regulated at the transcriptional and post-transcriptional levels (8–10), and the protein can be regulated by environmental conditions (10). The *E. coli* enzyme is the prototype of a widespread family of exoribonucleases, and RNase II homologues can be found in prokaryotes and eukaryotes (11). In the nucleus and in the cytoplasm of eukaryotic cells, RNase II homologues (Rrp44/Dis3) are part of the exosome, an essential multiprotein complex of exoribonucleases involved in processing, turnover, and quality control of different types of RNAs (12). Rrp44 is the only catalytically active nuclease in the human and yeast core exosome (13, 14). Moreover, it was recently demonstrated that apart from the RNB catalytic domain, Rrp44p has a second nuclease domain, the PINc domain, that confers endonucleolytic activity to the protein (15, 16). In prokaryotic cells, apart from RNase II, there is an additional RNase II-like enzyme, RNase R, that is involved in RNA degradation and RNA and protein quality control (17–20). RNase R has also been shown to be required for virulence (21).

The determination of *E. coli* RNase II structure (22–24) showed that, contrary to the sequence predictions, RNase II consisted of four domains; they are two N-terminal cold shock domains (CSD1 and CSD2) involved in RNA binding, one central RNB catalytic domain, and a third RNA binding domain at the C terminus, the S1 domain (Fig. 1*A*). Inside RNase II the RNA contacts the enzyme at two different and non-contiguous regions, the anchoring region (formed by the three RNA binding domains) and the catalytic region (buried inside the catalytic domain) (22, 25). The shortest RNA molecule able to retain contacts with these two regions simultaneously is a 10-nucleotide fragment, and this is also the minimum length necessary to maintain the processivity of the enzyme (22, 25, 26). Therefore, simultaneous binding of substrate to both sites is necessary for a processive degradation. Moreover, the structure of the RNA-bound complex revealed a tight packing of the five 3′-terminal nucleotides in the catalytic cavity, mediated by the conserved aromatic residues Tyr-253 and Phe-358 (22). When the RNA substrate is shorter than 5 nucleotides the required packing of the bases can no longer occur, impeding the translocation of the RNA and generating the typical 4-nt frag-

* The work was supported by Ministerio de Educación y Ciencia, Spain, Grant SAF2007-61926, an institutional grant from the "Fundación Ramón Arecesm," and by Fundação para a Ciência e a Tecnologia, Portugal.
[S] The on-line version of this article (available at http://www.jbc.org) contains supplemental Figs. S1 and S2.
[1] These authors contributed equally to this work.
[2] Recipient of a post-doctoral fellowship from the Fundação para a Ciência e a Tecnologia, Portugal.
[3] Recipient of a Ph.D. fellowship from the Fundação para a Ciência e a Tecnologia, Portugal.
[4] To whom correspondence should be addressed: Instituto de Tecnologia Química e Biológica/Universidade Nova de Lisboa, Apartado 127, 2781-901 Oeiras, Portugal. Tel.: 351-214469547; Fax: 351-214469549; E-mail: cecilia@itqb.unl.pt.
[5] The abbreviations used are: RNase, ribonuclease; CSD, cold shock domain; RNB, RNase II catalytic domain; MD, molecular dynamics; WT, wild type; nt, nucleotide(s).

ment as the end-product for RNase II. A mutational analysis of *E. coli* RNase II has been reported (26), confirming the crucial role of Tyr-253 in setting the end-product of RNase II degradation. In addition, this analysis showed that conserved acidic residues in the active site can have a different role during the degradation mechanism (26).

RNase II is specific for RNA. However, although it does not degrade DNA, it is still able to bind it. DNA oligonucleotides have been shown to act as reaction inhibitors of the *E. coli* RNase II, suggesting that both DNA and RNA compete for the same binding sites of the enzyme (25). Previous reports have demonstrated that the ribose specificity of RNase II is not for the scissile bond but for the nearby nucleotides (22, 25). The presence of a ribose between positions 2 through 5 from the 3′-end of the RNA substrate is required for cleavage to occur (25). The crystal structure of the RNase II-RNA-bound complex (22) revealed direct contacts between the residues Asp-201, Tyr-313, and Glu-390 and the O2′ ribose oxygens of nucleotides in positions 2, 4, and 6 (Fig. 1*B*). Such interactions seem to be responsible for the proper orientation of the RNA at the catalytic cavity and may account for the specificity of RNA *versus* DNA in RNase II.

Structural data also revealed that there are two other conserved residues at the active site that seem to be crucial for RNase II activity, Arg-500 and Glu-542 (22). In the RNA-complexed structure, the Arg-500 is positioned between the two nucleotides at the 3′-end interacting with their phosphate backbones (Fig. 1*B*). It was postulated that Arg-500 could assist in catalysis by fixing the phosphodiester bond at the cleavage position and enhancing the susceptibility of the leaving phosphorous atom to a nucleophilic attack (22). Glu-542 is in close proximity to the nitrogen atoms of the leaving nucleotide (Fig. 1*B*) and was suggested to facilitate the elimination of this nucleotide upon phosphor-ester cleavage by pulling it out of the base-stacked position (22).

In this report we analyze the role of some of these highly conserved amino acids in RNase II activity. We studied the function of Asp-201, Tyr-313, and Glu-390 in the cleavage discrimination of RNA *versus* DNA. Our results showed that only Tyr-313 and Glu-390 are crucial for RNA specificity of RNase II. We also demonstrate that Arg-500 is essential for RNase II activity, but it is not involved in RNA binding. Moreover, the most prominent findings presented are the extraordinary catalysis and binding abilities observed in the E542A mutant that turns RNase II into a super-enzyme.

EXPERIMENTAL PROCEDURES

Materials—Restriction enzymes, T4 DNA ligase, *Pfu* DNA polymerase, and T4 polynucleotide kinase were purchased from Fermentas. Unlabeled oligonucleotide primers were synthesized by STAB Vida, Portugal.

Strains—The *E. coli* strains used were DH5α (F′ *fhuA2* Δ(*argF-lacZ)U169 phoA glnV44* Φ*80* Δ(*lacZ)M15 gyrA96 recA1 relA1 endA1 thi-1 hsdR17*a) (27) for cloning experiments and BL21(DE3) ($F^- r_B^- m_B^-$ *gal ompT* (*int*::P_{lacUV5} *T7 gen1 imm21 nin5*) (28) for expression and purification of enzymes.

Construction of RNase II Mutants by PCR Overlapping—The point mutations Y313F, Y313A, E390A, R500K, R500A, and E542A, the double mutations D201N/Y313F, D201N/E390A, and Y313F/E390A, and the triple mutation D201N/Y313F/E390A were introduced into pFCT6.9 (10) or in the pFCT6.9/D201N (26) by PCR overlapping (29).

The primers used in this study were the following (base changes are indicated in small letters): forward primer Y313Fa, 5′-GCAAAGCTtGTGTtTGACCAGGTTTCT-GAC-3′, and reverse primer Y313Fb; 5′-GTCAGAAACCTG-GTCAaACACaAGCTTTGC-3′; forward primer, Y313Aa, 5′-GCAAAGCTtGTGgcTGACCAGGTTTCTGAC-3′, and reverse primer, Y313Ab; 5′-GTCAGAAACCTGGTCAgcC-ACaAGCTTTGC-3′, forward primer, E390Aa, 5′-CCAAC-CGTATCGTCGctGAAGCGATGATTGCC-3′, and reverse primer, E390Ab, 5′-GGCAATCATCGCTTCagCGACGAT-ACGGTTGG-3′; forward primer, R500Ka, 5′-CCACCTGG-ACgTCGCCGATCaagAAATATG-3′, and reverse primer, R500Kb, 5′-CATATTTcttGATCGGCGAcGTCCAGGTGG-3′; forward primer, R500Aa, 5′-CGCCACCTGGACTTCGCC-GATCgcTAAATA-3′, and reverse primer, R500Ab, 5′-CCATA-TTTAgcGATCGGCGAAGTCCAGGTG-3′; forward primer, E542Aa, 5′-CGCCGgCTCAACCGGATGGCAGcACGTGAT-GTT-3′, and reverse primer, E542Ab, 5′-AACATCACGTgCTG-CCATCCGGTTGAGcCGGCG-3′. All mutant constructs were confirmed by DNA sequencing at STAB Vida, Portugal.

Overexpression and Purification of Wild Type RNase II and Mutants—The plasmid used for expression of wild-type *E. coli* histidine-tagged RNase II protein was pFCT6.9 plasmid (10). This plasmid contains the *rnb* gene cloned into pET-15b vector (Novagen) under the control of φ10 promoter, allowing the expression of the His_6-tagged RNase II fusion protein.

All other plasmids bearing mutations were transformed into BL21(DE3) *E. coli* strain (Novagen) to allow the expression of the recombinant proteins. Cells were grown at 37 °C in 100 ml of LB medium supplemented with 150 μg/ml ampicillin to an A_{600} of 0.45 and then induced for 2 h by addition of 1 mM isopropyl 1-thio-β-D-galactopyranoside. Cell cultures were pelleted by centrifugation and stored at −80 °C.

Purification of all proteins was performed by histidine affinity chromatography using HiTrap Chelating HP columns (GE Healthcare) and the AKTA fast protein liquid chromatography system (GE Healthcare) following the protocol previously described (30, 31). Briefly, cell suspensions were lysed using a French press at 9000 p.s.i. in the presence of 0.1 mM phenylmethylsulfonyl fluoride. The crude extracts were treated with Benzonase (Sigma) to degrade the nucleic acids and clarified by a 30-min centrifugation at 10,000 × *g*. The clarified extracts were then added to a HiTrap chelating-Sepharose 1-ml column equilibrated in buffer A (20 mM Tris-HCl, 0.5 M NaCl, pH 8, 20 mM imidazole and 2 mM β-mercaptoethanol). Protein elution was achieved by a continuous imidazole gradient (from 20–500 mM) in buffer A. The fractions containing the purified protein were pooled together, and buffer was exchanged to buffer B (20 mM Tris-HCl, pH 8, 100 mM KCl, and 2 mM β-mercaptoethanol) using a desalting 5-ml column (GE Healthcare). Eluted proteins were concentrated by centrifugation at 15 °C with Amicon Ultra Centrifugal Filter Devices of 30,000 molecular weight cutoff (Millipore). Protein concentration was deter-

mined by spectrophotometry, and 50% (v/v) glycerol was added to the final fractions before storage at −20 °C. 0.5 μg of each purified protein was applied in a 8% SDS-PAGE and visualized by Coomassie Blue staining (Fig. 1*C*).

Activity Assays—Exoribonucleolytic activity was assayed using different RNA oligoribonucleotides as substrates (30): a poly(A) chain of 35 nt as a single-stranded substrate, a 30-mer oligoribonucleotide (5′-CCCGACACCAACCACUAAAAAA-AAAAAAAA-3′) annealed to the complementary 16-mer oligodeoxyribonucleotide (5′-AGTGGTTGGTGTCGGG-3′) as a double-stranded substrate with a 3′-single-stranded extension, and the DNA-RNA chimeric substrates Chi1 (5′-dTdTdTdTdTdTdTdTdTdTdTrCrCdTdT-3′) and Chi2 (5′-dTdTdT dTdTdTdTdTdTdTdTrCdTrCdT-3′). All the oligoribonucleotides were labeled at the 5′-end with [γ-^{32}ATP] and T4 polynucleotide kinase and further purified with Microcon YM-3 Centrifugal Filter Devices (Millipore) to remove the non-incorporated nucleotides. The hybridization between 30-mer and 16-mer oligomers was performed in a 1:1 (mol:mol) ratio in the Tris component of the activity by 5 min of incubation at 68 °C followed by 45 min as room temperature. The exoribonucleolytic reactions were carried out in a final volume of 10 μl containing 30 nM concentrations of substrate, 20 mM Tris-HCl, pH 8, 100 mM KCl, 1 mM $MgCl_2$, and 1 mM dithiothreitol. The amount of each enzyme added to the reaction was adjusted to obtain linear conditions and is indicated in the respective figures (Figs. 2–4). Reactions were started by the addition of the enzyme and incubated at 37 °C. Samples were withdrawn at the time points indicated in the figures (Figs. 2–4), and the reaction was stopped by adding formamide-containing dye supplemented with 10 mM EDTA. Reaction products were resolved in a 20% polyacrylamide, 7 M urea and analyzed by autoradiography. Autoradiograms were scanned, and the densities of the bands were quantified using ImageQuant 5.0 software. The exoribonucleolytic activity of the enzymes was determined by measuring and quantifying the disappearance of the substrate from gels in several distinct experiments, and each value obtained represents the mean of at least three independent assays. The specific activity of each enzyme is given as the nmol of substrate consumed/min/nmol of protein at 37 °C. Results obtained are shown in Table 1.

Formal Kinetic Analysis—To determine the 3′-5′ exoribonuclease rates of the WT and the E542A mutant, the reactions were carried out in 20 mM Tris-HCl, pH 8, 100 mM KCl, 1 mM $MgCl_2$, and 1 mM dithiothreitol using the 35-nt poly(A) RNA oligonucleotide as a substrate. Preliminary assays (not shown) showed that product formation proceeded linearly at the protein concentrations and for the incubation times used in the experiments reported here. As such, the protein activities were measured at the following substrate concentrations: 10, 25, 50, 100, 150, 200, 250 and 300 nM. The protein concentrations used were 5 pM and 0.1 fM for the WT and the E542A mutant, respectively. The reactions were carried out at 37 °C for 2 min with these protein concentrations as under these conditions less than 20% of substrate was degraded. Reactions were stopped by adding formamide-containing dye supplemented with 10 mM EDTA. Reaction products were resolved in a 20% polyacrylamide, 7 M urea and analyzed by autoradiography. Autoradiograms were scanned, and the densities of the bands were quantified using ImageQuant 5.0 software. The amount of product was calculated by using the original substrate concentration and the final ratio of remaining substrate and product formed. Lineweaver-Burk plots (32) were used to estimate kinetic parameters: K_m, V_{max}, and k_{cat}. Each value obtained represents the mean of at least three independent assays, and the S.D. was calculated from these data sets.

Surface Plasmon Resonance Analysis-BIACORE—Biacore SA chips were obtained from Biacore Inc. (GE Healthcare). The flow cells of the SA streptavidin sensor chip were coated with a low concentration of the following substrates. On flow cell 1 no substrate was added so this cell could be used as the control blank cell. On flow cell 2 a 5′-biotinylated 25-nucleotide RNA oligomer (5′-CCCGACACCAACCACUAAAAAAAAA-3′) was added to allow the study of the protein interaction with a single-stranded RNA molecule. On flow cell 3 a 5′-biotinylated 16-nucleotide DNA oligomer (5′-AGTGGTTGGTGTCGGG-3′) was added to allow the study of the protein interaction with a single-stranded DNA molecule. On flow cell 4 a 5′-biotinylated 35-nucleotide poly(A) oligomer was added to allow the study of the protein interaction with a single-stranded RNA molecule composed only of adenosines. The target RNA and DNA substrates were immobilized on flow cells 2 and 3 by injecting 20 μl of a 500 nM solution of the target RNA or DNA in 1 M NaCl at a 10 μl/min flow rate as described in previous reports (31, 33). The biosensor assay was run at 4 °C in 20 mM Tris-HCl, pH 8, 100 mM KCl, 1 mM dithiothreitol, and 25 mM EDTA. The proteins were injected over the flow cells for 2 min at concentrations of 10, 20, 30, 40, and 50 nM using a flow rate of 20 μl/min. All experiments included triple injections of each protein concentration to determine the reproducibility of the signal and control injections to assess the stability of the RNA or DNA surface during the experiment. Bound protein was removed with a 60-s wash with 2 M NaCl, which did not damage the substrate surface. Data from flow cell 1 were used to correct for refractive index changes and nonspecific binding. Rate constants and equilibrium constants were calculated using the BIA EVALUATION 3.0 software package according to the fitting model 1:1 Languimir binding.

Modeling of Wild-type RNase II and E542A Mutant—Using standard comparative modeling methods and the software DeepView (34), three-dimensional models of wild-type *E. coli* RNase II (RNB/ECOLI) and E542A mutant proteins were built up from the x-ray structure (PDB code 2IX1 (22)) of RNase II D209N mutant complexed with a 13-nt poly(A) RNA.

Molecular Dynamics (MD) Simulation of the E542A Mutant and RNase II Models Based on the 2ix1 Structure—To obtain a fine-grained theoretical model of wild-type RNase II and E542A mutant enzymes bound to a 13-nt poly(A) RNA, a 4-ns MD simulation was performed. To readjust side chains and domain conformations, the recreation was calculated using the PMEMD module of the AMBER9 package (35, 36) and the *parm99* parameter set from this distribution. Dynamically stabilized 2IX1 crystal structure model of RNase II in complex with RNA described elsewhere (26) was taken into consideration for subsequent molecular dynamics trajectory analyses. The details on MD methodology applied to the models were described (26).

MD Models of the Wild-type RNase II and E542A Mutant Proteins Bound to RNA—Theoretical models of RNase II wild-type and E542A mutant enzymes bound to a 13-nt poly(A) RNA were, respectively, built up from an energy-minimized average structure of the stabilized molecular dynamics simulation of the x-ray structure of RNase II D209N mutant complexed with a 13-nt poly(A) RNA (PDB code 2IX1 (22)), previously published (26). To obtain biophysically consistent models, 4-ns MD simulations were performed with each model. Calculations were done by using the PMEMD module and the *parm*99 parameter set in the AMBER9 package (35, 37, 38). MD simulations of both RNase II systems included the four RNase II domains (CSD1, CSD2, RNB, and S1), the RNA molecule, and the magnesium atom of the active center reported in the real structure of D209N mutant. To neutralize the electrostatic charge of the system, Na^+ counterions were placed in a shell around the system using a grid of coulombic potentials. Electrostatically neutralized complexes where then embedded in a truncated octahedron solvation box, keeping a distance of 12 Å between the limits of the box and the closest atom of the solute. Both counterions and solvent were added using the LEAP module in AMBER9. Initial relaxation of each complex was completed by performing 10,000 steps of energy minimization with a cut-off of 10.0 Å. Initial heating and equilibration were performed simultaneously by raising the temperature in two stages; a first one from 0 to 5 K to induce a slow adaptation of the system to the force field represented in parm99 and a second up to 298 K in 200-ps continuous heating phases. During this procedure stage velocities were reassigned at each new temperature according to the Maxwell-Boltzmann distribution, and positions of the Cα and P atoms of the solute were constrained with a force constant of 20 Kcal·mol^{-1} to impede spurious disorganizations of protein and RNA backbone structures. During the last 100 ps of the equilibration phase of the MD, the force constant was reduced stepwise down to 0 for all constrained atoms to progressively allow the stabilization of the system. Consecutively, a MD simulation of 4 ns over the complete systems was completed.

RESULTS

Comparing the Exoribonucleolytic Activity of the Different Mutant Proteins—E. coli RNase II is the prototype of the RNase II superfamily of exoribonucleases, and this protein has shown to be a good study model for all family members, as they share a similar mode of action (15, 26, 39–41). To better understand the reaction mechanism of *E. coli* RNase II and the processes underlying the specificity of RNA cleavage, we constructed a set of single, double, and triple mutants of RNase II and studied their effect in RNA binding and in catalytic activity. We introduced the following point mutations in RNase II: Y313F, Y313A, E390A, R500A, R500K, and E542A, the double mutations D201N/Y313F, D201N/E390A, and Y313F/E390A, and the triple mutation D201N/Y313F/E390A. All these mutant proteins were introduced in *E. coli* BL21(DE3) and were overproduced by isopropyl 1-thio-β-D-galactopyranoside induction. The optimal induction conditions were standardized for each mutant by analysis of protein production and solubility at different times of isopropyl 1-thio-β-D-galactopyranoside treatment. All the mutants were shown to be more than 80% soluble after induction, except for R500K, which was mainly in the insoluble fraction (data not shown). All the mutant proteins, with the exception of R500K were, purified (Fig. 1*C*) as described under "Experimental Procedures." The exoribonucleolytic activity of the purified mutant proteins was analyzed and compared with the wild type by performing activity assays using two different types of RNA substrates as described under "Experimental Procedures."

As previously demonstrated, the wild-type enzyme was able to degrade the single-stranded RNA substrate, and the end-product was a 4-nt fragment (26, 42) (Fig. 2). With the R500A mutant the shortest product observed was a 11 nt, even with 1000 nM concentration after a 30-min reaction. The double mutant D201N/Y313F was only able to degrade a few nucleotides in the conditions tested (1000 nM concentration of protein in a 30-min reaction). Previous reports had shown that D201N mutant accumulated a 10–11-nt fragment as a major degradation product, although longer reaction times resulted in the usual 4-nt fragment as a secondary product (26). This is probably because of a higher dissociation rate of RNA fragments shorter than 11 nt. A similar behavior was also observed for the double D201/E390A and triple D201N/Y313F/E390A mutants, which confirm the important role played by Asp-201 in the RNase II activity. Y313F, Y313A, Y313F/E390A, and E542A generated a 4-nt fragment like wild-type RNase II (Fig. 2). In the conditions tested (1 nM concentrations of protein in a 10-min reaction), the E390A mutant was able to degrade the substrate until it reached a 6-nt fragment (Fig. 2). However, in more extreme conditions (*i.e.* longer reaction times and/or higher enzyme concentrations) the mutant was also able to reach the typical final end-product of 4 nt (data no shown).

When the substrate tested was a double-stranded molecule with a 3′-single-stranded extension (16–30ds), the wild-type enzyme degraded the single-stranded portion, generating 23–25-nt oligomers (30). This shows that the enzyme stalls 7–9 nt before reaching the double-stranded region (30, 42) (Fig. 3). Similarly, most of the mutant enzymes rendered products ranging between 21 and 25 nt in length behaving like the wild-type does against secondary structures. The D201N, D201N/E390A, and R500A mutants, however, generated longer products than the wild type, with 26–27 nt in length. The E542A mutant was able to go closer to the double-stranded portion of the RNA, rendering a 19-nt product.

The exoribonucleolytic activity of wild-type and mutant enzymes was determined by measuring the substrate disappearance from the activity gels (Table 1). The results obtained suggested that although fully conserved in all domains of life, Glu-390 is not essential for RNase II catalysis because the activity of E390A was very similar to that of the wild-type enzyme (0.30 and 0.36 nmol·min^{-1}·nmol^{-1} for the wild-type and E390A mutant, respectively) (Table 1). In the case of Tyr-313, its substitution by Phe did not alter the enzymatic activity, whereas its replacement by an Ala resulted in a 100-fold reduction (Table 1). These observations imply that the aromatic moiety of Tyr-313, but not the hydroxyl group, is important for the maintenance of the enzymatic activity. Accordingly, the exori-

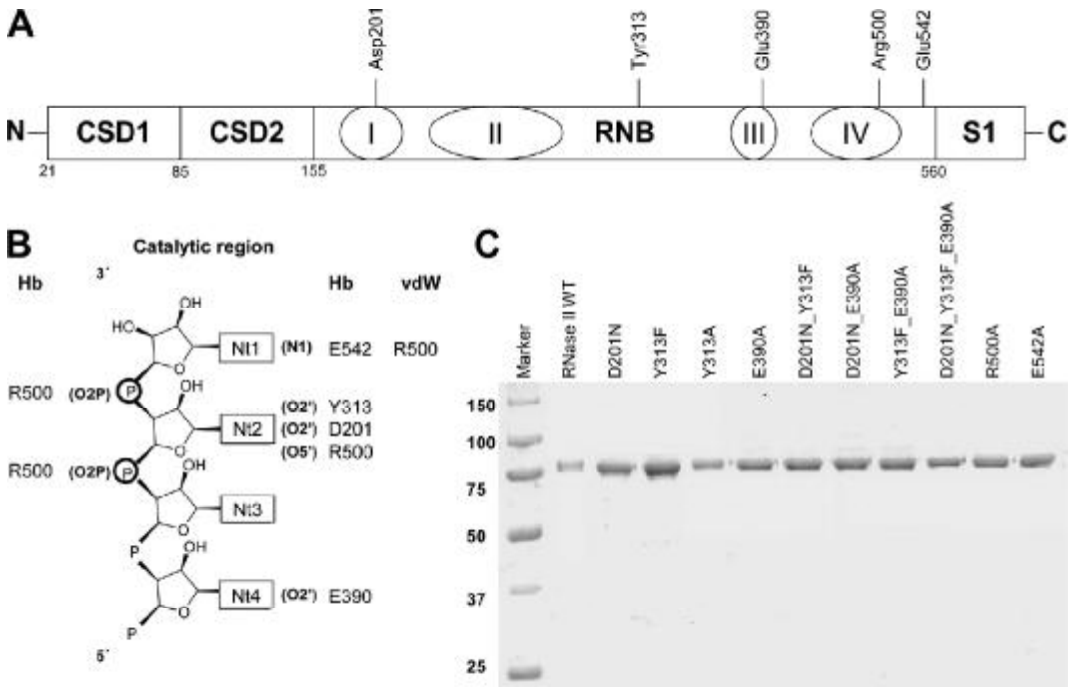

FIGURE 1. **RNase II and mutant proteins.** *A*, linear representation of RNase II domains with the specification of the position of the conserved residues within RNB domain. *B*, atomic interactions scheme between RNA and protein residues. *Hb* indicates hydrogen bonds up to 3.2 Å, and *vdW* indicates van der Waals interactions up to 3.6 Å. The labeling of the nucleotides starts from the 3′-end of the RNA, inversely to previous reports where the nucleotides at the 3′-end was labeled as nt 13 (22). *C*, purity of the enzymes. 0.5 μg of purified His_6-RNase II, His_6-D201N, His_6-Y313F, His_6-Y313A, His_6-E390A, His_6-D201N/Y313F, His_6-D201N/E390A, His_6-Y313F/E390A, His_6-D201N/Y313F/E390A, His_6-R500A, and His_6-E542A were applied and visualized by Coomassie Blue staining. Molecular weights of standard proteins are indicated on the *left*.

bonucleolytic activity of the double mutant Y313F/E390A was not affected by the presence of the two mutations simultaneously (Table 1). As previously reported, the activity of D201N was highly impaired (only 0.2% of the activity of wild-type enzyme), confirming the importance of this residue in RNase II activity (26). This effect was also reflected in the D201N/Y313F and the D201N/Y313F/E390A mutants, which showed less than 0.1% of the activity present in the wild type (Table 1). However, the D201N mutation did not have such a pronounced effect on the activity of the double mutant D201N/E390A, which had a very similar specific activity to the wild type (0.30 and 0.31 nmol·min^{-1}·nmol^{-1} for the wild type and D201N/E390A double mutant, respectively) (Table 1). This mutant was able to degrade the poly(A) substrate in a very processive manner until generating the 10-nt oligomer, as does the wild-type enzyme. However, further degradation of this 10-nt oligomer into shorter products seemed to occur with much more difficulty, and higher concentrations of enzyme were required to generate the typical 4-nt product. One explanation for the results obtained is the possible reconstitution of the catalytic site around the Mg^{2+} atom and the D201N, induced by the E390A mutation. The electrostatic environment in the catalytic center and in the cleft has to be preserved for the enzyme to continue to function; as such, an uncertain number of casual rearrangements might have taken place.

The Arg-500 residue seems to be very important for the RNase II activity, as the R500A mutant showed more than a 40,000-fold reduction in activity when compared with the wild type (7.0×10^{-6} *versus* 0.30 nmol·min^{-1}·nmol^{-1}) (Table 1). In fact, the side chain of this residue interacts with the phosphate backbone of the two nucleotides at the 3′-end of the RNA molecule, and it was postulated to assist in catalysis by fixing the phosphodiester bond at the cleavage position and enhancing the susceptibility of the leaving phosphorous atom to a nucleophilic attack (22). Its substitution by Ala would, therefore, prevent such an interaction, resulting in the inactivation of the enzyme.

Finally, the substitution of the Glu-542 by Ala rendered a mutant version of the RNase II that was much more active than the wild-type enzyme, with more than a 100-fold increase in the exoribonucleolytic activity. This residue is in close proximity to the leaving nucleotide and was suggested to facilitate the elimination of this nucleotide upon phosphor-ester cleavage by pulling it out of the base-stacked position (22). The elimination of the cleaved nucleotide from the catalytic cavity is essential for the enzymatic process to continue, and an alanine residue in this position seems to facilitate this process even more.

Determination of RNA Dissociation Constants (K_D) by Surface Plasmon Resonance Analysis—To determine the contribution of each residue in RNA binding, we calculated the dissoci-

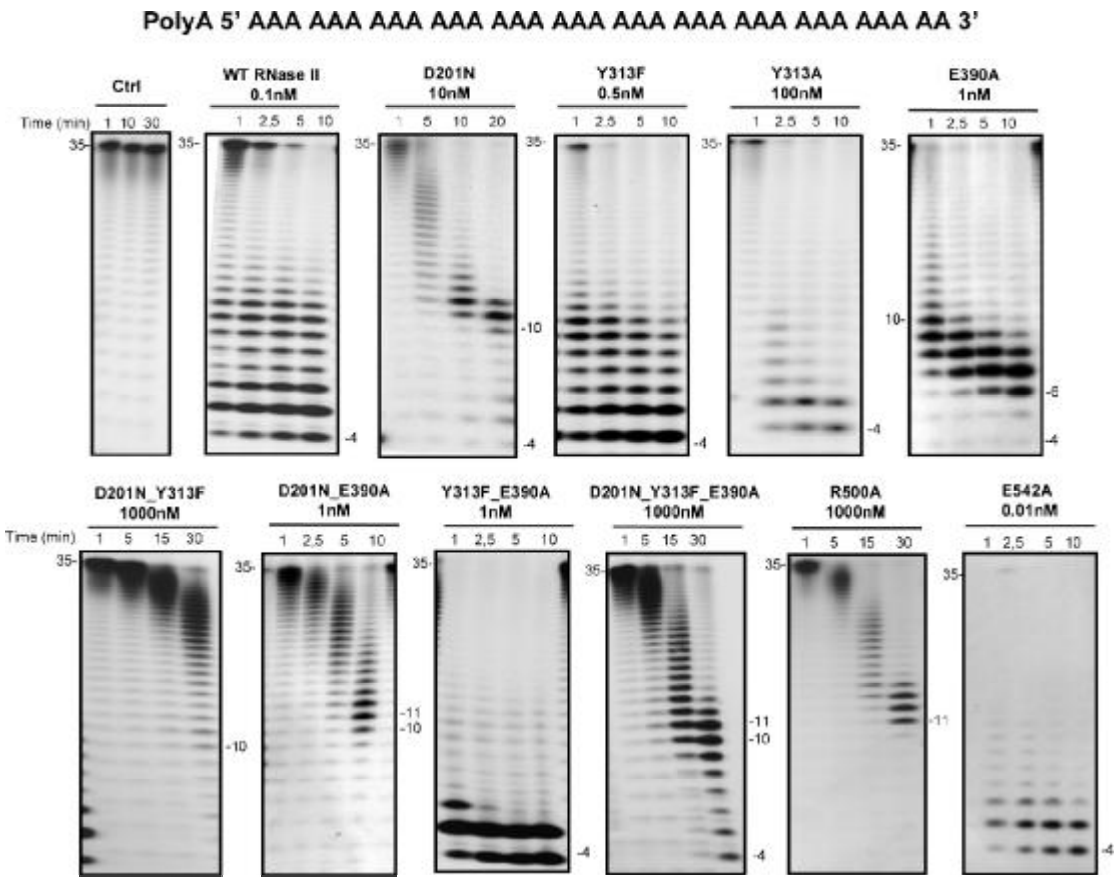

FIGURE 2. **Exoribonuclease activity with single-stranded RNA substrate; comparison of wild-type and mutant proteins.** Activity assays were performed as described under "Experimental Procedures" using a poly(A) chain of 35 nt as substrate. The mutants used and their respective protein concentrations are shown. The wild-type enzyme was used as control. Samples were taken during the reaction at the time points indicated, and reaction products were analyzed in a 20% polyacrylamide, 7 M urea gel. Control reactions with no enzyme added (*Ctrl*) were incubated at the maximum reaction time for each protein. Length of substrates and degradation products are indicated in the figure.

ation constants (K_D) of the wild-type and the mutant proteins by surface plasmon resonance analysis with Biacore 2000 using two different single-stranded RNA substrates as described under "Experimental Procedures." The results obtained are presented in Table 2. The dissociation constants for the 25-mer single-stranded RNA substrate of the wild-type RNase II and D201N enzymes were previously determined (6.5 ± 0.4 and 11.4 ± 0.7 nM, respectively) (26). When assaying the 25-mer single-stranded RNA substrate, almost all the mutant proteins tested in this work showed K_D values similar to that of the wild-type enzyme, except for the E542A mutant. This mutant enzyme presented a significant increase in RNA binding affinity with a much lower K_D value when compared with the wild type (0.5 ± 0.08 *versus* 6.5 ± 0.4 nM) (Table 2). When a poly(A) substrate was used almost all enzymes showed a moderate reduction on K_D values, indicating a higher affinity for this substrate. When compared with the wild type, most of the mutant enzymes showed no significant differences in K_D values except for the triple mutant, which showed a 9-fold reduction in poly(A) binding affinity. Once more, the E542A mutant presented a significant increase in RNA affinity for poly(A), with a ~20-fold higher K_D value when compared with that of the wild type (Table 2). The same result was obtained by electrophoretic mobility shift assay, with this mutant showing RNA-protein complex formation at much lower protein concentration than wild-type enzyme (supplemental Fig. S1). This means that the high level of activity of this mutant is, at least in part, because of a higher RNA binding affinity than the wild type.

Kinetic Analyses of Wild-type and E542A Mutant—Given the extraordinary properties of the E542A mutant, we wanted to better characterize its catalytic properties. With this aim, we performed a kinetic analysis of this E542A mutant and the wild-type enzyme and determined their kinetic parameters. The experiments were carried out using the poly(A) RNA substrate as described under "Experimental Procedures." The results obtained were plotted, and the reaction proceeded according to a Michaelis-Menten equation, as indicated by linearity in the Lineweaver-Burk plots (32) (data not shown). From this plot we

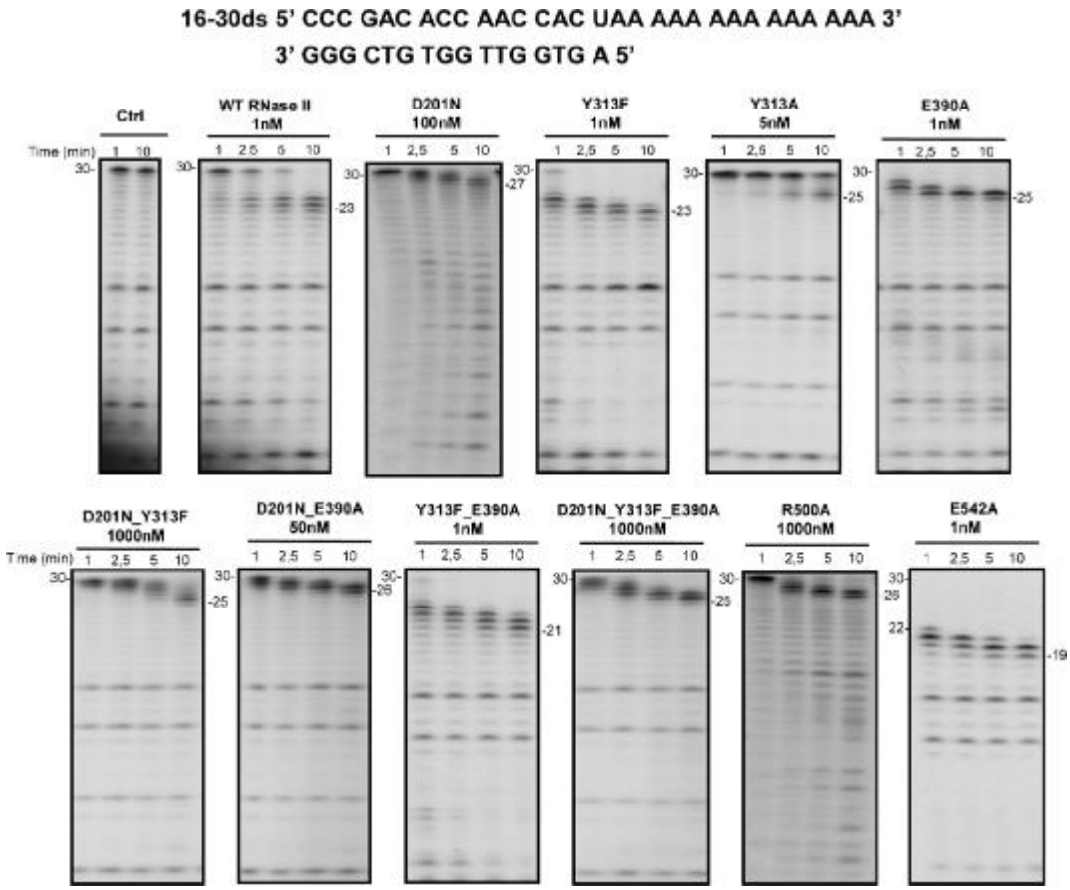

FIGURE 3. **Exoribonuclease activity with ds16–30 substrate; comparison of wild-type and mutant proteins.** Activity assays were performed as described under "Experimental Procedures" using a 30-mer oligoribonucleotide hybridized to the complementary 16mer oligodeoxyribonucleotide, thus obtaining the corresponding double-stranded substrate *16–30ds*. The mutants used and their respective protein concentrations are shown. The wild-type enzyme was used as control. Samples were taken during the reaction at the time points indicated, and reaction products were analyzed in a 20% polyacrylamide, 7 M urea gel. Control reactions with no enzyme added (*Ctrl*) were incubated at the maximum reaction time for each protein. Length of substrates and degradation products are indicated in the figure.

TABLE 1

Specific exoribonucleolytic activity of wild-type and mutant enzymes

Exoribonucleolytic activity was assayed using a 35-nt poly(A) chain as substrate. Activity assays were performed in triplicate as described under "Experimental Procedures." Each value represents nmol of substrate oligoribonucleotide consumed per min and per nmol of protein, and the exoribonucleolytic activity of the wild-type enzyme was taken as 100%.

Protein	Protein activity	Relative activity
	nmol min^{-1} *nmol*$^{-1}$	%
WT RNase II	0.30 ± 0.04	100
Y313F	0.35 ± 0.04	117
Y313A	<0.01	1
E390A	0.36 ± 0.03	120
D201N	<0.01	0.2
D201N/Y313F	<0.01	<0.1
D201N/E390A	0.31 ± 0.06	103
Y313F/E390A	0.33 ± 0.01	110
D210N/Y313F/E390A	≪0.01	≪0.1
E542A	33.75 ± 3.90	11,250
R500A	≪0.01	≪0.1

determined the kinetic parameters, V_{max}, K_m, and k_{cat} for the wild type and the E542A mutant, which are presented in Table 3. The K_m values obtained were 1.25 ± 0.17 μM for the wild type and 0.30 ± 0.05 μM for E542A (Table 3), suggesting that the E542A mutation significantly increased the affinity of RNase II enzyme for the poly(A) substrate and confirming the data obtained from the K_D values. In addition, the k_{cat} value of the E542A mutant was also much higher than that of the wild type (~200,000-fold), thus giving a final k_{cat}/K_m ratio of ~1,000,000-fold higher in the E542A mutant than in the wild type (Table 3). All these data explain why the E542A mutant is much more efficient in catalysis than the wild-type enzyme, confirming that, in fact, substitution of Glu-542 by Ala resulted in a super-enzyme.

Can the Discrimination of RNA Versus DNA by RNase II Be Dictated by Three Conserved Residues?—It was previously described that residues Asp-201, Tyr-313, and Glu-390 are involved in ribose binding (22); therefore, they are probably

important for the specificity of RNA cleavage. Particularly and starting from the 3′-end of the RNA molecule, Tyr-313 and Asp-201 interact with the O2′-ribose oxygen of the second nucleotide, and Glu-390 interacts with the O2′-ribose oxygen of the fourth nucleotide (Fig. 1*B*). To determine the role of these residues in the discrimination of RNA *versus* DNA, the activity of these mutants was assayed using two different 15-nt chimeric DNA-RNA oligomers. In the first chimeric substrate (Chi1), the 3rd and 4th positions from the 3′-end are occupied by ribonucleotides (rC) and the other 13 are deoxyribonucleotides (dT) (5′-dTdTdTdTdTdTdTdTdTdTrCrCdTdT-3′), whereas in the second substrate (Chi2) the ribonucleotides are located in the 2nd and 4th positions from the 3′-end (5′-dTdT-dTdTdTdTdTdTdTdTdTrCdTrCdT-3′). Our data showed that RNase II is only able to cleave DNA bases when having a ribose in the 2nd or the 4th positions. The results demonstrate that, with the Chi1 substrate, wild-type RNase II was only able to cleave three nucleotides, rendering a final degradation product of 12 nt (Fig. 4*A*). After the first cleavage event the RNA translocates, and the riboses now occupy the 2nd and 3rd positions. Because one of the riboses is still in the 2nd position, cleavage can pursue. The riboses then move to positions 1 and 2, and cleavage is still allowed. Finally, once there is only one ribose present, in the 1st position, cleavage halts. This explains why after three cleavage events the 12-nt fragment is released. With the Chi2 substrate only one cleavage event occurred with wild-type RNase II, converting the 15-mer into a 14-mer oligonucleotide (Fig. 4*B* and supplemental Fig. S2). After this first and unique cleavage event, the RNA translocates, the two riboses then occupy the 1st and the 3rd positions, and the enzyme is not able to continue degradation. Therefore, RNase II has a strict requirement for a ribose in the second and/or the fourth nucleotides from the 3′-end of the molecule and not in other positions, as previously described (43). This fact confirms that the specific contacts observed in the RNase II structure with the O2′ oxygen at these positions are essential for RNase II activity.

The substitution of the Asp-201 by Asn inhibited the degradation activity with both DNA-RNA substrates used (Fig. 4). However, this mutant has also been shown to be highly inactive in degradation of a poly(A) RNA substrate (with 0.2% of the wild-type activity) because of the role of Asp-201 in Mg^{2+} coordination (22, 26) (Fig. 2 and Table 1). Its role as an Mg^{2+} ligand at the active site of RNase II is so critical for the activity of the enzyme that we are unable to see the actual contribution of this residue in the interaction with the second ribose. The E390A mutant presented a similar degradation efficiency over an RNA substrate, like that of the wild type. However, this mutant was not able to degrade the Chi1 DNA-RNA substrate (Fig. 4*A*). The substitution of Glu-390 by Ala, which probably prevents the interaction with the 4th ribose, abolished the activity, confirming that the presence of a ribonucleotide in the 3rd position cannot support activity. With the Chi2 substrate, the E390A behaved like the wild type, although with less efficiency (Fig. 4B). Therefore, it seems that the single establishment of contacts with the ribose of 2nd nucleotide is enough to support catalysis to a certain extent. The importance of contacts between protein residues and the ribose of the 2nd nucleotide of the substrate for RNA recognition and cleavage was confirmed by mutations introduced in Tyr-313. Based on the crystal structure, the side chain of this residue is hydrogen-bonded to the O2′ oxygen of ribose of the 2nd nucleotide. Its substitution by Ala prevented the degradation of the Chi1 substrate, and the ability of the enzyme to degrade the Chi2 substrate was highly reduced, even at high protein concentrations (Fig. 4). This reduction seems to be similar to that observed with the poly(A) RNA substrate (Table 1). However, Y313F was shown to be highly active in degradation of both chimeric substrates (Fig. 4), even more active than the wild type over the Chi2. Furthermore, with this second substrate, Y313F was able to perform more than one cleavage event, behavior that was also observed in the Y313F/E390A double mutant (Fig. 4*B* and supplemental Fig. S2). Therefore, it seems that the absence of the side-chain hydroxyl group in Phe-313 could favor the degradation of certain substrates. The presence of a Phe instead of a Tyr may induce a local rearrangement of the nucleotides and/or the protein residues at the catalytic cavity, thus allowing the establishment of new contacts with a ribose in the 3rd or the 1st positions of the substrate. Such contacts, which are not present in the wild type, allow the enzyme to proceed in degradation of the Chi2 substrate even in the absence of the canonical interactions with the 2nd or the 4th riboses.

Determination of DNA Dissociation Constants (K_D) by Surface Plasmon Resonance Analysis—We wanted to explore the effect of these residues, Asp-201, Tyr-313, and Glu-390, in gen-

TABLE 2

RNA binding affinity of wild-type and mutant enzymes

The dissociation constants (K_D) were determined by surface plasmon resonance using BIACORE 2000 with a 25-nt RNA oligomer (5′-Biotin-CCC GAC ACC AAC CAC UAA AAA AAA A-3′) and 35-nt poly(A) RNA oligomer.

Proteins	25-mer ssRNA		Poly(A) ssRNA	
	K_D	Relative K_D	K_D	Relative K_D
	nM		nM	
WT RNase II	6.5 ± 0.4	1.0	1.3 ± 0.4	1.0
D201N	11.4 ± 0.7	1.8	1.1 ± 0.1	0.8
Y313F	12.9 ± 2.4	2.0	4.4 ± 0.1	3.4
Y313A	17.1 ± 0.8	2.6	4.2 ± 0.7	3.2
E390A	8.7 ± 1.4	1.3	2.3 ± 0.4	1.8
D201N/Y313F	3.4 ± 0.3	0.5	4.4 ± 0.6	3.4
D201N/E390A	17.8 ± 1.7	2.7	1.6 ± 0.1	1.2
Y313F/E390A	7.3 ± 0.3	1.1	6.0 ± 0.7	4.6
D201N/Y313F/E390A	22.1 ± 7.2	3.4	12.0 ± 2.9	9.2
R500A	10.9 ± 1.2	1.7	3.3 ± 0.6	2.5
E542A	0.5 ± 0.08	0.1	0.06 ± 0.005	0.05

TABLE 3

3′-5′-Exoribonuclease kinetic constants of wild-type and E542A mutant enzymes

The exoribonuclease rates were measured at different substrate concentrations using a 35-nt poly(A) chain as substrate, as indicated under "Experimental Procedures."

Proteins	V_{max}	K_m	k_{cat}	k_{cat}/K_m
	$\mu M s^{-1}$	μM	s^{-1}	$\mu M^{-1}.s^{-1}$
WT RNase II	0.25 ± 0.02	1.25 ± 0.17	0.41 ± 0.01	0.23 ± 0.06
E542A	(1.14 ± 0.48) × 10^4	0.30 ± 0.05	(8.08 ± 0.84) × 10^4	(2.36 ± 0.38) × 10^5

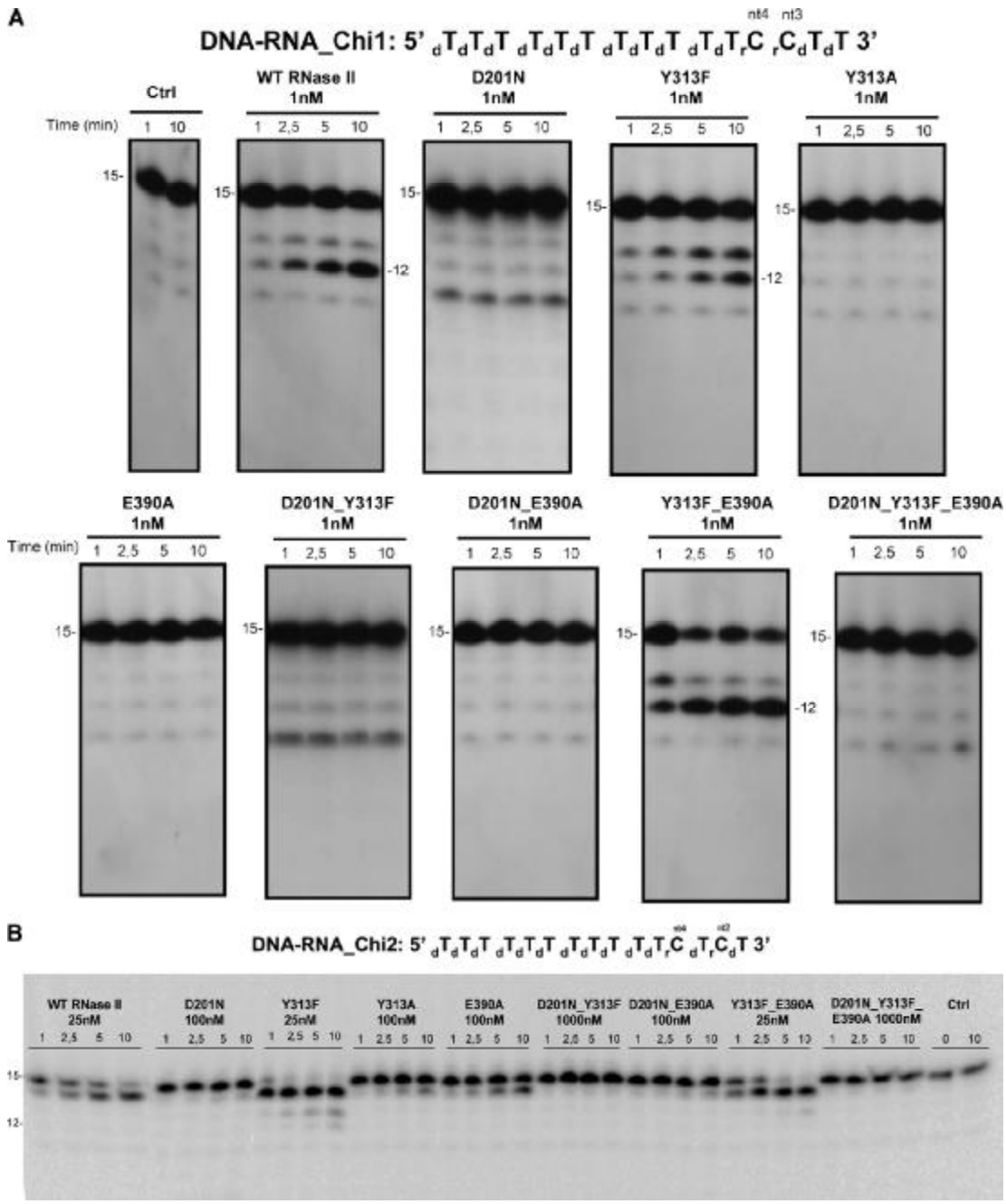

FIGURE 4. **Exoribonuclease activity with DNA-RNA chimeric substrates; comparison of wild-type and mutant proteins.** Activity assays were performed using two 15-mer chimeric substrates as described under "Experimental Procedures." *A*, activity assays with Chi 1 (5′-dTdTdTdTdTdTdTdTdTrCrCdTdT-3′) were the 3rd and 4th positions from the 3′-end are occupied by ribonucleotides (rC), and the other 13 are deoxyribonucleotides (dT). *B*, activity assays with Chi2 (5′-dTdTdTdTdTdTdTdTdTrCdTrCdT-3′) were the 2nd and 4th positions from the 3′-end are occupied by ribonucleotides, and the other 13 are deoxyribonucleotides. The mutants used and their respective protein concentrations are shown. The wild-type enzyme was used as control. Samples were taken during the reaction at the time points indicated, and reaction products were analyzed in a 20% polyacrylamide, 7 M urea gel. Control reactions with no enzyme added (*Ctrl*) were incubated at the maximum reaction time for each protein. Length of substrates and degradation products are indicated in the figure.

TABLE 4
DNA binding affinity of wild-type and mutant enzymes
The dissociation constants (K_D) were determined by surface plasmon resonance using BIACORE 2000 with a 16-nt DNA oligomer (5′-Biotin-AGT GGT TGG TGT CGG G-3′).

Proteins	16-mer ssDNA	
	K_D	Relative K_D
	nM	
WT RNase II	8.7 ± 0.7	1.0
D201N	15.9 ± 2.4	1.8
Y313F	6.9 ± 0.3	0.8
Y313A	≫100	≫100
E390A	75.7 ± 8.8	8.7
D201N/Y313F	6.4 ± 0.5	0.7
D201N/E390A	12.8 ± 2	1.5
Y313F/E390A	12.0 ± 0.4	1.4
D201N/Y313F/E390A	10.7 ± 0.3	1.2
R500A	14.2 ± 0.2	1.6
E542A	6.1 ± 0.3	0.7

eral DNA binding affinity. For this purpose we determined the K_D values by surface plasmon resonance using a DNA substrate. The results obtained (Table 4) showed that all mutants tested have a similar DNA affinity as the wild type. with the exceptions of E390A and Y313A derivatives, which showed a ~9-fold and a >100-fold reduction, respectively (Table 4). These results confirm that the contact of Tyr-313 and Glu-390 with the 2nd and 4th riboses are important not only for catalysis but also for a proper substrate binding at the catalytic cavity in the absence of the canonical interactions.

Our data indicate that inside the cavity the unique specific contacts for ribose established by RNase II are those with the 2nd and 4th nucleotides from the 3′-end of the RNA molecule. Moreover, these contacts are necessary and sufficient for cleavage to occur, and therefore, they seem to be responsible for the RNA specificity *versus* DNA in RNase II.

DISCUSSION

E. coli RNase II is the model of the RNase II family of enzymes, whose homologues are present in all three domains of life (1, 11, 12, 44, 45). The resolution of the structure of *E. coli* RNase II in the RNA-free and bound complex constituted a significant breakthrough (22, 24). The structural study together with biochemical analysis helped to explain certain aspects of the enzyme activity and led to the proposal of a model for RNA degradation by RNase II that can be extrapolated to other family members (13, 15, 22, 26, 41). However, some essential features remain unknown.

The structure of the D209N mutant complexed with a 13-nt poly(A) oligomer revealed specific contacts of several residues at the active site with the RNA oligomer, with most of these residues highly conserved in RNase II-like enzymes of all domains of life (22). To identify the specific role of these amino acids and verify their precise function in RNase II activity, we introduced several single, double, and triple mutations in residues Asp-201, Tyr-313, Glu-390, Arg-500, and Glu-542 and studied the exoribonucleolytic activity and substrate binding ability of the corresponding mutant proteins.

The results obtained in this report revealed that, except for the Glu-542, none of the residues analyzed is crucial for RNA binding, as only slight differences in RNA binding affinity (K_D values) were observed upon mutation (Table 2). However, the Glu-542 residue is very important in the prevention of the binding to the substrate, as its substitution by an Ala causes the protein to bind RNA more tightly than the wild-type enzyme. Moreover, our data demonstrate that, among the residues mutated in this study, Arg-500 plays a central role in catalysis. The R500A mutation practically inactivated the enzyme, although the protein was still able to bind RNA efficiently. A similar result had previously been obtained when mutating the conserved Asp-209 into an Asn (6, 26). Comparable results were obtained with the double mutant D201N/Y313F and the triple mutant D201N/Y313F/E390A, which also have their activities highly impaired.

The results obtained with R500A support the essential role of this residue in assisting catalysis (22). Arg-500 has been described as interacting with the phosphate backbone of the two nucleotides at the 3′-end of the substrate (Fig. 1*B*). It was suggested that the role of Arg-500 could be to fix the phosphodiester bond at the cleavage position, enhancing the susceptibility of the phosphorous atom of the leaving nucleotide to a nucleophilic attack. To confirm our experimental results, we performed a computational model of the putative binding mode of a 13-nt poly(A) RNA fragment to RNase II wild-type enzyme based on the x-ray structure of RNase II D209N-RNA-bound complex (22). The model obtained gave us precious information about the interactions established between the RNA substrate and protein residues and helped to clarify certain aspects (Fig. 5*A*). For instance, the computational model predicts that in the wild-type enzyme, the guanidinium group in the Arg-500 residue would contact directly with the phosphate of nt 2 from the 3′-end, stabilizing its position. This conformation keeps the enzyme catalytically competent and allows the outgoing nucleotide to remain coordinated with the magnesium atom and the rest of the active center elements. Thus, the model shows that changes in this position could induce an extensive reorganization of the region that would turn the enzyme catalytically incompetent, which correlates with the experimental results obtained for mutant R500A and confirms the hypothesis previously postulated (22).

The RNase II structure showed that Tyr-313, Asp-201, and Glu-390 hydrogen-bonded with the O2′-ribose oxygen of two nucleotides in the RNA molecule (Fig. 1*B*). Because this oxygen is absent in a deoxyribose, the three residues were postulated to be involved in RNA discrimination *versus* DNA.

Previous studies showed that Asp-201 residue was very important for RNase II activity but not for substrate binding (26). In this report we performed new experiments with the previously constructed D201N mutant, and we demonstrated that this mutant enzyme was unable to degrade DNA-RNA chimeras. The computational model performed in this report helped to explain all experimental data obtained with the D201N mutant, showing that different groups of the aspartate participate in different contacts. The carboxylic of its side chain coordinates the Mg^{2+} ion that is essential for catalysis, and therefore, its substitution by asparagine led to the loss of activity. However, interaction with the O2′-ribose is mediated by polar contacts with the carbonyl oxygen in the backbone trace, indicating that any other residue could account for such interaction as long as the substrate and protein residue conforma-

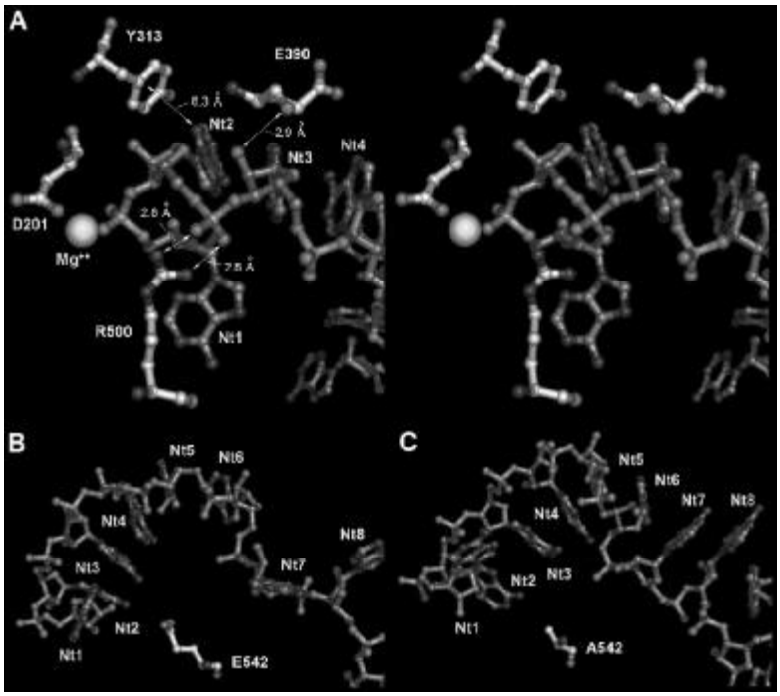

FIGURE 5. **Modeling of RNase II and E542A mutant proteins in RNA-bound conformations.** To obtain biophysically consistent models, minimal energy average structures of both models were obtained from stabilized trajectories of 4-ns molecular dynamics. Figures in sticks were depicted with Pymol© (DeLano Scientific LLC, San Carlos, CA). *A*, stereo diagram of wild-type protein active center showing Glu-390, Tyr-313, Arg-500, and Asp-201 residues from the RNB domain. Significant polar contacts distances and relative positions of Mg^{2+} atom and outgoing RNA nucleotides (nt 1) are also represented. Hydrogen bonding between the Glu-390 backbone trace carbonyl oxygen and nt 3 ribose 2′-OH group could be responsible for RNA *versus* DNA recognition. Mutation to alanine would have introduced soft changes in local RNB conformation that could affect RNA discrimination in chimeric substrates. The guanidinium phosphate-hydrogen-bonding network between Arg-500 and nt 2 would essentially result in stabilizing the catalytic complex while keeping the outgoing nucleotide conformation correct. Catalytic competence of mutant R500A would result in being completely abolished. Long range hydrogen-π facial interactions between nucleotide nt 12 and Tyr-313 or Phe-313 mutant aromatic side chains could contribute to avoiding harmful interactions in the active center during procession and/or catalysis. *B* and *C*, modeled conformations of the poly(A) RNA strand in the RNB domain procession cleft in the wild-type and Ala-542 mutant RNase II proteins, respectively. As depicted in *B*, after 4 ns of MD simulation, the RNB domain of RNase II Ala-542 mutant could be able to deploy 6 stacked nucleotides (from nt 8 to 2) in progression, ready for cleavage. As shown in *C*, the same region in the wild-type model could only allocate 4 nucleotides (from nt 5 to 2) simultaneously in the cleft during a catalytic event. Substitution in position 542 of the negatively charged glutamic side chain for the smaller neutral methyl group of alanine could significantly reduce both electrostatic and steric surfaces in the RNA binding interface.

tion is conserved. Therefore, although the actual contribution of Asp-201 to the RNA cleavage specificity cannot be deciphered with the D201N mutant because of its inactivation, computational model confirms the postulated contact between this residue and the 2nd ribose of the RNA molecule. According to our results Tyr-313 and Glu-390 seemed to be two essential contacts that RNase II establishes with the ribose of the substrate, demonstrating that these residues are responsible for the RNA cleavage specificity.

Substitution of Glu-390 by Ala caused a significant loss of activity over the chimeric substrates but did not affect degradation of a RNA molecule. The model predicts polar contacts between the ribose 2′-OH and the carbonyl oxygens of the glutamic. This means that its replacement by Ala should not destabilize the interaction. However, Glu-390 is also involved in polar contacts with neighboring arginine residues through its side chain. Therefore, E390A mutation will probably induce local conformational changes that may prevent the hydrogen bond formation between Ala (smaller residue than Glu) and the second ribose oxygen. The loss of this interaction would have a drastic effect in degradation of the chimeric substrate, where other canonical interactions may not be occurring. In the case of Tyr-313, our experimental results suggested that its aromatic moiety but not its hydroxyl group is crucial for activity and for RNA specificity of RNase II, as the Y313A but not Y313F mutation produced a drastic reduction of RNA and DNA-RNA substrate degradation efficiency. In fact, the computational modeling predicts contacts between the Tyr-313 aromatic ring and the OH of the ribose, but the hydroxyl group of the Tyr-313 does not participate in such interactions, confirming this hypothesis. In addition, our results demonstrate that the contact with Tyr-313 (or Phe) is critical for the degradation of DNA-RNA chimeric substrate and that this single contact is able to support catalysis of DNA bases. Therefore, the presence of a ribose in positions 2 or 4 from the 3′-end of the nucleic acid is the unique requirement for RNase II to perform degradation. RNA specificity shown by this ribonuclease resides in these two positions and interaction with Tyr-313 and Glu-390.

Finally, Glu-542 was shown to play a very important function in RNase II. The carboxylic group of this glutamate is in close proximity to the nitrogen atoms of the leaving nucleotide, and the establishment of one or more hydrogen-bonds between them could facilitate the elimination of this nucleotide after cleavage, thus allowing the degradation process to continue. Thus, Glu-542 seemed to be very important for the degradation to occur. Our experimental results demonstrate that its substitution by Ala resulted in a 110-fold increase in RNA degradation efficiency compared to the wild-type enzyme (Table 1) and a 10–20-fold increase in RNA affinity (Table 2). Moreover, the kinetic data suggest that this mutant not only has a much higher affinity for the poly(A) RNA substrate but also presents a much higher catalytic rate, confirming its role in the catalytic event. Such intriguing results led us to perform computational modeling with the E542A

mutant enzyme with the RNA bound and compared it with the model of the wild type. The model predicts that substitution of the negatively charged glutamic acid side chain for a short quasi-apolar alanine residue seems to induce a subtle conformational change in the Cα backbone of the RNB domain itself that leads to a reorganization of its RNA binding interface (Fig. 5*B*). Comparing the E542A mutant and wild-type models in this region (Fig. 5*B*), the RNA bound to E542A mutant shows that nucleotides in positions ranging from 2 to 8 are set out in a stable stacked conformation. In comparison, the wild-type model presents only nucleotides 2–6 in a similar conformation. The efficiency of E542A mutant to deploy 50% more residues within the catalytic domain in the model could determine an increased capability of binding the RNA substrate by the RNB domain during catalysis than the RNase II wild type. In addition, the higher degree of organization and density of packing of the nucleotide chain in the E542A mutant could favor the RNA translocation upon cleavage, leading to higher degradation efficiency. These two aspects together may, therefore, be responsible for the high enzymatic activity experimentally determined of this mutant.

The results we present in this study substantially improve the RNase II model for RNA degradation. We have identified the residues that are responsible for the discrimination of cleavage of RNA *versus* DNA, which are fully conserved in all domains of life. We also show that the Arg-500 residue, present in RNase II active site, is crucial for activity but not for RNA binding. Finally, we report a very interesting mutant that acts as a super-enzyme, in which the substitution of Glu-542 by Ala leads to an outstanding catalytic efficiency, because of the high increase of both the exoribonucleolytic activity and substrate binding.

Because Rrp44/Dis3 protein (an RNase II homologue) is the only catalytically active nuclease in the exosome, the understanding of the degradation mechanism will have a large impact in future studies of the exosome. Moreover, the recent determination of the structure of yeast Rrp44 showed that *E. coli* RNase II is a good study model (39, 40). Also, yeast Rrp44/Dis3 has a similar linear arrangement of domains in the sequence when compared with *E. coli* RNase II. Both proteins share a high degree of identity as their conservation is the highest at the active site. This suggests that these two exoribonucleases share a similar hydrolytic mechanism (40). As such, the results from this report on RNase II mutants can be extrapolated for the comprehension of the mode of action of other members of the RNase II family.

Acknowledgments—We thank Ambro Van-Hoof for critical reading. We also thank to Biomol-Informatics SL for bioinformatics consulting.

REFERENCES

1. Andrade, J. M., Pobre, V., Silva, I. J., Domingues, S., and Arraiano, C. M. (2009) *Prog. Mol. Biol. Transl. Sci.* **85,** 187–229
2. Gupta, R. S., Kasai, T., and Schlessinger, D. (1977) *J. Biol. Chem.* **252,** 8945–8949
3. McLaren, R. S., Newbury, S. F., Dance, G. S., Causton, H. C., and Higgins, C. F. (1991) *J. Mol. Biol.* **221,** 81–95
4. Coburn, G. A., and Mackie, G. A. (1996) *J. Biol. Chem.* **271,** 1048–1053
5. Marujo, P. E., Hajnsdorf, E., Le Derout, J., Andrade, R., Arraiano, C. M., and Régnier, P. (2000) *RNA* **6,** 1185–1193
6. Amblar, M., and Arraiano, C. M. (2005) *FEBS J.* **272,** 363–374
7. Deutscher, M. P., and Reuven, N. B. (1991) *Proc. Natl. Acad. Sci. U.S.A.* **88,** 3277–3280
8. Zilhão, R., Cairrão, F., Régnier, P., and Arraiano, C. M. (1996) *Mol. Microbiol.* **20,** 1033–1042
9. Zilhão, R., Camelo, L., and Arraiano, C. M. (1993) *Mol. Microbiol.* **8,** 43–51
10. Cairrão, F., Chora, A., Zilhão, R., Carpousis, J., and Arraiano, C. M. (2001) *Mol. Microbiol.* **276,** 19172–19181
11. Mian, I. S. (1997) *Nucleic Acids Res.* **25,** 3187–3195
12. Mitchell, P., Petfalski, E., Shevchenko, A., Mann, M., and Tollervey, D. (1997) *Cell* **91,** 457–466
13. Dziembowski, A., Lorentzen, E., Conti, E., and Séraphin, B. (2007) *Nat. Struct. Mol. Biol.* **14,** 15–22
14. Liu, Q., Greimann, J. C., and Lima, C. D. (2006) *Cell* **127,** 1223–1237
15. Schaeffer, D., Tsanova, B., Barbas, A., Reis, F. P., Dastidar, E. G., Sanchez-Rotunno, M., Arraiano, C. M., and van Hoof, A. (2009) *Nat. Struct. Mol. Biol.* **16,** 56–62
16. Lebreton, A., Tomecki, R., Dziembowski, A., and Séraphin, B. (2008) *Nature* **456,** 993–996
17. Cheng, Z. F., and Deutscher, M. P. (2005) *Mol. Cell* **17,** 313–318
18. Cairrão, F., Cruz, A., Mori, H., and Arraiano, C. M. (2003) *Mol. Microbiol.* **50,** 1349–1360
19. Andrade, J. M., Cairrão, F., and Arraiano, C. M. (2006) *Mol. Microbiol.* **60,** 219–228
20. Cairrão, F., and Arraiano, C. M. (2006) *Biochem. Biophys. Res. Commun.* **343,** 731–737
21. Cheng, Z. F., Zuo, Y., Li, Z., Rudd, K. E., and Deutscher, M. P. (1998) *J. Biol. Chem.* **273,** 14077–14080
22. Frazão, C., McVey, C. E., Amblar, M., Barbas, A., Vonrhein, C., Arraiano, C. M., and Carrondo, M. A. (2006) *Nature* **443,** 110–114
23. McVey, C. E., Amblar, M., Barbas, A., Cairrão, F., Coelho, R., Romão, C., Arraiano, C. M., Carrondo, M. A., and Frazão, C. (2006) *Acta Crystallogr. Sect. F Struct. Biol. Cryst. Commun.* **62,** 684–687
24. Zuo, Y., Vincent, H. A., Zhang, J., Wang, Y., Deutscher, M. P., and Malhotra, A. (2006) *Mol. Cell* **24,** 149–156
25. Cannistraro, V. J., and Kennell, D. (1994) *J. Mol. Biol.* **243,** 930–943
26. Barbas, A., Matos, R. G., Amblar, M., López-Viñas, E., Gomez-Puertas, P., and Arraiano, C. M. (2008) *J. Biol. Chem.* **283,** 13070–13076
27. Taylor, R. G., Walker, D. C., and McInnes, R. R. (1993) *Nucleic Acids Res.* **21,** 1677–1678
28. Studier, F. W., and Moffatt, B. A. (1986) *J. Mol. Biol.* **189,** 113–130
29. Higuchi, R. (1990) in *PCR Protocols. A Guide to Methods and Applications* (Innis, M. A., Gelfand, D. H., Sninsky, J. J., and White, T. J., eds) Academic Press, Inc., Harcourt Brace Jovanovich, Publishers, San Diego, CA
30. Amblar, M., Barbas, A., Fialho, A. M., and Arraiano, C. M. (2006) *J. Mol. Biol.* **360,** 921–933
31. Arraiano, C. M., Barbas, A., and Amblar, M. (2008) *Methods Enzymol.* **447,** 131–160
32. Lineweaver, H., and Burk, D. (1934) *J. Am. Chem. Soc.* **56,** 658–666
33. Park, S., Myszka, D. G., Yu, M., Littler, S. J., and Laird-Offringa, I. A. (2000) *Mol. Cell. Biol.* **20,** 4765–4772
34. Guex, N., and Peitsch, M. C. (1997) *Electrophoresis* **18,** 2714–2723
35. Case, D. A., Cheatham, T. E., 3rd, Darden, T., Gohlke, H., Luo, R., Merz, K. M., Jr., Onufriev, A., Simmerling, C., Wang, B., and Woods, R. J. (2005) *J. Comput. Chem.* **26,** 1668–1688
36. Case, D. A., Darden, T., Cheatham, T. E., 3rd, Simmerling, C., Wang, J., Duke, R. E., Luo, R., Merz, K. M., Jr., Wang, B., Pearlman, D. A., Crowley, M., Brozell, S., Tsui, V., Gohlke, H., Mongan, J., Hornak, V., Cui, G., Beroza, P., Schafmeister, C., Caldwell, J. W., Ross, W. S., and Kollman, P. A. (2004) AMBER 8, University of California, San Francisco
37. Pearlman, D. A., Case, D. A., Caldwell, J. W., Ross, W. S., Cheatham, T. E., DeBolt, S., Ferguson, D., Seibel, G., and Kollman, P. (1995) *Comput. Phys. Commun.* **91,** 1–41
38. Case, D. A., Darden, T. E., Cheatham, T. E., Simmerling, C. L., Wang, J., Duke, R. E., Luo, R., Merz, K. M., Pearlman, D. A., Crowley, M., Walker, R. C., Zhang, W., Wang, B., Hayik, S., Roitberg, A., Seabra, G., Wong, K. F.,

Paesani, F., Wu, X., Brozell, S., Tsui, V., Gohlke, H., Yang, L., Tan, C., Mongan, J., Hornak, V., Cui, G., Beroza, P., Mathews, D. H., Schafmeister, C., Ross, W. S., and Kollman, P. (2006) AMBER 9, University of California, San Franscisco
39. Wang, H. W., Wang, J., Ding, F., Callahan, K., Bratkowski, M. A., Butler, J. S., Nogales, E., and Ke, A. (2007) *Proc. Natl. Acad. Sci. U.S.A.* **104,** 16844–16849
40. Lorentzen, E., Basquin, J., Tomecki, R., Dziembowski, A., and Conti, E. (2008) *Mol. Cell* **29,** 717–728
41. Schneider, C., Anderson, J. T., and Tollervey, D. (2007) *Mol. Cell* **27,** 324–331
42. Amblar, M., Barbas, A., Gomez-Puertas, P., and Arraiano, C. M. (2007) *RNA* **13,** 317–327
43. Cannistraro, V. J., and Kennell, D. (2001) *Methods Enzymol.* **342,** 309–330
44. Grossman, D., and van Hoof, A. (2006) *Nat. Struct. Mol. Biol.* **13,** 760–761
45. Zuo, Y., and Deutscher, M. P. (2001) *Nucleic Acids Res.* **29,** 1017–1026

THE JOURNAL OF BIOLOGICAL CHEMISTRY VOL. 283, NO. 19, pp. 13070–13076, May 9, 2008

New Insights into the Mechanism of RNA Degradation by Ribonuclease II

IDENTIFICATION OF THE RESIDUE RESPONSIBLE FOR SETTING THE RNase II END PRODUCT[*] [S]

Received for publication, December 7, 2007, and in revised form, March 12, 2008 Published, JBC Papers in Press, March 12, 2008, DOI 10.1074/jbc.M709989200

Ana Barbas[‡], Rute G. Matos[‡], Mónica Amblar[‡1], Eduardo López-Viñas[§], Paulino Gomez-Puertas[§], and Cecília M. Arraiano[‡2]

From the [‡]Instituto de Tecnologia Química e Biológica/Universidade Nova de Lisboa, Apartado 127, 2781-901 Oeiras, Portugal and [§]Centro de Biologia Molecular "Severo Ochoa", Campus Universidad Autonoma de Madrid and CIBER-Obn, Physiopathology of Obesity and Nutrition (CB06/03/0026), Instituto de Salud Carlos III, Madrid 28049, Spain

RNase II is a key exoribonuclease involved in the maturation, turnover, and quality control of RNA. RNase II homologues are components of the exosome, a complex of exoribonucleases. The structure of RNase II unraveled crucial aspects of the mechanism of RNA degradation. Here we show that mutations in highly conserved residues at the active site affect the activity of the enzyme. Moreover, we have identified the residue that is responsible for setting the end product of RNase II. In addition, we present for the first time the models of two members of the RNase II family, RNase R from *Escherichia coli* and human Rrp44, also called Dis3. Our findings improve the present model for RNA degradation by the RNase II family of enzymes.

Escherichia coli RNase II is the prototype of the RNase II superfamily of exoribonucleases, whose homologues are present in all three domains of life (1–4). RNase II and its homologues can be environmentally (5, 6) and developmentally regulated (7), and other ribonucleases have been shown to be involved in their post-transcriptional control (8–10). Mutations in the *rnb* gene have been linked with abnormal chloroplast biogenesis (11), mitotic control, and cancer (12). RNase II is a ubiquitous enzyme that degrades single-stranded RNAs processively in the 3′- to 5′-direction, resulting in the generation of 5′-mononucleotides. Ten nucleotides is the minimum length of the RNA molecule needed to detect activity in RNase II, and the end product of degradation of this enzyme is a 4-nucleotide RNA oligomer (13–15). RNase II homologues Dis3/Rrp44 are components of the exosome, a complex of exoribonucleases involved in the maturation and turnover of RNA (2), in RNA interference (16), and in surveillance pathways that recognize and degrade aberrant RNAs (17, 18). Recent reports have shown that Dis3/Rrp44 is the only catalytically active nuclease in the yeast core exosome (19) and plays a direct role in RNA surveillance, contributing to the recognition and degradation of specific RNA targets (20). In addition, the human exosome has hydrolytic activity, similar to what happens in the yeast exosome (13, 18, 21).[3] The RNase II homologues present in the exosome have the same behavior regarding the minimum length of RNA substrate and the same final end product as the *E. coli* RNase II (13, 18, 21). Moreover, the recent determination of the electron microscopy structure of yeast Rrp44 (22) showed that *E. coli* RNase II is a good model and suggests that the RNA recruitment mechanism is conserved.

The three-dimensional structure of *E. coli* RNase II was recently determined (23–25). The structure of RNase II RNA-bound complex (23, 24), together with biochemical data, gave new insights into the mechanisms of catalysis, translocation, and processivity of this important RNA-degrading enzyme. The *E. coli* RNase II structure and its RNA-bound complex have been used as a model for the analysis of Dis3/Rrp44 (20). RNase II consists of four domains (Fig. 1*A*): two N-terminal cold shock domains (CSD1 and CSD2), one central RNB catalytic domain, and one C-terminal S1 domain. The RNA contacts the enzyme at two different and non-contiguous regions, the anchoring and the catalytic regions, which act synergistically to provide a processive degradation. Nucleotides 1 to 5 are located in the anchor region, situated in a deep cleft between the two cold shock domains and the S1 domain (Fig. 1*A*). The catalytic region forms a cavity that is only accessible to single-stranded RNA, where the last five nucleotides at the 3′-end of the RNA molecule (nt 9–13) are stacked and clamped between the aromatic residues Tyr-253 and Phe-358. In a recent report (23) we postulated a model for RNA degradation that involves one Mg^{2+} ion, four highly conserved aspartic acids (201, 207, 209, and 210), and the recruitment of a second Mg^{2+} for catalysis. In this study we mutated these highly conserved amino acids present in the active site and characterized the respective proteins. Here, we also show, for the first time, the models of two related members of the RNase II family, RNase R from *E. coli* and human Rrp44 (Fig. 1, *B* and *C*). These results shed new light on the mechanism of RNA degradation by RNase II

* The work at the CBMSO was supported by "Ministerio de Educación y Ciencia" Grant SAF2004-06843 and by an institutional grant from "Fundación Ramón Areces." The work at the ITQB was supported by Fundação para a Ciência e a Tecnologia (FCT), Portugal. The costs of publication of this article were defrayed in part by the payment of page charges. This article must therefore be hereby marked "*advertisement*" in accordance with 18 U.S.C. Section 1734 solely to indicate this fact.

[S] The on-line version of this article (available at http://www.jbc.org) contains supplemental experimental procedures, supplemental references, and supplemental Figs. S1–S6.

[1] Present address: Centro de Investigaciones Biológicas, C/Ramiro de Maeztu, 9, 28040 Madrid, Spain.

[2] To whom correspondence should be addressed. Tel.: 351-214469547; Fax: 351-214411277; E-mail: cecilia@itqb.unl.pt.

[3] C. D. Lima, personal communication.

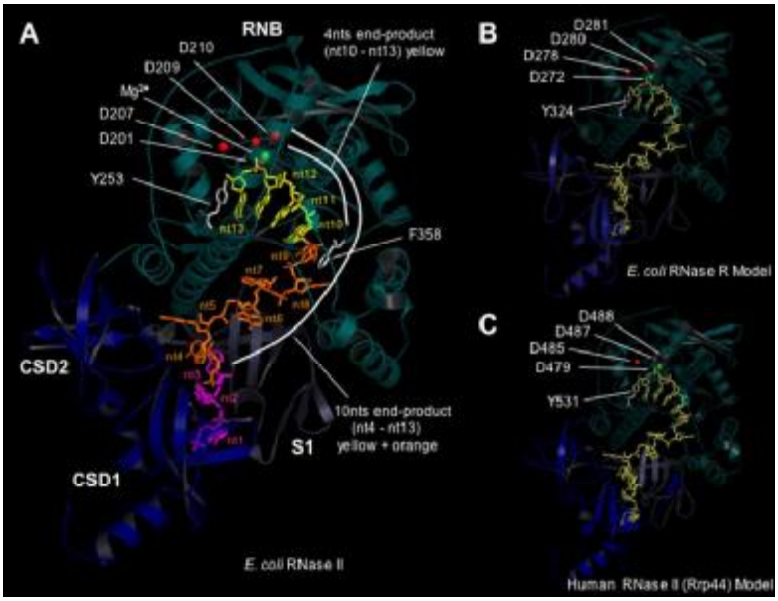

FIGURE 1. **Structure of *E. coli* RNase II-RNA complex and homology-based three-dimensional models of *E. coli* RNase R and human RNase II (*Rrp44*).** *A*, RNase II structure bound to a 13-nt RNA molecule (crystal 2ix1) indicating possible RNA degradation end products (4 nt, *yellow*, and 10 nt, *yellow plus orange*). Highly conserved residues mutated are indicated. The 5 nt at the 3′-end of the RNA molecule (nt 9–13) are stacked and clamped between the aromatic residues Tyr-253 and Phe-358. *B* and *C*, three-dimensional models of *E. coli* RNase R (amino acids 84–724) and human Rrp44 (amino acids 301–927) proteins, respectively, based on crystal structure 2ix1. Positions of all equivalent residues of the catalytic site of RNase II enzyme that were mutated in this report are indicated in all three proteins. Tyr-324 (*RNase R*) and Tyr-531 (*Rrp44*) are equivalent to RNase II Tyr-253 stacking residue. The human Rrp44 model does not include large insertions spanning residues Asp-166-Ser-254 and Ser-307-Arg-344 due to the lack of an appropriately aligned template structure.

and can therefore be important for comprehension of the mode of action of other members of the RNase II family.

EXPERIMENTAL PROCEDURES

Construction of RNase II Mutants by Site-directed Mutagenesis—Mutations D207N, D210N, F358A, and Y253A,F358A were introduced into pFCT6.9 (5) by PCR overlapping (26). D201N and Y253A mutations were generated by site-directed mutagenesis using QuikChange Site-directed Mutagenesis kit from Stratagene. The primers used in this study are described in supplemental experimental procedures.

Overexpression and Purification of Wild-type and RNase II Mutants—The plasmid used for expression of wild-type *E. coli* histidine-tagged RNase II protein was pFCT6.9 plasmid (5). All other plasmids bearing mutations were transformed into BL21(DE3) *E. coli* strain (Novagen) to allow the expression of the recombinant proteins. Purification of all proteins was performed by histidine affinity chromatography using HiTrap Chelating HP columns (GE Healthcare) and the AKTA HLPC system (GE Healthcare) following the protocol previously described (13). The purity of the enzymes was analyzed in an 8% SDS-PAGE (supplemental Fig. S1).

Activity Assays—Exoribonucleolytic activity was assayed using oligoribonucleotides as substrate (13). The 30-mer oligoribonucleotide (5′-CCCGACACCAACCACUAAAAAAA-AAAAAAA-3′) and the poly(A) chain of 35 nt were labeled at the 5′-end with [γ-^{32}P] ATP and T4 polynucleotide kinase. The RNA oligomers were then purified using Microcon YM-3 Centrifugal Filter Devices (Millipore). Reactions were carried out in a final volume of 10 μl containing 30 nM substrate, 20 mM Tris-HCl, pH 8, 100 mM KCl, 1 mM $MgCl_2$, and 1 mM dithiothreitol. The amount of each enzyme added to the reaction was adjusted to obtain linear conditions and is indicated in Fig. 2. Reactions were started by the addition of the enzyme and incubated at 37 °C. Samples were withdrawn at the time points indicated in the figure, and the reaction was stopped by adding formamide-containing dye supplemented with 10 mM EDTA. Reaction products were resolved in 20% polyacrylamide/7 M urea and analyzed by autoradiography. The exoribonucleolytic activity of the enzymes was determined by measuring and quantifying the disappearance of the substrate in three distinct experiments; each value obtained represents the mean of these independent assays (supplemental Fig. S2). The exoribonucleolytic activity of the wild-type enzyme was taken as 100%.

Surface Plasmon Resonance Analysis, Biacore—Biacore SA streptavidin chips were obtained from Biacore Inc. (GE Healthcare). The flow cells of the SA streptavidin sensor chip were coated with a low concentration of the substrates as described in supplemental experimental procedures. The biosensor assay was run at 4 °C in a buffer containing 20 mM Tris-HCl, pH 8, 100 mM KCl, 1 mM dithiothreitol, and 25 mM EDTA. The target RNA substrate was captured on flow cell 2, and the pure proteins were injected as indicated in supplemental experimental procedures. All experiments included triple injections of each protein concentration (10, 20, 30, 40, and 50 nM) to determine the reproducibility of the signal and to control injections to assess the stability of the RNA surface during the experiment. Dissociation constants were calculated using the BIA Evaluation 3.0 software package, according to the fitting model 1:1 Languimir binding.

Modeling of RNase R and Rrp44 Protein Structures—Three-dimensional models for *E. coli* RNase R (RNR_ECOLI) and human exosome complex exonuclease Rrp44 (Rrp44_HUMAN) proteins were performed using standard homology modeling methods based on the multiple sequence alignment of the family members, as described in supplemental experimental procedures.

TABLE 1

Exoribonucleolytic activity and RNA binding affinity of wild-type and mutant enzymes

Exoribonucleolytic activity was assayed using a 35-nt poly(A) chain as substrate. Activity assays were performed as described under "Experimental Procedures." The dissociation constants (K_D) were determined by surface plasmon resonance using Biacore 2000 with a 25-nt RNA oligomer (5′-biotin-CCC GAC ACC AAC CAC UAA AAA AAA A-3′).

Proteins	Exoribonucleolytic activity	Relative activity	Dissociation constants-K_D	Relative K_D
	nM/min	%	*nM*	
WT	29.9 ± 3.6	100[a]	6.48 ± 0.4	1.0
D201N	<0.1	0.2	11.4 ± 0.7	1.8
D207N	3.7 ± 0.6	12	13.4 ± 1.7	2.1
D209N	≪0.1	<0.1	5.3 ± 0.3	0.8
D210N	<0.1	0.3	11.4 ± 0.9	1.8
Y253A	7.7 ± 1.9	26	35.0 ± 3.5	5.5
F358A	62.6 ± 3.3	209	9.9 ± 0.3	1.5
Y253A,F358A	3.7 ± 0.3	12	5.1 ± 0.1	0.8

[a] Exoribonucleolytic activity of the wild-type enzyme was taken as 100%. The determination of the enzyme exoribonucleolytic activity was carried out by measuring and quantifying the disappearance of the substrate.

MD Simulation of 2ix1 Structure; Modeling of Wild-type Enzyme and Y253A Mutant—To obtain a theoretical dynamic model of RNase enzyme, the previously published x-ray structure of RNase II D209N mutant complexed with a 10-nt poly(A) RNA (Protein Data Bank code 2IX1) (23) was subjected to 4 ns of molecular dynamics (MD)[4] simulation. Re-creation was performed using the PMEMD module and the parm99 parameter set in the AMBER 8 package (27, 28). Based on the resultant *in silico* structure of the mutant, models for wild-type enzyme as well as for Y253A mutant were also generated by substituting appropriate residues using standard homology modeling procedures. Both structures were then subjected to a second MD running to simulate the possible modifications in the protein arrangement and its relationship to the substrate RNA as a result of the introduced changes. Details on the MD method are described in supplemental experimental procedures.

Multiple Sequence Alignment—Homologous sequences belonging to the RNase II, RNase R, and Rrp44 family of proteins were obtained in protein data bases using BLAST (29) and were aligned using ClustalW (30) and T-COFFEE (31) algorithms.

RESULTS AND DISCUSSION

Mutations in the Aromatic Residues That Clamp the RNA Can Alter the End Products—To further determine the role of Tyr-253 and Phe-358 in RNA decay, we mutated these aromatic residues into an alanine and constructed single (Y253A or F358A) and double (Y253A,F358A) mutants. In RNase II the RNA molecule (nt 9–13) is stacked and clamped between the aromatic residues Tyr-253 and Phe-358. Based on structure, we would predict that RNase II would be inactive in the absence of Tyr-253, because the unclamping of the RNA at the active site would disrupt the correct conformation of the substrate, thus impairing catalysis. However, by changing Tyr-253 to Ala 26% of the activity of the enzyme persisted (Table 1 and Fig. 2). Dynamic models built from the crystallographic structure of the RNase II-RNA complex reveal that, in fact, Tyr-253 remains firmly stacked to the putative outgoing nt 13 by its respective aromatic system, even after 4 ns of molecular dynamics simulation and despite the *anti* to *syn* conformational change exhibited by the adenine nucleotide (Fig. 3*A* and supplemental Fig. S3). This result supports that Tyr-253 is actually important for the maintenance of the RNA clamping in RNase II. However, despite its conservation, there must be other residues and contacts at the catalytic cavity that are sufficient for the RNA to bind to the protein. In fact, Phe-250 and Phe-257 residues, located in close vicinity to Tyr-253, could presumably account for such a role, although the corresponding model would require a conformational reorganization of the protein backbone around these positions. Nevertheless, the most surprising result was that the Y253A mutant changed the smallest product of degradation of RNase II from 4 to 10 nt (Fig. 2), an end product not observed before. It is known that for a processive degradation by RNase II the RNA molecule must bind simultaneously to the anchoring and catalytic regions (14, 23). Moreover, the three-dimensional model of the RNase II-RNA complex revealed that a 10-nt fragment is the minimum length of the RNA molecule that is still able to contact both the anchoring and the catalytic regions (23). RNA molecules shorter than 10 nt only establish interactions with the catalytic region, and consequently degradation becomes distributive. In Y253A the absence of Tyr-253 may cause the loosening of the RNA substrate at the catalytic site and, as a consequence, the binding at the anchoring region is essential for the RNA to remain attached to the enzyme. For this reason, RNA is degraded up to 10 nt and the RNA fragment is then released from the enzyme, being therefore the smallest degradation product generated in the Y253A mutant. As such, Tyr-253 must play an essential role in the attachment of the 3′-end of the RNA substrate to the catalytic region. In agreement, the K_D value obtained for Y253A by surface plasmon resonance analysis is 5.5-fold higher than that of the wild-type enzyme (Table 1 and supplemental Fig. S4), and this shows that Y253A substitution significantly impaired RNA binding. Moreover, the modeled structures of Y253A show that, once the Tyr-253-nt 13 stacking is lost, the RNA suffers a large rearrangement, coordinated by corresponding counter movements of contacting RNase II catalytic domain structure (Fig. 3*A* and supplemental Fig. S3*B*). Surprisingly, these movements do not appear to affect directly the geometry of the Asp residues in the active center, thus explaining the remaining catalytic activity of the Y253A mutant.

When analyzing the F358A mutant we found that, unexpectedly, the protein was 2-fold more active than the wild-type (Table 1). Although the smallest degradation product detected was 4 nt, similar to the wild-type, there was a visible product of 5 nt (Fig. 2). This may suggest that Phe-358 is acting as a "propeller," helping to push the last 5 nt toward the catalytic site, until the final product is a 4-nt fragment. However, the K_D was not dramatically affected by this mutation because it was <2-fold higher than that of the wild-type enzyme, suggesting that Phe-358 may be playing a more accessory role in the maintenance of the proper RNA conformation. This hypothesis was confirmed by MD of the structure, which contrary to the data revealed by the three-dimensional structure suggests that the dynamic stability of the Phe-358 stacking could be compromised in the simulation conditions in the general AMBER force

[4] The abbreviation used is: MD, molecular dynamics.

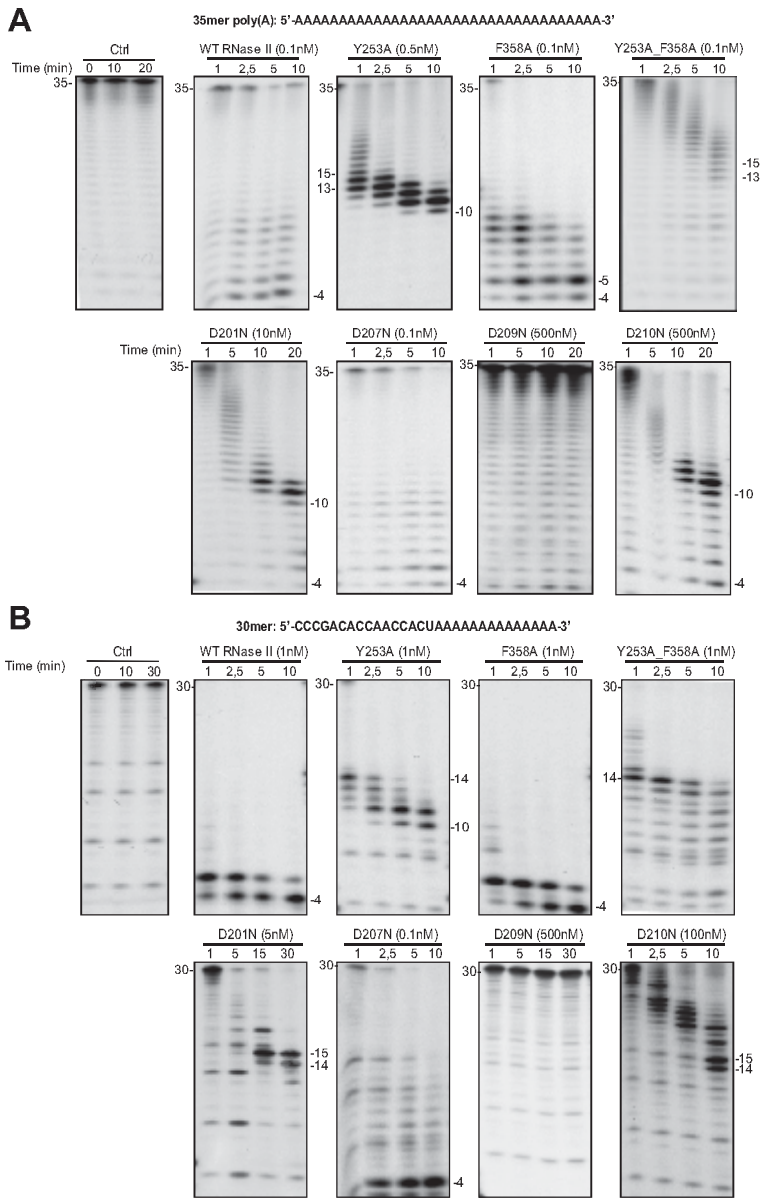

FIGURE 2. **Exoribonuclease activity: comparison of wild-type and mutants.** Activity assays were performed as described under "Experimental Procedures" using a poly(A) chain of 35 nt (*A*) or a 30-mer oligoribonucleotide (*B*) as substrate. The mutants used and their respective protein concentrations are shown. The wild-type enzyme was used as control. Samples were taken during the reaction at the time points indicated, and reaction products were analyzed in a 20% polyacrylamide/7 M urea gel. Control reactions with no enzyme added (*Ctrl*) were incubated at the maximum reaction time for each protein. Length of substrates and degradation products are indicated.

field (27, 28). Nevertheless, in accordance with the experimental results obtained for the F358A mutant, a less active structural role of this residue during catalysis could still be compatible with the real structural data. Therefore, Phe-358 is not equivalent in function to Tyr-253 and, unlike the latter, Phe-358 is not present in all members of the RNase II family (supplemental Fig. S5). Computational models also support that the structural role of these residues in RNA stabilization could also be quite different. Tyr-253 would be responsible for the stacking-mediated stabilization of the outgoing nucleotide at the 3′-end during catalysis (Fig. 3*A*), while the partially conserved Phe-358 position could mediate the transition of the RNA by providing the appropriate hydrophobic environment to prevent spurious contacts. In turn, substitution by a smaller hydrophobic residue, such as alanine, could modify the RNA stability in that region, thus biasing the rate of processing.

The double mutant Y253A,F358A behaved similar to Y253A regarding the size of the smallest product generated, because the end product obtained was 13–15 nt (Fig. 2). However, we detected a decrease in activity (12 *versus* 26%) although the RNA binding affinity was not significantly affected ($K_D = 5.1 \pm 0.1$ nM) (Table 1). Therefore, it seems that the F358A mutation may somehow compensate the absence of Tyr-253 in RNA binding, perhaps allowing an alternative accommodation of the RNA in the catalytic cavity.

To compare RNase II with other family members, we constructed the structural models of *E. coli* RNase R and human Rrp44 proteins based on the RNase II structure (Fig. 1, *B* and *C*). The results clearly indicate that these three enzymes share a common three-dimensional arrangement, being all the critical residues for exoribonucleolytic activity located in equivalent spatial positions. Comparing the three protein models (Fig. 1), it is noteworthy that they have a common arrangement of the clamping tyrosine amino acid. In contrast, the presence of Phe-358 is exclusive to RNase II (supplemental Fig. S5). RNase R protein presents a Phe residue in the immediate downstream position (Phe-429 in RNR_ECOLI sequence), perhaps with a similar functionality in RNA fixing. However, an equivalent residue is completely absent in Rrp44 sequences, where it is substituted mainly by polar residues with uncharged R-groups (Asn and Thr) (supple-

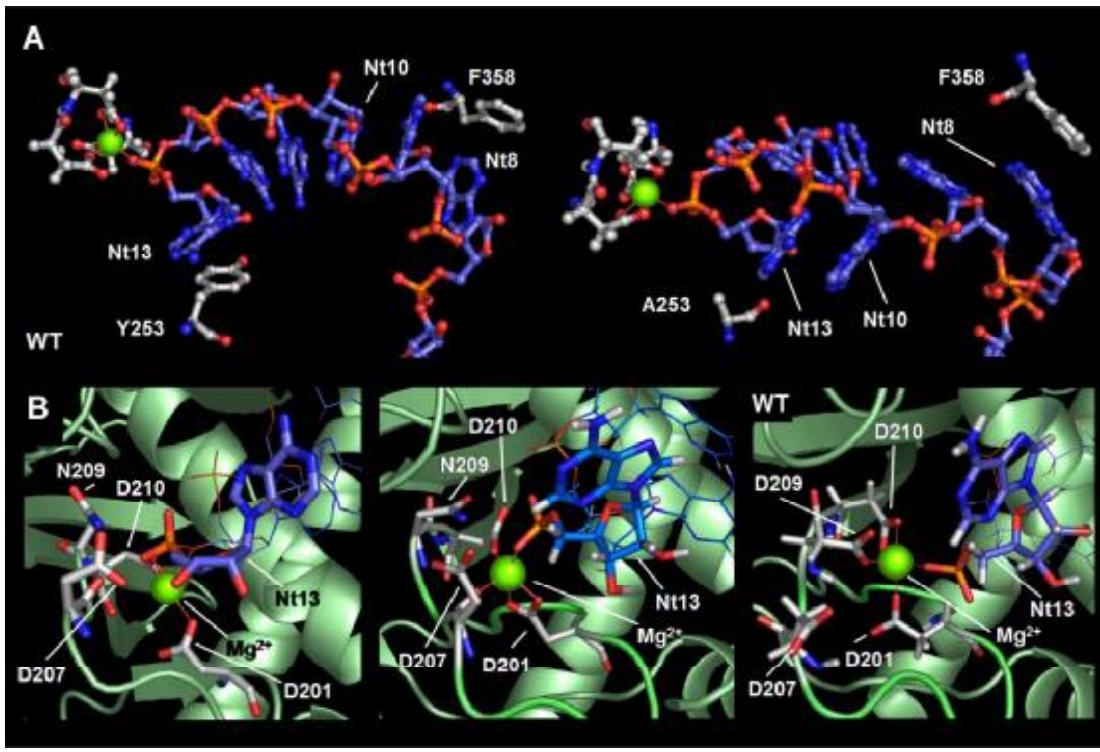

FIGURE 3. **Modeling active center and RNA binding in wild-type and mutant RNase II proteins.** Crystal structure 2ix1 (RNase II-Asp-209 mutant complexed with the RNA) was subjected to molecular dynamics equilibration for 4 ns. The wild-type enzyme and Y253A mutant were modeled and subjected again to equilibration for 1 ns. *A*, relative position of the RNA molecule in wild-type (*left*) and Y253A mutant (*right*) enzymes after 1 ns of molecular dynamics. Despite the lack of notable differences in Asp residues surrounding the Mg^{2+} ion in the active center, the Y253A mutation results in large reorganization of RNA, implicating differences in base-stacking among nucleotides themselves as well as between them and Tyr-253 and Phe-358 residues, probably resulting in loss of stability for RNA positioning. *B*, residues surrounding the active center of the enzyme. *Left*, initial 2ix1 -D209N- crystal structure. *Center*, model for the D209N mutant after 4 ns of MD, showing that whereas Asn-209 does not contact with the Mg^{2+} ion, Asp-207 coordinates it through its backbone CO group. *Right*, MD model for wild-type RNase II showing Asp-209, but not Asp-207, contacting Mg^{2+} in addition to Asp-201, Asp-210, and the phosphate group of nt 13.

mental Fig. S5). The differences in the equivalent amino acid Phe-358 in RNase II, RNase R, and Rrp44 enzymes could explain their differences in regard to RNA degradation. For instance, the final end product of both RNase II and Rrp44 is 4 nt, whereas for RNase R it is a 2-nt fragment (2, 13, 15, 23).

The Highly Conserved Aspartates in RNase II Active Site Are Not Equivalent in Their Role in Catalysis—Four highly conserved aspartic acids, Asp-201, Asp-207, Asp-209, and Asp-210, are located in the RNase II active site. It has been postulated that their function is to position the RNA substrate correctly and promote the nucleophilic attack of the phosphodiester bond (23, 32). The single substitution of Asp-209 by Asn in RNase II (D209N) has been shown to be responsible for the total loss of RNase II activity without affecting RNA binding ability (32) (Table 1 and Fig. 2). A similar mutation in the yeast RNase II homologue Dis3/Rrp44 (D551N) totally abolished activity without reducing substrate binding and was responsible for a very strong growth defect, suggesting that the phenotype of this mutant is very important for yeast physiology (19, 20).

To understand the precise role of these residues, we mutated residues Asp-201, Asp-207, and Asp-210 to asparagines. Our results revealed that mutations in both Asp-201 and Asp-210 lead to a significant loss of activity in degradation of poly(A) (0.2 and 0.3% of that of the wild-type enzyme, respectively) (Table 1). Aspartates 201 and 210 were proposed to be coordinating the Mg^{2+} ion that is essential for catalysis together with two water molecules and two oxygen atoms of the RNA substrate (23). The substitution of these aspartates by asparagines would result in the loss of one of the coordinations, thus destabilizing the cation at the active site and impairing the reaction. Similar reduction in activity was observed with the 30 single-stranded substrate (Fig. 2*B*). Both D201N and D210N mutants generated a 10–11-nt fragment as a major degradation product, although longer reaction times resulted in the usual 4-nt fragment as a secondary product (Fig. 2*A*). The absence of these aspartates may destabilize the attachment of the RNA at the catalytic site, because both residues are contributing to the binding of the RNA at this region, either directly (by Asp-201) or through the Mg^{2+} ion they chelate (Asp-201 and Asp-210) (23). As such, fragments below 10 nt in length, when the binding of the substrate to the anchor region is no longer possible, lead to a distributive degradation, explaining this destabilization. Interestingly, the degradation of the 30 single-stranded seems to stop

after digestion of 15–16 nt, thus generating a 14–15-nt fragment as a final product (Fig. 2*B*). This substrate contains a 16-nt poly(A) tail at its 3′-end, and both D201N and D210N mutant enzymes degrade this tail to completion and then stop. This effect reflects a marked preference by poly(A) substrate that has also been observed in the wild-type enzyme (13–15) but seems to be more pronounced in these two mutants.

The role of Asp-207 does not seem to be so critical for catalysis when compared with the other mutants because after its substitution by asparagine the enzyme still retains 12% activity (Table 1 and Fig. 2). This result differs from previously published data in which the mutation of Asp-207 to alanine led to a more significant loss of activity (2.5% of that of the wild-type enzyme) (25). However, the substitution of an aspartate by alanine may cause local conformational changes other than those generated by the substitution by asparagine in which only the acidic nature of the residue is altered. The structure of the RNase II D209N mutant revealed that Asp-207 is within H-bonding distance of the 3′-OH group of the RNA molecule (Fig. 3*B*). In contrast, after molecular dynamics equilibration during 4 ns, this close contact apparently disappeared and Asp-207 was then positioned in contact with the Mg^{2+} ion in the active center via its backbone CO group (Fig. 3*B*). Surprisingly, when the wild-type protein was modeled and subjected again to molecular dynamics processes, Asp-209 was located in contact with the Mg^{2+} atom, in the active center, resulting in the displacement of Asp-207 to a far position (Fig. 3*B*). As a result of this analysis, Asp-207 does not appear to play such a critical role. Perhaps it only contributes to the general maintenance of the appropriate position of both water and ions, which explains in part the remaining activity of D207N.

As expected, D209N was totally inactive in the degradation of the two substrates tested (Table 1 and Fig. 2), reinforcing the key role of Asp-209 in catalysis. In the three mutant proteins D201N, D207N, and D210N, the K_D ranged between 11 and 14 nM, only 2-fold higher than the wild-type RNase II enzyme (Table 1), thus showing only a slight reduction in the RNA binding affinity. Therefore it seems that aspartates 201, 207, and 210 are not directly involved in the RNA binding (Table 1). In fact, in the crystal structure these three residues interact with the RNA substrate at the active site via the Mg^{2+} ion or by being directly bound to the leaving nucleotide (23). Disruption of such interactions by these mutations would cause the loosening of the RNA at the active site.

Moreover, the three-dimensional models of *E. coli* RNase R and human Rrp44 proteins (Fig. 1, *B* and *C*) revealed that these four aspartic residues have spatial positions equivalent to those in RNase II. Therefore, we can propose similar catalytic roles for these residues in these two RNase II-like enzymes.

In this report we have improved the proposed model for RNA degradation by RNase II by defining the precise role and function of some highly conserved residues present in the active site of the enzyme. We conclude that Tyr-253 and Phe-358 are not essential for catalysis by RNase II, because the enzyme still retains activity after the substitution of these residues by alanines. However, Tyr-253 seems to be a critical residue in setting the smallest product generated by RNase II under the conditions tested. This accentuates the importance of this residue in the stabilization of the 3′-end of the RNA molecule. Tyr-253 is highly conserved and equivalent residues are present in many RNase II family members (supplemental Fig. S5). Taking into account the functional and structural similarities to Rrp44 (20), these conclusions will be particularly important for the evaluation of the role of this residue in recognition, binding, and degradation of different RNA targets. The substitution of Phe-358 results in the increase by 2-fold of the activity of the enzyme. This result suggests that Phe-358 could be preventing a faster degradation of the RNA by stalling its translocation, probably due to the stacking of its aromatic ring between the bases of contiguous nucleotides. Furthermore, we show that the highly conserved aspartates Asp-201, Asp-207, Asp-209, and Asp-210 are not equivalent and that their functions in RNA metabolism are distinct, with Asp-209 being the only residue essential for RNase II activity.

Moreover, the structural models of *E. coli* RNase R and human Rrp44 proteins showed an overall structure similar to that of the RNase II, with the critical residues in similar spatial positions. In addition, the structure of yeast Rrp44 showed that *E. coli* RNase II is a good model and suggests that the RNA recruitment mechanism is conserved. As such, we can hypothesize and extrapolate our findings to related members of the RNase II family.

This study sheds new light on the model previously proposed for RNA degradation by RNase II. In addition, the fact that the RNase II homologue is the only catalytically active nuclease in the exosome highlights the need to unravel the precise role of highly conserved residues. Finally, these results can be applied to better understand the decay mechanisms for all RNase II family members that have revealed a similar mode of action, including those present in the exosome.

Acknowledgments—We thank Ambro Van-Hoof for critical reading and Gonçalo da Costa for advice on the plasmon resonance analysis (Biacore). We also thank Jesús Mendieta for helpful discussions in molecular dynamics approaches and Biomol-Informatics SL for bioinformatics consulting.

REFERENCES

1. Mian, I. S. (1997) *Nucleic Acids Res.* **25,** 3187–3195
2. Mitchell, P., Petfalski, E., Shevchenko, A., Mann, M., and Tollervey, D. (1997) *Cell* **91,** 457–466
3. Grossman, D., and van Hoof, A. (2006) *Nat. Struct. Mol. Biol.* **13,** 760–761
4. Zuo, Y., and Deutscher, M. P. (2001) *Nucleic Acids Res.* **209,** 1017–1026
5. Cairrão, F., Chora, A., Zilhão, R., Carpousis, J., and Arraiano, C. M. (2001) *Mol. Microbiol.* **276,** 19172–19181
6. Andrade, J. M., Cairrão, F., and Arraiano, C. M. (2006) *Mol. Microbiol.* **60,** 219–228
7. Cairrão, F., Arraiano, C., and Newbury, S. (2005) *Dev. Dyn.* **232,** 733–737
8. Zilhão, R., Cairrão, F., Régnier, P., and Arraiano, C. M. (1996) *Mol. Microbiol.* **20,** 1033–1042
9. Zilhão, R., Regnier, P., and Arraiano, C. M. (1995) *FEMS Microbiol. Lett.* **130,** 237–244
10. Cairrão, F., and Arraiano, C. M. (2006) *Biochem. Biophys. Res. Commun.* **343,** 731–737
11. Bollenbach, T. J., Lange, H., Gutierrez, R., Erhardt, M., Stern, D. B., and Gagliardi, D. (2005) *Nucleic Acids Res.* **33,** 2751–2763
12. Lim, J., Kuroki, T., Ozaki, K., Kohsaki, H., Yamori, T., Tsuruo, T., Nakamori, S., Imaoka, S., Endo, M., and Nakamura, Y. (1997) *Cancer*

Res. **57,** 921–925
13. Amblar, M., Barbas, A., Fialho, A. M., and Arraiano, C. M. (2006) *J. Mol. Biol.* **360,** 921–933
14. Cannistraro, V. J., and Kennell, D. (1994) *J. Mol. Biol.* **243,** 930–943
15. Amblar, M., Barbas, A., Gomez-Puertas, P., and Arraiano, C. M. (2007) *RNA* (*N.Y.*) **13,** 317–327
16. Orban, T. I., and Izaurralde, E. (2005) *RNA* (*N.Y.*) **11,** 459–469
17. Lejeune, F., Li, X., and Maquat, L. E. (2003) *Mol. Cell* **12,** 675–687
18. LaCava, J., Houseley, J., Saveanu, C., Petfalski, E., Thompson, E., Jacquier, A., and Tollervey, D. (2005) *Cell* **121,** 713–724
19. Dziembowski, A., Lorentzen, E., Conti, E., and Seraphin, B. (2007) *Nat. Struct. Mol. Biol.* **14,** 15–22
20. Schneider, C., Anderson, J. T., and Tollervey, D. (2007) *Mol. Cell* **27,** 324–331
21. Liu, Q., Greimann, J. C., and Lima, C. D. (2006) *Cell* **127,** 1223–1237
22. Wang, H. W., Wang, J., Ding, F., Callahan, K., Bratkowski, J., Butler, J. S., Nogles, E., and Ke, A. (2007) *Proc. Natl. Acad. Sci. U. S. A.* **104,** 16844–16849
23. Frazão, C., McVey, C. E., Amblar, M., Barbas, A., Vonrhein, C., Arraiano, C. M., and Carrondo, M. A. (2006) *Nature* **443,** 110–114
24. McVey, C. E., Amblar, M., Barbas, A., Cairrão, F., Coelho, R., Romão, C., Arraiano, C. M., Carrondo, M. A., and Frazão, C. (2006) *Acta Crystallogr. Sect. F* **62,** 684–687
25. Zuo, Y., Vincent, H. A., Zhang, J., Wang, Y., Deutscher, M. P., and Malhotra, A. (2006) *Mol. Cell* **24,** 149–156
26. Higuchi, R. (1990) in *PCR Protocols, A Guide to Methods and Applications* (Innis, M. A., Gelfand, D. H., Sninsky, J. J., and White, T. J., eds) pp. 177–183 Academic Press, Inc./Harcourt Brace Jovanovich, San Diego, CA
27. Case, D. A., Cheatham, T. E., III, Darden, T., Gohlke, H., Luo, R., Merz, K. M., Jr., Onufriev, A., Simmerling, C., Wang, B., and Woods, R. J. (2005) *J. Comput. Chem.* **26,** 1668–1688
28. Case, D. A., Darden, T., Cheatham, T. E., III, Simmerling, C., Wang, J., Duke, R. E., Luo, R., Merz, K. M., Jr., Wang, B., Pearlman, D. A., Crowley, M., Brozell, S., Tsui, V., Gohlke, H., Mongan, J., Hornak, V., Cui, G., Beroza, P., Schafmeister, C., Caldwell, J. W., Ross, W. S., and Kollman, P. A. (2004) *AMBER 8*, University of California, San Francisco
29. Altschul, S. F., Madden, T. L., Schaffer, A. A., Zhang, J., Zhang, Z., Miller, W., and Lipman, D. J. (1997) *Nucleic Acids Res.* **25,** 3389–3402
30. Thompson, J. D., Higgins, D. G., and Gibson, T. J. (1994) *Nucleic Acids Res.* **22,** 4673–4680
31. Notredame, C., Higgins, D. G., and Heringa, J. (2000) *J. Mol. Biol.* **302,** 205–217
32. Amblar, M., and Arraiano, C. M. (2005) *FEBS J.* **272,** 363–374

ITQB-UNL | Av. da República, 2780-157 Oeiras, Portugal
Tel (+351) 214 469 100 | Fax (+351) 214 411 277

www.itqb.unl.pt